

REGULATORY PEPTIDES IN NEUROSCIENCE AND ENDOCRINOLOGY: A NEW ERA BEGINS

EDITED BY: Lee E. Eiden, Limei Zhang, Colin Brown and David Vaudry
PUBLISHED IN: Frontiers in Neuroscience and Frontiers in Endocrinology



frontiers

Frontiers eBook Copyright Statement

The copyright in the text of individual articles in this eBook is the property of their respective authors or their respective institutions or funders. The copyright in graphics and images within each article may be subject to copyright of other parties. In both cases this is subject to a license granted to Frontiers.

The compilation of articles constituting this eBook is the property of Frontiers.

Each article within this eBook, and the eBook itself, are published under the most recent version of the Creative Commons CC-BY licence.

The version current at the date of publication of this eBook is CC-BY 4.0. If the CC-BY licence is updated, the licence granted by Frontiers is automatically updated to the new version.

When exercising any right under the CC-BY licence, Frontiers must be attributed as the original publisher of the article or eBook, as applicable.

Authors have the responsibility of ensuring that any graphics or other materials which are the property of others may be included in the CC-BY licence, but this should be checked before relying on the CC-BY licence to reproduce those materials. Any copyright notices relating to those materials must be complied with.

Copyright and source acknowledgement notices may not be removed and must be displayed in any copy, derivative work or partial copy which includes the elements in question.

All copyright, and all rights therein, are protected by national and international copyright laws. The above represents a summary only. For further information please read Frontiers' Conditions for Website Use and Copyright Statement, and the applicable CC-BY licence.

ISSN 1664-8714

ISBN 978-2-88963-225-1

DOI 10.3389/978-2-88963-225-1

About Frontiers

Frontiers is more than just an open-access publisher of scholarly articles: it is a pioneering approach to the world of academia, radically improving the way scholarly research is managed. The grand vision of Frontiers is a world where all people have an equal opportunity to seek, share and generate knowledge. Frontiers provides immediate and permanent online open access to all its publications, but this alone is not enough to realize our grand goals.

Frontiers Journal Series

The Frontiers Journal Series is a multi-tier and interdisciplinary set of open-access, online journals, promising a paradigm shift from the current review, selection and dissemination processes in academic publishing. All Frontiers journals are driven by researchers for researchers; therefore, they constitute a service to the scholarly community. At the same time, the Frontiers Journal Series operates on a revolutionary invention, the tiered publishing system, initially addressing specific communities of scholars, and gradually climbing up to broader public understanding, thus serving the interests of the lay society, too.

Dedication to Quality

Each Frontiers article is a landmark of the highest quality, thanks to genuinely collaborative interactions between authors and review editors, who include some of the world's best academicians. Research must be certified by peers before entering a stream of knowledge that may eventually reach the public - and shape society; therefore, Frontiers only applies the most rigorous and unbiased reviews.

Frontiers revolutionizes research publishing by freely delivering the most outstanding research, evaluated with no bias from both the academic and social point of view. By applying the most advanced information technologies, Frontiers is catapulting scholarly publishing into a new generation.

What are Frontiers Research Topics?

Frontiers Research Topics are very popular trademarks of the Frontiers Journals Series: they are collections of at least ten articles, all centered on a particular subject. With their unique mix of varied contributions from Original Research to Review Articles, Frontiers Research Topics unify the most influential researchers, the latest key findings and historical advances in a hot research area! Find out more on how to host your own Frontiers Research Topic or contribute to one as an author by contacting the Frontiers Editorial Office: researchtopics@frontiersin.org

REGULATORY PEPTIDES IN NEUROSCIENCE AND ENDOCRINOLOGY: A NEW ERA BEGINS

Topic Editors:

Lee E. Eiden, National Institutes of Health (NIH) Bethesda, United States

Limei Zhang, National Autonomous University of Mexico, Mexico

Colin Brown, University of Otago, New Zealand

David Vaudry, Institut National de la Santé et de la Recherche Médicale (INSERM), France

Citation: Eiden, L. E., Zhang, L., Brown, C., Vaudry, D., eds. (2019). Regulatory Peptides in Neuroscience and Endocrinology: A New Era Begins. Lausanne: Frontiers Media SA. doi: 10.3389/978-2-88963-225-1

Table of Contents

- 05 Editorial: Regulatory Peptides in Neuroscience and Endocrinology: A New Era Begins**
Limei Zhang, David Vaudry, Colin H. Brown and Lee E. Eiden
- 10 Sex Dimorphic Responses of the Hypothalamus–Pituitary–Thyroid Axis to Maternal Separation and Palatable Diet**
Lorraine Jaimes-Hoy, Fidelia Romero, Jean-Louis Charli and Patricia Joseph-Bravo
- 26 Voluntary Exercise-Induced Activation of Thyroid Axis and Reduction of White Fat Depots is Attenuated by Chronic Stress in a Sex Dimorphic Pattern in Adult Rats**
Marco Antonio Parra-Montes de Oca, Mariana Gutiérrez-Mariscal, Ma Félix Salmerón-Jiménez, Lorraine Jaimes-Hoy, Jean-Louis Charli and Patricia Joseph-Bravo
- 39 Whole-Brain Mapping of Monosynaptic Afferent Inputs to Cortical CRH Neurons**
Shouhua Zhang, Fei Lv, Yuan Yuan, Chengyu Fan, Jiang Li, Wenzhi Sun and Ji Hu
- 53 Deletion of CRH From GABAergic Forebrain Neurons Promotes Stress Resilience and Dampens Stress-Induced Changes in Neuronal Activity**
Nina Dedic, Claudia Kühne, Karina S. Gomes, Jakob Hartmann, Kerry J. Ressler, Mathias V. Schmidt and Jan M. Deussing
- 69 Effect of Oxytocin on Hunger Discrimination**
Mitchell A. Head, David C. Jewett, Sarah N. Gartner, Anica Klockars, Allen S. Levine and Pawel K. Olszewski
- 79 A Synaptically Connected Hypothalamic Magnocellular Vasopressin-Locus Coeruleus Neuronal Circuit and its Plasticity in Response to Emotional and Physiological Stress**
Oscar R. Hernández-Pérez, Vito S. Hernández, Alicia T. Nava-Kopp, Rafael A. Barrio, Mohsen Seifi, Jerome D. Swinny, Lee E. Eiden and Limei Zhang
- 93 Dynamic Modulation of Mouse Locus Coeruleus Neurons by Vasopressin 1a and 1b Receptors**
Elba Campos-Lira, Louise Kelly, Mohsen Seifi, Torquil Jackson, Torsten Giesecke, Kerim Mutig, Taka-aki A. Koshimizu, Vito S. Hernandez, Limei Zhang and Jerome D. Swinny
- 112 Involvement of Vasopressin in the Pathogenesis of Pulmonary Tuberculosis: A New Therapeutic Target?**
Mario Zetter, Jorge Barrios-Payán, Dulce Mata-Espinosa, Brenda Marquina-Castillo, Andrés Quintanar-Stephano and Rogelio Hernández-Pando
- 123 Pituitary Adenylate Cyclase-Activating Peptide (PACAP)-Glutamate Co-transmission Drives Circadian Phase-Advancing Responses to Intrinsically Photosensitive Retinal Ganglion Cell Projections by Suprachiasmatic Nucleus**
Peder T. Lindberg, Jennifer W. Mitchell, Penny W. Burgoon, Christian Beaulé, Eberhard Weihe, Martin K.-H. Schäfer, Lee E. Eiden, Sunny Z. Jiang and Martha U. Gillette

- 136** *The Roles of the Kisspeptin System in the Reproductive Physiology of the Lined Seahorse (Hippocampus erectus), an Ovoviviparous Fish With Male Pregnancy*
Huixian Zhang, Bo Zhang, Geng Qin, Shuisheng Li and Qiang Lin
- 149** *Spexin-Based Galanin Receptor Type 2 Agonist for Comorbid Mood Disorders and Abnormal Body Weight*
Seongsik Yun, Arfaxad Reyes-Alcaraz, Yoo-Na Lee, Hyo Jeong Yong, Jeewon Choi, Byung-Joo Ham, Jong-Woo Sohn, Dong-Hoon Kim, Gi Hoon Son, Hyun Kim, Soon-Gu Kwon, Dong Sik Kim, Bong Chul Kim, Jong-Ik Hwang and Jae Young Seong
- 160** *Strategies for the Identification of Bioactive Neuropeptides in Vertebrates*
Auriane Corbière, Hubert Vaudry, Philippe Chan, Marie-Laure Walet-Balieu, Thierry Lecroq, Arnaud Lefebvre, Charles Pineau and David Vaudry
- 172** *Conceptualization of a Parasympathetic Endocrine System*
Jonathan Gorky and James Schwaber
- 180** *Neurotrophic, Gene Regulation, and Cognitive Functions of Carboxypeptidase E-Neurotrophic Factor- α 1 and its Variants*
Lan Xiao, Xuyu Yang and Y. Peng Loh
- 190** *Synthetic Peptides as Therapeutic Agents: Lessons Learned From Evolutionary Ancient Peptides and Their Transit Across Blood-Brain Barriers*
David A. Lovejoy, David W. Hogg, Thomas L. Dodsworth, Fernando R. Jurado, Casey C. Read, Andrea L. D'Aquila and Dalia Barsyte-Lovejoy



Editorial: Regulatory Peptides in Neuroscience and Endocrinology: A New Era Begins

Limei Zhang¹, David Vaudry², Colin H. Brown³ and Lee E. Eiden^{4*}

¹ Department of Physiology, Universidad Nacional Autonoma de México, Mexico City, Mexico, ² Normandie Univ, UNIROUEN, Inserm, Laboratory of Neuronal and Neuroendocrine Communication and Differentiation, Neuropeptides, Neuronal Death and Cell Plasticity Team, Rouen, France, ³ Department of Physiology, University of Otago, Dunedin, New Zealand, ⁴ National Institute of Mental Health, Intramural Research Program, NIH, Bethesda, MD, United States

Keywords: regulatory peptides, neuropeptide, incretin, gut-brain axes, translation

Editorial on the Research Topic

Regulatory Peptides in Neuroscience and Endocrinology: A New Era Begins

The Research Topic “Regulatory Peptides in Neuroscience and Endocrinology: A New Era Begins” represents the second such Research Topic gathered under the auspices of the International Regulatory Peptide Society, an international federation of scientists committed to progress in basic research on the biology and physiology of peptides, and translation of that basic research into clinical gains and public health benefit. The first summarized key contributions from RegPep2016 (1), held in Rouen, France July 13–17, 2016. This second corresponds to RegPep2018, held in Acapulco Diamante September 22–25, 2018, with the stated mission of emphasizing the emergence of peptides as therapeutic agents from the basic research on newly discovered regulatory peptides, and new roles of established regulatory peptides, *in vivo*.

We refer here to a new era in regulatory peptide research for two reasons. The first concerns the changing definition of “translation.” The concept of research translation as first formulated in the early twenty-first century, emphasized it as a separate discipline bridging basic and clinical research to accelerate public health gains. This included establishment of separate departments of translational science or translational medicine, to act as the “midwives” for rapidly carrying basic knowledge to the bedside of the patient. However, this formulation has risked the further “siloeing” of scientific and clinical endeavor which the very concept of translational research/science was meant to overcome. We now tend to view translational research as simply all of the research that practitioners do, but performed with a mindfulness of therapeutic application. This is achieved by conferences such as RegPep, at which the actual progress made toward therapeutic fulfillment of promising leads is shared, monitored and assessed. Hence, this editorial overview.

Are we learning both positive and negative lessons about what really works, in the lab and the clinic, to advance understanding of how regulatory peptides perform their roles in systems physiology? Here, several major questions are emerging. These include: (i) how redundant are the functions of multiple peptides that converge on the same circuit nodes in the endocrine and nervous systems? Insulin secretion, for example, is controlled by incretins, neurotransmitters, hormones, paracrine factors, and metabolites-including the focal regulatory point itself, namely glucose. Yet, none of these is “redundant” in the sense of being merely duplicative. Rather, fine regulation of insulin secretion apparently requires all, and therefore therapeutic application of any one target of “insulin regulation” must be seen in the context of this integrative regulation, lest one step forward result in two back, due to counter-regulatory mechanisms intersecting with drug presentation. Regulatory peptides in the central nervous system also regulate glucose indirectly via control of food intake, by a mix of allostatic and homeostatic (or “reward” and “metabolic”) drives.

OPEN ACCESS

Edited by:

Vincent Geenen,
University of Liège, Belgium

Reviewed by:

Gareth Leng,
University of Edinburgh,
United Kingdom

*Correspondence:

Lee E. Eiden
eidenl@mail.nih.gov

Specialty section:

This article was submitted to
Neuroendocrine Science,
a section of the journal
Frontiers in Endocrinology

Received: 14 October 2019

Accepted: 30 October 2019

Published: 04 December 2019

Citation:

Zhang L, Vaudry D, Brown CH and
Eiden LE (2019) Editorial: Regulatory
Peptides in Neuroscience and
Endocrinology: A New Era Begins.
Front. Endocrinol. 10:793.
doi: 10.3389/fendo.2019.00793

The wish to exploit this complexity rather than be overwhelmed by it, is exemplified by the latest batch of incretin-based peptide therapies for management of diabetes (2). So, the new era beginning is one in which it is acknowledged that various treatments will represent opportunities unique to the variations among human physiologies, diets, motivations, threats, and habitual behaviors, and that animal models relevant to human disease will require a subtlety matching these variations.

The presentations from RegPep2018 that have been contributed and selected here represent several distinct themes relevant to the new era of regulatory peptide research.

The systematic study of sex differences is an explosive growth area in “personalized medicine:” sex is the most obvious of the personal differences to be considered in tailoring of therapy in psychiatric, metabolic, oncologic, and immunologic disease arenas to the individual. Male/female differences are not confined to the gonads and their neuroendocrine regulation, but also to the mechanisms whereby appetitive and aversive drives are prioritized, reflecting the behavioral choices of individuals. This intersection of metabolic and hormonal sexual dimorphism penetrant to behavioral dimorphism is illustrated by the contributions of Jaimes-Hoy et al. and Parra-Montes De Oca et al., which represent the first two contributions of this Research Topic. Focusing on the hypothalamic-pituitary-thyroid axis, these laboratories studied two stressors, maternal separation, and restraint, and their effects on the metabolic outcomes of administration of a high-fat diet and voluntary exercise on HPT axis activation, and on the “final outcomes” of body weight and fat content. Clearly, elucidating chains of causality across multiple intersecting endocrine regulatory loops is problematic. However, these contributors emphasize the overall finding that the response of the HPT axis to stress, and stress/metabolism/feeding behavior interactions, shows sexually dimorphic patterns. Fitting this information to human metabolism, feeding behavior, and health outcomes to illuminate gender-specific patterns, both learned and hard-wired, is now an obligatory task for neuroendocrinologists.

The mapping of peptidergic brain circuits, particularly in the mouse in which genetic manipulations and virally-mediated tract tracing can be accomplished, is an area of regulatory peptide research that has been progressing at a rapid rate for the past decade, aided in large part by the Allen Brain Project (www.brain-map.org/). Zhang et al. present here the whole-brain mapping of the afferent inputs to cortical corticotropin-releasing hormone (CRH) neurons. The critically important GABAergic interneurons of the cerebral cortex are increasingly seen as coordinated but functionally independent arrays, and one of the means of distinguishing them is via the neuropeptides that they mutually exclusively express. Neuropeptide expression can provide a marker that in addition allows promoter-specific genetic manipulation of these subpopulations, and ultimately a way of linking neuron structure and neurochemistry to brain circuit function. In this particular case, rabies virus was injected into cerebral cortex in a recipient mouse with the correct trans-genetic trappings to produce virions only in host neurons that are CRHergic (harbor a CRH-promoter-specific Cre element), those virions having the property of uptake and fluorescent

marking of afferent cells (i.e., a retrogradely-labeling *in vivo*-generated “marker virion”). The plethora of inputs (to anterior cingulate cortical CRHergic interneurons) from cortex, thalamus, olfactory area, amygdala, basal forebrain, striatum, hippocampus, midbrain (e.g., ventral tegmental area), and hindbrain (e.g., raphe nuclei) raise several interesting questions, among them: (i) is the functional importance of such inputs proportional to their relative abundance (they range from <1% to 10–15%), (ii) is there any latent topology revealed by such studies?, (iii) if and when will such studies converge and combine to offer novel physiological insight into how CRH and other regulatory peptides function in different types of neurons, and can this information be parlayed into a “combinatorial signaling code” that can be exploited for therapeutical purposes in specific cerebral pathologies? The contribution of Dedic et al. suggests that there are specific neuropathology-related roles played by this very cerebral interneuronal population in the mouse. Thus, deleting CRH from these neurons, while sparing other CRHergic subpopulations throughout the brain, appears to promote stress resilience by damping stress-induced neuronal activation. Put another way, CRH function in this neuronal population seems to be to promote or exaggerate the importance of stress in altering brain function: in animals with CRH deficiency in these neurons but not in hypothalamus and other brain areas, CRH-related endocrine functions appear to be normal, while stress-triggered behaviors (anxiogenesis, for example) are blunted. This is very much in tune with results in other peptide systems, as in dissociation of endocrine and behavioral effects of PACAP in stress responding (3) and a potential harbinger of how sub-specialization of regulatory peptide synaptic function might be exploited therapeutically, should differential delivery to different brain regions (4), or biased signaling agonism and antagonism, be achievable in these functionally distinct systems.

A further intriguing example of discrimination between dynamic homeostatic states afforded by a brain peptidergic system is provided by the report of Head et al. for oxytocin (OT) effects on food intake at various stages of food intake, i.e., before vs. during food intake. A novel hunger discrimination protocol was employed to allow rats to distinguish, based on a two-lever operant procedure, between 2- and 22-h food deprivation, and the effect of i.p. OT. at a dose that diminishes food intake, on discrimination-driven response to these two “hunger states.” The authors conclude that OT affects neuronal activation (c-fos expression) in a broader network of neurons in the sated compared to the hungry state, and thus, with other supporting data including dynamic changes in OTR expression in brain, that OT likely has anorexigenic effects on continued feeding rather than on initiation of feeding when hungry. Given the complex interactions among peptide systems in hypothalamus that control both hunger and satiety, the notion that multiple phases of feeding (each in turn influenced by affect/mood, and other drives including threat aversion and thirst) can be modulated by peptidergic systems encourages further experiments that calibrate peptide effects on feeding to state and trait variables relevant to food intake. A more robust understanding of the motivation for feeding may mean that

combinatorial approaches to multi-peptide control of feeding are on the horizon (Head et al.).

Vasopressin, like the closely-related oxytocin, has effects mediated both in the telencephalon, through synaptic actions via projections from hypothalamus, and in brain stem, perhaps via a combination of hormonal and neuronal peptide action at receptors there. Two contributions (LZ and LE are co-authors of the first report, and LZ is co-author of the second) by Hernández-Pérez et al., and Campos-Lira et al., feature the elucidation of vasopressinergic projections to the locus coeruleus, which are likely to gate stress- and attention-related motivation for various appetitive and aversive behaviors. Similarly to the OT system (see Head et al. above), vasopressin receptor expression seems to be an important dynamic regulator of how important peptide influence on allostatic behavioral responses will be for a given state-sexual, hormonal, metabolic, hydromineral—that the animal finds itself in upon exposure to stressors and other environmental contingencies (and see the very interesting contribution of Zetter et al. re: vasopressin's ectopic production and role in acceleration of infection in tuberculosis, suggesting vasopressin antagonism as a target in TB).

An increasingly important aspect of regulatory peptide action is brought to the fore in considering vasopressin's actions in the brain: the role of classical transmitter co-transmission in the actions of neuropeptides and other regulatory peptides. This is of fundamental importance both centrally and peripherally. The Hernandez-Perez report (Hernández-Pérez et al.) (two authors of this commentary are co-authors of this report) reveals that the vasopressinergic projections to the locus coeruleus, like those to other brain areas including hippocampus, amygdala, and lateral habenula, are also glutamatergic. As pointed out by Hokfelt and colleagues some years ago (5), release of classical transmitters from small synaptic vesicles is likely to be a roughly linear function of neuronal firing frequency, whereas release of regulatory peptides from large dense-core vesicles occurs largely only at high firing frequencies, in part because a higher concentration of intraterminal calcium is required for LCDV vs. SSV release. Although peptides are preferentially released at high firing frequencies, however, this is also the point at which classical transmitter release is also maximal. Thus, attention to the role(s) of small transmitter-regulatory peptide secreted/released *together* must be a part of the analysis of how regulatory peptides act in both the central and peripheral nervous systems (though not for their actions as hormones).

The contribution of Lindberg et al. (LE is a co-author of this report) to the Research Topic emphasizes this latter point. It has previously been shown that the phase-advancing effects of light during late night in the mouse *in vivo*, but not the phase-delaying effects of light during early night, is PACAP-dependent (does not occur in PACAP-deficient mice). In slices of hypothalamus containing suprachiasmatic nucleus (SCN) *ex vivo*, glutamate substitutes for light in driving both late-night phase advance and early-night phase delay, and, as *in vivo*, the former does not occur in slices from PACAP-deficient mice, or from enucleated mice in which denervation of the retinohypothalamic tract input to the SCN has occurred. The permissive role of PACAP in glutamate-dependent phase

advance in the circadian pacemaker center of the brain, the suprachiasmatic nucleus, in response to PACAP/glutamate co-release from retinohypothalamic projections from intrinsically photosensitive retinal ganglion cells (ipRGCs) of the retina, correlates with waxing and waning of PACAP mRNA expression in the RGC layer of the retina *in vivo*.

The contribution on kisspeptin expression and function in the seahorse hypothalamus illustrates a critical mainstay of regulatory peptide research: comparative physiology and neuroendocrinology. Since the very inception of the field, comparisons between mammalian and non-mammalian systems have informed the understanding of regulatory peptides due to conservation of critical structural elements and conservation of critical homeostatic functions among diverse species. The report by Zhang et al. reveals that interaction between kisspeptin and GnRH neurons are critical for sexual maturation initiated in the hypothalamus in response to both brain-intrinsic and brain-extrinsic cues, and that these interacting systems have been honed by evolution not only for sexually segregated reproductive function as found in mammals, but for more variegated sexual options in other species. Knowledge of reproduction of all extant species enriches our understanding of the planetary lifeweb, with practical implications in this case for fish husbandry, as well as the co-evolution of ligand-receptor dyads, and dyadic interactions, that extends beyond these particular brain regulatory peptides (6–8).

Galanin is an intriguing peptide first discovered by chemical means as an amidated gut peptide, rather than based on a search for the structure of a known physiotropic “factor.” Following its structural elucidation, galanin was rapidly shown to be synthesized not only in gut but in brain, adrenal medulla, pituitary and peripheral nervous system. Galanin is truly a “jack of all trades,” even among regulatory peptides (9), and the contribution of Yun et al. exemplifies this. True to the theme of peptide/receptor duplication and redundancy, with evolutionarily acquisition of specialization for divergent ligand-receptor dyads, the novel neuropeptide spexin interacts with galanin receptors types 2 and 3. The structure of spexin, in comparison with that of galanin, has allowed spexin-based drug development with specificity for the latter receptors. In this case, the GALR-2-specific agonist CG2A, when administered intraventricularly in CORTI mice, led to recovery of body weight in these mice (but to weight loss in normal mice). Fear memory consolidation was attenuated, while extinction of fear memory was accelerated, in SG2A-treated mice. These results suggest multiple actions of CG2A along the neural axis, and interestingly, intranasal administration of CG2A showed a similar profile with respect to memory and feeding, suggesting that the compound penetrates the blood-brain-barrier, or at least reaches its key sites of action via specialized transport to those brain regions. These experiments may well be the beginning of further interest in spexin-related peptides as treatments for mood and metabolic disorders, which have a high degree of co-morbidity.

The last four contributions to this Research Topic are reviews rather than original reports, and offer an expanded view of past progress and anticipated future directions for the regulatory peptide field.

Corbière et al. review (DV is a co-author of this report) the cohort of biochemical, bioinformatic, genetic, and pharmacological tools available for combing the genomes, transcriptomes, proteomes, and peptidomes of diverse species and tissues for novel peptides in vertebrates with bona fide biological activity: the case of nociception is used as a primary illustration. The strategies for identifying bioactive neuropeptides depend largely upon the “game plan” of the investigating teams. Goals can be oriented toward discovery, systems biology, or a combination of both. A clear algorithm for identifying (novel) bioactive neuropeptides is not yet in view, likely because diversity of biology begets diversity of technology.

The neuroanatomical superficiality of the review of Gorky and Schwaber is, in a way, refreshing after decades of unnecessary obfuscation about whether to call intrinsic cholinergic gut innervation “parasympathetic” or “enteric.” Intrinsic cholinergic neurons of the gut are, in fact, parasympathetic, and in that sense the intrinsic cholinergic component of the enteric nervous system is in fact not magically different from intrinsic cholinergic parasympathetic innervation of heart, kidney, lung, and other visceral organs. What does make the gut unique, with respect to its parasympathetic innervation, is the plethora of peptide-elaborating cells populating the gastrointestinal tract that are contacted by parasympathetic post-ganglionic (intrinsic) cholinergic neurons, and release paracrine, incretin, autocrine, and hormonal factors (the authors emphasize CCK, VIP, somatostatin and GLP-1 but there are many others). While the “conceptualization of a parasympathetic endocrine system” is in some ways incompletely thought-out in this contribution, the idea of it is a useful heuristic for re-evaluation of many decades of classical physiological observations of the effects of vagotomy on gastrointestinal function, and of the signaling of the gut to the brain, with the aid of modern imaging, tracing, genetic, and biochemical tools. We recommend the excellent review of Powley et al. (10) as a companion to the one offered here in this collection of reports and reviews.

This Research Topic closes with two contributions on polypeptides that might at first blush not seem to fit neatly into the category of “regulatory peptides” yet illustrate several facets of current endeavor in this rich field. The report by Loh and colleagues reviews current information about a new role for carboxypeptidase E (CPE) in neuroprotection. The importance of CPE as a processing enzyme in the chain of intracellular transformations leading from prohormone to peptide hormone has been long appreciated in regulatory peptide biology. CPE has a second role, however, wholly independent of its prohormone processing function, which is to act as a bioactive secreted peptide in its own right, mediating rather dramatic effects on neuronal protection against stress, and primarily in the hippocampus, one of the brain centers for processing of associated sensory

signals in a way that allows basis of future behavior on past experience. It is fitting that the report of Lovejoy et al. is the final contribution of this collection, both original and synthetic, on the state-of-the-art of regulatory peptide research, and its translational potential. Teneurins are polypeptide ligands for receptors within the adhesion GPCR family. The ligand-receptor dyad mediates various facets of intracellular communication that must occur in synaptogenesis and other neurodevelopmental events. A peptide cleaved from the extracellular teneurin domain, called TCAP (teneurin C-terminal associated peptide) bears structural similarity to several family B peptides (including CRH, calcitonin, and secretin), and its receptor (latrophilin) is structurally related to the B family GPCRs. Whether or not TCAPs represent a primordial family B functional equivalent, TCAP-derived peptides may represent both tool pharmacological agents, and potential therapeutical avenues, for modifying family B-related neuroendocrine function and stress-related affective behaviors and disorders. TCAP pharmacology and, ultimately therapeutics, may reflect evolutionary either serendipity or the harvesting of evolutionary bricolage. In either case, regulatory peptide research is the richer for embracing both.

We urge the reader to peruse the contributions of this Research Topic as examples of this emerging new landscape, in which all aspects of regulatory peptide research are viewed in the largest possible physiological, clinical, and therapeutic perspective, so that all new experimental information, whether designed, of nature, or created from careful medical observation, is thoughtfully integrated.

AUTHOR CONTRIBUTIONS

All authors contributed to the writing and editing of this introduction.

ACKNOWLEDGMENTS

This Research Topic is one of the two special issues dedicated to RegPep2018, whose co-chairs (LZ and LE) express gratitude for generous support from the School of Medicine of the UNAM, through Dean Dr. German Fajardo, Secretary General Dr. Irene Durante, Chief Administrative and Legal officers Lics. Luis Arturo Gonzalez Nava, and Luis Gutierrez. We thank the Mexican Academy of Sciences, the International Brain Research Organization, the British Society for Neuroendocrinology, and Elsevier for their generous support. RegPep2018 was also supported by CONACYT-292881, CB-238744, and IN216918. LE acknowledges the support of NIMH-IRP through MH002386. DV acknowledges the support of INSERM (U1239), Rouen University, and Normandy Region and European Union (ERDF).

REFERENCES

- Vaudry H, Tonon MC, Vaudry D. Editorial: trends in regulatory peptides. *Front Endocrinol.* (2018) 9:125. doi: 10.3389/fendo.2018.00125
- Clemmensen C, Finan B, Muller TD, DiMarchi RD, Tschoep MH, Hofmann SM. Emerging hormonal-based combination pharmacotherapies for the treatment of metabolic diseases. *Nat Rev Endocrinol.* (2019) 15:90–104. doi: 10.1038/s41574-018-0118-x
- Jiang SZ, Eiden LE. Activation of the HPA axis and depression of feeding behavior induced by restraint stress are separately regulated by PACAPergic neurotransmission in the mouse. *Stress.* (2016) 19:374–82. doi: 10.1080/10253890.2016.1174851

4. Lee MR, Scheidweiler KB, Diao XX, Akhlaghi F, Cummins A, Huestis MA, et al. Oxytocin by intranasal and intravenous routes reaches the cerebrospinal fluid in rhesus macaques: determination using a novel oxytocin assay. *Mol Psychiatry*. (2018) 23:115–22. doi: 10.1038/mp.2017.27
5. Hokfelt T, Bartfai T, Bloom F. Neuropeptides: opportunities for drug discovery. *Lancet Neurol*. (2003) 2:463–72. doi: 10.1016/s1474-4422(03)00482-4
6. Darlison MG, Richter D. Multiple genes for neuropeptides and their receptors: co-evolution and physiology. *Trends Neurosci*. (1999) 22:81–8.
7. Hoyle CH. Neuropeptide families and their receptors: evolutionary perspectives. *Brain Res*. (1999) 848:1–25.
8. Katz PS, Harris-Warrick RM. The evolution of neuronal circuits underlying species-specific behavior. *Curr Opin Neurobiol*. (1999) 9:628–33.
9. Hokfelt T, Tatemoto K. Galanin—25 years with a multitasking neuropeptide. *Cell Mol Life Sci*. (2008) 65:1793–5. doi: 10.1007/s00018-008-8152-9
10. Powley TL, Jaffey DM, McAdams J, Baronowsky EA, Black D, Chesney L, et al. Vagal innervation of the stomach reassessed: brain-gut connectome uses smart terminals. *Ann N Y Acad Sci*. (2019) 1454:14–30. doi: 10.1111/nyas.14138

Conflict of Interest: The authors declare that the research was conducted in the absence of any commercial or financial relationships that could be construed as a potential conflict of interest.

Copyright © 2019 Zhang, Vaudry, Brown and Eiden. This is an open-access article distributed under the terms of the Creative Commons Attribution License (CC BY). The use, distribution or reproduction in other forums is permitted, provided the original author(s) and the copyright owner(s) are credited and that the original publication in this journal is cited, in accordance with accepted academic practice. No use, distribution or reproduction is permitted which does not comply with these terms.



Sex Dimorphic Responses of the Hypothalamus–Pituitary–Thyroid Axis to Maternal Separation and Palatable Diet

Lorraine Jaimes-Hoy*, Fidelia Romero, Jean-Louis Charli and Patricia Joseph-Bravo

Laboratorio de Neurobiología Molecular y Celular, Departamento de Genética del Desarrollo y Fisiología Molecular, Instituto de Biotecnología, Universidad Nacional Autónoma de México (UNAM), Cuernavaca, Mexico

OPEN ACCESS

Edited by:

Colin Brown,
University of Otago, New Zealand

Reviewed by:

Julie A. Chowen,
Niño Jesús University Children's
Hospital, Spain
Patricia Cristina Lisboa,
Rio de Janeiro State University, Brazil

*Correspondence:

Lorraine Jaimes-Hoy
ljaimes@ibt.unam.mx

Specialty section:

This article was submitted to
Neuroendocrine Science,
a section of the journal
Frontiers in Endocrinology

Received: 22 April 2019

Accepted: 20 June 2019

Published: 11 July 2019

Citation:

Jaimes-Hoy L, Romero F, Charli J-L
and Joseph-Bravo P (2019) Sex
Dimorphic Responses of the
Hypothalamus–Pituitary–Thyroid Axis
to Maternal Separation and Palatable
Diet. *Front. Endocrinol.* 10:445.
doi: 10.3389/fendo.2019.00445

Neonatal stress contributes to the development of obesity and has long-lasting effects on elements of the hypothalamus–pituitary–thyroid (HPT) axis. Given the importance of thyroid hormones in metabolic regulation, we studied the effects of maternal separation and a high-fat/high-carbohydrate diet (HFC), offered from puberty or adulthood, on HPT axis activity of adult male and female Wistar rats. Pups were non-handled (NH) or maternally separated (MS) 3 h/day at postnatal days (Pd) 2–21. In a first experiment, at Pd60, rats had access to chow or an HFC diet (cookies, peanuts, chow) for 1 month. Male and female NH and MS rats that consumed the HFC diet increased their caloric intake, body weight, and serum insulin levels; fat weight increased in all groups except in MS males, and serum leptin concentration increased only in females. Mediobasal hypothalamus (MBH) *Pomc* expression increased in NH-HFC females and *Npy* decreased in NH-HFC males. MS males showed insulinemia and hypercortisolemia that was attenuated by the HFC diet. The HPT axis activity response to an HFC diet was sex-specific; expression of MBH thyrotropin-releasing hormone-degrading ectoenzyme (*Trhde*) increased in NH and MS males; serum TSH concentration decreased in NH males, and T4 increased in NH females. In a second experiment, rats were fed chow or an HFC diet from Pd30 or 60 until Pd160 and exposed to 1 h restraint before sacrifice. Regardless of neonatal stress, age of diet exposition, or sex, the HFC diet increased body and fat weight and serum leptin concentration; it induced insulinemia in males, but in females only in Pd30 rats. The HFC diet's capacity to curtail the hypothalamus–pituitary–adrenal axis response to restraint was impaired in MS males. In restrained rats, expression of *Trh* in the paraventricular nucleus of the hypothalamus, *Dio2* and *Trhde* in MBH, and serum thyroid hormone concentration were altered differently depending on sex, age of diet exposition, and neonatal stress. In conclusion, metabolic alterations associated to an HFC-diet-induced obesity are affected by sex or time of exposition, while various parameters of the HPT axis activity are additionally altered by MS, pointing to the complex interplay that these developmental influences exert on HPT axis activity in adult rats.

Keywords: TRH, TRH-DE, thyroid hormones, maternal separation, stress, palatable diet, sex

INTRODUCTION

Obesity is a devastating human health problem in modern societies (1). Sedentarism and stress, together with access to cheap palatable food high in fats and carbohydrates (HFC), are strong contributors whose interacting effects may synergize and provoke the metabolic syndrome (2, 3). Early-life stress due to deficient maternal care, mimicked in rodents by separation of pups from their mother, alters hypothalamus–pituitary–adrenal (HPA) axis reactivity to stress, food intake, and body weight, and impairs learning and induces anxiety and depressive behaviors (4–7). Outcomes vary among studies and may depend on time, length, and mode of pups' separation, age, or sex (4, 8–10). Daily maternal separation (MS) for 3 h during at least the first 10 postnatal days (Pd) induces long-term stress hyper-reactivity related to changes in DNA methylation of several rat or mice gene promoters involved in HPA axis activity, such as hippocampal glucocorticoid receptor (*Gr*), hypothalamic corticotrophin-releasing hormone (*Crh*) and vasopressin, and pituitary pro-opiomelanocortin (*Pomc*) (11–14). Consumption of a palatable diet rich in carbohydrates and/or fats attenuates stress response in both adult humans and rats (15–17); likewise, MS rats fed an HFC diet present a blunted HPA response to restraint stress compared to chow-fed rats (6).

The sympathoadrenal and neuroendocrine systems, including the hypothalamus–pituitary–thyroid (HPT) axis, are major regulators of energy homeostasis activating adrenergic, glucocorticoid and thyroid hormone (TH) receptors that modulate carbohydrate, lipid, and protein metabolism in multiple organs (18, 19). THs regulate basal metabolic rate accounting for 30% of energy expenditure (20) and, together with noradrenergic stimulation of brown adipose tissue, are responsible for thermogenesis (18). The important role of TH in energy homeostasis includes enhancement of lipolysis in adipose tissue followed by fatty acid uptake by active metabolic tissues, as well as increase of glucose metabolism (18, 21). The HPT axis is controlled by thyrotropin-releasing hormone (TRH) synthesized in neurons of the hypothalamic paraventricular nucleus (PVN) and released at the median eminence near portal vessels that communicate with the anterior pituitary where TRH activates TRH-R1 receptor in thyrotrophs increasing synthesis and release of thyrotropin (TSH). TSH controls the synthesis of thyroxine (T4) at the thyroid; T4 is converted to 3,3',5-triiodo-L-thyronine (T3) by tissue deiodinases I or II (22–25). Released TRH at the median eminence may be degraded by the TRH-degrading ectoenzyme (TRH-DE), present in tanycytes, before it travels to the pituitary regulating the amount of TRH that reaches the thyrotrophs (Figure 5A) (26).

Chronic and some forms of acute stress inhibit various elements of the HPT axis in rats (24, 25, 27–29), and stress during critical periods of development may program its function. A history of physical/emotional abuse or neglect has been linked with reduced plasma levels of T3 in adolescents (30) and low plasma levels of TSH in adult women (31).

In a previous study, we showed that maternal separation causes long-term changes in the offspring in a sex-specific manner on some elements of the HPT axis of adult rats and

blunts fasting-induced inhibition of the HPT axis activity of male rats but not females (32). Thus, we hypothesized that stress early in life may cause sex-specific responses of the HPT axis activity to an HFC diet in adult rats. Given the importance of THs in lipid and glucose metabolism as well as energy expenditure (18), the biological and physiological differences between males and females in energy metabolism (33), and especially in the neuroendocrine responses to stress (34, 35), we studied the effects of maternal separation and an HFC diet, starting at puberty or adulthood, on the HPT axis activity under basal conditions or after an acute stress insult in male and female adult rats. We also evaluated some metabolic (leptin, insulin, glucose) and neuroendocrine and endocrine (*Pomc* and *Npy* expression, HPA axis) parameters related to diet-induced obesity and stress, some of which modulate the activity of TRH neurons in the PVN.

MATERIALS AND METHODS

Animals

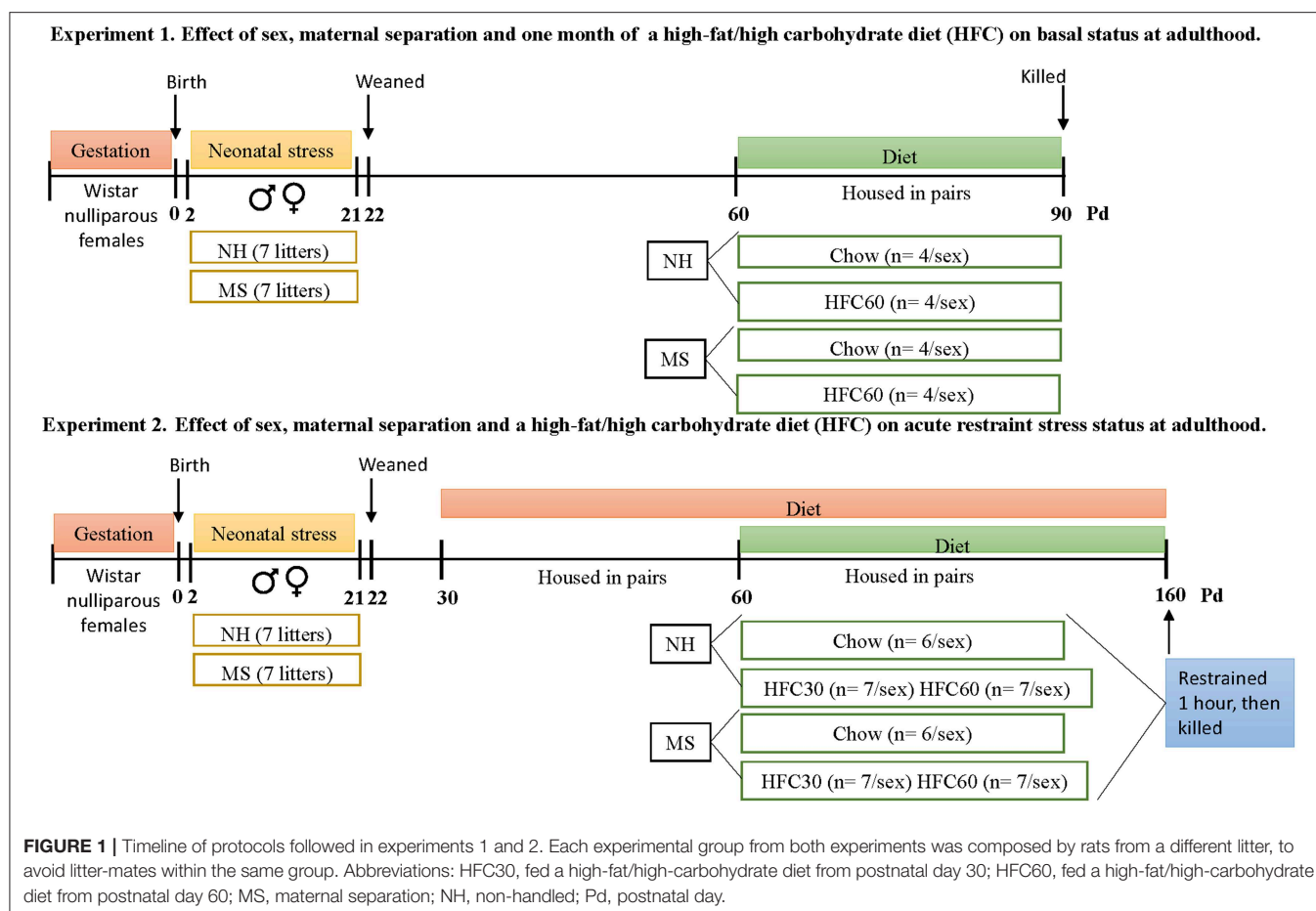
Protocols followed the NIH Guide for the Care and Use of Laboratory Animals and the Official Mexican Norm for production, care, and use of laboratory animals NOM-062-ZOO-1999. All experiments were approved by the Bioethics Committee of the Instituto de Biotecnología, UNAM (authorization project number 311). Protocols for experiments 1 and 2 are described in Figure 1.

Maternal Separation

Two independent experiments were performed, using a different cohort of nulliparous Wistar female rats ($n = 14/\text{experiment}$) from the Institute's outbred colony; pregnant rats were individually housed in a temperature ($22 \pm 1^\circ\text{C}$) and humidity (50–55%) controlled room on a 12-h dark–light cycle with chow (Teklad 2018SX, Envigo, USA) and water available *ad libitum*. As previously described (32), the day of birth was considered postnatal day 0 (Pd0); at Pd1, litters were culled to 8 pups/dam (4 males and 4 females) and were randomly assigned to the non-handled group (NH, $n = 7$ litters) for which pups were only manipulated once a week for cage cleaning or the maternal separation group (MS, $n = 7$ litters). Briefly, for the MS procedure, starting at Pd2 and until Pd21, pups were placed in a new cage with standard bedding material at 9:00 a.m. and moved to an adjacent room with controlled temperature ($30\text{--}32 \pm 0.5^\circ\text{C}$), 3 h/day. Pups were weaned at Pd22, and one rat from each litter was randomly selected to house four/cage according to sex and neonatal protocol (NH or MS); at Pd60, rats were housed two/cage, in separate rooms according to sex. In experiment 1, a total of 16 males and 16 females were used; in experiment 2, a total of 40 males and 40 females of a different cohort were used.

Diet

Maternal separation affects the metabolic response to a high-fat/high-sucrose diet later in life (4) and changes some elements of the HPT axis in adult rats (32); in addition, there is a clear relationship between palatable foods high in fats and carbohydrates and stress in humans and animals that suggests a therapeutic value of “comfort foods”; in turn, stress affects feeding



behavior and food choice (2, 5, 36). Thus, in the first experiment (Figure 1), we evaluated the response of the HPT axis of MS adult rats to 1 month of a palatable diet high in fat and high in carbohydrates (HFC). From Pd60 to 90, rats were randomly exposed to chow (C; NH, $n = 4/\text{sex}$; MS, $n = 4/\text{sex}$) or an HFC diet (NH, $n = 4/\text{sex}$; MS, $n = 4/\text{sex}$); all animals within each experimental group came from different litters. Basal activity of the HPT axis is inhibited in response to an acute stress (24), and the type of diet can alter the stress response of adult rats (2, 5, 36). In addition, adolescence is a vulnerable developmental period where feeding behavior is susceptible to insults (37) and availability of palatable foods increases female susceptibility to develop obesity and metabolic syndrome later in life (37, 38) and it may be exacerbated by MS in adult female rats (9). Thus, in the second experiment (Figure 1), we studied the effect of restraint stress on the activity of the HPT axis of adult obese animals with or without neonatal stress. To ensure an obese state in adult animals, chow (NH, $n = 6/\text{sex}$; MS, $n = 6/\text{sex}$) or an HFC diet (NH, $n = 7/\text{sex}$; MS, $n = 7/\text{sex}$) was offered to juvenile (Pd30) or adult (Pd60) rats for a longer period (until Pd160) compared to experiment 1. As in the first experiment, all animals within each experimental group came from different litters. NH and MS groups had *ad libitum* access to either chow (Teklad 2018SX, Envigo, USA) or an HFC diet and water. Each cage of HFC-fed rats contained three choices of food: chow [Teklad

2018SX, Envigo, USA, diet composition: 3.1 kcal/g; 21.03 g of protein, 7.01 g of fat (84% of unsaturated fatty acids, 16% of saturated fats), and 50.8 g of complex carbohydrates per 100 g], organic-animal cookies [3.9 kcal/g; 7.14 g of protein, 10.71 g of fat (66.6% of unsaturated fatty acids, 33.3% of saturated fat), and 67.85 g of carbohydrate (73.6% of complex carbohydrates, 26.3% of sugar) per 100 g; vanilla flavored, Kirkland, USA], or raw unsalted-skinned peanuts produced in Mexico [5.68 kcal/g; 25.75 g of protein, 49.4 g of fat (93.6% of unsaturated fatty acids, 6.4% of saturated fats), and 16.23 g of carbohydrate per 100 g]. Body weight was registered weekly and food intake was registered every fourth day (considering spilled food). Intake of some essential amino acids was calculated, since wheat (from cookies) is deficient in lysine, and peanuts in threonine and methionine (39, 40); digestibility and bioavailability of protein was considered (39, 41).

Restraint Stress

To evaluate the HPT axis sensitivity of adult male and female obese rats to an acute stress with or without maternal separation, in the second experiment at Pd160, rats were restrained from 9:00 to 10:00 a.m. in a prone position, and immediately sacrificed. Since body size of rats varied, a metal wire mesh was folded according to their size, with their tail hanging out to avoid heating. A baseline blood sample was taken by tail clipping within

3 min (250–300 μ l) and at 30 and 60 min following initiation of the restraint to quantify serum corticosterone levels (42). Blood glucose concentration was measured before and 60 min after introducing the rats to the restrainer using an Accutrend strip and analyzer (Roche Diagnostics, USA).

Tissue Collection

Non-fasted animals were killed (43) at Pd90 (experiment 1) or Pd160 (experiment 2) by decapitation (42), in an independent room, by an experienced technician; trunk blood was collected to obtain the serum and was stored in aliquots at -20°C for posterior hormone determinations. Brains were immediately removed and carefully placed on crushed dry ice; once frozen, they were stored at -70°C for mRNA purification and expression analyses of genes of interest. White adipose tissue (WAT) depots (gonadal, retroperitoneal, and interscapular) were dissected and weighed fresh.

mRNA Level Analyses

Coronal brains sections were dissected to obtain the hypothalamic PVN (Bregma -0.84 to -2.3 mm) or the mediobasal hypothalamus (MBH; Bregma -2.3 to -3.6 mm), which contains the arcuate nucleus, basal part of the third ventricle with tanycytes, and median eminence, using a 1- or a 0.5-mm-internal-diameter sample corer (Fine Science Tools, Foster City, CA), respectively. Total RNA was extracted from frozen PVN or MBH using the guanidine thiocyanate method (44); RNA concentration was quantified and its purity was verified, using a Nanodrop spectrophotometer (ThermoScientific 2000c). RNA integrity of every sample was verified by running an aliquot (0.5 μ g) of intact RNA on a denaturing agarose gel; a 28S/18S rRNA ratio above 1.5 was considered adequate to use for RT-PCR. Relative mRNA levels were measured by RT-PCR; PVN *Trh* and *Crh*, and MBH *Trhde* and deiodinase type 2 (*Dio2*) mRNAs were measured as previously described (45–47). Amplification conditions for MBH *Npy* (5'-TATCCCTGCTCG TGTGTTTG-3' and 5'-GTTCTGGGGGCATTTTCTG-3') and *Pomc* (5'-TTGATGATGGCGTTCTTGAA-3' and 5'-GAGATT CTGCTACAGTCGCTC-3') cDNAs were as follows: $T_m = 64^{\circ}\text{C}$, 26 and 27 cycles, respectively. The expression level of target genes was normalized against cyclophilin (experiment 1) or 18S ribosomal RNA (experiment 2; 5'-CGGACAGGATTGACAG ATTG-3', 5'-CAAATCGCTCCACCAACTAA-3'; $T_m = 64^{\circ}\text{C}$ and 17 cycles). Primers were synthesized in the synthesis and sequencing DNA unit of Instituto de Biología, UNAM.

Serum Hormone Analyses

Serum concentration of TSH (NIDDK reagents, Bethesda, MD; sensitivity range = 2.5–80 ng/ml) and corticosterone (reagents from Merck-Millipore, Perkin Elmer and Sigma; limits of detection, 20–2,000 ng/ml) were quantified by radioimmunoassay. Total T3 (limits of detection, 0.75–10 ng/ml) and T4 (limits of detection, 1–30 μ g/dl) were quantified by ELISA [kits from Diagnóstica Internacional (Zapopan, JAL., México)] following the manufacturer's instructions, except for one variation: standard curve was prepared by adding 25 μ l of rat hypothyroid serum to the calibrators provided in the kit,

as recommended (48). Leptin (assay range, 0.2–12.8 ng/ml) and insulin (sensitivity range, 0.1–12.8 ng/ml) were measured using rat ELISA kits from Crystal Chem Inc. (Downers Grove, IL), ACTH using an ELISA kit from USCNC Life Science (Wuhan P.R., China; detection range, 12.35–1,000 pg/ml), and 17β -estradiol using an ELISA kit from Arbor assays (Michigan, USA; limits of detection, 3.75–120 pg/ml). Experiments 1 and 2 were analyzed independently; for each experiment, samples from male and female rats were measured in duplicate within a single assay, and inter-assay and intra-assay coefficients of variation were below 10%.

Statistical Analyses

Results are reported as the mean \pm S.E.M. Data were analyzed by a three-way ANOVA to determine effects of neonatal stress (NH vs. MS), diet (chow vs. HFC), sex (male vs. female rats), and the interaction of these variables. If a significant main effect or interaction was found, ANOVA was followed by the Holm–Sidak multiple comparisons test; the level of significance was set at $p < 0.05$. Pearson's correlation coefficient was used to examine the association between serum leptin or insulin levels and some predictive variables of obesity. Statistical analyses were performed using the GraphPad Prism8 software.

RESULTS

Experiment 1. Effect of Sex, Maternal Separation, and 1 Month of an HFC Diet on Basal Status at Adulthood

Food Intake and Body Weight

Food intake and body weight were monitored from weaning until the end of the experiment (Pd90). There was no difference in the amount of chow consumed during Pd30–60 between MS and NH male rats (**Supplementary Figure 1A**), though MS males weighed slightly less than NH rats [stress effect $F_{(1, 548)} = 4.79$, $p = 0.04$; **Supplementary Figure 1B**]. MS did not affect chow intake and body weight of females at this age period (**Supplementary Figures 1A,B**). During Pd60–90, there was an effect of MS [$F_{(1, 80)} = 6.21$, $p = 0.02$], diet [$F_{(2, 80)} = 92.83$, $p < 0.0001$], sex [$F_{(1, 80)} = 281.22$, $p < 0.0001$], and an interaction of diet and sex [$F_{(2, 80)} = 4.5$, $p = 0.04$] on food intake. Chow-fed MS male rats, but not females, reduced their food intake compared to the NH group (**Supplementary Figure 2A**), but MS rats gained weight similarly to the NH group in both sexes; no differences were observed in intake of kcal/kg of body weight (BW) between MS-chow and NH-chow (**Table 1**). The HFC diet offered starting at adulthood (Pd60) for 1 month reduced chow intake in both sexes, and both NH and MS groups increased caloric intake, mainly from cookies and peanuts (**Supplementary Figures 2A,B**), body weight [except MS-HFC60 females; diet effect $F_{(1, 23)} = 53.18$, $p < 0.0001$; sex effect $F_{(1, 23)} = 17.63$, $p = 0.0003$; MS and diet $F_{(1, 23)} = 5.87$, $p = 0.02$; diet and sex $F_{(1, 23)} = 6.81$, $p = 0.015$; MS, diet and sex $F_{(1, 23)} = 11.22$, $p = 0.002$], and gonadal fat weight/kg [except in MS-HFC60 males; diet effect $F_{(1, 23)} = 15.4$, $p = 0.008$; **Table 1**]. NH and MS females had a smaller intake of total kilocalories than males

TABLE 1 | Effect of maternal separation and 1 month of a high-fat/high-carbohydrate diet on metabolic and HPT axis parameters (experiment 1).

	Males				Females			
	NH		MS		NH		MS	
	C	HFC60	C	HFC60	C	HFC60	C	HFC60
BWg (g)	103 ± 4	135 ± 10*	102 ± 4	150 ± 6***	29 ± 4 ^A	66 ± 5* ^A	36 ± 5 ^A	46 ± 3 ^A
kcal/kg BW	202 ± 4	241 ± 6*	181 ± 9	225 ± 4*	243 ± 7	334 ± 16*** ^A	240 ± 8	304 ± 19*
gWAT(g/kg)	45 ± 3	66 ± 6*	52 ± 4	61 ± 4	18 ± 4	26 ± 1.5*	15 ± 0.6	23 ± 0.5*
Leptin (ng/ml)	10.6 ± 3.5	16 ± 1.2	11.7 ± 0.4	15 ± 2	3.5 ± 0.9	9.7 ± 1.1*** ^A	3.9 ± 0.5	8.3 ± 2*
Insulin (ng/ml)	1.4 ± 0.09	3.1 ± 0.6*	2.4 ± 0.3 [†]	5 ± 1.5*	2 ± 0.4	3.7 ± 0.3*	2.2 ± 0.2	2 ± 0.09 ^A
ACTH (ng/ml)	348 ± 68	346 ± 54	407 ± 8	246 ± 50	81 ± 21	35 ± 9* ^A	125 ± 6 ^A	144 ± 38 ^A
Cort (ng/ml)	59 ± 9	56 ± 12	162 ± 26 [†]	54 ± 2*	194 ± 25	209 ± 45 ^A	174 ± 15 ^A	121 ± 6
<i>Pomc</i>	100 ± 8	122 ± 14	109 ± 14	114 ± 13	100 ± 10	132 ± 6* ^A	111 ± 12	89 ± 13
<i>Npy</i>	100 ± 4	80 ± 2*	97 ± 4	86 ± 4	100 ± 1	100 ± 2	84 ± 9	96 ± 4
<i>Trhde</i>	100 ± 15	228 ± 32*	226 ± 36 [†]	347 ± 31*	100 ± 13	140 ± 8* ^A	98 ± 10 ^A	108 ± 8 ^A
<i>Dio2</i>	100 ± 10	88 ± 8	91 ± 18	122 ± 6	100 ± 12	98 ± 2	109 ± 5	100 ± 6
TSH (ng/ml)	1.4 ± 0.01	0.75 ± 0.07*	1 ± 0.05 [†]	1.2 ± 0.04	0.7 ± 0.1	0.5 ± 0.1	0.78 ± 0.1	0.56 ± 0.05
T4 (ng/dl)	2.84 ± 0.1	2.97 ± 0.3	2.48 ± 0.4	2.66 ± 0.2	1.75 ± 0.3	2.59 ± 0.3*	2.04 ± 0.6	2.1 ± 0.2
T3 (ng/dl)	115 ± 6	118 ± 15	105 ± 30	104 ± 8	75 ± 7	94 ± 18	93 ± 12	78 ± 1.7

Non-handled (NH) or maternal separated (MS) male and female rats were either fed chow (C) or a high-fat/high-carbohydrate diet (HFC) from postnatal day (Pd) 60–90. Body weight gain (BWg) and intake of kcal/kg of body weight (BW) were registered during the adult period (Pd60–90), and gonadal white adipose tissue (gWAT) at Pd90. Metabolic and HPT axis parameters were quantified at the end of the experiment (Pd90). Expression of pro-opiomelanocortin (*Pomc*), neuropeptide Y (*Npy*), TRH degrading ectoenzyme (*Trhde*), and deiodinase type 2 (*Dio2*) were semi-quantified in the mediobasal hypothalamus (MBH) and are expressed as % of values of NH-chow rats. Data are presented as mean ± S.E.M. and were analyzed by a three-way ANOVA to determine effects of neonatal stress, diet, sex, and the interaction of these variables. If a significant main effect or interaction was found, ANOVA was followed by the Holm–Sidak multiple comparisons test; the level of significance was set at $p < 0.05$. [†] $p < 0.05$ MS-C vs. NH-C; * $p < 0.05$, *** $p < 0.001$ vs. chow; ^Avs. MS-HFC60; ^Avs. males. NH-C and NH-HFC60 $n = 4/\text{sex}$, MS-C and MS-HFC60 $n = 4/\text{sex}$. Cort, corticosterone.

[sex effect $F_{(1, 23)} = 281.2$, $p < 0.0001$], but given their lower body weight, the relative intake (kcal/kg BW) of NH-HFC60 in females was higher than in males [sex effect $F_{(1, 23)} = 6.78$, $p = 0.015$; **Table 1**].

Neuroendocrine and Endocrine Parameters

Serum insulin levels slightly increased in MS-chow-fed males but not females [sex effect $F_{(1, 23)} = 5.34$, $p = 0.03$; **Table 1**], as previously described (9). After 1 month of exposure to the HFC diet, although relative epididymal WAT weight increased in NH male rats, serum leptin concentration did not change, while insulinemia was induced in NH-HFC60- and MS-HFC60-fed male rats [diet effect $F_{(1, 23)} = 4.25$, $p = 0.05$; **Table 1**]. Serum insulin concentration correlated positively with epididymal WAT weight of HFC-60 groups ($r = 0.81$; $p = 0.01$) but not of chow-fed males, whose epididymal WAT weight correlated instead with serum leptin concentration ($r = 0.66$; $p = 0.03$). In contrast, in NH and MS females fed an HFC diet, serum leptin concentration increased [diet effect $F_{(1, 23)} = 22.43$, $p = 0.0002$; sex effect $F_{(1, 23)} = 5.96$, $p = 0.02$; diet and sex effect $F_{(1, 23)} = 5.51$, $p = 0.03$], while insulinemia was only present in NH-HFC60 rats (**Table 1**).

MS induced persistent stress in chow-fed male rats, evidenced by increased serum corticosterone concentration that was lowered by 1 month of feeding an HFC diet [MS and diet effect $F_{(1, 23)} = 6.48$, $p = 0.02$; MS and sex effect $F_{(1, 23)} = 5.82$, $p = 0.02$; **Table 1**], but no change in serum ACTH concentration was observed, compared to NH-chow-fed rats (**Table 1**). In contrast, neither an HFC diet nor MS affected stress markers in adult female rats, except for a lower serum ACTH concentration in

NH-HFC60 compared to chow-fed female rats [MS and sex effect $F_{(1, 23)} = 12.11$, $p = 0.0025$; MS, diet, and sex effect $F_{(1, 23)} = 5.41$, $p = 0.03$; **Table 1**]. Serum 17 β -estradiol concentration was not affected by MS or 1 month of feeding an HFC diet in female rats (**Supplementary Figure 3A**).

Expression of MBH peptides was modified by sex and/or the HFC diet, but not by MS; *Pomc* mRNA levels increased in NH-HFC60 females compared to NH-chow and MS-HFC60 groups [diet effect $F_{(1, 23)} = 5.04$, $p = 0.04$; **Table 1**], and *Npy* mRNA levels decreased in NH-HFC60 males compared to chow-fed rats [diet effect $F_{(1, 23)} = 5.51$, $p = 0.04$; diet and sex effect $F_{(1, 23)} = 13.5$, $p = 0.001$; **Table 1**] as reported by Obici et al. (49) and Schwinkendorf et al. (50).

MS modified elements involved in the HPT axis activity, including an increase of *Trhde* mRNA levels in the MBH [MS effect $F_{(1, 23)} = 6.67$, $p = 0.019$; sex effect $F_{(1, 23)} = 29.86$, $p < 0.0001$; MS and sex effect $F_{(1, 23)} = 10.28$, $p = 0.005$; **Table 1**] and a decrease of serum TSH concentration [MS effect $F_{(1, 23)} = 5.47$, $p = 0.04$; **Table 1**] compared to NH males, but not in females, as published (32). Consumption of an HFC diet increased MBH-*Trhde* expression in NH and MS males [diet effect $F_{(1, 23)} = 13.02$, $p = 0.002$; diet and sex effect $F_{(1, 23)} = 5.15$, $p = 0.03$; **Table 1**], while only in NH-HFC60 females compared to NH-chow-fed rats (**Table 1**). MBH-*Dio2* expression was not modified under any condition (**Table 1**). The HFC diet decreased serum TSH concentration in NH males compared to chow-fed rats [diet effect $F_{(1, 23)} = 4.31$, $p = 0.05$; **Table 1**], whereas that of T4 was higher only in female NH-HFC60 than in NH-chow rats [diet effect $F_{(1, 23)} = 4.28$, $p = 0.05$; **Table 1**].

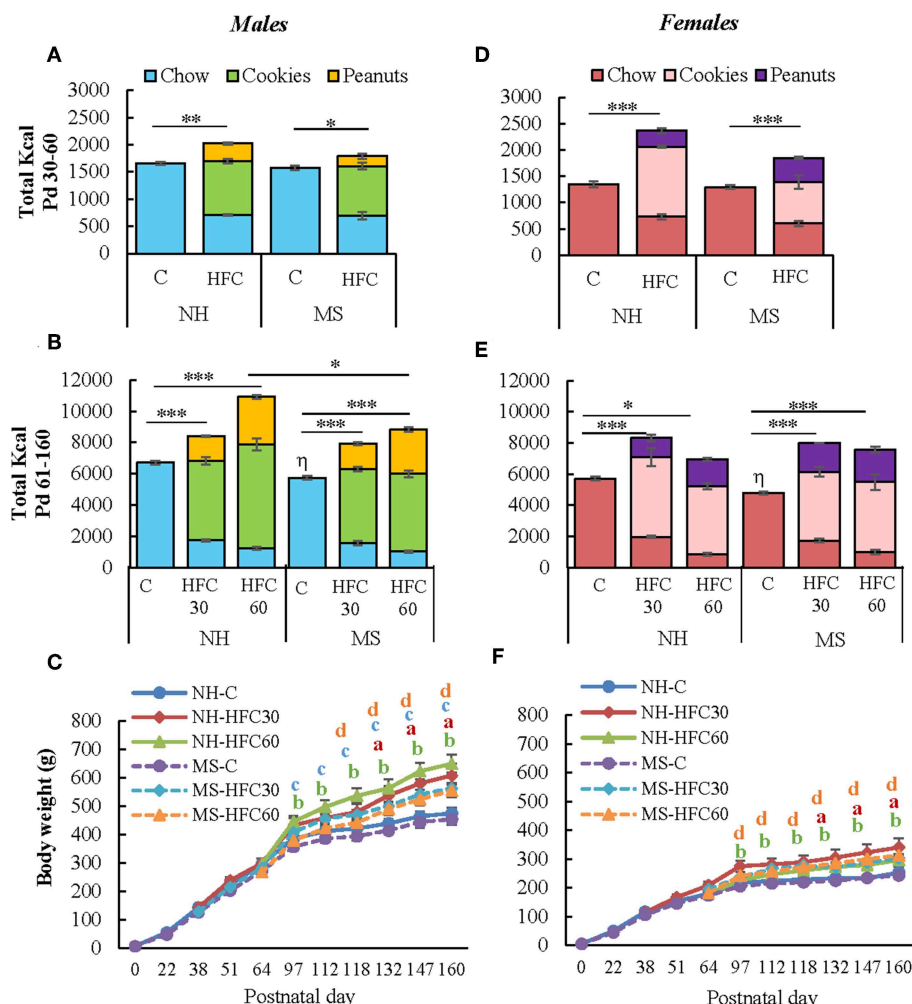


FIGURE 2 | Effect of maternal separation and a high-fat/high-carbohydrate diet on food intake and body weight. Male and female pups were non-handled (NH) or separated from the dam (MS) daily from postnatal day 2–21 (Pd) for 3 h. NH and MS rats had free access to either chow (C) or a high-fat/high-carbohydrate diet (HFC: cookies, peanuts, and chow) from Pd30 (HFC30) or 60 (HFC60) until Pd160. Total kilocalorie intake during the juvenile period (A,D) and adulthood (B,E). (C,F) Body weight of male and female rats from birth until Pd160. Food intake was calculated by dividing the daily kilocalorie intake per cage by the number of rats in the cage (two rats/cage). Data are expressed as mean \pm S.E.M. and were analyzed by a three-way ANOVA to determine effects of neonatal stress, diet, sex, and the interaction of these variables. If a significant main effect or interaction was found, ANOVA was followed by the Holm–Sidak multiple comparisons test; the level of significance was set at $p < 0.05$. * $p < 0.05$, ** $p < 0.01$, *** $p < 0.001$, ^avs. NH-C, ^bNH-HFC30 vs. NH-C, ^cNH-HFC60 vs. NH-C, ^dMS-HFC30 vs. MS-C, ^eMS-HFC60 vs. MS-C. NH-C $n = 6$ /sex, NH-HFC30 and NH-HFC60 $n = 7$ /sex, MS-C $n = 6$ /sex, MS-HFC30, and MS-HFC60 $n = 7$ /sex.

Experiment 2. Effect of Sex, Maternal Separation, and an HFC Diet on Acute Restraint Stress Status at Adulthood Food Intake and Diet Preference, Body Weight, and Composition

NH and MS rats were fed a chow or a high-fat/high-carbohydrate diet from Pd30 or 60 up to Pd160 and then exposed 1 h to restraint stress before sacrifice. As in experiment 1, MS males and females on a chow diet consumed similar kcal as their respective NH group during adolescence (Figures 2A,D). MS did not change food preference; however, MS-chow rats of both sexes had lower food intake than NH-chow animals during adulthood, with males consuming more kcal than females [MS effect $F_{(1, 80)} =$

10.8, $p < 0.0014$; sex effect $F_{(1, 80)} = 65.4$, $p < 0.0001$; MS and sex effect $F_{(1, 80)} = 5.66$, $p = 0.01$; Figures 2B,E]; thus, the proportion of each macronutrient contributing to total kilocalorie intake remained the same (Supplementary Table 1). Availability of palatable food diminished chow intake [diet effect $F_{(1, 80)} = 4011.23$, $p < 0.0001$; sex effect $F_{(1, 80)} = 20.45$, $p < 0.0001$; sex and diet effect $F_{(1, 80)} = 15.45$, $p = 0.0002$], with cookies being the largest contributor of kilocalorie intake in male and female rats followed by peanuts, at all ages (Figures 2A,B,D,E). NH and MS male and female rats that had access to the HFC from Pd30 (HFC30 group) consumed slightly more total kilocalories compared to chow-fed groups during the adolescence period [diet effect $F_{(1, 80)} = 157.24$, $p < 0.0001$; MS and diet effect $F_{(1, 80)} = 11.2$, $p = 0.001$; diet and sex effect $F_{(1, 80)} = 33.97$, $p < 0.0001$;

TABLE 2 | Effect of maternal separation and 3–4 months of a high-fat/high-carbohydrate diet on metabolic parameters in acutely restrained rats (experiment 2).

Males	NH			MS		
	C	HFC30	HFC60	C	HFC30	HFC60
Epididymal WAT (g/kg)	24.92 ± 2.6	47.4 ± 5.2*	43.8 ± 3.3*	27.54 ± 2.6	44.53 ± 4*	40.1 ± 3.9*
Retroperitoneal WAT (g/kg)	36.84 ± 4.9	70.05 ± 9.8*	88.02 ± 3.8**	37.85 ± 3.3	71.96 ± 4.8*	67.09 ± 5.1*
Interscapular WAT (g/kg)	5.43 ± 0.7	11.9 ± 3.3*	13.06 ± 0.4*	4.92 ± 0.4	9.55 ± 2.8*	11.1 ± 1.2*
Leptin (ng/ml)	6.19 ± 0.8	14.1 ± 1.5*	17.57 ± 1.2*	7.5 ± 0.7	10.7 ± 0.8*	14.4 ± 0.7*
Glucose before RES (mg/dL)	98 ± 2.2	123 ± 3.2**	120 ± 2.4*	102 ± 2.7	127 ± 3.5**	117 ± 2.5*
Glucose 60 min after RES (mg/dL)	164 ± 7.6 ⁺	174 ± 7.2 ⁺	192 ± 9.2 ⁺⁺	145 ± 2.6 ⁺	182 ± 5.7 ⁺⁺	185 ± 8.1 ⁺⁺
Insulin (ng/mL)	0.68 ± 0.04	1.07 ± 0.09*	1.6 ± 0.16*	0.63 ± 0.1	1.22 ± 0.08*	1.25 ± 0.1*
Females	NH			MS		
	C	HFC30	HFC60	C	HFC30	HFC60
Ovaric WAT (g/kg)	21.6 ± 2.4	71.7 ± 3.3***	56.73 ± 4.6***	27.08 ± 2.3	65.2 ± 6.2***	79.07 ± 9.7***
Retroperitoneal WAT (g/kg)	18.64 ± 1.7	60.3 ± 3.3***	52.24 ± 6.3***	24.9 ± 3	57.5 ± 4***	59.47 ± 4.6***
Interscapular WAT (g/kg)	3.91 ± 0.4	15.6 ± 3.8**	8.28 ± 1.5*	4.73 ± 0.5	15 ± 1.5**	15.9 ± 2.3**
Leptin (ng/mL)	2.47 ± 0.27	6.58 ± 0.8*	8.05 ± 1.13***	3.2 ± 0.2	9.2 ± 1.1***	10.26 ± 1.5***
Glucose before RES (mg/dL)	124 ± 5.3	119 ± 3.9	128 ± 4.6	115 ± 2.6	123 ± 4.9	120 ± 3.8
Glucose 60 min after RES (mg/dL)	162 ± 7.6 ⁺	161 ± 4.1 ⁺	169 ± 6.5 ⁺	141 ± 4.7 ⁺	165 ± 10 ⁺	160 ± 7.7 ⁺
Insulin (ng/mL)	0.1 ± 0.03	0.27 ± 0.05*	0.17 ± 0.01	0.13 ± 0.02	0.29 ± 0.05*	0.13 ± 0.01

Non-handled (NH) or maternal separated (MS) male and female rats fed a chow (C) or a high-fat/high-carbohydrate diet (HFC) from Pd30 (HFC30) or 60 (HFC60) until Pd160 were restrained 1 h before they were killed. White adipose tissue (WAT) depots and serum concentrations of leptin and insulin were determined at the end of the experiment (Pd160). Blood glucose concentration was quantified before restraint (RES) and 60 min after RES. Data are presented as mean ± S.E.M. and were analyzed by a three-way ANOVA to determine effects of neonatal stress, diet, sex, and the interaction of these variables. If a significant main effect or interaction was found, ANOVA was followed by the Holm–Sidak multiple comparisons test, the level of significance was set at $p < 0.05$, * $p < 0.05$, ** $p < 0.01$, and *** $p < 0.001$ vs. respective chow group; ⁺ $p < 0.01$ vs. glucose before RES. NH-C $n = 6/\text{sex}$, NH-HFC30 and NH-HFC-60 $n = 7/\text{sex}$, MS-C $n = 6$, MS-HFC30, and MS-HFC60 $n = 7/\text{sex}$.

Figures 2A,B]. During the adult period (Pd61–160), all NH-HFC and MS-HFC fed male and female rats consumed higher total kilocalories than chow-fed rats, but kilocalorie intake was even higher in the NH-HFC60 group compared to MS-HFC60 males [MS effect $F_{(1, 80)} = 10.8$, $p = 0.0014$; diet effect $F_{(2, 80)} = 77.45$, $p < 0.0001$; diet and sex effect $F_{(1, 80)} = 33.97$, $p < 0.0001$; **Figures 2B,E].**

Male and female rats fed an HFC diet, either from Pd30 or 60, ingested a similar proportion of macronutrients during Pd60–90 or Pd91–160, diminishing protein intake in favor of lipids (**Supplementary Table 1**). In HFC-fed animals, protein intake diminished, although to amounts and a proportion adequate for protein maintenance considering the quality of protein (51), and recommended intake of essential amino acids for growth maintenance was preserved (51) (**Supplementary Table 1**).

The slope of body weight gain was reduced after Pd97 in NH- and MS-chow-fed groups of both sexes while the reduction was less conspicuous in those receiving an HFC diet, especially in NH-HFC60 males compared to NH-chow and MS-HFC60 groups [diet effect $F_{(2, 80)} = 7.18$, $p = 0.007$; sex effect $F_{(1, 80)} = 130.85$, $p < 0.0001$; **Figures 2C,F].** NH-chow and NH-HFC60 males consumed more kilocalories per day than females [diet effect $F_{(1, 80)} = 21.9$, $p < 0.0001$; sex effect $F_{(1, 80)} = 65.4$, $p < 0.0001$] but not relative to their body weight (**Supplementary Table 1**); MS-chow and MS-HFC males also consumed more kilocalories per day than females during Pd91–160 [diet and sex effect $F_{(2, 80)} = 4.8$, $p = 0.04$;

Supplementary Table 1]. Food efficiency was lower in female than in male groups [diet and sex effect $F_{(2, 80)} = 8.18$, $p = 0.003$; **Supplementary Table 1**], as shown in adult rats (4).

Weights of gonadal fat [diet effect $F_{(2, 80)} = 55.52$, $p < 0.0001$; diet and sex $F_{(2, 80)} = 10.98$, $p < 0.0001$], retroperitoneal fat [diet effect $F_{(2, 80)} = 66.33$, $p < 0.0001$; diet and sex effect $F_{(2, 80)} = 4.23$, $p = 0.018$], and interscapular fat [diet effect $F_{(2, 80)} = 27.25$, $p < 0.0001$] increased with consumption of an HFC diet, to a similar extent whether diet started at Pd30 or 60 in NH and MS males and females compared to chow-fed rats (**Table 2**); MS-HFC60 female rats showed a tendency of higher interscapular WAT weight than NH-HFC60 but did not achieve statistical significance ($p = 0.06$) (**Table 2**).

Metabolic Parameters and Serum 17 β -Estradiol

Serum leptin concentrations of HFC-fed NH and MS male and female rats were higher than those of NH-chow-fed rats [diet effect $F_{(2, 80)} = 42.82$, $p < 0.0001$; **Table 2**]. Changes in serum insulin concentration followed a similar pattern to serum leptin in males; in contrast, in females, serum insulin concentration augmented only in NH-HFC30 and MS-HFC30 compared to chow and HFC60 groups [diet effect $F_{(2, 80)} = 10.22$, $p = 0.0001$; diet and sex effect $F_{(2, 80)} = 5.33$, $p = 0.007$; **Table 2**]. Basal glucose levels were not changed by MS in chow-fed animals, but levels were higher in HFC-fed NH and MS rats compared to chow-fed males, regardless of the age of access to the diet and were unchanged by an HFC diet in females [diet effect

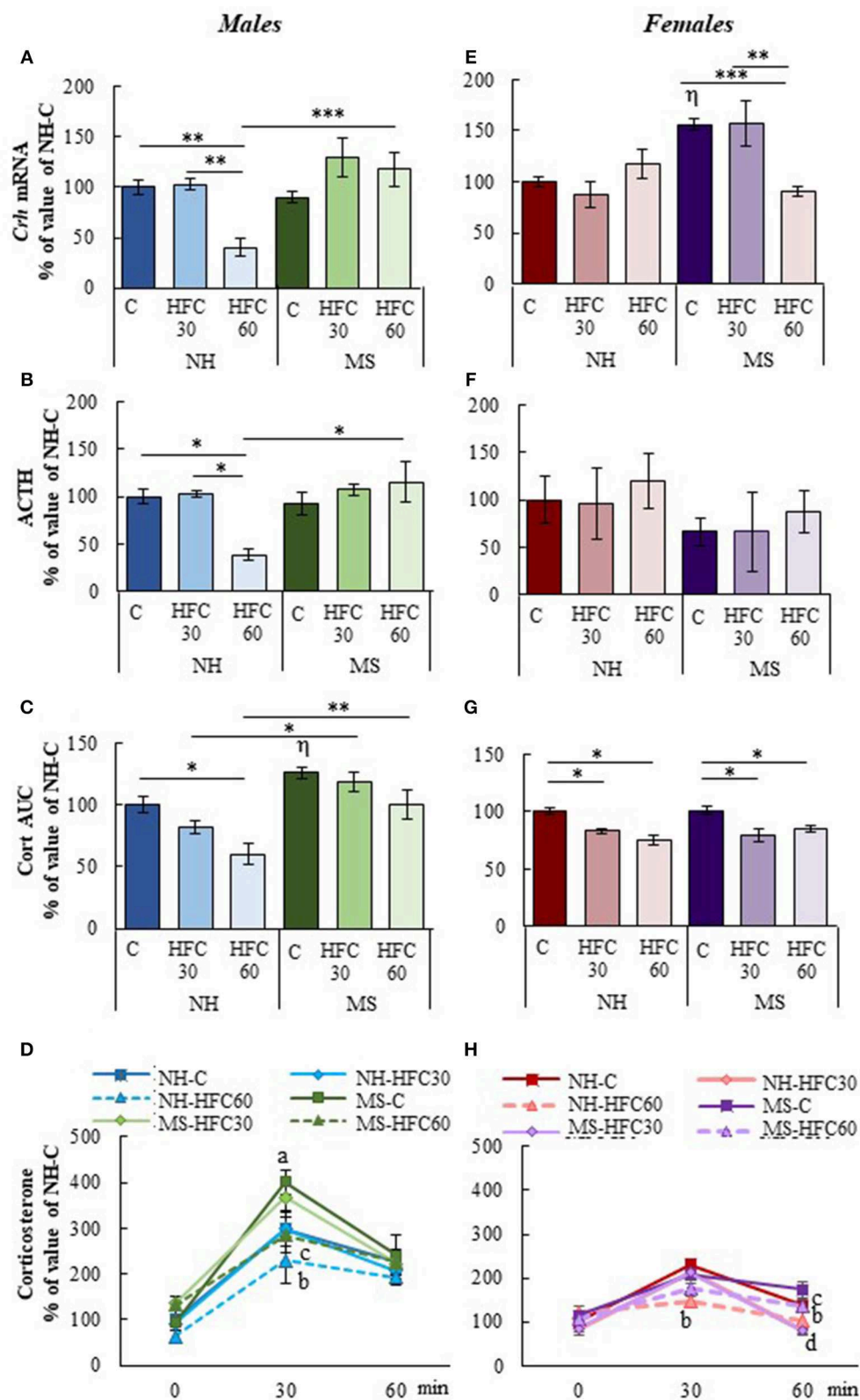


FIGURE 3 | Effect of maternal separation and a high-fat/high-carbohydrate diet on HPA axis parameters in acutely restrained rats. Non-handled (NH) or maternal separated (MS) male and female rats fed a chow (C) or a high-fat/high-carbohydrate diet (HFC) from Pd30 (HFC30) or 60 (HFC60) until Pd160 were restrained 1 h

(Continued)

FIGURE 3 | before they were killed. **(A,E)** Expression levels of *Crh* in the paraventricular nucleus. **(B,F)** Serum concentration of ACTH. **(C,G)** Area under the curve (AUC) of serum corticosterone concentration response to restraint shown in **(D,H)**; serum corticosterone values are presented in % of NH-chow groups to compare the extent of the stress response between males and females, as females present higher basal levels of serum corticosterone than male rats; absolute values are shown in **Supplementary Figure 4**. Data are mean \pm S.E.M. expressed as % of values of NH-chow rats. Data were analyzed by a three-way ANOVA to determine effects of neonatal stress, diet, sex, and the interaction of these. If a significant main effect or interaction was found, ANOVA was followed by the Holm-Sidak multiple comparisons test, the level of significance was set at $p < 0.05$. * $p < 0.05$, ** $p < 0.01$, *** $p < 0.001$, ^avs. NH-C, ^bMS vs. NH, ^cNH-HFC60 vs. NH-C, ^dMS-HFC60 vs. MS-C, ^eNH- and MS-HFC30 vs. NH-C and MS-C. NH-C $n = 6/\text{sex}$, NH-HFC30 and NH-HFC60 $n = 7/\text{sex}$, MS-C $n = 6/\text{sex}$, MS-HFC30 and MS-HFC60 $n = 7/\text{sex}$.

$F_{(2,80)} = 12.03$, $p < 0.0001$; sex effect $F_{(1,80)} = 8.77$, $p = 0.004$; **Table 2**]. In response to restraint, blood glucose levels increased in all chow and HFC groups in both sexes and were even higher in NH-HFC60, MS-HFC30, and MS-HFC60 males in comparison to chow-fed rats, with no differences between groups in females [diet effect $F_{(2,80)} = 11.37$, $p < 0.0001$; sex effect $F_{(1,80)} = 11.46$, $p = 0.001$; **Table 2**]. The concentration of 17β -estradiol was lower after 3–4 months of feeding an HFC diet to NH and MS female rats [diet effect $F_{(2,40)} = 6.51$, $p = 0.003$; **Supplementary Figure 3B**].

HPA Axis Parameters

After 1 h of restraint, serum corticosterone AUC was significantly higher in MS-chow than in NH-chow-fed male rats [MS effect $F_{(1,80)} = 20.5$, $p < 0.0001$; **Figure 3C**], but serum ACTH concentration and mRNA levels of *Crh* in the PVN were unchanged (**Figures 3A,B**). Ingestion of an HFC diet diminished the stress response only in NH males that consumed the diet from adulthood, but not of MS males, since PVN-*Crh* expression [MS effect $F_{(1,80)} = 18.3$, $p < 0.0001$; diet effect $F_{(2,80)} = 4.38$, $p = 0.016$; **Figure 3A**], serum concentration of ACTH [MS and sex effect $F_{(1,80)} = 10.1$, $p < 0.002$; **Figure 3B**], corticosterone at 30 min and corticosterone AUC were lower in NH-HFC60 than in chow-fed rats [MS effect $F_{(1,80)} = 20.5$, $p < 0.0001$; diet effect $F_{(2,80)} = 17.59$, $p < 0.0001$; MS and sex effect $F_{(1,80)} = 15.4$, $p = 0.0002$; **Figures 3C,D**]. Thus, MS impaired the inhibitory effect of an HFC diet on the restraint-induced activation of the HPA axis in male rats. Females responded differently; MS enhanced *Crh* expression in the PVN of chow-fed rats and was reduced in MS-HFC60 but not MS-HFC30 compared to chow-fed MS rats [sex effect $F_{(1,80)} = 13.92$, $p = 0.0004$; MS, diet and sex effect $F_{(2,80)} = 17.45$, $p < 0.0001$; **Figure 3E**]. No changes in serum ACTH concentration were found in females (**Figure 3F**), whereas serum corticosterone at 30 min and AUC was similar between NH- and MS-chow-fed groups and comparable lower in all groups fed an HFC diet regardless of neonatal stress or age of diet exposition [sex effect $F_{(1,80)} = 6.03$, $p = 0.016$; MS and sex effect $F_{(1,80)} = 15.4$, $p = 0.0002$; **Figures 3G,H**].

Mediobasal Hypothalamic Neuropeptides and HPT Axis Parameters

The PVN-*Trh* expression is regulated in part by peptides released from neurons located within the arcuate nucleus that project to TRH synthesizing neurons in the PVN of the hypothalamus, positively by POMC and negatively by NPY (22). MBH-*Pomc* expression in males was reduced by an HFC diet, with no effects of maternal separation or age of access to the HFC diet [diet effect

$F_{(2,80)} = 4.07$, $p = 0.022$; sex effect $F_{(1,80)} = 25.45$, $p < 0.0001$; diet and sex effect $F_{(2,80)} = 7.2$, $p = 0.001$; **Figure 4A**], whereas no changes were found in female rats (**Figure 4D**). MBH-*Npy* expression was enhanced in both MS-chow male and female rats compared to NH-chow groups (**Figures 4A,D**) and reduced in MS-HFC60 males compared to MS-chow-fed rats [MS effect $F_{(1,80)} = 22.2$, $p < 0.0001$; sex effect $F_{(1,80)} = 74.73$, $p < 0.0001$; diet and sex effect $F_{(2,80)} = 6.85$, $p = 0.002$; **Figure 4A**].

In adult male rats, acute restraint is reported to reduce PVN-*Trh* expression and serum TSH concentration (46), but serum T3 concentration only after a larger restraint span (52). Various parameters of the HPT axis in response to restraint stress were altered differently according to neonatal stress, sex, and age of access to the HFC diet. In male rats, MS-chow feeding regulated few HPT axis parameters, producing a small decrease in PVN-*Trh* mRNA levels [MS effect $F_{(1,80)} = 4.75$, $p = 0.03$; **Figure 4B**] and MBH-*Trhde* mRNA levels [MS effect $F_{(1,80)} = 6.74$, $p = 0.01$; **Figure 4B**] and lower serum T3 concentration than NH-chow males [MS effect $F_{(1,80)} = 13.3$, $p = 0.0005$; **Figure 4C**]. The HFC diet induced changes depending on age of diet initiation and neonatal stress; NH-HFC30 male rats had lower serum T4 [diet effect $F_{(2,80)} = 4.83$, $p = 0.04$; **Figure 4C**] and T3 concentration [diet effect $F_{(2,80)} = 4.27$, $p = 0.01$; **Figure 4C**] than the NH-chow fed group. Compared to MS-chow-fed animals, MS-HFC30 males had higher PVN-*Trh* expression [MS and diet effect $F_{(2,80)} = 14.95$, $p < 0.0001$; **Figure 4B**] and reduced serum concentration of TSH [diet effect $F_{(2,80)} = 6.05$, $p = 0.004$; MS, diet and sex effect $F_{(2,80)} = 3.87$, $p = 0.026$; **Figure 4C**], T4 [MS, diet and sex effect $F_{(2,80)} = 3.73$, $p = 0.02$; **Figure 4C**], and T3 [diet effect $F_{(2,80)} = 4.27$, $p = 0.01$; MS and diet effect $F_{(2,80)} = 8.62$, $p = 0.0004$; MS, diet and sex effect $F_{(2,80)} = 3.87$, $p = 0.026$; **Figure 4C**]. Different effects were observed in NH and MS male rats that had access to the HFC diet from Pd60; PVN-*Trh* expression and serum T4 concentration were lower in NH-HFC60 compared to NH-chow-fed animals (**Figures 4B,C**); in contrast, MS-HFC60 males had lower PVN-*Trh* and MBH-*Trhde* expression and serum TSH and T4 concentrations compared to MS-chow-fed rats (**Figures 4B,C**).

In female rats submitted to restraint, diet and neonatal stress effects were distinct from those observed in males. A decrease in mRNA levels of *Trhde* in MBH [sex effect $F_{(1,80)} = 3.73$, $p = 0.05$; MS and sex effect $F_{(1,80)} = 10.57$, $p = 0.001$; **Figure 4E**] and of serum TSH concentration [MS, diet and sex effect $F_{(2,80)} = 3.87$, $p = 0.026$; **Figure 4F**] was observed in MS compared to NH rats. In NH rats, access to an HFC diet, either starting at puberty or adulthood, reduced MBH-*Trhde* [sex effect $F_{(1,80)} = 3.73$, $p = 0.05$; MS and sex effect $F_{(1,80)} = 10.57$, $p = 0.001$; diet and sex effect $F_{(2,80)} = 4.32$, $p = 0.04$; **Figure 4E**] and *Dio2*

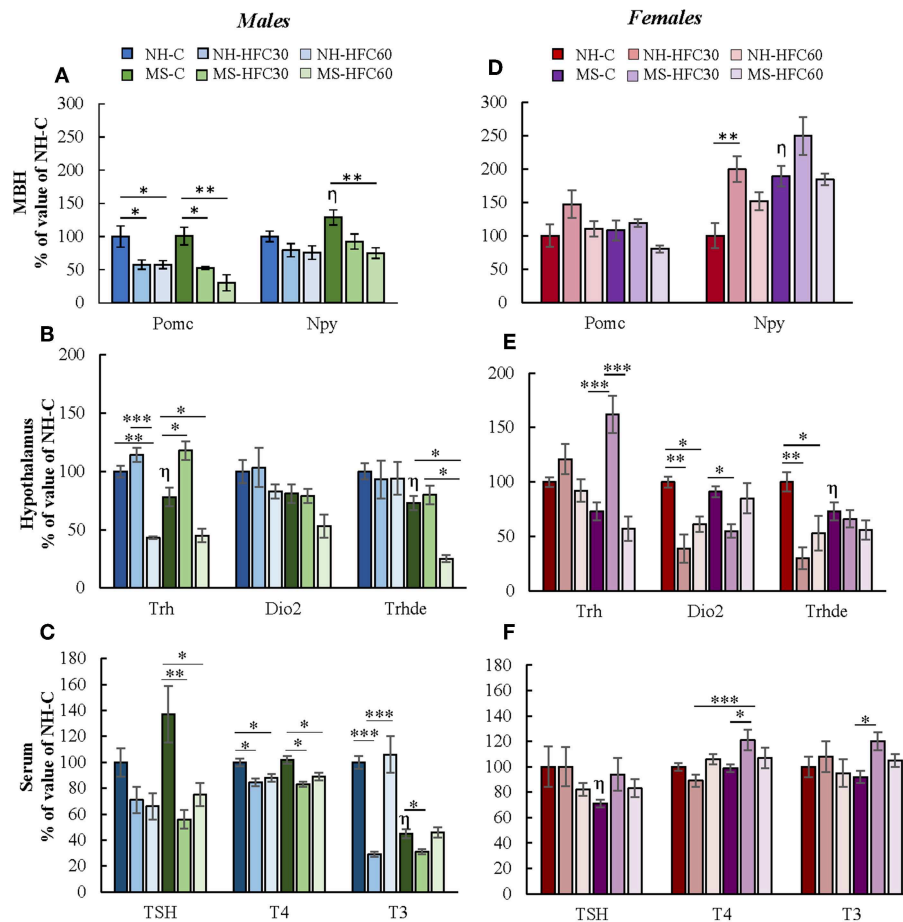


FIGURE 4 | Effect of maternal separation, and a high-fat/high-carbohydrate diet on the expression of arcuate peptides and HPT axis parameters in acutely restrained rats. Non-handled (NH) or maternal separated (MS) male and female rats fed a chow (C) or a high-fat/high-carbohydrate diet (HFC) from Pd30 (HFC30) or 60 (HFC60) until Pd160 were restrained 1 h before they were killed. **(A,D)** Expression levels of pro-opiomelanocortin (*Pomc*) and neuropeptide Y (*Npy*) in the mediobasal hypothalamus (MBH). **(B,E)** Expression levels of *Trh* in the paraventricular nucleus and of *Dio2* and *Trhde* in the MBH. **(C,F)** Serum concentrations of TSH, T4, and T3. Data are expressed as % of values of NH-chow illustrated as mean \pm S.E.M. Data were analyzed by a three-way ANOVA to determine effects of neonatal stress, diet, sex, and the interaction of these variables. If a significant main effect or interaction was found, ANOVA was followed by the Holm-Sidak multiple comparisons test; the level of significance was set at $p < 0.05$. * $p < 0.05$, ** $p < 0.01$, *** $p < 0.001$, η vs. NH-C. NH-C $n = 6$ /sex, NH-HFC30 and NH-HFC60 $n = 7$ /sex, MS-C $n = 6$ /sex, MS-HFC30 and MS-HFC60 $n = 7$ /sex.

mRNA levels [diet effect $F_{(2, 80)} = 7.25$, $p = 0.001$; sex effect $F_{(1, 80)} = 4.3$, $p = 0.01$; diet and sex effect $F_{(2, 80)} = 6.36$, $p = 0.003$; **Figure 4E**] compared to chow-fed females. In contrast, in MS rats, the HPT axis activity was altered in HFC30, but not in HFC60 rats compared to the chow-fed group: PVN-*Trh* expression was increased [sex effect $F_{(1, 80)} = 14.22$, $p = 0.0004$; MS, diet and sex effect $F_{(2, 80)} = 5.46$, $p = 0.0065$; **Figure 4E**], while MBH-*Dio2* expression was reduced [MS and sex effect $F_{(1, 80)} = 6.17$, $p = 0.01$; **Figure 4E**], and serum concentrations of T4 [MS, diet and sex effect $F_{(2, 80)} = 3.73$, $p = 0.02$; **Figure 4F**] and T3 increased [MS and sex effect $F_{(1, 80)} = 26.51$, $p < 0.0001$; MS, diet, and sex effect $F_{(2, 80)} = 3.24$, $p = 0.04$; **Figure 4F**].

DISCUSSION

Nutrition and stress play a major role in programming neuroendocrine systems that regulate energy homeostasis and

body weight (53), but whether early-life stress contributes to metabolic alterations later in life is controversial with evidence for both improved or worsened metabolic disease risk (3, 10). Our results support published data indicating that compared to NH rats, MS reduces food intake in both sexes at adulthood (8) and enhances serum corticosterone and insulin concentrations, but only in males (54–56), suggesting a degree of insulin insensitivity as in Mela et al. (57). An HFC feeding increased serum insulin concentration in MS males but reduced that of corticosterone, consistent with previous data (5). MS-induced insulinemia is prevented by mechanical and tactical stimulation of the pups (56), supporting the role of neonatal stress shown to alter the pancreatic beta-cell function and insulin sensitivity in rats, with males being more sensitive than females (58, 59).

During adolescence, development of feeding behavior is vulnerable to insults, especially in females (37). Some reports describe that constant availability of palatable foods increases

female susceptibility to develop obesity and metabolic syndrome later in life (37, 38), exacerbated by MS in adult female rats (9). Our results did not reproduce these findings; MS did not potentiate obesity in adult HFC-fed females, in agreement with other studies (5, 8). Differences could be due to the type and composition of the diet (10). It is interesting to notice the consistency in the proportion of macronutrient intake of NH and MS male and female rats with diet choice, even after 3–4 months of exposure to HFC foods; although their carbohydrate and fat intake was high, rats maintained the minimum protein intake required for growth maintenance (51). The high proportion of fats and carbohydrates consumed by the NH-HFC and MS-HFC groups most likely reinforced energy intake through enhanced hedonic feeding (60, 61).

MS and 1 Month of an HFC Diet Regulate the Basal Activity of the HPT Axis

Expression of MBH neuropeptides was evaluated due to their important role not only in food intake and energy balance but also in regulating the activity of PVN-TRH neurons (22). An HFC diet, but not MS, induced sex-specific changes in MBH-orexigenic and -anorexigenic peptides, with low *Npy* expression in NH-HFC males and elevated *Pomc* expression in NH-HFC females compared to chow-fed groups (49, 50). In contrast to previous reports of HPT axis activation with a high-fat saturated diet in male rodents (62–64), the HFC diet reduced serum TSH levels in NH males, coincident with increased expression of *Trhde*, supporting the lowering effect of a high-fat unsaturated diet on serum TSH concentration (65).

MS altered some parameters of the HPT axis activity only in males: expression of *Trhde* was higher in MS-HFC60 and MS-chow-fed rats than in NH animals, and serum TSH concentration decreased accordingly in MS-chow-fed rats as reported previously (32). NH females did show a slight activation of the HPT axis by an HFC diet, as serum T4 levels increased together with two activators of PVN-TRH neurons: serum leptin concentration and MBH-*Pomc* expression (22). Increased serum T4 could contribute to the enhanced expression of MBH-*Trhde* observed in NH-HFC females, as injection of this hormone increases the enzyme's expression in tanycytes (26). These changes, however, were not observed in MS females, in spite of having increased concentration of serum leptin.

MS and 3–4 Months of an HFC Diet Regulate Metabolic and Stress Parameters in Acutely Restrained Rats

Obesity and chronic hyperglycemia are risk factors in developing metabolic derangements (i.e., reduced insulin sensitivity) (66–68). Adolescent male rats appear to be more sensitive to a high-fat saturated diet-induced obesity than adults, producing more drastic metabolic effects when a high-fat diet is administered to young males compared to adult-fed rats (69, 70). Contrary to these reports, consumption of an HFC diet from either adolescence or adulthood induced a similar obese state and moderate basal hyperglycemia in MS and NH male rats, suggesting reduced insulin sensitivity (71) whether the HFC

diet was offered starting at adolescence or adulthood, although this remains to be confirmed. In addition, the HFC diet heightened the hyperglycemic response to restraint stress in males, and consequently, serum insulin levels were higher in comparison to chow-fed groups, although serum insulin concentration was slightly higher in NH-HFC60 males. In contrast, the HFC diet enhanced serum insulin concentration in restrained females (independently of MS), if initiated at adolescence but not at adulthood, despite lack of differences in basal blood glucose concentration and similar stress-induced hyperglycemia, suggesting insulin resistance in NH-HFC30 and MS-HFC30 females (71). These results support the idea that puberty is a vulnerable period for females with unrestricted access to palatable foods and could increase their risk to develop metabolic alterations in adulthood (37). Nevertheless, our results show that an HFC diet, but not neonatal stress, is a major determinant of serum metabolic markers after acute stress in a sex-specific manner.

The restraint-induced serum corticosterone response was higher in MS than in NH males (6, 11, 72), and the HFC diet dampened it, but only in NH rats as reported (16, 36, 73, 74). A sex dimorphism was evidenced in the effects of early-life stress since MS males' response to stress was independent of diet in contrast to MS females, which had lower *Crh* expression in HFC60 and corticosterone concentration in HFC30 and HFC60 than chow-fed rats. Furthermore, although NH females have higher basal corticosterone concentration, the extent of their response to acute stress was lower than that in NH males, in contrast to some reports (34, 35). Serum concentration of 17 β -estradiol could have contributed to the sex differences observed in the HPA axis activity in acutely restrained rats and to the effect of palatable foods to reduce restraint stress responses (34, 75), since serum 17 β -estradiol levels were reduced by an HFC diet in NH and MS females, as reported previously (76, 77). These results suggest that an HFC diet alters the HPA axis activity differently in male than in female rats, with MS being a contributing factor in males but not in females, and highlights the complex interaction of diet, gonadal steroids, and stress.

MS and 3–4 Months of an HFC Diet Regulate HPT Axis Activity in Acutely Restrained Rats

Expression of arcuate peptides *Pomc* and *Npy* are regulated by the animal's energy state but also by stress (78–81). MBH-*Npy* expression was higher in MS-chow-fed restrained male and female rats than in NH-chow groups; neonatal stress *per se* does not affect *Npy* expression in male and female rats (5, 57, 82), but it increases hyperreactivity to restraint stress in adulthood (6, 11). As glucocorticoids (83) and restraint increase mRNA levels of *Npy* in the arcuate nucleus (albeit 24-h after initiated the stress) (78–80), the combination of MS and adult acute stress may have heightened *Npy* expression. Sex differences were observed in MBH neuropeptide expression in HFC-fed rats; *Npy* expression was higher in NH females that had access to the HFC from adolescence compared to NH-chow rats, but not in males, suggesting an altered diet-induced arcuate

NPY activation and increased vulnerability of young females to chronic high-fat feeding (84). Restraint stress increases arcuate *Pomc* expression in adult male rats, although 4 h after stress (78, 79), its expression was inhibited in the MBH of NH-HFC30, MS-HFC30, and MSHFC-60 males compared to chow-fed rats, despite increased serum leptin levels, which is concordant with a hyperphagic behavior, a diet-induced obesity, and male rats' higher susceptibility to develop diet-induced leptin resistance compared to females (84–86). Thus, our results are in agreement with the reported impairment of the anorexigenic leptin–POMC system in males, whereas in females, there is an over-activation of the orexigenic NPY system in high-fat-fed rats (84).

Restraint and other forms of psychological stress rapidly inhibit HPT axis activity in adult male rats fed a standard diet and without a history of early-life stress (45, 46, 87). In contrast

to the blunting effect of an HFC diet on restraint-induced *Crh* expression, compared to chow-fed rats, that of *Trh* was inhibited in NH-HFC60 and MS-HFC60 males as observed with *Pomc* expression. The restraint-induced decrease of serum TSH concentration in NH-chow males (46) was presumably blunted in MS-chow rats, most probably due to the lower expression of *Trhde* in MS in comparison to NH-chow males. These changes are not explained by altered serum TH or corticosterone concentration but could be due to lowered PVN-*Trh* expression since it has recently been reported that TRH may upregulate mRNA levels of *Trhde* and activity in tanycytes (88). Serum T4 concentration was lower in HFC- than in chow-fed males in both NH and MS groups, but did not coincide with changes in serum concentration of T3, which varied the most, as strong decreases were observed in MS-chow compared to NH-chow

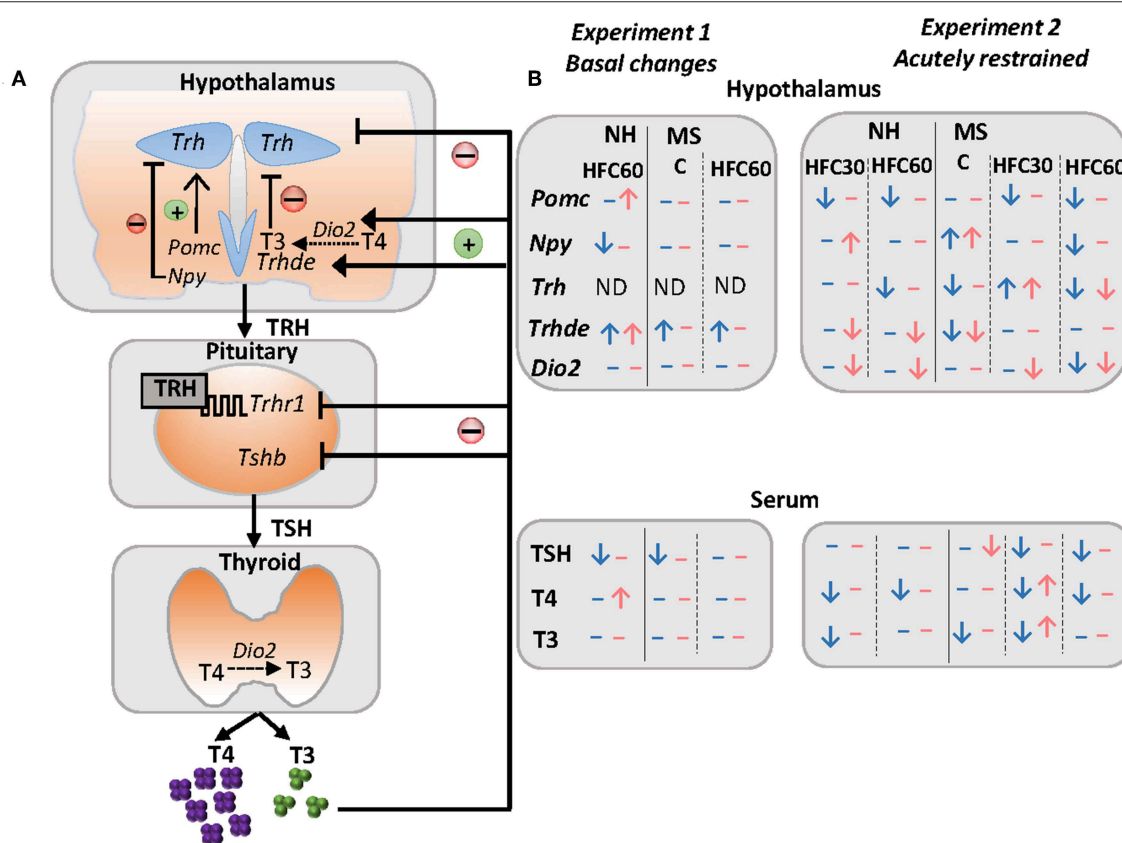


FIGURE 5 | Schema of some peripheral inputs regulating the HPT axis and summary of changes of the HPT axis parameters and arcuate neuropeptides in response to maternal separation and 1–4 months of a high-fat/high-carbohydrate diet under basal conditions or after an acute stress in adult rats. **(A)** The HPT axis is controlled by thyrotropin-releasing hormone (TRH), synthesized in neurons of the hypothalamic paraventricular nucleus (PVN), and released at the median eminence near portal vessels that communicate with the anterior pituitary, where TRH activates its receptor (TRH-R1) increasing synthesis and release of thyrotropin (TSH) that controls the synthesis of thyroxine (T4) at the thyroid; T4 is converted to 3,3',5-triiodo-L-thyronine (T3) by tissue deiodinases I or II (D1, D2). Released TRH at the median eminence may be degraded by the TRH-degrading ectoenzyme (TRH-DE) present in tanycytes before it travels to the pituitary, regulating the amount of TRH that reaches the thyrotrophs, and concomitantly, TSH and thyroid hormone synthesis and release, which in turn exert negative feedback at the pituitary and hypothalamus level. In addition, hypophysiotropic TRH neurons are negatively regulated by arcuate orexigenic neuropeptide Y (NPY), whereas anorexigenic neuropeptide pro-opiomelanocortin up-regulates *Trh* expression in the PVN. **(B)** Results summary of experiments 1 and 2. In experiment 1, we evaluated changes in maternal separated rats (MS) fed regular chow (C) vs. non-handled (NH), and the effect of 1 month of a high-fat/high-carbohydrate (HFC60) diet on NH and MS rats administered at Pd60. In experiment 2, we evaluated changes in NH and MS acutely restrained adult rats fed a C or an HFC diet starting at puberty (HFC30) or adulthood (HFC60) until postnatal day 160. NH and MS rats had free access to chow (C) or to an HFC diet from Pd30 or 60 until Pd160 and were restrained for 1 h before they were killed. Blue arrows and dashes represent males and pink denotes female rats; arrows indicate changes observed in NH-HFC30 and NH-HFC60 rats compared to the NH-C group; MS-C vs. NH-C; MS-HFC30 and MS-HFC60 compared to MS-C.

and in NH-HFC30 and MS-HFC30 groups compared to chow-fed animals.

Females responded differently to the acute stress situation dependent on diet initiation; NH-HFC30 and NH-HFC60 restrained females showed lower MBH expression of *Trhde* and *Dio2* without changes in PVN-*Trh*, serum TSH, or T3 concentration compared to NH-chow rats; it is tempting to speculate that acute stress modulated by an HFC diet regulates the expression of these enzymes, although this remains to be elucidated. Parallel changes of *Dio2* and *Trhde* expression are consistent with the proposal that T3 formed by D2 activates *Trhde* in MBH (26, 89). Even though *Dio2* expression and activity are not modified under basal conditions by a hypercaloric diet, as observed in our first experiment (Table 1) and other studies (62, 63), the combination of obesity with acute stress may have altered MBH-*Dio2* expression, since this enzyme is susceptible to various types of stimuli (47, 90–92). MS-HFC-fed females seemed to be less susceptible to stress than males, as reported previously (32). MS-HFC30 females had higher *Trh* expression and serum levels of T4 and T3 than MS-chow-fed rats, as well as decreased *Dio2* expression; this decrease may explain why expression of *Trh* was increased in MS-HFC30 animals in spite of a small increment in serum T4, not being sufficient to exert negative feedback on TRH at the PVN level (22, 93, 94). These changes were not observed in MS females that were exposed to an HFC diet until adulthood (HFC60), supporting females' susceptibility during adolescence, particularly to a diet that makes them more resilient to restraint stress.

CONCLUSIONS

The HPT axis activity is regulated by energy-related cues (Figure 5A) as well as by stressors (Figure 5B). In this study, we show that MS did not exacerbate an obese phenotype or related metabolic alterations as hyperglycemia and insulinemia in either sex when rats have unrestricted access to an HFC diet composed mainly by unsaturated fatty acids. However, neonatal stress and/or long-term intake of an HFC diet altered the HPT axis activity in restraint-stressed rats in a sex-specific manner, and dependent on diet introduction at puberty or adulthood. Results are summarized in Figure 5B. Altogether, they emphasize the complex interaction of various environmental and physiological factors such as neonatal stress, nutrition, and sex in the regulation of the HPT axis activity, underlining the importance of studying sex differences, confirming that neuroendocrine responses to stress and nutrition are sexually dimorphic. Finally, our results are in line with clinical studies that report that different adult or adolescent psychopathologies due to childhood trauma are associated with alterations in thyroid function (29–31, 95, 96). The HPT axis is a dynamic and adaptive system; however, in

this context, if adaptability is not met, psychological or metabolic pathologies may arise as observed in obese patients (97).

DATA AVAILABILITY

All datasets generated for this study are included in the manuscript and/or the **Supplementary Files**.

ETHICS STATEMENT

This study was carried out in accordance with the recommendations of the NIH guide for the care and use of laboratory animals and the Official Mexican Norm for production, care and use of laboratory animals NOM-062-ZOO-1999. The protocol and experiments were approved by the Bioethics Committee of Instituto de Biotecnología, UNAM, with authorization project number 311.

AUTHOR CONTRIBUTIONS

LJ-H performed the maternal separation and HFC diet protocol of both experiments, ELISA analyses, data analyses, and writing and text editing of the manuscript. FR performed the RNA extraction of hypothalamic tissues and RT-PCRs. J-LC contributed to manuscript editing. PJ-B contributed in the experimental design, data analyses, manuscript writing, and editing.

FUNDING

This work was supported by DGAPA IA200417 (LJ-H) and CONACyT 180009 and 284883 (PJ-B).

ACKNOWLEDGMENTS

We thank José Manuel Villa for his help in the care of animals during the experimental period, Q.F.B. Miguel Cisneros in radioimmunoassay analyses, and Mariana Gutiérrez-Mariscal, DSc, in assisting in the restraint stress protocol and sample collections. We also thank the synthesis and sequencing DNA unit of Instituto de Biotecnología, UNAM, for synthesizing primers used in these experiments and the computational unit for assisting in computer issues.

SUPPLEMENTARY MATERIAL

The Supplementary Material for this article can be found online at: <https://www.frontiersin.org/articles/10.3389/fendo.2019.00445/full#supplementary-material>

REFERENCES

1. Hruby A, Hu FB. The epidemiology of obesity: a big picture. *Pharmacoeconomics*. (2015) 33:673–89. doi: 10.1007/s40273-014-0243-x
2. Dallman MF. Stress-induced obesity and the emotional nervous system. *Trends Endocrinol Metabol*. (2010) 21:159–65. doi: 10.1016/j.tem.2009.10.004
3. Morris MJ, Beilharz JE, Maniam J, Reichelt AC, Westbrook RF. Why is obesity such a problem in the 21st century? The intersection of palatable food, cues

- and reward pathways, stress, and cognition. *Neurosci Biobehav Rev.* (2015) 58:36–45. doi: 10.1016/j.neubiorev.2014.12.002
4. Paternain L, Martisova E, Milagro FI, Ramírez MJ, Martínez JA, Campión J. Postnatal maternal separation modifies the response to an obesogenic diet in adulthood in rats. *Dis Model Mech.* (2012) 5:691–97. doi: 10.1242/dmm.009043
 5. Maniam J, Morris MJ. Palatable cafeteria diet ameliorates anxiety and depression-like symptoms following an adverse early environment. *Psychoneuroendocrinology.* (2010) 35:717–28. doi: 10.1016/j.psyneuen.2009.10.013
 6. Maniam J, Morris MJ. Voluntary exercise and palatable high-fat diet both improve behavioural profile and stress responses in male rats exposed to early life stress: role of hippocampus. *Psychoneuroendocrinology.* (2010) 35:1553–64. doi: 10.1016/j.psyneuen.2010.05.012
 7. Miller AL, Lumeng JC. Pathways of association from stress to obesity in early childhood. *Obesity.* (2018) 26:1117–24. doi: 10.1002/oby.22155
 8. Mela V, Llorente-Berzal A, Díaz F, Argente J, Viveros M-P, Chowen JA. Maternal deprivation exacerbates the response to a high fat diet in a sexually dimorphic manner. *PLoS ONE.* (2012) 7:e48915. doi: 10.1371/journal.pone.0048915
 9. Murphy MO, Herald JB, Wills CT, Unfried SG, Cohn DM, Loria AS. Postnatal treatment with metyrapone attenuates the effects of diet-induced obesity in female rats exposed to early-life stress. *Am J Physiol Endocrinol Metabol.* (2017) 312:E98–108. doi: 10.1152/ajpendo.00308.2016
 10. Maniam J, Antoniadis C, Morris MJ. Early-life stress, HPA axis adaptation, and mechanisms contributing to later health outcomes. *Front Endocrinol.* (2014) 5:73. doi: 10.3389/fendo.2014.00073
 11. Chen J, Evans AN, Liu Y, Honda M, Saavedra JM, Aguilera G. Maternal deprivation in rats is associated with corticotropin releasing hormone (CRH) promoter hypomethylation and enhances CRH transcriptional responses to stress in adulthood. *J Neuroendocrinol.* (2012) 24:1055–64. doi: 10.1016/j.biotechadv.2011.08.021.Secreted
 12. Murgatroyd C, Patchev AV, Wu Y, Micale V, Bockmühl Y, Fischer D, et al. Dynamic DNA methylation programs persistent adverse effects of early-life stress. *Nat. Neurosci.* (2009) 12:1559–66. doi: 10.1038/nn.2436
 13. Wu Y, Patchev AV, Daniel G, Almeida OFX, Spengler D. Early-life stress reduces DNA methylation of the Pomc gene in male mice. *Endocrinology.* (2014) 155:1751–62. doi: 10.1210/en.2013-1868
 14. Todkar A, Granholm L, Aljumah M, Nilsson KW, Comasco E, Nylander I. HPA axis gene expression and DNA methylation profiles in rats exposed to early life stress, adult voluntary ethanol drinking and single housing. *Front Mol Neurosci.* (2016) 8:90. doi: 10.3389/fnmol.2015.00090
 15. Foster MT, Warne JP, Ginsberg AB, Horneman HF, Pecoraro NC, Akana SF, et al. Palatable foods, stress, and energy stores sculpt corticotropin-releasing factor, adrenocorticotropin, and corticosterone concentrations after restraint. *Endocrinology.* (2009) 150:2325–33. doi: 10.1210/en.2008-1426
 16. Tannenbaum BM, Brindley DN, Tannenbaum GS, Dallman MF, McArthur MD, Meaney MJ. High-fat feeding alters both basal and stress-induced hypothalamic–pituitary–adrenal activity in the rat. *Am J Physiol.* (1997) 273:E1168–77.
 17. Macht M, Mueller J. Immediate effects of chocolate on experimentally induced mood states. *Appetite.* (2007) 49:667–74. doi: 10.1016/j.appet.2007.05.004
 18. Mullur R, Liu Y-Y, Brent GA. Thyroid hormone regulation of metabolism. *Physiol Rev.* (2014) 94:355–825. doi: 10.1152/physrev.00030.2013
 19. Rabasa C, Dickson SL. Impact of stress on metabolism and energy balance. *Curr Opin Behav Sci.* (2016) 9:71–7. doi: 10.1016/j.cobeha.2016.01.011
 20. Silva JE. The thermogenic effect of thyroid hormone and its clinical implications. *Ann Intern Med.* (2003) 139:205–13. doi: 10.7326/0003-4819-139-3-200308050-00010
 21. Klieverik LP, Coomans CP, Endert E, Sauerwein HP, Havekes LM, Voshol PJ, et al. Thyroid hormone effects on whole-body energy homeostasis and tissue-specific fatty acid uptake *in vivo*. *Endocrinology.* (2009) 150:5639–48. doi: 10.1210/en.2009-0297
 22. Fekete C, Lechan RM. Central regulation of hypothalamic–pituitary–thyroid under physiological and pathophysiological conditions. *Endocr Rev.* (2014) 35:159–94. doi: 10.1210/er.2013-1087
 23. Gereben B, McAninch EA, Ribeiro MO, Bianco AC. Scope and limitations of iodothyronine deiodinases in hypothyroidism. *Nat Rev Endocrinol.* (2015) 11:642–52. doi: 10.1038/nrendo.2015.155
 24. Joseph-Bravo P, Jaimes-Hoy L, Charli JL. Regulation of TRH neurons and energy homeostasis-related signals under stress. *J Endocrinol.* (2015) 224:R139–59. doi: 10.1530/JOE-14-0593
 25. Joseph-Bravo P, Jaimes-Hoy L, Uribe RM, Charli JL. TRH, the first hypophysiotropic releasing hormone isolated: control of the pituitary–thyroid axis. *J Endocrinology.* (2015) 226:T85–100. doi: 10.1530/JOE-15-0124
 26. Sánchez E, Vargas MA, Singru PS, Pascual I, Romero F, Fekete C, et al. Tanycyte pyroglutamate II contributes to regulation of the hypothalamic–pituitary–thyroid axis through glial–axonal associations in the median eminence. *Endocrinology.* (2009) 150:2283–91. doi: 10.1210/en.2008-1643
 27. Helmreich DL, Tylee D. Thyroid hormone regulation by stress and behavioral differences in adult male rats. *Horm Behav.* (2011) 60:284–91. doi: 10.1016/j.yhbeh.2011.06.003
 28. Olivares EL, Silva-Almeida C, Pestana FM, Sonoda-Côrtes R, Araujo IG, Rodrigues NC, et al. Social stress-induced hypothyroidism is attenuated by antidepressant treatment in rats. *Neuropharmacology.* (2012) 62:446–56. doi: 10.1016/j.neuropharm.2011.08.035
 29. Moog NK, Entringer S, Heim C, Wadhwa PD, Kathmann N, Buss C. Influence of maternal thyroid hormones during gestation on fetal brain development. *Neuroscience.* (2017) 342:68–100. doi: 10.1016/j.neuroscience.2015.09.070
 30. Machado TD, Salum GA, Bosa VL, Goldani MZ, Meaney MJ, Agranonik M, et al. Early life trauma is associated with decreased peripheral levels of thyroid-hormone T3 in adolescents. *Int J Dev Neurosci.* (2015) 47:304–8. doi: 10.1016/j.ijdevneu.2015.10.005
 31. Fischer S, Markert C, Strahler J, Doerr JM, Skoluda N, Kappert M, et al. Thyroid functioning and fatigue in women with functional somatic syndromes—Role of early life adversity. *Front Physiol.* (2018) 9:564. doi: 10.3389/fphys.2018.00564
 32. Jaimes-Hoy L, Gutiérrez-Mariscal M, Vargas Y, Pérez-Maldonado A, Romero F, Sánchez-Jaramillo E, et al. Neonatal maternal separation alters, in a sex specific manner, the expression of TRH, of TRH-degrading ectoenzyme in the rat hypothalamus, and the response of the thyroid axis to starvation. *Endocrinology.* (2016) 157:3253–65. doi: 10.1210/en.2016-1239
 33. Mauvais-Jarvis F. Sex differences in metabolic homeostasis, diabetes, and obesity. *Biol Sex Differ.* (2015) 6:14. doi: 10.1186/s13293-015-0033-y
 34. Oyola MG, Handa RJ. Hypothalamic–pituitary–adrenal and hypothalamic–pituitary–gonadal axes: sex differences in regulation of stress responsivity. *Stress.* (2017) 20:476–94. doi: 10.1080/10253890.2017.1369523
 35. Heck AL, Handa RJ. Sex differences in the hypothalamic–pituitary–adrenal axis' response to stress: an important role for gonadal hormones. *Neuropsychopharmacology.* (2019) 44:45–58. doi: 10.1038/s41386-018-0167-9
 36. Pecoraro N, Reyes F, Gomez F, Bhargava A, Dallman MF. Chronic stress promotes palatable feeding, which reduces signs of stress: feedforward and feedback effects of chronic stress. *Endocrinology.* (2004) 145:3754–62. doi: 10.1210/en.2004-0305
 37. Clawson RC, dela Cruz LN, Allen S, Wolgemuth T, Maner A, Dorsett A, et al. Continuous access to snacks from weaning onwards in female rats causes weight gain, insulin insensitivity, and sustained leptin resistance in adulthood. *Physiol Behav.* (2019) 201:165–74. doi: 10.1016/j.physbeh.2018.11.026
 38. Leibowitz SE, Akabayashi A, Alexander J, Karatayev O, Chang GQ. Puberty onset in female rats: relation to fat intake, ovarian steroids and the peptides, galanin and enkephalin, in the paraventricular and medial preoptic nuclei. *J Neuroendocrinol.* (2009) 21:538–49. doi: 10.1111/j.1365-2826.2009.01870.x.Puberty
 39. Suarez Lopez M, Kizlansky A, Lopez L. Evaluación de la calidad de las proteínas en los alimentos calculando el escore de aminoácidos corregido por digestibilidad. *Nutr Hosp.* (2006) 21:47–51.
 40. Venkatachalan M, Sathe SK. Chemical composition of selected edible nut seeds. *J Agric Food Chem.* (2006) 54:4705–14. doi: 10.1021/jf0606959
 41. Schaafsma G. *Criteria and Significance of Dietary Protein Sources in Humans.* The protein digestibility-corrected amino acid score 1 (2000). pp. 1865–67.
 42. Vahl TP, Ulrich-Lai YM, Ostrander MM, Dolgas CM, Elfers EE, Seeley RJ, et al. Comparative analysis of ACTH and corticosterone sampling

- methods in rats. *Am J Physiol Endocrinol Metabol.* (2005) 289:E823–8. doi: 10.1152/ajpendo.00122.2005
43. Sotelo-Rivera I, Jaimes-Hoy L, Cote-Velez A, Espinoza-Ayala C, Charli JL, Joseph-Bravo P. An acute injection of corticosterone increases thyrotrophin-releasing hormone expression in the paraventricular nucleus of the hypothalamus but interferes with the rapid hypothalamus pituitary thyroid axis response to cold in male rats. *J Neuroendocrinol.* (2014) 26:861–69. doi: 10.1111/jne.12224
 44. Chomczynski P, Sacchi N. The single-step method of RNA isolation by acid guanidinium thiocyanate-phenol-chloroform extraction: twenty-something years on. *Nat Protocols.* (2006) 1:581–85. doi: 10.1038/nprot.2006.83
 45. Aguilar-Valles A, Sánchez E, de Gortari P, García-Vázquez AI, Ramírez-Amaya V, Bermúdez-Rattoni F, et al. The expression of TRH, its receptors and degrading enzyme is differentially modulated in the rat limbic system during training in the Morris Water Maze. *Neurochem Int.* (2007) 50:404–17. doi: 10.1016/j.neuint.2006.09.009
 46. Gutiérrez-Mariscal M, Sánchez E, García-Vázquez A, Rebolledo-Solleiro D, Charli JL, Joseph-Bravo P. Acute response of hypophysiotropic thyrotropin releasing hormone neurons and thyrotropin release to behavioral paradigms producing varying intensities of stress and physical activity. *Regul Pept.* (2012) 179:61–70. doi: 10.1016/j.regpep.2012.08.010
 47. Uribe RM, Jaimes-Hoy L, Ramírez-Martínez C, García-Vázquez A, Romero F, Cisneros M, et al. Voluntary exercise adapts the hypothalamus-pituitary-thyroid axis in male rats. *Endocrinology.* (2014) 155:2020–30. doi: 10.1210/en.2013-1724
 48. Bianco AC, Anderson G, Forrest D, Galton VA, Gereben B, Kim BW, et al. American Thyroid Association guide to investigating thyroid hormone economy and action in rodent and cell models. *Thyroid.* (2014) 24:88–168. doi: 10.1089/thy.2013.0109
 49. Obici S, Feng Z, Morgan K, Stein D, Karkanias G, Rossetti L. Central administration of oleic acid inhibits glucose production and food intake. *Diabetes.* (2002) 51:271–75. doi: 10.2337/DIABETES.51.2.271
 50. Schwinkendorf DR, Tsatsos NG, Gosnell BA, Mashek DG. Effects of central administration of distinct fatty acids on hypothalamic neuropeptide expression and energy metabolism. *Int J Obes.* (2011) 35:336–44. doi: 10.1038/ijo.2010.159
 51. Subcommittee on Laboratory Animal Nutrition, Committee on Animal Nutrition, Board on Agriculture, National Research Council. 1995. *Nutrient Requirements of Laboratory Animals. Fourth Rev.* Washington, DC: National Academies Press (1995). doi: 10.17226/4758
 52. Bianco AC, Nunes MT, Hell NS, Maciel RMB. The role of glucocorticoids in the stress-induced reduction of extrathyroidal 3,5,3'-triiodothyronine generation in rats. *Endocrinology.* (1987) 120:1033–38. doi: 10.1210/endo-120-3-1033
 53. Reynolds CM, Gray C, Li M, Segovia SA, Vickers MH. Early life nutrition and energy balance disorders in offspring in later life. *Nutrients.* (2015) 7:8090. doi: 10.3390/NU7095384
 54. Vargas J, Junco M, Gomez C, Lajud N. Early life stress increases metabolic risk, HPA axis reactivity, and depressive-like behavior when combined with postweaning social isolation in rats. Edited by Cheryl M McCormick *PLoS ONE.* (2016) 11:e0162665. doi: 10.1371/journal.pone.0162665
 55. Viveros MP, Llorente R, López-Gallardo M, Suarez J, Bermúdez-Silva F, De la Fuente M, et al. Sex-dependent alterations in response to maternal deprivation in rats. *Psychoneuroendocrinology.* (2009) 34(Suppl. 1):S217–26. doi: 10.1016/j.psyneuen.2009.05.015
 56. Haley S, Neff K, Gulliver K, Gough G, Slater H, Lane RH, et al. Mechanical-tactile stimulation (MTS) intervention in a neonatal stress model alters adult adipose tissue deposition and prevents hyperinsulinemia in male rats. *Early Human Dev.* (2013) 89:387–92. doi: 10.1016/j.earlhumdev.2012.12.005
 57. Mela V, Díaz F, Vázquez MJ, Argente J, Tena-Sempere M, Viveros M-P, et al. Interaction between neonatal maternal deprivation and serum leptin levels on metabolism, pubertal development, and sexual behavior in male and female rats. *Biol Sex Differ.* (2016) 7:1–17. doi: 10.1186/s13293-015-0054-6
 58. Gehrand AL, Hoeync B, Jablonski M, Leonovicz C, Ye R, Scherer PE, et al. Sex differences in adult rat insulin and glucose responses to arginine: programming effects of neonatal separation, hypoxia, and hypothermia. *Physiol Rep.* (2016) 4:e12972. doi: 10.14814/phy2.12972
 59. Raff H, Hoeync B, Jablonski M, Leonovicz C, Phillips JM, Gehrand AL. Insulin sensitivity, leptin, adiponectin, resistin, and testosterone in adult male and female rats after maternal-neonatal separation and environmental stress. *Am J Physiol Regul Integr Comp Physiol.* (2018) 314:R12–21. doi: 10.1152/ajpregu.00271.2017
 60. Leigh S-J, Morris MJ. The role of reward circuitry and food addiction in the obesity epidemic: an update. *Biol Psychol.* (2018) 131:31–42. doi: 10.1016/j.biopsycho.2016.12.013
 61. Hoch T, Kreitz S, Gaffling S, Pischetsrieder M, Hess A. Fat/carbohydrate ratio but not energy density determines snack food intake and activates brain reward areas. *Sci. Rep.* (2015) 5:10041. doi: 10.1038/srep10041
 62. Araujo RL, Andrade BM, Padrón AS, Gaidhu MP, Perry RLS, Carvalho DP, et al. High-fat diet increases thyrotropin and oxygen consumption without altering circulating 3,5,3'-triiodothyronine (T3) and thyroxine in rats: the role of iodothyronine deiodinases, reverse T3 production, and whole-body fat oxidation. *Endocrinology.* (2010) 151:3460–69. doi: 10.1210/en.2010-0026
 63. Perello M, Çakir I, Cyr NE, Romero A, Stuart RC, Chiappini F, et al. Maintenance of the thyroid axis during diet-induced obesity in rodents is controlled at the central level. *Am J Physiol Endocrinol Metabol.* (2010) 299:E976–89. doi: 10.1152/ajpendo.00448.2010
 64. Shao SS, Zhao YF, Song YF, Xu C, Yang JM, Xuan SM, et al. Dietary high-fat lard intake induces thyroid dysfunction and abnormal morphology in rats. *Acta Pharmacologica Sinica.* (2014) 35:1411–20. doi: 10.1038/aps.2014.82
 65. Cano P, Jiménez-Ortega V, Larrad A., Reyes Toso CF, Cardinali DP, Esquifino AI. Effect of a high-fat diet on 24-h pattern of circulating levels of prolactin, luteinizing hormone, testosterone, corticosterone, thyroid-stimulating hormone and glucose, and pineal melatonin content, in rats. *Endocrine.* (2008) 33:118–25. doi: 10.1007/s12020-008-9066-x
 66. Chang J-S, You Y-H, Park S-Y, Kim J-W, Kim H-S, Yoon K-H, et al. Pattern of stress-induced hyperglycemia according to type of diabetes: a predator stress model. *Diabetes Metab J.* (2013) 37:475–83. doi: 10.4093/dmj.2013.37.6.475
 67. Plummer MP, Finnis ME, Phillips LK, Kar P, Bihari S, Biradar V, et al. Stress induced hyperglycemia and the subsequent risk of type 2 diabetes in survivors of critical illness. *PLoS ONE.* (2016) 11:e0165923. doi: 10.1371/journal.pone.0165923
 68. Beaudry JL, D'souza AM, Teich T, Tsushima R, Riddell MC. Exogenous glucocorticoids and a high-fat diet cause severe hyperglycemia and hyperinsulinemia and limit islet glucose responsiveness in young male Sprague-Dawley rats. *Endocrinology.* (2013) 154:3197–208. doi: 10.1210/en.2012-2114
 69. Barella LF, De Oliveira JC, Branco RCS, Camargo RL, Gomes RM, Mendes FCV, et al. Early exposure to a high-fat diet has more drastic consequences on metabolism compared with exposure during adulthood in rats. *Horm Metab Res.* (2012) 44:458–64. doi: 10.1055/s-0032-1306300
 70. Cheng HS, Ton SH, Phang SCW, Tan JBL, Abdul Kadir K. Increased susceptibility of post-weaning rats on high-fat diet to metabolic syndrome. *J Adv Res.* (2017) 8:743–52. doi: 10.1016/j.jare.2017.10.002
 71. Bowe JE, Franklin ZJ, Hauge-Evans AC, King AJ, Persaud SJ, Jones PM. Assessing glucose homeostasis in rodent models. *J. Endocrinology.* (2014) 222:13–25. doi: 10.1530/JOE-14-0182
 72. Lippmann M, Bress A, Nemeroff CB, Plotsky PM, Monteggia LM. Long-term behavioural and molecular alterations associated with maternal separation in rats. *Eur J Neurosci.* (2007) 25:3091–98. doi: 10.1111/j.1460-9568.2007.05522.x
 73. Dallman MF, Pecoraro N, Akana SF, La Fleur SE, Gomez F, Houshyar H, et al. Chronic stress and obesity: a new view of 'comfort food'. *Proc Natl Acad Sci USA.* (2003) 100:11696–701. doi: 10.1073/pnas.1934666100
 74. Kinzig KP, Hargrave SL, Honors MA. Binge-type eating attenuates corticosterone and hypophagic responses to restraint stress. *Physiol Behav.* (2008) 95:108–13. doi: 10.1016/j.physbeh.2008.04.026
 75. Egan AE, Thompson AMK, Buesing D, Fourman SM, Packard AEB, Terefe T, et al. Palatable food affects HPA axis responsivity and forebrain neurocircuitry in an estrous cycle-specific manner in female rats. *Neuroscience.* (2018) 384:224–40. doi: 10.1016/j.neuroscience.2018.05.030
 76. Balasubramanian P, Jagannathan L, Mahaley RE, Subramanian M, Gilbreath ET, MohanKumar PS, et al. High fat diet affects reproductive functions in female diet-induced obese and dietary resistant rats. *J Neuroendocrinol.* (2012) 24:748–55. doi: 10.1111/j.1365-2826.2011.02276.x

77. Lie MEK, Overgaard A, Mikkelsen JD. Effect of a postnatal high-fat diet exposure on puberty onset, estrous cycle regularity, and kisspeptin expression in female rats. *Reprod Biol.* (2013) 13:298–308. doi: 10.1016/J.REPBIO.2013.08.001
78. Larsen PJ, Mau SE. Effect of acute stress on the expression of hypothalamic messenger ribonucleic acids encoding the endogenous opioid precursors preproenkephalin A and proopiomelanocortin. *Peptides.* (1994) 15:783–90. doi: 10.1016/0196-9781(94)90030-2
79. Baubet V, Fèvre-Montange M, Gay N, Debilly G, Bobillier P, Cespuglio R. Effects of an acute immobilization stress upon proopiomelanocortin (POMC) mRNA levels in the mediobasal hypothalamus: a quantitative in situ hybridization study. *Mol Brain Res.* (1994) 26:163–68. doi: 10.1016/0169-328X(94)90087-6
80. Conrad CD, McEwen BS. Acute stress increases neuropeptide Y mRNA within the arcuate nucleus and hilus of the dentate gyrus. *Brain Res Mol Brain Res.* (2000) 79:102–9. doi: 10.1016/S0169-328X(00)00105-4
81. Makino S, Baker RA, Smith MA, Gold PW. Differential regulation of neuropeptide Y mRNA expression in the arcuate nucleus and locus coeruleus by stress and antidepressants. *J Neuroendocrinol.* (2000) 12:387–95. doi: 10.1046/j.1365-2826.2000.00451.x
82. Viveros MP, Llorente R, Díaz F, Romero-zerbo SY, Bermudez-silva FJ, Rodríguez F, et al. Maternal deprivation has sexually dimorphic long-term effects on hypothalamic cell-turnover, body weight and circulating hormone levels. *Horm Behav.* (2010) 58:808–19. doi: 10.1016/j.yhbeh.2010.08.003
83. Shimizu H, Arima H, Ozawa Y, Watanabe M, Banno R, Sugimura Y, et al. Glucocorticoids increase NPY gene expression in the arcuate nucleus by inhibiting MTOR signaling in rat hypothalamic organotypic cultures. *Peptides.* (2010) 31:145–49. doi: 10.1016/j.peptides.2009.09.036
84. Priego T, Sánchez J, Picó C, Palou A. Sex-associated differences in the leptin and ghrelin systems related with the induction of hyperphagia under high-fat diet exposure in rats. *Horm Behav.* (2009) 55:33–40. doi: 10.1016/j.yhbeh.2008.07.010
85. Fleur SE, La, Van Rozen AJ, Luijendijk MCM, Groeneweg F, Adan RAH. A free-choice high-fat high-sugar diet induces changes in arcuate neuropeptide expression that support hyperphagia. *Int J Obes.* (2010) 34:537–46. doi: 10.1038/ijo.2009.257
86. Heuvel J. K. van den, Eggels L, Fliers E, Kalsbeek A, Adan RAH, la Fleur SE. Differential modulation of arcuate nucleus and mesolimbic gene expression levels by central leptin in rats on short-term high-fat high-sugar diet. *PLoS ONE.* (2014) 9:e87729. doi: 10.1371/JOURNAL.PONE.0087729
87. Cizza G, Brady LS, Esclapes M, Blackman MR. Age and gender influence basal and stress-modulated hypothalamic–pituitary–thyroidal function in Fischer 344/N rats. *Neuroendocrinology.* (1996) 64:440–48.
88. Müller-Fielitz H, Stahr M, Bernau M, Richter M, Abele S, Krajka V, et al. Tanycytes control the hormonal output of the hypothalamic–pituitary–thyroid axis. *Nat Commun.* (2017) 8:484. doi: 10.1038/s41467-017-00604-6
89. Marsili A, Sanchez E, Singru P, Harney JW, Zavacki AM, Lechan RM, et al. Thyroxine-induced expression of pyroglutamyl peptidase II and inhibition of TSH release precedes suppression of TRH mRNA and requires type 2 deiodinase. *J. Endocrinology.* (2011) 211:73–78. doi: 10.1530/JOE-11-0248
90. Diano S, Naftolin F, Goglia F, Horvath TL. Fasting-induced increase in type II iodothyronine deiodinase activity and messenger ribonucleic acid levels is not reversed by thyroxine in the rat hypothalamus. *Endocrinology.* (1998) 139:2879–84.
91. Fekete C, Sarkar S, Christoffolete MA, Emerson CH, Bianco AC, Lechan RM. Bacterial lipopolysaccharide (LPS)-induced type 2 iodothyronine deiodinase (D2) activation in the mediobasal hypothalamus (MBH) is independent of the LPS-induced fall in serum thyroid hormone levels. *Brain Res.* (2005) 1056:97–99. doi: 10.1016/j.brainres.2005.07.021
92. Lazcano I, Cabral A, Uribe RM, Jaimes-Hoy L, Perello M, Joseph-Bravo P, et al. Fasting enhances pyroglutamyl peptidase II activity in tanycytes of the mediobasal hypothalamus of male adult rats. *Endocrinology.* (2015) 156:2713–23. doi: 10.1210/en.2014-1885
93. Segerson T, Kauer J, Wolfe H, Mobtaker H, Wu P, Jackson I, et al. Thyroid hormone regulates TRH biosynthesis in the paraventricular nucleus of the rat hypothalamus. *Science.* (1987) 238:78–80. doi: 10.1126/science.3116669
94. Perello M, Friedman T, Paez-Espinosa V, Shen X, Stuart RC, Nillni EA. Thyroid hormones selectively regulate the posttranslational processing of prothyrotropin-releasing hormone in the paraventricular nucleus of the hypothalamus. *Endocrinology.* (2006) 147:2705–165. doi: 10.1210/en.2005-1609
95. Plaza A, Garcia-Esteve L, Ascaso C, Navarro P, Gelabert E, Halperin I, et al. Childhood sexual abuse and hypothalamus–pituitary–thyroid axis in postpartum major depression. *J Affect Disord.* (2010) 122:159–63. doi: 10.1016/J.JAD.2009.07.021
96. Sinai C, Hirvikoski T, Nordström A-L, Nordström P, Nilsson A, Wilczek A, et al. Hypothalamic pituitary thyroid axis and exposure to interpersonal violence in childhood among women with borderline personality disorder. *Eur J Psychotraumatol.* (2014) 5:23911. doi: 10.3402/ejpt.v5.23911
97. Fontenelle L, Feitosa M, Severo J, Freitas T, Morais J, Torres-Leal F, et al. Thyroid function in human obesity: underlying mechanisms. *Horm Metab Res.* (2016) 48:787–94. doi: 10.1055/s-0042-121421

Conflict of Interest Statement: The authors declare that the research was conducted in the absence of any commercial or financial relationships that could be construed as a potential conflict of interest.

Copyright © 2019 Jaimes-Hoy, Romero, Charli and Joseph-Bravo. This is an open-access article distributed under the terms of the Creative Commons Attribution License (CC BY). The use, distribution or reproduction in other forums is permitted, provided the original author(s) and the copyright owner(s) are credited and that the original publication in this journal is cited, in accordance with accepted academic practice. No use, distribution or reproduction is permitted which does not comply with these terms.



Voluntary Exercise-Induced Activation of Thyroid Axis and Reduction of White Fat Depots Is Attenuated by Chronic Stress in a Sex Dimorphic Pattern in Adult Rats

Marco Antonio Parra-Montes de Oca, Mariana Gutiérrez-Mariscal, Ma Félix Salmerón-Jiménez, Lorraine Jaimes-Hoy, Jean-Louis Charli and Patricia Joseph-Bravo*

Departamento de Genética del Desarrollo y Fisiología Molecular, Instituto de Biotecnología, Universidad Nacional Autónoma de México, Cuernavaca, Mexico

OPEN ACCESS

Edited by:

Lee E. Eiden,
National Institutes of Health (NIH),
United States

Reviewed by:

Gábor B. Makara,
Hungarian Academy of Sciences
(MTA), Hungary
Joao Pedro Werneck De Castro,
University of Miami, United States

*Correspondence:

Patricia Joseph-Bravo
joseph@ibt.unam.mx

Specialty section:

This article was submitted to
Neuroendocrine Science,
a section of the journal
Frontiers in Endocrinology

Received: 22 March 2019

Accepted: 11 June 2019

Published: 26 June 2019

Citation:

Parra-Montes de Oca MA, Gutiérrez-Mariscal M, Salmerón-Jiménez MF, Jaimes-Hoy L, Charli J-L and Joseph-Bravo P (2019) Voluntary Exercise-Induced Activation of Thyroid Axis and Reduction of White Fat Depots Is Attenuated by Chronic Stress in a Sex Dimorphic Pattern in Adult Rats. *Front. Endocrinol.* 10:418. doi: 10.3389/fendo.2019.00418

The activity of the hypothalamus-pituitary-thyroid (HPT) axis is inhibited by energy deficit, by acute or chronic stress, but activated by cold exposure or exercise. Because stress curtails acute cold induced activation of HPT, we evaluated the effect of chronic stress on HPT axis response to voluntary exercise, a persistent energy-demanding situation. Adult male and female Wistar rats were exposed to restraint stress, 30 min/day for 2 weeks, or to isolation (Iso) [post-natal day [PND] 30–63]. Exercise was performed (7 p.m.–7 a.m.) in a running wheel, sedentary controls stayed in individual cages (Sed); at 7 a.m. they were housed with their cage mate or individually (Iso); food intake by the exercised group was measured day and night to pair-fed Sed. At sacrifice, hormones, mRNA levels and tissue weights were quantified. Control or restrained adult rats had access to running wheel daily for 2 weeks. Compared to C, exercise decreased white adipose tissue (WAT) mass in females and males, increased hypothalamic paraventricular nucleus (PVN)-*Trh* expression in males proportionally to exercise performed, and increased TSH and T4 serum concentration in females. These changes were not detected in restrained groups. Starting at PND 63 control (2/cage) and isolated (1/cage) rats either exercised on 10 alternated nights or were sedentary. In control male animals, compared to Sed rats, exercise did not decrease WAT mass, nor changed HPT axis activity, but increased *Pomc* and deiodinase 2 (*Dio2*) expression in mediobasal hypothalamus (MBH), adrenergic receptor $\beta 3$ and uncoupling protein-1 in brown adipose tissue. In control female animals, exercise decreased WAT mass, increased *Pomc*, *Dio2*, and *Trhde* expression in MBH, and TSH serum concentration. Iso females had lower TSH and T4 serum concentration, *Dio2* and *Trhde* expression in MBH than controls. The stress response was higher in isolated males than females, but in males it did not alter the effects of exercise, in contrast to isolated females that had a blunted response to exercise compared to controls. In conclusion, chronic stress interferes with metabolic effects produced by exercise, such as loss of WAT mass, coincident with dampening of HPT activity.

Keywords: TRH, WAT, HPT axis, restraint, social isolation, exercise

INTRODUCTION

Physical activity and food intake are the two most important controllable variable in setting body weight. Energy expenditure is produced by basal metabolism and thermogenesis required for everyday living and physical activity. In concert with the sympathetic nervous system, thyroid hormones (TH) contribute to thermogenesis and basal metabolic rate, but they also participate in several aspects of exercise performance as they are directly involved in muscle activity, mitochondrial biogenesis, lipolysis, glycolysis, and gluconeogenesis, and mobilization of fuel to metabolically active tissues (1, 2). Patients with hypothyroidism, overt or subclinical, have reduced exercise tolerance, endurance, muscle strength, cardiovascular functions, deficient control of energy expenditure, fatigue, and poor quality of life (3–6).

Tissue levels of thyroid hormones are regulated by the activity of the hypothalamic-pituitary-thyroid (HPT) axis, and at target cells by transporters, deiodinases, and membrane or intracellular TH receptors, the latter acting as transcription factors (1, 7–9). The HPT axis is subject to multifactorial regulation, initiating with neurons of the hypothalamic paraventricular nucleus (PVN) that synthesize thyrotropin releasing hormone (TRH) and release it in the median eminence, in the vicinity of portal vessels and β 2-tanycytes. These neurons receive multiple afferents from the arcuate nucleus and other brain areas that convey information of environmental, nutritional and metabolic status (10, 11). Tanycytes express deiodinase-2 (*Dio2*) that transforms T4 to T3, TH transporters, and TRH-degrading enzyme (*Trhde*) that inactivates released TRH (10). Once in portal vessels, TRH is transported to the adenohypophysis where it controls synthesis and release of thyrotropin (TSH). TSH activates synthesis of T4 in thyroid; some T4 is deiodinated to T3 in thyroid but most in target tissues (1, 12, 13). T3 is the active hormone at transcriptional level and responsible for feedback inhibition on TRH and TSH synthesis (7, 14, 15).

Multiple factors modulate the activity of the HPT axis; it is inhibited in situations of energy deficit as fasting, food restriction or chronic illness, and stimulated in certain conditions of energy excess (10, 16). Situations of energy demands as cold exposure and some types of exercise increase HPT axis activity (17–20). Rats running in a treadmill have increased serum concentration of T3 at the beginning of exercise (21) but lower after 120 min. In humans, contradictory results relate to the intensity and duration of exercise, nutritional status, and timing of blood samples; increased TSH serum concentrations are detected at short times after an exercise bout, and of T4 in some conditions although dehydration may give false results (22); increased TSH and TH concentration is detected after endurance training if measured before exhaustion but inhibited if energy reserves are temporarily depleted, or in conditions of high release of corticosterone or interleukins, for example (23). Research in animals has produced also inconsistent results; among the confounding factors, exercise usually diminishes food intake (19, 24), which by itself drives inhibition of HPT axis; likewise, for stress imposed by certain types of exercise (21). Access to a wheel provides rodents with the opportunity to exercise in voluntary non-stressed conditions

(25). Using this paradigm we previously demonstrated that compared to sedentary animals exercised rats decrease their food intake and mass of white adipose tissue (WAT), and diminish the parameters that reflect HPT axis activity; however, if values are compared to a pair-fed group there is still a strong decrease in WAT mass, but PVN *Trh* expression, TSH and T3 serum concentrations are higher and proportional to the loss of WAT mass (19).

Another important regulator on HPT activity is stress, either acute or chronic, which may cause inhibition. Stress diminishes synthesis and release of TRH, TSH, and TH, and hepatic conversion of T4 into T3 (26–30); some effects are mimicked by acute or chronic corticosterone injections (31, 32). Not only basal HPT axis activity is affected by acute stress but also its response to an energy demanding situation as cold exposure; rats subjected to an acute stress or to corticosterone injection prior to cold exposure do not present the expected activation of HPT axis activity, and of a target organ as brown adipose tissue (BAT) (19, 32). The interference of glucocorticoids on neuronal activation of TRH neurons has been demonstrated at the level of *Trh* transcription in hypothalamic cells *in vitro* (33, 34); *in vivo*, corticosterone administration inhibits cold-induced CREB phosphorylation in TRH neurons (34). All these data pertain to male rodents as data on females are scarce.

Although chronic exposure to stress or to corticosterone inhibits PVN *Trh* expression and serum TSH concentration (31), the response of the HPT axis in chronically stressed animals exposed to energy demands is unknown. There are several models to induce chronic stress in rodents and depending on the type, the response of the HP-adrenal (HPA) axis (CRH:ACTH:glucocorticoids) can either subside (animals habituate) or intensify. Chronic stress induced by daily intermittent short periods of restraint (Res) is a model of psychological stress that produces habituation of the response of the HPA axis, but if rodents are submitted to a new stressor, response is enhanced (35, 36). After 30 min of acute restraint, PVN *Trh* expression and TSH serum concentration decrease but levels normalize after 14 daily sessions (19, 37). The cold-induced activation of the HPT axis is also curtailed in male rats submitted to 14 days of intermittent repeated restraint (unpublished). Another type of stressor is individual housing; isolation (Iso) constitutes a continuous chronic stress recognized as a strong psychosocial stressor that causes hyperactivation of the HPA axis, and the lack of social stimuli prevent habituation (38); animals isolated since puberty have behavioral and physiological malfunctions, as puberty and adolescence are critical developmental periods for circuit formation between limbic areas (39, 40).

As an adequate response of the HPT axis to exercise favors mobilization of energy reserves (19, 41), we hypothesized that chronic stress attenuates the response of the HPT axis to voluntary exercise and this contributes to long-term consequences in WAT depots. We selected these two paradigms to distinguish the effect of stress on animals that habituated (Res) and no longer have high basal corticosterone levels but may show an exaggerated response to a novel situation as exercise (35–37), compared to isolated animals that do not habituate and

show dysfunction of HPA axis (42). As an acute corticosterone increase blunts the increase in TRH synthesis induced by cold-induced neuronal stimulation (32–34), we may expect a different response if effects depend only in corticosterone variations or, if they depend on limbic circuitry (43). We studied the response of the HPT and HPA axes (the latter as control) and WAT depots to voluntary wheel running in male and female rats submitted to two types of chronic stress: (a) 2 weeks of intermittent restraint in adult animals, and (b) isolation caused by keeping rats in individual housing since puberty.

MATERIALS AND METHODS

Animals

Male and female Wistar rats were raised at the Institute's Animal Facility, as described in Sotelo-Rivera et al. (32). Breeding colony management and care was carried out only by two technicians to avoid additional stress. The breeding procedure followed: an outbreed monogamous pair scheme in which the male is removed before the litter is born; litter is adjusted to 10 offspring at post-natal day 2 (PND 2) and culled if necessary. Animals are weaned at PND 21, placed by sex in groups of 2–4/cage and treated as described (44). Appropriate records assure non-inbreeding; colony breeders are renewed every 5 years. For these experiments, rats (PND 45–60) were placed in experimental independent rooms according to sex (2/cage). When males were near 350 g or 2.5 months, they were housed in groups of two per cage, in cages with a wire bar lid modified so that the rear 8.00" of lid is ~3.00" higher (total height of 11.00"), allowing rats to stand on their back legs (Y Corporation of America, INC.). Food (Teklad 2018SX, Envigo, USA) and water were offered *ad libitum* except where indicated otherwise. Maintenance and work with animals followed the Guide for the care and use of laboratory animals (8th ed.), as well as the Mexican norm NOM-062-ZOO-1999. These experiments were approved by the Bioethics Committee of the Institute, approval No. 273 and 318.

Experiment 1. Chronic Intermittent Restraint

Forty adult male rats at PND 86 (390 ± 6 g) were weighed and separated in five groups (eight rats per group). Two groups were taken to an empty room and introduced into a plexiglass tube (23.5×7 cm) with slots for ventilation and keeping tail out, in prone position during 30 min every day at 10:00 h for 2 weeks [restrained [Res] group]; two groups serving as experimental controls (C) were taken to a different room and placed in a small cage during 30 min (37). A group of 8 naïve (N) animals from the same cohort was kept undisturbed in the animal room to evaluate environmental conditions effect. Food intake was quantified by weight difference: A set measured amount of food was placed over the rack of the Res and N groups every 3 days, the amount left was weighted again after recovering small pieces from the bed. The mean of Res intake offered to controls (pair-fed).

At PND 101, rats of C and Res groups were divided; half of C (420 ± 13 g) and of Res (429 ± 14 g) animals were introduced every night (7:00 p.m.–7:00 a.m.), during 2 weeks, in a cage

with a running wheel of 25 cm diameter (AccuScan Instruments INC) for voluntary exercise (exercised: Ex), the other two halves of animals stayed in individual cages (sedentary: Sed) (19). All rats rejoined their cage mate in the morning. Food was offered during dark or light cycles and intake registered at every food change (between 7:00 a.m. and 9:00 a.m. in the morning and 5:00 p.m.–7:00 p.m. in the night). Sedentary rats were pair-fed to the intake of Ex rats.

The same paradigm was used to study female rats starting at PND 95 (before Res: 248 ± 4 g; after Res, before Ex: 253 ± 3 g).

Experiment 2. Social Isolation

At PND 30 male ($N = 32$; 110 ± 2 g) and female ($N = 32$; 100 ± 2 g) Wistar rats were separated in two groups that were housed, either in individual cages (Iso) ($N = 16$) or in groups of 2/cage (C) in the same room to expose isolated rats to visual, auditive, and olfactory cues of other rats (45). Rats were maintained as described (32), in separate rooms according to sex. Food and water were offered *ad libitum*, food intake (FI) was quantified every 3 days from PND 30 to PND 63 and body weight measured every week in the adolescence period. At PND 63 C (Males: 379 ± 8 g; Females: 223 ± 6 g) or Iso (Males: 363 ± 7 ; Females: 224 ± 5 g) rats of each sex were further separated in two groups, one was left undisturbed (Sed) and the other exposed to a running wheel (Ex) ($N = 8$ each) as described above and in Uribe et al. (19), with some modifications. Due to limited amount of running cages, rats had alternate access during 16 days for a total of 10 running days. At light change (7:00 a.m.), C animals were housed with their cage-mate or in an isolated cage (Iso group); food intake, and number of revolutions were recorded daily and body weight every 2 days. Sedentary rats received the amount of food consumed by the exercised group as described previously.

Sacrifice and Tissue Collection

On the last day of exercise, 3 h after lights on and cage change, animals were decapitated with a sharp guillotine by an experienced technician as described (19), in a separate laboratory near the animal rooms, taking one animal at a time, cleaning the guillotine in-between and with care of diminishing stress. Trunk blood was collected, serum separated and stored in aliquots. Adipose tissues (gonadal, retroperitoneal and interscapular) and adrenals were extracted and weighed in fresh; brain and BAT were placed in dry ice and stored at -70°C . Several experienced persons participated to limit time between initiation and termination of sacrifice to a maximum of 2 h. Dissection of hypothalamic regions is described in **Supplementary Figure 1**.

Hormone Assays

Radioimmunoassays were utilized for TSH (NIDDK reagents and protocols) and corticosterone (CORT; reagents from Merck-Millipore, PerkinElmer, and Sigma) quantification. Total T3 and T4 were quantified with ELISA kits (Diagnóstica Internacional Zapopan, JAL, México) adding to standard curves an aliquot of hypothyroid rat serum (46). All samples were measured in duplicate and the mean taken as one determination; intraassay and interassay coefficients of variation were $<10\%$.

Semi-quantification of mRNA

Total RNA was extracted from frozen tissues according to Chomzynsky et al. (47) with some modifications for BAT, for which a centrifugation (870 g, 4°C, and 10 min) and an extra chloroform wash were performed to remove fat. Relative mRNA levels were measured by RT-PCR according to reported conditions (19); for those not previously reported by our group, linearity was verified and optimized conditions described in **Supplementary Figure 2**.

Statistical Analysis

The mean of duplicate biochemical measurements was considered as one determination; results were calculated as percent of each experiment's control group mean. Two-way ANOVA was performed to analyze the effect of chronic stress and sex before exercise, and to analyze the effect of chronic stress and physical activity on the different variables. Three-way ANOVA was performed to analyze effects of chronic stress, physical activity and sex, and interaction between these variables. All data were analyzed by Sigma plot 11.0 (Systat Software, Inc.) and GraphPad Prism 8 (GraphPad Software, Inc.). Results of statistical analysis are described in **Supplementary Tables 1, 2**. *Post-hoc* comparisons were carried out with either Bonferroni or Holm-Sidak tests, and difference considered to be significant when $P < 0.05$.

RESULTS

Experiment 1. Effect of Chronic Restraint Stress on the Response to Voluntary Exercise

Chronic Restraint Decreased Food Intake and Body Weight Gain

During the period of intermittent restraint, there was no difference in the total food intake or body weight gain (BWg) of restrained male rats compared to naïve (**Table 1**). Res females ate 10% less than the naïve group and as controls were pair fed to Res, they ate all that was offered (**Table 1**). BWg was lowest in the pair-fed, followed by Res and highest by N. Restraint diminished voluntary food intake, pair-fed were probably stressed by hunger causing highest weight lost. Females ate less absolute food than males (**Table 1**) but ate more relatively to body weight, thus their food efficiency was lower (**Supplementary Table 3A**).

Chronic Restraint Diminished Motivation for Running Only in Males

Res males performed less exercise than controls (**Figure 1A**) whereas females were not affected as both groups gradually increased the total distance ran which were considerably higher than those ran by males (**Figure 1B**). As previously published (19), exercise diminished food intake more in C-Ex than in Res-Ex; body weight gain in Sed or Ex, C or Res was 5% lower than N but differences between C or Res groups were non-significant (**Table 2**). Compared to N, exercise decreased food intake in C or Res females but BWg was not significantly different (**Table 2** and **Supplementary Table 4A**).

TABLE 1 | Food intake (FI) and body weight gain (BWg) during restraint stress period of naïve (N) pair fed controls (C) and restraint (R) male and female rats.

	N	C	Res
MALES			
FI (g/day)	26.6 ± 9.4	27.2 ± 0.6	26.4 ± 0.8
BWg (g)	31.6 ± 3.5	27.4 ± 3.5	25.3 ± 2.4
FEMALES			
FI (g/day)	20.7 ± 0.11 ^A	18.41 ± 0.26 ^A	18.1 ± 0.2 ^A
BWg (g)	10.25 ± 3.9 ^A	−4 ± 2.12 ^A	5.5 ± 1.5 ^A

Male and female Wistar adult rats were restrained (R) or kept in single cage for 30 min/day for 14 consecutive days in two independent rooms, food intake of restrained group was pair-fed to control group (C). Results are expressed in mean ± SEM. Significant ANOVAs (**Supplementary Table 1A**) followed by post-hoc: * $P < 0.05$ vs. C group; ^A $P < 0.05$ vs. Sex; [°] $P < 0.05$ vs. N.

Chronic Restraint Blunted Exercise-Induced Loss of Fat Mass and Activation of HPT Axis in a Sex-Dependent Manner

Exercise induces WAT mass loss even if it is not evident in body weight (19, 48). C males reduced gonadal, retroperitoneal, and interscapular fat depots after exercise, but Res group did not (**Figure 1C**). C-Ex females also reduced them, although gonadal WAT loss was not significant; as in males, Res females did not lose WAT after exercise (**Figure 1D**).

Because chronic stress affects the HPA response to new stressors and exercise has been considered either to increase or diminish HPA activity (19, 49), we measured gene expression profile of *Crh* and *Gr* in PVN, and corticosterone in serum. There were no significant differences in any of these variables in groups of either sex (not shown), except for an increase in right-adrenal weight of Res males (N, 27 ± 3; C-Ex 31 ± 1; Res 31 ± 3; Res-Ex 39 ± 2^{**} mg, * $P = 0.007$ vs. N; ^x $P = 0.02$ vs. C-Ex) suggesting chronic stress (50). Females had higher basal corticosterone serum concentration (181 ± 7 ng/ml) than males (65 ± 4 ng/ml); but in contrast, values were increased similarly in all experimental groups compared to naïve (C-Sed 396 ± 56, C-ex 332 ± 19, Res-Sed 354 ± 30, Res-Ex 303 ± 16).

Trh expression was stimulated in C-Ex (**Figure 1E**) and values correlated negatively with WAT retroperitoneal mass ($r = -0.832$; $P = 0.003$). No other parameters of HPT axis varied among male groups. In females, *Trh* expression was not significantly different between C-Ex and C-Sed or between Res groups. In contrast to males, TSH serum concentration increased in C-Ex females as well as T4 (**Figure 1F**). In both sexes, activation of the HPT axis coincides with WAT mass decrease only in controls, but not in those previously stressed by daily restraint.

Experiment 2. Effect of Individual Housing on the Response to Voluntary Exercise Social Isolation Did Not Affect Food Intake and Body Weight Gain During Adolescence

We chose to analyze social isolation since adolescence because this stressor prevents proper development of brain, causing behavioral and physiological alterations that can remain until

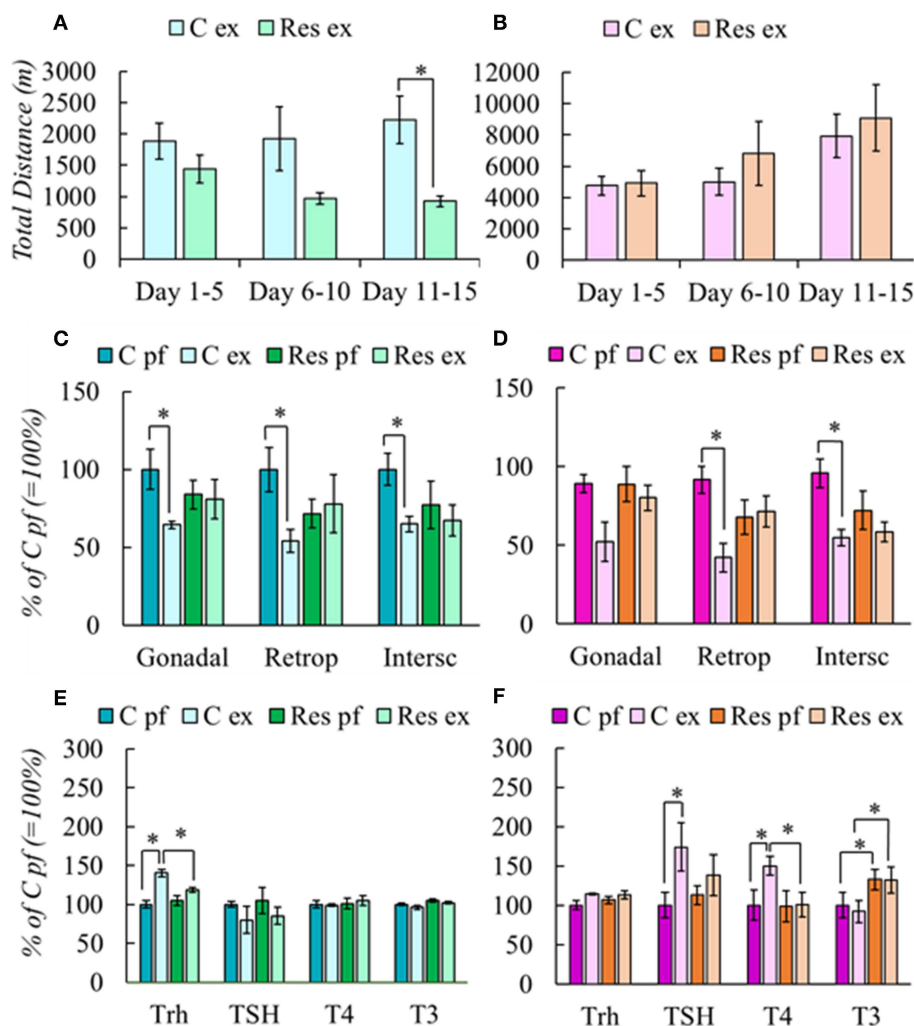


FIGURE 1 | Effect of chronic restraint on physical activity (A,B), fat mass (C,D), and HPT axis response (E,F) of male and female rats. Stress protocol and exercise conditions as described in **Tables 1, 2**, respectively. Physical activity was expressed in total distance in meters at periods stated in the abscissa. Results are expressed in percent of mean values of C pf. Significant ANOVAs (**Supplementary Table 2A**), followed by *post-hoc*: * $P < 0.05$.

adult stage (43, 51, 52). Social isolation in adulthood delays exercised-induced hippocampal neurogenesis in male and female rats, affecting more in males than in females (47, 53).

Rats were isolated at PND 30, as expected males grew faster than females; no difference was observed in body weight gain between C or Iso groups; by PND 60, body weight of C or Iso groups were similar so as their food intake (**Table 3** and **Supplementary Table 3B**). The lack of effect of social isolation since weaning on ponderal variables during the growing phase has been previously reported (54, 55).

Ponderal Changes and HPA Responses to Exercise Were Affected by Social Isolation Dependent on Sex

Exercise reduced their food intake 19% in C and 18% in Iso groups compared to average intake before exercise in both sexes (**Tables 3, 4**), but Iso-Ex ate more than exercised controls (**Table 4**), sedentary group were pair-fed accordingly.

After exercise, Iso gained more weight than controls (**Table 4**). If food intake was calculated in relation to body weight, females ate more and their food efficiency was lower than males (**Supplementary Table 4B**). Isolation did not diminish the amount of running in males or females compared to group-housed controls (**Figures 2A,B**), and as in the previous experiments, females ran more than males (**Table 4**). Total distance ran by C males in this experiment was similar to controls of experiment 1, whereas females ran more, even though they had access to the wheel only in alternate days for a total of 10 nights, instead of 14 daily nights in the previous experiment (**Supplementary Figure 3**); probably be due to the lighter weight of the latter (56), and/or the form of exercise, on alternate days in Iso that avoided habituation (25) compared to every day in Res.

C males had less gonadal and retroperitoneal WAT mass compared with Iso group, but there was no lost of any fat type by exercised (**Figure 2C**). C-Ex females lost gonadal and

TABLE 2 | Food intake (FI), Body weight gain (BWg) and distance per day (DPD) after exercise period of male and female rats.

	N	C pf	C ex	Res pf	Res ex
MALES					
FI (g/day)	25.15 ± 0.97	18.5 ± 0.9°	17.8 ± 1.1°	21.5 ± 1.9°	20.9 ± 1.2°
BWg (g)	19.8 ± 10.2	−6.5 ± 3.6°	−12.75 ± 2.9°	2.4 ± 4.7°	−9.2 ± 13.4°
DPD (m)	–	–	402 ± 78	–	280 ± 64
FEMALES					
FI (g/day)	23.27 ± 0.54	15.39 ± 1.58°	15.55 ± 1.52°	16.12 ± 1.35° ^A	16.28 ± 1.35° ^A
BWg (g)	15.3 ± 5.46	5.0 ± 4.0 ^A	7.6 ± 2.2 ^A	15.6 ± 3.8 ^A	15.8 ± 2.8 ^A
DPD (m)	–	–	1179 ± 186 ^A	–	1599 ± 248 ^A

Effect of restraint.

Restrained or control rats were either exposed to a running wheel (C ex and Res ex) or left individually in a cage (C pf and Res pf) overnight for 14 days. Food intake of exercised animals was pair-fed to control groups. Significant ANOVAs (**Supplementary Table 2A**) followed by post-hoc: ^AP < 0.05 vs. Sex; °P < 0.05 vs. N.

TABLE 3 | Food intake (FI) and body weight gain (BWg) during adolescence-adulthood period of group-housed (C) and isolated (Iso) male and female rats.

	C	Iso
MALES		
FI (g/day)	27.58 ± 0.37	27.14 ± 0.64
BWg (g)	232.63 ± 5.48	220.00 ± 4.34
FEMALES		
FI (g/day)	19.55 ± 0.23 ^A	19.81 ± 0.53 ^A
BWg (g)	104.94 ± 3.57 ^A	104.19 ± 3.06 ^A

Male and female Wistar rats were kept isolated (Iso) or in 2/cage (Controls, C) from PND 30 to PND 63. Results are expressed in mean ± SEM. Significant ANOVAs (**Supplementary Table 1B**) followed by post-hoc: ^AP < 0.001 vs. Sex.

TABLE 4 | Food intake (FI), body weight gain (BWg) and distance per day (DPD) after exercise period of group-housed (C) and isolated (Iso) male and female rats.

	C-Sed	C-Ex	Iso-Sed	Iso-Ex
MALES				
FI (g/day)	24.74 ± 0.02	25.24 ± 0.84	26.05 ± 0.04*	26.30 ± 0.92*
BWg (g)	16.67 ± 1.20	15.00 ± 3.84	30.83 ± 2.27*	25.50 ± 2.53* ^{&}
DPD (m)	–	542 ± 36	–	570 ± 74
FEMALES				
FI (g/day)	16.99 ± 0.01 ^A	17.07 ± 0.34 ^A	18.16 ± 0.02* ^A	18.00 ± 0.46* ^A
BWg (g)	10.86 ± 2.98 ^A	7.17 ± 3.63 ^A	14.00 ± 1.41* ^A	13.14 ± 1.98* ^A
DPD (m)	–	3,1061 ± 597 ^A	–	3,753 ± 522 ^A

At PND 63, group-housed (C) and isolated (Iso) rats were separated in two groups, one was left undisturbed (Sedentary, Sed) and the other was exposed to a running wheel in alternated days during the dark period. Sed group received the amount of food that Ex group. Results are expressed in mean ± SEM. Significant ANOVAs (**Supplementary Table 2B**) followed by post-hoc: *P < 0.05 vs. C group; [&]P < 0.05 vs. Sed group; ^AP < 0.05 vs. Sex.

subcutaneous WAT mass albeit only subcutaneous in the Iso-Ex group (**Figure 2D**).

HPA response differed between groups. Isolation increased PVN *Crh* expression whether or not they exercised; there was a tendency to increase PVN *Gr* expression and Cort serum concentration in C-Ex but did not achieve significance

(**Figure 2E**). Females in contrast, had lower PVN *Crh* expression and serum Cort concentration in Iso than C groups. PVN *Gr* mRNA levels increased although significant only in Iso-Sed (**Figure 2F**). Higher expression of *Gr* may contribute to overcome the reduced levels of corticosterone to lower *Crh* expression (57).

Social Isolation Altered the HPT Response to Voluntary Exercise in a Sex-Dependent Manner

Two important regions that regulate HPT axis activity reside in mediobasal hypothalamus (MBH), the arcuate nucleus and the median eminence. In the arcuate nucleus, neuronal populations that express anorexigenic (POMC/CART) and orexigenic (NPY/AgRP) peptides stimulate or inhibit *Trh* expression in PVN, respectively (10). Tanycytes in median eminence inhibit TRH expression through deiodinase 2 activity increasing T3 levels in the hypothalamus, and the activity of TRH-degrading enzyme controls TSH secretion (58). In the MBH, the expression of arcuate peptides varied due to rearing condition or exercise. *Pomc* expression increased in C-Ex males compared with C-Sed and Iso-Ex, and *Npy* expression decreased in Iso (**Figure 3A**). The pattern of *Pomc* expression was similar in female MBH, however *Npy* mRNA levels were higher in Iso than C groups (**Figure 3B**). *Dio2* expression was higher in C-Ex than C-sed in males but *Trhde* was not modified (**Figure 3A**). In females, *Dio2* was higher in C than in Iso; *Trhde* increased by exercise in C and slightly in Iso (**Figure 3B**).

HPT axis was not stimulated by exercise in C-males. In contrast, isolated males had diminished TSH serum concentration after exercise; that of T4 augmented but in both Iso groups compared to their controls (**Figure 3C**). Negative correlation was observed between T4 and WAT retroperitoneal mass in C-Ex group ($r = -0.856$; $P = 0.030$) whereas positive, in Iso-Ex ($r = 0.879$; $P = 0.009$). In females, *Trh* mRNA levels were lower in C-Ex than in C-Sed, TSH serum concentration increased by exercise in C, and T4 decreased compared to Iso-sed, while T3 concentration increase in both exercised groups (**Figure 3D**). T4:T3 ratio was higher in Iso than C, and was higher in females than males (**Supplementary Table 5**).

Brown adipose tissue (BAT) is a target of thyroid hormones that in concert with the adrenergic system is responsible for

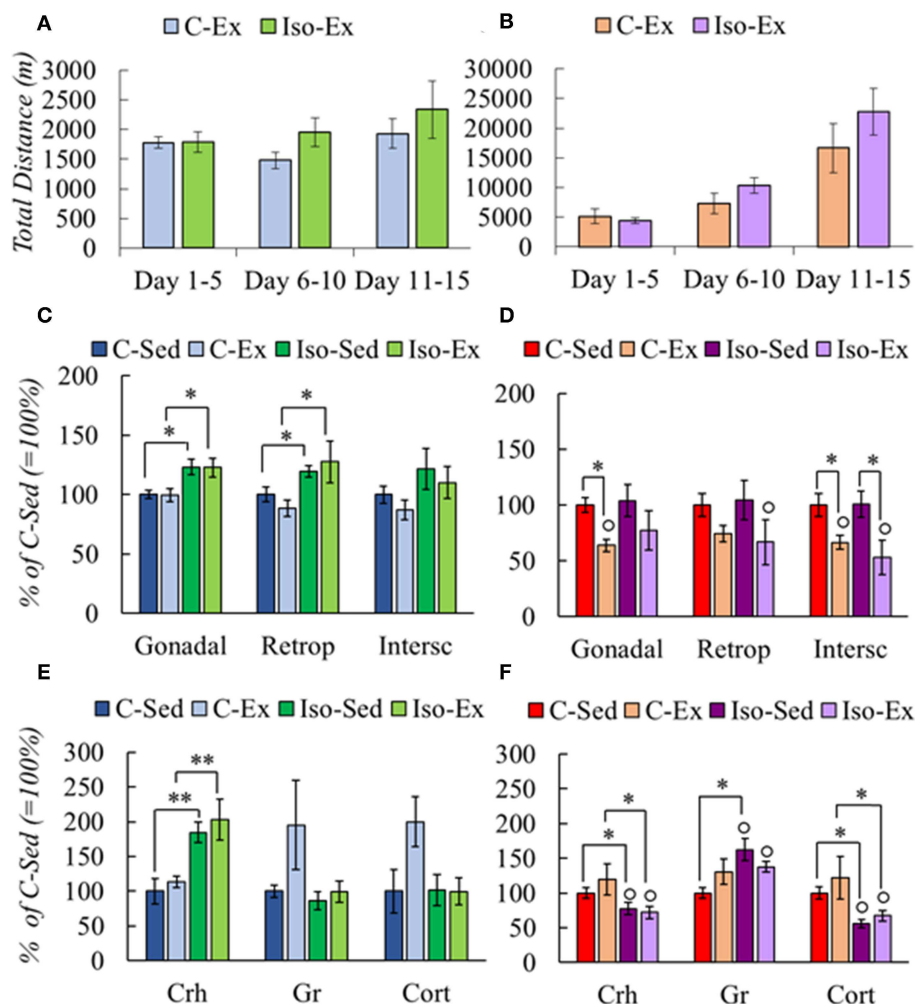


FIGURE 2 | Effect of social isolation on physical activity (A,B), fat mass (C,D), and HPA axis response (E,F) of male and female rats. Rearing and exercise conditions described in tables 3 and 4, respectively. Significant ANOVAs (Supplementary Table 2B) followed by *post-hoc*: * $P < 0.05$; ** $P < 0.001$; ° $P < 0.05$ vs. Males of the same group.

thermogenesis, activity that contributes to energy expenditure (19, 59). Noradrenergic signaling stimulates *Dio2* expression, rising T3 concentration in the tissue (60) and, in turn, stimulates the transcription of β -adrenergic receptors (β -AR) and UCP-1 (2, 61). We thus measured the expression of these molecules; mRNA levels of *Adrb3* or *Ucp1* were lower in Iso groups of males than C but increased in both by exercise, those of *Dio2* were not changed (Figure 3E). Females showed no changes in *Adrb3* expression, decreased that of *Ucp1* in Iso-Sed compared to C-Sed while increased, as *Dio2*, in Iso-Ex (Figure 3F).

DISCUSSION

Life of laboratory rodents, in controlled environments, is very distant from that in natural conditions. Experimental rats have little stimuli and space for physical activity, and usually become obese (62). Although distinct from training exercise, voluntary running for short bouts provides many benefits for animals'

health (63), and allows comparing the physiology of a sedentary animal with an active one. In just 2 weeks of daily running during their active phase, male rats lose WAT mass proportionally to their physical activity and to the levels of serum thyroid hormones or PVN *Trh* expression (19). Stress inhibits the response of the HPT axis to the short-term energy needs of an acute exposure to cold [(32, 34) and unpublished], but its effect on long-term energy demands was not known. We considered voluntary running a suitable model of energy demand, to study the effects of two types of chronic stress on the responses of the HPT axis to exercise in both male and female rats, given the sex dimorphism in metabolic and stress responses. A short time of exercise was selected to avoid allostatic adjustments that could make it difficult to validate results with previously reported results (19).

The chronic stressors chosen were intermittent restraint at adulthood, and isolation from puberty to adulthood. Restraint is a well-studied model of psychological homotypic stress that

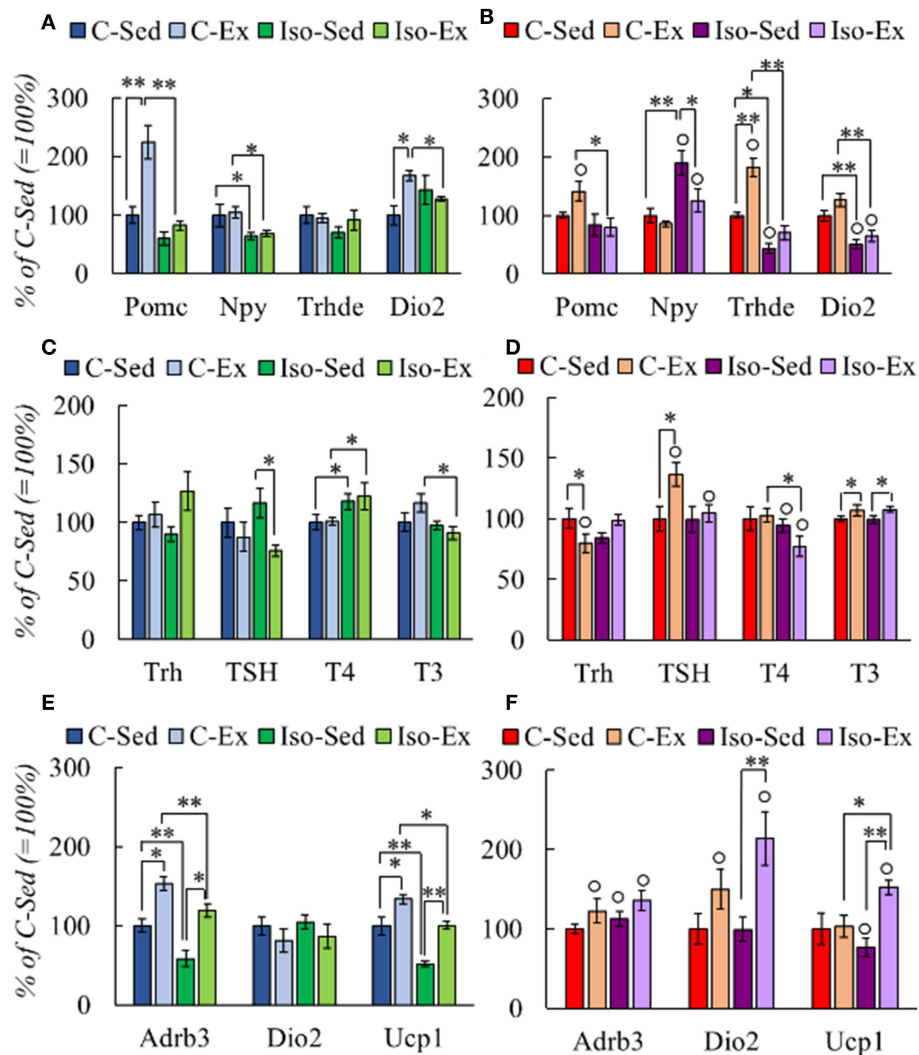
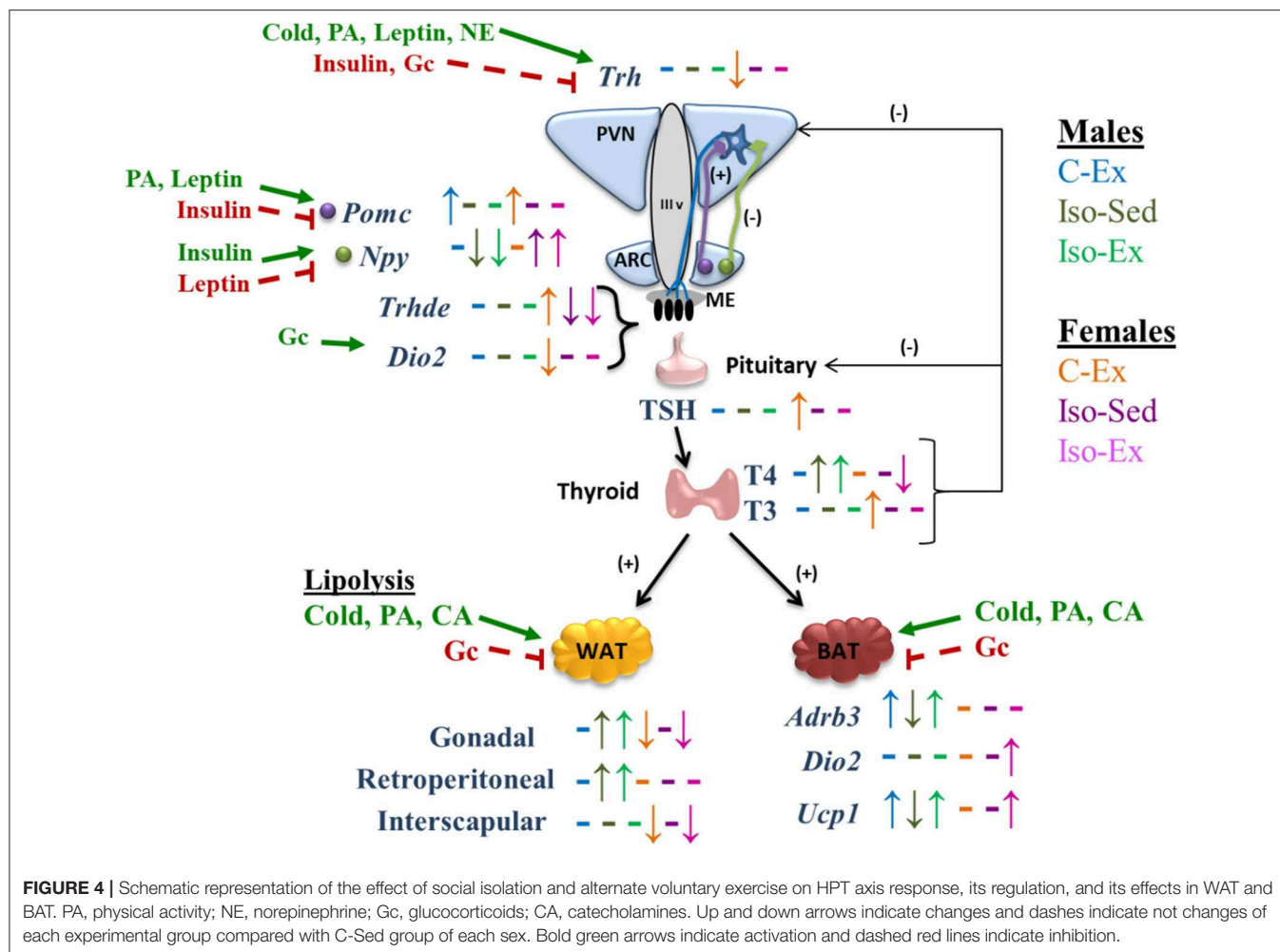


FIGURE 3 | Effect of social isolation and alternate exercise on the expression of HPT status-related genes (A,B), HPT axis response (C,D), and genes that respond to thyroid hormones in BAT (E,F) of male and female rats. Rearing and exercise conditions described in tables 3 and 4, respectively. Results are expressed in percent of mean values of C-Sed. Significant ANOVAs (Supplementary Table 2B) followed by *post-hoc*: * $P < 0.05$; ** $P < 0.001$; * $P < 0.05$ vs. Males of the same group.

causes habituation (35) as well as neurological changes that cause a hyper-reactive response to a new stressor, persistence of oxidative stress, modifications in immune responses, to name a few (64). In contrast, social isolation is a model of psychosocial stress that alters glucocorticoid feedback through changes in neurochemical functions of limbic and cortical systems, affecting the maturation of some of these circuits leading to long lasting alterations that induce depression and anxiety in adult rodents (38, 65, 66); isolation during adolescence produces HPA axis malfunction at adult stage, decreasing basal levels of serum corticosterone and producing a hyper-reactive response to acute stress (67–69). Voluntary exercise attenuates various deleterious effects produced by stress, and although it may cause increases in serum corticosterone concentration it is not considered a strong stressor, in contrast to forced training or exhaustive exercise (70, 71). The exercise paradigm utilized was not considered as a new

stressor since variables of HPA axis were not different in exercised to those of sedentary rats. In our experiments, both types of stress affected feeding and exercise task; Res males exercised less and ate more, whereas Iso animals, especially females, increased food intake and body weight gain, suggesting stress-induced imbalances in eating behavior. Decreased fat mass was expected in exercised rats (19, 72, 73), and was detected in adult males and females that exercised every night (experiment 1). However, animals that exercised alternately (experiment 2) did not reduce food intake as did those running every night (this experiment, and 19). In males, lipolysis induced by daily exercise appeared to reduce hunger; signals required for this and for losing WAT mass might not be enough if exercise is not done daily. Conversely, female controls of both experiments did lose WAT mass in response to voluntary exercise but also ran considerably more than males, as is generally recognized in rodents (74, 75).



They lost subcutaneous WAT (interscapular) and only one of the abdominal types (gonadal or retroperitoneal) of WAT depending on the experiment. Previous Res-stress reduced the amount of exercise performed only in males that showed no WAT mass loss; less exercise may account for the lack of fat mass lost however, stressed females that ran the same amount as controls did not lose WAT mass either, despite not differing in food intake. In isolated females, exercise induced similar tendencies in WAT mass reduction, which was significant only in subcutaneous type. These results point for a negative effect of chronic stress on the adequate WAT-metabolic response to exercise.

Voluntary and forced exercise increase basal corticosterone serum concentration (47, 69, 76) without affecting the expression of *Crh* and *Gr* in PVN (77, 78). Adult control animals of both experiments showed no exercise-induced variations in any of the HPA axis parameters, and neither those that had been previously restrained. Isolation induced HPA malfunction differently in males and females; males had increased PVN *Crh* expression but no changes in serum corticosterone concentration, whereas females had decreased serum corticosterone concentration and *Crh* mRNA levels, suggesting hypoactivity of the axis (79). These findings agree with a higher susceptibility of females to stress

(80), isolation (81) and depression (82, 83), the latter usually coincident with hypoactivity of HPA (79); this might be due to the effect of stress at adolescent stage (84), and exercise could reverse the deleterious effects of stress (53, 71).

Exercise promotes the expression of *Pomc* in arcuate nucleus (ARC) (85), in agreement with what we found in C male and female rats, albeit it was not according to the amount of exercise performed, as Iso males ran similar distances and their response was blunted. Isolation and not wheel running increased ARC *Npy* expression in females, coincident with higher food intake and some reports (86, 87).

The HPT axis is subject to multiple metabolic, hormonal and neuronal effectors that regulate its activity at multiple levels (8, 11, 56). Elements of the HPT axis showed a sex-dimorphic regulation (Figure 4). Change-dynamics of HPT axis parameters depend on the type of stimulus; PVN *Trh* expression changes can be rapid and transient (17, 18), half-lives of serum TSH and T3 are short (min to h) compared to that of serum T4 (8). Furthermore, since the activity of tissue deiodinases is also regulated, circulating thyroid hormones (TH) concentrations are difficult to interpret (12), making it necessary to evaluate as many variables as possible, if only one time point is studied.

Exercise increased *Dio2* expression in median eminence (ME) in C males, possibly because of increased serum corticosterone concentration (88). If *DIO2* activity was indeed increased, it should have augmented local T3 concentration which in turn, would be expected to stimulate ME *Trhde* expression (58) or inhibit PVN *Trh* expression (10), albeit with unknown dynamics. None of these changes were found in males; since animals were sacrificed 3 h after switching to a wheel-free cage, and time since the last exercise boot was not recorded, it is possible that the time-point was inadequate. However, exercise did increase ME *Trhde* expression in C females, with only a slight non-significant tendency for *Dio2* expression, and diminished PVN *Trh* expression. In females, isolation decreased ME *Dio2* and *Trhde* expression, coincident only with decreased corticosterone serum concentration, which stimulates *Dio2* expression (88); parallel changes in *Dio2* and *Trhde* reflect the dependence of *DIO2* activity to set the levels of T3 in tanycytes, which activate *Trhde* expression (58). However, despite increased *Trhde* expression in ME, TSH serum concentration was increased, most probably by an exercise-induced effect that could either increase TRH release in spite of not finding a higher expression or, increased TSH release due to higher expression of TRH-R1 or in response to events distinct from TRH.

Thyroid hormones regulate the activity of adipose tissue genes which constitute additional markers of HPT axis activity. BAT can promote energy expenditure through facultative thermogenesis induced by sympathetic nervous system activity (89). The impact of exercise on BAT is still not well-understood (90) since *Adrb3* and *Ucp1* regulation in BAT by exercise depends on species and training time; in mice, treadmill training increases *Ucp1* expression but *Adrb3* expression does not change (91), while in rat *Ucp1* and *Adrb3* mRNA levels do not change after one session of treadmill exercise (92), in contrast to an increase during progressive treadmill (93). The increase in the expression of *Adrb3* and *Ucp1* in Iso-Ex males, and of *Dio2* and *Ucp1* in Iso-Ex females, suggests that voluntary exercise promotes the effect of thyroid hormones on BAT, promoting energy expenditure as heat instead of muscle work, and being able to revert the effects of social isolation.

To conclude, present results demonstrate that a history of chronic stress curtails the adequate metabolic response to voluntary exercise characterized by loss of WAT depots, in male and female rats. Females ran much more than males, which allowed them to lose fat independent of schedule (daily or alternate days). Restraint stress reduced exercise in males, either due to fatigue or lack of motivation. Some changes in the HPT

axis (PVN *Trh* expression or serum concentrations of TSH or TH) were related to WAT loss, but only in controls and not in stressed groups. We propose that in control animals the HPT axis is activated transiently at each exercise boot contributing to lipolysis, event inhibited by previous chronic stress, leading to problems with fuel availability.

DATA AVAILABILITY

The raw data generated are available on request to corresponding author.

ETHICS STATEMENT

The experiments were approved by the Bioethics Committee of the Institute, approval No. 273 and 318.

AUTHOR CONTRIBUTIONS

MP-M, MG-M, and MS-J performed the experiments. MP-M, LJ-H, and PJ-B analyzed the data. MP-M and PJ-B wrote the manuscript draft. LJ-H and J-LC helped with manuscript edition. MP-M is a doctorate student and main contributor. PJ-B is principal investigator of grant and project director. J-LC and PJ-B are co-directors of the Neuroendocrinology group.

FUNDING

This work was supported by DGAPA IN204316 (PJ-B) and IA200417 (LJ-H); CONACYT 0284883 (PJ-B). MP-M is recipient of CONACYT 273496 post-graduate scholarship.

ACKNOWLEDGMENTS

Authors express their gratitude to technicians QFB, Miguel Cisneros and Q. Fidelia Romero for their aid in experimental work, and to Roberto Rodríguez Bahena, Shirley Ainsworth, David Santiago Castañeda, and Eugenio López Bustos for providing reagents and computer assistance.

SUPPLEMENTARY MATERIAL

The Supplementary Material for this article can be found online at: <https://www.frontiersin.org/articles/10.3389/fendo.2019.00418/full#supplementary-material>

REFERENCES

- McAninch EA, Bianco A. Thyroid hormone signaling in energy homeostasis and energy metabolism. *Ann N Y Acad Sci.* (2014) 1311:77–87. doi: 10.1111/nyas.12374
- Mullur R, Liu Y-Y, Brent GA. Thyroid hormone regulation of metabolism. *Physiol Rev.* (2014) 94:355–82. doi: 10.1152/physrev.00030.2013
- Gonçalves A, Resende ES, Fernandes MLMP, da Costa AM. Effect of thyroid hormones on cardiovascular and muscle systems on exercise tolerance: a brief review. *Arq Bras Cardiol.* (2006) 86:e42–4. doi: 10.1590/s0066-782x2006001600033
- Louwerens M, Appelhof BC, Verloop H, Medici M, Peeters RP, Visser TJ, et al. Fatigue and fatigue-related symptoms in patients treated for different causes of hypothyroidism. *Eur J Endocrinol.* (2012) 167:809–15. doi: 10.1530/EJE-12-0501
- Lankhaar JAC, de Vries WR, Jansen JACG, Zelissen PMJ, Backx FJG. Impact of overt and subclinical hypothyroidism on exercise tolerance: a systematic review. *Res Q Exer Sport.* (2014) 85:365–89. doi: 10.1080/02701367.2014.930405

6. Tanriverdi A, Ozcan Kahraman B, Ozsoy I, Bayraktar F, Ozgen Saydam B, Acar S, et al. Physical activity in women with subclinical hypothyroidism. *J Endocrinol Invest.* (2018) 1–7. doi: 10.1007/s40618-018-0981-2
7. Mendoza A, Hollenberg AN. New insight into thyroid hormone action. *Pharmacol Ther.* (2017) 173:135–45. doi: 10.1016/j.pharmthera.2017.02.012
8. Chatzitomaris A, Hoermann R, Midgley JE, Hering S, Urban A, Dietrich B, et al. Thyroid allostasis-adaptative responses of thyrotropic feedback control to conditions of strain, stress, and developmental programming. *Front Endocrinol.* (2017) 8:1–28. doi: 10.3389/fendo.2017.00163
9. Visser WE, Friesema EC, Visser TJ. Minireview: thyroid hormone transporters: the knowns and the unknowns. *Mol Endocrinol.* (2011) 25:1–14. doi: 10.1210/me.2010-0095
10. Fekete C, Lechan RM. Central regulation of hypothalamic-pituitary-thyroid axis under physiological and pathophysiological conditions. *Endocr Rev.* (2014) 35:159–94. doi: 10.1210/er.2013-1087
11. Joseph-Bravo P, Jaimes-Hoy L, Charli J-L. Advances in TRH signaling. *Rev Endocr Metab Disord.* (2016) 17:545–58. doi: 10.1007/s11154-016-9375-y
12. Bianco AC, Kim BW. Deiodinases: implications of the local control of thyroid hormone action. *J Clin Invest.* (2006) 116:2571–9. doi: 10.1172/JCI29812
13. Gereben B, Zavacki AM, Ribich S, Kim BW, Huang SA, Simonides WS, et al. Cellular and molecular basis of deiodinase-regulated thyroid hormone signaling. *Endocr Rev.* (2008) 29:898–938. doi: 10.1210/er.2008-0019
14. Dyess EM, Segerson TP, Liposits Z, Paull WK, Kaplan MM, Wu P, et al. Triiodothyronine exerts direct cell-specific regulation of thyrotropin-releasing hormone gene expression in the hypothalamic paraventricular nucleus. *Endocrinology.* (1988) 123:2291–7. doi: 10.1210/endo-123-5-2291
15. Chiamolera MI, Wondisford FE. Thyrotropin-releasing hormone and the thyroid hormone feedback mechanism. *Endocrinology.* (2009) 150:1091–6. doi: 10.1210/en.2008-1795
16. Fliers E, Kalsbeek A, Boelen A. Mechanisms in endocrinology: beyond the fixed setpoint of the hypothalamus–pituitary–thyroid axis. *Eur J Endocrinol.* (2014) 171: R197–208. doi: 10.1530/EJE-14-0285
17. Zoeller RT, Kabber N, Albers E. Cold exposure elevates cellular levels of messenger ribonucleic acid encoding thyrotropin-releasing hormone in paraventricular nucleus despite elevated levels of thyroid hormones. *Endocrinology.* (1990) 127:2955–62. doi: 10.1210/endo-127-6-2955
18. Uribe RM, Redondo JL, Charli JL, Joseph-Bravo P. Suckling and cold stress rapidly and transiently increase TRH mRNA in the paraventricular nucleus. *Neuroendocrinology.* (1993) 58:140–45. doi: 10.1159/000126523
19. Uribe RM, Jaimes-Hoy L, Ramírez-Martínez C, García-Vázquez A, Romero F, Cisneros M, et al. Voluntary exercise adapts the hypothalamus-pituitary-thyroid axis in male rats. *Endocrinology.* (2014) 155:2020–30. doi: 10.1210/en.2013-1724
20. Arkader R, Rosa MR, Moretti G. Physiological changes of exercise of thermogenesis, thyroid homeostasis and inflammation. *Endocrinol Metab Int J.* (2016) 3:85–8. doi: 10.15406/emij.2016.03.00055
21. Fortunato RS, Ignácio DL, Padron AS, Peçanha R, Marassi M P, Rosenthal D, et al. The effect of acute exercise session on thyroid hormone economy in rats. *J Endocr.* (2008) 198:347–53. doi: 10.1677/JOE-08-0174
22. Hackney AC, Dodbridge JD. Thyroid hormone and the interrelationship of cortisol and prolactin: influence of prolonged, exhaustive exercise. *Pol J Endocrinol.* (2009) 60:252–7.
23. Leal LG, Lopes MA, Batista ML Jr. Physical exercise-induced myokines and muscle-adipose tissue crosstalk: a review of current knowledge and the implications for health and metabolic diseases. *Front Physiol.* (2018) 9:1–17. doi: 10.3389/fphys.2018.01307
24. Afonso VM, Eikelboom R. Relationship between wheel running, feeding, drinking, and body weight in male rats. *Physiol Behav.* (2003) 80:19–26. doi: 10.1016/S0031-9384(03)00216-6
25. Basso JC, Morrell JI. Using wheel availability to shape running behavior of the rats towards improved behavioral and neurobiological outcomes. *J Neurosci Methods.* (2017) 290:13–23. doi: 10.1016/j.jneumeth.2017.07.009
26. Joseph-Bravo P, Jaimes-Hoy L, Uribe RM, Charli JL. TRH, the first hypophysiotropic releasing hormone isolated: control of the pituitary-thyroid axis. *J Endocrinol.* (2015) 226:T85–100. doi: 10.1530/JOE-15-0124
27. Olivares EL, Silva-Almeida C, Pestana FM, Sonoda-Cortes R, Araujo IG, Rodrigue NC, et al. Social stress-induced hypothyroidism is attenuated by antidepressant treatment in rats. *Neuropharmacology.* (2012) 62:446–56. doi: 10.1016/j.neuropharm.2011.08.035
28. Joseph-Bravo P, Jaimes-Hoy L, Charli JL. Regulation of TRH neurons and energy homeostasis-related signals under stress. *J Endocrinol.* (2015) 224:R139–59. doi: 10.1530/JOE-14-0593
29. Moog NK, Entringer S, Heim C, Wadhwa PD, Kathmann N, Buss C. Influence of maternal thyroid hormones during gestation on fetal brain development. *Neuroscience.* (2017) 342:68–100. doi: 10.1016/j.neuroscience.2015.09.070
30. Bianco AC, Nunes MT, Hell NS, Maciel RMB. The role of glucocorticoids in the stress-induced reduction of extrathyroidal 3,5,3'-triiodothyronine generation in rats. *Endocrinology.* (1987) 120:1033–8. doi: 10.1210/endo-120-3-1033
31. Kakucska I, Qi Y, Lechan RM. Changes in adrenal status affect hypothalamic thyrotropin-releasing hormone gene expression in parallel with corticotropin-releasing hormone. *Endocrinology.* (1995) 136:2795–802. doi: 10.1210/endo.136.7.7789304
32. Sotelo-Rivera I, Jaimes-Hoy L, Cote-Vélez A, Espinoza-Ayala C, Charli J-L, Joseph-Bravo P. An acute injection of corticosterone increases thyrotropin-releasing hormone in paraventricular nucleus of the hypothalamus but interferes with the rapid hypothalamus pituitary thyroid axis response to cold in male rats. *J Endocr.* (2014) 26:882–90. doi: 10.1111/jne.12224
33. Díaz-Gallardo MY, Cote-Vélez A, Charli JL, Joseph-Bravo P. A rapid interference between glucocorticoids and cAMP-activated signaling in hypothalamic neurons prevents binding of phosphorylated cAMP response element binding protein and glucocorticoid receptor at the CRE-like and composite GRE sites of thyrotropin-releasing hormone gene promoter. *J Neuroendocrinol.* (2010) 22:282–93. doi: 10.1111/j.1365-2826.2010.01966.x
34. Sotelo-Rivera I, Cote-Vélez A, Uribe RM, Charli JL, Joseph-Bravo P. Glucocorticoids curtail stimuli-induced CREB phosphorylation in TRH neurons through interaction of the glucocorticoid receptor with the catalytic subunit of protein kinase A. *Endocrine.* (2017) 55:861–71. doi: 10.1007/s12020-016-1223-z
35. Bhatnagar S, Dallman M. Neuroanatomical basis for facilitation of hypothalamic-pituitary-adrenal responses to a novel stressor after chronic stress. *Neuroscience.* (1998) 84:1025–39. doi: 10.1016/S0306-4522(97)00577-0
36. Herman JP, Tasker JG. Paraventricular hypothalamic mechanism of chronic stress adaptation. *Front Endocrinol.* (2014) 7:1–10. doi: 10.3389/fendo.2016.00137
37. Gutiérrez-Mariscal M, Sánchez E, García-Vázquez A, Rebolledo-Solleiro D, Charli JL, Joseph-Bravo P. Acute response of hypophysiotropic thyrotropin releasing hormone neurons and thyrotropin release to behavioral paradigms producing varying intensities of stress and physical activity. *Regul Pept.* (2012) 179:61–70. doi: 10.1016/j.regpep.2012.08.010
38. Filipović D, Todorovic N, Bernardi RE, Gass P. Oxidative and nitrosative stress pathways in the brain of socially isolated adult male rats demonstrating depressive- and anxiety-like symptoms. *Brain Struct Funct.* (2017) 222:1–20. doi: 10.1007/s00429-016-1218-9
39. Romeo RD, Patel R, Pham L, So VM. Adolescence and the ontogeny of the hormonal stress response in male and female rats and mice. *Neurosci Biobehav Rev.* (2016) 70:206–16. doi: 10.1016/j.neubiorev.2016.05.020
40. Burke AR, McCormick CM, Pellis SM, Lukkes JL. Impact of adolescent social experiences on behavior and neural circuits implicated in mental illnesses. *Neurosci Biobehav Rev.* (2017) 76:280–300. doi: 10.1016/j.neubiorev.2017.01.018
41. Ciloglu F, Peker I, Pehlivan A, Karacabey K, Ilan N, Saygin O, et al. Exercise intensity and its effects on thyroid hormones. *Neuroendocrinol Lett.* (2005) 26:830–4.
42. McCormick CM, Green MR, Simone JJ. Translational relevance of rodents models of hypothalamic-pituitary-adrenal function and stressors in adolescence. *Neurobiol Stress.* (2017) 6:31–43. doi: 10.1016/j.jynstr.2016.08.003
43. Radley JJ, Sawchenko PE. Evidence of involvement of a limbic paraventricular hypothalamic inhibitory network in hypothalamic-pituitary-adrenal axis adaptations to repeated stress. *J Comp Neurol.* (2015) 523:2769–87. doi: 10.1002/cne.23815
44. Jaimes-Hoy L, Gutiérrez-Mariscal M, Vargas Y, Pérez-Maldonado A, Romero F, Sánchez-Jaramillo E, et al. Neonatal maternal separation alters, in a sex-specific manner, the expression of TRH, TRH-degrading ectoenzyme in

- the rat hypothalamus, and the response of the thyroid axis to starvation. *Endocrinology*. (2016) 157:3253–5. doi: 10.1210/en.2016-1239
45. Fone KCF, Porkess MV. Behavioral and neurochemical effects of post-weaning social isolation in rodents-Relevance to developmental neuropsychiatric disorders. *Neurosci Behav Rev.* (2008) 32:1087–102. doi: 10.1016/j.neubiorev.2008.03.003
 46. Bianco AC, Anderson G, Forrest D, Galton VA, Gereben V, Kim BW, et al. American thyroid association guide to investigating thyroid hormone economy and action in rodent and cell models. *Thyroid*. (2014) 24:88–168. doi: 10.1089/thy.2013.0109
 47. Chomzynsky P, Sacchi N. Single-step method of RNA isolation by acid guanidinium thiocyanate-phenol-chloroform extraction. *Anal Biochem.* (1987) 162:156–9. doi: 10.1006/abio.1987.9999
 48. Horowitz JF. Fatty acid mobilization from adipose tissue during exercise. *Trends Endocrinol Metab.* (2003) 14:386–92. doi: 10.1016/S1043-2760(03)00143-7
 49. Stranahan AM, Khalil D, Gould E. Social isolation delays the positive effects of running on adult neurogenesis. *Nat Neurosci.* (2006) 9:526–33. doi: 10.1038/nn1668
 50. Ulrich-Lai YM, Figueiredo HF, Ostrander MM, Choi DC, Engelan WC, Herman JP. Chronic stress induced adrenal hyperplasia and hypertrophy in a subregion-specific manner. *Am J Physiol Endocr Metab.* (2006) 291:E965–73. doi: 10.1152/ajpendo.00070.2006
 51. Lukkes JD, Watt MJ, Lowry CA, Forster GL. Consequences of post-weaning social isolation on anxiety behavior and related neural circuits in rodents. *Front Behav Neurosci.* (2009) 3:1–12. doi: 10.3389/neuro.08.018.2009
 52. Arakawa H. Ethological approach to social isolation effects in behavioral studies of laboratory rodents. *Behav Brain Res.* (2018) 341:98–108. doi: 10.1016/j.bbr.2017.12.022
 53. Leasure JL, Decker L. Social isolation prevents exercise-induced proliferation of hippocampal progenitor cells in female rats. *Hippocampus.* (2009) 19:907–12. doi: 10.1002/hipo.20563
 54. Krolow R, Noschang C, Arcego DM, Huffell AP, Marcolin ML, Benitz AN, et al. Sex-specific effects of isolation stress and consumption of palatable diet during the prepubertal period on metabolic parameters. *Metabolism.* (2013) 62:1268–78. doi: 10.1016/j.metabol.2013.04.009
 55. Arcego DM, Krolow R, Lampert C, Noschang C, Ferreira AGK, Scherer E, et al. Isolation during the pubertal period associated with chronic access to palatable diets: effects on plasma lipids profile and liver oxidative stress. *Physiol Behav.* (2014) 124:23–32. doi: 10.1016/j.physbeh.2013.10.029
 56. Soch A, Bradburn S, Sominsky L, De Luca SN, Murgatroyd C, Spencer SJ. Effects of exercise on adolescent and adult hypothalamic and hippocampal neuroinflammation. *Hippocampus.* (2016) 26:1435–46. doi: 10.1002/hipo.22620
 57. Jeanneteau FD, Lambert WM, Ismaili N, Bath KG, Lee FS, Garabedian MJ, et al. BDNF and glucocorticoids regulate corticotrophin releasing hormone (CRH) homeostasis in the hypothalamus. *Proc Natl Acad Sci USA.* (2012) 109:1305–10. doi: 10.1073/pnas.1114122109
 58. Sánchez E, Vargas MA, Singru PF, Pascual I, Romero F, Fekete C, et al. Tanycyte pyroglutamate II contributes to regulation of the hypothalamic-pituitary-thyroid axis through glial-axonal associations in the median eminence. *Endocrinology.* (2009) 150:2283–91. doi: 10.1210/en.2008-1643
 59. Sánchez-Delgado G, Martínez-Téllez B, Olza J, Aguilera CM, Gil A, Ruiz JR. Role of exercise in the activation of brown adipose tissue. *Ann Nutr Metab.* (2015) 67:21–32. doi: 10.1159/000437173
 60. Arrojo e Drigo R, Fonseca TL, Werneck-de-Castro JPS, Bianco AC. Role of the type 2 iodothyronine deiodinase (D2) in the control of thyroid hormone signaling. *Biochim Biophys Acta Gen Subj.* (2013) 1083:3956–64. doi: 10.1016/j.bbagen.2012.08.019
 61. Rubio A, Raasmaja A, Silv JE. Thyroid hormone and norepinephrine signaling in Brown adipose tissue. II. Differential effects of thyroid hormone on beta 3-adrenergic receptors in brown and white adipose tissue. *Endocrinology.* (1995) 136:3277–84. doi: 10.1210/en.136.8.3277
 62. Martin B, Ji S, Maudsley S, Mattson MP. “Control” laboratory rodents are metabolically morbid: why it matters. *Proc Natl Acad Sci USA.* (2010) 107:6127–33. doi: 10.1073/pnas.0912955107
 63. Novak CM, Burghardt PR, Levine JA. The use of a running wheel to measure activity in rodents: relationship to energy balance, general activity, and reward. *Neurosci Biobehav Rev.* (2012) 36:1001–14. doi: 10.1016/j.neubiorev.2011.12.012
 64. Buynitsky T, Mostofsky DI. Restrain stress in behavioral research: recent developments. *Neurosci Behav Rev.* (2009) 33:1089–98. doi: 10.1016/j.neubiorev.2009.05.004
 65. Cacioppo JT, Cacioppo S, Capotanio JP, Cole SW. The neuroendocrinology of social isolation. *Annu Rev Psychol.* (2015) 66:733–67. doi: 10.1146/annurev-psych-010814-015240
 66. Mumtaz F, Khan MI, Zubair M, Dehpour AR. Neurobiology and consequences of social isolation stress in animal model-A comprehensive review. *Biomed Pharmacother.* (2018) 105:1205–22. doi: 10.1016/j.biopha.2018.05.086
 67. Biggio F, Pisu MG, Garau A, Boero G, Locci V, Mostallino MC, et al. Maternal separation attenuates the effect of adolescent social isolation on HPA axis responsiveness in adult rats. *Eur Neuropsychopharm.* (2014) 24:1152–61. doi: 10.1016/j.euroneuro.2014.03.009
 68. Butler TR, Ariwodola OJ, Weiner JL. The impact of social isolation on HPA axis function, anxiety-like behavior, and ethanol drinking. *Front Interg Neurosci.* (2014) 7:102. doi: 10.3389/fnint.2013.00102
 69. Pisu MG, Garau A, Boero G, Biggio F, Pibiri V, Dore R, et al. Sex differences in the outcome of juvenile social isolation on HPA axis function in rats. *Neuroscience.* (2016) 320:172–82. doi: 10.1016/j.neuroscience.2016.02.009
 70. Stranahan AM, Lee K, Mattson MP. Central mechanisms of HPA axis regulation by voluntary exercise. *Neuromolecular Med.* (2008) 10:118–27. doi: 10.1007/s12017-008-8027-0
 71. Chen C, Nakagawa S, An Y, Ito K, Kitaichi Y, Kusumi I. The exercise-glucocorticoid paradox: how exercise is beneficial to cognition, mood, and the brain while increasing glucocorticoid levels. *Front Neuroendocrinol.* (2017) 44:83–102. doi: 10.1016/j.yfrne.2016.12.001
 72. Gollisch KSC, Brandauer J, Jessen N, Toyoda T, Nayer A, Hirshman MF, et al. Effects of exercise training on subcutaneous and visceral adipose tissue in normal- and high-fat diet-fed rats. *Am J Physiol Endocrinol Metab.* (2009) 297:E495–504. doi: 10.1152/ajpendo.90424.2008
 73. Stanford KI, Goodyear LJ. Exercise regulation of adipose tissue. *Adipocyte.* (2016) 5:153–62. doi: 10.1080/21623945.2016.1191307
 74. Blizard DA. Sex differences in running-wheel behaviour in the rat: the inductive and activational effects of gonadal hormones. *Anim Behav.* (1983) 31:378–84. doi: 10.1016/S0003-3472(83)80056-6
 75. Jones LC, Bellingham WP, Ward LC. Sex differences in voluntary locomotor activity of food-restricted and *ad libitum*-fed rats. Implications for the maintenance of a body weight set-point. *Comp Biochem Physiol A Comp Physiol.* (1990) 96:287–90. doi: 10.1016/0300-9629(90)90694-N
 76. Brannan KW, DeVallance ER, Lemaster KA, Skinner RC, Bryner RW, Olfert IM, et al. Role of chronic stress and exercise on microvascular function in metabolic syndrome. *Med Sci Sports.* (2018) 50:957–66. doi: 10.1249/MSS.0000000000001531
 77. Kawashima H, Saito T, Yoshizato H, Fujikawa T, Sato Y, McEwen BS, et al. Endurance treadmill training in rats alters CRH activity in the hypothalamic paraventricular nucleus at rest and during acute running according to its period. *Life Sci.* (2004) 76:763–74. doi: 10.1016/j.lfs.2004.09.014
 78. Droste SK, Chandromohan Y, Hill LE, Linthorst ACE, Reul JMHM. Voluntary exercise impacts on the rat hypothalamic-pituitary-adrenocortical axis mainly at the adrenal level. *Neuroendocrinology.* (2007) 86:26–37. doi: 10.1159/000104770
 79. Ostrander MM, Ulrich-Lai YM, Choi DC, Richtand NM, Herman JP. Hypoactivity of the hypothalamo-pituitary-adrenocortical axis during recovery from chronic variable stress. *Endocrinology.* (2006) 147:2008–17. doi: 10.1210/en.2005-1041
 80. Heck AL, Handa RJ. Sex differences in the hypothalamic-pituitary-adrenal axis’ response to stress: an important role for gonadal hormones. *Neuropsychopharmacology.* (2019) 44:45–58. doi: 10.1038/s41386-018-0167-9
 81. Beery AK, Kaufer D. Stress, social behavior and resilience: insights for rodents. *Neurobiol Stress.* (2015) 1:116–27. doi: 10.1016/j.ynstr.2014.10.004
 82. Weintraub A, Singaravelu J, Bhatnagar S. Enduring and sex-specific effects of adolescent social isolation in rats on adult stress reactivity. *Brain Res.* (2010) 1343:83–92. doi: 10.1016/j.brainres.2010.04.068

83. Janhg JW, Yoo SB, Ryu V, Lee J-H. Hyperphagia and depression-like behavior by adolescence social isolation in female rats. *Int J Dev Neurosci.* (2012) 30:47–53. doi: 10.1016/j.ijdevneu.2011.10.001
84. Bale TL, Epperson CN. Sex differences and stress across the lifespan. *Nat Neurosci.* (2015) 18:1413–20. doi: 10.1038/nn.4112
85. Jiaxu C, Weiyl Y. Influence of acute and chronic treadmill exercise on rat brain POMC gene expression. *Med Sci Sport Exerc.* (2000) 32:954–7. doi: 10.1097/00005768-200005000-00012
86. Bi S, Scott KA, Hyun J, Ladenheim EE, Moran TH. Running wheel activity prevents hyperphagia and obesity in Otsuka Long-Evans Tokushima Fatty rats: role of hypothalamic signaling. *Endocrinology.* (2005) 146:1676–85. doi: 10.1210/en.2004-1441
87. Chen J-X, Zhao X, Yue G-X, Wang Z-F. Influence of acute and chronic treadmill exercise on rat plasma lactate and brain NPY, L-ENK, DYN A1-13. *Cell Mol Neurobiol.* (2007) 27:1–10. doi: 10.1007/s10571-006-9110-4
88. Coppola A, Meli R, Diano S. Inverse shift in circulating corticosterone and leptin levels elevates hypothalamic deiodinase type 2 in fasted rats. *Endocrinology.* (2005) 146:2827–33. doi: 10.1210/en.2004-1361
89. Morrison SF, Madden CJ, Tupone D. Central neural regulation of brown adipose tissue thermogenesis and energy expenditure. *Cell Metab.* (2014) 19:741–56. doi: 10.1016/j.cmet.2014.02.007
90. Dewal RS, Stanford KI. Effects of exercise on brown and beige adipocytes. *Biochim Biophys Acta Mol Cell Biol Lipids.* (2019) 1864:71–8. doi: 10.1016/j.bbalip.2018.04.013
91. Slocum N, Durrant JR, Bailey D, Yoon L, Jordan H, Barton J. Responses of brown adipose tissue to diet-induced obesity, exercise, dietary restriction and ephedrine treatment. *Exp Toxicol Pathol.* (2013) 65:549–57. doi: 10.1016/j.etp.2012.04.001
92. De Matties R, Lucertini F, Guescini M, Polidori E, Zeppa S, Stocchi V, et al. Exercise as new physiological stimulus for brown adipose tissue activity. *Nutr Metab Cardiovasc Dis.* (2013) 23:582–90. doi: 10.1016/j.numecd.2012.01.013
93. Barbosa de Queiroz K, Rodovalho GV, Guimaraes JB, Carvalho de Lima D, Coimbra CC, Evangelista EA, et al. Endurance training blocks uncoupling protein 1 up-regulation in brown adipose tissue while increasing uncoupling protein 3 in the muscle tissue of rats fed with high-sugar diet. *Nutr Res.* (2012) 32:709–17. doi: 10.1016/j.nutres.2012.06.020

Conflict of Interest Statement: The authors declare that the research was conducted in the absence of any commercial or financial relationships that could be construed as a potential conflict of interest.

Copyright © 2019 Parra-Montes de Oca, Gutiérrez-Mariscal, Salmerón-Jiménez, Jaimes-Hoy, Charli and Joseph-Bravo. This is an open-access article distributed under the terms of the Creative Commons Attribution License (CC BY). The use, distribution or reproduction in other forums is permitted, provided the original author(s) and the copyright owner(s) are credited and that the original publication in this journal is cited, in accordance with accepted academic practice. No use, distribution or reproduction is permitted which does not comply with these terms.



Whole-Brain Mapping of Monosynaptic Afferent Inputs to Cortical CRH Neurons

Shouhua Zhang^{1,2,3}, Fei Lv^{2,3,4,5}, Yuan Yuan^{2,3,5}, Chengyu Fan², Jiang Li¹, Wenzhi Sun^{2,4,6} and Ji Hu^{2*}

¹ Division of Physical Biology and Bioimaging Center, Shanghai Synchrotron Radiation Facility, Shanghai Institute of Applied Physics, Chinese Academy of Sciences, Shanghai, China, ² School of Life Sciences and Technology, ShanghaiTech University, Shanghai, China, ³ University of Chinese Academy of Sciences, Beijing, China, ⁴ iHuman Institute, ShanghaiTech University, Shanghai, China, ⁵ Institute of Neuroscience, Chinese Academy of Sciences, Shanghai, China, ⁶ Chinese Institute for Brain Research, Beijing, China

OPEN ACCESS

Edited by:

Limei Zhang,
National Autonomous University
of Mexico, Mexico

Reviewed by:

Shovan Naskar,
National Institute of Mental Health
(NIMH), United States
Jan M. Deussing,
Max Planck Institute of Psychiatry
(MPI), Germany

*Correspondence:

Ji Hu
huji@shanghaitech.edu.cn

Specialty section:

This article was submitted to
Neuroendocrine Science,
a section of the journal
Frontiers in Neuroscience

Received: 22 March 2019

Accepted: 16 May 2019

Published: 04 June 2019

Citation:

Zhang S, Lv F, Yuan Y, Fan C, Li J,
Sun W and Hu J (2019) Whole-Brain
Mapping of Monosynaptic Afferent
Inputs to Cortical CRH Neurons.
Front. Neurosci. 13:565.
doi: 10.3389/fnins.2019.00565

Corticotropin-releasing hormone (CRH) is a critical neuropeptide modulating the mammalian stress response. It is involved in many functional activities within various brain regions, among which there is a subset of CRH neurons occupying a considerable proportion of the cortical GABAergic interneurons. Here, we utilized rabies virus-based monosynaptic retrograde tracing system to map the whole-brain afferent presynaptic partners of the CRH neurons in the anterior cingulate cortex (ACC). We find that the ACC CRH neurons integrate information from the cortex, thalamus, hippocampal formation, amygdala, and also several other midbrain and hindbrain nuclei. Furthermore, our results reveal that ACC CRH neurons receive direct inputs from two neuromodulatory systems, the basal forebrain cholinergic neurons and raphe serotonergic neurons. These findings together expand our knowledge about the connectivity of the cortical GABAergic neurons and also provide a basis for further investigation of the circuit function of cortical CRH neurons.

Keywords: corticotropin-releasing hormone, the anterior cingulate cortex, whole-brain mapping, monosynaptic inputs, rabies virus

INTRODUCTION

Corticotropin-releasing hormone (CRH) is an important widely expressed neuropeptide with neuroendocrine and neurotransmitter properties, which is essential for brain function (Vale et al., 1981; Young, 2007). Since its initial identification and characterization, CRH has been indicated to play an important role in coordinating endocrine, autonomic, and behavioral responses to stress (Bale and Vale, 2004; Henckens et al., 2016). Previous studies have shown that a group of parvocellular neuroendocrine cells (PNCs) of the hypothalamic–pituitary–adrenal (HPA) axis the HPA axis, through somatic cells production and released into capillaries entering pituitary portal circulation, directly control pituitary corticotroph function, and downstream glucocorticoid secretion by the adrenal glands, of which most widely studied is CRH (Wamsteeker Cusulin et al., 2013). CRH has a major role in the regulation of the HPA axis, and it is the chief organizer of the body's response to stress (Wang et al., 2011, 2013; Yang et al., 2015; Fang et al., 2016; Peng et al., 2017; Zhou and Fang, 2018). The anatomical distribution of CRH in the brain that this peptide is not only a key regulator of neuroendocrine stress, but also regulates neuronal

activity in a neuromodulated manner (Dedic et al., 2018a). An increase of CRH expression is associated with several neurological disorders, such as Alzheimer's disease (AD), major depression and anxiety disorders (Raadsheer et al., 1995). According to previous studies, CRH shows the most widespread expression in brain, but strongly expressed in several subcortical nuclei, such as paraventricular hypothalamic nucleus (PVN), amygdala, and the bed nucleus of the stria terminalis (BNST) (Chen et al., 2015; Dedic et al., 2018b; Deussing and Chen, 2018). Also, there is a subset of CRH neurons occupying a considerable proportion of the cortical GABAergic interneurons (Kubota et al., 2011). GABAergic interneurons are crucial in regulating the balance, flexibility, and functional architecture of cortical circuits (Markram et al., 2004; Klausberger and Somogyi, 2008). Their various intrinsic, synaptic, and dynamic properties allow interneurons to generate a rich range of inhibitory outputs (Jonas et al., 2004). Moreover, their different connectivity patterns confirm differential recruitment through appropriate inputs from specific brain regions (Somogyi et al., 1998; Buzsaki et al., 2004). They are of very importance in distinct forms of network oscillations that provide spatial-temporal frameworks to dynamically organize functional neural ensembles as well (Bartos et al., 2007; Klausberger and Somogyi, 2008; Taniguchi et al., 2011). The anterior cingulate cortex (ACC) is especially crucial for the performance of executive functions and emotional processing (Gasquoin, 2013; Kim et al., 2014; Meechan et al., 2015). There is evidence from electrophysiology and lesion studies indicating that the ACC plays an essential role in emotional self-control as well as focused problem-solving, error recognition, and adaptive response to changing conditions, which are central to intelligent behavior (Allman et al., 2001). It consists of several subdivisions, each with distinct functions that are provided by different input and output projections (Vogt and Paxinos, 2014). However, there is no comprehensive and systemic investigation of CRH neurons in the ACC. Therefore, characterizing the whole brain afferent pathways of CRH neurons in the ACC can expand the field of knowledge about molecular functions and neural circuit mechanism of CRH neurons.

The recent developed viral tracing system with modified rabies virus, which can map the monosynaptic afferents to a genetically defined neuronal subtype, has been applied to identify the whole-brain presynaptic partners of a specific type of neurons within a complex neural network (Wickersham et al., 2007; Ogawa et al., 2014; Grealish et al., 2015; Hu et al., 2016). Here, we applied such viral tracing system to illustrate the whole-brain afferent inputs of the ACC CRH neurons and investigated what kind of information it integrated from several important upstream brain regions. We identified the presynaptic partners of ACC CRH neurons from neocortex and thalamus. Also, we found that hippocampal information, amygdala and olfactory areas sent direct projections to the ACC CRH neurons. Interestingly, two neuromodulatory systems, the basal forebrain cholinergic system and raphe serotonergic system, provide direct innervation onto the ACC CRH neurons. Therefore, our results should be valuable to guide further investigations of the functional roles of the ACC CRH neurons, such as the normal and neurological disease states.

MATERIALS AND METHODS

Ethical Approval

This study was carried out in accordance with the recommendations of the guidelines issued by the Institutional Animal Care and Use Committees (IACUC) at Wuhan Institute of Physics and Mathematics, the Chinese Academy of Sciences, China. The protocol was approved by IACUC at ShanghaiTech University. Every effort was made to ensure the mice used were treated humanely and any discomfort was kept to a minimum.

Animals

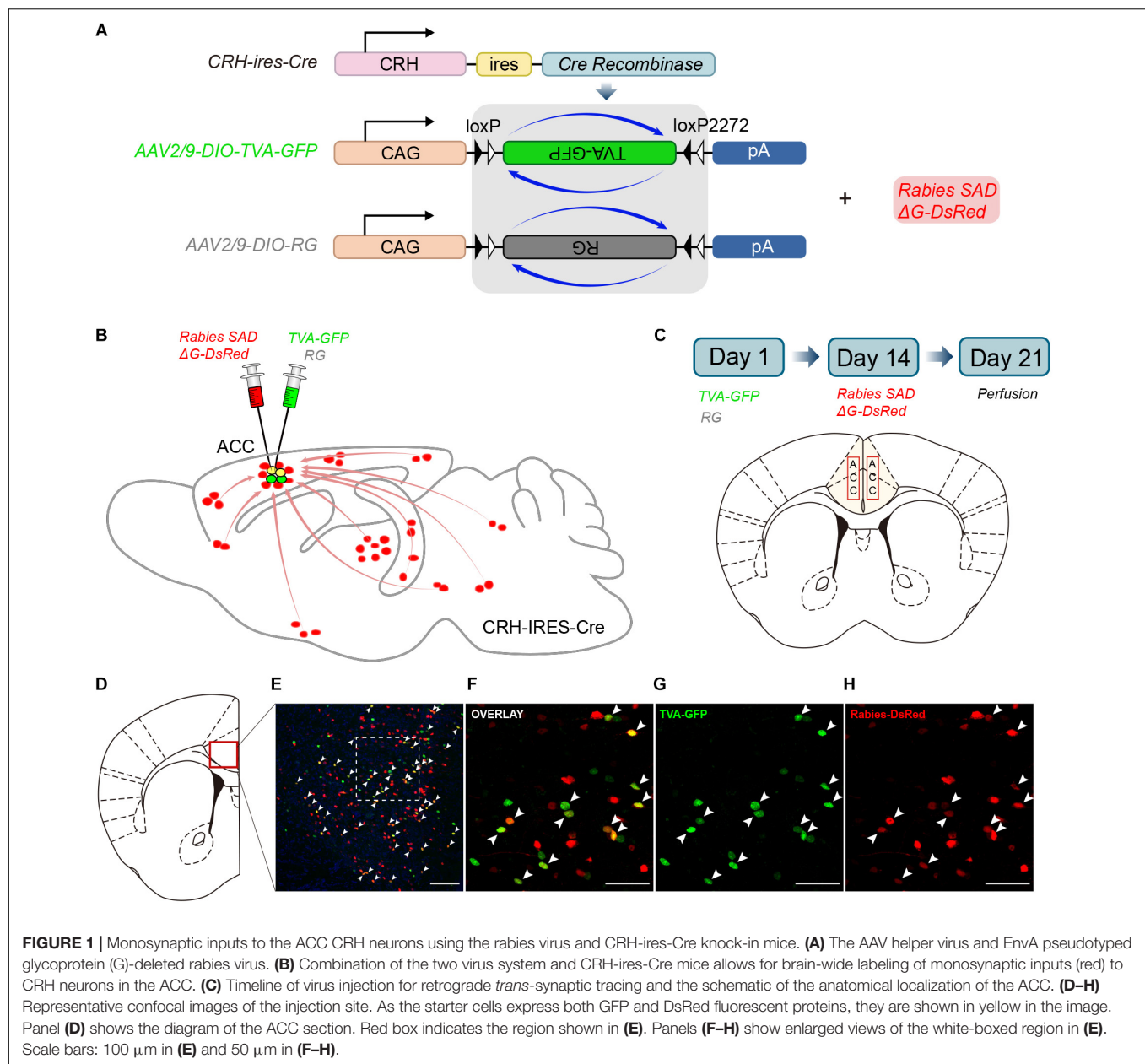
All mice were housed under a 12/12 day/night cycle at the temperature of 22–25°C, with *ad libitum* access to rodent food and water freely available in environmentally controlled conditions. The mice used in the study were adult (8–15 weeks) CRH-ires-Cre knock-in mice (Stock No. 012704) (Jackson Laboratory, Bar Harbor, ME) and C57BL/6 mice (N/A) (Shanghai Model Organisms).

Viral Microinjection and Stereotactic Surgery

All the viruses used in the *trans*-synaptic retrograde tracing experiments included AAV-CAG-DIO-TVA-GFP (AAV2/9, 1.7×10^{13} genomic copies per ml), AAV-CAG-DIO-RG (AAV2/9, 6.8×10^{12} genomic copies per ml), and EnvA-pseudotyped, glycoprotein (RG)-deleted and DsRed-expressing rabies virus (RV-EvnA-DsRed, RV) (5.0×10^8 genomic copies per ml), which were packaged and provided by F. Xu (Wuhan, China). Surgical procedures generally followed previous studies (Liu et al., 2014; Hu et al., 2017). In brief, mice were anesthetized under isoflurane, kept warm (37°C) with an electric heating pad (BrainKing Biotech, Beijing), and placed in a stereotaxic apparatus to adjust the skulls of experimental mice in parallel to the reference panel. Using a microsyringe pump (Nanoject III #3-000-207, DRUMMOND), 150 nl~300 nl of AAV-CAG-DIO-TVA-GFP and AAV-CAG-DIO-RG were stereotactically injected (20 nl/min) into the bilateral ACC (+1.10 mm AP, ± 0.20 mm ML, -1.30 mm DV, relative to Bregma) of CRH-ires-Cre mice and C57BL/6 mice, an additional 5 min being allowed for viral particles to diffuse away from the injection site before the pump was slowly withdrawn. After 2 weeks of helper viruses expression, 300 nl of RV-EvnA-DsRed was injected into the same location of the previous injection of CRH-ires-Cre mice. C57BL/6 mice were directly perfused.

Histology and Image Analysis

One week after injection of the rabies virus, CRH-ires-Cre mice were deeply anesthetized by intraperitoneal injection of an overdose of pentobarbital and then intracardially perfused with 0.9% saline solution followed by 4% paraformaldehyde (PFA) in PBS. After 2 h of post-fixation in 4% PFA, brain samples were transferred to 30% sucrose (m/v) in 1 \times PBS over one night. Then brains prepared with the optimum cutting temperature compound (O.C.T Compound) were sectioned coronally in



50 μm thickness on a freezing microtome (Leica CM1900). One out of every three sections was counterstained with nucleus dye DAPI (Molecular Probes, Eugene, OR, United States) and these sections were imaged for all subsequent analyses with an Olympus VS120 microscope. For the quantifications of starter cells and afferent input cells, we divided the boundaries of the subregions, according to the Allen Institute's reference atlas (Lein et al., 2007). Further data analyses were carried out using Olympus analysis software, ImageJ software and GraphPad Prism7. All values were presented as the Mean \pm SEM. To characterize the rabies-labeled cells in different regions, some of the remaining sections were selected for immunostained with various antibodies, including the primary goat anti-choline acetyltransferase (ChAT) antibody (1:200, Abcam,

United Kingdom), primary mouse anti-tyrosine hydroxylase (TH) antibody (1:1000, Abcam, United Kingdom), primary rabbit anti-tryptophan hydroxylase 2 (Tph2) antibody (1:1000, Abcam, United Kingdom), Alexa Fluor 488 donkey anti-rabbit second antibody (1:1000, Abcam, United Kingdom), Alexa Fluor 488 goat anti-mouse second antibody (1:1000, Abcam, United Kingdom) and Alexa Fluor 488 donkey anti-goat second antibody (1:1000, Abcam, United Kingdom). Briefly, the sections were first blocked with 3% BSA in PBS-0.3% Triton X-100 for 30 min and incubated with the primary antibodies for 48 h at 4°C. After washing, the sections were incubated with second antibodies for 2 h at room temperature. Brain sections were imaged with 20 \times and 60 \times objectives on a confocal microscope (Nikon Ti-E+A1 R SI).

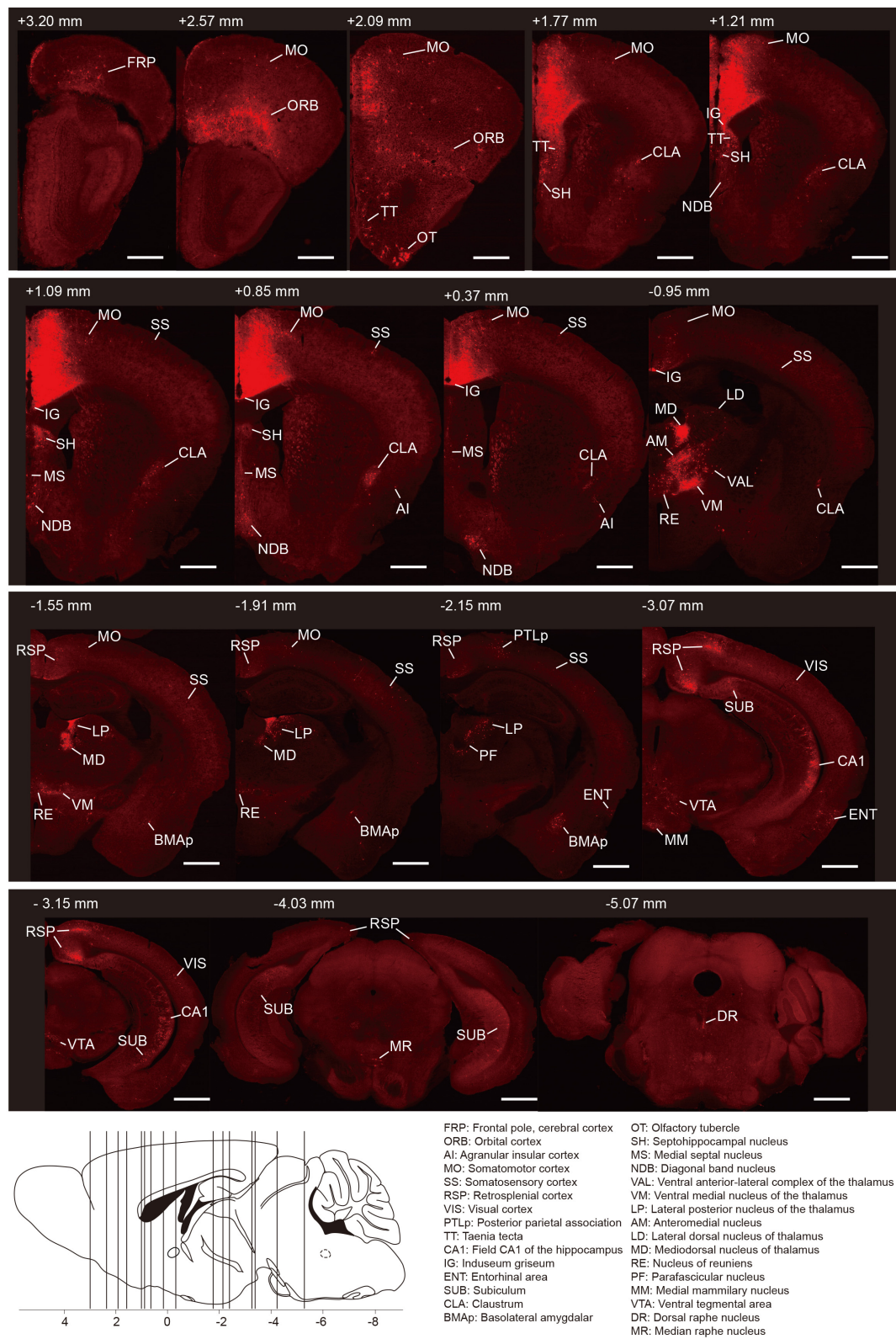


FIGURE 2 | Whole-brain distributions of monosynaptic inputs to the ACC CRH neurons. Representative coronal sections showing labeling of monosynaptic inputs to the ACC CRH neurons. For some sections, only the unilateral side is shown. Scale bar, 1 mm. Bottom-left: illustration of the anatomical localization of the sections shown above.

RESULTS

Strategies for Tracing Monosynaptic Inputs to the ACC CRH Neurons

CRH-ires-Cre mice, a genetically engineered mouse line, were used to target CRH neurons specifically. We utilized rabies-based viral strategy to map the whole-brain monosynaptic inputs to the ACC CRH neurons (Wall et al., 2010; **Figure 1A**). The rabies virus was pseudotyped with an avian virus envelope protein (EnvA), so they could not infect mammalian cells without a cognate receptor (e.g., TVA) (Watabe-Uchida et al., 2012). In addition, RG gene, which was required for transsynaptic spread, had been genetically replaced by fluorescent protein DsRed.

In Day 1, the mixture of two helper viruses (equal amount of AAV2/9-DIO-TVA-GFP and AAV2/9-DIO-RG) was stereotactically micro-injected into the bilateral ACC of CRH-ires-Cre mice (**Figures 1B,C**). The helper viruses were Cre dependent, so TVA-GFP and RG proteins were only expressed in CRH neurons where the Cre recombinase existed. In order to verify the specificity of the helper virus, we also injected the same amount of virus into the ACC of C57BL/6 mice. After 2 weeks, C57BL/6 mice were perfused and the brains were sectioned at 50 μm . As for CRH-ires-Cre mice, the rabies virus, Rabies SAD Δ G-DsRed was injected into the same area. Rabies virus only infected CRH cells expressing the TVA receptor and then retrograde spread to the upstream cells with the help of RG. The mice were sacrificed seven days after the last injection; then the whole brains were sectioned at 50 μm for further anatomic analysis. Starter cells were both GFP⁺ (from the TVA-GFP fusion) and DsRed⁺ (from rabies virus) (**Supplementary Figure S1**), whereas their presynaptic partners were only DsRed⁺ (**Figures 1D–H**). 2010 ± 200 (Mean \pm SEM) GFP⁺ cells were counted in CRH-ires-Cre mice, whereas no GFP⁺ cell in C57BL/6 mice (**Supplementary Figure S2**). In summary, the joint use of CRH-ires-Cre line and rabies virus validated our strategy of monosynaptic retrograde tracing of the ACC CRH neurons.

Overview of the Whole-Brain Inputs to the ACC CRH Neurons

To generate the overall distribution of the rabies-labeled presynaptic partners of the ACC CRH neurons, we imaged serial whole-brain coronal sections (**Figure 2**). Then we identified each input area manually based on the Allen Institute's reference atlas and found the ACC CRH neurons integrate monosynaptic inputs from widespread brain regions, ranging from the cerebral cortex to the hindbrain (Bregma +3.2 mm \sim -5.4 mm).

In order to quantify each upstream brain area, all the inputs were divided into 31 regions of interest belonging to 11 large brain regions. Then we counted the number of input neurons in each area and computed their proportions of total inputs (**Figure 3A**). The results showed that most of the afferents to the ACC CRH neurons originated from the cortex. Among different cortical subregions, the majority of the projections ($83.75\% \pm 1.56\%$, Mean \pm SEM) were received from somatomotor (MO), retrosplenial (RSP) and orbital cortex (ORB) (**Figures 2, 3A**) and the ACC afferents in the secondary motor

cortex (MOs) were more than that in the primary motor cortex (Mop) (**Supplementary Figure S4A**). The thalamus was the second largest inputs source ($34.42\% \pm 2.30\%$, Mean \pm SEM), in which over a third of inputs ($38.45\% \pm 1.90\%$, Mean \pm SEM) come from the anteromedial nucleus (AM) (**Figures 2, 3A**). Additionally, hippocampal formation and amygdala accounted for minor direct projections ($10.97\% \pm 1.44\%$, Mean \pm SEM) to the ACC CRH neurons (**Figures 2, 3A**). There were also a few other areas in midbrain and hindbrain that yielded weak innervations ($1.39\% \pm 0.24\%$, Mean \pm SEM) (**Figures 2, 3A**). We further calculated the cell densities of input neurons in each area (**Figure 3B**) and the ratios of rabies-labeled neurons to starter neurons in the ACC (**Figure 3C**). For some brain regions with high cell density, such as the ORB, RSP, AM, and the mediodorsal nucleus of the thalamus (MD), we showed their high-resolution pictures in the **Supplementary Figure S3**.

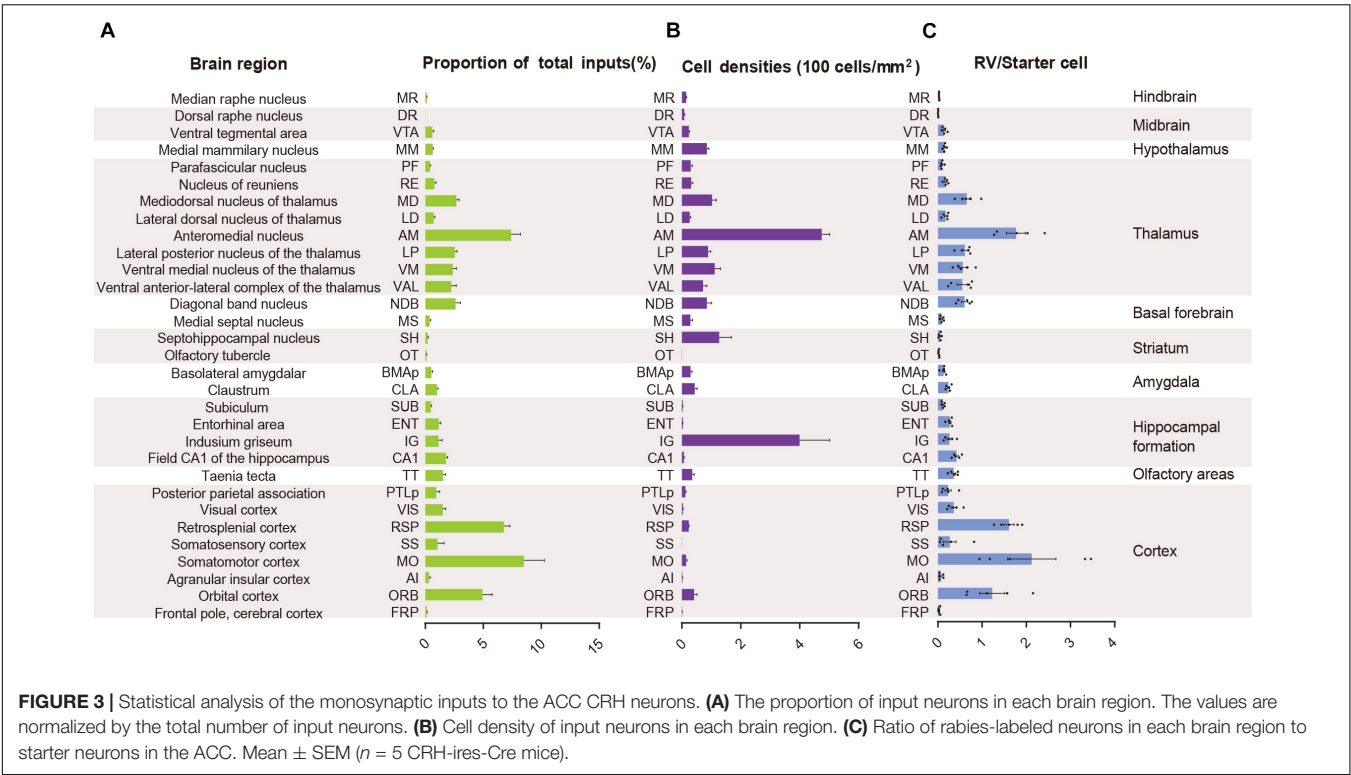
The ACC CRH Neurons Receive Extensive Cortical Inputs

We found significant monosynaptic inputs from cortical areas (**Figures 2, 3A**). In the neocortex, rabies-labeled neurons were widely distributed across cortical areas, including the frontal pole (FRP), ORB, agranular insular cortex (AI), MO, somatosensory cortex (SS), RSP, visual cortex (VIS), and posterior parietal association (PTLp) (**Figures 2, 6**).

Overall, the MO, RSP, and ORB comprised a significant portion of the cortical projection to the ACC which were about $8.50\% \pm 1.79\%$, $6.79\% \pm 0.51\%$, and $4.94\% \pm 0.81\%$ (Mean \pm SEM), respectively (**Figure 3A**). Among them, the RSP was implicated in a wide range of cognitive functions including navigation, episodic memory, and imagining future events in human fMRI studies (Spreng et al., 2009; Vann et al., 2009). Furthermore, the VIS, SS, and PTLp occupied a medium proportion that were about $1.51\% \pm 0.26\%$, $1.06\% \pm 0.57\%$, and $0.96\% \pm 0.30\%$ (Mean \pm SEM) (**Figure 3A**). We also found that input neurons in the FRP and AI accounted for only about $0.31\% \pm 0.12\%$ and $0.13\% \pm 0.04\%$ (Mean \pm SEM) of the rabies-labeled neurons (**Figure 3A**). Notably, the major input neurons in cortical areas were found in deep layer 2/3 or layer 5, such as in the MO, SS, PTLp, and VIS (**Supplementary Figure S4**). These results suggested that the ACC CRH neurons received projections primary from the motor cortex and sensory cortex, which may provide insights for the further investigation of the ACC CRH neurons in somatic movement and cognition processing.

The ACC CRH Neurons Receive Strong Thalamic Inputs

The thalamus has complex functions, generally viewed as a relay station to transfer and integrate sensory signals, including motor signals to the cortical areas, and the modulation of sleep, alertness, learning, and decision-making (Mitchell, 2015; Feng et al., 2017; Hwang et al., 2017). The thalamus is globally connected with different cortical areas, yet the cell types of connections between each thalamus nucleus and distributed cortical regions remain elusive.



Our results demonstrated that the thalamus was the second largest inputs source ($34.42\% \pm 2.30\%$, Mean \pm SEM) of the ACC CRH neurons, showing pervasive and widespread monosynaptic input neurons (Figures 2, 3). Among different sub-nuclei of the thalamus, more than a third of projections ($38.45\% \pm 1.90\%$, Mean \pm SEM) were received from the AM (Figure 3A). The anterior thalamic nuclei have been shown to support multiple and complementary forms of learning and social defeat-associated contextual fear memory (Rangel et al., 2018). Our results may provide the new perspectives for the functional role of the ACC CRH neurons in learning and memory process. Also, the mediodorsal nucleus (MD), lateral posterior nucleus (LP), ventral medial nucleus (VM) and ventral anterior-lateral complex (VAL) of thalamus contributed almost equally and made moderate direct projections to the ACC CRH neurons (Figures 2, 3A). Furthermore, many regions of the thalamus were sparsely labeled, including the parafascicular nucleus (PF), the nucleus of reuniens (RE) and the lateral dorsal nucleus of the thalamus (LD) (Figure 2). Our results revealed that thalamus sent broad projections to CRH neurons in the ACC, indicating that the cortical CRH neurons should be considered in the future exploration of the thalamic functions in the processing of learning, memory, and cognition.

The ACC CRH Neurons Receive Inputs From the Basal Forebrain

Previous studies have demonstrated that the basal forebrain is a complex nucleus which provides GABAergic, glutamatergic neurons and cholinergic inputs to cortical areas

(Gritti et al., 1997; Hur and Zaborszky, 2005; Zaborszky et al., 2015). Functionally, it has suggested that the projections from the basal forebrain to the cortex played an important role for cortical states and was also implicated in attention, sensory processing and learning (Buzsaki et al., 1988; Everitt and Robbins, 1997; Duque et al., 2000; Fuller et al., 2011; Pinto et al., 2013). Consistent with these studies, our retrograde tracing results indicated that the basal forebrain provided significant inputs to the ACC CRH neurons (Figures 2, 3). Moreover, the cholinergic neurons have been associated with plasticity and selective attention (Wenk, 1997; Rasmusson, 2000). The dysfunction of the cholinergic neurons in the basal forebrain has also been related to neurological disorders such as Alzheimer's disease (AD) and schizophrenia (Cuello et al., 2010; Marra et al., 2012; Burke et al., 2013). To further understand the nature of the basal forebrain projections to the ACC, we performed neurochemical characterization of rabies-labeled input neurons to explore the potential difference of cell types in diagonal band nucleus (NDB) as it comprised a major portion of the basal forebrain inputs to the ACC (Figure 3A). Immunochemical staining against ChAT allowed for the identification of cholinergic NDB-projecting cells (Figures 4A–O). Interestingly, we found that $30.79\% \pm 4.08\%$ (Mean \pm SEM) of the rabies-labeled NDB cells were cholinergic (Figures 4P,Q), which suggested that the ACC CRH neurons may contribute to some vital brain functions of the cholinergic circuit. The basal forebrain contains cholinergic, GABAergic, glutamatergic and peptidergic neurons (Amaral and Kurz, 1985; Freund and Antal, 1988; Gulyás et al., 1990). Maybe the ChAT negative neurons labeled by rabies virus were other cell types.

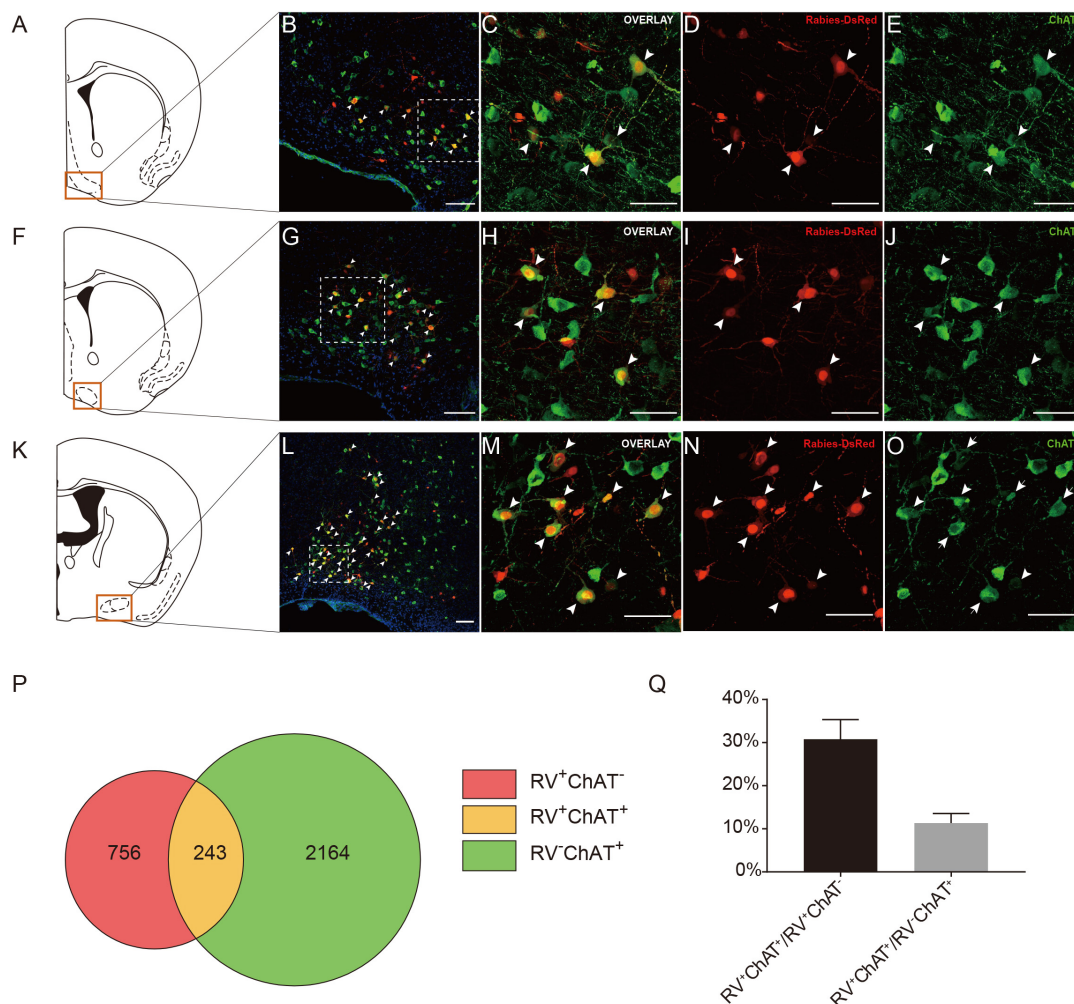
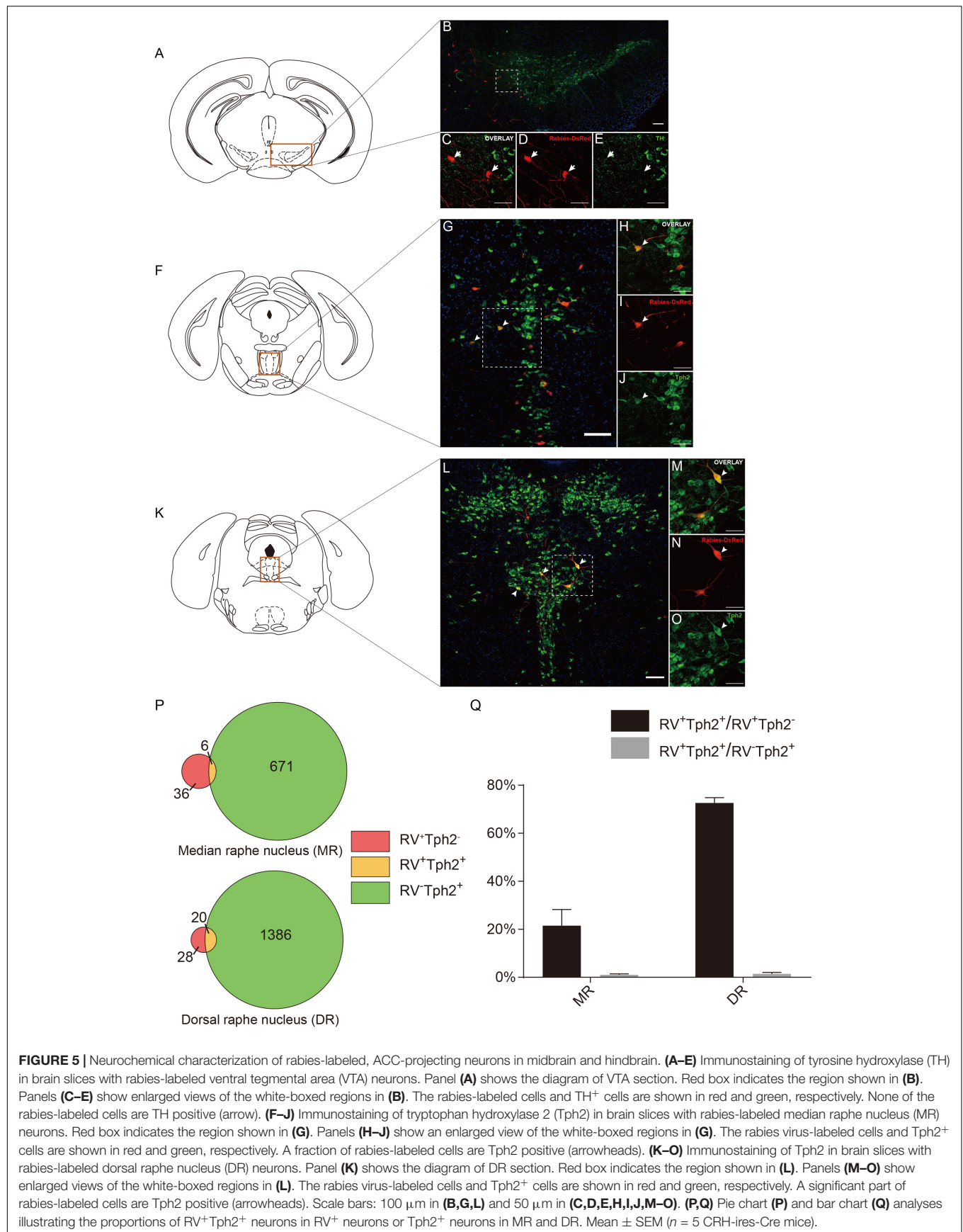


FIGURE 4 | Immunohistochemical characterization and quantification of rabies-labeled neurons in NDB presynaptic to the ACC CRH neurons. (A–O) Immunostaining of choline acetyltransferase (ChAT) in brain slices with rabies-labeled diagonal band nucleus (NDB) neurons. Panels (A, F, K) show three diagrams of anterior-posterior NDB sections. Red boxes indicate the regions shown in (B, G, L). Panels (C–E) show enlarged views of the white-boxed regions in (B). Panels (H–J) show enlarged views of the white-boxed regions in (G). Panels (M–O) show enlarged views of the white-boxed regions in (L). The rabies-labeled cells and ChAT⁺ cells are shown in red and green, respectively. Scale bars: 100 μ m in (B, G, L) and 50 μ m in (C, D, E, H, I, J, M–O). (P, Q) Pie chart (P) and bar chart (Q) analyses illustrating the proportions of RV⁺ChAT⁺ neurons in RV⁺ neurons or ChAT⁺ neurons. Mean \pm SEM ($n = 5$ CRH-ires-Cre mice).

The ACC CRH Neurons Receive Inputs From the Midbrain and Hindbrain

There were a few areas in the midbrain and hindbrain that provided weak but important innervations. The dopamine (DA) neurons originated from either the ventral tegmental area (VTA) or substantia nigra pars compacta (SNc) have been proposed to have complex and multifaceted functions, including modulating appetitive, reward-related behaviors (Holly and Miczek, 2016; Zhang et al., 2017). There are many brain areas conveying information to DA neurons, and DA neurons, in turn, send projections to the prefrontal cortex, thalamus, hippocampus, amygdala and striatum, demonstrating the “feedback” nature of this circuit (Avery and Krichmar, 2017). However, many questions remain to date regarding cortical inputs to the dopaminergic system.

To further provide the new perspectives for the function of the dopaminergic system, we examined the cell type of rabies-labeled neurons in the VTA by immunostaining experiments (Figures 5A–F). The TH, a marker of DA neurons was used to identify DA neurons in the VTA. After immunostaining, the densest TH positive staining was observed in the middle and anterior portion of the VTA, including parabrachial pigmented area (PBP) and parafasciculus retroflexus area (PFR) (Figure 5B). We observed that none of the rabies-labeled cells are TH positive (Figures 5C–E), which may imply not the CRH neurons in the ACC, but other types, involve in the VTA dopaminergic circuitry. Although DA neurons in the VTA are widely studied, GABAergic and glutamatergic neurons are also abundant (Faget et al., 2016). So in this *trans-synaptic* retrograde tracing experiment, the TH negative neurons maybe GABAergic or glutamatergic.



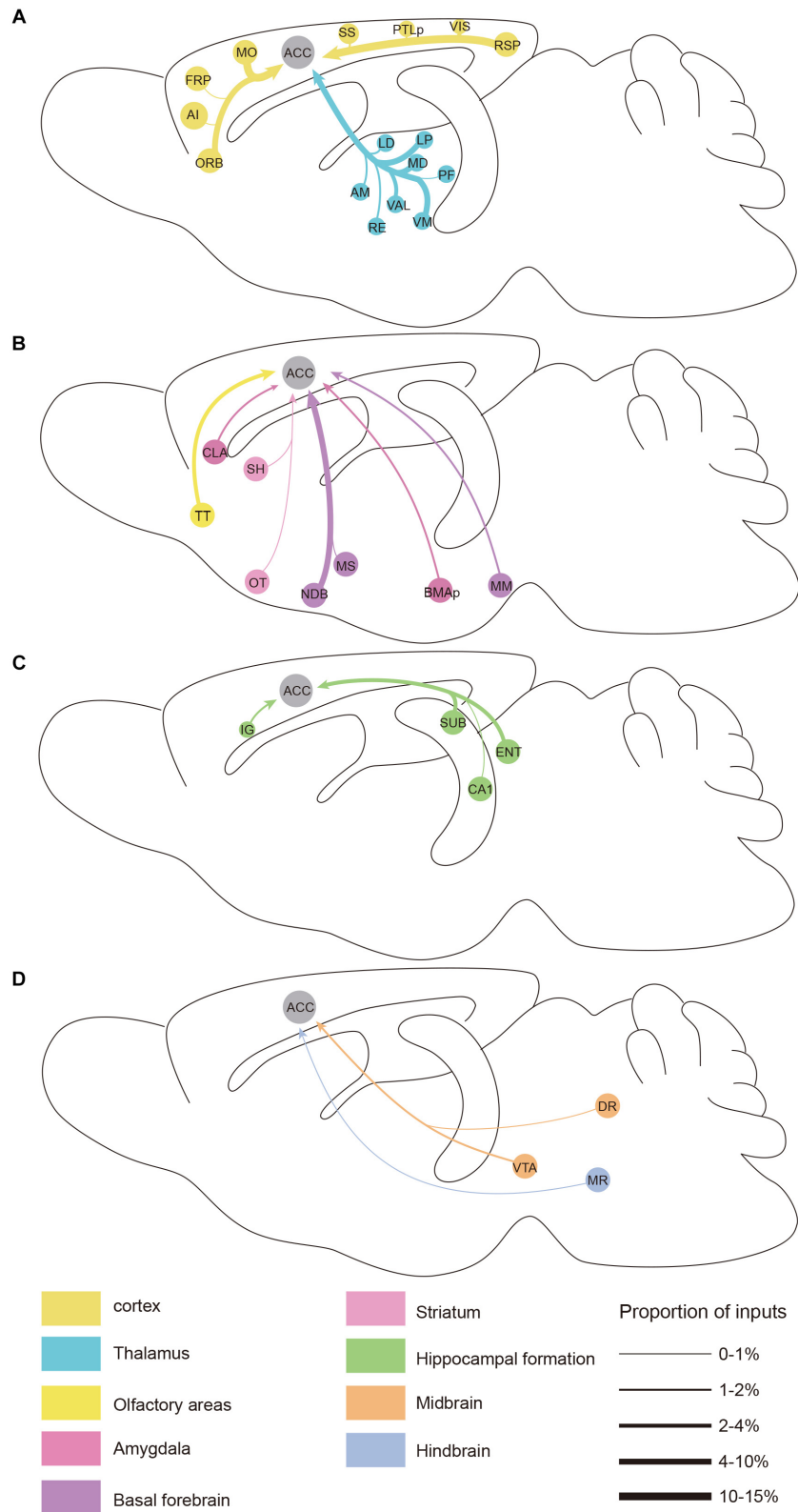


FIGURE 6 | Summarized whole brain monosynaptic inputs to the ACC CRH neurons. **(A)** Schematic of the cortical and thalamic inputs. **(B)** Schematic of the olfactory areas and forebrain subcortical inputs. **(C)** Schematic of the hippocampal inputs. **(D)** Schematic of inputs from the midbrain and hindbrain. Brain regions of the same color belong to the same brain structure shown below. The thickness of each line indicates the proportion of input neurons in each area as defined at the bottom right.

Serotonin (5-hydroxytryptamine, 5-HT), another neuromodulator, has been proposed to have an essential impact on brain functions. Several studies have revealed 5-HT's involvement in predicting punishment or harm aversion, impulsivity, stress and anxiety, and a wide variety of functions including emotion, sleep, reward, attention, and memory (Millan, 2003; Winstanley et al., 2003; Cools et al., 2008; Crockett et al., 2008, 2015; Jasinska et al., 2012; Nakamura, 2013; Seyedabadi et al., 2014; Quentin et al., 2018). The raphe nuclei, including the median raphe (MR) and dorsal raphe (DR), produce the major serotonergic populations in the central nervous system (CNS). Previous investigations have proposed that the principal targets of the raphe nucleus are "limbic cortices" including the ACC. Also, there was evidence demonstrating that the raphe nucleus received input back from "limbic cortices" (Vertes and Linley, 2008; Pollak Dorocic et al., 2014). Interestingly, the MR and DR serotonergic projections are two distinct systems differing in their morphology and physiology (Hensler, 2006). Previous studies revealed that there are few or partially overlapping in the final projections in the cortex of these two sets of serotonergic nuclei (Hensler, 2006; Vertes and Linley, 2008).

To further identify the disparity between the monosynaptic inputs to the ACC CRH neurons in the MR and DR, we carried out the immunostaining experiments (Figures 5F–O) and made some statistical analysis (Figures 5P,Q) afterward. Tph2 immunostaining was performed to identify 5-HT neurons in the raphe nucleus. Our results revealed, among rabies-labeled neurons, the proportion of 5-HT neurons in the MR ($21.49\% \pm 6.05\%$, Mean \pm SEM) was significantly lower than the DR ($72.61\% \pm 2.24\%$, Mean \pm SEM) (Figure 5Q). Besides 5-HT neurons, GABAergic neurons in the DR also project to the forebrain (Bang and Commons, 2012). These RV⁺TPH2[−] cells we labeled may be GABAergic neurons. This difference may be quite important for understanding how these two distinct serotonergic systems modulate the limbic system in normal brain and psychiatric disorders. This may give us a more rigorous cue of the circuitry of 5-HT neurons in the brain and help to understand how serotonergic and CRH system interconnected in normal and disease conditions.

DISCUSSION

The ACC has been linked to some of the most pivotal behaviors, such as decision-making, conflict monitoring and pain processing (Kolling et al., 2016; Xiao and Zhang, 2018). In order to understand the circuit mechanism associated with these behaviors more accurately, it is necessary to investigate the whole-brain inputs to the specific cell-type neurons in the ACC. In the present study, our viral tracing results efficiently mapped a comprehensive list of monosynaptic inputs to the ACC CRH neurons. We demonstrated the ACC CRH neurons receive major direct inputs from cortical regions and thalamus nucleus. Furthermore, we showed that the cholinergic system and serotonergic system in the basal forebrain and raphe nuclei, respectively, provide neuromodulatory inputs to the ACC CRH neurons. Though our results were almost identical to those

afferents of ACC neurons labeled by traditional reverse tracer FG, in a few brain areas labeled by FG, there were no RV⁺ cells in our results, such as the substantia nigra, *pars compacta* (SNc) (Fillinger et al., 2017).

Monosynaptic Reverse Tracing by Rabies Virus With Cre Recombinase Transgenic Mice

Compared with conventional retrograde tracing techniques, rabies virus system allows for mapping of monosynaptic inputs to defined neuronal subtypes by combining Cre-loxp system. In this study, we used CRH-ires-Cre mice to target CRH neurons specifically. Through the joint use of CRH-ires-Cre line and rabies virus system, we exclusively distinguished the CRH cell-specific inputs from the general inputs to ACC. As previous studies showed, this method with the combination of these two systems was efficient in labeling the monosynaptic inputs of the cell-type specific neurons (Watabe-Uchida et al., 2012; Pollak Dorocic et al., 2014; Weissbourd et al., 2014). During the data analysis, we found that some patterns of labeling produced by the rabies virus are not in accordance with known brain connectivity, but the rabies-labeled brain areas projecting to ACC CRH neurons in all mice in our experiments were consistent, for example, the labeling of the olfactory tubercle. In addition, the monosynaptic tracing of CRH neurons revealed a comprehensive atlas of the presynaptic partners of the ACC CRH neurons with a high resolution. We mapped average 12,214 neurons per animal and showed the ACC CRH neurons receive direct inputs from raphe nuclei even though there were just a minimal number of rabies-labeled inputs (0.15% roughly). Moreover, the number of starter cells is available, which makes it possible to carry out the statistical analysis and generate a quantitative and precise map of whole-brain monosynaptic inputs to the ACC CRH neurons. On the other hand, there are still a few drawbacks that may influence the statistical results because of the limitation of rabies retrograde tracing. For example, some CRH neurons expressing TVA-GFP but not express RG due to two separate helper virus. Consequently, the number of starter cells may be overestimated, then the ratios of rabies-labeled neurons in each brain region to starter neurons may be underestimated. Apart from that, there are a few TVA-GFP positive but RV negative neurons in the ACC, suggesting that this system has certain limitations on the transduction efficiency of the rabies virus. The characteristics of RV-based monosynaptic retrograde tracing strategy make it more suitable for exploring the long-range brain neuronal connectivity by mapping the monosynaptic inputs onto defined cell types in a specific region, facilitating related more in-depth research in the future.

Implications for the Role of the ACC CRH Neurons in Pain Processing

Pain is a distressing sensory and emotional experience often associated with intense or damaging stimuli alert the individual to withdraw from harmful damage (Bushnell et al., 2013; Bliss et al., 2016). Anatomical and physiological studies have revealed that the ACC and other cortical areas, including the somatosensory

cortex, prefrontal cortex and the insular cortex, are activated by various painful stimuli (Talbot et al., 1991; Schnitzler and Ploner, 2000; Xiao and Zhang, 2018). Previous studies showed that CRH had an important function on the modulation of pain resulted from bone cancer or inflammatory nociceptive stimuli and acted on important brain structures in pain regulatory (Lariviere and Melzack, 2000; Lariviere et al., 2011; Fan et al., 2015). Under pain processing, neurons in the thalamus play important effects in relaying the ascending information to the ACC, somatosensory cortex, prefrontal cortex, insular cortex and amygdala (Apkarian et al., 2005; Zhuo, 2014; Bliss et al., 2016). Then, the ACC, as a critical brain area involved in pain processing, projecting to periaqueductal gray, prefrontal cortex, and insular cortex. As well, neurons in the deep layers in the ACC innervate directly or indirectly to the spinal dorsal horn. All of these connections make up a spinal dorsal horn–thalamus–cortex–spinal dorsal horn loop in pain processing (Fuchs et al., 2014; Bliss et al., 2016). Our results showed that CRH neurons in the ACC receive a great number of projections from the somatosensory cortex and thalamus. Besides, amygdala, which has been linked to emotion, also provides moderate inputs to CRH neurons in the ACC. These connections may point out the ACC CRH neurons take part in the signal transmission and emotion storage in pain processing.

Implications for the Role of the ACC CRH Neurons in Emotion

The function of emotion has been described as to decouple stimulus and response, thus modulating cognition to allow for a suitable adaptation to the environment (Scherer, 1994; Brosch et al., 2013). Emotion has a critical contribution to perceiving the world, the enhancement of memory and decision-making (Brosch et al., 2013; Desmedt et al., 2015). Because of its complexity, there are a set of neural mechanisms that modulate many brain regions simultaneously in emotional behavior and neuromodulatory systems play a crucial part in the experience and expression of emotion (Fellous, 1999; LeDoux, 2000). Neuromodulatory systems, including the cholinergic system, serotonergic system, noradrenergic and dopaminergic system, are suggested to be important for many crucial behaviors, such as rewards, aversion, risks, cooperation, and novelty (Krichmar, 2008). The cholinergic system has been linked with various functions including attention, learning and memory, sleep, cognition, and emotion (Hasselmo, 2006; Platt and Riedel, 2011; Picciotto et al., 2012; Ballinger et al., 2016; Mu and Huang, 2019). Besides, several studies have revealed 5-HT's involved in many brain functions, such as emotion, reward, attention, and memory (Cools et al., 2008; Nakamura, 2013; Seyedabadi et al., 2014; Li et al., 2016; Quentin et al., 2018). The interactions between these systems and the other regions, like the ACC, frontal cortex, hippocampus, sensory and striatum, provide a foundation for higher cognitive functions, including emotion (Avery and Krichmar, 2017). Also, previous studies proposed that the ventral hippocampus (anterior in primates) relates to emotion (Fanselow and Dong, 2010; Grigoryan and Segal, 2016). Our retrograde tracing revealed that the ACC CRH neurons receive projections from (1) the cholinergic neurons

in the basal forebrain (about 31% rabies-labeled neurons in the NDB); (2) the serotonergic neurons in the raphe nucleus (about 73% rabies-labeled neurons in the DR and 21% in the MR); (3) neurons in the ventral hippocampus (mainly in the CA1). These results give us more indications about the functions of the ACC CRH neurons with neuromodulatory systems and hippocampus in emotion processing, illustrating such connection is a critical component for developing a circuit-level understanding of emotion, even other higher cognitive functions.

DATA AVAILABILITY

The raw data supporting the conclusions of this manuscript will be made available by the authors, without undue reservation, to any qualified researcher.

ETHICS STATEMENT

This study was carried out in accordance with the recommendations of the guidelines issued by the Institutional Animal Care and Use Committees (IACUC) at Wuhan Institute of Physics and Mathematics, the Chinese Academy of Sciences, China. The protocol was approved by IACUC at ShanghaiTech University. Every effort was made to ensure the mice used were treated humanely and any discomfort was kept to a minimum.

AUTHOR CONTRIBUTIONS

JH, JL, WS, YY, and SZ conceptualized the project. SZ and FL performed the majority of experiments. JH, SZ, FL, and CF analyzed the data. JH, SZ, and FL wrote the manuscript with the participation of all other authors.

FUNDING

This work was supported by the National Natural Science Foundation of China (Grant Nos. 31671086, 61890951, and 61890950 to JH) and Shanghai Pujiang Talent Award (Grant No. 2018X0302-101-01 to WS).

ACKNOWLEDGMENTS

We thank all members of JH and WS labs at ShanghaiTech University.

SUPPLEMENTARY MATERIAL

The Supplementary Material for this article can be found online at: <https://www.frontiersin.org/articles/10.3389/fnins.2019.00565/full#supplementary-material>

FIGURE S1 | Overview of the distribution of starter cells in the ACC. Schematic representation of starter cells (yellow) on coronal sections from anterior to posterior ACC.

FIGURE S2 | Control experiment demonstrating specificity of retrograde trans-synaptic tracing approach. **(A)** Timeline of virus injection into the ACC of C57BL/6 mice for retrograde trans-synaptic tracing. **(B)** The diagram of the ACC (injection site). Red box indicates the regions in **(C)**. **(C)** Representative confocal images of GFP⁺ neurons in C57BL/6 mice and CRH-ires-Cre mice. No evidence of TVA-GFP fluorescence positive cells was observed in C57BL/6 mice. Scale bars, 100 μ m.

FIGURE S3 | Distribution of input neurons in the ORB, RSP, AM and MD. The rabies virus-labeled cells are shown in red. Scale bar, 100 μ m. Ald, agranular insular area, dorsal part; AON, anterior olfactory nucleus; MOB, main olfactory bulb; SUBd, subiculum, dorsal part; CM, central medial nucleus of the thalamus; IAD, interanterodorsal nucleus of the thalamus; AV, anteroventral nucleus of thalamus; PVT, paraventricular nucleus of the thalamus; MH, medial habenula; LH, lateral habenula; sm, stria medullaris; AD, anterodorsal nucleus; IMD, Intermediodorsal nucleus of the thalamus.

FIGURE S4 | Layer specificity of diverse cortical inputs. Representative confocal images of input neurons in the MO, SS, PTLp, and VIS. Scale bar, 100 μ m.

REFERENCES

- Allman, J. M., Hakeem, A., Erwin, J. M., Nimchinsky, E., and Hof, P. (2001). The anterior cingulate cortex: the evolution of an interface between emotion and cognition. *Ann. N. Y. Acad. Sci.* 935, 107–117. doi: 10.1111/j.1749-6632.2001.tb03476.x
- Amaral, D. G., and Kurz, J. (1985). An analysis of the origins of the cholinergic and noncholinergic septal projections to the hippocampal formation of the rat. *J. Comp. Neurol.* 240, 37–59. doi: 10.1002/cne.902400104
- Apkarian, A. V., Bushnell, M. C., Treede, R. D., and Zubietta, J. K. (2005). Human brain mechanisms of pain perception and regulation in health and disease. *Eur. J. Pain* 9, 463–484. doi: 10.1016/j.ejpain.2004.11.001
- Avery, M. C., and Krichmar, J. L. (2017). Neuromodulatory systems and their interactions: a review of models, theories, and experiments. *Front. Neural Circ.* 11:108. doi: 10.3389/fncir.2017.00108
- Bale, T. L., and Vale, W. W. (2004). CRF and CRF receptors: role in stress responsivity and other behaviors. *Annu. Rev. Pharmacol. Toxicol.* 44, 525–557. doi: 10.1146/annurev.pharmtox.44.101802.121410
- Ballinger, E. C., Ananth, M., Talmage, D. A., and Role, L. W. (2016). Basal forebrain cholinergic circuits and signaling in cognition and cognitive decline. *Neuron* 91, 1199–1218. doi: 10.1016/j.neuron.2016.09.006
- Bang, S. J., and Commons, K. G. (2012). Forebrain GABAergic projections from the dorsal raphe nucleus identified by using GAD67-GFP knock-in mice. *J. Comp. Neurol.* 520, 4157–4167. doi: 10.1002/cne.23146
- Bartos, M., Vida, I., and Jonas, P. (2007). Synaptic mechanisms of synchronized gamma oscillations in inhibitory interneuron networks. *Nat. Rev. Neurosci.* 8, 45–56. doi: 10.1038/nrn2044
- Bliss, T. V., Collingridge, G. L., Kaang, B. K., and Zhuo, M. (2016). Synaptic plasticity in the anterior cingulate cortex in acute and chronic pain. *Nat. Rev. Neurosci.* 17, 485–496. doi: 10.1038/nrn.2016.68
- Brosch, T., Scherer, K. R., Grandjean, D., and Sander, D. (2013). The impact of emotion on perception, attention, memory, and decision-making. *Swiss. Med. Wkly.* 143:w13786. doi: 10.4414/smw.2013.13786
- Burke, R. M., Norman, T. A., Haydar, T. F., Slack, B. E., Leeman, S. E., Blusztajn, J. K., et al. (2013). BMP9 ameliorates amyloidosis and the cholinergic defect in a mouse model of Alzheimer's disease. *Proc. Natl. Acad. Sci.* 110, 19567–19572. doi: 10.1073/pnas.1319297110
- Bushnell, M. C., Ceko, M., and Low, L. A. (2013). Cognitive and emotional control of pain and its disruption in chronic pain. *Nat. Rev. Neurosci.* 14, 502–511. doi: 10.1038/nrn3516
- Buzsaki, G., Bickford, R. G., Ponomareff, G., Thal, L., Mandel, R., and Gage, F. H. (1988). Nucleus basalis and thalamic control of neocortical activity in the freely moving rat. *J. Neurosci.* 8, 4007–4026. doi: 10.1523/jneurosci.08-11-04007.1988
- Buzsaki, G., Geisler, C., Henze, D. A., and Wang, X. J. (2004). Interneuron diversity series: circuit complexity and axon wiring economy of cortical interneurons. *Trends Neurosci.* 27, 186–193. doi: 10.1016/j.tins.2004.02.007
- Chen, Y., Molet, J., Gunn, B. G., Ressler, K., and Baram, T. Z. (2015). Diversity of reporter expression patterns in transgenic mouse lines targeting corticotropin-releasing hormone-expressing neurons. *Endocrinology* 156, 4769–4780. doi: 10.1210/en.2015-1673
- Cools, R., Roberts, A. C., and Robbins, T. W. (2008). Serotonergic regulation of emotional and behavioural control processes. *Trends Cogn. Sci.* 12, 31–40. doi: 10.1016/j.tics.2007.10.011
- Crockett, M. J., Clark, L., Tabibnia, G., Lieberman, M. D., and Robbins, T. W. (2008). Serotonin modulates behavioral reactions to unfairness. *Science* 320, 1739–1739. doi: 10.1126/science.1155577
- Crockett, M. J., Siegel, J. Z., Kurth-Nelson, Z., Ousdal, O. T., Story, G., Friband, C., et al. (2015). Dissociable effects of serotonin and dopamine on the valuation of harm in moral decision making. *Curr. Biol.* 25, 1852–1859. doi: 10.1016/j.cub.2015.05.021
- Cuello, A. C., Bruno, M. A., Allard, S., Leon, W., and Iulita, M. F. (2010). Cholinergic involvement in Alzheimer's disease. A link with NGF maturation and degradation. *J. Mol. Neurosci.* 40, 230–235. doi: 10.1007/s12031-009-9238-z
- Dedic, N., Chen, A., and Deussing, J. M. (2018a). The CRF family of neuropeptides and their receptors - mediators of the central stress response. *Curr. Mol. Pharmacol.* 11, 4–31. doi: 10.2174/1874467210666170302104053
- Dedic, N., Kuhne, C., Jakovcsevski, M., Hartmann, J., Genewsky, A. J., Gomes, K. S., et al. (2018b). Chronic CRH depletion from GABAergic, long-range projection neurons in the extended amygdala reduces dopamine release and increases anxiety. *Nat. Neurosci.* 21, 803–807. doi: 10.1038/s41593-018-0151-z
- Desmedt, A., Marighetto, A., Richter-Levin, G., and Calandreau, L. (2015). Adaptive emotional memory: the key hippocampal-amygdalar interaction. *Stress* 18, 297–308. doi: 10.3109/10253890.2015.1067676
- Deussing, J. M., and Chen, A. (2018). The corticotropin-releasing factor family: physiology of the stress response. *Physiol. Rev.* 98, 2225–2286. doi: 10.1152/physrev.00042.2017
- Duque, A., Balatoni, B., Detari, L., and Zaborszky, L. (2000). EEG correlation of the discharge properties of identified neurons in the basal forebrain. *J. Neurophysiol.* 84, 1627–1635. doi: 10.1152/jn.2000.84.3.1627
- Everitt, B. J., and Robbins, T. W. (1997). Central cholinergic systems and cognition. *Annu. Rev. Psychol.* 48, 649–684. doi: 10.1146/annurev.psych.48.1.649
- Faget, L., Osakada, F., Duan, J., Ressler, R., Johnson, A. B., Proudfoot, J. A., et al. (2016). Afferent inputs to neurotransmitter-defined cell types in the ventral tegmental area. *Cell Rep.* 15, 2796–2808. doi: 10.1016/j.celrep.2016.05.057
- Fan, H. B., Zhang, T., Sun, K., Song, S. P., Cao, S. B., Zhang, H. L., et al. (2015). Corticotropin-releasing factor mediates bone cancer induced pain through neuronal activation in rat spinal cord. *Tumour Biol.* 36, 9559–9565. doi: 10.1007/s13277-015-3670-1
- Fang, H., Sun, Y. J., Lv, Y. H., Ni, R. J., Shu, Y. M., Feng, X. Y., et al. (2016). High activity of the stress promoter contributes to susceptibility to stress in the tree shrew. *Sci. Rep.* 6:24905. doi: 10.1038/srep24905
- Fanselow, M. S., and Dong, H. W. (2010). Are the dorsal and ventral hippocampus functionally distinct structures? *Neuron* 65, 7–19. doi: 10.1016/j.neuron.2009.11.031
- Fellous, J.-M. (1999). Neuromodulatory basis of emotion. *Neuroscientist* 5, 283–294. doi: 10.1177/107385849900500514
- Feng, L., Motelow, J. E., Ma, C., Biche, W., McCafferty, C., Smith, N., et al. (2017). Seizures and sleep in the thalamus: focal limbic seizures show divergent activity patterns in different thalamic nuclei. *J. Neurosci.* 37, 11441–11454. doi: 10.1523/JNEUROSCI.1011-17.2017
- Fillinger, C., Yalcin, I., Barrot, M., and Veinante, P. (2017). Afferents to anterior cingulate areas 24a and 24b and midcingulate areas 24a' and 24b' in the mouse. *Brain Struct. Funct.* 222, 1509–1532. doi: 10.1007/s00429-016-1290-1
- Freund, T. F., and Antal, M. (1988). GABA-containing neurons in the septum control inhibitory interneurons in the hippocampus. *Nature* 336:170. doi: 10.1038/336170a0

- Fuchs, P. N., Peng, Y. B., Boyette-Davis, J. A., and Uhelski, M. L. (2014). The anterior cingulate cortex and pain processing. *Front. Integr. Neurosci.* 8:35. doi: 10.3389/fnint.2014.00035
- Fuller, P. M., Sherman, D., Pedersen, N. P., Saper, C. B., and Lu, J. (2011). Reassessment of the structural basis of the ascending arousal system. *J. Comp. Neurol.* 519, 933–956. doi: 10.1002/cne.22559
- Gasquoin, P. G. (2013). Localization of function in anterior cingulate cortex: from psychosurgery to functional neuroimaging. *Neurosci. Biobehav. Rev.* 37, 340–348. doi: 10.1016/j.neubiorev.2013.01.002
- Grealish, S., Heuer, A., Cardoso, T., Kirkeby, A., Jonsson, M., Johansson, J., et al. (2015). Monosynaptic tracing using modified rabies virus reveals early and extensive circuit integration of human embryonic stem cell-derived neurons. *Stem Cell Rep.* 4, 975–983. doi: 10.1016/j.stemcr.2015.04.011
- Grigoryan, G., and Segal, M. (2016). Lasting differential effects on plasticity induced by prenatal stress in dorsal and ventral hippocampus. *Neural Plast.* 2016:2540462. doi: 10.1155/2016/2540462
- Gritti, I., Mainville, L., Mancina, M., and Jones, B. E. (1997). GABAergic and other noncholinergic basal forebrain neurons, together with cholinergic neurons, project to the mesocortex and isocortex in the rat. *J. Comp. Neurol.* 383, 163–177. doi: 10.1002/(sici)1096-9861(19970630)383:2<163::aid-cne4>3.3.co;2-t
- Gulyás, A., Görös, T., and Freund, T. (1990). Innervation of different peptide-containing neurons in the hippocampus by GABAergic septal afferents. *Neuroscience* 37, 31–44. doi: 10.1016/0306-4522(90)90189-b
- Hasselmo, M. E. (2006). The role of acetylcholine in learning and memory. *Curr. Opin. Neurobiol.* 16, 710–715. doi: 10.1016/j.conb.2006.09.002
- Henckens, M. J., Deussing, J. M., and Chen, A. (2016). Region-specific roles of the corticotropin-releasing factor–urocortin system in stress. *Nat. Rev. Neurosci.* 17:636. doi: 10.1038/nrn.2016.94
- Hensler, J. G. (2006). Serotonergic modulation of the limbic system. *Neurosci. Biobehav. Rev.* 30, 203–214. doi: 10.1016/j.neubiorev.2005.06.007
- Holly, E. N., and Miczek, K. A. (2016). Ventral tegmental area dopamine revisited: effects of acute and repeated stress. *Psychopharmacology* 233, 163–186. doi: 10.1007/s00213-015-4151-3
- Hu, R., Jin, S., He, X., Xu, F., and Hu, J. (2016). Whole-brain monosynaptic afferent inputs to basal forebrain cholinergic system. *Front. Neuroanat.* 10:98. doi: 10.3389/fnana.2016.00098
- Hu, R., Zhang, J., Luo, M., and Hu, J. (2017). Response patterns of GABAergic neurons in the anterior piriform cortex of awake mice. *Cereb. Cortex* 27, 3110–3124. doi: 10.1093/cercor/bhw175
- Hur, E. E., and Zaborszky, L. (2005). Vglut2 afferents to the medial prefrontal and primary somatosensory cortices: a combined retrograde tracing in situ hybridization study [corrected]. *J. Comp. Neurol.* 483, 351–373. doi: 10.1002/cne.20444
- Hwang, K., Bertolero, M. A., Liu, W. B., and D'Esposito, M. (2017). The human thalamus is an integrative hub for functional brain networks. *J. Neurosci.* 37, 5594–5607. doi: 10.1523/JNEUROSCI.0067-17.2017
- Jasinska, A. J., Lowry, C. A., and Burmeister, M. (2012). Serotonin transporter gene, stress and raphe–raphe interactions: a molecular mechanism of depression. *Trends Neurosci.* 35, 395–402. doi: 10.1016/j.tins.2012.01.001
- Jonas, P., Bischofberger, J., Fricker, D., and Miles, R. (2004). Interneuron diversity series: fast in, fast out—temporal and spatial signal processing in hippocampal interneurons. *Trends Neurosci.* 27, 30–40. doi: 10.1016/j.tins.2003.10.010
- Kim, B. S., Lee, J., Bang, M., Am Seo, B., Khalid, A., Jung, M. W., et al. (2014). Differential regulation of observational fear and neural oscillations by serotonin and dopamine in the mouse anterior cingulate cortex. *Psychopharmacology* 231, 4371–4381. doi: 10.1007/s00213-014-3581-7
- Klausberger, T., and Somogyi, P. (2008). Neuronal diversity and temporal dynamics: the unity of hippocampal circuit operations. *Science* 321, 53–57. doi: 10.1126/science.1149381
- Kolling, N., Behrens, T., Wittmann, M. K., and Rushworth, M. (2016). Multiple signals in anterior cingulate cortex. *Curr. Opin. Neurobiol.* 37, 36–43. doi: 10.1016/j.conb.2015.12.007
- Krichmar, J. L. (2008). The neuromodulatory system: a framework for survival and adaptive behavior in a challenging world. *Adapt. Behav.* 16, 385–399. doi: 10.1177/1059712308095775
- Kubota, Y., Shigematsu, N., Karube, F., Sekigawa, A., Kato, S., Yamaguchi, N., et al. (2011). Selective coexpression of multiple chemical markers defines discrete populations of neocortical GABAergic neurons. *Cereb. Cortex* 21, 1803–1817. doi: 10.1093/cercor/bhq252
- Lariviere, W. R., Fiorenzani, P., Ceccarelli, I., Massafra, C., Sorda, G., Di Canio, C., et al. (2011). Central CRH administration changes formalin pain responses in male and female rats. *Brain Res.* 1383, 128–134. doi: 10.1016/j.brainres.2011.01.106
- Lariviere, W. R., and Melzack, R. (2000). The role of corticotropin-releasing factor in pain and analgesia. *Pain* 84, 1–12. doi: 10.1016/s0304-3959(99)00193-1
- LeDoux, J. E. (2000). Emotion circuits in the brain. *Annu. Rev. Neurosci.* 23, 155–184. doi: 10.1146/annurev.neuro.23.1.155
- Lein, E. S., Hawrylycz, M. J., Ao, N., Ayres, M., Bensinger, A., Bernard, A., et al. (2007). Genome-wide atlas of gene expression in the adult mouse brain. *Nature* 445, 168–176. doi: 10.1038/nature05453
- Li, Y., Zhong, W., Wang, D., Feng, Q., Liu, Z., Zhou, J., et al. (2016). Serotonin neurons in the dorsal raphe nucleus encode reward signals. *Nat. Commun.* 7:10503. doi: 10.1038/ncomms10503
- Liu, Z., Zhou, J., Li, Y., Hu, F., Lu, Y., Ma, M., et al. (2014). Dorsal raphe neurons signal reward through 5-HT and glutamate. *Neuron* 81, 1360–1374. doi: 10.1016/j.neuron.2014.02.010
- Markram, H., Toledo-Rodriguez, M., Wang, Y., Gupta, A., Silberberg, G., and Wu, C. (2004). Interneurons of the neocortical inhibitory system. *Nat. Rev. Neurosci.* 5, 793–807. doi: 10.1038/nrn1519
- Marra, C., Quaranta, D., Profice, P., Pilato, F., Capone, F., Iodice, F., et al. (2012). Central cholinergic dysfunction measured “in vivo” correlates with different behavioral disorders in Alzheimer's disease and dementia with lewy body. *Brain Stimul.* 5, 533–538. doi: 10.1016/j.brs.2011.08.009
- Meechan, D. W., Rutz, H. L., Fralish, M. S., Maynard, T. M., Rothblat, L. A., and LaMantia, A. S. (2015). Cognitive ability is associated with altered medial frontal cortical circuits in the LgDel mouse model of 22q11.2DS. *Cereb. Cortex* 25, 1143–1151. doi: 10.1093/cercor/bht308
- Millan, M. J. (2003). The neurobiology and control of anxious states. *Prog. Neurobiol.* 70, 83–244. doi: 10.1016/s0301-0082(03)00087-x
- Mitchell, A. S. (2015). The mediodorsal thalamus as a higher order thalamic relay nucleus important for learning and decision-making. *Neurosci. Biobehav. Rev.* 54, 76–88. doi: 10.1016/j.neubiorev.2015.03.001
- Mu, P., and Huang, Y. H. (2019). Cholinergic system in sleep regulation of emotion and motivation. *Pharmacol. Res.* 143, 113–118. doi: 10.1016/j.phrs.2019.03.013
- Nakamura, K. (2013). The role of the dorsal raphe nucleus in reward-seeking behavior. *Front. Integr. Neurosci.* 7:60. doi: 10.3389/fnint.2013.00060
- Ogawa, S. K., Cohen, J. Y., Hwang, D., Uchida, N., and Watabe-Uchida, M. (2014). Organization of monosynaptic inputs to the serotonin and dopamine neuromodulatory systems. *Cell Rep.* 8, 1105–1118. doi: 10.1016/j.celrep.2014.06.042
- Peng, J., Long, B., Yuan, J., Peng, X., Ni, H., Li, X., et al. (2017). A quantitative analysis of the distribution of CRH Neurons in whole mouse brain. *Front. Neuroanat.* 11:63. doi: 10.3389/fnana.2017.00063
- Picciotto, M. R., Higley, M. J., and Mineur, Y. S. (2012). Acetylcholine as a neuromodulator: cholinergic signaling shapes nervous system function and behavior. *Neuron* 76, 116–129. doi: 10.1016/j.neuron.2012.08.036
- Pinto, L., Goard, M. J., Estandian, D., Xu, M., Kwan, A. C., Lee, S. H., et al. (2013). Fast modulation of visual perception by basal forebrain cholinergic neurons. *Nat. Neurosci.* 16, 1857–1863. doi: 10.1038/nn.3552
- Platt, B., and Riedel, G. (2011). The cholinergic system, EEG and sleep. *Behav. Brain Res.* 221, 499–504. doi: 10.1016/j.bbr.2011.01.017
- Pollak Dorocic, I., Furth, D., Xuan, Y., Johansson, Y., Pozzi, L., Silberberg, G., et al. (2014). A whole-brain atlas of inputs to serotonergic neurons of the dorsal and median raphe nuclei. *Neuron* 83, 663–678. doi: 10.1016/j.neuron.2014.07.002
- Quentin, E., Belmer, A., and Maroteaux, L. (2018). Somato-dendritic regulation of raphe serotonin neurons; a key to antidepressant action. *Front. Neurosci.* 12:982. doi: 10.3389/fnins.2018.00982
- Raadshere, F. C., Heerikhuizen, J. J. V., Lucassen, P. J., Hoogendijk, W. J., Tilders, F. J., and Swaab, D. F. (1995). Corticotropin-releasing hormone mRNA levels in the paraventricular nucleus of patients with Alzheimer's disease and depression. *Am. J. Psychiatry* 152, 1372–1376. doi: 10.1176/ajp.152.9.1372

- Rangel, M. J. Jr., Baldo, M. V. C., and Canteras, N. S. (2018). Influence of the anteromedial thalamus on social defeat-associated contextual fear memory. *Behav. Brain Res.* 339, 269–277. doi: 10.1016/j.bbr.2017.10.038
- Rasmusson, D. (2000). The role of acetylcholine in cortical synaptic plasticity. *Behav. Brain Res.* 115, 205–218. doi: 10.1016/s0166-4328(00)00259-x
- Scherer, K. R. (1994). “Emotion serves to decouple stimulus and response,” in *The Nature of Emotion: Fundamental Questions*, eds P. Egan and R. J. Davidson (New York, NY: Oxford University Press), 127–130.
- Schnitzler, A., and Ploner, M. (2000). Neurophysiology and functional neuroanatomy of pain perception. *J. Clin. Neurophysiol.* 17, 592–603. doi: 10.1097/00004691-200011000-00005
- Seyedabadi, M., Fakhfouri, G., Ramezani, V., Mehr, S. E., and Rahimian, R. (2014). The role of serotonin in memory: interactions with neurotransmitters and downstream signaling. *Exp. Brain Res.* 232, 723–738. doi: 10.1007/s00221-013-3818-4
- Somogyi, P., Tamas, G., Lujan, R., and Buhl, E. H. (1998). Salient features of synaptic organization in the cerebral cortex. *Brain Res. Rev.* 26, 113–135. doi: 10.1016/s0165-0173(97)00061-1
- Spreng, R. N., Mar, R. A., and Kim, A. S. (2009). The common neural basis of autobiographical memory, prospection, navigation, theory of mind, and the default mode: a quantitative meta-analysis. *J. Cogn. Neurosci.* 21, 489–510. doi: 10.1162/jocn.2008.21029
- Talbot, J. D., Marrett, S., Evans, A. C., Meyer, E., Bushnell, M. C., and Duncan, G. H. (1991). Multiple representations of pain in human cerebral cortex. *Science* 251, 1355–1358. doi: 10.1126/science.2003220
- Taniguchi, H., He, M., Wu, P., Kim, S., Paik, R., Sugino, K., et al. (2011). A resource of cre driver lines for genetic targeting of GABAergic neurons in cerebral cortex. *Neuron* 72:1091. doi: 10.1016/j.neuron.2011.12.010
- Vale, W., Spiess, J., Rivier, C., and Rivier, J. (1981). Characterization of a 41-residue ovine hypothalamic peptide that stimulates secretion of corticotropin and β -endorphin. *Science* 213, 1394–1397. doi: 10.1126/science.6267699
- Vann, S. D., Aggleton, J. P., and Maguire, E. A. (2009). What does the retrosplenial cortex do? *Nat. Rev. Neurosci.* 10, 792–802. doi: 10.1038/nrn2733
- Vertes, R. P., and Linley, S. B. (2008). “Efferent and afferent connections of the dorsal and median raphe nuclei in the rat,” in *Serotonin and Sleep: Molecular, Functional and Clinical Aspects*, eds J. M. Monti, B. L. Jacobs, D. Nutt, and S. R. Pandi-Perumal (Berlin: Springer), 69–102. doi: 10.1007/978-3-7643-8561-3_3
- Vogt, B. A., and Paxinos, G. (2014). Cytoarchitecture of mouse and rat cingulate cortex with human homologies. *Brain Struct. Funct.* 219, 185–192. doi: 10.1007/s00429-012-0493-3
- Wall, N. R., Wickersham, I. R., Cetin, A., De La Parra, M., and Callaway, E. M. (2010). Monosynaptic circuit tracing in vivo through Cre-dependent targeting and complementation of modified rabies virus. *Proc. Natl. Acad. Sci.* 107, 21848–21853. doi: 10.1073/pnas.1011756107
- Wamsteeker Cusulin, J. I., Fuzesi, T., Watts, A. G., and Bains, J. S. (2013). Characterization of corticotropin-releasing hormone neurons in the paraventricular nucleus of the hypothalamus of Crh-IRES-Cre mutant mice. *PLoS One* 8:e64943. doi: 10.1371/journal.pone.0064943
- Wang, X. D., Rammes, G., Kraev, I., Wolf, M., Liebl, C., Scharf, S. H., et al. (2011). Forebrain CRF(1) modulates early-life stress-programmed cognitive deficits. *J. Neurosci.* 31, 13625–13634. doi: 10.1523/JNEUROSCI.2259-11.2011
- Wang, X. D., Su, Y. A., Wagner, K. V., Avrabos, C., Scharf, S. H., Hartmann, J., et al. (2013). Nectin-3 links CRHR1 signaling to stress-induced memory deficits and spine loss. *Nat. Neurosci.* 16, 706–713. doi: 10.1038/nn.3395
- Watabe-Uchida, M., Zhu, L., Ogawa, S. K., Vamanrao, A., and Uchida, N. (2012). Whole-brain mapping of direct inputs to midbrain dopamine neurons. *Neuron* 74, 858–873. doi: 10.1016/j.neuron.2012.03.017
- Weissbourd, B., Ren, J., DeLoach, K. E., Guenther, C. J., Miyamichi, K., and Luo, L. (2014). Presynaptic partners of dorsal raphe serotonergic and GABAergic neurons. *Neuron* 83, 645–662. doi: 10.1016/j.neuron.2014.06.024
- Wenk, G. L. (1997). The nucleus basalis magnocellularis cholinergic system: one hundred years of progress. *Neurobiol. Learn. Mem.* 67, 85–95. doi: 10.1006/nlme.1996.3757
- Wickersham, I. R., Lyon, D. C., Barnard, R. J., Mori, T., Finke, S., Conzelmann, K. K., et al. (2007). Monosynaptic restriction of transsynaptic tracing from single, genetically targeted neurons. *Neuron* 53, 639–647. doi: 10.1016/j.neuron.2007.01.033
- Winstanley, C. A., Dalley, J. W., Theobald, D. E., and Robbins, T. W. (2003). Global 5-HT depletion attenuates the ability of amphetamine to decrease impulsive choice on a delay-discounting task in rats. *Psychopharmacology* 170, 320–331. doi: 10.1007/s00213-003-1546-3
- Xiao, X., and Zhang, Y. Q. (2018). A new perspective on the anterior cingulate cortex and affective pain. *Neurosci. Biobehav. Rev.* 90, 200–211. doi: 10.1016/j.neubiorev.2018.03.022
- Yang, X. D., Liao, X. M., Uribe-Marino, A., Liu, R., Xie, X. M., Jia, J., et al. (2015). Stress during a critical postnatal period induces region-specific structural abnormalities and dysfunction of the prefrontal cortex via CRF1. *Neuropsychopharmacology* 40, 1203–1215. doi: 10.1038/npp.2014.304
- Young, W. S. III, (2007). “Regulation of gene expression in the hypothalamus: hybridization histochemical studies,” in *Proceedings of the Ciba Foundation Symposium 168-Functional Anatomy of the Neuroendocrine Hypothalamus: Functional Anatomy of the Neuroendocrine Hypothalamus: Ciba Foundation Symposium 168*, (Hoboken, NJ: Wiley Online Library), 127–143. doi: 10.1002/9780470514283.ch9
- Zaborszky, L., Duque, A., Gielow, M., Gombkoto, P., Nadasdy, Z., and Somogyi, J. (2015). “Organization of the basal forebrain cholinergic projection system,” in *The Rat Nervous System*, ed. G. Paxinos (Amsterdam: Elsevier), 491–507. doi: 10.1016/b978-0-12-374245-2.00019-x
- Zhang, Z., Liu, Q., Wen, P., Zhang, J., Rao, X., Zhou, Z., et al. (2017). Activation of the dopaminergic pathway from VTA to the medial olfactory tubercle generates odor-preference and reward. *eLife* 6:e25423. doi: 10.7554/eLife.25423
- Zhou, J. N., and Fang, H. (2018). Transcriptional regulation of corticotropin-releasing hormone gene in stress response. *IBRO Rep.* 5, 137–146. doi: 10.1016/j.ibror.2018.08.003
- Zhuo, M. (2014). Long-term potentiation in the anterior cingulate cortex and chronic pain. *Philos. Trans. R. Soc. Lond. B Biol. Sci.* 369:20130146. doi: 10.1098/rstb.2013.0146

Conflict of Interest Statement: The authors declare that the research was conducted in the absence of any commercial or financial relationships that could be construed as a potential conflict of interest.

Copyright © 2019 Zhang, Lv, Yuan, Fan, Li, Sun and Hu. This is an open-access article distributed under the terms of the Creative Commons Attribution License (CC BY). The use, distribution or reproduction in other forums is permitted, provided the original author(s) and the copyright owner(s) are credited and that the original publication in this journal is cited, in accordance with accepted academic practice. No use, distribution or reproduction is permitted which does not comply with these terms.



Deletion of CRH From GABAergic Forebrain Neurons Promotes Stress Resilience and Dampens Stress-Induced Changes in Neuronal Activity

Nina Dedic^{1,2}, Claudia Kühne¹, Karina S. Gomes^{1,3}, Jakob Hartmann^{2,4}, Kerry J. Ressler², Mathias V. Schmidt⁴ and Jan M. Deussing^{1*}

¹ Molecular Neurogenetics, Max Planck Institute of Psychiatry, Munich, Germany, ² Department of Psychiatry, Harvard Medical School and McLean Hospital, Belmont, MA, United States, ³ Laboratory of Neuropsychopharmacology, Paulista State University, Araraquara, Brazil, ⁴ Stress Resilience, Max Planck Institute of Psychiatry, Munich, Germany

OPEN ACCESS

Edited by:

Lee E. Eiden,
National Institutes of Health (NIH),
United States

Reviewed by:

Kazuhiro Nakamura,
Nagoya University, Japan
Jerome D. Swinny,
University of Portsmouth,
United Kingdom

*Correspondence:

Jan M. Deussing
deussing@psych.mpg.de

Specialty section:

This article was submitted to
Neuroendocrine Science,
a section of the journal
Frontiers in Neuroscience

Received: 20 May 2019

Accepted: 02 September 2019

Published: 20 September 2019

Citation:

Dedic N, Kühne C, Gomes KS,
Hartmann J, Ressler KJ, Schmidt MV
and Deussing JM (2019) Deletion
of CRH From GABAergic Forebrain
Neurons Promotes Stress Resilience
and Dampens Stress-Induced
Changes in Neuronal Activity.
Front. Neurosci. 13:986.
doi: 10.3389/fnins.2019.00986

Dysregulation of the corticotropin-releasing hormone (CRH) system has been implicated in stress-related psychopathologies such as depression and anxiety. Although most studies have linked CRH/CRH receptor 1 signaling to aversive, stress-like behavior, recent work has revealed a crucial role for distinct CRH circuits in maintaining positive emotional valence and appetitive responses under baseline conditions. Here we addressed whether deletion of CRH, specifically from GABAergic forebrain neurons (*Crh*^{CKO-GABA} mice) differentially affects general behavior under baseline and chronic stress conditions. Expression mapping in *Crh*^{CKO-GABA} mice revealed absence of *Crh* in GABAergic neurons of the cortex and limbic regions including the hippocampus, central nucleus of the amygdala and the bed nucleus of the stria terminalis, but not in the paraventricular nucleus of hypothalamus. Consequently, conditional CRH knockout animals exhibited no alterations in circadian and stress-induced corticosterone release compared to controls. Under baseline conditions, absence of *Crh* from forebrain GABAergic neurons resulted in social interaction deficits but had no effect on other behavioral measures including locomotion, anxiety, immobility in the forced swim test, acoustic startle response and fear conditioning. Interestingly, following exposure to chronic social defeat stress, *Crh*^{CKO-GABA} mice displayed a resilient phenotype, which was accompanied by a dampened, stress-induced expression of immediate early genes *c-fos* and *zif268* in several brain regions. Collectively our data reveals the requirement of GABAergic CRH circuits in maintaining appropriate social behavior in naïve animals and further supports the ability of CRH to promote divergent behavioral states under baseline and severe stress conditions.

Keywords: corticotropin-releasing hormone (CRH), stress, anxiety, resilience, GABAergic circuits, corticosterone, HPA (hypothalamic-pituitary-adrenal) axis

INTRODUCTION

Since its discovery in 1981 by Wylie Vale and colleagues (Vale et al., 1981), the neuropeptide corticotropin-releasing hormone (CRH) has become known as the key orchestrator of the neuroendocrine, autonomic and behavioral responses to stress (Deussing, 2013; Janssen and Kozicz, 2013; Dedic et al., 2017; Deussing and Chen, 2018). CRH is densely expressed in the paraventricular nucleus of the hypothalamus (PVN) from where it regulates hypothalamic-pituitary-adrenal (HPA) axis activity and consequently the circadian and stress-mediated release of glucocorticoids. Together with its high affinity type 1 receptor (CRHR1), CRH is also involved in modulating behavioral adaptations to stress, which can be attributed to their wide distribution within the mammalian brain including the cortex, key limbic structures and midbrain monoaminergic nuclei (Swanson et al., 1983; Van Pett et al., 2000; Rodaros et al., 2007; Refojo et al., 2011; Dedic et al., 2018a).

We and others have shown that CRHR1 is expressed in forebrain glutamatergic and GABAergic neurons, dopaminergic neurons of the ventral tegmental area (VTA) as well as a limited subset of serotonergic neurons of the dorsal raphe nucleus (Van Pett et al., 2000; Refojo et al., 2011). In contrast, cortical and limbic CRH expression is largely confined to GABAergic neurons with the exception of the piriform cortex (Pir) and PVN, where CRH is found in glutamatergic cells (Chen et al., 2001; Kubota et al., 2011; Dabrowska et al., 2013; Kubota, 2013; Dedic et al., 2018a; Gunn et al., 2019). Although it is well established that CRH/CRHR1 signaling mediates aversive responses, including anxiety and depression-like behaviors, several recent studies have challenged this viewpoint by revealing anxiolytic and appetitive properties of specific CRH/CRHR1 circuits. Genetic dissection of CRHR1-expressing cell populations demonstrated a bidirectional role for the receptor in anxiety, suggesting that glutamatergic and dopaminergic systems mediate anxiogenic and anxiolytic effects of CRHR1, and might function in a concerted but antagonist manner to keep emotional responses to stressful situations in balance (Refojo et al., 2011). More recently, our work extended these findings by identifying the source of the “anxiolytic” CRH neurons. These represent a distinct subpopulation of GABAergic, long-range projecting neurons in the extended amygdala that target CRHR1 on dopaminergic VTA neurons to positively modulate emotional behavior by regulating dopaminergic neurotransmission (Dedic et al., 2018a). Importantly, these findings were obtained from naïve animals, which poses the question as to whether specific CRH circuits might modulate different behaviors under baseline and stressful conditions. In fact, Lemos and colleagues demonstrated that CRH acts in the nucleus accumbens (NAc) to increase dopamine release and promote appetitive behavior in mice; an effect which was lost following repeated stress exposure, suggesting that CRH differentially affects the reward circuitry under basal and stress conditions (Lemos et al., 2012). However, whether severe stress is able to switch CRH action from positive to negative in the context of anxiety, social and/or depression-like behavior, remains largely unexplored.

In order to address this question, we assessed whether conditional deletion of CRH from forebrain GABAergic neurons (*Crh*^{CKO-GABA} mice) would differently affect anxiety, social behavioral and cognitive parameters under baseline and chronic stress conditions. In contrast to utilizing full CRH knockout mice, this approach enabled the dissection of GABAergic CRH circuits in a genetically defined manner, without altering CRH levels in the PVN and thus not affecting peripheral glucocorticoid release. Our results demonstrate that absence of CRH from forebrain GABAergic neurons increases social avoidance, thus highlighting CRH's capacity to positively regulate specific behaviors under physiological conditions. In contrast, *Crh*^{CKO-GABA} mice exhibited resilience to chronic social defeat stress (CSDS) and showed a decrease in stress-induced neuronal activation in multiple forebrain regions. Collectively, our data demonstrates that CRH can promote divergent effects on specific emotional states under physiological and chronic stress conditions.

MATERIALS AND METHODS

Animals

Adult, male mice were used in all experiments. *Crh*^{CKO-GABA} mice were obtained by breeding the recently generated *Crh*^{lox} mice (Dedic et al., 2018a) to *Dlx5/6-Cre* driver mice (Monory et al., 2006) to obtain *Crh*^{Ctrl} (*Crh*^{lox/lox}) and *Crh*^{CKO-GABA} (*Crh*^{lox/lox}; *Dlx5/6-Cre*) mice. Mice were of a mixed 129S2/Sv × C57BL/6J genetic background. All animals were group housed (maximum 4 mice per cage) under standard laboratory conditions (22 ± 1°C, 55 ± 5% humidity) and were maintained on a 12:12 h light–dark cycle (lights on from 07:00 to 19:00 h), with food and water provided *ad libitum*. Behavioral testing was conducted between 8:30 a.m. and 12:30 p.m. during the light cycle. Mice were single housed 1 week before behavioral testing or hormone assessment. For the assessment of initial baseline behavior, the following behavioral tests were performed in one cohort of animals in the following order: open field test, elevated plus-maze, dark/light box test and forced swim test (FST). The acoustic startle response and fear conditioning were assessed in a second cohort of animals. A third cohort of mice was used for the CSDS experiment. All experiments were conducted in accordance with the Guide for the Care and Use of Laboratory Animals of the Government of Upper Bavaria, Germany.

In situ Hybridization (ISH)

ISH was performed as previously described (Refojo et al., 2011). Mice were killed with an overdose of isoflurane (Floren, Abbott) and decapitated immediately after. The brains were carefully removed and immediately shock-frozen on dry ice. Brains were sectioned coronally at 20 µm using a cryostat (Microm, Walldorf, Germany). The sections were thaw-mounted onto SuperFrost slides, dried, and kept at –80°C. The following riboprobes were used: *Crh* (3'UTR): bp 2108–2370 of AY128673; *c-fos*: bp 608–978 of NM_010234; *zif268*: bp 245–786 of NM_00791. Images were analyzed with Adobe Photoshop CS2 and Adobe Illustrator CS2.

Corticosterone Measurements

To determine basal plasma corticosterone hormone levels, blood sampling was performed in the early morning (08:30–09:30 h) and afternoon (04:30–05:30 h) by collecting blood from the tail vein. Samples were collected in 1.5 ml EDTA-coated microcentrifuge tubes (Kabe Labortechnik, Germany). All blood samples were kept on ice and later centrifuged at 8000 rpm at 4°C for 15 min. Plasma was transferred to new labeled microcentrifuge tubes and stored at –20°C until further processing. Plasma corticosterone concentrations were measured using a commercially available RIA kit (MP Biomedicals, Eschwege, Germany) according to the manufacture's manual.

Open Field (OF) Test

The OF test was used to characterize locomotor activity in a novel environment. Testing was performed in an open field arena (50 × 50 × 50 cm) dimly illuminated (about 15 lux) in order to minimize anxiety effects on locomotion. All mice were placed into a corner of the apparatus at the beginning of the trial. The distance traveled, and time spent in the outer and inner zones was assessed with the ANY-maze software (4.20, Stoelting).

Dark/Light (DaLi) Box Test

The DaLi box test was used to assess anxiety-related behavior and performed in a rectangular apparatus (15 × 20 × 25 cm) consisting of an aversive brightly lit compartment (700 lux) and a more protective dark compartment (5 lux). At the start of the test, all mice were placed in the dark compartment and were allowed to freely explore the apparatus for 5 min. Lit zone entries were counted if at least the two front paws and half of the animal's body were inside the lit compartment. Automatic tracking was employed using the ANY-maze software (4.20, Stoelting).

Elevated Plus Maze (EPM) Test

In addition to the DaLi, the EPM was used to assess anxiety-related behavior. The apparatus consisted of a plus-shaped platform with four intersecting arms, elevated 37 cm above the floor. Two opposing open (30 × 5 cm) and closed (30 × 5 × 15 cm) arms were connected by a central zone (5 × 5 cm). Animals were placed in the center of the apparatus facing the closed arm and were allowed to freely explore the maze for 5 min. Automatic tracking was employed using the ANY-maze software (4.20; Stoelting). Percent open arm time was calculated as follows: open arm time (%) = open arm time/(open arm time + closed arm time).

Social Avoidance Test

The two-trial social avoidance test was modified from Berton et al. (2006), Golden et al. (2011). In the first trial, each experimental mouse was introduced into the open field arena for 2.5 min containing an empty wire mesh cage, placed at one side of the apparatus (marked as the interaction zone). During the second 2.5 min trial, test animals were confronted with an unfamiliar male CD1 mouse, which had previously been introduced into the wire mesh cage. The

ratio between the time in the interaction zone of the non-target trial and the time in the interaction zone of the target trial was calculated.

Forced Swim Test (FST)

The FST represents a well-established antidepressant-screening paradigm (Porsolt et al., 1977). Animals were carefully placed into a 2 l glass beaker (diameter: 13 cm, height: 24 cm) filled with tap water (22 ± 1°C) to a height of 15 cm, so that the mouse could not touch the bottom with its hind paws or tail. Testing duration was 6 min. The time spent immobile was scored by an experienced observer, blind to genotype or condition of the animals.

Acoustic Startle Response (ASR)

The ASR was modified from Golub et al. (2009). Mice were introduced into a non-restrictive plexiglas cylinder, which was mounted to a plastic platform located in a sound attenuated chamber (SR-LAB, San Diego Instruments SDI, San Diego, CA, United States). This set-up quantified changes in the conductance as a response to varying acoustic stimuli, which are then detected by a piezoelectric sensor located underneath each cylinder. The background noise was set to 50 dB. After an acclimatization period of 5 min, the mice were subjected to white noise bursts of varying intensities (75, 90, 105, and 115 dB) in a random order. The data are represented as mean peak startle amplitude in mV ± SEM in response to 136 randomized trials of the mentioned intensities including background noise measurements.

Fear Conditioning

Contextual and cued fear conditioning was performed in conditioning chambers (ENV-307A, MED Associates Inc.) as previously described (Dedic et al., 2018a). Foot shock (FS) delivery and context-dependent fear memory were assessed in a cube-shaped chamber with metal grid floors, which was thoroughly cleaned and sprayed with 70% ethanol before the animals were introduced (shock context). A neutral context consisting of a Plexiglas cylinder with bedding was used to investigate cued (tone-dependent) fear memory; it was cleaned and sprayed with 1% acetic acid (novel context).

For foot shock application (day 0), mice were placed into the conditioning chamber for 3 min. After 180 s, a sine wave tone (80 dB, 9 kHz) was presented for 20 s, which co-terminated with a 2 s scrambled electric foot shock of 1.5 mA. The mice remained in the shock chamber for another 60 s. To measure the freezing responses to the tone, mice were placed into the novel environment (cylinder) on the following day (day 1). Three minutes later, a 3 min tone was presented (80 dB, 9 kHz). The animals were returned to their home cages 60 s after the end of tone presentation. Contextual fear was tested by re-exposing the animals to the shock context for 3 min on day 2. In order to assess potential differences in long-term memory, all animals were exposed to the novel and familiar (shock) context 30 days later (days 31 and 32 respectively). As a measure of fear memory, freezing behavior was recorded and analyzed by an observer blind to genotype. Freezing was scored if the animals adopted an immobile posture (except for breathing-related movement)

with all four paws on the ground and the head in a horizontal position. Data were analyzed in 60 s bins and normalized to the observation interval.

Chronic Social Defeat Stress Paradigm

The chronic social defeat stress (CSDS) paradigm is commonly utilized to induce anxiety- and depression-related endophenotypes in mice and was performed as previously described (Wagner et al., 2011; Wang et al., 2011; Hartmann et al., 2012a, 2016; Gassen et al., 2014; Metzger et al., 2017; Dedic et al., 2018b). *Crh*^{Ctrl} and *Crh*^{CKO-GABA} mice (10–15 male mice per group between 3 and 4 months of age) were submitted to CSDS for 21 consecutive days. They were introduced into the home cage (45 cm × 25 cm) of a dominant CD1 resident for no longer than 5 min during which they experienced multiple bouts of defeat. Following defeat, animals spent 24 h in the same cage, which was separated via a perforated steel partition, enabling sensory but not physical contact. Every day experimental mice were exposed to a new unfamiliar resident. Defeat encounters were randomized, with variations in starting time in order to decrease the predictability to the stressor and minimize habituation effects. Control animals were housed in their home cages throughout the course of the experiment. Control and stressed mice were housed in the same room, but in different racks. All animals were handled daily and weighed. Behavioral testing was conducted during the last week of the CSDS paradigm in the following order: OF test, Social avoidance test, EPM, DaLi, and the FST. For evaluation of the corticosterone response to an acute stressor, blood samples were collected 30 min (response levels) after the start of FST by tail cut. All animals were killed by an overdose of isoflurane at the end of the experiment (1 day after the last CSDS encounter). Trunk blood was collected after decapitation for the assessment of basal corticosterone levels. Adrenal and thymus glands were removed, dissected from fat, and weighed.

Assessment of Immediate Early Gene (IEG) Expression

Stress-induced expression of IEGs c-fos and zif268 (also known as Krox-24, NGF1-A, Egr1, TIS8, and Zenk), was assessed in naïve *Crh*^{Ctrl} and *Crh*^{CKO-GABA} mice following FST. The animals were euthanized 30 min following the onset of the FST. The brains were carefully removed and immediately shock-frozen on dry ice and stored at −80°C until further processing for ISH.

Statistical Analyses

Statistical analyses were performed using the commercially available software SPSS v16.0 (SPSS, Chicago, IL, United States) and GraphPad Prism v7.0 (GraphPad Software, La Jolla, CA, United States). All results are presented as mean ± s.e.m. Statistical significance was defined as $p < 0.05$. Normality and equality of variance were analyzed with the D'Agostino-Pearson omnibus test and Bartlett's test, respectively. In cases where sample sizes were too small, data distribution was assumed to be normal. All data were tested for outliers using the Grubbs' test. Based on the results of these tests,

appropriate parametric (two-tailed unpaired *t*-test) or non-parametric (Mann-Whitney *U*-test) tests were performed. For CSDS experiments, the effects of genotype and condition on all other behavioral and neuroendocrine parameters were assessed by two factorial ANOVA (2-way ANOVA). Time-dependent measures were analyzed with repeated-measures ANOVA followed by Bonferroni *post hoc* analysis. Whenever significant main or interaction effects were found by the ANOVAs, Bonferroni *post hoc* tests were carried out to locate simple effects. Conditional knockout mice and control littermates were assigned to the experimental group on the basis of genotype. Age-matched littermates were used as controls in all experiments. Animals were allocated to the experimental groups in a semi-randomized manner and data analysis was performed blinded to the group allocation.

RESULTS

Crh mRNA Expression Mapping in *Crh*^{CKO-GABA} Mice

Using sensitive *in situ* hybridization (ISH) methods, we recently mapped the neurochemical identity of *Crh* neurons across the mouse brain, revealing an overwhelming majority of GABAergic (*Gad65/67*-positive) CRH neurons in the cortex, hippocampus, central nucleus of the amygdala (CeA) and the bed nucleus of the stria terminalis (BNST), which has also been reported by others (Kubota et al., 2011; Kubota, 2013; Dedic et al., 2018a; Gunn et al., 2019). In contrast, *Crh* neurons in the Pir and PVN primarily coexpressed the glutamatergic markers *Vglut1* and *Vglut2*, respectively (Dedic et al., 2018a). In order to dissect the role of *Crh* in GABAergic circuits we crossed the recently generated *Crh*^{flox/flox} mice with *Dlx5/6-Cre* transgenic mice (Rodríguez et al., 2000; Kamprath et al., 2006; Monory et al., 2006), in which *Cre* is driven by the regulatory sequences of the *Dlx5/Dlx6* homeobox genes expressed in migrating, forebrain GABAergic neurons during development (E10). Consequently, the resulting *Crh* deletion pattern in *Crh*^{CKO-GABA} mice was restricted specifically to GABAergic neurons of the forebrain (Figure 1) and was largely in line with the previously published *Crh* expression maps obtained with double ISH (Dedic et al., 2018a). Thus, absence of *Crh* mRNA expression was observed in the CeA, hippocampus and throughout the cortex of *Crh*^{CKO-GABA} mice (Figure 1B). Expectedly, *Crh* mRNA levels were comparable between control and *Crh*^{CKO-GABA} mice in the Pir, PVN and throughout the hindbrain and brainstem areas.

HPA Axis Activity, Baseline Locomotion, Anxiety, and Fear Memory Are Not Altered in *Crh*^{CKO-GABA} Mice

In order to assess whether lack of *Crh* from GABAergic forebrain neurons would affect HPA axis activity, we measured corticosterone release in *Crh*^{CKO-GABA} mice (Figure 2B). No differences in plasma corticosterone levels were detected between *Crh*^{CKO-GABA} mice and control littermates in the morning

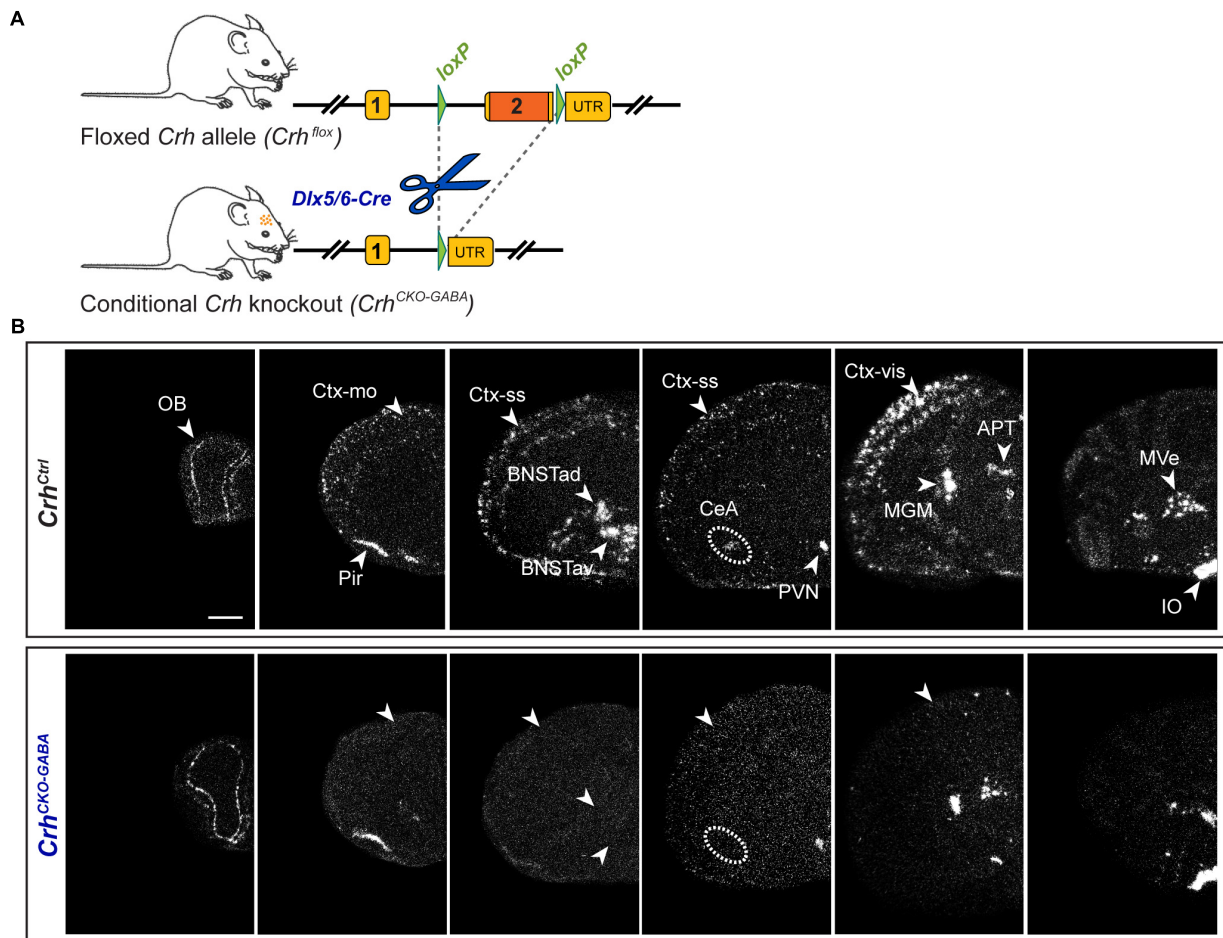


FIGURE 1 | *Crh* deletion pattern in conditional *Crh*^{CKO-GABA} mice. **(A)** Schematic representation of the previously established conditional inactivation of the *Crh* gene (Dedic et al., 2018a). Exon 2 is flanked by *loxP* sites. Breeding of *Crh*^{lox} mice to *Dlx5/6-Cre* driver mice resulted in *Crh* deletion specifically in GABAergic forebrain neurons. UTR, untranslated region. **(B)** Expression of *Crh* mRNA was assessed by ISH in control and *Crh*^{CKO-GABA} mice using a riboprobe, which detects the 3'UTR of *Crh*. Dark-field photomicrographs depict the specific *Crh* deletion pattern in *Crh*^{CKO-GABA} mice. Areas of interest are highlighted with arrowheads and dashed lines. Images are representative of three separate experiments. APT, anterior pretectal nucleus; CeA, central amygdala; BNSTad/v, anterior bed nucleus of the stria terminalis dorsal/ventral; CtxL/III, CtxV/VI, cortical layers; IO, inferior olive; MGM, medial geniculate nucleus; MVe, medial vestibular nucleus; Ctx-mo, motor cortex; OB, olfactory bulb; Pir, piriform cortex; PVN, paraventricular nucleus of the hypothalamus; Ctx-ss, somatosensory cortex; Ctx-vis, visual cortex. Scale bar represents 1 mm.

(am: unpaired *t*-test, $t_{26} = 0.57$, $p = 0.6$), evening (pm: unpaired *t*-test, $t_{22} = 0.19$, $p = 0.85$), as well as 10 and 90 min after restraint stress (stress: unpaired *t*-test, $t_{24} = 1.1$, $p = 0.29$ /recovery: unpaired *t*-test, $t_{19} = 1.15$, $p = 0.27$). In addition, no significant, genotype-mediated changes were observed in body weight (unpaired *t*-test, $t_{27} = 1.1$, $p = 0.3$; **Figure 2A**). To functionally dissect whether GABAergic neurons are mediating the effects of CRH on aspects of emotional behavior, *Crh*^{CKO-GABA} mice were subjected to a series of behavioral tests. In the Open field (OF) test, locomotor activity [repeated measures ANOVA, genotype $F_{(1, 27)} = 0.12$, $p = 0.73$], inner zone time (unpaired *t*-test, $t_{27} = 1.7$, $p = 0.1$) and the number of inner zone entries (unpaired *t*-test, $t_{27} = 1.0$, $p = 0.3$) were not significantly altered in *Crh*^{CKO-GABA} mice compared to controls (**Figure 2C**). Interestingly, *Crh*^{CKO-GABA} mice displayed no changes in anxiety-related behavior (**Figures 2D,E**) assessed

in the dark/light box (DaLi) and elevated plus maze (EPM) test [DaLi, unpaired *t*-test: lit zone time (%), $t_{25} = 0.42$, $p = 0.6$; lit zone entries, $t_{25} = 0.46$, $p = 0.6$; latency lit zone time (%), $t_{25} = 0.61$, $p = 0.5$ /EPM, unpaired *t*-test: open arm time (%), $t_{22} = 0.4$, $p = 0.7$; open arm entries (%), $t_{22} = 0.66$, $p = 0.5$; latency, $t_{22} = 0.46$, $p = 0.7$]. Similarly, immobility in the FST did not differ between *Crh*^{CKO-GABA} mice and littermate controls (unpaired *t*-test, $t_{27} = 0.46$, $p = 0.65$; **Figure 2F**).

The CRH system has been implicated in modulating aspects of the acoustic startle response, although both increased and decreased startle amplitudes have been observed following CRH overexpression and/or injection (Lee and Davis, 1997; Groenink et al., 2002, 2008; Flandreau et al., 2015). Control and *Crh*^{CKO-GABA} mice exhibited a characteristic, decibel-dependent increase in the acoustic startle response (**Figure 2G**), but no differences were observed between genotypes [repeated

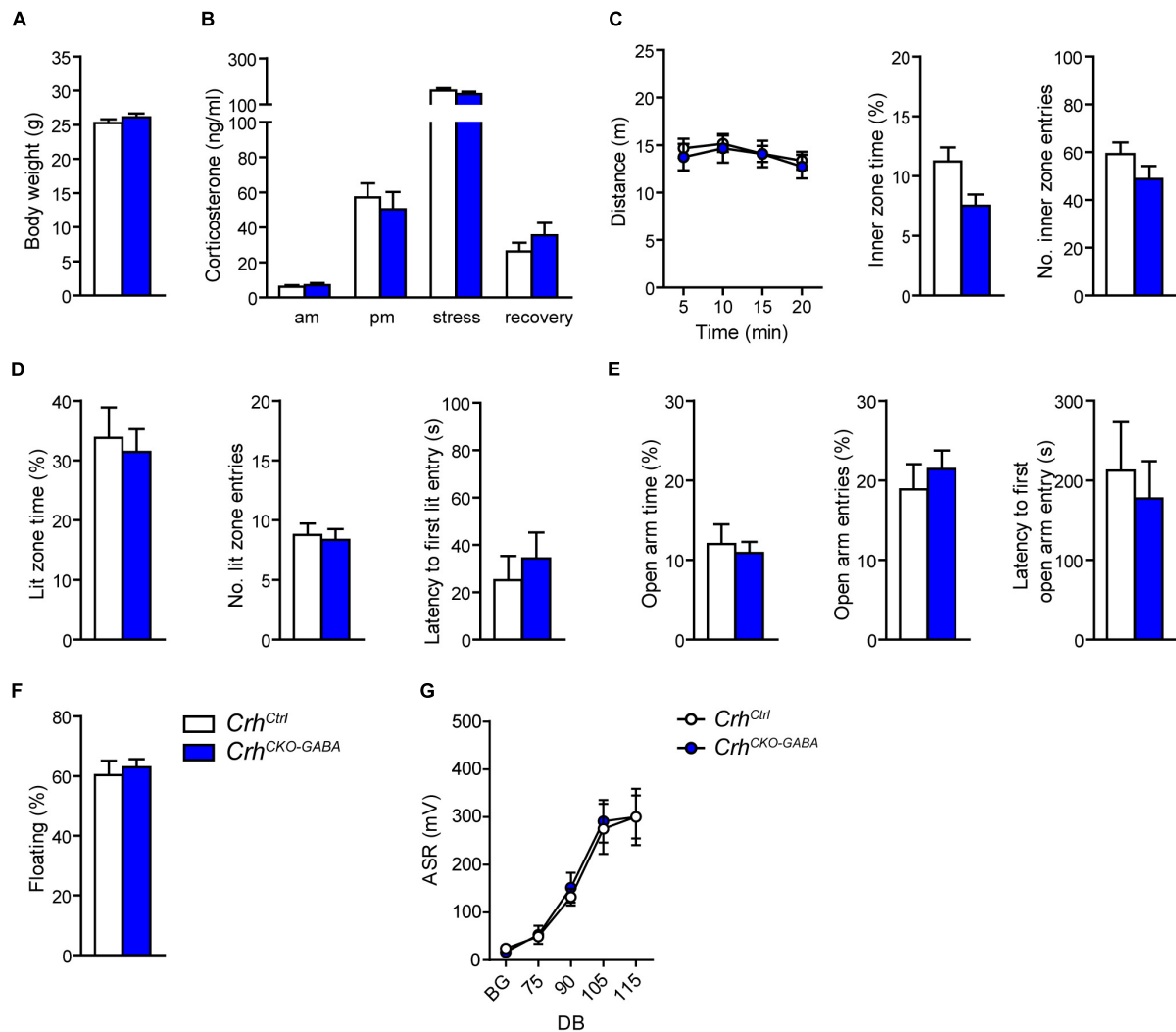


FIGURE 2 | *Crh* deletion in GABAergic forebrain neurons does not alter HPA axis activity, locomotion and anxiety-related behavior under baseline conditions. Body weight (A) as well as circadian and stress-induced corticosterone release (B) were not significantly changed in *Crh*^{CKO-GABA} mice compared to littermate controls. Similarly, spontaneous locomotion in the OF test (C), anxiety-related behavior in the DaLi (D) and EPM (E), immobility in the FST (F), and the acoustic startle response (G) did not significantly differ between genotypes. Unpaired two-tailed *t*-test; time- and decibel-dependent measures: repeated-measures ANOVA; $p < 0.05$; $n = 12$ –15/group). Data are shown as mean \pm s.e.m.

measures ANOVA; db $F_{(1, 96)} = 39.1$, $p < 0.0001$; genotype $F_{(1, 24)} = 0.04$, $p = 0.8$]. In view of CRH's important role in conditioned fear (Haubensak et al., 2010; Isogawa et al., 2013; Tovote et al., 2015; Sanford et al., 2016; Fadok et al., 2017; Dedic et al., 2018a), we additionally assessed auditory and contextual fear memory. *Crh*^{CKO-GABA} mice showed no significant changes in tone- and context-dependent freezing compared to control littermates (Figure 3). This was also the case when re-tested 30 days later, suggesting that long term fear memory is also not altered in *Crh*^{CKO-GABA} mice [repeated measures ANOVA; tone: genotype $F_{(1, 24)} = 0.06$, $p = 0.8$; tone d30: genotype $F_{(1, 23)} = 0.19$, $p = 0.7$ /context: genotype $F_{(1, 24)} = 0.05$, $p = 0.8$; context d30: genotype $F_{(1, 23)} = 0.006$, $p = 0.9$]. Overall, deletion of *Crh* from GABAergic forebrain neurons did not produce significant

differences in HPA axis activity or any of the evaluated behavioral endpoints.

Crh^{CKO-GABA} Mice Exhibit Deficits in Baseline Social Behavior and Resilience to Chronic Social Defeat Stress

Recent work has suggested that the CRH/CRHR1 system might exert different effects on emotional valence under physiological and severe stress conditions (Lemos et al., 2012; Dedic et al., 2018a). To assess whether deletion of *Crh* from GABAergic forebrain neurons would alter stress susceptibility, *Crh*^{CKO-GABA} mice were subjected to 3 weeks of CSDS, a paradigm commonly applied to induce anxiety- and depression-related endophenotypes in mice (Berton et al., 2006;

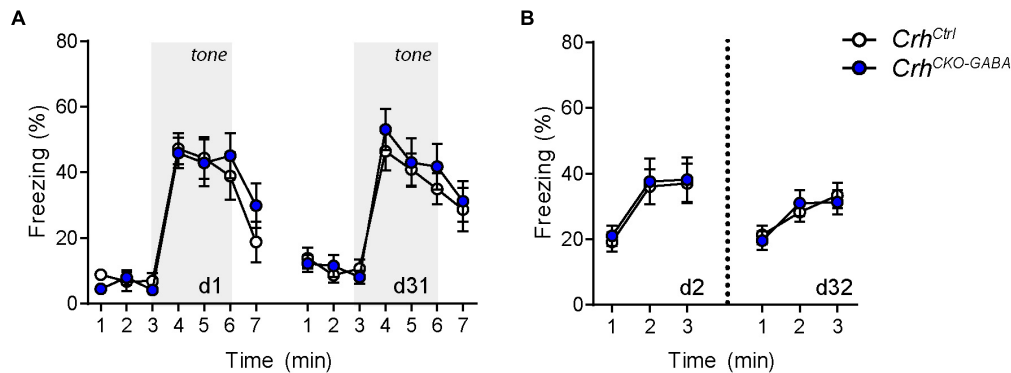


FIGURE 3 | Cued and context-dependent fear condition is not altered in *Crh*^{CKO-GABA} mice. **(A)** Auditory fear memory assessed one and 30 days after conditioning was not significantly altered in *Crh*^{CKO-GABA} mice compared to littermate controls. Both groups expressed similar levels of freezing in the novel context under baseline conditions (initial 3 min) and following exposure to the tone (3–6 min). **(B)** Expression of contextual fear memory was also not altered between genotypes. Repeated-measures ANOVA; $p < 0.05$; $n = 13/\text{group}$. Data are shown as mean \pm s.e.m.

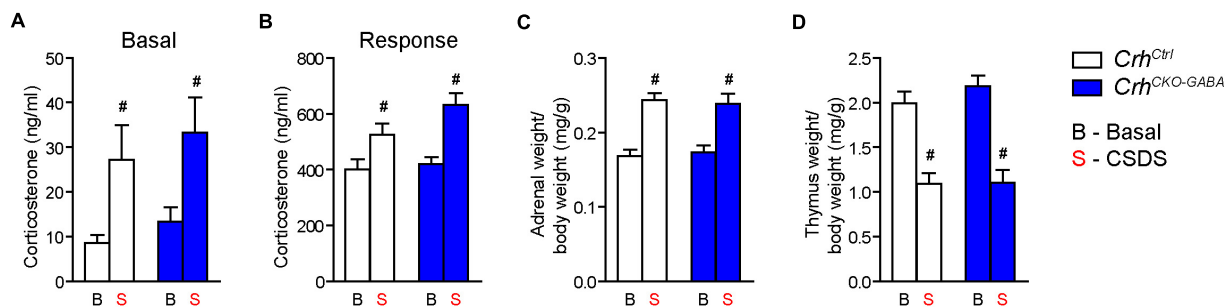


FIGURE 4 | CSDS induced similar neuroendocrine and physiological alterations in *Crh*^{CKO-GABA} and control mice. **(A)** Control and *Crh*^{CKO-GABA} mice showed increased basal corticosterone levels following exposure to 3 weeks of CSDS. **(B)** Corticosterone response levels assessed 30 min after a FST challenge, were significantly increased in chronically stressed mice independent of genotype. The efficacy of the CSDS paradigm was further demonstrated by a significant enlargement of the adrenal glands **(C)** and a substantial decrease in thymus size **(D)** in chronically stressed mice. Two-way ANOVA + Bonferroni *post hoc* test; #significantly different from the basal condition of the same genotype, $p < 0.05$; $n = 10\text{--}15/\text{group}$. Data are shown as mean \pm s.e.m.

Golden et al., 2011; Gassen et al., 2014; Hartmann et al., 2016; Dedic et al., 2018b).

Basal (Figure 4A) and acute-stress induced corticosterone levels (Figure 4B) were significantly elevated in chronically stressed mice independent of genotype [Basal: 2-way ANOVA, stress $F_{(1, 46)} = 10.4$, $p < 0.005$; Bonferroni *post hoc* test, $p < 0.05$ /Response: 2-way ANOVA, stress $F_{(1, 44)} = 20.4$, $p < 0.0001$; Bonferroni *post hoc* test, $p < 0.05$]. In addition, CSDS resulted in enhanced adrenal gland weight and decreased thymus weight in stressed *Crh*^{Ctrl} and *Crh*^{CKO-GABA} mice [AG: 2-way ANOVA, stress $F_{(1, 48)} = 42.5$, $p < 0.0001$; Bonferroni *post hoc* test, $p < 0.05$ /Thymus: 2-way ANOVA, stress $F_{(1, 48)} = 58.9$, $p < 0.0001$; Bonferroni *post hoc* test, $p < 0.05$; Figures 4C,D). These robust physiological and neuroendocrine changes evoked by CSDS validate the efficacy of the paradigm and are in line with previous studies (Wagner et al., 2011; Hartmann et al., 2012a,b, 2016; Gassen et al., 2014; Metzger et al., 2017; Dedic et al., 2018b). Spontaneous locomotion in the OF tests was significantly reduced in *Crh*^{Ctrl} and *Crh*^{CKO-GABA} mice following CSDS (Figure 5A), whereas inner zone time and number of entries were not affected [repeated measures-ANOVA, time \times

stress $F_{(1, 47)} = 4.8$, $p < 0.05$; stress $F_{(1, 48)} = 16.9$, $p < 0.0001$; Bonferroni *post hoc* test, $p < 0.05$; Figure 5B]. Locomotion was not significantly altered by genotype, both under basal and chronic stress conditions. The OF test was conducted under low illumination (15 lux) in order to minimize potential effects of anxiety on locomotion. This likely explains the lack of CSDS effects on inner zone time and number of entries.

Interestingly, *Crh*^{CKO-GABA} mice were less susceptible to the anxiety-inducing effects of CSDS (Figures 5C,D). The latencies to enter the aversive lit zone of the DaLi and open arms of the EPM were significantly increased in chronically stressed *Crh*^{Ctrl} but not *Crh*^{CKO-GABA} mice [DaLi: 2-way ANOVA, genotype \times stress $F_{(1, 43)} = 4.3$, $p < 0.05$; stress $F_{(1, 43)} = 4.2$, $p < 0.05$; Bonferroni *post hoc* test, $p < 0.05$ /EPM: 2-way ANOVA, genotype $F_{(1, 44)} = 4.6$, $p < 0.05$; stress $F_{(1, 44)} = 4.0$, $p = 0.051$; Bonferroni *post hoc* test, $p < 0.05$]. In accordance, lit zone time and number of entries were significantly reduced in controls following CSDS; this stress effect was absent in *Crh*^{CKO-GABA} mice [time: 2-way ANOVA, stress $F_{(1, 44)} = 4.9$, $p < 0.05$; Bonferroni *post hoc* test, $p < 0.05$ /entries: 2-way ANOVA, stress $F_{(1, 44)} = 12.2$, $p < 0.005$; Bonferroni *post hoc* test,

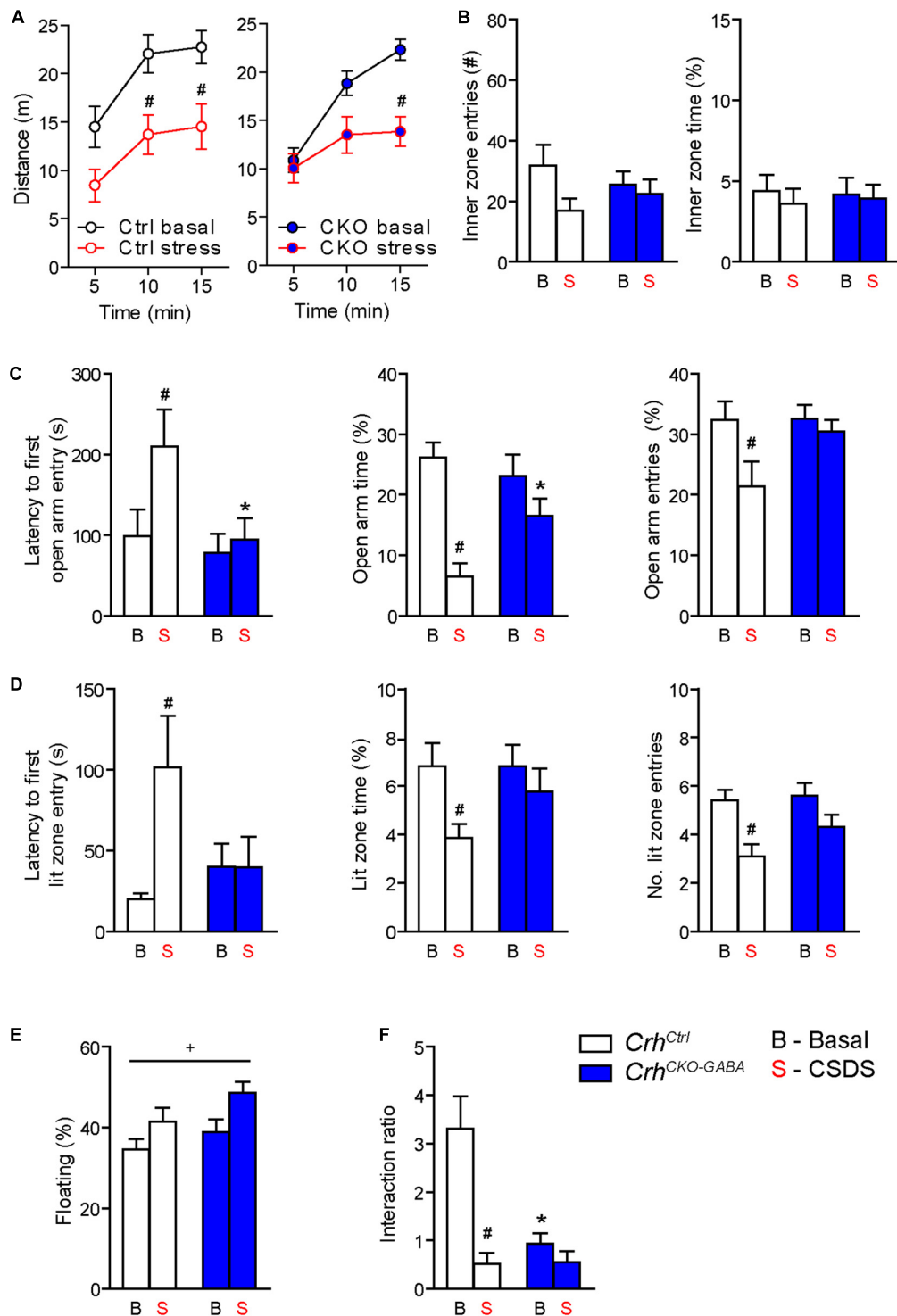


FIGURE 5 | *Crh* deletion from forebrain GABAergic neurons induces social deficits under baseline conditions and reduces the susceptibility to CSDS-induced anxiety. **(A,B)** CSDS reduced locomotion in the OF test, independent of genotype. Inner zone time and the number of inner zone entries were not significantly affected by stress or genotype. Following CSDS, anxiety-related behavior in the DaLi **(C)** and EPM **(D)** was significantly increased in control but not *Crh*^{CKO-GABA} mice. This is depicted by increased latencies to enter the aversive lit zone of the DaLi and open arms of the EPM, as well as significantly reduced lit/open arm times and entries in stressed control but not stressed *Crh*^{CKO-GABA} mice. **(E)** CSDS increased immobility in the FST independent of genotype. **(F)** CSDS reduced interaction ratios in control mice during the social avoidance test. This effect was absent in *Crh*^{CKO-GABA} mice, which displayed a significant reduction in social interaction already under baseline conditions. Two-way ANOVA or repeated measures ANOVA + Bonferroni *post hoc* test; * Significant from control of the same condition, #significant from the basal group of the same genotype, +significant condition effect; $p < 0.05$; $n = 10-15$ /group. Data are shown as mean \pm s.e.m.

$p < 0.05$). These results indicate that CRH in GABAergic neurons modulates the effects of CSDS on anxiety-related behavior. In addition, immobility in the FST was increased in chronically stressed mice, independent of genotype [2-way ANOVA, stress $F_{(1, 48)} = 12.2$, $p < 0.05$; **Figure 5E**]. As initially observed, no genotype effects were detected under baseline conditions in the DaLi, EPM, and FST.

Alterations in social behavior are observed in many psychiatric disorders including major depressive disorder, bipolar disorder, schizophrenia and autism (Nestler and Hyman, 2010; Kaiser and Feng, 2015). In addition, CSDS has repeatedly been shown to reduce social interaction and enhance avoidance behavior in rodents (Berton et al., 2006; Golden et al., 2011; Dedic et al., 2018b). To test whether *Crh* deletion from GABAergic forebrain neurons would affect social behavior under basal and chronic stress conditions, we performed the social avoidance test. Chronically stressed control mice spent significantly less time in close proximity to a social counterpart, indicated by a decreased interaction ratio (**Figure 5F**). Interestingly, compared to controls, *Crh*^{CKO-GABA} mice exhibited reduced social interaction already under basal conditions, which was not further aggravated following CSDS [2-way ANOVA, genotype \times stress $F_{(1, 41)} = 9.8$, $p < 0.005$; stress $F_{(1, 41)} = 17.0$, $p < 0.0005$; genotype $F_{(1, 41)} = 9.3$, $p < 0.005$; Bonferroni post-test, $p < 0.05$]. This suggests that CRH in GABAergic neurons is required for the expression of “normal” social behavior.

Stress-Induced Expression of Immediate Early Genes Is Reduced in *Crh*^{CKO-GABA} Mice

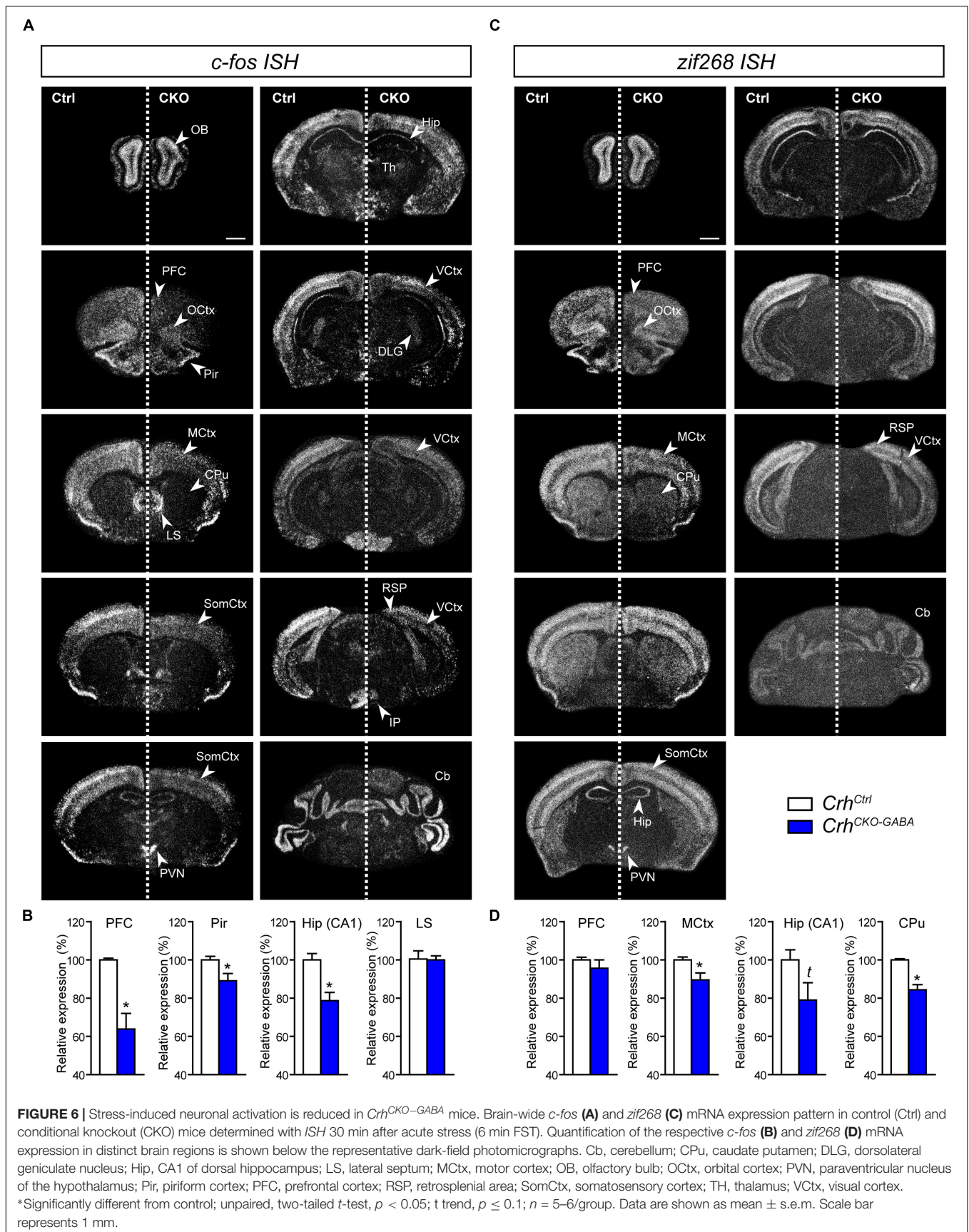
Following the observation that lack of *Crh* from forebrain GABAergic neurons promotes resilience to CSDS, we asked whether stress would induce similar patterns of neuronal activation in control and *Crh*^{CKO-GABA} mice. Thus, the mRNA expression of the immediate early genes *c-fos* and *zif268* was analyzed in naïve animals 30 min after exposure to an acute stressor (6 min of FST) using ISH. *C-fos* and *zif268* have been commonly used to map neuronal activity in different brain regions of various species. Both are rapidly and transiently induced by a variety of stimuli including stress, and show overlapping as well as distinct expression patterns following specific stimuli (Sagar et al., 1988; Sheng and Greenberg, 1990; Cullinan et al., 1995; Guzowski et al., 2001; Leslie and Nedivi, 2011; Veyrac et al., 2014; Farina and Commins, 2016; Gallo et al., 2018; Bisagno and Cadet, 2019). *C-fos* and *zif268* expression is consistently low under baseline conditions and was not significantly different between control and *Crh*^{CKO-GABA} mice (data not shown). Following acute FST-stress, a marked increase of *c-fos* and *zif268* expression was detected throughout the brain of *Crh*^{Ctrl} and *Crh*^{CKO-GABA} mice (**Figure 6**). However, diminished *c-fos* expression was observed in the dorsal hippocampus and most cortical areas of *Crh*^{CKO-GABA} compared to control animals (**Figures 6A,B**). Similar effects were observed for *zif268*, where decreased activation was additionally detected in the caudate putamen of *Crh*^{CKO-GABA} mice compared to

controls (**Figures 6C,D**). These results demonstrate that CRH depletion from GABAergic neurons attenuates stress-induced neuronal activity changes in CRHR1-expressing brain regions such as the cortex and hippocampus. This is further supported by the fact that *c-fos* expression was not differentially altered in the PVN of *Crh*^{CKO-GABA} mice, a structure largely devoid of CRHR1 and CRHR2 (Van Pett et al., 2000). Our findings suggest that deletion of *Crh* in GABAergic neurons protects from the adverse effects of CSDS, possibly by reducing stress-induced neuronal activation.

DISCUSSION

The central peptidergic CRH/CRHR1 system impinges on a broad spectrum of physiological processes that are the basis for successful adaptation and concomitantly integrate autonomic, neuroendocrine, and behavioral stress responses. Accordingly, dysregulation of the CRH/CRHR1 system has been observed in stress-related psychopathologies including depression and anxiety disorders (Laryea et al., 2012; Deussing, 2013; Janssen and Kozicz, 2013; Henckens et al., 2016; Dedic et al., 2017). It has widely been accepted that CRH-CRHR1 signaling promotes the stress response and aversive behaviors, but more recent findings provide clear evidence for a requirement of specific CRH circuits in positive emotional valence and appetitive responses (Lemos et al., 2012; Dedic et al., 2018a). Thus, a more complex picture has emerged, suggesting that there are brain region- and cell type-specific effects of CRH/CRHR1 signaling that are influenced by the individual's prior experience and that shape molecular, cellular and ultimately behavioral responses to stressful challenges (Henckens et al., 2016; Dedic et al., 2017).

We recently demonstrated that a specific subpopulation of VTA-projecting, GABAergic CRH neurons in the extended amygdala (CeA and BNST) act anxiety-suppressing by positively modulating dopamine release under physiological conditions (Dedic et al., 2018a). These neurons are characterized by the co-expression of *Camk2a* and account for approximately one third of the CRH population in the CeA and BNST. Since absence of *Crh* specifically in GABAergic, *Camk2a*-expressing CRH neurons increased anxiety, we wondered whether deletion of the neuropeptide from the entire GABAergic forebrain population would produce a similar or distinct phenotype. Moreover, we addressed whether *Crh*^{CKO-GABA} mice would display differential behaviors under baseline and chronic stress conditions. Mapping analyses in *Crh*^{CKO-GABA} mice showed complete lack of *Crh* mRNA in the CeA, BNST, hippocampus and throughout most of the cortex, which is in line with previous studies reporting predominant expression of cortical and limbic CRH in GABAergic neurons (Chen et al., 1998, 2001; Kubota et al., 2011; Kubota, 2013; Dedic et al., 2018a; Gunn et al., 2019). To our initial surprise, *Crh*^{CKO-GABA} mice showed no gross behavioral changes in locomotion, anxiety, startle response and fear memory, but exhibited social deficits under baseline conditions. This is partially in line with earlier studies reporting normal baseline locomotor activity, exploration, anxiety, startle response and learning in conventional *Crh* knockout (*Crh* null)



mice (Weninger et al., 1999). In contrast, specific deletion of *Crh* from GABAergic, *Camk2α*-expressing neurons increases anxiety and fear memory expression (Dedic et al., 2018a). A possible explanation for the discrepancy in anxiety- and fear-related behavior between the two mouse lines could be the fact that *Crh*^{CKO-GABA} mice lack *Crh* in GABAergic circuits that modulate positive and negative emotional valence. In addition, *Camk2α-CreERT2*-induced deletion of *Crh* is initiated during adulthood as opposed to *Dlx5/6-Cre*-driven recombination in *Crh*^{CKO-GABA} mice, which occurs during embryonic development (E10). Thus, differences in deletion time points and/or subsequent compensatory mechanisms between *Crh*^{CKO-Camk2α} and *Crh*^{CKO-GABA} mice might account for the difference in anxiety-related behavior. Along these lines, mice carrying a PVN-restricted deletion of *Crh* (*Sim1CrhKO*) exhibit reduced anxiety under baseline conditions (Zhang et al., 2017). These suggest that PVN CRH neurons are likely modulating aversive responses in naïve animals, which has also been observed by others (Füzesi et al., 2016; Kim et al., 2019). The lack of effect on baseline anxiety in *Crh*^{CKO-GABA} mice further support this, given the fact *Crh* expression is absent from cortical and limbic regions but preserved in the PVN of these animals.

Overexpression of CRH has repeatedly been shown to induce stress-like behavioral responses including increased fear and anxiety under baseline conditions (Stenzel-Poore et al., 1994; Van Gaalen et al., 2002; Lu et al., 2008; Kolber et al., 2010; Dedic et al., 2012; Flandreau et al., 2012). However, overexpression studies are limited in their ability to accurately reflect the endogenous function of specific CRH subpopulations, which is primarily due to ectopic and non-physiological expression of the peptide in the brain. In addition, corticosterone release is dysregulated in many CRH overexpressing lines as well as CRH null mice (Muglia et al., 1995; Dedic et al., 2018a), which can obscure the interpretations of the behavioral results. In contrast, HPA axis activity was not significantly altered in *Crh*^{CKO-GABA} mice, due to the lack of *Dlx5/6-Cre* mediated recombination in CRH-expressing neurons of the PVN. This suggests that CRH drive in the PVN, rather than other extrahypothalamic sites, is primarily responsible for regulating HPA axis function.

Interestingly, *Crh*^{CKO-GABA} mice exhibited significantly reduced social interaction (increased social avoidance) compared to controls under basal conditions. This implies a requirement of CRH in forebrain GABAergic neurons for the expression of “normal” social behavior. These observations are partially in line with the work of Kasahara and colleagues, which demonstrated enhanced social investigation in CRH overexpressing mice (Kasahara et al., 2011). In contrast, BNST and amygdala-specific CRH administration were shown to decrease social interaction (Dunn and File, 1987; Sajdyk et al., 1999; Lee et al., 2008). Along these lines, CRH infusion into the nucleus accumbens propagates stress-induced social avoidance (mimicked by optogenetic activation of VTA-NAc projections). However, in the absence of stress or optical stimulation, CRH application to the NAc produced no alterations in social behavior (Walsh et al., 2014). Similarly, knockdown of *Crh* in the PVN attenuated social avoidance in chronic social defeated mice, without altering social interaction under basal conditions (Elliott et al., 2010). However,

possible alterations in HPA axis function, which could have been caused by *Crh* knockdown in the PVN, were not assessed in that study. Thus, it cannot be excluded that the observed phenotype is partially caused by reduced glucocorticoid levels. Importantly, results obtained after exogenous CRH application have to be interpreted with caution considering that these experiments are only mimicking acute effects of CRH hyperdrive. In addition, enhanced receptor activation following exogenous CRH application or overexpression might overshadow normal patterns of endogenous CRH release. Furthermore, co-activation of CRHR2 might obscure the relevance of CRH-CRHR1 signaling in social behavior. This is supported by the fact that *Ucn3*-, *Ucn2*- (specific CRHR2 ligands), and *Crhr2*-deficient mice display alterations in social behavior (Deussing et al., 2010; Breu et al., 2012). Importantly, social avoidance/approach paradigms are often confounded by anxiety, such that anxious animals are more likely to display reduced social engagement. This was not the case for *Crh*^{CKO-GABA} mice, which displayed no alterations in anxiety under baseline conditions.

In accordance with recent studies, our data further support the presence of distinct CRH circuits that have the ability to positively regulate emotional valence under physiological (non-stress) conditions. Importantly, severe stress was previously reported to switch the action of CRH from appetitive to aversive (Lemos et al., 2012). Specifically, CRH produces an appetitive effect in the nucleus accumbens under basal conditions, which resulted from CRH's ability to positively regulate dopamine release (Lemos et al., 2012). However, repeated stress exposure was shown to induce a persistent dysregulation of CRH-dopamine interactions that normally produce a positive affective state, resulting in an aversive phenotype. Along these lines, we showed that enhanced CRH/CRHR1 signaling in the VTA produces an anxiolytic effect in naïve animals (Dedic et al., 2018a); an effect that is lost following chronic drug exposure, in which CRH action in the VTA becomes aversive/anxiogenic (George et al., 2012; Grieder et al., 2014). In addition to the effects on emotional and reward behavior, recent experiments showed that CRH within the inferior olive of the brain stem modulates motor capabilities of mice under challenging, but not baseline conditions (Ezra-Nevo et al., 2018). In line of these results, we investigated whether deletion of *Crh* from forebrain GABAergic neurons might confer resilience to a severe, long-term stressor. Following exposure to CSDS, increased anxiety-related behavior was detected in control but not *Crh*^{CKO-GABA} mice. These findings are in line with a large body of work demonstrating the ability of CRHR1 antagonists to block stress-induced behavioral alterations (Heinrichs et al., 1992; Swiergiel et al., 1993; Liebsch et al., 1995; Shaham et al., 1998; Weninger et al., 1999; Habib et al., 2000; Gully et al., 2002; Zorrilla et al., 2002; Ducottet et al., 2003; Robison et al., 2004; Roozendaal et al., 2008; Bruijnzeel et al., 2009; Ivy et al., 2010; Gilpin et al., 2016). Along these lines, forebrain-specific deletion of *Crhr1* decreases the susceptibility to chronic stress-induced cognitive deficits (Wang et al., 2011, 2012, 2013). Of note, the protective effects in *Crh*^{CKO-GABA} mice were specifically observed for anxiety behavior. Neither locomotion, immobility in the FST or any of the physiological parameters were differentially affected by CSDS in control and *Crh*^{CKO-GABA} mice. Thus, the

effects on anxiety were independent of altered locomotion or HPA axis function. Social avoidance in *Crh*^{CKO-GABA} mice was not further aggravated by CSDS most likely due to the established floor effect under basal conditions.

Subsequent molecular assessment in *Crh*^{CKO-GABA} mice revealed a significant reduction in stress-induced mRNA levels of immediate early genes *c-fos* and *zif268* in CRHR1-expressing brain regions, including the hippocampus and cortex. Whether lack of *Crh* from GABAergic forebrain neurons induces compensatory regulation of CRHR1, CRHR2, and Urocortin expression remains to be investigated. Overall, the results in *Crh*^{CKO-GABA} mice mirror the activating effects of central CRH application on *c-fos* expression (Dunn and Berridge, 1990; Liebsch et al., 1995; Benoit et al., 2000; Bittencourt and Sawchenko, 2000; Rostkowski et al., 2013; Wiersielis et al., 2016; Salvatore et al., 2018). Along these lines, CRHR1-antagonist treatment block CRH- and stress-induced increases in *c-fos* expression (Doyon et al., 2007; Skórzewska et al., 2008). Given its ability to facilitate excitatory neurotransmission in regions such as the amygdala and hippocampus, CRH is generally denoted as an activating neuropeptide (Aldenhoff et al., 1983; Hollrigel et al., 1998; Giesbrecht et al., 2010; Refojo et al., 2011; Kratzer et al., 2013). As previously mentioned, CRH administration into different brain regions can induce *c-fos* expression and mimic acute-stress effects. In addition, CNS-specific CRH overexpressing mice demonstrate enhanced *c-fos* and *zif268* activation of the locus coeruleus following forced-swim stress (Lu et al., 2008). Thus, it seems plausible that deletion of *Crh* from most cortical and all limbic regions would produce a net inhibitory effect, exhibited by decreased stress-induced *c-fos* activation. Dampened neuronal activity in response to an acute challenge likely underlies aspects of stress-resilience in *Crh*^{CKO-GABA} mice. The necessity to uncover the precise mechanisms by which CRH acts in an excitatory fashion becomes evident inline of the fact that CRH is primarily released from inhibitory GABAergic neurons.

It is still not entirely understood how sensory information is represented and evaluated by specific CRH/CRHR1 circuits to produce discrete autonomic and behavioral outputs. An earlier study reported demethylation of the CRH-promoter region, which resulted in enhanced *Crh* gene expression in the PVN of mice that were susceptible to chronic defeat stress (Elliott et al., 2010). Knockdown of *Crh* in the PVN attenuated defeat-induced behavioral alterations. To what extent CSDS alters *Crh* methylation in other brain regions remains to be explored. Thus, epigenetic regulation of CRH likely constitutes a mechanism by which the brain regulates long-term behavioral responses to stress. Moreover, stress was shown to induce metaplasticity in PVN CRH neurons at glutamate synapses, which ultimately primed behavioral and physiological responses (Sterley et al., 2018). In addition, recent calcium imaging experiments revealed the ability of PVN CRH neurons to respond in a rapid and biphasic manner to encode positive and negative valence of specific stimuli (Kim et al., 2019). More specifically, PVN CRH neurons are immediately activated by aversive cues (e.g., FST, predator odor or food deprivation)

and are rapidly suppressed by appetitive stimuli (e.g., palatable food or social interaction). These findings are consistent with previous work showing that activation of hypothalamic and amygdalar CRH circuits results in aversive or fear-related responses (Füzesi et al., 2016; Sanford et al., 2016; Fadok et al., 2017; Zhang et al., 2017; Sterley et al., 2018). However, it will be important to address whether the diverse behavioral effects are actually driven by changes in CRH release or potentially modulated by other, co-expressed neurotransmitters and/or neuromodulators.

In addition to the repeatedly described limbic CRH networks that drive aversive behavioral responses, our current and previous work have revealed the presence of specific GABAergic CRH circuits that modulate positive emotional and social valence under baseline conditions. This suggests the presence of distinct GABAergic CRH circuits that function in a concerted but antagonistic manner to keep emotional responses under physiological conditions in balance. This concept was initially observed for CRHR1, showing that CRHR1-controlled glutamatergic and dopaminergic circuits modulate anxiogenic and anxiolytic responses under baseline conditions (Refojo et al., 2011). Whether CRHR1 signaling in dopaminergic neurons retains anxiety-suppressing properties following exposure to chronic stress remains to be investigated. Interestingly, deletion of *Crh* from GABAergic forebrain neurons confers resilience to chronic stress-induced anxiety, supporting the hypothesis that CRH action can switch from positive to negative in the presence of chronic, uncontrollable stress. In contrast to acute stressors, which can be highly beneficial by priming the brain toward optimal alertness, behavioral and cognitive performance, adverse life events such as trauma and/or chronic stress represent strong risk factors for multiple neuropsychiatric disorders and can exacerbate mood-related psychopathologies. Thus, understanding the underlying molecular mechanisms by which specific stress circuits lose their motivational properties to become pathological is of utter importance for the development of novel treatments for stress-related psychiatric disorders.

DATA AVAILABILITY

All datasets generated for this study are included in the manuscript and/or the supplementary files.

ETHICS STATEMENT

The animal study was reviewed and approved by the Regierung von Oberbayern, Munich.

AUTHOR CONTRIBUTIONS

ND and JD conceived and designed the study, and wrote the manuscript. ND performed the experiments and analyzed the data. CK generated the conditional knockout mutants. CK, KG, and JH assisted with behavioral experiments and data acquisition.

KR and MS contributed to the interpretation of the data and revised the manuscript.

FUNDING

This work was supported by grants from the Max Planck Society, the German Federal Ministry of Education and Research, within the framework of the e:Med research and funding concept (IntegraMent: FKZ 01ZX1314H to JD), the Marie Skłodowska-Curie innovative training network PurinesDX (JD); and by the

program supporting scientific and technological cooperation between Germany and Argentina (FKZ 01DN16028 to JD). KG was a recipient of a scholarship from FAPESP (2013/03445-3).

ACKNOWLEDGMENTS

Partially included content first appeared in the thesis of ND (Dedic, 2015). We thank Sabrina Bauer, Daniela Harbich, and Bianca Schmid for excellent technical support and Carsten T. Wotjak for providing core unit infrastructure.

REFERENCES

- Aldenhoff, J., Gruol, D., Rivier, J., Vale, W., and Siggins, G. (1983). Corticotropin releasing factor decreases postburst hyperpolarizations and excites hippocampal neurons. *Science* 221, 855–857.
- Benoit, S. C., Thiele, T. E., Heinrichs, S. C., Rushing, P. A., Blake, K. A., and Steeley, R. J. (2000). Comparison of central administration of corticotropin-releasing hormone and urocortin on food intake, conditioned taste aversion, and c-Fos expression. *Peptides* 21, 345–351. doi: 10.1016/S0196-9781(00)00153-4
- Berton, O., McClung, C. A., Dileone, R. J., Krishnan, V., Renthal, W., Russo, S. J., et al. (2006). Essential role of BDNF in the mesolimbic dopamine pathway in social defeat stress. *Science* 311, 864–868. doi: 10.1126/science.1120972
- Bisagno, V., and Cadet, J. L. (2019). Expression of immediate early genes in brain reward circuitries: differential regulation by psychostimulant and opioid drugs. *Neurochem. Int.* 124, 10–18. doi: 10.1016/j.neuint.2018.12.004
- Bittencourt, J. C., and Sawchenko, P. E. (2000). Do centrally administered neuropeptides access cognate receptors? an analysis in the central corticotropin-releasing factor system. *J. Neurosci.* 20, 1142–1156. doi: 10.1523/jneurosci.20-03-01142.2000
- Breu, J., Touma, C., Hölter, S. M., Knapman, A., Wurst, W., and Deussing, J. M. (2012). Urocortin 2 modulates aspects of social behaviour in mice. *Behav. Brain Res.* 233, 331–336. doi: 10.1016/j.bbr.2012.05.031
- Buijzeel, A. W., Prado, M., and Isaac, S. (2009). Corticotropin-releasing factor-1 receptor activation mediates nicotine withdrawal-induced deficit in brain reward function and stress-induced relapse. *Biol. Psychiatry* 66, 110–117. doi: 10.1016/j.biopsych.2009.01.010
- Chen, Y., Bender, R. A., Frotscher, M., and Baram, T. Z. (1998). Novel and transient populations of corticotropin-releasing hormone-expressing neurons in developing hippocampus suggest unique functional roles: a quantitative spatiotemporal analysis. *J. Neurosci.* 21, 7171–7181. doi: 10.1523/jneurosci.21-18-07171.2001
- Chen, Y., Bender, R. A., Frotscher, M., and Baram, T. Z. (2001). Novel and transient populations of corticotropin-releasing hormone-expressing neurons in developing hippocampus suggest unique functional roles: a quantitative spatiotemporal analysis. *J. Neurosci.* 21, 7171–7181. doi: 10.1523/jneurosci.21-18-07171.2001
- Cullinan, W. E., Herman, J. P., Battaglia, D. F., Akil, H., and Watson, J. (1995). Pattern and time course of immediate early gene expression in rat brain following acute stress. *Neuroscience* 64, 477–505. doi: 10.1016/0306-4522(94)00355-9
- Dabrowska, J., Hazra, R., Guo, J. -D., Dewitt, S., and Rannin, D. G. (2013). Central CRF neurons are not created equal: phenotypic differences in CRF-containing neurons of the rat paraventricular hypothalamus and the bed nucleus of the stria terminalis. *Front. Neurosci.* 7:156. doi: 10.3389/fnins.2013.00156
- Dedic, N. (2015). *Genetic Dissection of CRH-Controlled Neurocircuitries of Stress*. Ph.D. Thesis, Technical University of Munich, Munich.
- Dedic, N., Chen, A., and Deussing, J. (2017). The CRF family of neuropeptides and their receptors - mediators of the central stress response. *Curr. Mol. Pharmacol.* 11, 4–31. doi: 10.2174/1874467210666170302104053
- Dedic, N., Kühne, C., Jakovcevski, M., Hartmann, J., Genewsky, A. J., Gomes, K. S., et al. (2018a). Chronic CRH depletion from GABAergic, long-range projection neurons in the extended amygdala reduces dopamine release and increases anxiety. *Nat. Neurosci.* 21, 803–807. doi: 10.1038/s41593-018-0151-z
- Dedic, N., Pöhlmann, M. L., Richter, J. S., Mehta, D., Czamara, D., Metzger, M. W., et al. (2018b). Cross-disorder risk gene CACNA1C differentially modulates susceptibility to psychiatric disorders during development and adulthood. *Mol. Psychiatry* 23, 533–543. doi: 10.1038/mp.2017.133
- Dedic, N., Touma, C., Romanowski, C. P., Schieven, M., Kühne, C., Ableitner, M., et al. (2012). Assessing behavioural effects of chronic HPA axis activation using conditional CRH-overexpressing mice. *Cell. Mol. Neurobiol.* 32, 815–828. doi: 10.1007/s10571-011-9784-9780
- Deussing, J. M. (2013). Targeted mutagenesis tools for modelling psychiatric disorders. *Cell Tissue Res.* 354, 9–25. doi: 10.1007/s00441-013-1708-1705
- Deussing, J. M., Breu, J., Kühne, C., Kallnik, M., Bunck, M., Glasl, L., et al. (2010). Urocortin 3 modulates social discrimination abilities via corticotropin-releasing hormone receptor type 2. *J. Neurosci.* 30, 9103–9116. doi: 10.1523/JNEUROSCI.1049-10.2010
- Deussing, J. M., and Chen, A. (2018). The corticotropin-releasing factor family: physiology of the stress response. *Physiol. Rev.* 98, 2225–2286. doi: 10.1152/physrev.00042.2017
- Doyon, C., Samson, P., Lalonde, J., and Richard, D. (2007). Effects of the CRF1 receptor antagonist SSR125543 on energy balance and food deprivation-induced neuronal activation in obese Zucker rats. *J. Endocrinol.* 193, 11–19. doi: 10.1677/joe.1.07064
- Ducottet, C., Griebel, G., and Belzung, C. (2003). Effects of the selective nonpeptide corticotropin-releasing factor receptor 1 antagonist antalarmin in the chronic mild stress model of depression in mice. *Prog. Neuro Psychopharmacol. Biol. Psychiatry* 27, 625–631. doi: 10.1016/S0278-5846(03)00051-4
- Dunn, A. J., and Berridge, C. W. (1990). Physiological and behavioral responses to corticotropin-releasing factor administration: is CRF a mediator of anxiety or stress responses? *Brain Res. Rev.* 15, 71–100. doi: 10.1016/0165-0173(90)90012-d
- Dunn, A. J., and File, S. E. (1987). Corticotropin-releasing factor has an anxiogenic action in the social interaction test. *Horm. Behav.* 21, 193–202. doi: 10.1016/0018-506x(87)90044-4
- Elliott, E., Ezra-Nevo, G., Regev, L., Neufeld-Cohen, A., and Chen, A. (2010). Resilience to social stress coincides with functional DNA methylation of the Crf gene in adult mice. *Nat. Neurosci.* 13, 1351–1353. doi: 10.1038/nn.2642
- Ezra-Nevo, G., Volk, N., Ramot, A., Kuehne, C., Tsoory, M., Deussing, J., et al. (2018). Inferior olive CRF plays a role in motor performance under challenging conditions. *Transl. Psychiatry* 8:107. doi: 10.1038/s41398-018-0145-3
- Fadok, J. P., Krabbe, S., Markovic, M., Courtin, J., Xu, C., Massi, L., et al. (2017). A competitive inhibitory circuit for selection of active and passive fear responses. *Nature* 542, 96–100. doi: 10.1038/nature21047
- Farina, F. R., and Commins, S. (2016). Differential expression of immediate early genes Zif268 and c-Fos in the hippocampus and prefrontal cortex following spatial learning and glutamate receptor antagonism. *Behav. Brain Res.* 307, 194–198. doi: 10.1016/j.bbr.2016.04.002
- Flandreau, E. I., Ressler, K. J., Owens, M. J., and Nemeroff, C. B. (2012). Chronic overexpression of corticotropin-releasing factor from the central amygdala produces HPA axis hyperactivity and behavioral anxiety associated with gene-expression changes in the hippocampus and paraventricular nucleus of the hypothalamus. *Psychoneuroendocrinology* 37, 27–38. doi: 10.1016/j.psyneuen.2011.04.014
- Flandreau, E., Risbrough, V., Lu, A., Ableitner, M., Geyer, M. A., Holsboer, F., et al. (2015). Cell type-specific modifications of corticotropin-releasing factor (CRF)

- and its type 1 receptor (CRF1) on startle behavior and sensorimotor gating. *Psychoneuroendocrinology* 53, 16–28. doi: 10.1016/j.psyneuen.2014.12.005
- Füzesi, T., Daviu, N., Wamsteeker Cusulin, J. I., Bonin, R. P., and Bains, J. S. (2016). Hypothalamic CRH neurons orchestrate complex behaviours after stress. *Nat. Commun.* 7:11937. doi: 10.1038/ncomms11937
- Gallo, F. T., Kathe, C., Morici, J. F., Medina, J. H., and Weisstaub, N. V. (2018). Immediate early genes, memory and psychiatric disorders: focus on c-fos, Egr1 and Arc. *Front. Behav. Neurosci.* 12:79. doi: 10.3389/fnbeh.2018.00079
- Gassen, N. C., Hartmann, J., Zschocke, J., Stepan, J., Hafner, K., Zellner, A., et al. (2014). Association of FKBP51 with priming of autophagy pathways and mediation of antidepressant treatment response: evidence in cells, mice, and humans. *PLoS Med.* 11:e1001755. doi: 10.1371/journal.pmed.1001755
- George, O., Le Moal, M., and Koob, G. F. (2012). Allostasis and addiction: role of the dopamine and corticotropin-releasing factor systems. *Physiol. Behav.* 106, 58–64. doi: 10.1016/j.physbeh.2011.11.004
- Giesbrecht, C. J., Mackay, J. P., Silveira, H. B., Urban, J. H., and Colmers, W. F. (2010). Countervailing modulation of Ih by neuropeptide Y and corticotropin-releasing factor in basolateral amygdala as a possible mechanism for their effects on stress-related behaviors. *J. Neurosci.* 30, 16970–16982. doi: 10.1523/JNEUROSCI.2306-10.2010
- Gilpin, N. W., Richardson, H. N., Baynes, B. B., Lu, Y. -L., and Schreiber, A. L. (2016). Corticotropin-releasing factor in ventromedial prefrontal cortex mediates avoidance of a traumatic stress-paired context. *Neuropharmacology* 113, 323–330. doi: 10.1016/j.neuropharm.2016.05.008
- Golden, S. A., Covington, H. E., Berton, O., and Russo, S. J. (2011). A standardized protocol for repeated social defeat stress in mice. *Nat. Protoc.* 6, 1183–1191. doi: 10.1038/nprot.2011.361
- Golub, Y., Mauch, C. P., Dahlhoff, M., and Wotjak, C. T. (2009). Consequences of extinction training on associative and non-associative fear in a mouse model of posttraumatic stress disorder (PTSD). *Behav. Brain Res.* 205, 544–549. doi: 10.1016/j.bbr.2009.08.019
- Grieder, T. E., Herman, M. A., Contet, C., Tan, L. A., Vargas-Perez, H., Cohen, A. E., et al. (2014). VTA CRF neurons mediate the aversive effects of nicotine withdrawal and promote intake escalation. *Nat. Neurosci.* 17, 1751–1758. doi: 10.1038/nn.3872
- Groenink, L., Dirks, A., Verdouw, P. M., de Graaff, M., Peeters, B. W., Millan, M. J., et al. (2008). CRF1 not glucocorticoid receptors mediate prepulse inhibition deficits in mice overexpressing CRF. *Biol. Psychiatry* 63, 360–368. doi: 10.1016/j.biopsych.2007.06.002
- Groenink, L., van der Gugten, J., Schipholt, M. I., Geyer, M. A., Dirks, A., Hijzen, T. H., et al. (2002). Reduced startle reactivity and plasticity in transgenic mice overexpressing corticotropin-releasing hormone. *Biol. Psychiatry* 51, 583–590. doi: 10.1016/s0006-3223(01)01323-3
- Gully, D., Geslin, M., Serva, L., Fontaine, E., Roger, P., Lair, C., et al. (2002). 4-(2-Chloro-4-methoxy-5-methylphenyl)-N-[(1S)-2-cyclopropyl-1-(3-fluoro-4-methylphenyl)ethyl]-5-methyl-N-(2-propenyl)-1,3-thiazol-2-amine hydrochloride (SSR125543A): a potent and selective corticotrophin-releasing factor1 receptor antagonist. II. characterization in rodent models of stress-related disorders. *J. Pharmacol. Exp. Ther.* 301, 333–345. doi: 10.1124/jpet.301.1.333
- Gunn, B. G., Sanchez, G. A., Lynch, G., Baram, T. Z., and Chen, Y. (2019). Hyperdiversity of CRH interneurons in mouse hippocampus. *Brain Struct. Funct.* 224, 583–598. doi: 10.1007/s00429-018-1793-z
- Guzowski, J. F., Setlow, B., Wagner, E. K., and McGaugh, J. L. (2001). Experience-dependent gene expression in the rat hippocampus after spatial learning: a comparison of the immediate-early genes Arc, c-fos, and zif268. *J. Neurosci.* 21, 5089–5098. doi: 10.1523/jneurosci.21-14-05089.2001
- Habib, K. E., Weld, K. P., Rice, K. C., Pushkas, J., Champoux, M., Listwak, S., et al. (2000). Oral administration of a corticotropin-releasing hormone receptor antagonist significantly attenuates behavioral, neuroendocrine, and autonomic responses to stress in primates. *Proc. Natl. Acad. Sci.* 97, 6079–6084. doi: 10.1073/pnas.97.11.6079
- Hartmann, J., Dedic, N., Pohlmann, M. L., Hausl, A., Karst, H., Engelhardt, C., et al. (2016). Forebrain glutamatergic, but not GABAergic, neurons mediate anxiogenic effects of the glucocorticoid receptor. *Mol. Psychiatry* 22, 466–475. doi: 10.1038/mp.2016.87
- Hartmann, J., Wagner, K. V., Liebl, C., Scharf, S. H., Wang, X. D., Wolf, M., et al. (2012b). The involvement of FK506-binding protein 51 (FKBP5) in the behavioral and neuroendocrine effects of chronic social defeat stress. *Neuropharmacology* 62, 332–339. doi: 10.1016/j.neuropharm.2011.07.041
- Hartmann, J., Wagner, K. V., Dedic, N., Marinescu, D., Scharf, S. H., Wang, X. D., et al. (2012a). Fkbp52 heterozygosity alters behavioral, endocrine and neurogenetic parameters under basal and chronic stress conditions in mice. *Psychoneuroendocrinology* 37, 2009–2021. doi: 10.1016/j.psyneuen.2012.04.017
- Haubensak, W., Kunwar, P. S., Cai, H., Ciochi, S., Wall, N. R., Ponnusamy, R., et al. (2010). Genetic dissection of an amygdala microcircuit that gates conditioned fear. *Nature* 468, 270–276. doi: 10.1038/nature09553
- Heinrichs, S. C., Merlo-Pich, E., Miczek, K. A., Britton, K. T., and Koob, G. F. (1992). Corticotropin-releasing factor antagonist reduces emotionality in socially defeated rats via direct neurotropic action. *Brain Res.* 581, 190–197. doi: 10.1016/0006-8993(92)90708-h
- Henckens, M. J., Deussing, J. M., and Chen, A. (2016). Region-specific roles of the corticotropin-releasing factor-urocortin system in stress. *Nat. Rev. Neurosci.* 17, 636–651. doi: 10.1038/nrn.2016.94
- Hollrigel, G. S., Chen, K., Baram, T. Z., and Soltesz, I. (1998). The pro-convulsant actions of corticotropin-releasing hormone in the hippocampus of infant rats. *Neuroscience* 84, 71–79. doi: 10.1016/s0306-4522(97)00499-5
- Isogawa, K., Bush, D. E. A., and LeDoux, J. E. (2013). Contrasting effects of pretraining, posttraining, and pretesting infusions of corticotropin-releasing factor into the lateral amygdala: attenuation of fear memory formation but facilitation of its expression. *Biol. Psychiatry* 73, 353–359. doi: 10.1016/j.biopsych.2012.08.021
- Ivy, A. S., Rex, C. S., Chen, Y., Dube, C., Maras, P. M., Grigoriadis, D. E., et al. (2010). Hippocampal dysfunction and cognitive impairments provoked by chronic early-life stress involve excessive activation of CRH receptors. *J. Neurosci.* 30, 13005–13015. doi: 10.1523/jneurosci.1784-10.2010
- Janssen, D., and Kozicz, T. (2013). Is it really a matter of simple dualism? Corticotropin-releasing factor receptors in body and mental health. *Front. Endocrinol.* 4:28. doi: 10.3389/fendo.2013.00028
- Kaiser, T., and Feng, G. (2015). Modeling psychiatric disorders for developing effective treatments. *Nat. Med.* 21, 979–988. doi: 10.1038/nm.3935
- Kamprath, K., Marsicano, G., Tang, J., Monory, K., Bisogno, T., Marzo, V. D., et al. (2006). Cannabinoid CB1 receptor mediates fear extinction via habituation-like processes. *J. Neurosci.* 26, 6677–6686. doi: 10.1523/JNEUROSCI.0153-06.2006
- Kasahara, M., Groenink, L., Kas, M. J. H., Bijlsma, E. Y., Olivier, B., and Sarthyai, Z. (2011). Influence of transgenic corticotropin-releasing factor (CRF) overexpression on social recognition memory in mice. *Behav. Brain Res.* 218, 357–362. doi: 10.1016/j.bbr.2010.12.029
- Kim, J., Lee, S., Fang, Y. Y., Shin, A., Park, S., Hashikawa, K., et al. (2019). Rapid, biphasic CRF neuronal responses encode positive and negative valence. *Nat. Neurosci.* 22, 556–585. doi: 10.1038/s41593-019-0342-2
- Kolber, B. J., Boyle, M. P., Wiczorek, L., Kelley, C. L., Onwuzurike, C. C., Nettles, S. A., et al. (2010). Transient early-life forebrain corticotropin-releasing hormone elevation causes long-lasting anxiogenic and despair-like changes in mice. *J. Neurosci.* 30, 2571–2581. doi: 10.1523/JNEUROSCI.4470-09.2010
- Kratzer, S., Mattusch, C., Metzger, M. W., Dedic, N., Noll-Hussong, M., Kafitz, K. W., et al. (2013). Activation of CRH receptor type 1 expressed on glutamatergic neurons increases excitability of CA1 pyramidal neurons by the modulation of voltage-gated ion channels. *Front. Cell. Neurosci.* 7:91. doi: 10.3389/fncel.2013.00091
- Kubota, Y. (2013). Untangling GABAergic wiring in the cortical microcircuit. *Curr. Opin. Neurobiol.* 26, 7–14. doi: 10.1016/j.conb.2013.10.003
- Kubota, Y., Shigematsu, N., Karube, F., Sekigawa, A., Kato, S., Yamaguchi, N., et al. (2011). Selective coexpression of multiple chemical markers defines discrete populations of neocortical GABAergic neurons. *Cereb. Cortex* 21, 1803–1817. doi: 10.1093/cercor/bhq252
- Laryea, G., Arnett, M. G., and Muglia, L. J. (2012). Behavioral studies and genetic alterations in corticotropin-releasing hormone (crh) neurocircuitry: insights into human psychiatric disorders. *Behav. Sci.* 2, 135–171. doi: 10.3390/bs2020135
- Lee, Y., and Davis, M. (1997). Role of the hippocampus, the bed nucleus of the stria terminalis, and the amygdala in the excitatory effect of corticotropin-releasing hormone on the acoustic startle reflex. *J. Neurosci.* 17, 6434–6446. doi: 10.1523/JNEUROSCI.17-16-06434.1997

- Lee, Y., Fitz, S., Johnson, P. L., and Shekhar, A. (2008). Repeated stimulation of CRF receptors in the BNST of rats selectively induces social but not panic-like anxiety. *Neuropsychopharmacology* 33, 2586–2594. doi: 10.1038/sj.npp.1301674
- Lemos, J. C., Wanat, M. J., Smith, J. S., Reyes, B. A. S., Hollon, N. G., Van Bockstaele, E. J., et al. (2012). Severe stress switches CRF action in the nucleus accumbens from appetitive to aversive. *Nature* 490, 402–406. doi: 10.1038/nature11436
- Leslie, J. H., and Nedivi, E. (2011). Activity-regulated genes as mediators of neural circuit plasticity. *Prog. Neurobiol.* 94, 223–237. doi: 10.1016/j.pneurobio.2011.05.002
- Liebsch, G., Landgraf, R., Gerstberger, R., Probst, J. C., Wotjak, C. T., Engelmann, M., et al. (1995). Chronic infusion of a CRH1 receptor antisense oligodeoxynucleotide into the central nucleus of the amygdala reduced anxiety-related behavior in socially defeated rats. *Regul. Pept.* 59, 229–239. doi: 10.1016/0167-0115(95)00099-w
- Lu, A., Steiner, M. A., Whittle, N., Vogl, A. M., Walser, S. M., Ableitner, M., et al. (2008). Conditional mouse mutants highlight mechanisms of corticotropin-releasing hormone effects on stress-coping behavior. *Mol. Psychiatry* 13, 1028–1042. doi: 10.1038/mp.2008.51
- Metzger, M. W., Walser, S., Dedic, N., Aprile-Garcia, F., Jakubcakova, V., Adamczyk, M., et al. (2017). Heterozygosity for the mood disorder-associated variant Gln460Arg Alters P2X7 receptor function and sleep quality. *J. Neurosci.* 37, 11688–11700. doi: 10.1523/jneurosci.3487-16.2017
- Monory, K., Massa, F., Egertová, M., Eder, M., Blaudzun, H., Westenbroek, R., et al. (2006). The endocannabinoid system controls key epileptogenic circuits in the hippocampus. *DLX-Cre. Neuron* 51, 455–466. doi: 10.1016/j.neuron.2006.07.006
- Muglia, L. J., Jacobson, L., Dikkes, P., and Majzoub, J. A. (1995). Corticotropin-releasing hormone deficiency reveals major fetal but not adult glucocorticoid need. *Nature* 373, 427–432. doi: 10.1038/373427a0
- Nestler, E. J., and Hyman, S. E. (2010). Animal models of neuropsychiatric disorders. *Nat. Neurosci.* 13, 1161–1169. doi: 10.1038/nn.2647
- Porsolt, R. D., Le Pichon, M., and Jalfre, M. (1977). Depression: a new animal model sensitive to antidepressant treatments. *Nature* 267, 730–732. doi: 10.1038/266309a0
- Refojo, D., Schweizer, M., Kuehne, C., Ehrenberg, S., Thoeniger, C., Vogl, A. M., et al. (2011). Glutamatergic and dopaminergic neurons mediate anxiogenic and anxiolytic effects of CRHR1. *Science* 333, 1903–1907. doi: 10.1126/science.1202107
- Robison, C. L., Meyerhoff, J. L., Saviolakis, G. A., Chen, W. K., Rice, K. C., and Lumley, L. A. (2004). A CRH1 antagonist into the amygdala of mice prevents defeat-induced defensive behavior. *Ann. N. Y. Acad. Sci.* 1032, 324–327. doi: 10.1196/annals.1314.052
- Rodaro, D., Caruana, D., Amir, S., and Stewart, J. (2007). Corticotropin-releasing factor projections from limbic forebrain and paraventricular nucleus of the hypothalamus to the region of the ventral tegmental area. *Neuroscience* 150, 8–13. doi: 10.1016/j.neuroscience.2007.09.043
- Rodríguez, C., Buchholz, F., Galloway, J., Sequerra, R., Kasper, J., Ayala, R., et al. (2000). High-efficiency deleter mice show that FLPe is an alternative to Cre-loxP. *Nat. Genet.* 25, 139–140. doi: 10.1038/75973
- Roosendaal, B., Schelling, G., and McGaugh, J. L. (2008). Corticotropin-releasing factor in the basolateral amygdala enhances memory consolidation via an interaction with the adrenoceptor-cAMP pathway: dependence on glucocorticoid receptor activation. *J. Neurosci.* 28, 6642–6651. doi: 10.1523/jneurosci.1336-08.2008
- Rostkowski, A. B., Leitermann, R. J., and Urban, J. H. (2013). Differential activation of neuronal cell types in the basolateral amygdala by corticotropin releasing factor. *Neuropeptides* 47, 273–280. doi: 10.1016/j.npep.2012.12.004
- Sagar, S. M., Sharp, P. A., and Curran, T. (1988). Expression of c-fos protein in brain: metabolic mapping at the cellular level. *Science* 240, 1328–1331. doi: 10.1126/science.3131879
- Sajdyk, T. J., Schober, D. A., Gehlert, D. R., and Shekhar, A. (1999). Role of corticotropin-releasing factor and urocortin within the basolateral amygdala of rats in anxiety and panic responses. *Behav. Brain Res.* 100, 207–215. doi: 10.1016/S0166-4328(98)00132-6
- Salvatore, M., Wiersielis, K. R., Luz, S., Waxler, D. E., Bhatnagar, S., and Bangasser, D. A. (2018). Sex differences in circuits activated by corticotropin releasing factor in rats. *Horm. Behav.* 97, 145–153. doi: 10.1016/j.yhbeh.2017.10.004
- Sanford, C. A., Soden, M. E., Baird, M. A., Miller, S. M., Schulkin, J., Palmiter, R. D., et al. (2016). A central amygdala CRF circuit facilitates learning about weak threats. *Neuron* 93, 164–178. doi: 10.1016/j.neuron.2016.11.034
- Shaham, Y., Erb, S., Leung, S., Buczek, Y., and Stewart, J. (1998). CP-154,526, a selective, non-peptide antagonist of the corticotropin-releasing factor1 receptor attenuates stress-induced relapse to drug seeking in cocaine- and heroin-trained rats. *Psychopharmacology* 137, 184–190. doi: 10.1007/s002130050608
- Sheng, M., and Greenberg, M. E. (1990). The regulation and function of c-fos and other immediate early genes in the nervous system. *Neuron* 4, 477–485. doi: 10.1016/0896-6273(90)90106-p
- Skórzcawska, A., Bidziński, A., Hamed, A., Lehner, M., Turzyńska, D., Sobolewska, A., et al. (2008). The influence of CRF and α -helical CRF(9–41) on rat fear responses, c-Fos and CRF expression, and concentration of amino acids in brain structures. *Horm. Behav.* 54, 602–612. doi: 10.1016/j.yhbeh.2008.06.002
- Stenzel-Poore, M. P., Heinrichs, S. C., Rivest, S., and Koob, G. F. (1994). Overproduction of corticotropin-releasing a genetic model of anxiogenic behavior factor in transgenic mice. *J. Neurosci.* 14(5 Pt 1), 2579–2584. doi: 10.1523/jneurosci.14-05-02579.1994
- Sterley, T. L., Baimoukhametova, D., Füzesi, T., Zurek, A. A., Daviu, N., Rasiah, N. P., et al. (2018). Social transmission and buffering of synaptic changes after stress. *Nat. Neurosci.* 21, 393–403. doi: 10.1038/s41593-017-0044-6
- Swanson, L., Sawchenko, P., Rivier, J., and Vale, W. (1983). Organization of ovine corticotropin-releasing factor immunoreactive cells and fibers in the rat brain: an immunohistochemical study. *Neuroendocrinology* 36, 165–186. doi: 10.1159/000123454
- Swiergiel, A. H., Takahashi, L. K., and Kalin, N. H. (1993). Attenuation of stress-induced behavior by antagonism of corticotropin-releasing factor receptors in the central amygdala in the rat. *Brain Res.* 623, 229–234. doi: 10.1016/0006-8993(93)91432-r
- Tovote, P., Fadok, J. P., and Lüthi, A. (2015). Neuronal circuits for fear and anxiety. *Nat. Rev. Neurosci.* 16, 317–331. doi: 10.1038/nrn3945
- Vale, W., Spiess, J., Rivier, C., and Rivier, J. (1981). Characterization of a 41-residue ovine hypothalamic peptide that stimulates secretion of corticotropin and beta-endorphin. *Science* 213, 1394–1397. doi: 10.1126/science.6267699
- Van Gaalen, M. M., Stenzel-Poore, M. P., Holsboer, F., and Steckler, T. (2002). Effects of transgenic overproduction of CRH on anxiety-like behaviour. *Eur. J. Neurosci.* 15, 2007–2015. doi: 10.1046/j.1460-9568.2002.02040.x
- Van Pett, K., Viau, V., Bittencourt, J. C., Chan, R. K. W., Li, H. Y., Arias, C., et al. (2000). Distribution of mRNAs encoding CRF receptors in brain and pituitary of rat and mouse. *J. Comp. Neurol.* 428, 191–212. doi: 10.1002/1096-9861(20001211)428:2<191::aid-cne1>3.0.co;2-u
- Veyrac, A., Besnard, A., Caboche, J., Davis, S., and Laroche, S. (2014). The transcription factor Zif268/Egr1, brain plasticity, and memory. *Prog. Mole. Biol. Trans. Sci.* 122, 89–129. doi: 10.1016/B978-0-12-420170-5.00004-0
- Wagner, K. V., Wang, X. D., Liebl, C., Scharf, S. H., Müller, M. B., and Schmidt, M. V. (2011). Pituitary glucocorticoid receptor deletion reduces vulnerability to chronic stress. *Psychoneuroendocrinology* 36, 579–587. doi: 10.1016/j.psyneuen.2010.09.007
- Walsh, J. J., Friedman, A. K., Sun, H., Heller, E. A., Ku, S. M., Juarez, B., et al. (2014). Stress and CRF gate neural activation of BDNF in the mesolimbic reward pathway. *Nat. Neurosci.* 17, 27–29. doi: 10.1038/nn.3591
- Wang, X. D., Chen, Y., Wolf, M., Wagner, K. V., Liebl, C., Scharf, S. H., et al. (2011). Forebrain CRHR1 deficiency attenuates chronic stress-induced cognitive deficits and dendritic remodeling. *Neurobiol. Dis.* 42, 300–310. doi: 10.1016/j.nbd.2011.01.020
- Wang, X. D., Labermaier, C., Holsboer, F., Wurst, W., Deussing, J. M., Müller, M. B., et al. (2012). Early-life stress-induced anxiety-related behavior in adult mice partially requires forebrain corticotropin-releasing hormone receptor 1. *Eur. J. Neurosci.* 36, 2360–2367. doi: 10.1111/j.1460-9568.2012.08148.x
- Wang, X. D., Su, Y. A., Wagner, K. V., Avrabos, C., Scharf, S. H., Hartmann, J., et al. (2013). Nectin-3 links CRHR1 signaling to stress-induced memory deficits and spine loss. *Nat. Neurosci.* 16, 706–713. doi: 10.1038/nn.3395

- Weninger, S. C., Dunn, A. J., Muglia, L. J., Dikkes, P., Miczek, K. A., Swiergiel, A. H., et al. (1999). Stress-induced behaviors require the corticotropin-releasing hormone (CRH) receptor, but not CRH. *Proc. Natl. Acad. Sci. U.S.A.* 96, 8283–8288. doi: 10.1073/pnas.96.14.8283
- Wiersielis, K. R., Wicks, B., Simko, H., Cohen, S. R., Khantsis, S., Baksh, N., et al. (2016). Sex differences in corticotropin releasing factor-evoked behavior and activated networks. *Psychoneuroendocrinology* 73, 204–216. doi: 10.1016/j.psyneuen.2016.07.007
- Zhang, R., Asai, M., Mahoney, C. E., Joachim, M., Shen, Y., Gunner, G., et al. (2017). Loss of hypothalamic corticotropin-releasing hormone markedly reduces anxiety behaviors in mice. *Mol. Psychiatry* 22, 733–744. doi: 10.1038/mp.2016.136
- Zorrilla, E. P., Valdez, G. R., Nozulak, J., Koob, G. F., and Markou, A. (2002). Effects of antalarmin, a CRF type 1 receptor antagonist, on anxiety-like behavior and motor activation in the rat. *Brain Res.* 952, 188–199. doi: 10.1016/s0006-8993(02)03189-x
- Conflict of Interest Statement:** The authors declare that the research was conducted in the absence of any commercial or financial relationships that could be construed as a potential conflict of interest.

Copyright © 2019 Dedic, Kühne, Gomes, Hartmann, Ressler, Schmidt and Deussing. This is an open-access article distributed under the terms of the Creative Commons Attribution License (CC BY). The use, distribution or reproduction in other forums is permitted, provided the original author(s) and the copyright owner(s) are credited and that the original publication in this journal is cited, in accordance with accepted academic practice. No use, distribution or reproduction is permitted which does not comply with these terms.



Effect of Oxytocin on Hunger Discrimination

Mitchell A. Head¹, David C. Jewett², Sarah N. Gartner¹, Anica Klockars¹, Allen S. Levine³ and Pawel K. Olszewski^{1,3*}

¹ Faculty of Science and Engineering, University of Waikato, Hamilton, New Zealand, ² Department of Psychology, University of Wisconsin-Eau Claire, Eau Claire, WI, United States, ³ Department of Food Science and Nutrition, University of Minnesota, St. Paul, MN, United States

OPEN ACCESS

Edited by:

Limei Zhang,
National Autonomous University of
Mexico, Mexico

Reviewed by:

Laura Marta Vivas,
Medical Research Institute Mercedes
and Martín Ferreyra
(INIMEC), Argentina
Rafael Lujan,
Universidad de Castilla-La
Mancha, Spain
Lee E. Eiden,
National Institutes of Health (NIH),
United States

*Correspondence:

Pawel K. Olszewski
pawel@waikato.ac.nz

Specialty section:

This article was submitted to
Neuroendocrine Science,
a section of the journal
Frontiers in Endocrinology

Received: 27 February 2019

Accepted: 25 April 2019

Published: 15 May 2019

Citation:

Head MA, Jewett DC, Gartner SN,
Klockars A, Levine AS and
Olszewski PK (2019) Effect of
Oxytocin on Hunger Discrimination.
Front. Endocrinol. 10:297.
doi: 10.3389/fendo.2019.00297

Centrally and peripherally administered oxytocin (OT) decreases food intake and activation of the endogenous OT systems, which is associated with termination of feeding. Evidence gathered thus far points to OT as a facilitator of early satiation, a peptide that reduces the need for a meal that has already begun. It is not known, however, whether OT can diminish a feeling of hunger, thereby decreasing a perceived need to seek calories. Therefore, in the current project, we first confirmed that intraperitoneal (i.p.) OT at 0.3–1 mg/kg reduces food intake in deprived and non-deprived rats. We then used those OT doses in a unique hunger discrimination protocol. First, rats were trained to discriminate between 22- and 2-h food deprivation (hungry vs. sated state) in a two-lever operant procedure. After rats acquired the discrimination, they were food-restricted for 22 h and given i.p. OT before a generalization test session. OT did not decrease 22-h deprivation-appropriate responding to match that following 2-h food deprivation, thus, it did not reduce the perceived level of hunger. In order to better understand the mechanisms behind this ineffectiveness of OT, we used c-Fos immunohistochemistry to determine whether i.p. OT activates a different subset of feeding-related brain sites under 22- vs. 2-h deprivation. We found that in sated animals, OT induces c-Fos changes in a broader network of hypothalamic and brain stem sites compared to those affected in the hungry state. Finally, by employing qPCR analysis, we asked whether food deprivation vs. sated state have an impact on OT receptor expression in the brain stem, a CNS “entry” region for peripheral OT. Fasted animals had significantly lower OT receptor mRNA levels than their *ad libitum*-fed counterparts. We conclude that OT does not diminish a feeling of hunger before a start of a meal. Instead OT’s anorexigenic properties are manifested once consumption has already begun which is—at least to some extent—driven by changes in brain responsiveness to OT treatment in the hungry vs. fed state. OT should be viewed as a mediator of early satiation rather than as a molecule that diminishes perceived hunger.

Keywords: oxytocin, satiety, hunger, feeding, hypothalamus

INTRODUCTION

A nine amino acid neuropeptide, oxytocin (OT), synthesized primarily in the hypothalamic paraventricular (PVN) and supraoptic (SON) nuclei, released throughout the CNS and, via the neurohypophysis, into general circulation, has been known to regulate a number of functions, including parturition, lactation, and social behaviors. In 1989, Arletti et al. reported for the first time

that intracerebral and intraperitoneal (i.p.) administration of OT in rats causes a marked reduction in food intake (1). Since then, a plethora of evidence has emerged that supports the involvement of OT in termination of feeding.

Injections of OT in the third and fourth cerebral ventricles as well as in numerous brain areas, including the hypothalamic ventromedial nucleus (VMH), dorsal vagal complex, central (CEA), and basolateral (BLA) amygdala, ventral tegmental area (VTA) and nucleus accumbens core (AcbC), and the limbic system, produce cessation of ingestive behavior (2–10). This early termination of feeding after OT treatment pertains to relatively bland laboratory chow, as well as those that are highly palatable (2, 3, 10, 11). Despite its limited ability to cross the blood-brain barrier (BBB), peripherally administered OT (including via intraperitoneal (i.p.), subcutaneous, and intravenous routes) also potentially decreases food intake, most likely by engaging the brainstem where the BBB protection is weak (1, 2, 9, 12–14).

Increased c-Fos immunoreactivity in OT neurons and elevated OT plasma levels coincide with meal cessation (15). Hypothalamic OT mRNA expression is downregulated during fasting and restored by re-feeding (16). Administration of molecules that support satiation, such as cholecystokinin (CCK), alpha-melanocyte stimulating hormone, and glucagon-like peptide-1 (GLP-1), increases activity of the OT system (17–21). Furthermore, OT release has been associated with peripheral changes that typically occur as ingestive behavior nears its end, such as elevated osmolality, an increase in select nutrient levels, and excessive stomach distension (9, 22–25).

Overall, those findings strongly point to the role of OT in promoting satiety, facilitating early termination of consumption, and reducing meal size. On the other hand, one aspect of OT's involvement in feeding control that has not been investigated in detail is whether OT has a capacity to reduce a feeling of hunger. That, e.g., peripherally administered OT increases latency to begin a meal, might suggest it to some extent, but direct evidence is lacking. Scarcity of data also stems from methodological difficulties in assessing hunger in laboratory animals.

There is a unique protocol, however, that relies on rats reporting their hunger status using an operant behavior. Animals are trained to discriminate between acute food deprivation lasting 22 h (hunger) or 2 h (no actual energy depletion). In one such study, Corwin et al. trained rats maintained at 80% of their free-feeding body weight to discriminate between food consumed 22 or 3 h before experimental sessions (26). The anorexigen CCK or ingestion of sweetened condensed milk induced effects similar to chow consumption occurring 3 h before a test session, in contrast to fenfluramine which did not reliably produce effects similar to 3-h food ingestion. Thus, CCK produced effects that resembled a lack of hunger. Similar outcomes to those induced by CCK were seen in response to an anti-obesity drug, sibutramine (27, 28).

In the current project, we employed this unique hunger discrimination protocol (employing 22-h vs. 2-h deprivation) to examine whether OT administered i.p. prior to discrimination testing in rats reduces a feeling of hunger. We used OT doses based on previous reports and on the results of two additional feeding studies in hungry and sated animals performed here. In

order to better understand whether i.p. OT activates a different subset of feeding-related brain sites depending on the lack of access to food for 22 or 2 h, we conducted an analysis of c-Fos immunoreactivity. Finally, since i.p. OT is thought to directly act at the brain stem, we asked whether food deprivation vs. a sated state has an impact on OT receptor expression established with real-time PCR.

MATERIALS AND METHODS

Animals

Male Sprague-Dawley rats aged 12-weeks old (average b. wt. 400 g) were housed individually in standard plastic cages with wire tops in a temperature-controlled (22°C) animal facility with a 12:12 light:dark cycle (lights on at 08:30 in the discrimination studies and 07:00 in the remaining experiments). Water and standard laboratory chow were available *ad libitum* unless stated otherwise. Animals were treated in accordance with the National Institute of Health Guide for the Care and Use of Laboratory Animals. The University of Waikato Animal Ethics Committee and the University of Wisconsin-Eau Claire Institutional Animal Care and Use Committee approved all procedures described here.

Behavioral Studies

Establishing Effective Doses of OT That Reduce Feeding in Animals Deprived for 22 h and 2 h

As we sought to investigate effects of OT on consumption of the same kind of diet in both 22-h deprived (thus, driven to eat by energy needs) and 2-h deprived (thus, not motivated to eat by energy needs) animals, we chose to give them episodic access to palatable high-fat high-sugar (HFHS; Research Diets) chow. Rodents avidly consume HFHS diet even in the absence of hunger. This was done to test whether i.p. OT retained its anorexigenic properties in the context of 2 and 22 h deprivation scenarios as they were slightly different from previously described protocols that typically relied either on depriving animals overnight, 16 or 24 h (hunger) or on giving animals episodic 2–4 h access to palatable food without depriving them even for 2 h (relative satiety).

Effect of OT on palatable food intake in rats deprived for 2 h

In order to examine whether OT decreases the consumption of HFHS food, we adjusted our previously published protocol (14, 29). Rats maintained on *ad libitum* food and water had standard chow taken away at 10:00 (water remained in the cage). Two hour later, HFHS chow was placed in the cages for 2 h. Fifteen minutes prior to the HFHS food presentation, animals received an i.p. injection of isotonic saline or 0.1, 0.3, or 1 mg/kg OT Sigma, St. Louis, MO, USA ($n = 9/\text{group}$). The animals had had previous episodic (2 h per day, 5 and 10 days before the study) exposure to this HFHS chow to avoid neophobia. Data were analyzed with a one-way ANOVA followed by Dunnett's *post-hoc* analysis, with a significance level set at $p \leq 0.05$.

Effect of OT on palatable food intake in rats deprived for 22 h

The cohort of rats used in the previous experiment (2.2.1.1) was studied here. A 2-week “washout” period elapsed between the

experiments. Animals that had had access to standard chow were food-deprived for 22 h (deprivation ending at 12:00). They were then given access for 4 h to the HFHS chow. Fifteen minutes prior to the HFHS food presentation, animals received an i.p. injection of isotonic saline or 0.1, 0.3, or 1 mg/kg OT. HFHS chow intake after 22 h of deprivation was measured at 1 and 4 h. Data were analyzed with a one-way ANOVA followed by Dunnett's *post-hoc* analysis, with a significance level set at $p \leq 0.05$.

Establishing Effects of OT on Discrimination Between 22 and 2 h of Food Deprivation

Experimentally naïve male Sprague Dawley rats (Harlan, Madison, WI) were ~12-weeks old at the beginning of the procedures. Food (Harlan Teklad chow, Madison, WI) and water were continuously available unless otherwise stated.

Apparatus

Daily discrimination sessions were conducted in standard operant chambers equipped with two response levers (Med-Associates, St. Albans, VT), placed in ventilated, sound-attenuating cubicles. Forty-five mg food pellets (Bio-Serve F#0021, Frenchtown, NJ) reinforced lever pressing and were delivered by a pellet dispenser into a food pellet trough located between the two levers. A house light in the back wall of the operant chamber illuminated the chambers during sessions. Experimental contingencies and data recording were performed with Med Associates software and a computer located in an adjacent room.

Discrimination training

Rats were initially food deprived to ~85% of their free feeding body weight and trained to press a lever via the method of successive approximations. First, a single lever press was reinforced with a 45 mg food pellet (Bio-Serv F#0021, Frenchtown NJ). Response requirements were increased gradually until 15 presses (fixed ratio (FR) 15) were needed to generate food. When reliable responding to both levers was achieved, rats were given free access to food for 305 days before subsequent discrimination training began. Rats were trained to discriminate between 22 and 2 h of acute food deprivation using multiple cycle training. Under 22-h conditions, food was removed 22 h before the training session. Rats were placed into the operant chamber 5 min before the first training cycle. When the first training cycle started, the house light was turned on and 15 left lever presses were reinforced with 45 mg food pellet delivery (FR 15 reinforcement schedule). Incorrect (right) lever presses were punished with 8 s of darkness under an FR 15 schedule. Training continued until 5 reinforcers were earned or 5 min elapsed. At least one more additional training cycle, identical to the first, was conducted 30–120 min after the previous cycle. Under 2-h conditions, the contingencies were reversed: right lever presses were reinforced and left lever presses were punished under the FR 15 schedule. Conditions were quasi-random with the provision that the same training condition (22 or 2 h of food deprivation) could not be given for more than two consecutive sessions.

Discrimination training continued until the subject emitted 80% or greater condition-appropriate responses prior to delivery of the first reinforcer and for the entire training session during all training cycles for 8 of 10 consecutive daily sessions.

Generalization test: evaluation of the ability of OT to reduce the discriminative stimulus effects of 22-h food deprivation

The final discrimination tests assessed the ability of OT to reduce the discriminative stimulus effects of 22-h food deprivation. These tests were conducted under 22-h deprivation conditions. During the first response period, only left lever presses were reinforced. Following the first response period, rats were injected i.p. with isotonic saline or OT (0.01–1 mg/kg range). After injections, rats were placed in stainless steel cages without food or water. During the next response period occurring 30 min after the injection, responses toward both levers were reinforced. Generalization tests lasted until the subject earned 5 reinforcers or until 5 min elapsed, whichever occurred first. Appropriate discriminative performance for at least 2 training days (one preceded by 22-h deprivation, one preceded by 2-h deprivation) was required between generalization tests.

Immediately after generalization tests, subjects were placed in stainless steel cages and had access to a pre-weighed amount of regular food (~25 g of Teklad rat chow) placed on the floor of the cage, and water available in a bottle attached to the cage. Food intake was measured at the end of 1 h. Afterwards, rats were returned to their home cage and had free access to food and water until 2 h before the next training session.

Data analysis

One-way ANOVA was calculated (SPSS, Chicago, IL, USA) by assessing the effects of OT versus control conditions on the discriminative stimulus effects of 22-h food deprivation, lever pressing rate, and food intake. Tukey HSD *post hoc* tests were performed following significant ANOVA values to determine pairwise differences among conditions. Significance was set at $p \leq 0.05$.

Establishing OT-induced c-Fos Immunoreactivity in Feeding-Related Brain Sites in Rats Deprived for 2 and 22 h

For practical reasons, including the transfer of rats between cages and behavioral manipulations that could have affected baseline Fos expression, we chose a different cohort of animals here than those used in behavioral studies. Experimentally naïve, age-matched male Sprague Dawley rats were divided into two cohorts ($n = 12$ per cohort) which were subjected to either 2 or 22 h of food deprivation (in both cases, deprivation period ended at 12:00). At the end of the deprivation, half of the animals in each cohort received an i.p. injection of isotonic saline, and the other half, 1 mg/kg OT. An hour after drug administration, animals were deeply anesthetized with urethane (35% dissolved in 0.9% saline, i.p.), and perfused through the aorta with 50 ml of saline followed by 500 ml of 4% paraformaldehyde in 0.1 phosphate buffer (pH 7.4). Brains were excised and post-fixed overnight in the same fixative at 4°C. 60 μ m-thick coronal sections were cut

with a vibratome (Leica, Germany) and later processed as free-floating sections for standard single antigen immunostaining of c-Fos.

Immunohistochemistry

Sections were rinsed in 50 nM TBS (pH 7.4–7.6), and then pre-treated for 10 min in 3% H₂O₂, 10% methanol (diluted in TBS). After rinsing in TBS they were incubated overnight at 4°C in the primary rabbit-anti-Fos antibody (diluted 1:3000; Synaptic Systems, Australia) washed in TBS, and subsequently incubated for 1 h at room temperature in the secondary goat-anti-rabbit antibody (1:400; Vector Laboratories). Following four washes in TBS, sections were incubated for 1 h with the avidin–biotin peroxidase complex (1:800; Elite Kit, Vector Laboratories). The vehicle for all incubations was a solution of 0.25% gelatin and 0.5% Triton X-100 in TBS. The peroxidase in the tissue was visualized with 0.05% diaminobenzidine (DAB), 0.01% H₂O₂ and 0.3% nickel sulfate (12-min incubation). Sections were washed four times in TBS to stop the reaction, mounted onto gelatin-coated slides, air-dried, dehydrated in ascending concentrations of ethanol, soaked in xylene (Merck KGaA, Germany) and embedded in Entellan (Merck KGaA, Germany). The number of Fos-positive nuclei per 1 mm² was counted bilaterally for each neuroanatomical region of interest using ImageJ Software, with boundaries defined according to the Paxinos and Watson brain atlas, on 2–4 sections per animal. Images provided by a CCD camera attached to a Nikon Eclipse 400 microscope were analyzed using Nikon NIS Elements image software. The following areas were analyzed (in the parentheses, anterior-posterior ranges of bregma levels of sections used to analyze each site are shown): AcbC—nucleus accumbens core (1.28–0.96); AcbS—nucleus accumbens shell (1.28–0.96); AP—area postrema (–13.92 to –14.16); ARC—arcuate nucleus (–2.16 to –2.52); BLA—basolateral amygdala (–2.64 to –2.92); CEA—central nucleus of the amygdala (–2.64 to –2.92); DMH—dorsomedial nucleus of the hypothalamus (–3.00 to –3.24); DMV—dorsal motor nucleus of the vagus (–13.76 to –14.16); NTS—nucleus of the solitary tract (–13.76 to –14.16); PVN—paraventricular nucleus of the hypothalamus (–1.56 to –1.92); SON—supraoptic nucleus (–0.96 to –1.2); VMH—ventromedial nucleus (–3.00 to –3.24); VTA—ventral tegmental area (–6.72 to –6.84).

Data Analysis

Densities of Fos-positive nuclear profiles (per 1 mm²) were averaged per individual, and then per group. Data between the two groups (saline vs. OT) in each cohort were compared using a *t*-test. Values were considered significantly different for $p \leq 0.05$.

Establishing the Effect of Food Deprivation on Brainstem Expression of the OT Receptor Gene

Deprivation and Brain Stem Collection

The rats were divided to two groups. One group ($n = 9$) had unlimited access to standard chow and water, whereas the other had food taken away ~24 h before the animals were sacrificed by decapitation ($n = 13$). The brain stem was dissected and put in

RNAlater (Ambion) for 2 h at room temperature and the samples were then frozen at –80°C until further preparation.

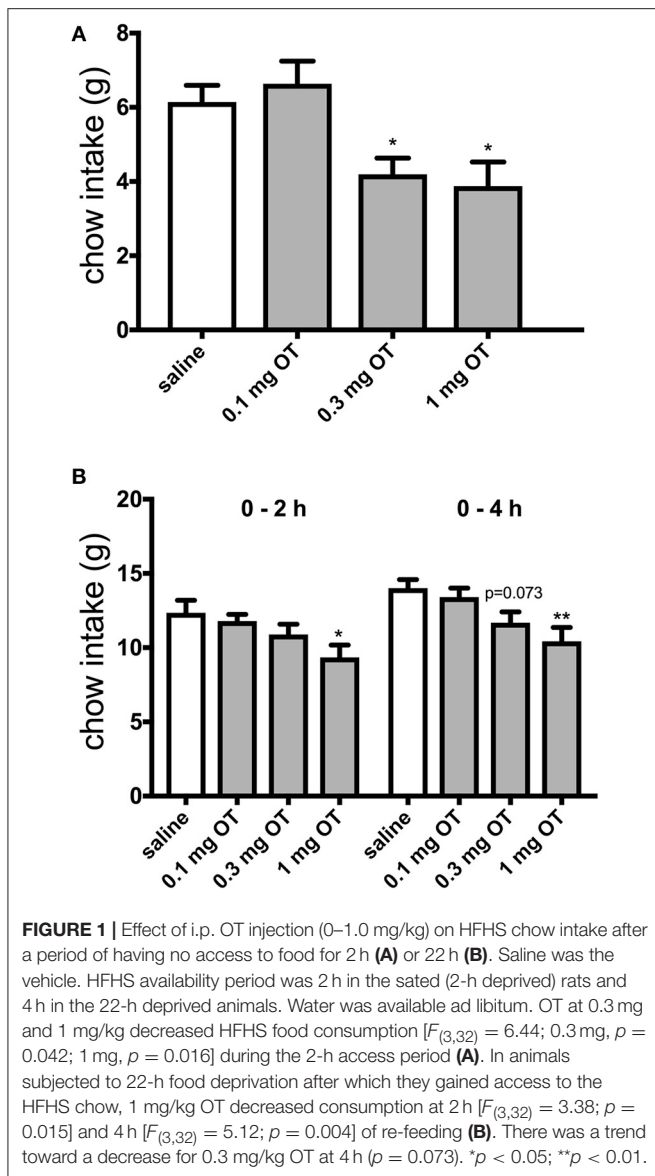
rtPCR Protocol and Data Analysis

A standard protocol of sample preparation and rtPCR was used and, for brevity reasons, the main steps are described here [see (30) for details]. Samples were homogenized in TRIzol (Ambion); RNA was extracted with chloroform and precipitated in isopropanol. After centrifuging, the pellet was washed, air-dried, and dissolved in the DNase buffer (NEB). The samples were treated with RNase-free DNase I (Merck) and the absence of genomic DNA was established by PCR of a 5% template. 100 ng/μl genomic DNA served as a positive control, whereas MilliQ H₂O as a negative one. The product was analyzed by electrophoresis. 5 μg RNA samples were diluted with MilliQ H₂O. RNA was reverse-transcribed in the master mix (Promega; 20 μl). Samples were incubated for 1 h (37°C), followed by PCR to confirm cDNA synthesis. RtPCR reactions were performed in duplicates. Sample cDNA template (25 ng) was used per primer [OT receptor primer sequences: ttctctgctgctgctgctg (fwd) and tcattgctgaagatggctgaga (rev)]. Expression of three housekeeping genes (glyceraldehyde-3-phosphate-dehydrogenase, β-actin, and β-tubulin) was used to calculate normalization factors (GeNorm). Primer efficiencies were calculated with LinRegPCR (HFRC) and Ct values were corrected for differences in primer efficiencies. rtPCR results were analyzed with a Student's *t*-test. Values are presented as means ± S.E.M and they were deemed significantly different when $p \leq 0.05$.

RESULTS

The effects of 0.1, 0.3, and 1.0 mg/kg OT i.p. on HFHS palatable chow intake were investigated after 2 h and after 22 h of food deprivation. Control animals that had standard food taken away for 2 h and subsequently gained short-term access to the HFHS chow (thus, these rats were in effect sated) ate approximately 6 grams of the HFHS diet. OT at 0.3 mg/kg and 1 mg/kg decreased HFHS food consumption [$F_{(3,32)} = 6.44$; 0.3 mg, $p = 0.042$; 1 mg, $p = 0.016$] during the 2-h access period by approximately 33% (Figure 1A). In animals subjected to 22-h food deprivation (which is a much more challenging energy deprivation scenario and it promotes search of and intake of caloric tastants) after which they gained access to the HFHS chow, 1 mg/kg OT decreased consumption by approximately 25% at 2 h [$F_{(3,32)} = 3.38$; $p = 0.015$] and 4 h [$F_{(3,32)} = 5.12$; $p = 0.004$] of re-feeding (Figure 1B). There was a trend toward a decrease for 0.3 mg/kg OT at 4 h ($p = 0.073$).

Rats learned to discriminate between 22- and 2-h food deprivation in a mean of 90 sessions. Operant studies revealed that OT even at doses that reduced HFHS diet intake in the experiments described above, did not alter the discriminative stimulus effects of 22-h food deprivation [$F_{(4,16)} = 1.00$, $p = 0.436$, Figure 2A]. OT did significantly alter response rates in rats [$F_{(4,31)} = 8.08$, $p = 0.0001$, Figure 2B]. OT significantly reduced rates of lever pressing following 0.1 mg/kg OT ($p = 0.044$), 0.32 ($p = 0.001$) and 1 mg/kg OT i.p. ($p < 0.0001$) (Figure 2B). As shown in Figure 2C, OT-treated animals deprived for 22 h and



subjected to the hunger discrimination paradigm, did not show significantly reduced consumption of regular chow when they were transferred to a transition cage for 1 h after the operant test was concluded.

In a separate set of studies, we sought to investigate the effects of i.p. OT on neuronal activation in animals that are hungry and in animals that are sated. Intraperitoneal injection of OT at 1 mg/kg in rats deprived for 2 h affected c-Fos immunoreactivity in eight of the 13 feeding-related brain sites studied here (Figure 3). The number of c-Fos positive nuclei per mm² in response to OT was elevated in the PVN ($p = 0.011$), SON ($p < 0.001$), NTS ($p = 0.003$), DMV ($p < 0.001$), and CEA ($p < 0.001$). A decrease was noted in the ARC ($p = 0.019$), VMH ($p < 0.001$), and DMH ($p < 0.001$). On the other hand, in animals deprived for 22 h (Figure 4), six areas showed differences in c-Fos levels: an increase was noted in the PVN ($p = 0.042$), SON ($p < 0.001$),

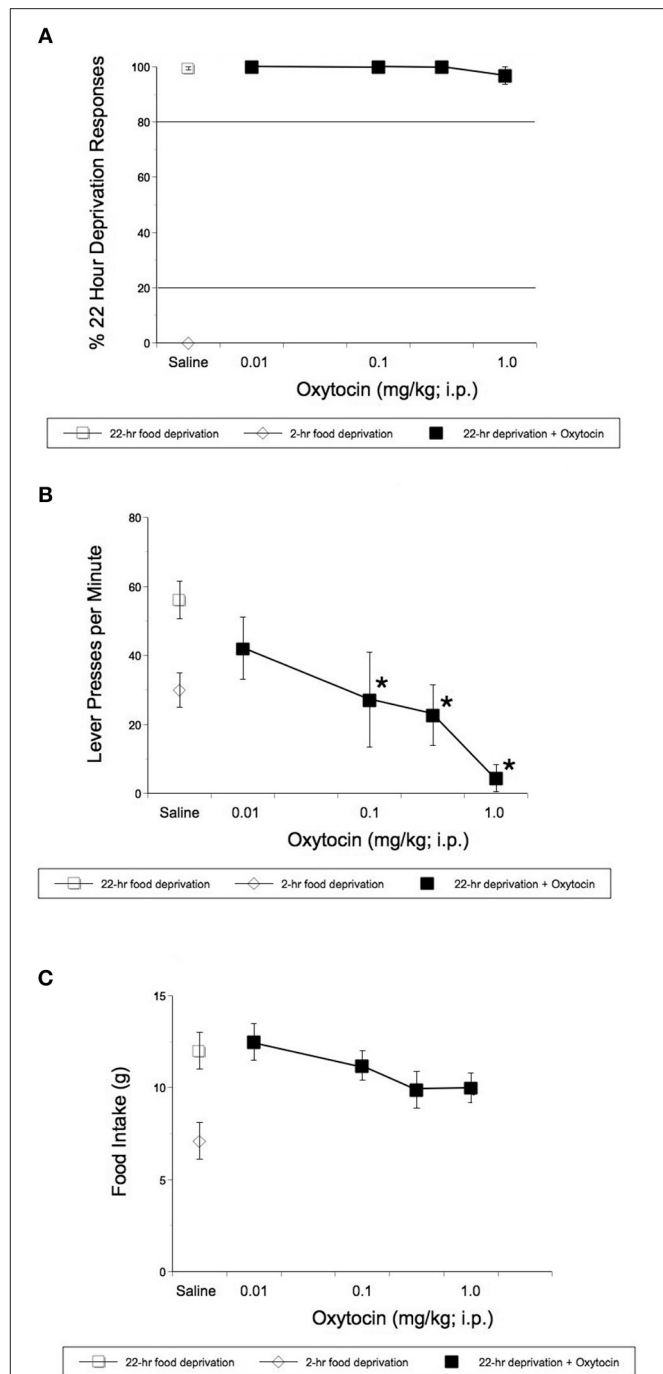


FIGURE 2 | Effect of i.p. OT on the stimulus effects of 22-h food deprivation (A), lever pressing response rates (B), and regular laboratory chow intake in 1 h immediately following the completion of the discrimination test (C). Animals had access to regular chow ad lib, before chow was withheld for 22 h and animals were injected. Saline was the vehicle. Operant studies revealed that OT did not alter the discriminative stimulus effects of 22-h food deprivation [$F_{(4,16)} = 1.00$, $p = 0.436$ (A)]. OT did significantly alter response rates in rats [$F_{(4,31)} = 8.08$, $p = 0.0001$ (B)]. OT significantly reduced rates of lever pressing following 0.1 ($p = 0.044$), 0.32 ($p = 0.001$), and 1 mg/kg OT i.p. ($p < 0.0001$) (B). (C) Shows that animals deprived for 22 h and treated with OT, did not show significantly reduced consumption of regular chow in 1 hr after the completion of the operant test. * $p < 0.05$.

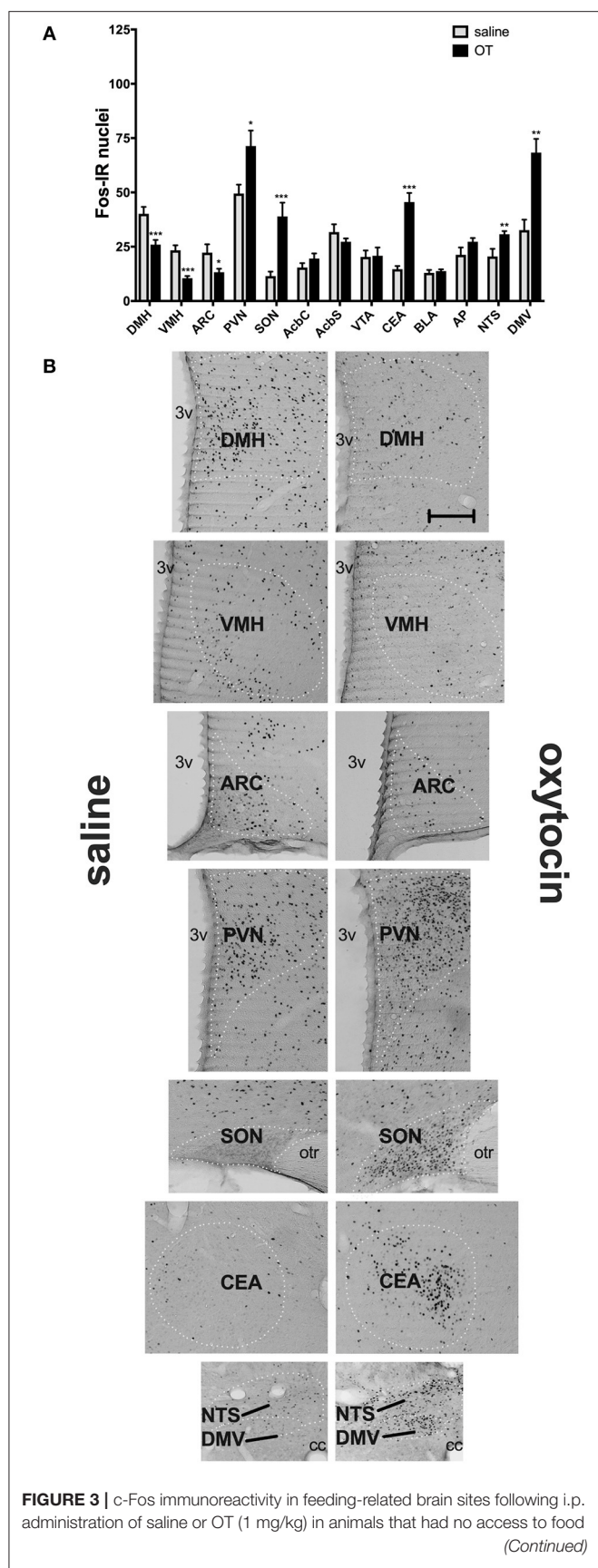


FIGURE 3 | for 2 h (A). Panel (B) presents photomicrographs depicting sites that showed a significant difference in c-Fos levels (saline-treated rats—left side; OT-treated rats—right side). Densities of Fos-positive nuclear profiles (per 1 mm² of a site) were averaged per individual, and then per group. AcbC, nucleus accumbens core; AcbS, nucleus accumbens shell; AP, area postrema; ARC, arcuate nucleus; BLA, basolateral amygdala; CEA, central nucleus of the amygdala; DMH, dorsomedial nucleus of the hypothalamus; DMV, dorsal motor nucleus of the vagus; NTS, nucleus of the solitary tract; PVN, paraventricular nucleus of the hypothalamus; SON, supraoptic nucleus; VMH, ventromedial nucleus; VTA, ventral tegmental area. * $p < 0.05$; ** $p < 0.01$; *** $p < 0.001$.

VMH ($p = 0.013$), CEA ($p < 0.001$), and BLA ($p = 0.012$), whereas a decrease, in the AP ($p < 0.001$).

Finally, by applying rtPCR analysis, we showed a downregulation of the OT receptor gene in the brain stem of rats that underwent deprivation compared to their sated counterparts ($p = 0.0024$; Figure 5).

DISCUSSION

The fundamental drive that initiates food intake is a feeling of hunger. Hunger increases our motivation to seek high-energy foods and generates an avid feeding behavior upon encountering such ingestants. There are evolutionarily conserved neural and endocrine processes, such as those involving ghrelin or neuropeptide Y (NPY) (31–33), that promote eating for hunger, thereby ensuring that enough energy is obtained in order for the organism to maintain its functioning. However, in the obesogenic environment, where highly palatable and energy-rich diets are readily available, those mechanisms coupled with reward processes appear to be active even in the absence of actual energy needs, producing a feeling of hunger that leads to excessive food intake. Therefore, an important question that arises in the context of peptides that reduce consumption that can be potentially used clinically is whether they are capable of diminishing hunger responsiveness. Several decades of research on anorexigenic properties of OT have indicated that administration of OT supports early cessation of ingestive behavior [for review, see (34)]. Evidence gathered thus far has strongly linked OT with termination of feeding due to enhanced satiation or in response to adverse physiological changes (such as plasma osmolality or stomach distension) that endanger homeostasis. The current set of data shows for the first time that anorexigenic effects of OT do not stem from promoting a reduced feeling of hunger.

Previous experiments have shown beyond reasonable doubt that peripherally injected OT decreases consumption. It seems that OT is particularly effective in reducing intake of energy-dense solid foods regardless of their composition and/or palatability (2, 8, 13, 14). On the other hand, unlike central OT (particularly, targeting the VTA, AcbC or amygdala) or OT receptor ligands that cross the BBB, peripheral OT is not effective in modifying consumption of calorie-dilute sweet solutions that are ingested primarily for pleasure (3, 5, 10, 35). Our feeding experiments indicate that i.p. OT decreases calorie-dense palatable food consumption regardless of whether intake

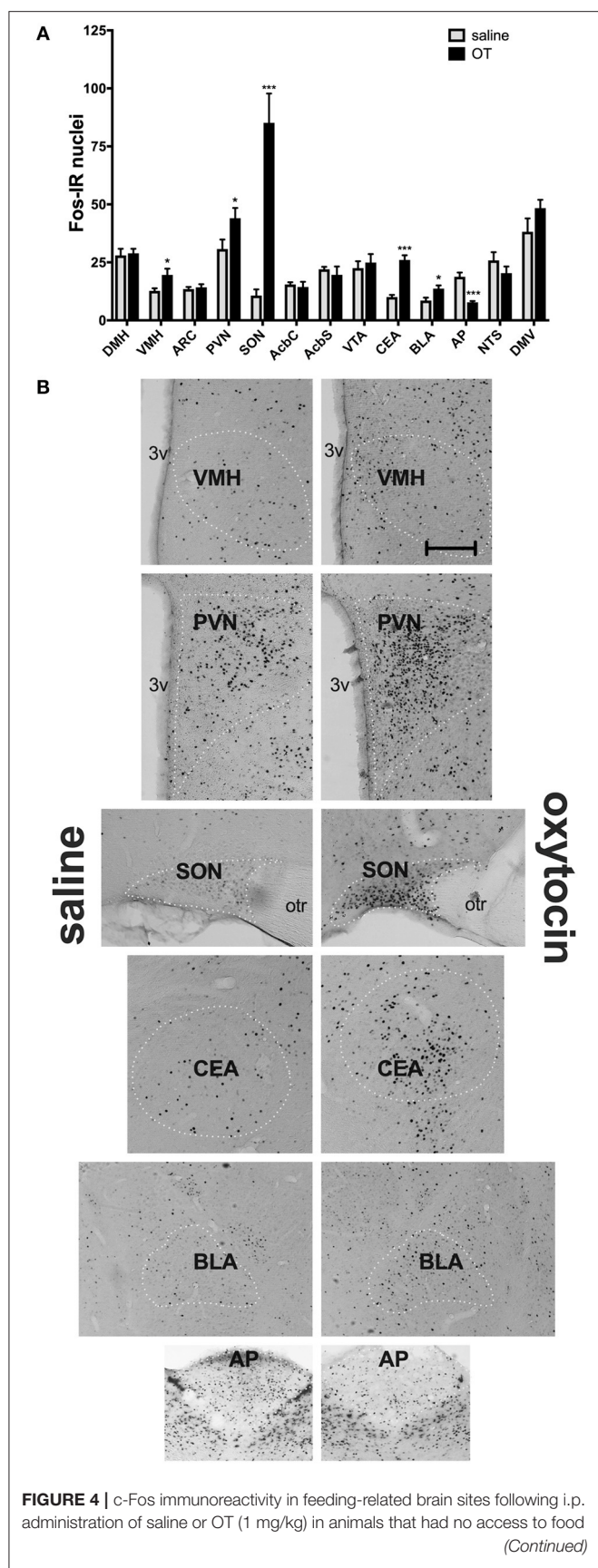
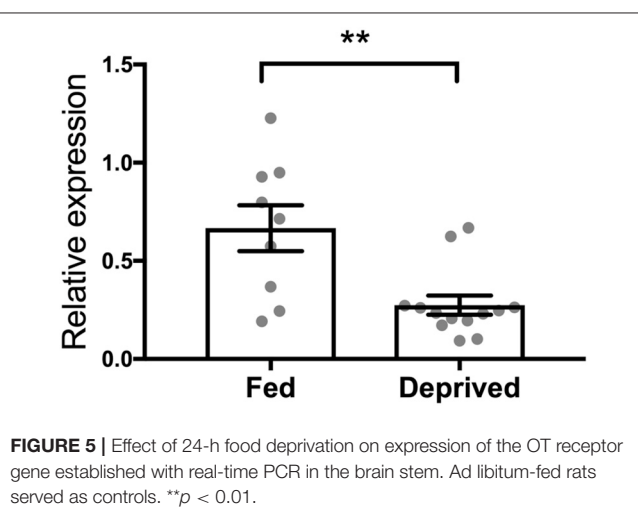


FIGURE 4 | for 22 h (A). Panel (B) presents photomicrographs depicting sites that showed a significant difference in c-Fos levels (saline-treated rats—left side; OT-treated rats—right side). Densities of Fos-positive nuclear profiles (per 1 mm² of a site) were averaged per individual, and then per group. AcbC, nucleus accumbens core; AcbS, nucleus accumbens shell; AP, area postrema; ARC, arcuate nucleus; BLA, basolateral amygdala; CEA, central nucleus of the amygdala; DMH, dorsomedial nucleus of the hypothalamus; DMV, dorsal motor nucleus of the vagus; NTS, nucleus of the solitary tract; PVN, paraventricular nucleus of the hypothalamus; SON, supraoptic nucleus; VMH, ventromedial nucleus; VTA, ventral tegmental area. * $p < 0.05$; *** $p < 0.001$.



is stimulated predominantly by hunger (as in animals deprived for 22 h) or by palatability (as in animals that had the standard chow removed only 2 h prior to episodic access to the HFHS diet). Hence, the relative calorie needs do not impact the ability of OT to produce hypophagia. The effective dose range (0.3–1 mg/kg) is also similar regardless of a feeding paradigm used here and by others.

It should be noted that craving and motivation are not factors that are directly measurable in either our discrimination or consumption procedures. As we and others have reported, simple measures of food consumption do not necessarily relate to motivation to work to obtain food [e.g., (36, 37)]. Assuming there are only two motivating factors driving consumption (reward/pleasure or “free or hedonic” drives) and energy, the “free” or “hedonic” drives would be the key influence mediating consumption under the 2 h deprivation. In our experiments, OT was somewhat more potent in reducing HFHS consumption in subjects that were 2 h-deprived compared to subjects that were 22 h-deprived. OT (0.3 and 1.0 mg reduced HFHS consumption by approximately 33% in the former group. OT (0.3 mg) did not reduce consumption of the HFHS diet in the subjects food-restricted for 22 h. The reduction in intake under 22-h deprivation was about 25% suggesting that the contribution of the “free or hedonic” food intake may be at least to some extent reduced following the 22-h deprivation. We and others have shown that opioid antagonists are more potent in reducing consumption of sweet food compared to regular chow [for review, see e.g., (38, 39)]. These findings would also support the

statement above. Craving is often associated with dependence-like behaviors during times of restriction or deprivation of the item inducing the “cravings.” We noted no dependence-like behaviors in subjects in either of our paradigms.

The hunger discrimination protocol that relies on the animals' ability to discriminate between short- (2–3 h) and long-term (e.g., 22 h) food deprivation and “report” it through operant behavior, has defined anorexigenic and orexigenic characteristics of several molecules. As food preloads appropriately change animals' perception of the length of deprivation, the parallel effect of anorexigens given instead of a food preload, indicates that they reduce a feeling of hunger. This approach allowed to implicate CCK and sibutramine as agents that can aid in controlling hunger (and deemed rimonabant ineffective in this process) (26, 27). Of note is the fact that, in contrast to anorexigens, some orexigens (NPY or ghrelin) make animals perceive the short 2-h deprivation as the state of hunger (28, 40). The fact that i.p. OT did not reduce operant responding to 22 h of deprivation strongly suggests that OT does not interfere with mechanisms that promote a feeling of hunger. It did not have an effect on hunger discrimination even though it was used at doses that are anorexigenic, and despite the fact that it did decrease bar pressing rate in general. It also produced a trend toward a reduction in chow intake in the 1 h after the completion of the operant test when animals were placed in a transition cage with chow present on the floor. Consequently, it can be inferred that OT induces hypophagia by being part of neuroendocrine processes that facilitate satiation and early cessation of feeding. This is in line with experiments showing a functional relationship between OT and numerous other mediators of satiety [for example, see (41, 42)], including melanocortins, which appear to form a common circuit with OT to support satiation. On the other hand, to our knowledge, there is no evidence that OT might be able to silence activation of, e.g., the NPY system, which could potentially suggest a link with hunger processing.

That i.p. OT differently affects neural processing under deprivation than in satiety is further substantiated by the outcomes of the c-Fos mapping study that revealed distinct patterns of c-Fos immunoreactivity in response to the OT treatment in hungry vs. sated animals. In individuals subjected to 2 h of deprivation, OT affected c-Fos immunoreactivity in a number of hypothalamic and brain stem sites: an increase in c-Fos staining occurred in the PVN, SON, NTS, and DMV, whereas a decrease was noted in the DMH, ARC, and VMH. The broad change in c-Fos levels in this network of sites that regulate energy intake is consistent with the role of OT as an anorexigen. Outside the hypothalamic-brainstem circuit, elevated c-Fos levels were in the CEA, which might potentially be related to emotional processing related to feeding (43–45) and it aligns well with the ability of OT itself to decrease consumption by acting at this site (5). Overall, the subset of sites activated by OT is quite similar to what had been reported before in various paradigms unrelated to food intake. For example, Carson et al. found an increase in the PVN, SON and CEA after 2 mg/kg OT in rats subjected to 80-min locomotor testing (46), and Hicks et al. found elevated activation in the PVN, SON, CEA and NTS after 1 mg/kg OT and a brief locomotor test (47). In another study, Hicks and colleagues

reported an increase in the PVN, CEA, and NTS in adolescent animals (48).

In hungry (thus, 22-h deprived) rats, systemic OT induced c-Fos in a smaller subset of areas. In the hypothalamus and brain stem, the PVN, SON, VMH, and—unlike under 2-h deprivation—the AP showed a significant change (it should be noted though that the AP c-Fos levels in hungry animals treated with OT were higher too, though only a trend was observed). No difference was noted in the DMH, ARC, NTS, and DMV. It appears therefore that in the hungry state, OT loses the capacity to engage as broad a network of sites that regulate energy balance as that activated during satiety. rtPCR data showing a decreased expression of the OT receptor gene in the brain stem, a region thought to mediate anorexigenic properties of systemic OT, provide an additional insight into a mechanistic change that might be a key contributor to the changed, hunger/satiety-dependent receptivity of the CNS to OT. Of note is the fact that the rtPCR analysis revealed global brain stem expression changes and did not include individual areas. Considering that specific brain stem sites (and within these sites, specific neuronal populations) play distinct roles in appetite regulation, future studies will have to refine our understanding of a relationship between energy state, OT receptor, and these particular circuits within the brain stem. Finally, it should be noted that in both 22-h and 2-h deprived rats the amygdala was affected by OT, however in hungry animals, not only the CEA, but also the BLA expressed higher c-Fos immunoreactivity. It allows us to speculate that—considering the role of the amygdala in emotional processing (43–45)—OT affects emotional aspects of feeding regardless of the deprivation level.

We conclude that systemic OT does not diminish a feeling of hunger before the start of a meal. Instead, OT's anorexigenic properties can be manifested once consumption has already begun and this, at least to some extent, is driven by changes in brain responsiveness to OT treatment in the hungry vs. fed state. Therefore, OT's role in feeding control should be viewed as a mediator of early satiation rather than as a molecule that diminishes a perceived need to seek calories.

ETHICS STATEMENT

This study was carried out in accordance with the recommendations of the University of Waikato animal ethics committee. The protocol was approved by the Institutional Animal Ethics Committee at the University of Waikato.

AUTHOR CONTRIBUTIONS

MH, DJ, SG, and AK performed the experiments. DJ, AL, and PO devised the project and the main conceptual ideas. MH, DJ, AK, PO, and SG processed and analyzed the data. MH, DJ, AL, and PO contributed to the organization and writing the manuscript.

FUNDING

Support was provided by the Royal Society of New Zealand (Marsden Grant 1203) and DGC Ltd.

REFERENCES

- Arletti R, Benelli A, Bertolini A. Influence of oxytocin on feeding behavior in the rat. *Peptides*. (1989) 10:89–93. doi: 10.1016/0196-9781(89)90082-X
- Blevins JE, Thompson BW, Anekonda VT, Ho JM, Graham JL, Roberts ZS, et al. Chronic CNS oxytocin signaling preferentially induces fat loss in high fat diet-fed rats by enhancing satiety responses and increasing lipid utilization. *Am J Physiol Regul Integr Comp Physiol*. (2016) 310:R640–58. doi: 10.1152/ajpregu.00220.2015
- Herisson FM, Waas JR, Fredriksson R, Schioth HB, Levine AS, Olszewski PK. Oxytocin acting in the nucleus accumbens core decreases food intake. *J Neuroendocrinol*. (2016) 28. doi: 10.1111/jne.12381
- Ho JM, Anekonda VT, Thompson BW, Zhu M, Curry RW, Hwang BH, et al. Hindbrain oxytocin receptors contribute to the effects of circulating oxytocin on food intake in male rats. *Endocrinology*. (2014) 155:2845–57. doi: 10.1210/en.2014-1148
- Klockars OA, Klockars A, Levine AS, Olszewski PK. Oxytocin administration in the basolateral and central nuclei of amygdala moderately suppresses food intake. *Neuroreport*. (2018) 29:504–10. doi: 10.1097/WNR.0000000000001005
- Klockars OA, Waas JR, Klockars A, Levine AS, Olszewski PK. Neural basis of ventromedial hypothalamic oxytocin-driven decrease in appetite. *Neuroscience*. (2017) 366:54–61. doi: 10.1016/j.neuroscience.2017.10.008
- Olszewski PK, Allen K, Levine AS. Effect of oxytocin receptor blockade on appetite for sugar is modified by social context. *Appetite*. (2015) 86:81–7. doi: 10.1016/j.appet.2014.10.007
- Roberts ZS, Wolden-Hanson T, Matsen ME, Ryu V, Vaughan CH, Graham JL, et al. Chronic hindbrain administration of oxytocin is sufficient to elicit weight loss in diet-induced obese rats. *Am J Physiol Regul Integr Comp Physiol*. (2017) 313:R357–71. doi: 10.1152/ajpregu.00169.2017
- Arletti R, Benelli A, Bertolini A. Oxytocin inhibits food and fluid intake in rats. *Physiol Behav*. (1990) 48:825–30. doi: 10.1016/0031-9384(90)90234-U
- Melis MR, Melis T, Cocco C, Succu S, Sanna F, Pillolla G, et al. Oxytocin injected into the ventral tegmental area induces penile erection and increases extracellular dopamine in the nucleus accumbens and paraventricular nucleus of the hypothalamus of male rats. *Eur J Neurosci*. (2007) 26:1026–35. doi: 10.1111/j.1460-9568.2007.05721.x
- Wu Z, Xu Y, Zhu Y, Sutton AK, Zhao R, Lowell BB, et al. An obligate role of oxytocin neurons in diet induced energy expenditure. *PLoS ONE*. (2012) 7:e45167. doi: 10.1371/journal.pone.0045167
- Maejima Y, Iwasaki Y, Yamahara Y, Kodaira M, Sedbazar U, Yada T. Peripheral oxytocin treatment ameliorates obesity by reducing food intake and visceral fat mass. *Aging*. (2011) 3:1169–77. doi: 10.18632/aging.100408
- Morton GJ, Thatcher BS, Reidelberger RD, Ogimoto K, Wolden-Hanson T, Baskin DG, et al. Peripheral oxytocin suppresses food intake and causes weight loss in diet-induced obese rats. *Am J Physiol Endocrinol Metab*. (2012) 302:E134–44. doi: 10.1152/ajpendo.00296.2011
- Klockars A, Brunton C, Li L, Levine AS, Olszewski PK. Intravenous administration of oxytocin in rats acutely decreases deprivation-induced chow intake, but it fails to affect consumption of palatable solutions. *Peptides*. (2017) 93:13–9. doi: 10.1016/j.peptides.2017.04.010
- Mitra A, Gosnell BA, Schioth HB, Grace MK, Klockars A, Olszewski PK, et al. Chronic sugar intake dampens feeding-related activity of neurons synthesizing a satiety mediator, oxytocin. *Peptides*. (2010) 31:1346–52. doi: 10.1016/j.peptides.2010.04.005
- Kublaoui BM, Gemelli T, Tolson KP, Wang Y, Zinn AR. Oxytocin deficiency mediates hyperphagic obesity of Sim1 haploinsufficient mice. *Mol Endocrinol*. (2008) 22:1723–34. doi: 10.1210/me.2008-0067
- Verbalis JG, McCann MJ, McHale CM, Stricker EM. Oxytocin secretion in response to cholecystokinin and food: differentiation of nausea from satiety. *Science*. (1986) 232:1417–9. doi: 10.1126/science.3715453
- Ohlsson B, Forsling ML, Rehfeld JF, Sjolund K. Cholecystokinin stimulation leads to increased oxytocin secretion in women. *Eur J Surg*. (2002) 168:114–8. doi: 10.1080/11024150252884340
- Renaud LP, Tang M, McCann MJ, Stricker EM, Verbalis JG. Cholecystokinin and gastric distension activate oxytocinergic cells in rat hypothalamus. *Am J Physiol*. (1987) 253(4 Pt 2):R661–5. doi: 10.1152/ajpregu.1987.253.4.R661
- Bojanowska E, Stempniak B. tGLP-1 and release of vasopressin and oxytocin from the isolated rat hypothalamo-neurohypophyseal system: effects of a tGLP-1 receptor agonist and antagonist. *J Physiol Pharmacol*. (2001) 52(4 Pt 2):781–93.
- Ladyman SR, Augustine RA, Scherf E, Philipps HR, Brown CH, Grattan DR. Attenuated hypothalamic responses to alpha-melanocyte stimulating hormone during pregnancy in the rat. *J Physiol*. (2016) 594:1087–101. doi: 10.1113/JP271605
- Gartner SN, Aidney F, Klockars A, Prosser C, Carpenter EA, Isgrove K, et al. Intragastric preloads of L-tryptophan reduce ingestive behavior via oxytocinergic neural mechanisms in male mice. *Appetite*. (2018) 125:278–86. doi: 10.1016/j.appet.2018.02.015
- Gartner SN, Klockars A, Prosser C, Carpenter EA, Levine AS, Olszewski PK. Identification of central mechanisms underlying anorexigenic effects of intraperitoneal L-tryptophan. *Neuroreport*. (2018) 29:1293–300. doi: 10.1097/WNR.0000000000001110
- Lawson EA, Marengi DA, DeSanti RL, Holmes TM, Schoenfeld DA, Tolley CJ. Oxytocin reduces caloric intake in men. *Obesity*. (2015) 23:950–6. doi: 10.1002/oby.21069
- Olson BR, Drutarosky MD, Chow MS, Hruby VJ, Stricker EM, Verbalis JG. Oxytocin and an oxytocin agonist administered centrally decrease food intake in rats. *Peptides*. (1991) 12:113–8. doi: 10.1016/0196-9781(91)90176-P
- Corwin RL, Woolverton WL, Schuster CR. Effects of cholecystokinin, d-amphetamine and fenfluramine in rats trained to discriminate 3 from 22 h of food deprivation. *J Pharmacol Exp Therapeut*. (1990) 253:720–8.
- Jewett DC, Hahn TW, Smith TR, Fiksdal BL, Wiebelhaus JM, Dunbar AR, et al. Effects of sibutramine and rimonabant in rats trained to discriminate between 22- and 2-h food deprivation. *Psychopharmacology*. (2009) 203:453–9. doi: 10.1007/s00213-008-1350-1
- Jewett DC, Lefever TW, Flashinski DP, Koffarnus MN, Cameron CR, Ehli DJ, et al. Intraparaventricular neuropeptide Y and ghrelin induce learned behaviors that report food deprivation in rats. *Neuroreport*. (2006) 17:733–7. doi: 10.1097/01.wnr.0000215767.94528.f8
- Olszewski PK, Klockars A, Olszewski PK, Fredriksson R, Schioth HB, Levine AS. Molecular, immunohistochemical, and pharmacological evidence of oxytocin's role as inhibitor of carbohydrate but not fat intake. *Endocrinology*. (2010) 151:4736–44. doi: 10.1210/en.2010-0151
- Fredriksson R, Hagglund M, Olszewski PK, Stephansson O, Jacobsson JA, Olszewska AM, et al. The obesity gene, FTO, is of ancient origin, up-regulated during food deprivation and expressed in neurons of feeding-related nuclei of the brain. *Endocrinology*. (2008) 149:2062–71. doi: 10.1210/en.2007-1457
- Stanley BG, Kyrkouli SE, Lampert S, Leibowitz SF. Neuropeptide Y chronically injected into the hypothalamus: a powerful neurochemical inducer of hyperphagia and obesity. *Peptides*. (1986) 7:1189–92. doi: 10.1016/0196-9781(86)90149-X
- Bailey AR, Giles M, Brown CH, Bull PM, Macdonald LP, Smith LC, et al. Chronic central infusion of growth hormone secretagogues: effects on fos expression and peptide gene expression in the rat arcuate nucleus. *Neuroendocrinology*. (1999) 70:83–92. doi: 10.1159/000054462
- Wren AM, Small CJ, Abbott CR, Dhillo WS, Seal LJ, Cohen MA, et al. Ghrelin causes hyperphagia and obesity in rats. *Diabetes*. (2001) 50:2540–7. doi: 10.2337/diabetes.50.11.2540
- Olszewski PK, Klockars A, Levine AS. Oxytocin: a conditional anorexigen whose effects on appetite depend on the physiological, behavioural and social contexts. *J Neuroendocrinol*. (2016) 28. doi: 10.1111/jne.12376
- Herisson FM, Brooks LL, Waas JR, Levine AS, Olszewski PK. Functional relationship between oxytocin and appetite for carbohydrates versus saccharin. *Neuroreport*. (2014) 25:909–14. doi: 10.1097/WNR.0000000000000201
- Jewett DC, Cleary J, Levine AS, Schaal DW, Thompson T. Effects of neuropeptide Y on food-reinforced behavior in satiated rats. *Pharmacol Biochem Behav*. (1992) 42:207–12. doi: 10.1016/0091-3057(92)90517-J
- Jewett DC, Cleary J, Levine AS, Schaal DW, Thompson T. Effects of neuropeptide Y, insulin, 2-deoxyglucose, and food deprivation on food-motivated behavior. *Psychopharmacology*. (1995) 120:267–71. doi: 10.1007/BF02311173

38. Olszewski PK, Wood EL, Klockars A, Levine AS. Excessive consumption of sugar: an insatiable drive for reward. *Curr Nutr Rep.* (2019) 8:120–8. doi: 10.1007/s13668-019-0270-5
39. Olszewski PK, Levine AS. Central opioids and consumption of sweet tastants: when reward outweighs homeostasis. *Physiol Behav.* (2007) 91:506–12. doi: 10.1016/j.physbeh.2007.01.011
40. Davidson TL, Kanoski SE, Tracy AL, Walls EK, Clegg D, Benoit SC. The interoceptive cue properties of ghrelin generalize to cues produced by food deprivation. *Peptides.* (2005) 26:1602–10. doi: 10.1016/j.peptides.2005.02.014
41. Olson BR, Drutarosky MD, Stricker EM, Verbalis JG. Brain oxytocin receptor antagonism blunts the effects of anorexigenic treatments in rats: evidence for central oxytocin inhibition of food intake. *Endocrinology.* (1991) 129:785–91. doi: 10.1210/endo-129-2-785
42. Olszewski PK, Wirth MM, Shaw TJ, Grace MK, Billington CJ, Giraudo SQ, et al. Role of alpha-MSH in the regulation of consummatory behavior: immunohistochemical evidence. *Am J Physiol Regul Integr Comp Physiol.* (2001) 281:R673–80. doi: 10.1152/ajpregu.2001.281.2.R673
43. Sun X, Kroemer NB, Veldhuizen MG, Babbs AE, de Araujo IE, Gitelman DR, et al. Basolateral amygdala response to food cues in the absence of hunger is associated with weight gain susceptibility. *J Neurosci.* (2015) 35:7964–76. doi: 10.1523/JNEUROSCI.3884-14.2015
44. Beckman TR, Shi Q, Levine AS, Billington CJ. Amygdalar opioids modulate hypothalamic melanocortin-induced anorexia. *Physiol Behav.* (2009) 96:568–73. doi: 10.1016/j.physbeh.2008.12.007
45. Alvarez-Crespo M, Skibicka KP, Farkas I, Molnar CS, Egecioglu E, Hrabovszky E, et al. The amygdala as a neurobiological target for ghrelin in rats: neuroanatomical, electrophysiological and behavioral evidence. *PLoS ONE.* (2012) 7:e46321. doi: 10.1371/journal.pone.0046321
46. Carson DS, Hunt GE, Guastella AJ, Barber L, Cornish JL, Arnold JC, et al. Systemically administered oxytocin decreases methamphetamine activation of the subthalamic nucleus and accumbens core and stimulates oxytocinergic neurons in the hypothalamus. *Addict Biol.* (2010) 15:448–63. doi: 10.1111/j.1369-1600.2010.00247.x
47. Hicks C, Ramos L, Dampney B, Baracz SJ, McGregor IS, Hunt GE. Regional c-Fos expression induced by peripheral oxytocin administration is prevented by the vasopressin 1A receptor antagonist SR49059. *Brain Res Bull.* (2016) 127:208–18. doi: 10.1016/j.brainresbull.2016.10.005
48. Hicks C, Jorgensen W, Brown C, Fardell J, Koehbach J, Gruber CW, et al. The nonpeptide oxytocin receptor agonist WAY 267,464: receptor-binding profile, prosocial effects and distribution of c-Fos expression in adolescent rats. *J Neuroendocrinol.* (2012) 24:1012–29. doi: 10.1111/j.1365-2826.2012.02311.x

Conflict of Interest Statement: The authors declare that the research was conducted in the absence of any commercial or financial relationships that could be construed as a potential conflict of interest.

Copyright © 2019 Head, Jewett, Gartner, Klockars, Levine and Olszewski. This is an open-access article distributed under the terms of the Creative Commons Attribution License (CC BY). The use, distribution or reproduction in other forums is permitted, provided the original author(s) and the copyright owner(s) are credited and that the original publication in this journal is cited, in accordance with accepted academic practice. No use, distribution or reproduction is permitted which does not comply with these terms.



A Synaptically Connected Hypothalamic Magnocellular Vasopressin-Locus Coeruleus Neuronal Circuit and Its Plasticity in Response to Emotional and Physiological Stress

Oscar R. Hernández-Pérez^{1†}, Vito S. Hernández^{1†}, Alicia T. Nava-Kopp^{1†}, Rafael A. Barrio², Mohsen Seifi³, Jerome D. Swinny³, Lee E. Eiden⁴ and Limei Zhang^{1*}

OPEN ACCESS

Edited by:

Vincent Geenen,
University of Liège, Belgium

Reviewed by:

Tomas Hokfelt,
Karolinska Institute (KI), Sweden
Gábor B. Makara,
Hungarian Academy of Sciences
(MTA), Hungary

*Correspondence:

Limei Zhang
limei@unam.mx

[†] These authors have contributed
equally to this work

Specialty section:

This article was submitted to
Neuroendocrine Science,
a section of the journal
Frontiers in Neuroscience

Received: 09 January 2019

Accepted: 19 February 2019

Published: 20 March 2019

Citation:

Hernández-Pérez OR,
Hernández VS, Nava-Kopp AT,
Barrio RA, Seifi M, Swinny JD,
Eiden LE and Zhang L (2019) A
Synaptically Connected Hypothalamic
Magnocellular Vasopressin-Locus
Coeruleus Neuronal Circuit and Its
Plasticity in Response to Emotional
and Physiological Stress.
Front. Neurosci. 13:196.
doi: 10.3389/fnins.2019.00196

¹ Departamento de Fisiología, Facultad de Medicina, Universidad Nacional Autónoma de México, Mexico City, Mexico,
² Instituto de Física, Universidad Nacional Autónoma de México, Mexico City, Mexico, ³ School of Pharmacy and Biomedical
Sciences, Institute for Biomedical and Biomolecular Science, University of Portsmouth, Portsmouth, United Kingdom,
⁴ Section on Molecular Neuroscience, National Institute of Mental Health-IRP, Bethesda, MD, United States

The locus coeruleus (LC)-norepinephrine (NE) system modulates a range of salient brain functions, including memory and response to stress. The LC-NE system is regulated by neurochemically diverse inputs, including a range of neuropeptides such as arginine-vasopressin (AVP). Whilst the origins of many of these LC inputs, their synaptic connectivity with LC neurons, and their contribution to LC-mediated brain functions, have been well characterized, this is not the case for the AVP-LC system. Therefore, our aims were to define the types of synapses formed by AVP+ fibers with LC neurons using immunohistochemistry together with confocal and transmission electron microscopy (TEM), the origins of such inputs, using retrograde tracers, and the plasticity of the LC AVP system in response to stress and spatial learning, using the maternal separation (MS) and Morris water maze (MWM) paradigms, respectively, in rat. Confocal microscopy revealed that AVP+ fibers contacting tyrosine hydroxylase (TH)+ LC neurons were also immunopositive for vesicular glutamate transporter 2, a marker of presynaptic glutamatergic axons. TEM confirmed that AVP+ axons formed Gray type I (asymmetric) synapses with TH+ dendrites thus confirming excitatory synaptic connections between these systems. Retrograde tracing revealed that these LC AVP+ fibers originate from hypothalamic vasopressinergic magnocellular neurosecretory neurons (AVPMNNs). MS induced a significant increase in the density of LC AVP+ fibers. Finally, AVPMNN circuit upregulation by water-deprivation improved MWM performance while increased Fos expression was found in LC and efferent regions such as hippocampus and prefrontal cortex, suggesting that AVPMNN projections to LC could integrate homeostatic responses modifying neuroplasticity.

Keywords: arginine vasopressin, RNAscope, Fluoro-Gold, Morris water maze, electron microscopy

INTRODUCTION

Converging pharmacological, physiological and behavioral data indicate that the neurohormone arginine vasopressin (AVP) system is principally linked to the homeostatic regulation of fluid balance (Armstrong, 2004), yet ascending vasopressinergic projections that connect the physiology of water regulation with emotional context and adaptive behaviors have been reported (de Wied et al., 1993; Hernandez et al., 2012; Zhang et al., 2012, 2016, 2018; Zhang and Eiden, 2018). Historically, the actions of AVP within the brain were considered to primarily occur in a paracrine manner, for example, via dendritic release from hypothalamic neurons and further diffusion to target brain regions via the cerebrospinal or interstitial fluids (Leng et al., 1992; Landgraf and Neumann, 2004; Ludwig and Leng, 2006). However, we and others have since demonstrated direct synaptic connections between vasopressinergic magnocellular neurosecretory neurons (AVPMNNs) of the hypothalamus and other brain regions including hippocampus (Cui et al., 2013; Zhang and Hernandez, 2013), amygdala (Hernandez et al., 2016), and lateral habenula (Zhang et al., 2016, 2018) via dual AVPMNN projections to these regions and to the neurohypophysis (Hernandez et al., 2015). This raises the possibility of direct AVPMNN projections to additional brain nuclei that participate in integrating homeostatic with behavioral regulation (Zhang and Eiden, 2018). AVP-immunopositive (AVP+) axons have indeed been identified in a myriad of brain regions involved in such functions, including the pontine nucleus *locus coeruleus* (LC) (Buijs, 1978; Rood and De Vries, 2011). However, the source of these inputs, and therefore the putative regulatory circuits in which they participate, have not been identified.

The LC (also called nucleus pigmentosus ponti) are bilateral dense groups of cells located in the pontine tegmentum, specifically in the lateral-rostral part of the floor of the 4th ventricle. LC neurons are identified by their expression of the norepinephrine synthesizing enzymes tyrosine hydroxylase (TH) and dopamine-beta-hydroxylase (DBH), but not phenylethanolamine N-methyltransferase, thereby confirming their principal neurochemical signature of norepinephrine (NE) (Kobayashi et al., 1974; Swanson, 1976; Levitt and Moore, 1979). LC neurons provide the major source of NE throughout most of the brain (Robertson et al., 2013; Schwarz and Luo, 2015). The LC-NE system modulates some of the most salient brain functions, such as arousal, learning and memory and the cognitive response to stress (Berridge and Waterhouse, 2003; Atzori et al., 2016). At the synaptic level, NE facilitates synaptic plasticity by recruiting and modifying multiple molecular elements of synaptic signaling, including specific transmitter receptors, intracellular protein kinases, and translation initiation (Maity et al., 2015; Nguyen and Gelin, 2018). All such LC-NE functions are strongly aligned with the levels of LC neuronal activity. While LC neurons are spontaneously active, their firing rates are strongly influenced by their afferent inputs, many of which contain an array of neuropeptides (Palkovits and Brownstein, 1983), including corticotropin-releasing factor (CRF) (Swinny and Valentino, 2006; Swinny et al., 2010) and AVP (Buijs, 1978). Regarding the former, there is consensus that

CRF fibers in LC are of hypothalamic (PVN parvocellular) origin (Valentino and Van Bockstaele, 2008). While a large body of data demonstrate the origins of CRF and other LC afferents (Schwarz and Luo, 2015), the precise source of AVP+ axons in the LC has yet to be identified, even though hypothalamic paraventricular and supraoptic regions are known sources for afferents to LC (Schwarz et al., 2015). Furthermore, conclusive evidence for AVP+ fibers making synaptic contact with LC neurons has yet to be reported.

We recently reported on the molecular and physiological correlates of the AVP-receptor system in the mouse LC (Campos-Lira et al., 2018). In the current study, we expand upon these data to demonstrate that AVP+ axons make excitatory synaptic contact with TH neurons, at the ultrastructural level, and that these axons originate from discrete hypothalamic nuclei, thereby identifying specific AVP hypothalamic-LC circuits. We further demonstrate the potential engagement of these circuits in response to life experiences which require the homeostatic properties of both the LC and the hypothalamus.

MATERIALS AND METHODS

Animals

Wistar rats from a local animal breeding facility were used throughout this study. All procedures were approved by the Research and Ethics Committee of the Faculty of Medicine, Universidad Nacional Autónoma de México (CIEFM 062/2016). Animals were housed three per cage under controlled temperature (22°C) and illumination (12 h), with water and food *ad libitum*. After surgery, animals were kept warm until fully recovered from anesthesia and then kept individually under the above-mentioned conditions for 1 week and returned to the original housing conditions.

Immunohistochemistry (IHC) for Light and Transmission Electron Microscopy (LM and TEM)

Male rats of 270 ± 30 g were deeply anesthetized with an overdose of sodium pentobarbital (63 mg/kg, Sedalpharma, Mexico) and perfused transaortically with 0.9% saline followed by cold fixative containing 4% of paraformaldehyde in 0.1 M sodium phosphate buffer (PB, pH 7.4) plus 15% v/v saturated picric acid for 15 min (0.05% of glutaraldehyde was added to fixative for the samples intended for TEM). Brains were immediately removed, blocked, then thoroughly rinsed with 0.1 M PB until they were clear of fixative. The brains were then sectioned using a Leica VT 1000S vibratome, at 70 µm thickness in the horizontal plane.

For LM IHC, non-specific binding of the secondary antibodies was minimized by incubating sections containing LC with 20% normal donkey serum (NDS) in Tris-buffered (0.05 M, pH 7.4) saline (0.9%) plus 0.3% of Triton X-100 (TBST) for 1 h at room temperature (RT). The sections were then incubated with the following primary antibodies: rabbit anti-AVP antibody (kind gift of Dr. Ruud M. Buijs; Buijs et al., 1989), mouse

anti-AVP antibody (kind gift of Dr. Hal Gainer; Alstein et al., 1988), rabbit anti-AVP (Abcam, ab39363, for **Figure 1B**) sheep anti-tyrosine hydroxylase (TH) [Abcam, ab113; guinea pig anti-VGLUT2 (Frontier Institute, VGLUT2, GP-Af810)]. The next day, the sections were washed with TBST for 30 min after

which they were incubated at RT in a cocktail of an appropriate mixture of secondary antibodies, conjugated with Alexa Fluor 488, Alexa 594 and indocarbocyanine (Cy5), all provided by Jackson ImmunoResearch, for 2 h. The sections were washed in TBST and were mounted on glass slides, air dried and

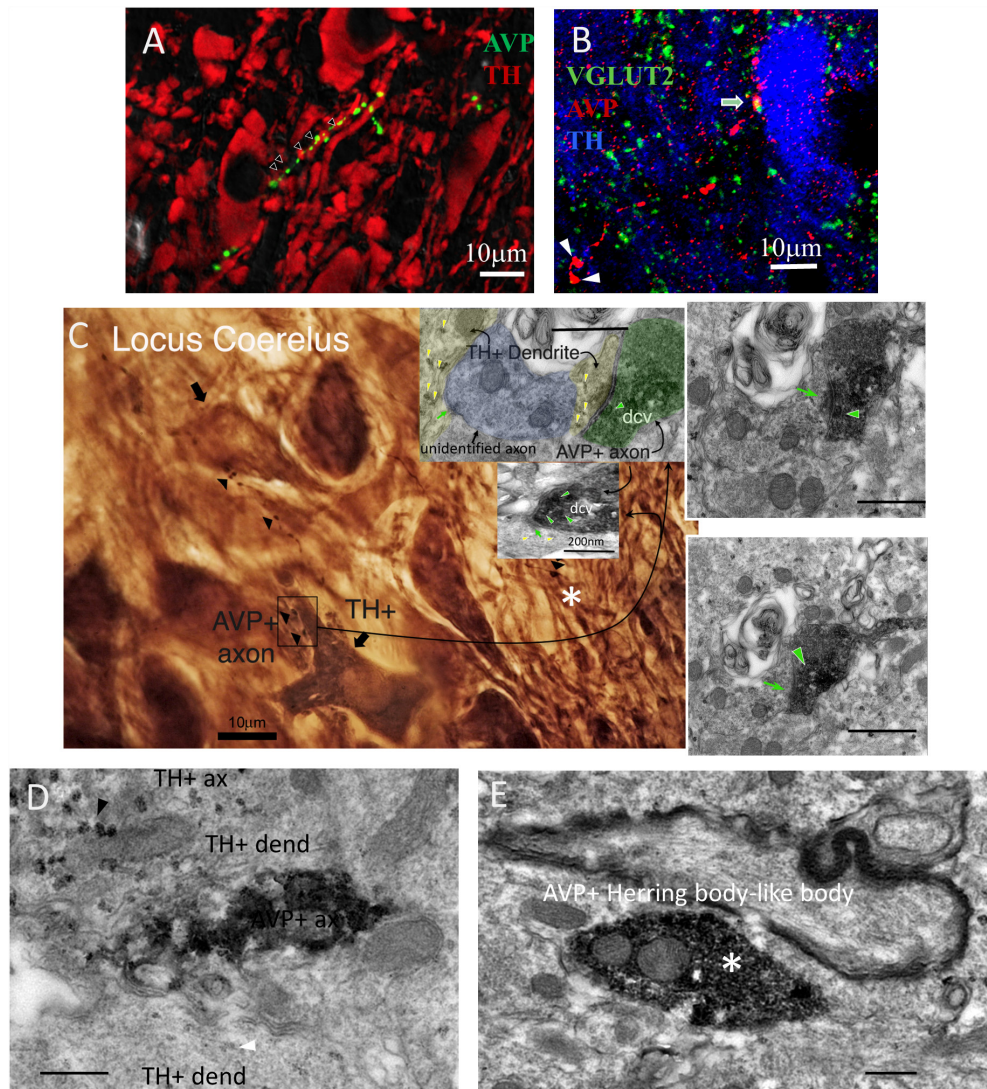


FIGURE 1 | AVP-VGLUT2 immunopositive (AVP+/VGLUT2+) fibers establish Gray type I (asymmetric) synapses onto tyrosine hydroxylase immunopositive (TH+) dendrites within the LC. **(A,B)** Confocal photomicrographs showing AVP+ fibers making contacts with TH+ dendrites **(A)** and the co-localization of AVP+/VGLUT2+ segments **(B)**, two Herring body-like bodies were indicated by arrow heads). **(A)** AVP reaction was made using the antibody gifted from H. Gainer laboratory and image was taken at 0.5 AU (Airy Units, using Leica SP5 confocal system) optical section thickness of around 0.596 μm . This measure helps to improve the optical resolution to visualize the contact points in a strongly labeled tissue. The panel **B** was from mouse LC tissue using a different antibody (Abcam ab39363) and taken at 1 AU (optical section thickness was around 0.892 μm). **(C)** Photomicrograph taken from a pre-embedding immunoreaction of trimmed resin capsule surface (the "pyramid," osmicated losing the purple color under LM), containing LC prepared for electron microscopy (EM), using DAB/VIP (Very Intense Purple) double peroxidase-chromogen immunostaining for electron microscopy. AVP+ fibers were evidently making contact with TH+ dendritic segments indicated by arrowheads. The inserts are TEM micrographs from serial samples of the region indicated by rectangle area in **C**. The image shows an AVP+ axon with a terminal (depicted in four serial sections) containing AVP+ dense-core vesicles (dcv, indicated with green arrowhead), establishing a Gray-type I synapse onto a TH+ dendrite (TH is demonstrated by granular labeling produced by VIP reagent at electron microscopy level, yellow arrowheads). Postsynaptic density (PSD), a TEM feature of a Gray type I synapse, which is generally indicative of a glutamatergic synapse, are indicated by green arrows. **(D)** TEM micrograph showing one segment of the same AVP+ profile (DAB-nickel labeling) coursing in parallel with two TH+ (VIP labeling) dendrites. Note that the VIP labeling for dendrite (white arrowhead) was weaker than for axonal segment (black arrowhead). **(E)** An Herring body-like body (large axonal varicosity), an anatomical feature of the vasopressinergic magnocellular neurosecretory neurons (white asterisks of panel **B,E**) examined under EM. Scale bars: 400 nm unless stated otherwise.

coverslipped using Vectashield mounting medium (H-1000, Vector Laboratories Inc.).

For double peroxidase-chromogen immunostaining and electron microscopy (TEM), brain sections containing LC, were cryoprotected with 10% and then 20% sucrose in PB (under gentle agitation until the sections sank). Permeability of the tissue was then enhanced by rapidly freezing and thawing sections using liquid nitrogen. Sections were then thoroughly rinsed with PB 0.1 M and non-specific secondary antibody binding was minimized with 20% NDS in TBS for 1 h at RT. The sections were then incubated with rabbit anti-AVP and sheep anti-TH antibodies (see above) in TBS plus 1% NDS for 48 h at 4°C with gentle agitation. After rinsing in TBS, incubation was continued with first secondary antibody swine anti-rabbit IgG conjugated with horseradish peroxidase (HRP) (1:100, Dako P021702, Copenhagen, Denmark), in TBS containing 1% of NDS, overnight at 4°C. Sections were then rinsed and peroxidase enzyme reaction was carried out using the chromogen 3,3'-diaminobenzidine (DAB, 0.05%, Electron Microscopy Sciences) and hydrogen peroxide (H₂O₂, 0.01%) as the substrate. The reaction end product in some sections was intensified with nickel. Subsequently, sections were incubated with 2nd secondary antibody, biotinylated goat anti sheep antibody (Jackson ImmunoResearch Laboratories) and then incubated with Vectastain standard ABC kit [VECTASTAIN®Elite®ABC HRP Kit (Peroxidase, Standard), Cat. No: PK-6100, Vector Laboratories, Burlingame, CA, United States]. The TH immunoreactivity was then visualized by using a Vector-VIP (*very intense purple*) peroxidase substrate kit [VECTOR®VIP Peroxidase (HRP) Substrate Kit; Vector Laboratories]. This procedure yields a reaction product that appears purple in the light microscope and granular or particulate in the electron microscope. Sections were then post-fixed with 1% osmium tetroxide in 0.1 M PB for 1 h and dehydrated through a series of graded alcohols (including 45 min of incubation in 1% uranyl acetate in 70% ethanol), then transferred to propylene oxide, followed by Durcupan ACM epoxy resin (Cat. No. 100503-434, Electron Microscopy Sciences). Sections were flat embedded on glass microscope slides, and the resin was polymerized at 60°C for 2 days. After removing the coverslip, LC containing regions, identified by TH immunoreactivity, were sectioned and carefully re-embedded in capsules in Durcupan resin. Ultrathin serial sections (70 nm) were prepared with an ultramicrotome, collected on pioloform-coated single slot grids and examined with a Philips CM100 transmission electron microscope. Digital electron micrographs were obtained with a digital micrograph 3.4 camera (Gatan Inc., Pleasanton, CA, United States).

RNAscope ISH Assays

Rats were deeply anesthetized and decapitated using a small animal guillotine (Kent Scientific corp.). Brains were removed and rapidly frozen using dry-ice powder. The fresh-frozen tissue was sectioned (12 µm thick) using a cryostat (Leica CM-1520) and mounted on positively charged glass slides (Fisher Scientific, Pittsburgh, PA, United States). The RNA probes for *in situ* hybridization used in this study to identify the genes of tyrosine hydroxylase (TH), V1a (Avpr1a), and V1b (Avpr1b) receptors

were designed and provided by Advanced Cell Diagnostics (Hayward, CA, United States). All staining steps were performed following RNAscope®2.5 HD Duplex Assay protocol for fresh frozen sections.

Fluoro-Gold Retrograde Tracing

The FG retrograde injection method was according to previously described protocols (Schmued and Fallon, 1986; Morales and Wang, 2002; Yamaguchi et al., 2011; Zhang and Hernandez, 2013). A total of twenty 300g Wistar male rats were used in this experiment. Rats were anesthetized with xylazine (Procin, Mexico) (20 mg/ml) and ketamine (Inoketam, Virbac, Mexico) (100 mg/ml) in a 1:1 volume ratio and administered intraperitoneally (*i.p.*) at a dose of 1 ml/kg of body weight. Deeply anesthetized rats were placed in a stereotaxic apparatus and the retrograde tracer Fluoro-Gold (FG, Fluorochrome, LLC, Denver, Colorado 80218, United States), dissolved 1% in 0.1 M cacodylate buffer (pH 7.5), was delivered iontophoretically (Value Kation Sci VAB-500) at the following coordinates: Bregma −9.48 mm, lateral 1.20 mm, and dorso-ventral 7.30 mm, via a glass micropipette (inner tip diameter of approximately 20 µm, current pulses of 0.1 µA, at 0.2 Hz, with a 50% duty cycle) for 20 min. The micropipette was left in place for an additional 10 min to prevent backflow of the tracer up the injection track after each injection. Upon recovery, the rats were administered 0.4 mg/kg *i.p.* Ketorolac (Apotex, Mexico) and 50 mg/kg *i.p.* ceftriaxone (Kendric, Mexico) as analgesic/anti-inflammatory and antibiotic agents, respectively. One week after the FG injections, the rats were perfused and brains sectioned in the coronal plane. Injection sites were evaluated and the inclusion criteria include: (1) the center of the injection was within the 300 µm of the core of LC and (2) there was no visible cerebrospinal-fluid (CSF) leaking of FG, evidenced by diffused and bilateral signals. The selected cases were further processed for IHC against TH in the brain stem and AVP in the anterior hypothalamus sections.

Maternal Separation (MS) Protocol

The MS (3 h daily, MS 3 h) procedure is described in detail elsewhere (Zhang et al., 2012). Briefly, female and male adult rats were mated for 2 days. During the last week of gestation, female rats were single-housed in standard rat Plexiglas cages and maintained under standard laboratory conditions. On the day after parturition, postnatal day (PND) 2, each litter was culled to 7–8 pups, of which 5–6 were males. During the period from PND 2–PND 16, the pups were separated daily from their dams, and placed into an incubator at 29°C ± 1°C, between 09:00 and 12:00 h. After this period rats were returned to their home cages. After ending the MS protocol, animals were left undisturbed until the weaning at PND 28, when male and female rats were separated. Bedding was changed twice a week, with minimum disturbance. At PND 75, male rats of 270 ± 30 g were not allowed access to water for 24 h (WD24h) before perfusion-fixation, according to the above-mentioned protocols, in order to minimize variability in basal AVP immunoreactivity, as demonstrated previously (Verney, 1947; Fitzsimons and O'Connor, 1976; Robertson et al., 1976; Zhang et al., 2010),

thereby enhancing comparability of subjects. Following fixation, tissue sections were prepared and immunoreactivity for AVP within the LC was carried out as above described.

Optical Density Analysis

For optical density analysis of IHC, the area occupied by the signal was calculated in 10 fields in control and MS animals using a modification of the protocol described elsewhere (Ying et al., 2017). Briefly, all images were acquired under identical conditions. Using ImageJ, images were converted to grayscale. Thresholds were manually set until the majority of the area occupied by the labeled fibers was highlighted and maximally separated from the background noise. Images were converted to binary format and the threshold areas were measured. The results were expressed as mean \pm SEM percentage of control and compared with a Student *t*-test.

Morris Water Maze Test

The Morris water maze (MWM) (Morris, 1984) assesses spatial learning and memory retention. The experimental design we used consisted of a black circular pool (diameter: 156 cm; height: 80 cm) filled with water to a height of 30 cm and temperature of $25 \pm 1^\circ\text{C}$, with visual cues placed on the wall of the pool. Four virtual quadrants were named I, II, III, IV (see **Figure 5**, panes C and D for a graphical description). A circular black escape platform (diameter 12 cm) was submerged 1 cm below the water surface to serve as an escape platform. The tests were video recorded under dim red light. This setting has proved to be useful for spatial learning and memory retention assessments as previously described (Zhang et al., 2008; Hernandez et al., 2012).

Ten rats participated in this test. Animals were kept in a light-dark cycle 12:12, with light on at 7:00 am of solar time, which is denominated as the *zeitgeber* time 0, i.e., circadian time 0 (CT0) and were separated in two groups: control with food and water *ad libitum* and water deprivation 24 h group (WD24h). The test was performed during rat inactivity period aiming to avoid the spontaneous high Fos expression in LC during the early activity period. Two assessments were made sequentially: the “morning” test (MT: performed between CT3–CT5) and the “afternoon” test (AT: performed between CT8–CT10). Before the MT, a pre-test habituation was done, which consisted in placing subjects from one group into the pool for 2 min to allow them to habituate the water. Rats are natural swimmers. Hence, this procedure reduces the possible stress of being immersed into water during the tests as well as to activate the innate swimming ability while making them acquainted to the environment.

The MT of MWM started by placing the escape platform in the quadrant II. Each subject was carefully introduced into the pool starting at quadrant I. Time elapsed between this event and subject arrival at the escape platform was recorded. In the first trial, subjects were allowed to explore the entire pool for 60 s, then the experimenter guided them to the platform, allowing them to climb onto the platform and to observe the location and environment for 5 s (see **Figure 5**, panels C and D, symbolized with dashed lines for a graphical description).

Six trials were completed for each subject, with intervals of 5 min between each of them. The rats were returned to the resting room with water and food *ad libitum* for 3 h. Then the AT started

at CT8 repeating the same procedure modifying the location of the escape platform to the quadrant I and the starting point to the quadrant III.

Fos IHC and Assessment

To evaluate the neuronal activity of LC, hippocampus and prefrontal cortex, the protein product of the proto-oncogene Fos was used. Since Fos is best detected in the interval between 60 and 120 min after a neuron is activated (Kovacs, 1998, 2008), we perfused the rats 90 min post-AT (MWM). For IHC, every third section containing the brain nuclei was blocked with 10% NDS in Tris-buffered (0.05M, pH 7.4) saline (0.9%) plus 0.3% of Triton X-100 (TBST) for 1 h at RT and then immunoreacted overnight with rabbit anti-Fos primary antibody (SC52, 1:1000, Santa Cruz Biotechnology, Santa Cruz, CA, United States) in TBST + 1% NDS at 4°C with gentle shaking. Afterward, sections were rinsed three times for 10 min with TBST and then incubated for 2 h at RT with biotinylated goat anti-rabbit secondary antibody (1:200; Vector Labs, Burlingame, CA, United States). Finally, sections were incubated in avidin-biotin-peroxidase complex (Elite ABC Kit, Vector Labs) for 1 h at RT. Peroxidase was detected using diaminobenzidine 0.05% as chromogen. Sections were rinsed and permanently mounted with Permount mounting medium (Electron Microscopy Sciences, Hatfield, PA, United States). Fos immunoreactive nuclei per 0.0346 mm^2 (area of a visual field: VF through the $100\times$ objective) were counted using a Nikon Eclipse 50i microscope. The results were expressed as mean \pm SEM nuclei/VF and compared with a Student *t*-test.

RESULTS

Synaptic Connectivity Between AVP+ Axons and LC Neurons

In mouse, sparse AVP+ axons have been reported in the region occupied by LC, using single labeling light microscopy (Rood and De Vries, 2011). We recently expanded upon these data to demonstrate that AVP+ axons in the mouse LC are located in close apposition to inhibitory and excitatory synaptic marker proteins (Campos-Lira et al., 2018). However, it is unclear whether the same association of AVP with synaptic molecular machinery exists in other species such as the rat, and whether the signal is located within synaptic junctions, or on neighboring compartments. We therefore began by examining the association of AVP+ profiles with such molecular signatures of synaptic transmission, in rat LC at the light microscopical level.

Using widely validated AVP antibodies (rabbit and mouse anti AVP), generous gifts from Ruud Buijs and Harold Gainer, respectively, we detected sparse AVP+ fibers in the LC which were closely apposed to tyrosine hydrolase (TH) immunoreactive dendrites (**Figure 1A**) and somata (**Figure 1B**). In contrast to previously reported (Aston-Jones and Waterhouse, 2016), no AVP+ cell bodies were detected in the LC. This suggests that there was no local source of AVP within the LC and these AVP+ axons originate from other brain regions. AVP+ varicosities were also immunopositive for the vesicular glutamate transporter 2 (VGLUT2) (**Figure 1B**), a protein expressed exclusively in

glutamatergic axon terminals. This suggests that AVP+ axons could form excitatory synapses with LC neurons.

To confirm this, we performed double peroxidase-chromogen immunostaining and TEM, using V – VIP (VECTOR®VIP Peroxidase (HRP) Substrate Kit; Vector Laboratories) and DAB as chromogens (see the “Materials and Methods” Section for details). It is worth noting that in EM preparations, the VIP reaction product was granular in appearance and easily distinguishable from the diffuse reaction product of DAB (Zhou and Grofova, 1995; Smiley et al., 1997; Muller et al., 2006, 2011). Visualization of the DAB reaction product at the light microscopical level revealed several AVP+ profiles (Figure 1C arrowheads and Figure 1D labeled as “AVP+ ax”). An AVP+ Herring body-like large varicose (Figure 1B white arrow and asterisk in Figures 1C,E), which is an anatomical feature of AVP-containing magnocellular axons, was also evident (Figure 1C, asterisk). Within this field of view, two AVP+ bouton closely apposed to a TH+ dendrite (Figure 1C, boxed area). Examination of serial EM sections taken from the boxed area revealed that one of these AVP+ boutons formed an asymmetric (Gray type I) synapse with a TH+ dendrite (Figure 1C, insert). The presynaptic bouton contained abundant DAB precipitate and labeled dense core vesicles (dcv, AVP+, green arrowhead), characteristic of neuropeptide-containing axon terminals. Collectively, this demonstrates that AVP is contained in a set of LC afferents, which make excitatory synaptic connections with noradrenergic profiles of the LC.

LC-NE Neurons Co-express mRNA for AVP V1a and V1b Receptors

We recently demonstrated, using immunohistochemistry, that in the mouse, V1a and V1b, but not V2 receptors are expressed in the LC (Campos-Lira et al., 2018). Whilst the V1b was expressed by both noradrenergic and non-noradrenergic LC neurons, the V1a was exclusively expressed by LC noradrenergic neurons. We used a high resolution double *in situ* hybridization technique (RNAscope®2.5 HD Duplex Assay) to assess the comparative AVP receptor expression profile in rat LC. LC noradrenergic neurons, identified by mRNA signal for TH (Figure 2D) co-expressed signal for both the V1a (Figure 2A) and V1b (Figure 2B) receptors. This indicates that AVP, released at excitatory synapses, uses both V1a and V1b receptors for postsynaptic signaling within LC neurons. Figures 2C,D shows neurons located in the dorsal raphe nucleus and LC, respectively, which expressed either V1b mRNA but not TH mRNA (Figure 2C) or TH mRNA but not V1b mRNA (Figure 2D), from the same samples as experimental controls.

AVP+ Axons in the LC Originate From the Magnocellular Neurosecretory Neurons of the PVN and SON

Our LM analysis revealed that the rat LC is devoid of AVP+ somata. This indicates that all AVP+ axons originate from regions beyond the LC. The presentation of LC AVP+ axons as large diameter profiles, with frequent varicosities and Herring body-like structures which co-expressed the glutamatergic synaptic marker protein VGLUT2 is typical of hypothalamic

AVPMNNs (Ziegler et al., 2002; Hrabovszky and Liposits, 2007), thus making this brain region the likely source of these afferents.

To assess this hypothesis, the retrograde tracer FG was stereotactically injected in LC, and the transported signal then evaluated in target regions. A total of four animals were confirmed to have FG injections within the core of the LC, confirmed with TH IHC (see the “Materials and Methods” Section for detailed description) (Figure 3A). Inspection of AVP immunofluorescence in conjunction with FG signal, in regions of the anterior hypothalamus confirmed the co-expression of AVP-FG in the hypothalamic paraventricular (PVN) and supraoptic (SON) nuclei (Figure 3, panels C–H). This confirms that AVPMNNs provide AVP-immunopositive innervation of LC-NE neurons. Further interpretations and discussion of this finding are developed in the Section of “Technical Considerations” at the end of this paper.

Table 1 describes the semi-quantitative analysis of the four cases matching the inclusion criteria. Interestingly, AVP/FG double labeled neurons were not found inside the suprachiasmatic nucleus.

Early Life Stress (ELS) Increases the Expression of AVP in the LC in Adulthood

We recently reported in mouse that acute stress significantly alters the expression of AVP terminals and AVP receptor expression in the mouse LC (Campos-Lira et al., 2018). The question therefore arises whether such stress-induced plasticity in the LC AVP system is enduring following exposure to chronic stress. One type of stress which induces long lasting molecular, physiological and structural plasticity in different brain regions (Caldji et al., 2003) including the LC (Swinney et al., 2010) is early life stress (ELS). Given the above data which indicate that LC AVP axons originate from, in part, the same center that integrates the stress response, i.e., the PVN, we assessed whether prior ELS alters the expression profile of AVP+ axons in the LC, using the maternal separation as a model of ELS. As previously reported for other brain regions (Zhang et al., 2012; Hernandez et al., 2016), MS resulted in a noticeable increase in the intensity of AVP immunoreactivity in the LC, in adulthood (Figures 4A,B). Quantification of AVP immunofluorescence intensity revealed a significant increase in MS samples (Figure 4C), $p < 0.001$, unpaired Student's *t*-test; $n = 5$ animals.

Water Deprivation 24 h (WD24h) Subtly Enhances Improvement in Spatial Learning and Memory Retention, Accompanied by a Significant Increase in Fos Expression in LC, Hippocampus and Prefrontal Cortex, After MWM Assessment

To answer our question whether the hypothalamic AVPMNN system's sub-chronic upregulation exerts modulatory effects on the LC-NE neurons activation and subsequent projection regions, which could be reflected in their behavioral modifications, we devised an experiment to assess the spatial learning and memory retention in water-maze-naive rats using water deprivation (WD)

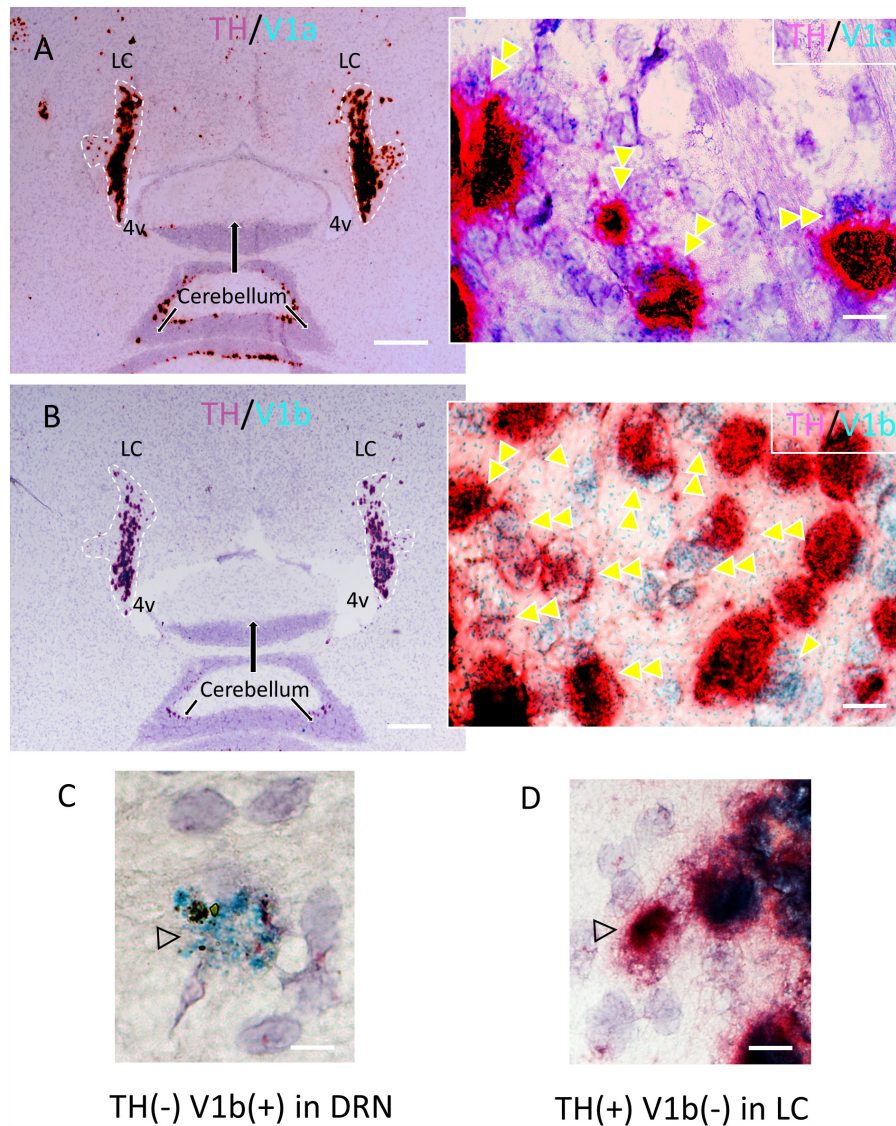


FIGURE 2 | Confirmation of the expression of V1a and V1b receptor mRNA in noradrenergic LC neurons using a high resolution *in situ* hybridization method (RNAscope® 2.5 HD Duplex Assay). **(A,B)** Horizontal sections of rat LC with inserts showing the co-localization (double arrowheads) of V1a/TH **(A)** and V1b/TH **(B)**. The TH mRNA signal was amplified using RNAscope channel 2 related probes and alkaline phosphatase (AP) – based Fast Red chromogen to result in a strongly detectable red signal and either V1a and V1b signals were amplified using RNAscope channel 1 related probes and horseradish peroxidase (HRP) – based green chromogen (the green punctuated signal). This newly developed technology allows a same-day ISH for two mRNAs detection with cellular resolution and being permanently mounted and examined under conventional light microscopy. Panels **(C,D)** are controls showing the labeling with V1b only, in the dorsal raphe nucleus and TH only in LC respectively. Scale bars: **A,B**: 0.5 mm; rest, 10 μ m.

as our experimental variable. From 12 h of water deprivation, the plasma AVP concentration in rat reaches to its maximum level and continues for the next 12 h (Zhang et al., 2010). Hence, this physiological model could up-regulate the AVP afference to LC.

As shown in **Figure 5A**, in the morning test, the WD group already showed a subtle improvement of spatial learning with a smoother learning course and a significant reduction of time to reach the escape-platform in the 2nd trial compared to control. This improvement is further confirmed in the afternoon session with significant reduction of time to reach the escape-platform

in the 2nd and 3rd trials compared to control (**Figure 5B**). An interesting phenomenon was observed in the first trial of the afternoon test, in which the WD subjects spent more time swimming in the quadrant II where the escape-platform was located in the morning test, while the control rats did not show this preference (**Figures 5C,D**).

The expression of c-Fos, a marker of neuronal plasticity, assessed 90 min after the end point of MWM, revealed significant increase in the LC, as well as in the granule cell layer (gcl) of the dentate gyrus (DG) of dorsal hippocampus and prefrontal

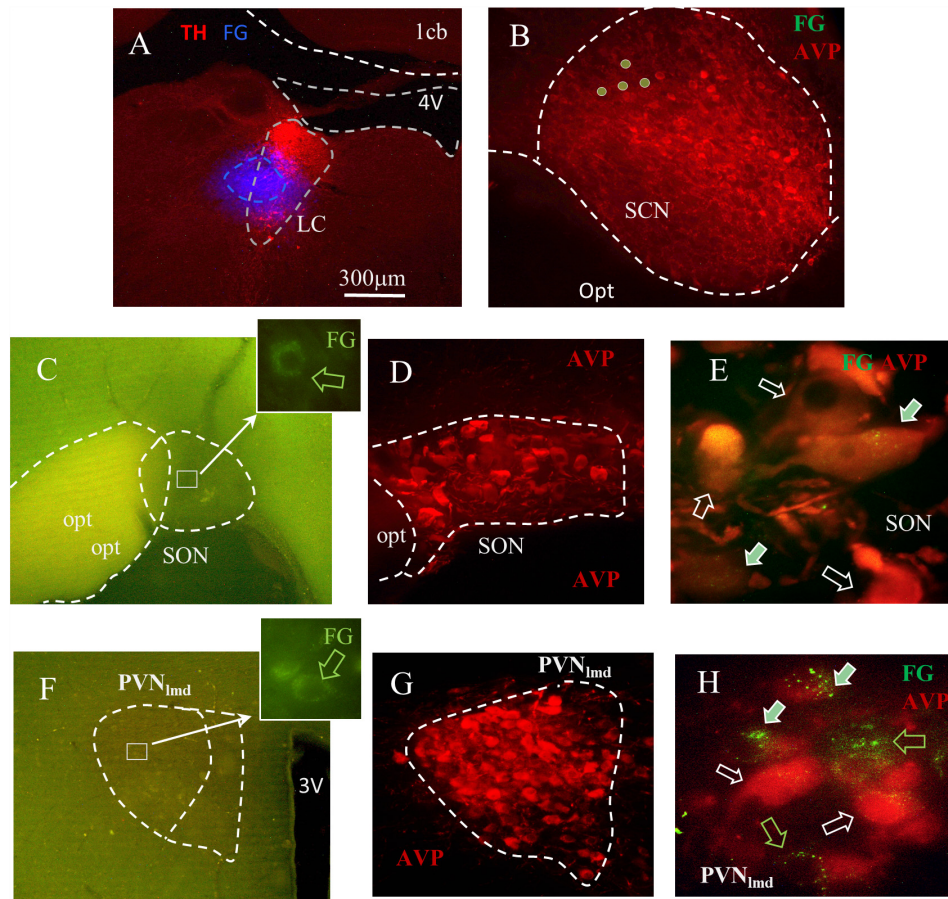


FIGURE 3 | Fluoro-Gold (FG) retrograde tracing identifies the SON and PVN nuclei as the sources of LC AVP afferents. **(A)** Coronal section of pontine tegmentum, Bregma -9.84 mm; red TH+ IHC showing LC and blue FG labeling site of about $300\ \mu\text{m}$ of diameter. **(B)** Within the suprachiasmatic nucleus (SCN), the FG labeled cells were found immuno-negative for AVP. In both SON **(C–E)** and the lateral magnocellular division of PVN (PVN_{lmd}, **F–H**), around 20–60% of AVP+ neurons were positively labeled. **(C,F)** Photomicrographs from freshly vibratome sectioned coronal hypothalamic slices indicate the sparse FG labeled magnocellular neurons (perinuclear lysosome labeling pattern). FG and AVP immunohistochemistry were co-localized (filled arrows) in a population of the magnocellular neurons in SON **(D,E)** and PVN_{lmd} **(G,H)**. White hollow arrows indicate AVP+ cells without FG and green hollow arrows show the FG+ cells without AVP. See “Technical Considerations” Section in the “Discussion” for further considerations. Scale bars: $20\ \mu\text{m}$ for **E,H**; rest $300\ \mu\text{m}$.

cortex. The panel E of **Figure 5** shows a higher number of Fos+ nuclei in all regions evaluated comparing control vs. WD24h rats, i.e., LC: 9.62 ± 0.9 vs. 13.14 ± 1.2 , $p < 0.05$; DG: 6.0 ± 0.7 vs. 11.62 ± 1.3 , $p < 0.001$; and PFC: 12.45 ± 0.5 vs. 19.73 ± 1.5 , $p < 0.001$. It is worth noting that both of the latter regions receive abundant NE innervations from LC (Schwarz et al., 2015) but no AVP direct innervations have been reported (Rood and De Vries, 2011; Zhang and Hernandez, 2013). Hence, it is coherent to interpret that these c-Fos expression increases are secondary to the potentiation of LC-NE afference to those regions.

DISCUSSION





In the current study, we provide the first demonstration that AVP-containing axons make synaptic connections with LC neurons. Furthermore, we provide evidence that these AVP afferents originate from magnocellular neurosecretory neurons

(AVPMNNs) of the hypothalamic PVN and SON. Finally, our data suggest the recruitment of this AVPMNN circuit during periods of psychological and physiological challenges. Collectively, the study identifies the anatomical substrates linking two different neural systems with a common responsibility for ensuring homeostasis in complex environments.

The Molecular and Structural Components of AVP-LC Communication

In contrast to its well-characterized role as a hormone in the periphery, within the brain, AVP has been shown to also exhibit the features of a neuromodulator by directly altering neuronal excitability (Zhang and Eiden, 2018). Axons containing such neuropeptide modulators generally adopt a range of release mechanisms, thereby increasing the versatility of their communication patterns. For example, volume transmission (VT) is a key feature of such hypothalamic neuropeptide

TABLE 1 | Fluoro-Gold (FG) retrograde labeling experimental survey and anatomical description*.

Subject's Pons at Breg. - 9.84 mm	Main hypoth. AVP + Regions	Ipsi-lateral	Contra-lateral	Observation	Subject's Pons at Breg. - 9.84 mm	Main hypoth. AVP+ Regions	Ipsi-lateral	Contra-lateral	Observation
 VH07	PVN SON SCN	+ ++ -	+ ++ -	++ in AVP- cell in dorso-lateral portion	 OH02	PVN SON SCN	+ ++ -	+ ++ -	++ in AVP- cell in dorso-lateral portion
 VH09	PVN SON SCN	+ ++ -	+ ++ -	++ in AVP- cell in dorso-lateral portion	 OH05	PVN SON SCN	+ ++ -	+ ++ -	++ in AVP- cell in dorso-lateral portion

*Twenty young male rats were used in this experiment. Sixteen rat's injection sites did not meet the criteria for inclusion (see "Materials and Methods" Section), hence they were not included here. FG+/AVP+ cell number per 0.229 mm²: +, 1-5; ++, 6-10; +++ > 10. "VH" and "OH" are the initials of the two experimenters and the number followed indicate the subject sequential number.

neurotransmitters and facilitates the modulation of large ensembles of neurons (Alpar et al., 2018). The sparsity of AVP+ axons throughout the LC, in comparison to the vast expression of AVP receptors in virtually all LC neurons, suggests that the LC AVP system relies heavily on VT as a means of influencing LC neuronal excitability. However, our ultrastructural data indicate that AVP+ axons also employ the wired form of transmission in terms of forming conventional synapses with LC profiles. This suggests that AVP afferents impart highly directed, synaptic modulation of a sub-population of LC neurons, whilst maintaining a more general influence over the entire nucleus via VT. Since synaptic connectivity imparts speed and precision in neuronal network signaling, this raises the question whether the synaptically connected AVP-LC neurons represent a group of cells essential for mediating specific aspects of AVP-mediated brain functions, in a strict temporally constrained manner. This could result in the parcellation of the LC into different populations of neurons within AVP-LC pathways. Evidence for this heterogeneity of the LC AVP system stems from our recent report which demonstrated that the pharmacological activation of LC neurons resulted in contrasting effects on spontaneous firing rates (Campos-Lira et al., 2018). If so, identifying the anatomical and molecular signatures of this sub-populations of LC neurons, together with the source/s of such synapse innervating AVP+ axons, will be the crucial in furthering our understanding of the contribution of neurochemical systems to overall LC function.

The Source of LC AVP+ Afferents

There are at least five major brain AVP centers, and therefore likely sources of the AVP+ axons innervating LC neurons, namely, the PVN, suprachiasmatic nucleus, supraoptic nucleus, bed nucleus of the stria terminalis (BNST), and medial amygdala (Goodson and Bass, 2001). AVP+ inputs to the LC have been reported since the late 1970s in both the core and pericoeruleus sub-regions (Buijs, 1978). These axons were considered to originate from parvocellular vasopressinergic neurons located within the caudal paraventricular nucleus and the BNST (Urban et al., 1999). However, the retrograde tracing data in this current studies point to magnocellular neurons of the PVN (AVPMNNs) being the major source. Our ancillary molecular data, in the form of VGLUT2-AVP co-expression, a signature of AVPMNNs, further supports the notion that these axons originate from this region of the brain. Further arguments to support the notion that these axons most likely arise from the hypothalamus rather than from extra-hypothalamic AVP-positive neurons include (i) AVPMNNs are known to be glutamatergic (Ziegler et al., 2002; Hrabovszky and Liposits, 2007); (ii) most, if not all, of the AVP-parvocellular populations, in hypothalamic suprachiasmatic nucleus (SCN), central (CeA) and medial (MeA) amygdala, bed nucleus of stria terminalis, intra-amygdala (BNSTIA) and medial posterior internal (BNSTmpi) divisions have been found to express VGAT hence to be GABAergic (Zhang and Eiden, unpublished; Zhang and Eiden, 2018). As such, the data reveal a synaptically connected circuit between PVN AVP+ neurons and the LC. Future studies focused on dissecting the roles of other PVN-LC pathways, such as those using CRF as a

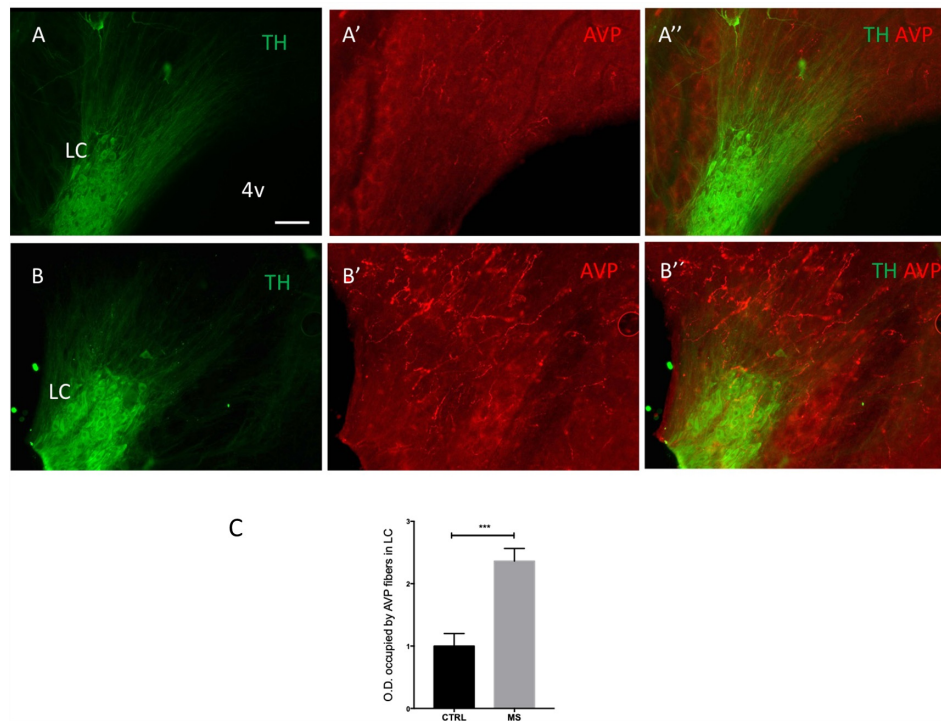


FIGURE 4 | Early life stress in the form of neonatal maternal separation (MS) increases LC AVP immunoreactivity. Photomicrographs of rat brain horizontal sections (around dorso-ventral 7.30 mm), showing immunoreactivity for TH and AVP in the LC of control (**As**) and MS (**Bs**) subjects, treated as described in Materials and Methods, Maternal Separation (MS) Protocol. Note that all tissue was processed and imaged under identical conditions. (**C**) Quantification of AVP immunoreactivity. The columns represent the means and the errors represent the SEM; ($n = 5$); *** $p < 0.001$. Scale bar: 100 μ m.

neuromodulator, are crucial in gaining a composite view of the contributions of such circuits to brain functions mediated by these respective centers.

The LC-AVP System and Its Role in the Stress Response

A common feature of the LC and the PVN nuclei are their involvement in ensuring that the individual is capable of mediating a coordinated response to a variety of psychological and physiological stressors (Atzori et al., 2016). CRF has historically been considered the messenger of choice for both brain regions (Swinny and Valentino, 2006; Swinny et al., 2010). The current study, as well as our previous report, identifies AVP, within the LC, as an additional molecule in the arsenal of mediators used by these brain regions in times of stress. Our recent report showed that acute stress, in the form of restraint for 1 h, significantly increased the density of V1b receptors, while decreasing the density of AVP immunoreactivity. V1a receptors were unaffected (Campos-Lira et al., 2018). In the current study, we show that a more severe form of stress, namely MS, has the opposite effect on AVP expression, by significantly increasing the density of immunoreactive axons in the LC. Furthermore, a mild stress which is known to engage the PVN-AVP system, namely WD, together with novelty of being subjected to the MWM test, also appeared to engage the LC (in addition to other brain regions), based on the expression of the early gene marker Fos

(Figure 5). Therefore, different life experiences have contrasting effects on LC-AVP plasticity. This stress-induced plasticity of the AVP in the brain has been replicated in other brain regions. For example, MS has been shown to potentiate the hypothalamic AVPMNN system as well as increase the fiber density in amygdala resulting in stress hyper-responsivity such as hyper-anxiety tested by Vogel-conflict test and elevated plus maze (Zhang et al., 2012; Hernandez et al., 2016). Remarkably, post-mortem analysis of the brains of suicide victims has indicated an increase in the immunoreactivity for AVP in the LC, in addition to other brain regions important in regulating emotions (Merali et al., 2006). Therefore, targeting the AVPMNNs system and the LC, in mental illnesses could unearth novel therapeutic strategies for debilitating stress-induced mental illnesses which remain poorly treated with currently available drug options.

Does the Activation of This Pathway by 24 h Water Deprivation Lead to Enhancement of Memory and/or Learning?

Using MWM, we assessed spatial learning in rats after undergoing 24 h water-deprivation (WD), during which time the AVPMNNs are physiologically hyper-activated with only minimal changes in blood osmolality (Dunn et al., 1973; Zhang et al., 2010). We found here the memory retention and learning course were both

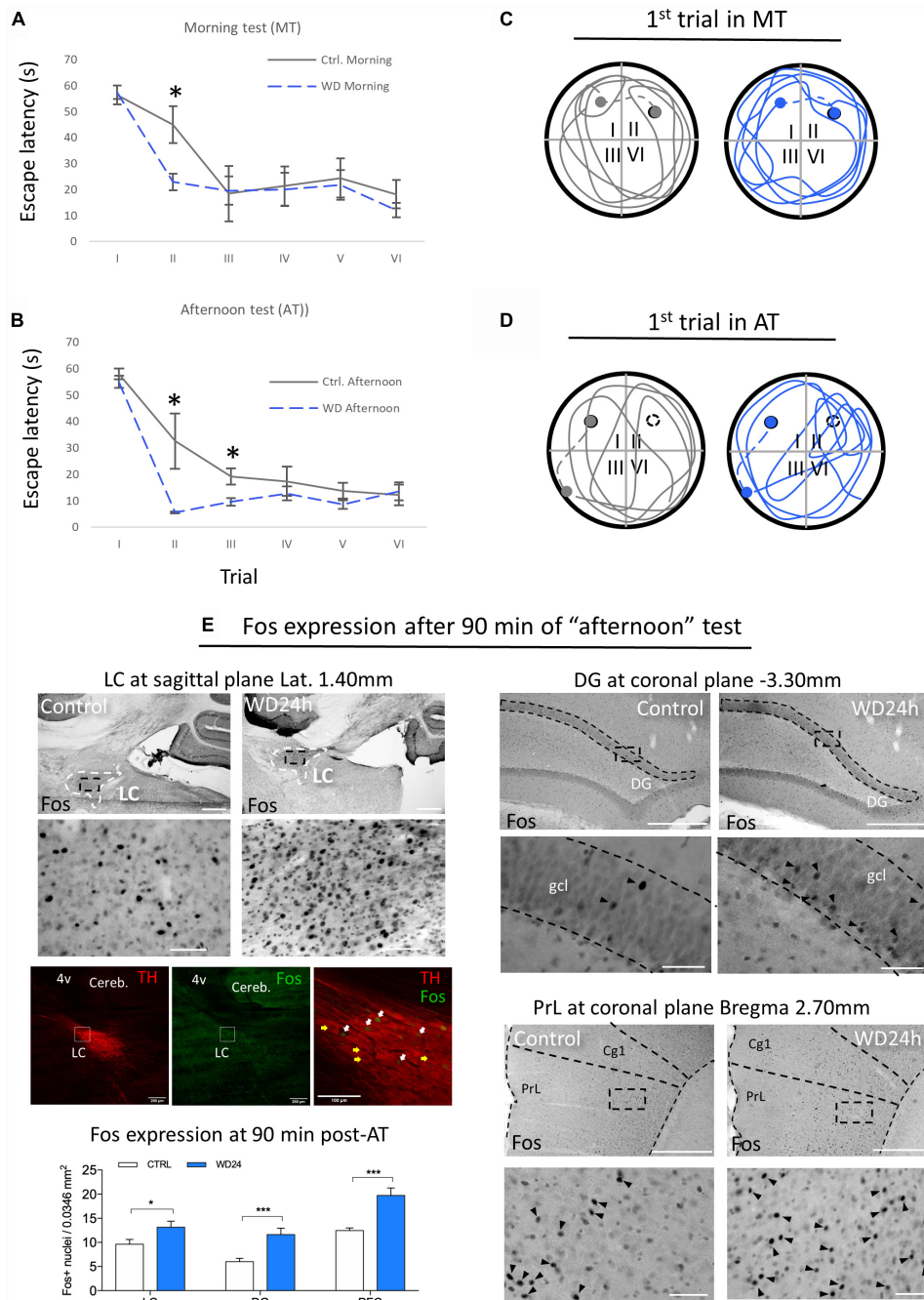


FIGURE 5 | Morris water maze (MWM) test showed that WD24h improved spatial learning and memory retention as well as increasing neuronal activity in LC, hippocampus (assessed at suprapyramidal branch of granule cell layer (gcl) of dorsal dentate gyrus (DG) and prefrontal cortex [assessed at the layer 5 of prelimbic cortex (PrL), regions relevant for working memory]. **(A)** “Morning testing” (MT, see the “Materials and Methods” Section) showed that WD24h rats learned to locate the hidden platform (quadrant II) faster than control rats, as shown by a reduction in the latency to reach the platform in the second trial. **(B)** “Afternoon testing” (AT, see the “Materials and Methods” Section) confirmed the previous observation with a significant reduction of time to reach the escape-platform (quadrant I) in the second and third trials compared to control. **(C)** No apparent differences in the swimming strategy were seen as shown in a tracing of the swimming path of the first trial of MT. **(D)** A different swimming strategy was observed in the AT, with WD24h rats spending more time swimming in the quadrant where the platform was located (quadrant II) before finding the new location (quadrant I). In panels **(C,D)** filled circles symbolize the escape platform; hollow circles symbolize the old platform location; dots symbolize the rat location when 60 s exploration lapse ends; dashed lines symbolize the route that the experimenter guided the subject to the platform. **(E)** Photomicrographs and bar graphs show an increase in the number of Fos+ nuclei in the LC, granule cell layer (gcl) of dorsal dentate gyrus (DG), and prefrontal cortex assessed at the prelimbic cortex (PrL, layer 5), 90 min post the AT. Immuno-fluorescence images from WD subject’s LC (sagittal section) depict examples of Fos activation in LC-NE neurons (white arrows) after the MWM test. Note that some LC-NE neurons are not activated (yellow arrows). Scale bars 500 μ m for the low amplifications photomicrographs and 50 μ m for the high amplification; * $p < 0.05$; *** $p < 0.001$.

improved in WD subject, while Fos-expression in LC, as well as in LC-NE projecting regions relevant for working memory, dorsal hippocampus and prefrontal cortex, were significantly increased. NE facilitates synaptic plasticity by recruiting and modifying multiple molecular elements of synaptic signaling, including specific transmitter receptors, intracellular protein kinases, and translation initiation have been extensively reported (Maity et al., 2015; Nguyen and Gelinas, 2018).

These results, adding to our previous studies, suggest that the AVPMNN system, a water homeostasis regulator, works centrally modulating the adaptive responses.

The postulated function of AVP as a modulator of LC principal neuron activity in response to osmotic stress is further supported by the finding of V1a receptors on TH+ (principal) LC neurons. Consistent with a role for AVP in linking osmotic stress to LC function, is enhancement of Fos up-regulation in LC neurons during a learning/orientation task (the MWM) after 24 h of water deprivation (WD) a reliable maneuver for enhancing AVPMNN tone in the PVN, SON and their vasopressinergic projections. In fact, performance during the MWM is also enhanced by WD. Since Fos activity is also up-regulated during MWM learning in LC target areas of the brain, some of which also receive AVPMNN inputs, it is not possible to know at this time if the effects of WD on MWM performance, though likely mediated through AVPMNN activity, are indirect (via action at the LC) or direct (via AVP release directly in these LC projection areas). Nevertheless, our findings reveal a novel neuroanatomical substrate for AVPMNN direct influence over LC neuronal function, and a new avenue for exploration of both homeostatic as well as allostatic modulation of behavior via the LC.

We take the data as a whole as indicating that the AVPMNN projections to LC likely act to potentiate a pattern of LC neuronal activity consistent with increased learning or enhanced attention under conditions of physiological stress (WD24h). This suggests that physiological need/motivation/stress enhances attention and learning under conditions in which acquisition of new information is especially critical to survival (Glennon et al., 2018).

Technical Considerations: Limitations for Quantitative Conclusions

This study describes for the first time that the hypothalamic AVPMNNs innervate the LC using FG neurotracing, immunohistochemical, and neuroanatomical methods. FG injection into the LC revealed retrogradely labeled AVP-positive cells in hypothalamic supraoptic (SON) and paraventricular nuclei (PVN). There are several technical issues concerning this observation that we considered important to discuss here. The LC are bilateral dense groups of cells located in the pontine tegmentum, specifically in the lateral-rostral part of the floor of the 4th ventricle. Here, there are two technical challenges for neuro-circuit tracing. First, the rat LC is a relatively small nucleus (for instance, dimensions measured from confocal microcopy images from one rat were rostro-caudal 566 μm , dorso-ventral 306 μm , medio-lateral 320 μm). Second, it is located just below the 4th ventricle, thus it is extremely easy to have the tracer leaking into the cerebro-spinal fluid (CSF).

Due the AVPMNNs neuro-secretion functional capacity, any leakage of FG can result in variable degree of magnocellular labeling, bilaterally. To avoid this leaking risk, we aimed to inject the tracer into the latero-ventral site of the LC as well as to use the method described in “Materials and Methods” which should yield a labeling region of less than 300 μm of diameter. In 20 attempts (20 rats used), only 4 resulted matching our inclusion criteria (20% of success rate). Although the stereotaxic coordinates and the rat body weights were kept identical, to the best of our knowledge, the first anatomical assessments for each rat yielded rather variable labeling sites. A more than 30 μm deviation, >10% of LC's diameter, resulted in other structure's labeling, which did not provide valid data for this study's aims and were excluded for further analysis. The four successful cases were analyzed and reported in the **Table 1** where we aimed to be rigorous and quantitative providing objective description of those four cases. We are fully aware that each injection only cover a small fraction of the LC's dendritic field, in a variable degree. Hence, not global quantitative conclusion should be generated from those individual descriptions of the 4 rats. The value of this discovery is that only a small portion of the AVPMNNs were labeled resulting from a given local-injection of one region of LC, and we showed AVPMNNs without FG labeling but adjacent to the double labeled cells, which suggests that the labeling was not likely, at least part of them, to be through the humoral leakage. Hence, it demonstrates the existence of a monosynaptic pathway from AVPMNN to LC.

In summary, establishment of a linkage between the AVPMNN system and the LC adds a significant component to the already-established communication to the LC from the hypothalamus, via CRF projections from the PVN. That thirst enhances performance in the MWM concomitantly with enhanced activation of LC neurons during the conduct of the MWM test may indicate either enhancement of innate learning, or increased attention to cues presented during this test, and this too is an important new avenue that we intend to develop in the future. The resolution of this question will be helpful in determining the relative functional impact of increased vasopressinergic tone in LC compared to other brain regions which are supplied with AVPMNN afferents from the PVN and SON.

AUTHOR CONTRIBUTIONS

LZ conceived and led the study. VH, AN-K, OH-P, and LZ designed the experiments. OH-P, VH, AN-K, MS, and LZ performed the experiments. All authors analyzed the data. LZ, JS, RB, and LE contributed experimental reagents and resources. LZ wrote the manuscript with contribution of JS and LE, and feedback from the remaining authors.

FUNDING

This work was supported by DGAPA-UNAM-PAPIIT, IN216918, CONACYT, CB-238744 (LZ) and CB-283279 (RB), NIMH-IRPMH002386 (LE).

ACKNOWLEDGMENTS

We thank Ruud M. Buijs and Harold Gainer for generous antibody donations, Enrique Pinzón for animal facility care, and Ben Micklem (Oxford) and Yorgui Santiago for kind technical helps. A part of the results presented here was obtained during LZ's sabbatical leave at Oxford University,

United Kingdom, for that she would like to thank Peter Somogyi for his guidance and continuous support. AN-K is a doctoral student from the *Programa de Doctorado en Ciencias Biomedicas, Universidad Nacional Autonoma de México* (UNAM) and received a scholarship (No. 468300) from the *Consejo Nacional de Ciencia y Tecnología* (CONACyT) of Mexico.

REFERENCES

- Alpar, A., Benevento, M., Romanov, R. A., Hokfelt, T., and Harkany, T. (2018). Hypothalamic cell diversity: non-neuronal codes for long-distance volume transmission by neuropeptides. *Curr. Opin. Neurobiol.* 56, 16–23. doi: 10.1016/j.conb.2018.10.012
- Alstein, M., Whitnall, M. H., House, S., Key, S., and Gainer, H. (1988). An immunochemical analysis of oxytocin and vasopressin prohormone processing in vivo. *Peptides* 9, 87–105. doi: 10.1016/0196-9781(88)90014-9
- Armstrong, W. (2004). "Hypothalamic supraoptic and paraventricular nuclei," in *The Rat Nervous System*, ed. G. Paxinos (Amsterdam: Elsevier), 369–388. doi: 10.1016/B978-012547638-6/50016-X
- Aston-Jones, G., and Waterhouse, B. (2016). Locus coeruleus: from global projection system to adaptive regulation of behavior. *Brain Res.* 1645, 75–78. doi: 10.1016/j.brainres.2016.03.001
- Atzori, M., Cuevas-Olguin, R., Esquivel-Rendon, E., Garcia-Oscos, F., Salgado-Delgado, R., Saderi, C., et al. (2016). Locus coeruleus norepinephrine release: a central regulator of CNS spatio-temporal activation? *Front. Synaptic Neurosci.* 8:25. doi: 10.3389/fnsyn.2016.00025
- Berridge, C. W., and Waterhouse, B. D. (2003). The locus coeruleus-noradrenergic system: modulation of behavioral state and state-dependent cognitive processes. *Brain Res. Brain Res. Rev.* 42, 33–84. doi: 10.1016/S0165-0173(03)00143-7
- Buijs, R. M. (1978). Intra- and extrahypothalamic vasopressin and oxytocin pathways in the rat. Pathways to the limbic system, medulla oblongata and spinal cord. *Cell Tissue Res.* 192, 423–435. doi: 10.1007/BF00224932
- Buijs, R. M., Pool, C. W., Van Heerikhuizen, J. J., Sluiter, A. A., Van der Sluis, P. J., Ramkema, M., et al. (1989). Antibodies to small transmitter molecules and peptides: production and application of antibodies to dopamine, serotonin, GABA, vasopressin, vasoactive intestinal peptide, neuropeptide y, somatostatin and substance P. *Biomed. Res.* 10(Suppl. 3), 213–221.
- Caldji, C., Diorio, J., and Meaney, M. J. (2003). Variations in maternal care alter GABA(A) receptor subunit expression in brain regions associated with fear. *Neuropsychopharmacology* 28, 1950–1959. doi: 10.1038/sj.npp.1300237
- Campos-Lira, E., Kelly, L., Seifi, M., Jackson, T., Giesecke, T., Mutig, K., et al. (2018). Dynamic modulation of mouse locus coeruleus neurons by vasopressin 1a and 1b receptors. *Front. Neurosci.* 12:919. doi: 10.3389/fnins.2018.00919
- Cui, Z., Gerfen, C. R., and Young, W. S. III (2013). Hypothalamic and other connections with dorsal CA2 area of the mouse hippocampus. *J. Comp. Neurol.* 521, 1844–1866. doi: 10.1002/cne.23263
- de Wied, D., Diamant, M., and Fodor, M. (1993). Central nervous system effects of the neurohypophyseal hormones and related peptides. *Front. Neuroendocrinol.* 14, 251–302. doi: 10.1006/frne.1993.1009
- Dunn, F. L., Brennan, T. J., Nelson, A. E., and Robertson, G. L. (1973). The role of blood osmolality and volume in regulating vasopressin secretion in the rat. *J. Clin. Invest.* 52, 3212–3219. doi: 10.1172/JCI107521
- Fitzsimons, J. T., and O'Connor, W. J. (1976). E. B. Verney's demonstration of 'The antidiuretic hormone and the factors which determine its release' [proceedings]. *J. Physiol.* 263, 92–93.
- Glennon, E., Carcea, I., Martins, A. R. O., Multani, J., Shehu, I., Svirsky, M. A., et al. (2018). Locus coeruleus activation accelerates perceptual learning. *Brain Res.* doi: 10.1016/j.brainres.2018.05.048 [Epub ahead of print].
- Goodson, J. L., and Bass, A. H. (2001). Social behavior functions and related anatomical characteristics of vasotocin/vasopressin systems in vertebrates. *Brain Res. Brain Res. Rev.* 35, 246–265. doi: 10.1016/S0165-0173(01)00043-1
- Hernandez, V. S., Hernandez, O. R., Perez de la Mora, M., Gomora, M. J., Fuxe, K., Eiden, L. E., et al. (2016). Hypothalamic vasopressinergic projections innervate central amygdala GABAergic neurons: implications for anxiety and stress coping. *Front. Neural Circuits* 10:92. doi: 10.3389/fncir.2016.00092
- Hernandez, V. S., Ruiz-Velazco, S., and Zhang, L. (2012). Differential effects of osmotic and SSR149415 challenges in maternally separated and control rats: the role of vasopressin on spatial learning. *Neurosci. Lett.* 528, 143–147. doi: 10.1016/j.neulet.2012.09.002
- Hernandez, V. S., Vazquez-Juarez, H., Marquez, E., Jauregui, M. M., Huerta, F., Barrio, R. A., et al. (2015). Extra-neurohypophyseal axonal projections from individual vasopressin-containing magnocellular neurons in rat hypothalamus. *Front. Neuroanat.* 9:130. doi: 10.3389/fnana.2015.00130
- Hrabovszky, E., and Liposits, Z. (2007). Glutamatergic phenotype of hypothalamic neurosecretory systems: a novel aspect of central neuroendocrine regulation. *Idegygyg. Sz.* 60, 182–186.
- Kobayashi, R. M., Palkovits, M., Kopin, I. J., and Jacobowitz, D. M. (1974). Biochemical mapping of noradrenergic nerves arising from the rat locus coeruleus. *Brain Res.* 77, 269–279. doi: 10.1016/0006-8993(74)90790-2
- Kovacs, K. J. (1998). c-Fos as a transcription factor: a stressful (re)view from a functional map. *Neurochem. Int.* 33, 287–297. doi: 10.1016/S0197-0186(98)00023-0
- Kovacs, K. J. (2008). Measurement of immediate-early gene activation-c-fos and beyond. *J. Neuroendocrinol.* 20, 665–672. doi: 10.1111/j.1365-2826.2008.01734.x
- Landgraf, R., and Neumann, I. D. (2004). Vasopressin and oxytocin release within the brain: a dynamic concept of multiple and variable modes of neuropeptide communication. *Front. Neuroendocrinol.* 25, 150–176. doi: 10.1016/j.yfrne.2004.05.001
- Leng, G., Dyball, R. E., and Luckman, S. M. (1992). Mechanisms of vasopressin secretion. *Horm. Res.* 37, 33–38. doi: 10.1159/000182278
- Levitt, P., and Moore, R. Y. (1979). Origin and organization of brainstem catecholamine innervation in the rat. *J. Comp. Neurol.* 186, 505–528. doi: 10.1002/cne.901860402
- Ludwig, M., and Leng, G. (2006). Dendritic peptide release and peptide-dependent behaviours. *Nat. Rev. Neurosci.* 7, 126–136. doi: 10.1038/nrn1845
- Maity, S., Rah, S., Sonenberg, N., Gkogkas, C. G., and Nguyen, P. V. (2015). Norepinephrine triggers metaplasticity of LTP by increasing translation of specific mRNAs. *Learn. Mem.* 22, 499–508. doi: 10.1101/lm.039222.115
- Merali, Z., Kent, P., Du, L., Hrdina, P., Palkovits, M., Faludi, G., et al. (2006). Corticotropin-releasing hormone, arginine vasopressin, gastrin-releasing peptide, and neuromedin B alterations in stress-relevant brain regions of suicides and control subjects. *Biol. Psychiatry* 59, 594–602. doi: 10.1016/j.biopsych.2005.08.008
- Morales, M., and Wang, S. D. (2002). Differential composition of 5-hydroxytryptamine₃ receptors synthesized in the rat CNS and peripheral nervous system. *J. Neurosci.* 22, 6732–6741. doi: 10.1523/JNEUROSCI.22-15-06732.2002
- Morris, R. (1984). Developments of a water-maze procedure for studying spatial learning in the rat. *J. Neurosci. Methods* 11, 47–60. doi: 10.1016/0165-0270(84)90007-4
- Muller, J. F., Mascagni, F., and McDonald, A. J. (2006). Pyramidal cells of the rat basolateral amygdala: synaptology and innervation by parvalbumin-immunoreactive interneurons. *J. Comp. Neurol.* 494, 635–650. doi: 10.1002/cne.20832
- Muller, J. F., Mascagni, F., and McDonald, A. J. (2011). Cholinergic innervation of pyramidal cells and parvalbumin-immunoreactive interneurons in the rat basolateral amygdala. *J. Comp. Neurol.* 519, 790–805. doi: 10.1002/cne.22550

- Nguyen, P. V., and Gelinas, J. N. (2018). Noradrenergic gating of long-lasting synaptic potentiation in the hippocampus: from neurobiology to translational biomedicine. *J. Neurogenet.* 32, 171–182. doi: 10.1080/01677063.2018.1497630
- Palkovits, M., and Brownstein, M. J. (1983). "Locus coeruleus," in *Advances in Cellular Neurobiology*, Vol. 4, eds S. Fedoroff and L. Hertz (Amsterdam: Elsevier), 81–103. doi: 10.1016/B978-0-12-008304-6.50008-7
- Robertson, G. L., Shelton, R. L., and Athar, S. (1976). The osmoregulation of vasopressin. *Kidney Int.* 10, 25–37. doi: 10.1038/ki.1976.76
- Robertson, S. D., Plummer, N. W., de Marchena, J., and Jensen, P. (2013). Developmental origins of central norepinephrine neuron diversity. *Nat. Neurosci.* 16, 1016–1023. doi: 10.1038/nn.3458
- Rood, B. D., and De Vries, G. J. (2011). Vasopressin innervation of the mouse (*Mus musculus*) brain and spinal cord. *J. Comp. Neurol.* 519, 2434–2474. doi: 10.1002/cne.22635
- Schmued, L. C., and Fallon, J. H. (1986). Fluoro-Gold: a new fluorescent retrograde axonal tracer with numerous unique properties. *Brain Res.* 377, 147–154. doi: 10.1016/0006-8993(86)91199-6
- Schwarz, L. A., and Luo, L. (2015). Organization of the locus coeruleus-norepinephrine system. *Curr. Biol.* 25, R1051–R1056. doi: 10.1016/j.cub.2015.09.039
- Schwarz, L. A., Miyamichi, K., Gao, X. J., Beier, K. T., Weissbourd, B., DeLoach, K. E., et al. (2015). Viral-genetic tracing of the input-output organization of a central noradrenergic circuit. *Nature* 524, 88–92. doi: 10.1038/nature14600
- Smiley, J. F., Morrell, F., and Mesulam, M. M. (1997). Cholinergic synapses in human cerebral cortex: an ultrastructural study in serial sections. *Exp. Neurol.* 144, 361–368. doi: 10.1006/exnr.1997.6413
- Swanson, L. W. (1976). The locus coeruleus: a cytoarchitectonic, Golgi and immunohistochemical study in the albino rat. *Brain Res.* 110, 39–56. doi: 10.1016/0006-8993(76)90207-9
- Swinny, J. D., O'Farrell, E., Bingham, B. C., Piel, D. A., Valentino, R. J., and Beck, S. G. (2010). Neonatal rearing conditions distinctly shape locus coeruleus neuronal activity, dendritic arborization, and sensitivity to corticotrophin-releasing factor. *Int. J. Neuropsychopharmacol.* 13, 515–525. doi: 10.1017/S146114570999037X
- Swinny, J. D., and Valentino, R. J. (2006). Corticotropin-releasing factor promotes growth of brain norepinephrine neuronal processes through Rho GTPase regulators of the actin cytoskeleton in rat. *Eur. J. Neurosci.* 24, 2481–2490. doi: 10.1111/j.1460-9568.2006.05129.x
- Urban, I. J. A., Burbach, J. P. H., and De Wied, D. (1999). *Advances in Brain Vasopressin*. Amsterdam: Elsevier.
- Valentino, R. J., and Van Bockstaele, E. (2008). Convergent regulation of locus coeruleus activity as an adaptive response to stress. *Eur. J. Pharmacol.* 583, 194–203. doi: 10.1016/j.ejphar.2007.11.062
- Verney, E. B. (1947). The antidiuretic hormone and the factors which determine its release. *Proc. R. Soc. Lond. B Biol. Sci.* 135, 25–106. doi: 10.1098/rspb.1947.0037
- Yamaguchi, T., Wang, H. L., Li, X., Ng, T. H., and Morales, M. (2011). Mesocorticolimbic glutamatergic pathway. *J. Neurosci.* 31, 8476–8490. doi: 10.1523/JNEUROSCI.1598-11.2011
- Ying, C., Qi, Y., and Cang-Bao, X. (2017). A convenient method for quantifying collagen fibers in atherosclerotic lesions by ImageJ software. *Int. J. Clin. Exp. Med.* 10, 14904–14910.
- Zhang, L., and Eiden, L. E. (2018). Two ancient neuropeptides, PACAP and AVP, modulate motivated behavior at synapses in the extrahypothalamic brain: a study in contrast. *Cell Tissue Res.* 375, 103–122. doi: 10.1007/s00441-018-2958-z
- Zhang, L., and Hernandez, V. S. (2013). Synaptic innervation to rat hippocampus by vasopressin-immuno-positive fibres from the hypothalamic supraoptic and paraventricular nuclei. *Neuroscience* 228, 139–162. doi: 10.1016/j.neuroscience.2012.10.010
- Zhang, L., Hernandez, V. S., Liu, B., Medina, M. P., Nava-Kopp, A. T., Irls, C., et al. (2012). Hypothalamic vasopressin system regulation by maternal separation: its impact on anxiety in rats. *Neuroscience* 215, 135–148. doi: 10.1016/j.neuroscience.2012.03.046
- Zhang, L., Hernández, V. S., Medina-Pizarro, M., Valle-Leija, P., Vega-González, A., and Morales, T. (2008). Maternal hyperthyroidism in rats impairs stress coping of adult offspring. *J. Neurosci. Res.* 86, 1306–1315. doi: 10.1002/jnr.21580
- Zhang, L., Hernandez, V. S., Swinny, J. D., Verma, A. K., Giesecke, T., Emery, A. C., et al. (2018). A GABAergic cell type in the lateral habenula links hypothalamic homeostatic and midbrain motivation circuits with sex steroid signaling. *Transl. Psychiatry* 8:50. doi: 10.1038/s41398-018-0099-5
- Zhang, L., Hernandez, V. S., Vazquez-Juarez, E., Chay, F. K., and Barrio, R. A. (2016). Thirst is associated with suppression of habenula output and active stress coping: is there a role for a non-canonical vasopressin-glutamate pathway? *Front. Neural Circuits* 10:13. doi: 10.3389/fncir.2016.00013
- Zhang, L., Medina, M. P., Hernandez, V. S., Estrada, F. S., and Vega-Gonzalez, A. (2010). Vasopressinergic network abnormalities potentiate conditioned anxious state of rats subjected to maternal hyperthyroidism. *Neuroscience* 168, 416–428. doi: 10.1016/j.neuroscience.2010.03.059
- Zhou, M., and Grofova, I. (1995). The use of peroxidase substrate Vector VIP in electron microscopic single and double antigen localization. *J. Neurosci. Methods* 62, 149–158. doi: 10.1016/0165-0270(95)00069-0
- Ziegler, D. R., Cullinan, W. E., and Herman, J. P. (2002). Distribution of vesicular glutamate transporter mRNA in rat hypothalamus. *J. Comp. Neurol.* 448, 217–229. doi: 10.1002/cne.10257

Conflict of Interest Statement: The authors declare that the research was conducted in the absence of any commercial or financial relationships that could be construed as a potential conflict of interest.

Copyright © 2019 Hernández-Pérez, Hernández, Nava-Kopp, Barrio, Seifi, Swinny, Eiden and Zhang. This is an open-access article distributed under the terms of the Creative Commons Attribution License (CC BY). The use, distribution or reproduction in other forums is permitted, provided the original author(s) and the copyright owner(s) are credited and that the original publication in this journal is cited, in accordance with accepted academic practice. No use, distribution or reproduction is permitted which does not comply with these terms.



Dynamic Modulation of Mouse Locus Coeruleus Neurons by Vasopressin 1a and 1b Receptors

Elba Campos-Lira^{1†}, Louise Kelly^{2††}, Mohsen Seifi², Torquil Jackson², Torsten Giesecke³, Kerim Mutig^{3,4}, Taka-aki A. Koshimizu⁵, Vito S. Hernandez¹, Limei Zhang^{1*} and Jerome D. Swinny^{2*}

OPEN ACCESS

Edited by:

Vincent Geenen,
University of Liège, Belgium

Reviewed by:

David Murphy,
University of Bristol, United Kingdom
Antoine Adamantidis,
University of Bern, Switzerland

*Correspondence:

Limei Zhang
limei.zhangdebarrio@gmail.com
Jerome D. Swinny
jerome.swinny@port.ac.uk

[†] These authors have contributed
equally to this work

*Present address:

Louise Kelly,
Faculty of Medicine, University
of Southampton, Southampton,
United Kingdom

Specialty section:

This article was submitted to
Neuroendocrine Science,
a section of the journal
Frontiers in Neuroscience

Received: 28 August 2018

Accepted: 22 November 2018

Published: 10 December 2018

Citation:

Campos-Lira E, Kelly L, Seifi M,
Jackson T, Giesecke T, Mutig K,
Koshimizu TA, Hernandez VS,
Zhang L and Swinny JD (2018)
Dynamic Modulation of Mouse Locus
Coeruleus Neurons by Vasopressin
1a and 1b Receptors.
Front. Neurosci. 12:919.
doi: 10.3389/fnins.2018.00919

¹ Departamento de Fisiología, Facultad de Medicina, Universidad Nacional Autónoma de México, Mexico City, Mexico,

² Institute for Biomedical and Biomolecular Sciences, School of Pharmacy and Biomedical Sciences, University of Portsmouth, Portsmouth, United Kingdom, ³ Department of Anatomy, Charité - Universitätsmedizin Berlin, Berlin, Germany, ⁴ I.M. Sechenov First Moscow State Medical University of the Ministry of Healthcare of the Russian Federation (Sechenovskiy University), Moscow, Russia, ⁵ Division of Molecular Pharmacology, Department of Pharmacology, Jichi Medical University, Shimotsuke, Japan

The locus coeruleus (LC) is a brainstem nucleus distinguished by its supply of noradrenaline throughout the central nervous system. Apart from modulating a range of brain functions, such as arousal, cognition and the stress response, LC neuronal excitability also corresponds to the activity of various peripheral systems, such as pelvic viscera and the cardiovascular system. Neurochemically diverse inputs set the tone for LC neuronal activity, which in turn modulates these adaptive physiological and behavioral responses essential for survival. One such LC afferent system which is poorly understood contains the neurohormone arginine-vasopressin (AVP). Here we provide the first demonstration of the molecular and functional characteristics of the LC-AVP system, by characterizing its receptor-specific modulation of identified LC neurons and plasticity in response to stress. High resolution confocal microscopy revealed that immunoreactivity for the AVP receptor 1b (V1b) was located on plasma membranes of noradrenergic and non-noradrenergic LC neurons. In contrast, immunoreactivity for the V1a receptor was exclusively located on LC noradrenergic neurons. No specific signal, either at the mRNA or protein level, was detected for the V2 receptor in the LC. Clusters immunoreactive for V1a-b were located in proximity to profiles immunoreactive for GABAergic and glutamatergic synaptic marker proteins. AVP immunopositive varicosities were also located adjacent to labeling for such synaptic markers. Whole-cell patch clamp electrophysiology revealed that the pharmacological activation of V1b receptors significantly increased the spontaneous activity of 45% (9/20) of recorded noradrenergic neurons, with the remaining 55% (11/20) of cells exhibiting a significant decrease in their basal firing patterns. Blockade of V1a and V1b receptors on their own significantly altered LC neuronal excitability in a similar heterogeneous manner, demonstrating that endogenous AVP sets the basal LC neuronal firing rates. Finally, exposing animals to acute stress increased V1b, but not V1a receptor expression, whilst decreasing AVP immunoreactivity. This study reveals the AVP-V1a-b system as

a considerable component of the LC molecular architecture and regulator of LC activity. Since AVP primarily functions as a regulator of homeostasis, the data suggest a novel pathway by modulating the functioning of a brain region that is integral to mediating adaptive responses.

Keywords: V1b, desmopressin, patch clamp, TASP 0390325, restraint stress

INTRODUCTION

The LC is a cluster of neurons located within the pons distinguished from surrounding cell groups by their production of the neurotransmitter noradrenaline (NA) (Dahlstroem and Fuxe, 1964). Despite the compact size of this nucleus, the principal neurons project to almost all regions of the brain and spinal cord, thereby serving as the primary source of NA for the central nervous system (Schwarz and Luo, 2015). The result is a LC-NA system that modulates some of the most salient aspects of brain function such as arousal (Carter et al., 2010), attention (Usher et al., 1999), and memory (Sara, 2015). These neural processes are combined to mediate a core responsibility of the LC-NA system, that being the modulation of adaptive responses to emotional and physiological stressors, which is a process essential for survival in an ever dynamic world (Valentino and Van Bockstaele, 2008). This is accomplished by a highly dynamic excitability profile of LC neurons, which results in the release of NA in precise spatiotemporal and brain-state specific patterns. However, this contribution of the LC-NA system to homeostasis extends beyond the CNS. Indeed, changes in the activity of LC neurons have been associated with diverse peripheral physiological states, such as intestinal contractility (Lechner et al., 1997), changes in blood pressure (Curtis et al., 1993), bladder contractility (Rickenbacher et al., 2008) and fluid balance (Godino et al., 2005). Therefore, the factors that govern LC neuronal excitability have the potential to impact on a vast array of physiological processes both within the CNS and in a number of major peripheral organs in health and disease.

The principal noradrenergic neurons of the LC have the ability to fire action potentials spontaneously and independently of synaptic inputs (Williams et al., 1991). However, their firing frequency is strongly modulated by conventional neurotransmitters (Cherubini et al., 1988; Singewald and Philippu, 1998). Often co-expressed with GABAergic and glutamatergic inputs are an assortment of neuropeptides which either exert direct effects on LC neuronal excitability or modulate the effects of the co-released neurotransmitters, and are thus considered as neuromodulators (Zitnik, 2016). In contrast, the role of another LC afferent system, distinguished by the expression of the neurohormone AVP (Rood and De Vries, 2011) is relatively poorly understood in terms of its contribution to LC function.

The primary signature of AVP is that of a hormone that acts on a range of physiological systems and is integral for the maintenance of homeostasis. Primarily produced by the hypothalamus, its multitude of functions include contributing to the regulation of fluid balance (Bankir et al., 2017), blood pressure (Lozic et al., 2018), thermoregulation (Daikoku et al., 2007),

stress, (Caldwell et al., 2017) as well as emotional and social behavior (Wu et al., 2015). Although many of these functions mirror those of the LC-NA system detailed above, evidence for the cooperativity of these two homeostatic systems is rather limited. This is due to the dearth of information on the molecular, cellular and behavioral correlates of the AVP system within brain pathways such as the LC.

In the mouse, AVP-immunoreactive axonal profiles have been demonstrated in the region of the pons occupied by the LC (Rood and De Vries, 2011). However, this single labeling study failed to demonstrate the association of such fibers with identified LC neurons or other LC neuromodulatory afferent systems. This is important because the LC is composed of morphologically diverse noradrenergic (Schwarz and Luo, 2015) and neurochemically diverse non-noradrenergic neurons (Corteen et al., 2011). Furthermore, the specific receptors, through which AVP might communicate with LC neurons remain to be identified. Three AVP receptor subtypes have been identified, namely AVP receptor 1a (V1a), 1b (V1b) and 2 (V2) (Thibonnier et al., 2002). Expression of the V1b receptor at the mRNA level has been reported in the pons, but not on identified LC neurons (Young et al., 2006). Evidence for the association of AVP with LC is more developed at the functional level. Recordings from neurons in the LC showed an excitatory effect of AVP in gerbil (Olpe et al., 1987) and rat (Berecek et al., 1987), whilst the injection of AVP into the LC complex, not on identified LC neurons, of cats, altered posture and vestibulospinal reflexes (Andre et al., 1992). However, such effects on LC excitability have yet to be demonstrated in other species, which is an important caveat given the demonstrated species differences of the CNS AVP system (Tribollet et al., 1998). Finally, although the contribution of AVP in the stress response has been demonstrated in specific stress circuits (Herman and Tasker, 2016), the activation of the LC AVP system, during stress, has yet to be demonstrated. Here we provide the first demonstration of the molecular and physiological characteristics of AVP-receptor system within neurochemically defined cellular networks of the mouse LC. We also show that exposing mice to a single episode of stress dramatically alters the expression of the LC AVP-receptor system, providing evidence for the direct interaction of two major homeostatic systems.

MATERIALS AND METHODS

All procedures involving animal experiments were approved by the Animal Welfare and Ethical Review Body of the University of Portsmouth and were performed by a personal license holder,

under a Home Office-issued project license, in accordance with the Animals (Scientific Procedures) Act, 1986 (United Kingdom) and associated procedures.

Tissue Preparation for Immunohistochemistry

Adult male C57BL/6J, as well as V1a and V1b receptor specific gene-deleted (Tanoue et al., 2004; Koshimizu et al., 2006) mice, 2 months of age, were used to determine the native AVP and AVP receptor subtype expression patterns, according to a previously published protocol (Corteen et al., 2011). Briefly, under anesthesia, animals were perfused transcardially with 0.9% saline solution for 2 min, followed by 12 min fixation with a fixative consisting of 1% paraformaldehyde and 15% v/v saturated picric acid in 0.1 M phosphate buffer (PB), pH 7.4. The brains were post-fixed overnight at room temperature in the same perfusion fixative, sectioned with a vibratome and stored in 0.1 M PB and 0.05% sodium azide until further processing.

Immunohistochemistry

Non-specific binding of the secondary antibodies was minimized by incubating the sections in TBS-Tx containing 20% normal horse serum (S-2000, Vector Laboratories Inc.) for 2 h. Sections were incubated in a cocktail of primary antibodies overnight at 4°C (**Supplementary Table S1**). The next day, the sections were washed with TBS-Tx for 30 min after which they were incubated at room temperature in a cocktail of an appropriate mixture of secondary antibodies, conjugated with Alexa Fluor 488, indocarbocyanine (Cy3) and indocarbocyanine (Cy5), all provided by Jackson ImmunoResearch, for 2 h. The sections were washed in TBS-Tx for 30 min after which they were mounted on glass slides, air dried and coverslipped using Vectashield mounting medium (H-1000, Vector Laboratories Inc.).

Image Acquisition

Sections were examined with a confocal laser-scanning microscope (LSM710 or LSM 880; Zeiss, Oberkochen, Germany) using a Plan Apochromatic 63 x DIC oil objective (NA 1.4, pixel size 0.13 μm). Z-stacks were used for routine evaluation of the labeling. All images presented represent a single optical section. These images were acquired using sequential acquisition of the different channels to avoid cross-talk between fluorophores, with the pinholes adjusted to one Airy unit. Images were processed with the software Zen 2009 Light Edition (Zeiss, Oberkochen, Germany) and exported into Adobe Photoshop. Only brightness and contrast were adjusted for the whole frame, and no part of a frame was enhanced or modified in any way.

Quantitative Real-Time Polymerase Chain Reaction (qPCR) Detection of V2 mRNA

For complete methods, please see **Supplementary Information**.

Whole Cell Patch Clamp Electrophysiology Recordings in Acute Brain Slices of the LC

Recordings were performed in juvenile (postnatal day 25–30) mice according to previously published protocols (Swinney et al., 2010). Briefly, animals were rapidly decapitated and the head placed in ice-cold oxygenated sucrose-cutting solution containing (mM): sucrose (234), KCl (2.5), NaH_2PO_4 (1.25), NaHCO_3 (26), dextrose (10), MgSO_4 (10), CaCl_2 (0.5). The brain was rapidly removed and blocked to isolate the brainstem region. The trimmed brain was affixed to a Vibratome equipped with a ceramic blade and submerged in ice cold oxygenated sucrose cutting solution. Horizontal 200 μm slices of the brainstem containing the LC were cut and placed in a holding vial containing extracellular solution (ECS) containing (mM): NaCl (126), KCl (2.95), NaH_2PO_4 (1.25), NaHCO_3 (26), dextrose (10), MgSO_4 (2), CaCl_2 (Sigma) for 1 h at 37°C, after which they were kept at room temperature, and transferred one at a time to the recording chamber.

A single slice was placed in the recording chamber and continuously superfused with ECS at 1 ml/min at 32°C. LC neurons were visualized using an Olympus B50 upright microscope fitted with a 40x water-immersion objective, differential interference contrast and infrared filter. Recording pipettes were fashioned from borosilicate glass capillary tubing (1.2 mm o.d., 0.69 mm i.d.; Warner Instruments) using a Narishige PC-10 micropipette puller. Pipettes were filled with potassium gluconate intracellular solution containing: K-Gluconate (70), KCl (70), HEPES (10), EGTA (10), MgCl_2 (2), CaCl_2 (1), ATP (2) (Maguire et al., 2014) and 0.1 % biocytin (pH 7.3) to allow *post-hoc* identification of the cell.

A visualized cell was approached with the electrode, a G Ω seal established and the cell membrane ruptured to obtain a whole-cell recording using a Multiclamp 700B amplifier (Molecular Devices, United States). Series resistance was monitored throughout the experiment. If the series resistance of the electrode was unstable or exceeded four times the electrode resistance, electrophysiological data from the cell were discarded. The main criteria for accepting a recording were an action potential amplitude of 65–70 mV, action potential shape characteristic of an LC neuron and membrane potential between –50 and –60 mV. If the cell retained a stable baseline and resistance and did not depolarize over time, the cell was retained for analysis. Signals were digitized by Digidata 1320-series analog-to-digital converter and stored online using pClamp 9 software (Molecular Devices). Only one cell per slice was recorded. The experimental protocol involved recording baseline cell characteristics in current clamp, including FR (Hz), input resistance [derived from the linear portion of a voltage–current plot of hyperpolarizing current steps (M Ω), resting membrane potential (mV), membrane time constant (τ , ms), action potential amplitude (mV) and duration (ms) and AHP amplitude (mV), and AHP $t_{1/2}$ duration (measured from the peak of the AHP to half the amplitude of the AHP, in ms)]. After determining baseline characteristics, the drugs were bath-applied for at least 10 min after which the cell characteristics were measured

again. Data were analyzed with Clampfit software (Molecular Devices).

Following the recording, the pipette was gently retracted, the slice removed from the recording chamber and submerged in a vial containing 1% paraformaldehyde fixative overnight. Following washing in TBS-Tx buffer, the sections were then incubated with 20% normal horse serum for 1 h at room temperature, followed by incubation with an antibody against TH overnight at 4°C. Following further washing with TBS-Tx, the sections were incubated with a streptavidin conjugated to Alexa Fluor 488 secondary antibody (1:1000) (Molecular Probes, United States), in addition to an appropriate secondary antibody to visualize TH, for 2 h at room temperature. Sections were then imaged on a confocal microscope (Zeiss LSM 710) in order to confirm that the recorded cell was located within the LC and was immunopositive for TH.

Drugs

All chemicals for the recording solutions were obtained from Sigma. Desmopressin, [d(CH₂)⁵, Tyr(Me)², Arg⁸]-Vasopressin and TASP 0390325 were obtained from Tocris, United Kingdom, and dissolved in ECS.

Acute Restraint Stress

A total of 10 (5 control and 5 stress) male mice, aged 2 months were used in this part of the study. The animals were placed in a rodent Plexiglas restrainer (Harvard Apparatus) for 60 min. The animals were then returned to their home cages for a further 60 min, after which they were killed, using the perfusion-fixation protocol above and the tissue used for quantitative immunohistochemistry.

Quantification of AVP and V1a-b Receptor Immunoreactivity in the LC of Tissue From Restraint Stress and Control Mice

One hour after the cessation of the stress period, animals were killed by perfusion fixation and the tissue prepared for semi-quantitative analyses of AVP and V1a-b receptor immunoreactivity as above. The quantitative method has been previously described (Gunn et al., 2013) and is detailed in **Supplementary Method**.

Statistical Analysis

All quantitative data are presented as the mean ± SEM. Statistical differences between means were assessed using GraphPad Prism software, with the names of statistical tests used indicated in the Results section. A *p*-value less than 0.05 was considered statistically significant.

RESULTS

The overall aims of the project were to identify the AVP receptor subtypes expressed by LC neurons, the location of these receptors within the cellular networks of the LC, their contribution to

LC neuronal excitability and whether they are engaged by acute stress.

Verification of the Specificity of AVP Receptor Immunoreactivity

A key determinant of a direct AVP influence on LC function would be the presence, and subtype, of AVP receptors in this brain region. Since there is evidence for the expression of all AVP receptor subtypes in the brain, from the outset, we sought to identify whether specific AVP receptor subtypes are expressed on identified LC neurons. In tissue from wild type (WT) mice, V1a receptor immunoreactivity presented as individual clusters enriched on the somata and dendrites of LC noradrenergic neurons, identified by immunoreactivity for the NA synthesizing enzyme tyrosine hydroxylase (TH) (**Figure 1A1**). In tissue from V1a receptor knockout mice, no such specific V1a receptor labeling pattern was detectable, with most of the signal enriched in nuclei or scattered diffusely showing no clear association with any cellular profiles, thus confirming the specificity of the V1a antibody used (**Figure 1A2**). In WT tissue, immunoreactivity for the V1b receptor also presented as clustered signal on somatodendritic compartments of LC noradrenergic neurons. However, in contrast to V1a, signal for V1b appeared more widespread and was likely contained on LC non-noradrenergic neurons as well (**Figure 1B1**). This labeling pattern was absent in tissue from V1b receptor knockout mice, thus confirming the specificity of the V1b antibody used (**Figure 1B2**). No specific labeling for the V2 receptor was detectable in the LC (**Figures 1C1,C2**). We further verified the lack of V2 receptor expression in the LC, at the mRNA level, by performing quantitative RT-PCR on tissue from the LC and another tissue site known to express this receptor, namely the kidney (*N* = 5 mice). Whilst robust V2 receptor mRNA expression was detected in kidney samples, only negligible amounts were evident in LC samples (**Figure 1C3**). We therefore conclude that V1a-b receptors are the major subtypes expressed in the mouse LC.

The V1b Receptor Is Expressed by Noradrenergic and Non-noradrenergic Neurons of the LC in Close Proximity to Excitatory and Inhibitory Synapses

We first examined the expression profile of the V1b receptor as it appeared to be more widely distributed throughout the LC, compared to the V1a receptor, and is possibly associated with both noradrenergic and non-noradrenergic profiles (compare **Figures 1A1,B1**). We have shown that the LC is composed of not only noradrenergic neurons, but also a range of neurochemically diverse non-noradrenergic neurons (**Figure 2A1**) (Corteen et al., 2011). In order to gain an integrative perspective of the role of the AVP system within the cellular networks of the LC, we sought to characterize the location of the V1b receptor throughout LC circuitry. High resolution imaging revealed that V1b receptor immunoreactivity was enriched on the plasma membranes of LC neurons with significantly lower levels of signal located in their cytoplasmic compartments, characteristic of a metabotropic receptor (**Figure 2A2**). Signal

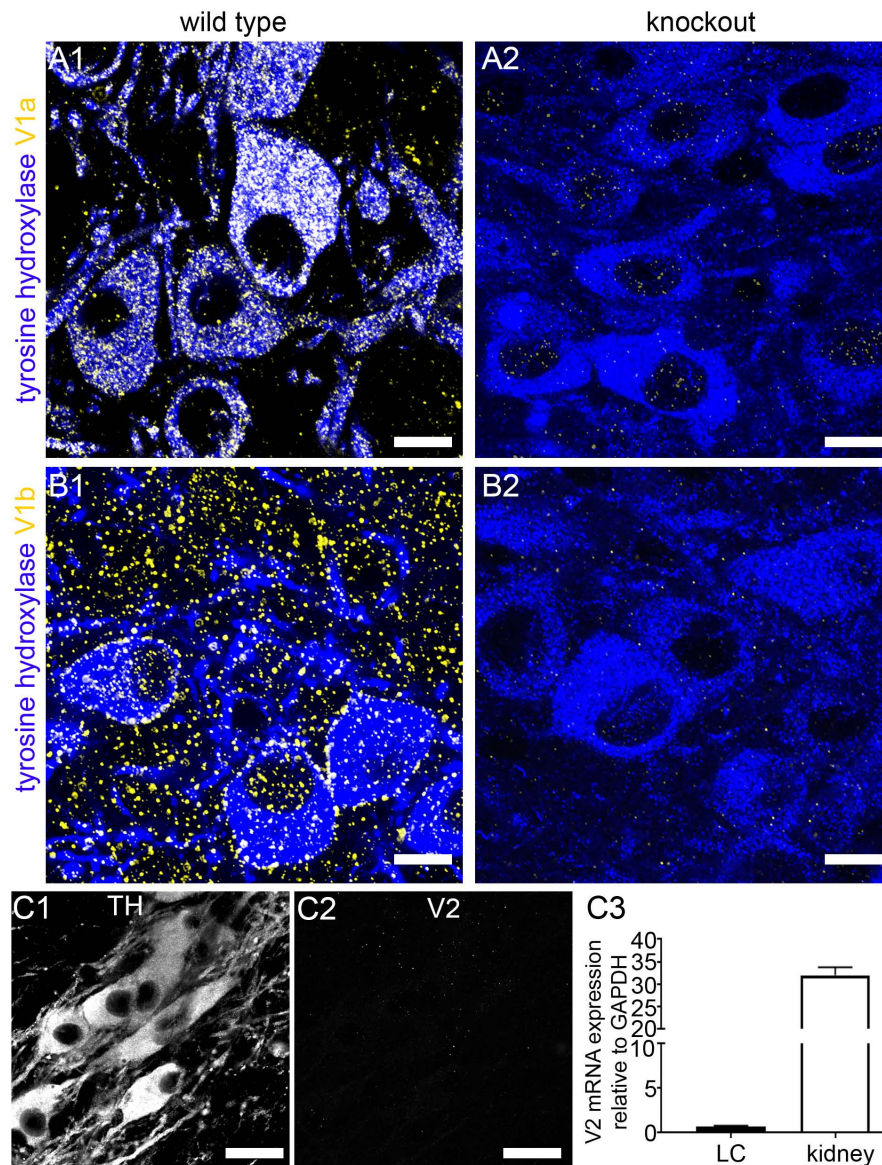


FIGURE 1 | Confirmation of the specificity of the V1a and V1b receptor antibody labeling in the LC. **(A1)** Shows immunoreactivity for tyrosine hydroxylase (TH) (blue) and the V1a receptor (yellow) in tissue from WT mouse. TH is the enzyme essential for noradrenaline synthesis and thus identifies the principal neurons of the LC. V1a signal is exclusively associated with TH-immunopositive profiles. **(A2)** Shows, immunoreactivity for TH (blue) and V1a receptor (yellow) in tissue from a V1a knock out mouse. Only weak, non-specific nuclear signal is evident confirming the specificity of the V1a antibody labeling pattern. **(B1)** Shows immunoreactivity for tyrosine hydroxylase (TH) (blue) and the V1b receptor (yellow) in tissue from WT mouse. V1b signal is associated with TH-immunopositive cells as well as areas not containing TH-immunopositive profiles. **(B2)** Shows, immunoreactivity for TH (blue) and V1b receptor (yellow) in tissue from a V1b knock out mouse. Only weak, non-specific signal is evident confirming the specificity of the V1b antibody labeling pattern. **(C1)** Shows TH immunoreactivity. **(C2)** Shows, in the corresponding field of view, labeling for an antibody against the V2 receptor. No specific signal was detectable. **(C3)** Shows the expression of mRNA for the V2 receptor in tissue from the LC and the kidney which is known to express this receptor subtype. Whilst robust mRNA expression was detected in kidney, negligible expression was evident in LC samples. $N = 5$ animals, with the bars representing the means and the error bars, the SEM. Scale bars **(A,B)**, 10 μm ; **(C)** 20 μm .

was also located on the somata of non-noradrenergic LC neurons (**Figure 2A3**), identified by immunoreactivity for the pan-neuronal marker protein HuC (Okano and Darnell, 1997) (**Figures 2A3,A4**). In addition to somatic labeling, V1b receptor was also located on dendritic profiles, delineated by immunoreactivity for microtubule associated protein 2 (MAP2) (**Figure 2B**).

This clustered distribution of V1b receptor immunoreactivity across the surfaces of LC neurons overlapped with the locations of previously demonstrated GABAergic (Corteen et al., 2011) and glutamatergic (Seifi et al., 2014) inputs. Furthermore, since AVP has been shown to modulate synaptic transmission (Ostergaard et al., 2014), we investigated the proximity of V1b receptor-immunoreactive clusters to excitatory and

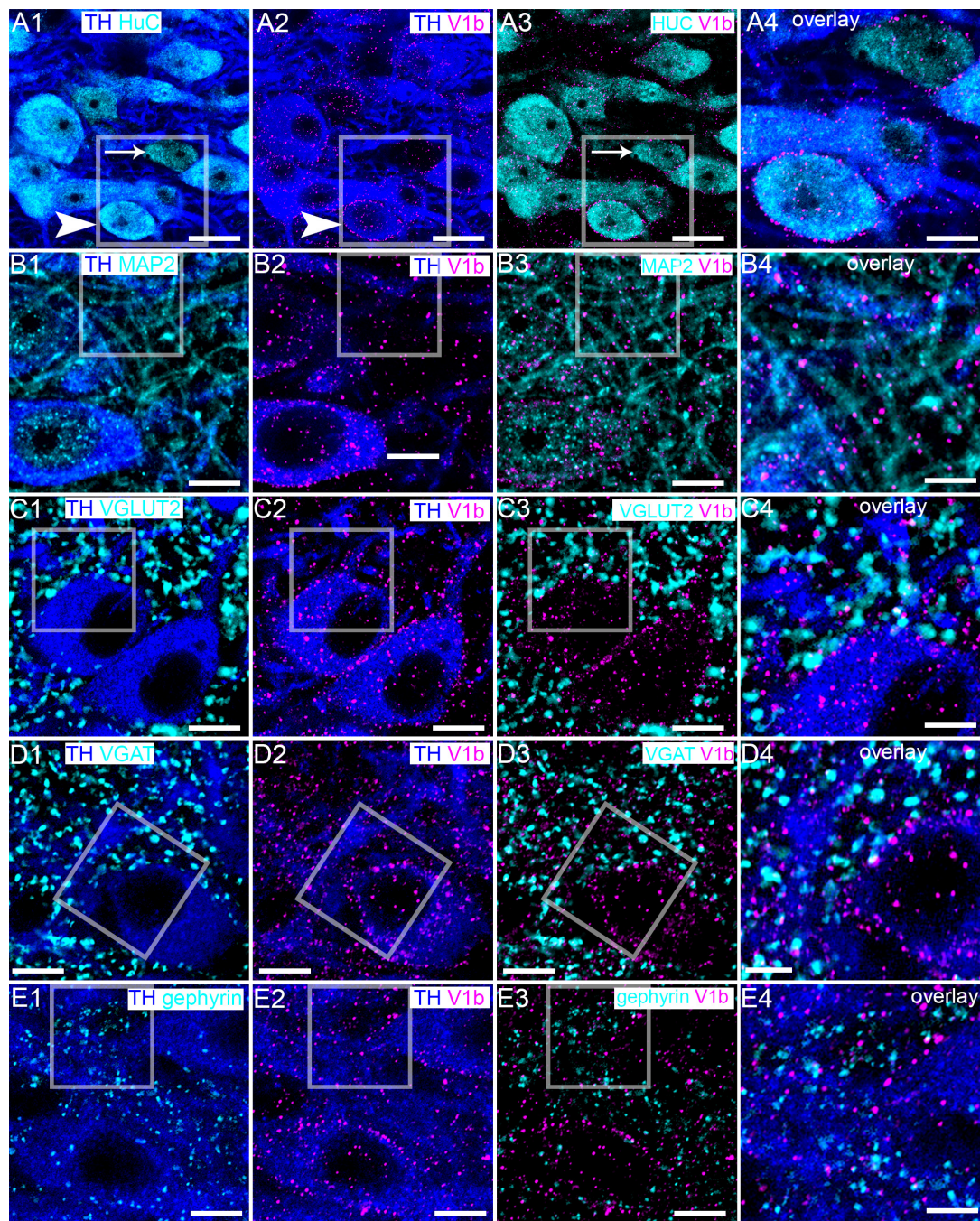


FIGURE 2 | V1b receptor is expressed on noradrenergic and non-noradrenergic LC neurons in close proximity to glutamatergic and GABAergic synapses. **(A1)** Shows immunoreactivity for TH (blue), a marker of noradrenergic neurons and HuC (cyan), a pan-neuronal marker. Thus, in this brain region, HuC identifies noradrenergic (arrowhead) and non-noradrenergic (arrow) neurons of the LC. **(A2)** Shows, in the same field of view, immunoreactivity for TH (blue) and V1b receptor (magenta), confirming its expression in LC noradrenergic neurons (arrowhead). V1b receptor signal presents as individual clusters concentrated on somatodendritic plasma membranes, typifying the expression pattern of a metabotropic receptor. **(A3)** shows, in the same field of view, immunoreactivity for V1b receptor (magenta) and HuC (cyan), confirming V1b receptor expression in LC non-noradrenergic neurons as well (arrow). **(A4)** Is an overlay and magnified view of the boxed area in **(A1–A3)**. **(B1)** Shows immunoreactivity for TH (blue), and microtubule associated protein 2 (MAP2) (cyan), a protein enriched in dendrites. **(B2)** shows, in the same field of view, immunoreactivity for TH (blue) and V1b receptor (magenta), which confirms V1b expression on dendritic compartments. **(B3)** Shows, in the same field of view, the association of immunoreactivity for V1b (magenta) with MAP2 (cyan), confirming V1b expression in dendritic compartments as well. **(B4)** Is an overlay and magnified view of the boxed area in **(B1–B3)**. **(C1)** Shows immunoreactivity for TH (blue), and vesicular glutamate transporter 2 (VGLUT2) (cyan), a protein enriched in glutamatergic axon terminals and used here to identify presynaptic domains of excitatory synapses. **(C2)** Shows, in the same field of view, immunoreactivity for TH (blue) and V1b receptor (magenta). **(C3)** Shows, in the same field of view, the association of immunoreactivity for V1b receptor (magenta) with VGLUT2 (cyan). The

(Continued)

FIGURE 2 | Continued

close association suggests that the V1b receptor in LC neurons is expressed in close proximity to excitatory synapses. **(C4)** Is an overlay and magnified view of the boxed area in **(C1–C3)**. **(D1)** Shows immunoreactivity for TH (blue), and vesicular GABA transporter (VGAT) (cyan), a protein enriched in GABAergic and glycinergic axon terminals and used here to identify presynaptic domains of inhibitory synapses. **(D2)** Shows, in the same field of view, immunoreactivity for TH (blue) and V1b (magenta). **(D3)** Shows, in the same field of view, the association of immunoreactivity for V1b (magenta) with VGAT (cyan). The close association suggests that V1b on LC neurons is expressed in close proximity to inhibitory synapses as well. **(D4)** Is an overlay and magnified view of the boxed area in **(D1–D3)**. **(E1)** Shows immunoreactivity for TH (blue), and gephyrin (cyan), a protein that anchors GABA_A and glycine receptors in inhibitory synapses and used here to identify postsynaptic domains of inhibitory synapses. **(E2)** Shows, in the same field of view, immunoreactivity for TH (blue) and V1b (magenta). **(E3)** Shows, in the same field of view, the association of immunoreactivity for V1b (magenta) with gephyrin (cyan). There is sparse colocalization of clusters immunoreactive for V1b and gephyrin suggesting a limited incorporation of V1b in inhibitory postsynaptic domains, with this receptors located most likely on perisynaptic compartments. **(E4)** Is an overlay and magnified view of the boxed area in **(E1–E3)**. Scale bars **(A1–A3)** 20 μ m; **(A4,B–D1–D3)** 10 μ m; **(B–D4)** 5 μ m.

inhibitory synaptic marker proteins. Clusters immunoreactive for the vesicular glutamate transporter 2 (VGLUT2) contacted the somatic and dendritic surfaces of TH-immunopositive neurons, thereby identifying glutamate release sites on these neurons (**Figure 2C1**). Evaluation of immunoreactivity for VGLUT2 alongside the V1b receptor revealed a proportion of closely apposed clusters for either molecule, suggesting that a proportion of V1b receptors function in proximity to glutamatergic synapses (**Figures 2C2,C3**). However, there was also a notable proportion of V1b receptor-immunoreactive clusters located on cell surfaces which were devoid of VGLUT2-immunoreactive contacts (**Figures 2C3,C4**). Immunoreactivity for the vesicular GABA transporter (VGAT) was used to identify the domains of inhibitory synaptic inputs. VGAT signal was widely distributed across the somatodendritic surfaces of LC neurons (**Figure 2D1**). In a similar manner, a proportion of V1b receptor immunoreactive clusters were adjacent to clusters immunoreactive for VGAT, although some, particularly those on somatic membranes were not associated with VGAT signal (**Figures 2D2–D4**). Since VGAT and VGLUT2 identify presynaptic compartments, we used gephyrin, a protein that anchors GABA_A and glycine receptors in the postsynaptic compartments of inhibitory synapses, in order to assess any enrichment of the V1b receptor in postsynaptic junctions. A relatively sparse association of V1b and gephyrin immunoreactivity was evident (**Figure 2E**). However, at the light microscopical level, it is not possible to determine the precise location of these receptors, or other proteins, in proximity to presynaptic, postsynaptic, perisynaptic or extrasynaptic compartments. Therefore, further ultrastructural analyses, using immunohistochemistry and transmission electron microscopy is required to unequivocally determine the location of these receptors in proximity to synaptic junctions.

V1b Receptor Activation Has Contrasting Effects on the Spontaneous Firing of LC Noradrenergic Neurons

Given the close proximity of V1b receptor signal to synaptic inputs, we next investigated whether the pharmacological activation of V1b receptors alters the spontaneous excitability of identified LC neurons by using whole cell patch clamp electrophysiology in acute brain slices containing the LC. In light of the LC consisting of noradrenergic and non-noradrenergic neurons, all cells were loaded with biocytin during the recording

in order to verify their location within the LC and their neurochemical identity. Only cells positively identified as TH-immunopositive and located within the LC core, were included in the analyses (**Figure 3A**). The spontaneous firing rates (FR) of the recorded neurons were indistinguishable from previously published studies, with the mean \pm SEM FR of 1.7 ± 0.1 Hz, ranging from 0.2 Hz to 3.2 Hz, $N = 50$ cells from 15 animals (**Supplementary Tables S2–S7**). The associated membrane properties of the neurons are also detailed in **Supplementary Tables S2–S7**. It was noticeable from the outset that V1b receptor activation, by applying the synthetic vasopressin analog desmopressin (200 μ M), which acts as an agonist at V1b and V2 receptors, either increased, or decreased the spontaneous FRs of LC neurons. We therefore categorized the recorded neurons into groups which exhibited either an increase or decrease in their activity in response to the drug. Desmopressin significantly increased the FR of LC neurons from 1.7 ± 0.3 Hz to 2.9 ± 0.3 Hz, $p = 0.01$, paired Student's *t*-test; $N = 9$ cells (**Figures 3B1,B2**). Desmopressin also significantly decreased the afterhyperpolarization (AHP) time constant from 65 ± 6 ms to 53 ± 5 ms, $p = 0.005$, paired Student's *t*-test; $N = 8$ cells (**Figure 3B3**). There were no significant differences in any other cell characteristics following the application of desmopressin (**Supplementary Table S2**). In a separate cohort of cells, recorded under identical conditions, desmopressin significantly decreased the FR of LC neurons from 1.4 ± 0.3 Hz to 0.9 ± 0.2 Hz, $p = 0.02$, paired Student's *t*-test; $N = 11$ cells (**Figures 3C1,C2**). In this group of cells, desmopressin also significantly decreased the action potential amplitude (69 ± 1.8 mV to 45.5 ± 9.3 mV, $p = 0.02$, paired Student's *t*-test; $N = 11$ cells, **Figure 3C1**) and increased the AHP time constant from 67 ± 8 ms to 167 ± 44 ms, $p = 0.03$, paired Student's *t*-test; $N = 11$ cells (**Figure 3C3**). In this group of cells, there were no significant differences in any other cell characteristics following the application of desmopressin (**Supplementary Table S2**). Thus, the activation of V1b receptors bi-directionally modulates the excitability of LC neurons.

We then explored whether locally released AVP contributes to the basal FR of LC neurons by recording the FR of LC neurons following the blockade of V1b receptors in the presence of the V1b receptor selective antagonist TASP 0390325 (Iijima et al., 2014). In a similar trend to desmopressin, TASP 0390325, 20 nM, either increased (2.2 ± 0.1 Hz to 3.2 ± 0.3 Hz, $p = 0.01$, paired Student's *t*-test, $N = 8$ cells, **Figures 3D1,D2**) or decreased (1.7 ± 0.2 Hz to 1.3 ± 0.3 Hz, $p = 0.03$, paired Student's *t*-test, $N = 6$ cells, **Figures 3E1,E2**) the spontaneous FR of neurons.

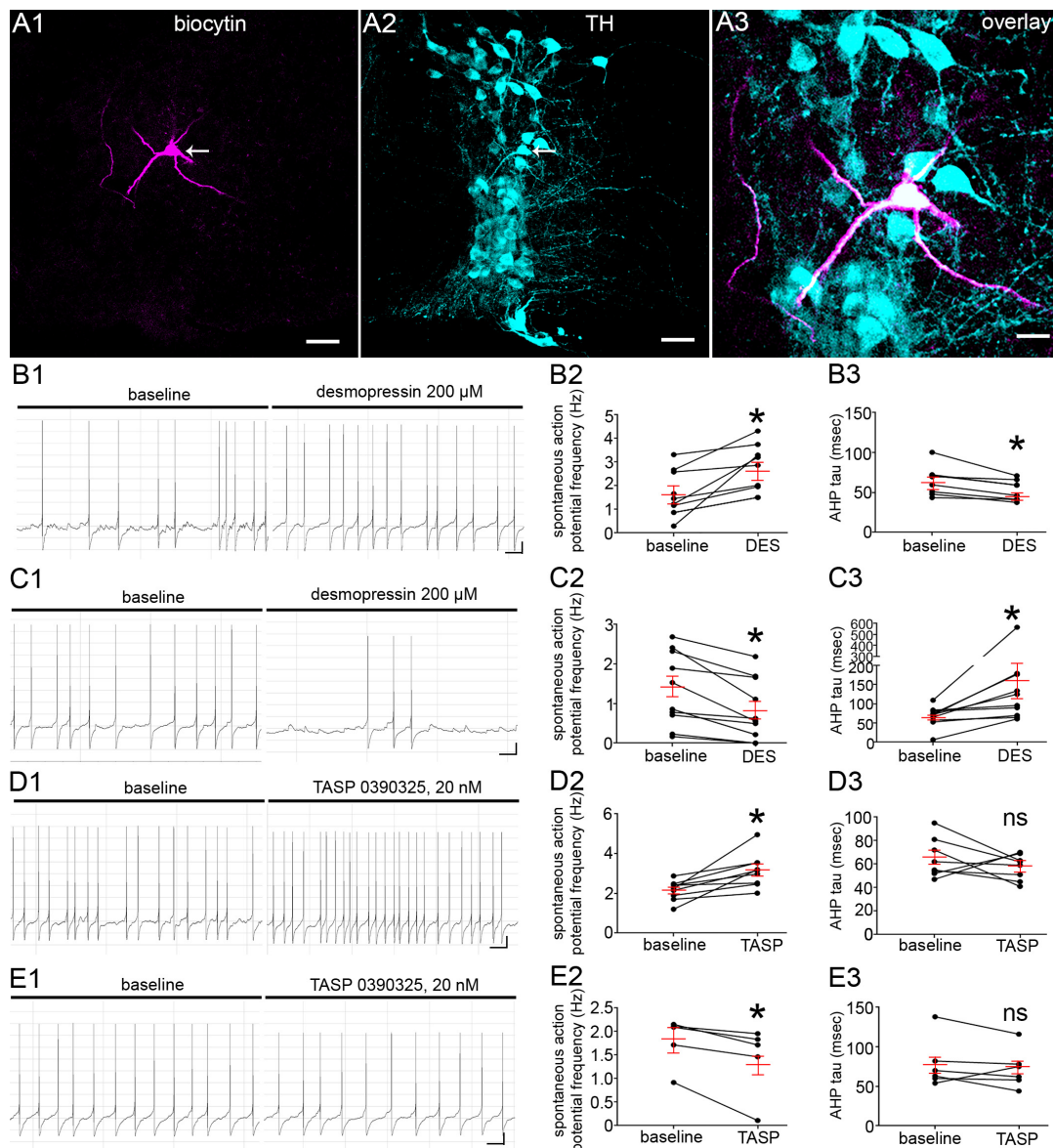


FIGURE 3 | V1b receptor modulation directly alters LC noradrenergic neuronal activity. **(A)** *Post hoc* microscopical confirmation of the molecular identity and location of recorded neurons. **(A1)** Shows immunoreactivity for biocytin which was originally contained within the intracellular solution used for recording the neuron in the whole-cell configuration. Note that immunoreactivity is located exclusively within the single neuron (arrow). **(A2)** Shows immunoreactivity for TH within the same field of view as **(A1)**, confirming that the recording was from the LC, with the arrow highlighting the recorded cell. **(A3)** Is an overlay and magnified view the cell in **(A1,A2)** confirming that the recorded cell is TH immunopositive and thus a noradrenergic LC neuron. **(B1)** Representative traces of the spontaneous firing pattern of an LC neuron before and after the application of the V1b receptor agonist desmopressin 200 μ M, from a cohort of neurons that responded with a significant increase in the frequency of spontaneous action potentials. **(B2)** Quantification of the spontaneous firing rates (Hz) of LC neurons before and after the application of desmopressin (DES). **(B3)** Quantification of the after hyperpolarization time constant (msec) of LC neurons before and after the application of desmopressin. **(C1)** Representative traces of the spontaneous firing pattern of an LC neurons before and after the application of the V1b receptor agonist desmopressin 200 μ M, from a cohort of neurons that responded with a significant decrease in the frequency of spontaneous action potentials. **(C2)** Quantification of the spontaneous firing rates (Hz) of LC neurons before and after the application of desmopressin. **(C3)** Quantification of the after hyperpolarization time constant (msec) of LC neurons before and after the application of desmopressin. **(D1)** Representative traces of the spontaneous firing pattern of an LC neuron before and after the application of the V1b receptor antagonist TASP 0390325, 20 nM, from a cohort of neurons that responded with a significant increase in the frequency of spontaneous action potentials. **(D2)** Quantification of the spontaneous firing rates (Hz) of LC neurons before and after the application of TASP 039325. **(D3)** Quantification of the afterhyperpolarization time constant (msec) of LC neurons before and after the application of TASP 039325. **(E1)** Representative traces of the spontaneous firing pattern of an LC neuron before and after the application of the V1b antagonist TASP 0390325, 20 nM, from a cohort of neurons that responded with a significant decrease in the frequency of spontaneous action potentials. **(E2)** Quantification of the spontaneous firing rates (Hz) of LC neurons before and after the application of TASP 039325. **(E3)** Quantification of the afterhyperpolarization time constant (msec) of LC neurons before and after the application of TASP 039325. For graphs in **(B-E)**, the dots represent the values for individual cells, the long red bars represents the mean for all cells within that group, and the short red bars represent the SEM. * $p < 0.05$, paired Student's t -test. Scale bars **(A1,A2)** 50 μ m; **(A3)** 20 μ m; **(B1,C1,D1,E1)** horizontal bar 1 s, vertical bar 10 mV.

However, in contrast to desmopressin, TASP 0390325 did not significantly alter the AHP time constant either in those cells that showed an increased (65 ± 6 ms to 58 ± 4 , $p = 0.3442$, paired Student's *t*-test; $N = 8$ cells, **Figure 3D3**) or decreased FR (78 ± 13 ms to 72 ± 10 ms, $p = 0.3442$, paired Student's *t*-test; $N = 6$ cells, **Figure 3E3**). This provides evidence that endogenous AVP and V1b receptor activation contributes to the basal level of LC activity.

The V1a Receptor Is Expressed Exclusively by Noradrenergic Neurons of the LC

In contrast to the V1b receptor, V1a receptor immunoreactivity was restricted to LC TH-immunopositive neurons, both on somatic (**Figure 4A**) and dendritic (**Figure 4B**) compartments, with TH immunonegative cell, identified by HUC immunoreactivity devoid of any TH signal. In common with the V1b receptor, clusters immunoreactive for V1a were also located, on occasion, in proximity to puncta immunoreactive for VGLUT2 (**Figure 4C**) and VGAT (**Figure 4D**).

V1a Receptor Blockade Has Contrasting Effects on the Spontaneous Firing of LC Noradrenergic Neurons

In a similar trend to the V1b receptor, blockade of the V1a receptor with the antagonist [(d(CH₂)51, Tyr(Me)₂, Arg₈)-Vasopressin, 30 nM] ($n = 16$) also had contrasting effects on LC FR. Indeed, 62% of the cells responded with an increase in their FR (1.6 ± 0.2 Hz to 2.1 ± 0.3 Hz; $p = 0.0016$, paired Student's *t*-test, $N = 8$ cells, **Figures 5A1,A2**). However, in contrast to the effects of the V1b antagonist, V1a blockade did result in a significant decrease in AHP of the neurons (73 ± 9 ms to 60 ± 6 , $p = 0.0185$, paired Student's *t*-test; $N = 8$ cells, **Figure 5A3**). The remaining cells responded with a decrease in their FR (2.0 ± 0.2 Hz to 1.4 ± 0.2 Hz; $p = 0.0172$, paired Student's *t*-test, $N = 6$ cells, **Figures 5B1,B2**). However, in these subset of cells, there were no significant differences between the AHP (61 ± 4 ms to 69 ± 10 , $p = 0.5117$, paired Student's *t*-test; $N = 6$ cells, **Figure 5B3**). This provides evidence that endogenous AVP and V1a-b receptors contributes to the basal level of LC activity. These data are summarized in **Supplementary Tables S6, S7**.

AVP-Containing Axons Contact Noradrenergic and Non-noradrenergic Neurons of the LC in Close Proximity to Excitatory and Inhibitory Synapses

The V1a-b antagonist data above provide evidence that AVP within the LC regulates the basal levels of neuronal activity. This could identify a novel pathway that modulates behavioral states associated with changes in both AVP production (Caldwell et al., 2017), and LC neuronal activity (McCall et al., 2015), such as psychosocial stress. For native AVP to exert a significant control over LC-mediated brain functions, there would need to be a considerable distribution of afferents containing this neurohormone throughout the LC. Since previous reports

provide only low resolution images of AVP-immunoreactive profiles within the region of the pons occupied by the LC (Rood and De Vries, 2011), we undertook a high resolution characterization of the native association of AVP-containing profiles with identified LC neurons.

The specificity of the LC AVP labeling pattern was replicated using two different AVP antibodies, and the paraventricular nucleus (PVN) as a positive control brain region. Both antibodies provided a pattern of immunoreactivity within the PVN that was consistent with previously published reports (Zhang and Hernandez, 2013) (**Figure 6A**). However, antibody AC39363 produced a superior signal to noise ratio and was therefore used for remainder of the study. Within the LC, AVP immunoreactivity presented as a mixture of varicose plexuses and individual clusters contacting LC neurons (**Figures 6B,C**). Importantly, AVP immunoreactivity was distributed through the entire extent of the LC, both within the nuclear core, as well as in the pericoeruleur dendritic region (**Figures 6B,C**). We found no evidence of specific AVP-immunoreactive neurons within the LC.

Upon close inspection, AVP immunoreactive varicosities contacted both noradrenergic (**Figures 7A1,A2**) and non-noradrenergic (**Figures 7A3,A4**) neurons of the LC. In addition to this association with somatic compartments, AVP-immunoreactive varicosities also contacted dendritic profiles (**Figure 7B**), thus closely mirroring the distribution of V1a-b receptors in this brain region. Unfortunately, both antibodies for AVP and V1a-b receptors were raised in the same species, thus precluding co-association studies. Nevertheless, we evaluated the association of AVP immunoreactivity alongside the synaptic marker proteins used for the V1a-b receptors receptor analyses, in an attempt to extrapolate the degree of coherence for their respective locations within these neurons. AVP-immunoreactive profiles were strongly associated with VGLUT2 immunopositive clusters (**Figure 7C**). However, AVP immunoreactivity showed relatively less association with the inhibitory synaptic markers proteins VGAT (**Figure 7D**) and gephyrin (**Figure 7E**). Thus, AVP-immunoreactive axonal profiles are distributed throughout the LC, suggesting a pool of this neurohormone that has the potential to impact on LC neurons.

AVP-Immunoreactive Profiles Show Sparse Association With Other LC Neuromodulatory Afferent Pathways

It is currently unclear whether LC AVP-immunopositive fibers contain other neuropeptides known to provide modulatory input to this nucleus. We therefore assessed the degree of colocalization between AVP-immunoreactive profiles and varicosities immunopositive for the predominant neuropeptides that have been shown to directly contact LC neurons and alter their excitability, namely substance P (Guyenet and Aghajanian, 1979; Pickel et al., 1979), enkephalin (Valentino and Wehby, 1989; Van Bockstaele et al., 1995), orexin A (Hagan et al., 1999; Horvath et al., 1999), and CRH (Valentino et al., 1983; Van Bockstaele et al., 1996). Only subsets of AVP-immunoreactive varicosities showed colocalization with substance P-immunopositive puncta with the vast majority

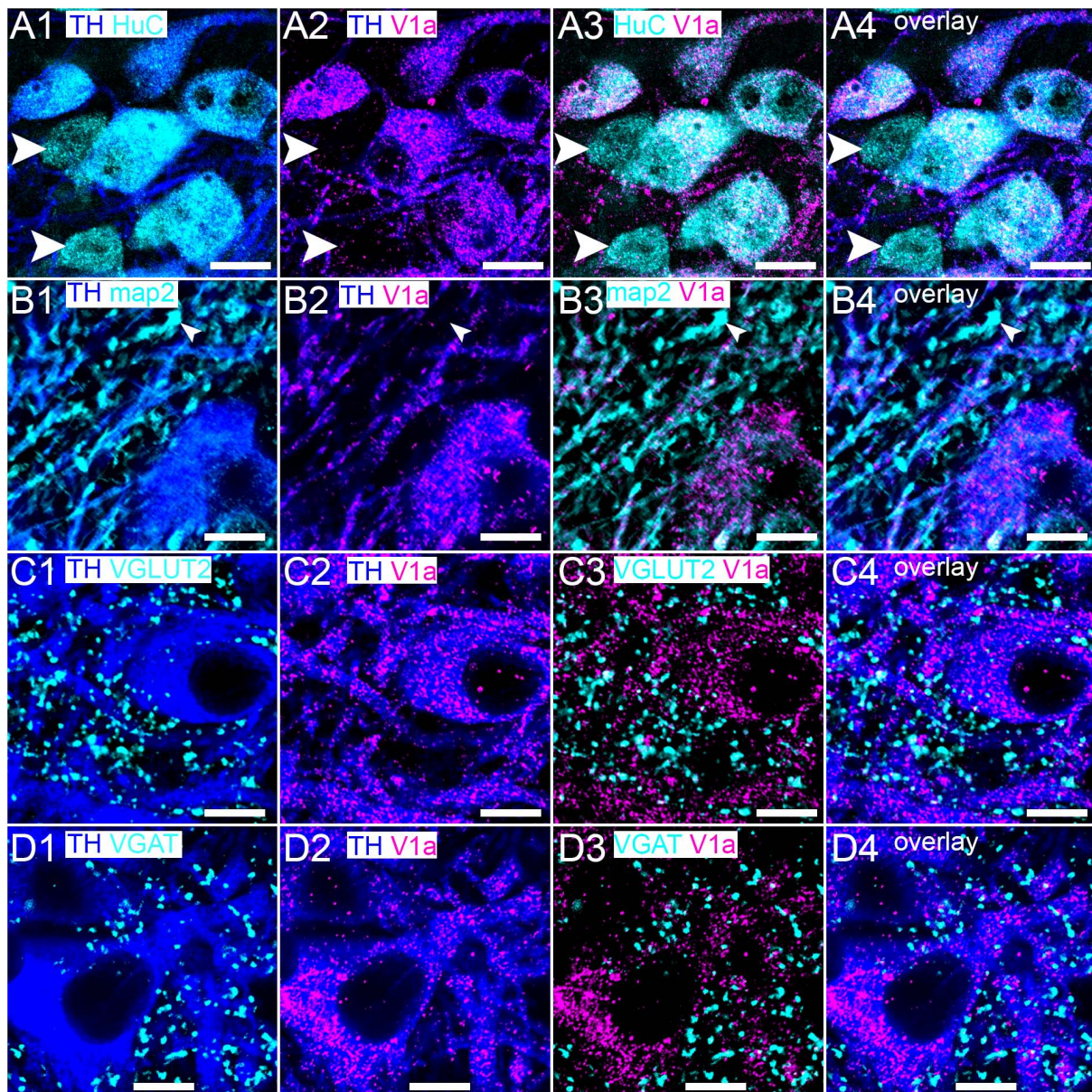


FIGURE 4 | Within the LC, the V1a receptor is expressed exclusively on noradrenergic neurons. **(A1)** Shows immunoreactivity for TH (blue) and HuC (cyan), with the arrowheads highlighting non-noradrenergic neurons of the LC. **(A2)** Shows, in the same field of view, immunoreactivity for TH (blue) and V1a receptor (magenta), confirming that its expression, within the LC, is restricted to noradrenergic neurons and **(A3)** is not located on non-noradrenergic neurons (arrowheads). **(A4)** Is an overlay of **(A1–A3)**. **(B1)** Shows immunoreactivity for TH (blue) and MAP2 (cyan) with the arrowhead highlighting a non-noradrenergic dendritic profile. **(B2)** shows, in the same field of view, immunoreactivity for TH (blue) and V1a receptor (magenta), which confirms V1a expression on noradrenergic profiles and **(B3)** not on non-noradrenergic profiles (arrowhead). **(B4)** Is an overlay of **(B1–B3)**. **(C)** and **(D)** show the association of V1a immunoreactivity with VGLUT2 and VGAT labeling respectively. Scale bars **(A)** 15 μm ; **(B–D)** 10 μm .

appearing mutually exclusive (**Figure 8A**). There was no detectable association between profiles immunoreactive for AVP and enkephalin (**Figure 8B**), orexin A (**Figure 8C**), and CRH (**Figure 8D**). An obvious caveat is that whilst AVP and these other neuropeptides may be contained in the same axons, they may not necessarily be located within the same regions of the axon, thus precluding the confirmation of their co-expression using colocalization analysis. Nevertheless, the data suggests

that AVP-containing afferents could represent a distinct axonal pathway within the LC.

Acute Stress Engages the LC-AVP System

A key contribution of the LC to brain function is the modulation of behavior that allows for adaptation to psychosocial stress

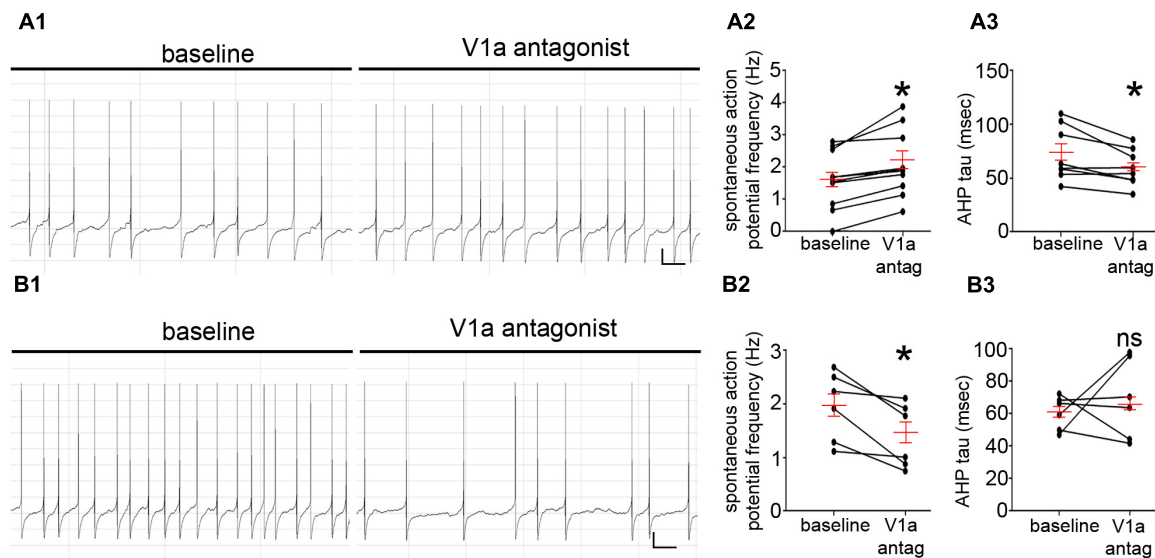


FIGURE 5 | V1a receptor modulation directly alters LC noradrenergic neuronal activity. **(A1)** Representative traces of the spontaneous firing patterns of an LC neuron before and after the application of the V1a receptor antagonist [d(CH₂)51, Tyr(Me)2, Arg8]-Vasopressin, 30 nM, from a cohort of neurons that responded with a significant increase in the frequency of spontaneous action potentials. **(A2)** Quantification of the spontaneous firing rates (Hz) of LC neurons before and after the application of the V1a receptor antagonist. **(A3)** Quantification of the afterhyperpolarization time constant (msec) of LC neurons before and after the application of the V1a receptor antagonist. **(B1)** Representative traces of the spontaneous firing patterns of an LC neuron before and after the application of the V1a receptor antagonist, from a cohort of neurons that responded with a significant decrease in the frequency of spontaneous action potentials. **(B2)** Quantification of the spontaneous firing rates (Hz) of LC neurons before and after the application of the V1a receptor antagonist. **(B3)** Quantification of the afterhyperpolarization time constant (msec) of LC neurons before and after the application of the V1a receptor antagonist. In the graphs, the dots represent the values for individual cells, the long red bars represents the mean for all cells within that group, and the short red bars represent the SEM. * $p < 0.05$, paired Student's *t*-test. Scale bars **(A1,B1)** horizontal bar 1 s, vertical bar 10 mV.

(Valentino and Van Bockstaele, 2008). The neurohormone corticotrophin releasing hormone (CRH) (Vale et al., 1981), released from afferents originating from the amygdala (Van Bockstaele et al., 2001), is the primary driver of the increased activity of LC neurons that underlies this behavioral response (Valentino et al., 1983; McCall et al., 2015). However, AVP is also released, together with CRH, from the hypothalamus, as part of the hypothalamic-pituitary-adrenal stress axis (O'Connor et al., 2000). Given the evidence that both AVP and CRH are contained in afferents that target LC neurons and both have now been shown to alter LC neuronal activity (this study for AVP), we explored whether acute stress engages the LC-AVP system following exposure to 1 h of restraint stress (Buynitsky and Mostofsky, 2009).

The intensity and pattern of V1a receptor immunoreactivity was indistinguishable in tissue from control and stress animals, processed and imaged under identical conditions (**Figure 9A**). Semi-quantitative analysis of the density (number of clusters per area) of V1a receptor immunoreactive clusters revealed no significant differences between control and stress subjects (control: 5782 ± 409 clusters per $100 \mu\text{m}^2$ versus stress: 4844 ± 753 clusters per $100 \mu\text{m}^2$; $p = 0.3054$, unpaired Student's *t*-test, $N = 5$ animals).

In contrast, we detected a significant increase in the number of V1b receptor immunoreactive clusters, especially within cytoplasmic domains (**Figure 9B**). Semi-quantitative analysis of the density (number of clusters per area) of V1b receptor

immunoreactive clusters revealed a significant increase in tissue in stress subjects (control: 945 ± 173 clusters per $100 \mu\text{m}^2$ versus stress: 4462 ± 307 clusters per $100 \mu\text{m}^2$; $p < 0.0001$ unpaired Student's *t*-test, $N = 5$ animals). This dramatic stress-induced alteration in V1b receptor immunoreactivity was accompanied by a change in the AVP immunoreactivity pattern. In tissue from control animals, AVP immunoreactivity presented as a mixture of varicose plexuses and individual clusters throughout the LC (**Figures 9C1–C3**). However, in tissue from stress subjects, processed and imaged under conditions identical to control, there was a noticeable decrease in the intensity of AVP immunoreactivity within the LC, with a relative lack of varicose plexuses (**Figures 9C4–C6**). Because AVP signal presented as a mixture of varicose plexuses and individual clusters, we performed the semi-quantitative analysis using fluorescence intensity which will incorporate both patterns of signal. Stress induced a moderate, though statistically significant decrease in the AVP fluorescence intensity [control: 35 ± 2 arbitrary units (AU) versus stress: 27 ± 2 AU, $p = 0.04$, unpaired Student's *t*-test, $N = 5$ animals]. This suggests that stress engages the LC AVP-receptor system.

DISCUSSION

The current study provides the first demonstration of the association of AVP-immunopositive axons with identified

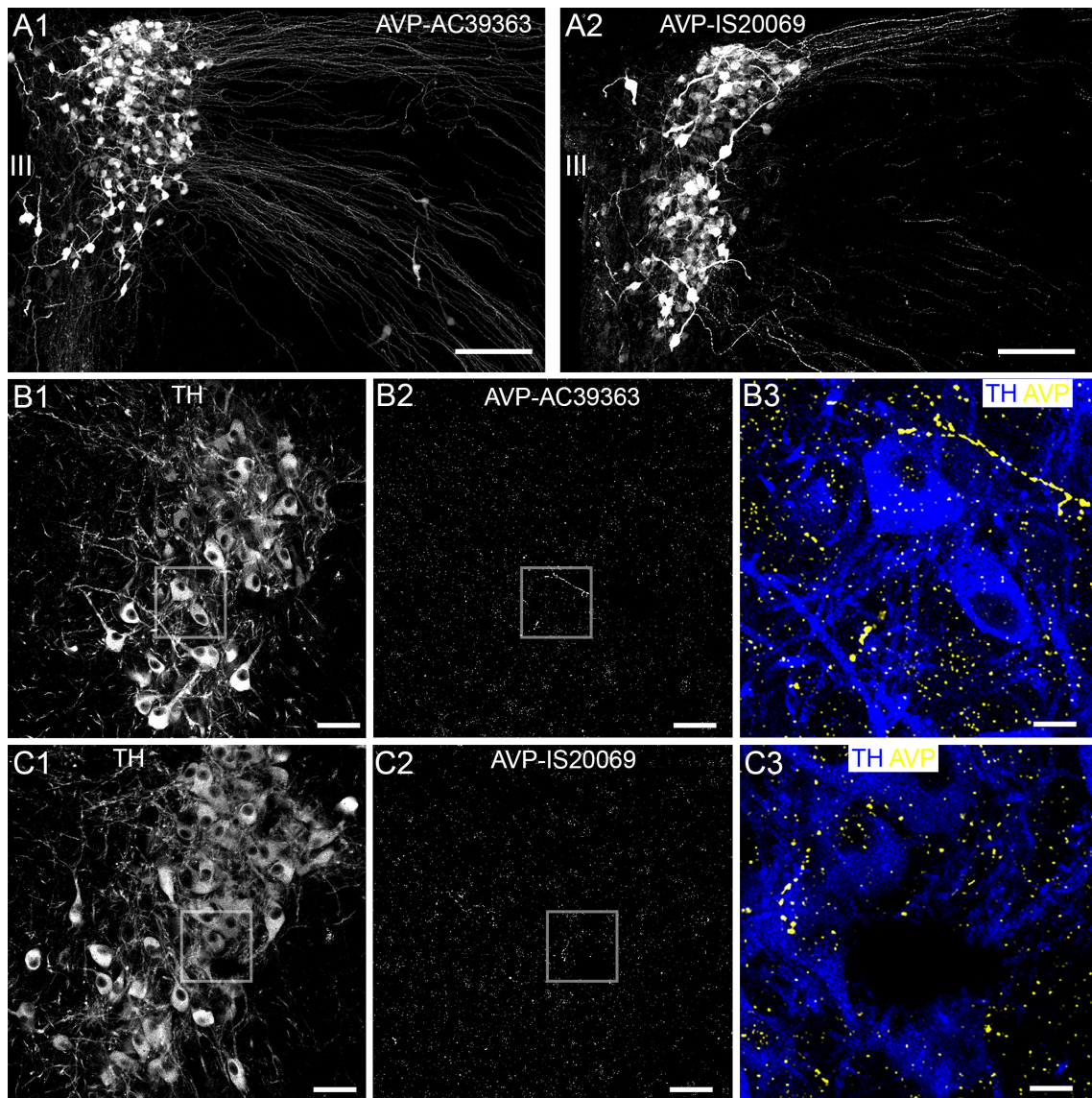


FIGURE 6 | Confirmation of AVP immunoreactivity, in the hypothalamus and LC. **(A1,A2)** Show the comparative immunoreactivity patterns of two different AVP antibodies, in the paraventricular nucleus of the hypothalamus. AC39363 is the antibody obtained from Abcam and IS20069 is the antibody obtained from ImmunoStar, with further details provided in **Supplementary Table S1**. Both antibodies replicate the characteristic pattern of AVP expression expected in this brain region (Zhang and Hernandez, 2013). **(B,C)** Show the comparative labeling patterns of these AVP antibodies in the LC, when used under conditions identical to those for hypothalamic tissue. **(B3,C3)** Shows that within the LC, AVP immunoreactivity presented as a combination of varicose plexuses and individual clusters contacting somatodendritic surfaces. Scale bars **(A)** 100 μm; **(B1,B2,C1,C2)** 50 μm; **(B3,C3)** 10 μm. III, third ventricle.

noradrenergic and non-noradrenergic neurons of the LC. These AVP-containing axons showed only a sparse association with another neuropeptide afferent system within this brain region, namely substance P. This suggests that AVP input to the LC represents a pathway distinct to the myriad of neuropeptide systems that modulate information transfer to this nucleus. Furthermore, we identify the specific AVP receptors within the LC, by localizing the V1a and V1b receptors to the somatodendritic surfaces of these different LC cell types. The modulation of both receptor subtypes induced heterogeneity in the excitability of LC noradrenergic

neurons, manifesting as either an increase or decrease in their spontaneous FR. Given the strong association between LC FR and the level of NA release, this suggests that this individual neurohormone is capable of both increasing and diminishing CNS NA levels. Finally, we provide evidence that exposing mice to a form of stress which generally induces adaptive behavioral and physiological responses, results in molecular plasticity in the AVP-receptor system. This potentially identifies AVP as an integral component of the molecular machinery utilized in LC-mediated homeostatic responses.

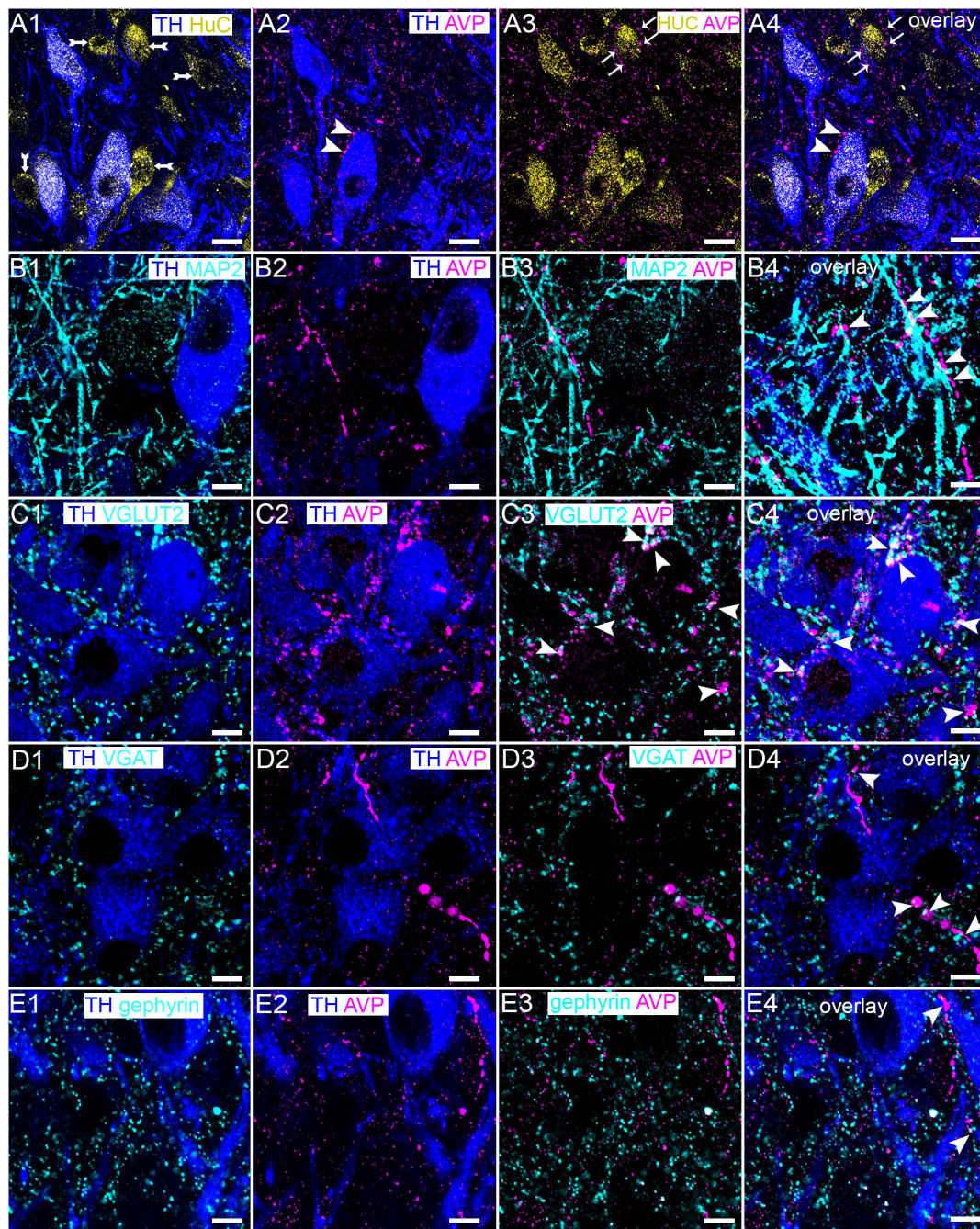


FIGURE 7 | Native AVP-containing axonal profiles contact both noradrenergic and non-noradrenergic LC neurons in close proximity to glutamatergic and GABAergic synapses. **(A1)** Shows immunoreactivity for TH (blue) and HuC (yellow), indicating the distribution of noradrenergic and non-noradrenergic neurons (double arrow) **(A2)** shows, in the same field of view, immunoreactivity for TH (blue) and AVP (magenta) immunoreactive profiles contacting LC noradrenergic neurons (arrowhead). **(A3)** Shows, in the same field of view, immunoreactivity for AVP (magenta) and HuC (yellow), confirming the association of AVP with LC non-noradrenergic neurons as well (arrows). **(A4)** Is an overlay of **(A1–A3)**. **(B1)** Shows immunoreactivity for TH (blue), and MAP2 (cyan). **(B2)** Shows, in the same field of view, immunoreactivity for TH (blue) and AVP (magenta). **(B3)** Shows, in the same field of view, the association of immunoreactivity for AVP (magenta) with MAP2 (cyan). Note the close apposition of the AVP-immunopositive varicosity with the dendritic profile (arrowheads). **(B4)** Is an overlay of **(B1–B3)**. **(C1)** Shows immunoreactivity for TH (blue), and VGLUT2 (cyan). **(C2)** Shows, in the same field of view, immunoreactivity for TH (blue) and AVP (magenta). **(C3)** Shows, in the same field of view, the strong association of immunoreactivity for AVP (magenta) with VGLUT2 (cyan) (arrowheads). **(C4)** Is an overlay of **(C1–C3)**. **(D1)** Shows immunoreactivity for TH (blue), and VGAT (cyan). **(D2)** Shows, in the same field of view, immunoreactivity for TH (blue) and AVP (magenta). **(D3)** Shows, in the same field of view, the association of immunoreactivity for AVP (magenta) with a few VGAT-immunopositive clusters (cyan). **(D4)** Is an overlay of **(D1–D3)**. **(E1)** Shows immunoreactivity for TH (blue), and gephyrin (cyan). **(E2)** Shows, in the same field of view, immunoreactivity for TH (blue) and AVP (magenta). **(E3)** Shows, in the same field of view, the relatively sparse association of immunoreactivity for AVP (magenta) with gephyrin (cyan). **(E4)** Is an overlay of **(E1–E3)**. Scale bars **(A)** 15 μm ; **(B–E)** 10 μm .

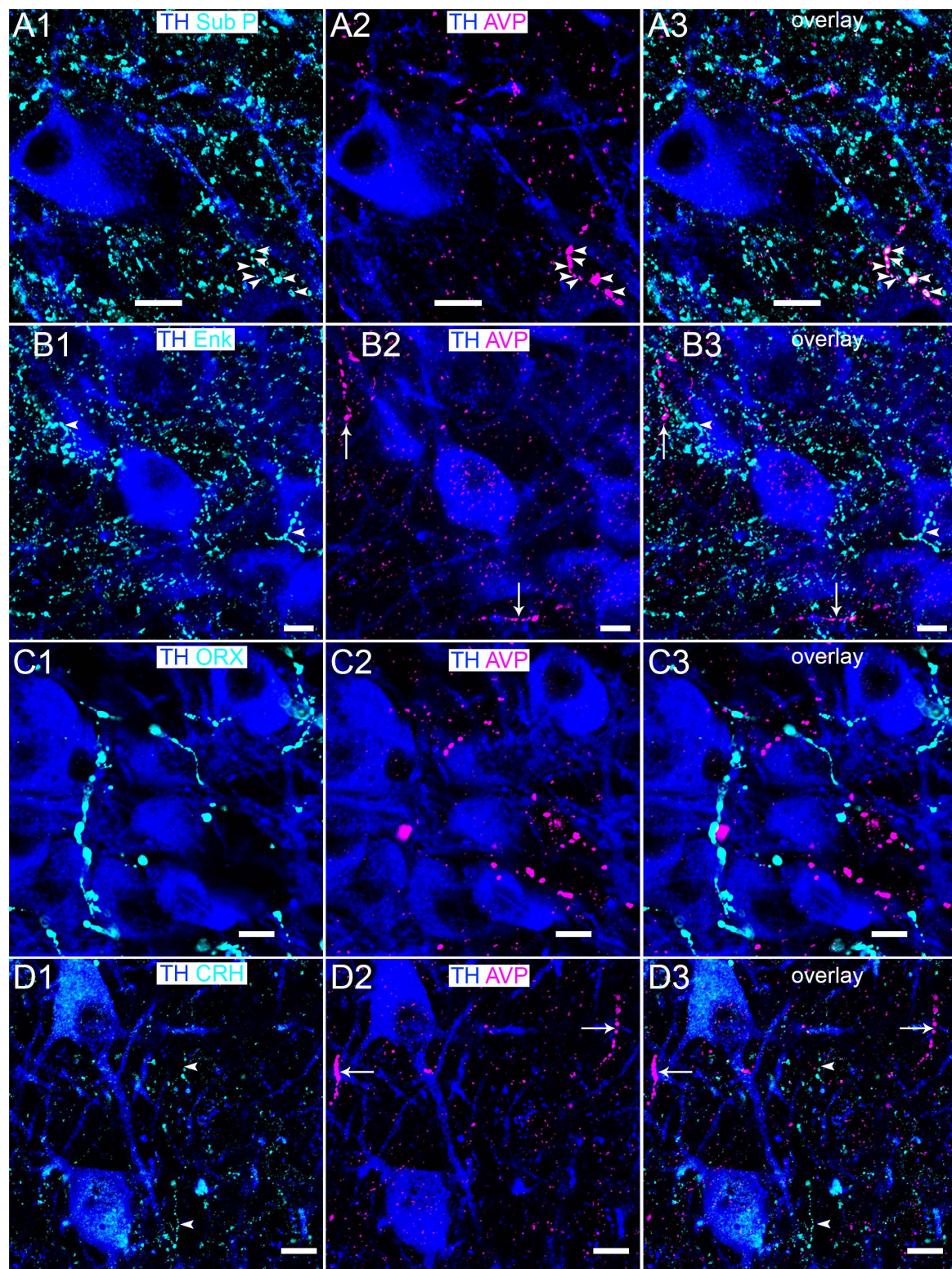


FIGURE 8 | Association of AVP with LC neuromodulatory afferent systems. **(A1)** Immunoreactivity for TH (blue) and substance P (Sub P) (cyan). In the same field of view, **(A2)** immunoreactivity of TH with AVP. **(A3)** Is an overlay of **(A1,A2)** showing isolated instances of colocalization of immunoreactivity for substance P and AVP (arrowheads). Immunoreactivity for TH with **(B1)** enkephalin (ENK), **(C1)** orexin A (ORX) and **(D1)** CRH, with arrowheads highlighting a subset of varicosities in **(B1,D1)**. **(B2,C2,D2)** Show immunoreactivity of TH with AVP in the corresponding fields of view, with AVP immunopositive varicosities highlighted by arrows in **(B2,D2)**. **(B3,C3,D3)** Are overlays of **(B,C,D1,D2)** showing the lack of colocalization of AVP signal with that of the corresponding neuropeptides. Scale bars 10 μ m.

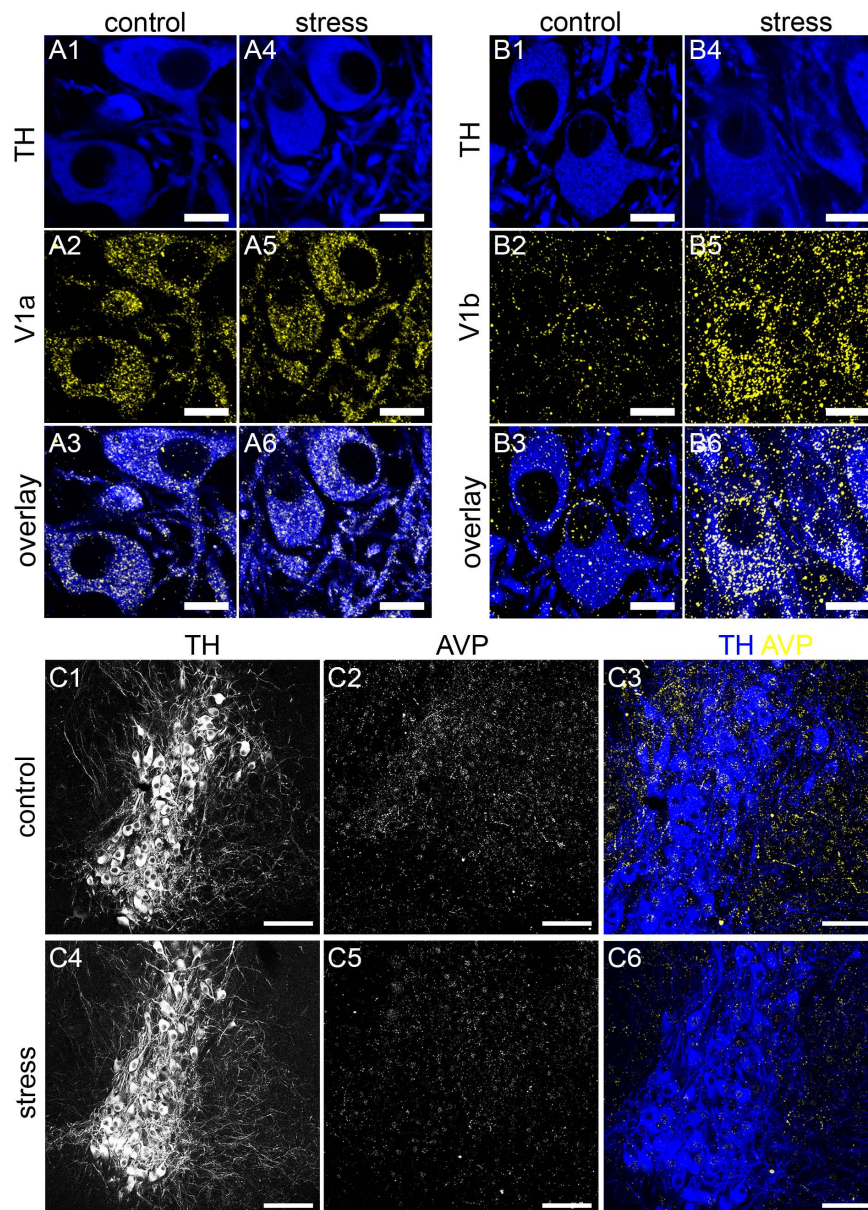


FIGURE 9 | Acute stress engages the AVP-V1a-b system in the LC. **(A1)** Shows TH immunoreactivity in the LC from a control mouse. **(A2)** Shows, in the same field of view, immunoreactivity for the V1a receptor. **(A3)** Is an overlay of **(A1,A2)**. **(A4)** Shows TH immunoreactivity in the LC from tissue of a mouse exposed to 1 h of restraint stress and killed an hour later, processed and imaged under conditions identical to control subjects. **(A5)** Shows, in the same field of view, immunoreactivity for V1a, with no discernible difference in labeling pattern and intensity evident between stress and control samples. **(A6)** Is an overlay of **(A4,A5)**. **(B1)** Shows TH immunoreactivity in the LC from a control mouse. **(B2)** Shows, in the same field of view, immunoreactivity for the V1b receptor. **(B3)** Is an overlay of **(B1,B2)**. **(B4)** Shows TH immunoreactivity in the LC from tissue of a mouse exposed to 1 h of restraint stress. **(B5)** Shows, the same field of view, immunoreactivity for V1b. A dramatic stress-induced increase in the intensity of V1b signal is noticeable, both on cell surfaces but also in cytoplasmic components, suggesting a stress-induced internalization, presumably via prolonged activation. **(B6)** Is an overlay of **(B4,B5)**, which exemplifies the differences between the immunoreactivity patterns in control and stress samples. **(C1)** Shows TH immunoreactivity in the LC from a control mouse. **(C2)** Shows, the same field of view, immunoreactivity for AVP. **(C3)** Is an overlay of **(C1,C2)** with TH and AVP pseudo-colored blue and yellow respectively. **(C4)** Shows TH immunoreactivity in the LC from tissue of a mouse exposed to 1 h of restraint stress and killed an hour later, processed and imaged under conditions to identical control subjects. **(C5)** Shows, the same field of view, immunoreactivity for AVP. A stress-induced decrease in the intensity of AVP signal is noticeable as well as the relative lack of immunoreactive varicosities. This is exemplified in **(C6)**, when compared to **(C3)**. Scale bars **(A,B)** 10 μm ; **(C)** 100 μm .

One of the most intriguing findings of the study is that V1a-b receptor ligands had contrasting effects on the spontaneous firing activity of LC neurons. *Post hoc* neurochemical analyses

confirmed that all recorded neurons were located within the LC and were noradrenergic. There could be a number of reasons why, presumably, the activation of a single receptor

type, on a specific cell type, induces contrasting effects on cellular excitability. Firstly, contrasting downstream receptor signaling cascades could be induced in different populations of LC noradrenergic neurons, following their activation. As receptors coupled to G protein (GPCRs), V1a and V1b receptors conventionally couple to the Gq and phospholipase C (PLC) pathway with the V2 receptor engaging the Gs and adenylyl cyclase (Gs-cAMP) pathway (Koshimizu et al., 2012). However, individual AVP receptors engaging differing secondary messenger cascades is not unprecedented. Indeed, multiple mechanisms have been identified which result in the differential activation of secondary messenger pathways by individual GPCRs. These include receptors adopting different active and inactive conformational states when bound to ligands (Kenakin, 2003), having the ability to homo- or heterodimerise, leading to variations in their pharmacological properties (Park and Palczewski, 2005) and the location of receptors within specialized microdomains of the plasma membrane such as rafts or caveolae (Guzzi et al., 2002). Such versatility in signal transduction has been exemplified by the V1b receptor which has been shown to activate either the IP or cAMP pathways (Jard et al., 1986; Thibonnier et al., 1997; Sabatier et al., 1998). Furthermore, the V1b receptor is capable of simultaneously activating both the Gq/11-inositol phosphate (IP) and Gs-cAMP pathways (Orcel et al., 2009). We are unable to distinguish from our data which of the above variables could contribute to the differences in the effects of desmopressin on the recorded neurons. A fundamental question is whether the directionality of the AVP response depends on the activity or metabolic state of the neuron, or it is a central feature of specific sub-populations of LC neurons. If the former, this could identify a role for AVP driving LC activity toward basal levels following various triggers which elevate excitability, such as stress (discussed below), or those which decrease LC activity, such the release of opioids, thus in keeping with its universal role of a homeostatic regulator. If the latter applies, this could be a mechanism for magnifying the diversity of LC noradrenergic neuron sub-populations. Indeed, the LC has been shown to be composed of genetically diverse noradrenergic neurons which are considered to represent different cell types (Robertson et al., 2013; Plummer et al., 2017). Future high resolution molecular, physiological and behavioral correlative studies are required to address these questions. Irrespective, and given the correlation between LC FR and NA release, these data identify the AVP-V1a-b receptor system as possibly being capable of both enhancing or diminishing NA release within the brain.

Precisely how AVP receptors change the spontaneous FR of LC neurons is unclear. This could be an indirect response to the modulation of local neurotransmitters, given the close association of these receptors with GABA and glutamate synaptic molecular machinery demonstrated in this study, and functional evidence in other brain regions (Raggenbass, 2008; Rood and Beck, 2014). Although we recorded from only noradrenergic neurons of the LC, our immunohistochemical data confirm the presence of V1b receptors in non-noradrenergic LC neurons. These neurons bear the neurochemical hallmarks of inhibitory interneurons (Aston-Jones et al., 2004; Corteen et al., 2011). If so, applied desmopressin could induce the release of their neurotransmitter content

locally, thereby impacting on the excitability of the recorded noradrenergic neuron. Paired recordings between identified interneuron-principal cell pairs would be essential to understand this dynamic of the AVP-LC system.

However, based on the changes in membrane properties induced by desmopressin, AVP could also directly alter LC neuronal excitability. In addition to changes in spontaneous action potential frequency, desmopressin also altered the membrane time constant for the AHP, thus impacting on the time taken for the neuron to repolarise and thus be capable of initiating the next action potential. This effect on the LC inter-spike interval, by other neurohormones such as CRH, has been shown to be modulated by potassium conductances (Jedema and Grace, 2004). Furthermore, CRH, in different cell types, has been shown to engage different secondary messenger pathways (Grammatopoulos et al., 2001), resulting in either the activation or inhibition of specific ion channels (Aldenhoff et al., 1983; Rainnie et al., 1992; Yu and Shinnick-Gallagher, 1998). Finally, desmopressin also significantly altered the action potential amplitude, but only in those cells which exhibited a decreased FR. It is therefore reasonable to speculate that AVP directly alters LC activity via the downstream modulation of ion channels associated with spontaneous FR. However, desmopressin did not alter the input resistance of the entire cell, thus arguing against any potential impact on membrane channel gating. Future studies investigating LC neuronal excitability in AVP receptor subtype-specific knock out mice will hopefully confirm the receptor subtype signaling cascaded in individual LC neurons.

A novel discovery was the changes in the patterns of AVP and V1b receptor immunoreactivity following exposure to acute stress. Importantly, V1a receptor immunoreactivity remained unchanged. An indicator of metabotropic receptor activation is receptor internalization from plasma membranes and incorporation within cytoplasmic compartments. Thus, the dramatic stress-induced internalization of V1b localization suggests engagement of stress signals with this receptor system and a potential pathway mediating the LC stress response. Future functional and behavioral studies are essential to identify the underlying mechanisms. We deliberately chose an acute stress protocol that is likely to engage adaptive or homeostatic pathways throughout the body including the LC. This has been widely demonstrated with the acute exposure to restraint stress used in this study (Buynitsky and Mostofsky, 2009). LC neurons are exquisitely sensitive to both emotional and physiological stressors, responding with an increased FR (Valentino and Van Bockstaele, 2008). The principal mediator of this stress-induced LC excitability is CRH, originating from a variety of brain centers (Valentino et al., 1992). Although AVP release from the hypothalamus coincides with that of CRH and the stress response (Kormos and Gaszner, 2013), its involvement in the LC stress pathways has yet to be documented. However, this would not be surprising, given the overlap of the LC, and AVP in general, in mediating adaptive or homeostatic responses to various psychological and physiological challenges (Valentino and Van Bockstaele, 2008; Koshimizu et al., 2012). If so, this could signal a novel partnership with CRH in regulating LC activity during

times of stress. Precisely how these systems might cooperate is unclear. An important distinction would be their contribution to resting LC FR. CRH antagonists do not alter resting LC FR thus indicating that this aspect of LC physiology is not mediated by the CRH system. In contrast, this study demonstrated that selective V1a-b receptor antagonists, on their own, significantly altered basal LC FR, indicating that endogenous AVP sets the tone of LC activity. Another difference would be the ability of the AVP-V1a-b receptor system to bi-directionally modulate LC activity. This distinguishes AVP-V1a-b system not only from the CRH but other neuropeptide systems that influence LC activity by either selectively increasing or decreasing activity, but never both (Zitnik, 2016). It would be intriguing to explore whether AVP would increase, or decrease, the activity of LC neurons, in a behavioral or physiological state-dependent manner. CRH is called upon during the stress response to elevate LC activity and enhance NA release. However, central to an adaptive or healthy stress system is the appropriate cessation of the stress response once the organism has effectively contended with the challenge. If AVP did work in tandem with CRH in this process, it could provide a counter measure by reversing any increase in LC activity, thereby ensuring effective resetting of basal LC activity. This could provide unique opportunities for V1a-b receptor ligands in psychiatric disorders associated with an impaired stress response and LC dysregulation, such as anxiety and depression (Itoi and Sugimoto, 2010). Indeed, in humans, the dysregulation of brain and CSF AVP levels are associated with a number of anxiety disorders (Neumann and Landgraf, 2012). Furthermore, the pharmacological blockade of either the V1a or V1b receptors showed anxiolytic and antidepressant actions (Koshimizu et al., 2012; Caldwell et al., 2017). The actions of these receptors on such emotional states have been attributed to changes in the functions of a range of brain regions such as the hypothalamus, the bed nucleus of the stria terminalis and amygdala, with the LC largely ignored. The current data suggest that the LC should be considered as a site of action for such agents in altering such psychiatric

symptoms. The use of cell type-specific AVP receptor knock out mice will be instrumental in dissecting the association of specific brain regions and AVP receptor subtypes in these brain functions.

In summary, the study provides a new vista on the central AVP system, by providing the molecular and physiological constructs of this neurohormone, and its associated receptor system, in the mouse LC. The data will serve as the basis to further dissect the contribution of what is conventionally a homeostatic system, to the functioning of a brain region that is integral to mediating adaptive responses to a variety of threats.

AUTHOR CONTRIBUTIONS

JS conceived and led the study. EC-L, LK, MS, and JS designed the experiments. EC-L, LK, MS, TJ, VH, LZ, and JS performed the experiments and analyzed the data. VH, TG, KM, TK, and LZ contributed unique resources. JS wrote the manuscript with all authors approving the final version.

FUNDING

EC-L was funded by the Posgrado en Ciencias Biológicas program of Universidad Nacional Autónoma de México (CVU/Becario: 365662/245546) and a traveling scholarship from the Mexican National Council of Science and Technology Academy of Sciences (CONACYT Becas Mixtas) and grant CONACYT CB-238744 (LZ).

SUPPLEMENTARY MATERIAL

The Supplementary Material for this article can be found online at: <https://www.frontiersin.org/articles/10.3389/fnins.2018.00919/full#supplementary-material>

REFERENCES

- Aldenhoff, J. B., Gruol, D. L., Rivier, J., Vale, W., and Siggins, G. R. (1983). Corticotropin releasing factor decreases postburst hyperpolarizations and excites hippocampal neurons. *Science* 221, 875–877. doi: 10.1126/science.6603658
- Andre, P., D'asciano, P., Ioffe, M., and Pompeiano, O. (1992). Microinjections of vasopressin in the locus coeruleus complex affect posture and vestibulospinal reflexes in decerebrate cats. *Pflugers Arch.* 420, 376–388. doi: 10.1007/BF00374473
- Aston-Jones, G., Zhu, Y., and Card, J. P. (2004). Numerous GABAergic afferents to locus coeruleus in the pericellular dendritic zone: possible interneuronal pool. *J. Neurosci.* 24, 2313–2321. doi: 10.1523/JNEUROSCI.5339-03.2004
- Bankir, L., Bichet, D. G., and Morgenthaler, N. G. (2017). Vasopressin: physiology, assessment and osmosensation. *J. Intern. Med.* 282, 284–297. doi: 10.1111/joim.12645
- Berecek, K. H., Olpe, H. R., and Hofbauer, K. G. (1987). Responsiveness of locus coeruleus neurons in hypertensive rats to vasopressin. *Hypertension* 9, 3110–3113. doi: 10.1161/01.HYP.9.6.Pt_2.III110
- Buynitsky, T., and Mostofsky, D. I. (2009). Restraint stress in biobehavioral research: Recent developments. *Neurosci. Biobehav. Rev.* 33, 1089–1098. doi: 10.1016/j.neubiorev.2009.05.004
- Caldwell, H. K., Aulino, E. A., Rodriguez, K. M., Witche, S. K., and Yaw, A. M. (2017). Social context, stress, neuropsychiatric disorders, and the vasopressin 1b receptor. *Front. Neurosci.* 11:567. doi: 10.3389/fnins.2017.00567
- Carter, M. E., Yizhar, O., Chikahisa, S., Nguyen, H., Adamantidis, A., Nishino, S., et al. (2010). Tuning arousal with optogenetic modulation of locus coeruleus neurons. *Nat. Neurosci.* 13, 1526–1533. doi: 10.1038/nn.2682
- Cherubini, E., North, R. A., and Williams, J. T. (1988). Synaptic potentials in rat locus coeruleus neurons. *J. Physiol.* 406, 431–442. doi: 10.1113/jphysiol.1988.sp017389
- Corteen, N. L., Cole, T. M., Sarna, A., Sieghart, W., and Swinny, J. D. (2011). Localization of GABA-A receptor alpha subunits on neurochemically distinct cell types in the rat locus coeruleus. *Eur. J. Neurosci.* 34, 250–262. doi: 10.1111/j.1460-9568.2011.07740.x
- Curtis, A. L., Drolet, G., and Valentino, R. J. (1993). Hemodynamic stress activates locus coeruleus neurons of unanesthetized rats. *Brain Res. Bull.* 31, 737–744. doi: 10.1016/0361-9230(93)90150-A

- Dahlstroem, A., and Fuxe, K. (1964). Evidence for the existence of monoamine-containing neurons in the central nervous system. I. demonstration of monoamines in the cell bodies of brain stem neurons. *Acta Physiol. Scand. Suppl.* 232, 1–55.
- Daikoku, R., Kunitake, T., Kato, K., Tanoue, A., Tsujimoto, G., and Kannan, H. (2007). Body water balance and body temperature in vasopressin V1b receptor knockout mice. *Auton. Neurosci.* 136, 58–62. doi: 10.1016/j.autneu.2007.04.002
- Godino, A., Giusti-Paiva, A., Antunes-Rodrigues, J., and Vivas, L. (2005). Neurochemical brain groups activated after an isotonic blood volume expansion in rats. *Neuroscience* 133, 493–505. doi: 10.1016/j.neuroscience.2005.02.035
- Grammatopoulos, D. K., Rande, H. S., Levine, M. A., Kanellopoulou, K. A., and Hillhouse, E. W. (2001). Rat cerebral cortex corticotropin-releasing hormone receptors: evidence for receptor coupling to multiple G-proteins. *J. Neurochem.* 76, 509–519. doi: 10.1046/j.1471-4159.2001.00067.x
- Gunn, B. G., Cunningham, L., Cooper, M. A., Corteen, N. L., Seifi, M., Swinny, J. D., et al. (2013). Dysfunctional astrocytic and synaptic regulation of hypothalamic glutamatergic transmission in a mouse model of early-life adversity: relevance to neurosteroids and programming of the stress response. *J. Neurosci.* 33, 19534–19554. doi: 10.1523/JNEUROSCI.1337-13.2013
- Guyenet, P. G., and Aghajanian, G. K. (1979). ACh, substance P and met-enkephalin in the locus coeruleus: pharmacological evidence for independent sites of action. *Eur. J. Pharmacol.* 53, 319–328. doi: 10.1016/0014-2999(79)90455-2
- Guzzi, F., Zanchetta, D., Cassoni, P., Guzzi, V., Francolini, M., Parenti, M., et al. (2002). Localization of the human oxytocin receptor in caveolin-1 enriched domains turns the receptor-mediated inhibition of cell growth into a proliferative response. *Oncogene* 21, 1658–1667. doi: 10.1038/sj.onc.1205219
- Hagan, J. J., Leslie, R. A., Patel, S., Evans, M. L., Wattam, T. A., Holmes, S., et al. (1999). Orexin A activates locus coeruleus cell firing and increases arousal in the rat. *Proc. Natl. Acad. Sci. U.S.A.* 96, 10911–10916. doi: 10.1073/pnas.96.19.10911
- Herman, J. P., and Tasker, J. G. (2016). Paraventricular hypothalamic mechanisms of chronic stress adaptation. *Front. Endocrinol.* 7:137. doi: 10.3389/fendo.2016.00137
- Horvath, T. L., Peyron, C., Diano, S., Ivanov, A., Aston-Jones, G., Kilduff, T. S., et al. (1999). Hypocretin (orexin) activation and synaptic innervation of the locus coeruleus noradrenergic system. *J. Comp. Neurol.* 415, 145–159. doi: 10.1002/(SICI)1096-9861(19991213)415:2<145::AID-CNE1>3.0.CO;2-2
- Iijima, M., Yoshimizu, T., Shimazaki, T., Tokugawa, K., Fukumoto, K., Kurosu, S., et al. (2014). Antidepressant and anxiolytic profiles of newly synthesized arginine vasopressin V1b receptor antagonists: TASP0233278 and TASP0390325. *Br. J. Pharmacol.* 171, 3511–3525. doi: 10.1111/bph.12699
- Itoi, K., and Sugimoto, N. (2010). The brainstem noradrenergic systems in stress, anxiety and depression. *J. Neuroendocrinol.* 22, 355–361. doi: 10.1111/j.1365-2826.2010.01988.x
- Jard, S., Gaillard, R. C., Guillon, G., Marie, J., Schoenenberg, P., Muller, A. F., et al. (1986). Vasopressin antagonists allow demonstration of a novel type of vasopressin receptor in the rat adenohypophysis. *Mol. Pharmacol.* 30, 171–177.
- Jedema, H. P., and Grace, A. A. (2004). Corticotropin-releasing hormone directly activates noradrenergic neurons of the locus coeruleus recorded in vitro. *J. Neurosci.* 24, 9703–9713. doi: 10.1523/JNEUROSCI.2830-04.2004
- Kenakin, T. (2003). Ligand-selective receptor conformations revisited: the promise and the problem. *Trends Pharmacol. Sci.* 24, 346–354. doi: 10.1016/S0165-6147(03)00167-6
- Kormos, V., and Gaszner, B. (2013). Role of neuropeptides in anxiety, stress, and depression: from animals to humans. *Neuropeptides* 47, 401–419. doi: 10.1016/j.neup.2013.10.014
- Koshimizu, T. A., Nakamura, K., Egashira, N., Hiroyama, M., Nonoguchi, H., and Tanoue, A. (2012). Vasopressin V1a and V1b receptors: from molecules to physiological systems. *Physiol. Rev.* 92, 1813–1864. doi: 10.1152/physrev.00035.2011
- Koshimizu, T. A., Nasa, Y., Tanoue, A., Oikawa, R., Kawahara, Y., Kiyono, Y., et al. (2006). V1a vasopressin receptors maintain normal blood pressure by regulating circulating blood volume and baroreflex sensitivity. *Proc. Natl. Acad. Sci. U.S.A.* 103, 7807–7812. doi: 10.1073/pnas.0600875103
- Lechner, S. M., Curtis, A. L., Brons, R., and Valentino, R. J. (1997). Locus coeruleus activation by colon distention: role of corticotropin-releasing factor and excitatory amino acids. *Brain Res.* 756, 114–124. doi: 10.1016/S0006-8993(97)00116-9
- Lozic, M., Sarenac, O., Murphy, D., and Japundzic-Zigon, N. (2018). Vasopressin, central autonomic control and blood pressure regulation. *Curr. Hypertens. Rep.* 20:11. doi: 10.1007/s11906-018-0811-0
- Maguire, E. P., Macpherson, T., Swinny, J. D., Dixon, C. I., Herd, M. B., Belelli, D., et al. (2014). Tonic inhibition of accumbal spiny neurons by extrasynaptic alpha4betadelta GABAA receptors modulates the actions of psychostimulants. *J. Neurosci.* 34, 823–838. doi: 10.1523/JNEUROSCI.3232-13.2014
- McCall, J. G., Al-Hasani, R., Siuda, E. R., Hong, D. Y., Norris, A. J., Ford, C. P., et al. (2015). CRH engagement of the locus coeruleus noradrenergic system mediates stress-induced anxiety. *Neuron* 87, 605–620. doi: 10.1016/j.neuron.2015.07.002
- Neumann, I. D., and Landgraf, R. (2012). Balance of brain oxytocin and vasopressin: implications for anxiety, depression, and social behaviors. *Trends Neurosci.* 35, 649–659. doi: 10.1016/j.tins.2012.08.004
- O'Connor, T. M., O'halloran, D. J., and Shanahan, F. (2000). The stress response and the hypothalamic-pituitary-adrenal axis: from molecule to melancholia. *QJM* 93, 323–333. doi: 10.1093/qjmed/93.6.323
- Okano, H. J., and Darnell, R. B. (1997). A hierarchy of Hu RNA binding proteins in developing and adult neurons. *J. Neurosci.* 17, 3024–3037. doi: 10.1523/JNEUROSCI.17-09-03024.1997
- Olpe, H. R., Steinmann, M. W., Pozza, M. F., and Haas, H. L. (1987). Comparative investigations on the actions of ACTH1-24, somatostatin, neurotensin, substance P and vasopressin on locus coeruleus neuronal activity in vitro. *Naunyn Schmiedeberg's Arch. Pharmacol.* 336, 434–437. doi: 10.1007/BF00164879
- Orcel, H., Albizu, L., Perkowska, S., Durroux, T., Mendre, C., Ansanay, H., et al. (2009). Differential coupling of the vasopressin V1b receptor through compartmentalization within the plasma membrane. *Mol. Pharmacol.* 75, 637–647. doi: 10.1124/mol.108.049031
- Ostergaard, L., Rudiger, A., Wellmann, S., Gammella, E., Beck-Schimmer, B., Struck, J., et al. (2014). Arginine-vasopressin marker copeptin is a sensitive plasma surrogate of hypoxic exposure. *Hypoxia* 2, 143–151. doi: 10.2147/HP.S57894
- Park, P. S., and Palczewski, K. (2005). Diversifying the repertoire of G protein-coupled receptors through oligomerization. *Proc. Natl. Acad. Sci. U.S.A.* 102, 8793–8794. doi: 10.1073/pnas.0504016102
- Pickel, V. M., Joh, T. H., Reis, D. J., Leeman, S. E., and Miller, R. J. (1979). Electron microscopic localization of substance P and enkephalin in axon terminals related to dendrites of catecholaminergic neurons. *Brain Res.* 160, 387–400. doi: 10.1016/0006-8993(79)91068-0
- Plummer, N. W., Scappini, E. L., Smith, K. G., Tucker, C. J., and Jensen, P. (2017). Two subpopulations of noradrenergic neurons in the locus coeruleus complex distinguished by expression of the dorsal neural tube marker pax7. *Front. Neuroanat.* 11:60. doi: 10.3389/fnana.2017.00060
- Raggenbass, M. (2008). Overview of cellular electrophysiological actions of vasopressin. *Eur. J. Pharmacol.* 583, 243–254. doi: 10.1016/j.ejphar.2007.11.074
- Rainnie, D. G., Fernhout, B. J., and Shinnick-Gallagher, P. (1992). Differential actions of corticotropin releasing factor on basolateral and central amygdaloid neurones, in vitro. *J. Pharmacol. Exp. Ther.* 263, 846–858.
- Rickenbacher, E., Baez, M. A., Hale, L., Leiser, S. C., Zderic, S. A., and Valentino, R. J. (2008). Impact of overactive bladder on the brain: central sequelae of a visceral pathology. *Proc. Natl. Acad. Sci. U.S.A.* 105, 10589–10594. doi: 10.1073/pnas.0800969105
- Robertson, S. D., Plummer, N. W., De Marchena, J., and Jensen, P. (2013). Developmental origins of central norepinephrine neuron diversity. *Nat. Neurosci.* 16, 1016–1023. doi: 10.1038/nn.3458
- Rood, B. D., and Beck, S. G. (2014). Vasopressin indirectly excites dorsal raphe serotonin neurons through activation of the vasopressin1A receptor. *Neuroscience* 260, 205–216. doi: 10.1016/j.neuroscience.2013.12.012
- Rood, B. D., and De Vries, G. J. (2011). Vasopressin innervation of the mouse (Mus musculus) brain and spinal cord. *J. Comp. Neurol.* 519, 2434–2474. doi: 10.1002/cne.22635
- Sabatier, N., Richard, P., and Dayanithi, G. (1998). Activation of multiple intracellular transduction signals by vasopressin in vasopressin-sensitive neurones of the rat supraoptic nucleus. *J. Physiol.* 513(Pt 3), 699–710. doi: 10.1111/j.1469-7793.1998.699ba.x

- Sara, S. J. (2015). Locus Coeruleus in time with the making of memories. *Curr. Opin. Neurobiol.* 35, 87–94. doi: 10.1016/j.conb.2015.07.004
- Schwarz, L. A., and Luo, L. (2015). Organization of the locus coeruleus-norepinephrine system. *Curr. Biol.* 25, R1051–R1056. doi: 10.1016/j.cub.2015.09.039
- Seifi, M., Corteen, N. L., Van Der Want, J. J., Metzger, F., and Swinny, J. D. (2014). Localization of NG2 immunoreactive neuroglia cells in the rat locus coeruleus and their plasticity in response to stress. *Front. Neuroanat.* 8:31. doi: 10.3389/fnana.2014.00031
- Singewald, N., and Philippu, A. (1998). Release of neurotransmitters in the locus coeruleus. *Prog. Neurobiol.* 56, 237–267. doi: 10.1016/S0301-0082(98)00039-2
- Swinny, J. D., O'farrell, E., Bingham, B. C., Piel, D. A., Valentino, R. J., and Beck, S. G. (2010). Neonatal rearing conditions distinctly shape locus coeruleus neuronal activity, dendritic arborization, and sensitivity to corticotrophin-releasing factor. *Int. J. Neuropsychopharmacol.* 13, 515–525. doi: 10.1017/S146114570999037X
- Tanoue, A., Ito, S., Honda, K., Oshikawa, S., Kitagawa, Y., Koshimizu, T. A., et al. (2004). The vasopressin V1b receptor critically regulates hypothalamic-pituitary-adrenal axis activity under both stress and resting conditions. *J. Clin. Invest.* 113, 302–309. doi: 10.1172/JCI200419656
- Thibonnier, M., Coles, P., Thibonnier, A., and Shoham, M. (2002). Molecular pharmacology and modeling of vasopressin receptors. *Prog. Brain Res.* 139, 179–196. doi: 10.1016/S0079-6123(02)39016-2
- Thibonnier, M., Preston, J. A., Dulin, N., Wilkins, P. L., Berti-Mattera, L. N., and Mattera, R. (1997). The human V3 pituitary vasopressin receptor: ligand binding profile and density-dependent signaling pathways. *Endocrinology* 138, 4109–4122. doi: 10.1210/endo.138.10.5432
- Tribollet, E., Arsenijevic, Y., and Barberis, C. (1998). Vasopressin binding sites in the central nervous system: distribution and regulation. *Prog. Brain Res.* 119, 45–55. doi: 10.1016/S0079-6123(08)61561-7
- Usher, M., Cohen, J. D., Servan-Schreiber, D., Rajkowski, J., and Aston-Jones, G. (1999). The role of locus coeruleus in the regulation of cognitive performance. *Science* 283, 549–554. doi: 10.1126/science.283.5401.549
- Vale, W., Spiess, J., Rivier, C., and Rivier, J. (1981). Characterization of a 41-residue ovine hypothalamic peptide that stimulates secretion of corticotropin and beta-endorphin. *Science* 213, 1394–1397. doi: 10.1126/science.6267699
- Valentino, R. J., Foote, S. L., and Aston-Jones, G. (1983). Corticotropin-releasing factor activates noradrenergic neurons of the locus coeruleus. *Brain Res.* 270, 363–367. doi: 10.1016/0006-8993(83)90615-7
- Valentino, R. J., Page, M., Van Bockstaele, E., and Aston-Jones, G. (1992). Corticotropin-releasing factor innervation of the locus coeruleus region: distribution of fibers and sources of input. *Neuroscience* 48, 689–705. doi: 10.1016/0306-4522(92)90412-U
- Valentino, R. J., and Van Bockstaele, E. (2008). Convergent regulation of locus coeruleus activity as an adaptive response to stress. *Eur. J. Pharmacol.* 583, 194–203. doi: 10.1016/j.ejphar.2007.11.062
- Valentino, R. J., and Wehby, R. G. (1989). Locus coeruleus discharge characteristics of morphine-dependent rats: effects of naltrexone. *Brain Res.* 488, 126–134. doi: 10.1016/0006-8993(89)90701-4
- Van Bockstaele, E. J., Bajic, D., Proudfit, H., and Valentino, R. J. (2001). Topographic architecture of stress-related pathways targeting the noradrenergic locus coeruleus. *Physiol. Behav.* 73, 273–283. doi: 10.1016/S0031-9384(01)00448-6
- Van Bockstaele, E. J., Branchereau, P., and Pickel, V. M. (1995). Morphologically heterogeneous met-enkephalin terminals form synapses with tyrosine hydroxylase-containing dendrites in the rat nucleus locus coeruleus. *J. Comp. Neurol.* 363, 423–438. doi: 10.1002/cne.903630307
- Van Bockstaele, E. J., Colago, E. E., and Valentino, R. J. (1996). Corticotropin-releasing factor-containing axon terminals synapse onto catecholamine dendrites and may presynaptically modulate other afferents in the rostral pole of the nucleus locus coeruleus in the rat brain. *J. Comp. Neurol.* 364, 523–534. doi: 10.1002/(SICI)1096-9861(19960115)364:3<523::AID-CNE10>3.0.CO;2-Q
- Williams, J. T., Bobker, D. H., and Harris, G. C. (1991). Synaptic potentials in locus coeruleus neurons in brain slices. *Prog. Brain Res.* 88, 167–172. doi: 10.1016/S0079-6123(08)63806-6
- Wu, N., Shang, S., and Su, Y. (2015). The arginine vasopressin V1b receptor gene and prosociality: mediation role of emotional empathy. *Psych J.* 4, 160–165. doi: 10.1002/pchj.102
- Young, W. S., Li, J., Wersinger, S. R., and Palkovits, M. (2006). The vasopressin 1b receptor is prominent in the hippocampal area CA2 where it is unaffected by restraint stress or adrenalectomy. *Neuroscience* 143, 1031–1039. doi: 10.1016/j.neuroscience.2006.08.040
- Yu, B., and Shinnick-Gallagher, P. (1998). Corticotropin-releasing factor increases dihydropyridine- and neurotoxin-resistant calcium currents in neurons of the central amygdala. *J. Pharmacol. Exp. Ther.* 284, 170–179.
- Zhang, L., and Hernandez, V. S. (2013). Synaptic innervation to rat hippocampus by vasopressin-immuno-positive fibres from the hypothalamic supraoptic and paraventricular nuclei. *Neuroscience* 228, 139–162. doi: 10.1016/j.neuroscience.2012.10.010
- Zitnik, G. A. (2016). Control of arousal through neuropeptide afferents of the locus coeruleus. *Brain Res.* 1641, 338–350. doi: 10.1016/j.brainres.2015.12.010

Conflict of Interest Statement: The authors declare that the research was conducted in the absence of any commercial or financial relationships that could be construed as a potential conflict of interest.

Copyright © 2018 Campos-Lira, Kelly, Seifi, Jackson, Giesecke, Mutig, Koshimizu, Hernandez, Zhang and Swinny. This is an open-access article distributed under the terms of the Creative Commons Attribution License (CC BY). The use, distribution or reproduction in other forums is permitted, provided the original author(s) and the copyright owner(s) are credited and that the original publication in this journal is cited, in accordance with accepted academic practice. No use, distribution or reproduction is permitted which does not comply with these terms.



Involvement of Vasopressin in the Pathogenesis of Pulmonary Tuberculosis: A New Therapeutic Target?

Mario Zetter¹, Jorge Barrios-Payán¹, Dulce Mata-Espinosa¹, Brenda Marquina-Castillo¹, Andrés Quintanar-Stephano² and Rogelio Hernández-Pando^{1*}

¹ Experimental Pathology Section, Department of Pathology, Instituto Nacional de Ciencias Médicas y Nutrición Salvador Zubirán, Mexico City, Mexico, ² Departamento de Fisiología y Farmacología, Centro de Ciencias Básicas, Universidad Autónoma de Aguascalientes, Aguascalientes, Mexico

OPEN ACCESS

Edited by:

David Vaudry,
Institut National de la Santé et de la
Recherche Médicale
(INSERM), France

Reviewed by:

Selvakumar Subbian,
Public Health Research Institute
(PHRI), United States
Gábor B. Makara,
Hungarian Academy of Sciences
(MTA), Hungary

*Correspondence:

Rogelio Hernández-Pando
rhdezpando@hotmail.com

Specialty section:

This article was submitted to
Neuroendocrine Science,
a section of the journal
Frontiers in Endocrinology

Received: 27 February 2019

Accepted: 16 May 2019

Published: 06 June 2019

Citation:

Zetter M, Barrios-Payán J,
Mata-Espinosa D,
Marquina-Castillo B,
Quintanar-Stephano A and
Hernández-Pando R (2019)
Involvement of Vasopressin in the
Pathogenesis of Pulmonary
Tuberculosis: A New Therapeutic
Target? *Front. Endocrinol.* 10:351.
doi: 10.3389/fendo.2019.00351

Tuberculosis (TB) is a highly complex infectious disease caused by the intracellular pathogen *Mycobacterium tuberculosis* (Mtb). It is characterized by chronic granulomatous inflammation of the lung and systemic immune-neuroendocrine responses that have been associated with pathophysiology and disease outcome. Vasopressin (VP), a neurohypophysial hormone with immunomodulatory effects, is abnormally high in plasma of some patients with pulmonary TB, and is apparently produced ectopically. In this study, a BALB/c mouse model of progressive pulmonary TB was used to determine whether VP may play a role in TB pathophysiology. Our results show that VP gene is expressed in the lung since early infection, increasing as the infection progressed, and localized mainly in macrophages, which are key cells in mycobacterial elimination. Pharmacologic manipulation using agonist and antagonist compounds showed that high and sustained stimulation of VPR resulted in increased bacillary burdens and fibrosis at lungs, while blockade of VP receptors reduced bacterial loads. Accordingly, treatment of infected alveolar macrophages with VP in cell cultures resulted in high numbers of intracellular Mtb and impaired cytokine production. Thus, we show that VP is ectopically produced in the tuberculous lungs, with macrophages being its most possible target cell. Further, it seems that chronic vasopressinergic stimulation during active late disease causes anti-inflammatory and tissue reparative effects, which could be deleterious while its pharmacologic suppression reactivates protective immunity and contributes to shorten conventional chemotherapy, which could be a new possible form of immune-endocrine therapy.

Keywords: vasopressin, lung, tuberculosis, immunopathology, fibrosis, therapy

INTRODUCTION

Tuberculosis (TB) is the leading cause of death by a single infectious agent worldwide (1). It is caused by the intracellular bacillus *Mycobacterium tuberculosis* (Mtb) that affects the lungs mainly and is characterized by chronic and excessive inflammation, in which innate and adaptive immune responses are profoundly affected (2, 3). Infection starts through inhalation of saliva droplets with

mycobacteria that reaches alveoli and is then engulfed by alveolar macrophages. Macrophages are key cells in bacilli elimination through different mechanisms (3). Nevertheless, Mtb has evolved several mechanisms to avoid immune responses, and eventually, phagocytic cells become incapable of bacilli clearance (4). Mycobacterial antigens are then processed by dendritic cells and presented to T lymphocytes in regional lymph nodes, and so, a type IV (delayed) hypersensitivity response is generated. Lymphocytes migrate to the lung and, together with fibroblasts, surround infected macrophages and form containment structures known as granulomas, which are the histopathological hallmark of TB (5). Thus, complex interactions between bacterium and host cells occur, determining the outcome of infection. In early stages of active infection, Th1 cellular immune responses are protective, as interferon gamma (IFN γ) and interleukin 12 (IL-12) induce macrophage activation, allowing bacterial growth control; nevertheless, during late active disease, extensive inflammation leads to a shift toward a Th-2 immune response in which IL-4, IL-10, and transforming growth factor- β (TGF- β) induce a local anti-inflammatory and immunosuppressive milieu resulting in poor containment of infection and progression of tissue damage, necrosis, and fibrosis, driving host to death (6). Besides these immunologic features, an intense neuroendocrine response during pulmonary mycobacterial infection creates a complex network of cytokines, hormones, and neurotransmitters that contribute to the outcome of TB pathogenesis (7, 8).

During pulmonary TB, different hormonal and neuroendocrine pathways are dysregulated, modifying the immune response to Mtb and influencing the outcome of infection. Neuroendocrine dysfunction and hormonal resistance have been found during human and experimental pulmonary TB (9). Further, the hypothalamus–pituitary–adrenal (HPA) axis seems to be chronically activated, a situation that worsens immunopathology, allowing disease progression (10). The hypothalamus is indeed a central anatomical area in which neuroimmune responses are integrated. Frequently, it is also affected by peripheral inflammation, and noteworthy, after intense inflammatory stress such as caused by Mtb.

The inappropriate production of VP during TB has been extensively reported; in fact, evidence of altered water metabolism was observed more than half a century ago (11). Furthermore, an “antidiuretic principle” was found in lungs of patients with active pulmonary TB that appears to be independent from the hypothalamus (12, 13), suggesting a direct involvement of the vasopressinergic system (VS) in the pathophysiology of TB.

Vasopressin (VP) is a well-evolutionary-conserved cyclic peptide conformed by nine amino acid residues, produced physiologically in parvocellular and magnocellular neurons in the paraventricular and supraoptic nucleus of the hypothalamus. It is synthesized as a long precursor molecule (Neurophysin II–VP–copeptin) (14), which is cleaved by endoproteases and released to median eminence and general circulatory system as a response of different central and peripheral stressors including hypovolemia, hyperosmolarity, and dehydration (15–18). Furthermore,

it has been shown that a VP is released as a response to peripheral inflammation (19, 20) and that this response could result deleterious in different immune-mediated diseases. VP exerts biological effects via at least three G-protein-coupled receptors named V1a, V1b, and V2, which are ubiquitously distributed (21).

Immune modulatory effects of VP are required early during monocyte/lymphoid ontogeny, and it is necessary to homeostatic lymphoid and myeloid development, as seemed in VP-deficient rats (Brattleboro strain), which present subtle but basal immunodeficiency, particularly in macrophage function (22, 23). In the context of inflammatory challenges, vasopressinergic activity is required during early and late stages, as VP coactivates the HPA axis among corticotrophin-releasing factors (CRFs), inducing cortisol production (24, 25). Conversely, in chronic inflammation, VP appears to be the main cortisol secretagogue (26, 27). Besides, in endothelial cells, VP regulates the expression of chemokines responsible for leukocyte migration and modulates the production of inflammatory cytokines by fibroblasts and macrophages (28–30). Adaptive immunity is also influenced by VP as it replaces IL-2 requirement of T lymphocytes for cytokine production and acts like a mitogen (31–33). Basal vasopressinergic *tone* is required for antibody production while it down-regulates the expression of B cell receptor (34, 35). Immunomodulatory effects of VP are dose and time dependent and differ between organs and tissues. In the urinary tract, vasopressinergic activity results in an epithelial milieu that impairs immune response against pathogenic bacteria (36). Further, in lungs, it has been reported that VP inhibits the translocation of nuclear factor kappa B (NF- κ B), resulting in a decreased IL-6 production and reduced pulmonary inflammation in response to lipopolysaccharide (LPS) (37). VP is a pleiotropic molecule that participates in the maintenance of homeostasis, but also seems to contribute to the establishment of certain diseases characterized by excessive inflammation and tissue remodeling such as cancer and autoimmunity and probably in chronic infections like TB. Nevertheless, this last point has not been studied in detail.

Thus, the aim of this study was to determine the role of the VS in Mtb infection. Using a model of progressive pulmonary TB in BALB/c mice, the kinetics of gene expression and production of VP in the lungs during mycobacterial infection was determined. To study the VP contribution in the pathogenesis of the disease, infected mice were treated with VP agonist and antagonist during the early and late phase of the disease and cell culture bacterial killing assays were made.

MATERIALS AND METHODS

Ethics Statements

All the animal work was done according to the guidelines of the Mexican law NOM 061-Z00-1999 and approved by the Internal Committee for the Care and Use of Laboratory Animals (CICUAL) of the National Institute of Medical Sciences and Nutrition in México (Protocol number PAT-1861-16/20).

Experimental Model of Progressive Pulmonary TB in BALB/c Mice

The experimental model of progressive pulmonary Tb has been described previously (6). Briefly, the *M. tuberculosis* reference strain H37Rv (ATCC No. 25618) was grown in Middlebrook 7H9 broth (DIFCO) supplemented with 0.2% glycerol, 10% OADC enrichment, and 0.02% Tween-80 and maintained at 37°C in agitation. Mid log-phase cultures were used for all the experiments. Mycobacteria were counted and stored at –80°C until use. Bacterial aliquots were thawed and pulse-sonicated to remove clumps. For the infection, male BALB/c mice ($n = 36$), 8 weeks old and weighing 21–23 g, were anesthetized in gas chamber using Sevoflurane and infected intratracheally with 2.5×10^5 live bacilli using a cannula inside a biosafety level III cabinet. Mice were maintained in vertical position until spontaneous recovery and maintained in groups of five in cages fitted with microisolators connected to negative pressure in animal biosafety level III facilities. Groups of five animals were euthanized inside a cabinet of biosecurity level III at 1, 3, 7, 14, 21, 28, and 60 days post-infection by exsanguination under anesthesia with 210 mg/kg of intraperitoneal pentobarbital. Three left lungs per time were perfused with absolute ethanol, fixed, and prepared for histopathological studies. After eliminating hilar lymph nodes and thymic tissues, seven lungs were frozen and kept to –80°C for bacilli loads determination and gene expression studies in two separated experiments. Animals were monitored daily and humanely euthanized under pentobarbital anesthesia if respiratory insufficiency, accentuated cachexia, or total immobilization was noted.

Preparation of Lung Tissue for Morphological and Immunohistochemical Analysis

Lungs of infected mice were perfused with absolute ethanol by endotracheal route and fixed for 24 h and then embedded in paraffin blocks. Sections of 4 μ m were obtained with a microtome, mounted on glass slides, deparaffinized, and stained with hematoxylin and eosin or with Masson's trichrome staining method. For quantification and morphometric analysis, three different mouse lungs per time point were evaluated. Pneumonic areas were measured with a histology automated system (Leica Microsystems), and then the percentage of affected area in microns was reported from two different experiments. For immunohistochemistry, lung tissues were sectioned and mounted on glass slides and then deparaffinized. Slides were first blocked for unspecific activity of peroxidase with methanol peroxide 3% for 1 h. For VP tissue detection, a rabbit anti-mouse polyclonal antibody (Genetex, USA) was used at a concentration of 1:100, incubated overnight in agitation, followed by incubation with secondary anti-rabbit IgG labeled with peroxidase. For TGF- β immunostaining, a rabbit anti-mouse polyclonal antibody directed to TGF- β 1 isoform was used at a final concentration of 1:250. In both cases, bound antibodies were detected with diaminobenzidine and counterstained with hematoxylin.

Gene Expression Kinetics of VP, VPR, and TGF- β in Lung Homogenates

The right lungs of three of the euthanized mice were obtained and stored in 1.5-ml cryotubes, immediately frozen in liquid nitrogen, and maintained at –80°C until processing. For homogenization, lungs were slowly defrosted and zirconium flint beads were added to each tube and lung tissue was homogenized in the FastPrepR-24 (MP Biomedicals). RNA extraction was performed with the RNeasyR Mini kit (Qiagen) following the manufacturer's instructions. The RNA obtained was quantified by spectrophotometry (A260/280), 100 ng of RNA from lung was used for the production of cDNA by retro-transcription following the indications of the Omniscript kit (Qiagen), and later an endpoint PCR was run to amplify the constitutive gene RPLP0 (Ribosomal protein large P0, Gen ID:11837, GenBank, NCBI) and its integrity was analyzed by running at 2% agarose gel stained with SYBR green. Complementary DNA (cDNA) obtained from each sample was analyzed by real-time PCR (qPCR) using the Real-Time PCR system 7500 (Applied Biosystems) and the Quantitech SYBR Green Mastermix kit (Qiagen) with specific primers (Invitrogen) designed with the first-BLAST (ncbi.nlm.nih.gov) for VP, V1aR, and V2R. For absolute quantification, the number of copies of each target gene was normalized to 1 million amplicons of mRNA of the housekeeping gene RPLP0, including the standard curves and a negative control. Cycling conditions used were as follows: initial denaturation at 95°C for 15 min, followed by 40 cycles at 95°C for 20 s, 60°C for 20 s, and 72°C for 34 s. In the case of TGF- β , for relative quantification, the Ct values were determined by 7500 real-time PCR system (Applied Biosystems, Foster City, CA, USA), and the fold change of gene expression was calculated by the $2^{-(\Delta\Delta Ct)}$ method (38). Sequences of primer probes can be found in **Supplementary Table 1**.

Pharmacological Manipulation of Vasopressinergic System

For the pharmacological treatment during early infection, male mice ($n = 60$) were infected as mentioned above and divided into two different groups: (1) saline control group (SS, $n = 30$) and (2) desmopressin (DdAVP, $n = 30$). Treatments were administered twice a day from day 1 post-infection and during the first 2 months. Animals were euthanized in groups of five in each time point (days 3, 7, 14, 21, 28, and 60). Three lungs were perfused and embedded in paraffin, and seven lungs were frozen immediately and stored at –80°C until processing for CFU counting as mentioned above and used for PCR analysis. In another set of experiments (late disease treatment), infected mice ($n = 120$) were divided into four groups: (1) saline control group (SS, $n = 30$), (2) desmopressin (DdAVP, $n = 30$), (3) conivaptan (CVP, $n = 30$), and (4) control vehicle (DMSO 10%) group ($n = 30$). Treatments were administered twice a day for 2 months, starting on day 60 of infection. Groups of 5 mice were euthanized on days 75, 90, and 120 post-infection (days 15, 30, and 60 of treatment). It is important to mention that DdAVP is a selective agonist of V2 receptor with weak affinity for V1a

and V1b receptors, while CVP is a non-peptidic antagonist of V1aR/V2R with weak effects on V1b receptor. Two independent experiments were performed. The dose of DdAVP was 0.75 µg/kg twice a day in a volume of 10 µl (vehicle was 0.9% NaCl solution) administered intramuscularly, which is the necessary dose to restore antidiuresis in neurointermediate-lobectomized animals (39). CVP obtained from BiochemPartner (BCP07817, Shanghai) was diluted in sterile water for injection with DMSO [10%] and administered via intramuscular (1 mg/kg twice a day in a final volume of 10 µl).

As shown later in the Results section, the group of infected mice treated with CVP during the advanced phase of the disease showed a significant decrease in the lung bacillary load, which suggests that the administration of this VP receptor blocker could have synergistic effect when administered in conjunction with conventional antibiotics used in the treatment of TB, with the objective of shortening the treatment. To study this aspect, mice ($n = 120$) on the 60th day of infection were divided into four groups ($n = 15$, each): the first group was a vehicle control (DMSO 10%); the second group received CVP at the same dose mentioned above; a third group (AB) was treated with first-line antibiotics, which are isoniazid (10 mg/kg of weight), rifampicin (10 mg/kg of weight), and pyrazinamide (30 mg/kg of weight), administered every day with an intragastric cannula in a volume of 100 µl; and a fourth group of antibiotic plus conivaptan (AB + CVP, $n = 15$) received the same type of antibiotic therapy plus CVP intramuscularly (1 mg/kg twice a day). All experimental groups were treated for 2 months. Groups of five animals were euthanized on days 15, 30, and 60 post-treatment. The right lungs were used to determine bacillary load and the left lungs were used to analyze the extent of the pneumonic damage by automated morphometry.

Collagen Quantification by Hydroxyproline Assay

To determine the extent of fibrosis during the advanced phase of pulmonary Tb, the amount of hydroxyproline was determined as an indirect measure of the amount of collagen in lung expressed in milligrams per gram of dry tissue. All reagents were obtained from the Hydroxyproline Quantification Kit (Sigma-Aldrich). Briefly, the right lungs of three mice per group treated with DdAVP or controls were dehydrated at 60°C and hydrolyzed with 1 ml of HCl (6N) and incubated at 110°C overnight. Subsequently, the samples were neutralized with NaOH (pH 7) and filtered and 50 µl of sample was diluted in 2 ml of distilled water. Chloramine T was added to each tube (1 ml), mixed, and incubated for 25 min at room temperature. Then, 1 ml of perchloric acid (3.15 M) was added and incubated for 5 min at room temperature. Finally, 1 ml of *p*-dimethylaminobenzaldehyde and ethylene glycol was added. The tubes were placed in a water bath at 60°C for 20 min and then cooled in water for 5 min. Samples were placed and a standard curve was made from a hydroxyproline standard of 10 µg/ml. Each sample was analyzed in triplicate. The absorbance was read at 557 nm in a spectrophotometer. To determine the collagen concentration, the values obtained from hydroxyproline

were multiplied by the dilution factor and then by the constant 7.23.

Mycobacterial Killing Assay in Cell Cultures

Murine Balb/c alveolar macrophages (cell line MH-S, ATCC® CRL-2019) were seeded in 96-well plates (1×10^4 cells per well) in RPMI medium (Caisson Labs, USA, Cat. RPL03) supplemented with 5% fetal bovine serum (Gibco, USA) and pre-stimulated and treated with three different doses: low (10^{-8} M), medium (10^{-7} M), and high (10^{-6} M) doses of DdAVP (Merck, Ger) or CVP (10^{-6} M) for 12 h. The dose of CVP corresponded to the molar higher dose of DdAVP making an equimolar inhibition. Subsequently, cells were infected with Mtb strain H37Rv at an MOI of 1:3 for 1 h. The wells were then washed with RPMI/Amikacin medium to eliminate non-phagocytosed bacteria. Infected cells in wells corresponding to 1 h post-infection time were lysed with 1% SDS and incubated for 10 min, and then 20% bovine serum albumin (BSA) was added to stop reaction. Serial dilutions from an initial volume of 10 µl were made in culture broth (7H9, Middlebrook, USA) and seeded in solid culture medium (7H10). The number of live bacteria was determined by counting colony-forming units (CFUs) as previously described (40). In the 24-h wells, the infected macrophages were supplemented every 12 h with different doses of DdAVP or CVP, and at the end of the experiment, the same procedure of preparation and sowing of bacteria in 7H10 medium was performed. A second experiment was performed in order to study the effects of sustained vasopressinergic stimulus on infected macrophages. 1×10^5 MH-S cells were seeded and infected as mentioned above in 12-well plates, with 1 ml of RPMI medium, and treated with the highest dose of VP and CVP. Culture medium (RPMI) was daily supplemented with VP or CVP at 9:00 h and followed in a kinetic of 72 h. Cells were harvested as described above for CFU count and culture supernatants were collected in 1.5-ml tubes containing 50 µl of protease inhibitor for cytokine detection.

Cytokine Detection

Cytokines IL-6 and TNFα were measured in pools of culture supernatants from control-infected treatment groups and non-infected macrophages employing commercially available ELISA kits according to the manufacturer's instructions (BioLegend Company, CA, USA). Detection limits were 63.0–4,000 pg/ml for IL-6 and 15.6–1,000 pg/ml for TNFα.

Mycobacterial Culture Assays

In order to test the possibility of the effect of AVP directly on mycobacteria, 1×10^5 CFU of *M. tuberculosis* (H37Rv) were seeded on 96-well plates in 200 µl of liquid broth media supplemented with the higher (1×10^6 M) and lower (1×10^{10} M) dose of synthetic AVP (Sigma-Aldrich, Germany) or DdAVP in groups of three for each experimental condition, and incubated in soft helicoidal agitation at 37°C in a CO₂ (3%) atmosphere for a 7-day period. At the end of this experiment, 40 µl of [3-(4,5-dimethylthiazol-2-yl)-5-(3-carboxymethoxyphenyl)-2-(4-sulfophenyl)-2H-tetrazolium, inner salt; MTS] (Cell-titer 96) was added to each experimental well, and the transformation of

the resulting formazan was read 4 h before. This compound is turned enzymatically to formazan by electron transport chain of viable mycobacteria (41). Before the MTS assay, 10 μ l was seeded in solid (7H10) medium and counted on day 21 as mentioned above.

Statistical Analysis

All the statistical analysis was performed using GraphPad Prism Software (version 6.0, La Jolla, USA). The data were analyzed using paired *t*-test, one- and two-tailed ANOVA with Bonferroni correction for multiple comparisons. *P*-values < 0.05 were considered significant.

RESULTS

Local Vasopressinergic Activity During Pulmonary Tb

In our TB murine model, there are two phases, an early phase of approximately 21 days in which the Th1-type response in the lung increases progressively and is predominant at the end of this stage, and the progressive phase that starts at day 28 post-infection in which the Th1 cytokine pattern decreases and the Th2-type response emerges in co-existence with extensive inflammatory infiltrate and progressive pneumonia, as well as an increase in the bacillary loads, which leads the animal to death (6).

Previously, it was reported that during active TB, there is a compound in the lung that has the same antidiuretic activity as VP, which suggested a possible ectopic production (12, 13). We studied this in our pulmonary TB model. In mice, during the early phase of the infection, there is a gradual granuloma formation since day 14 that coincides with a progressive increase in VP gene expression in the lungs (**Figure 1A**). Noteworthy, no VP mRNA was found at the healthy lung. These results well-coincided with an increase in the VP positivity detected by immunohistochemistry on the surface of some pneumocytes and strongly positive in macrophages that were forming part of the granulomas (**Figure 1B**). As the infection progressed, in the pneumonic areas, numerous macrophages with extensive cytoplasm vacuolization (foamy cells) exhibited strong VP immunostaining (**Figure 1C**) in co-existence with the high number of VP transcripts and progressive decrease of both VP receptors determined by qPCR that was pronounced in V2R (**Figures 1D,E**).

Effects of Vasopressinergic Pharmacological Manipulation in the Course of the TB

Due to the above results and the observations described previously on the immunomodulatory effects of VP, we decided to study its possible effects on experimental TB by pharmacological manipulation. To do this, groups of infected mice were treated with the synthetic agonist desmopressin (8-deamino-arginine VP, DdAVP) or the non-peptide antagonist conivaptan hydrochloride (CVP). DdAVP is a potent agonist of the V2 receptors and has a prolonged half-life in comparison with

VP. Treatment with DdAVP during the first month, during the early phase of murine TB, show no effects on histopathology; however, at the end of the infection, a higher number of bacilli was observed in the lungs of these mice in comparison with the controls (**Figure 2A**). This prompted us to study VP effects during the late infection. In the group of mice treated during the progressive phase of the disease, when the Th2 response and the anti-inflammatory and repair phenomena were predominant (from day 60), a significant increase in the bacillary loads (**Figure 2B**) and histologically extensive areas of fibrosis in the pulmonary interstitium was observed in mice treated with DdAVP (**Figure 2C**), which correlated with higher amount of collagen (hydroxyproline) (**Figure 2D**).

Regarding the possible mechanism of the highly fibrotic response produced by DdAVP administration, we considered the possibility that this could be induced indirectly by increased production of TGF- β , a potent fibrogenic and immunosuppressing cytokine related to poor protection against infection. It has been previously reported that VP promotes collagen synthesis and proliferation of fibroblasts through TGF- β , modifying fibrotic responses (42, 43). In this regard, mice treated with DdAVP showed higher TGF- β immunostaining after 60 days of treatment (**Figure 2E**, images), which correlated with relative increase in its gene expression (**Figure 2F**). Thus, it is possible that in advanced TB, VP promotes anti-inflammatory and fibrotic repair by the induction of TGF- β production.

In contrast, in animals treated during the advanced phase of the disease with the competitive non-selective VP antagonist CVP, when the effects of VP agonism were more pronounced, a significant reduction of the bacillary loads was observed (**Figure 3A**). These results prompted us to test a possible synergistic effect of CVP with conventional antibiotics (rifampin, isoniazid, and ethambutol) on animals in the chronic phase of H37Rv mycobacterial infection.

Although TB can be cured with these antibiotics, the treatment extend at least half a year, which frequently provokes therapeutic abandoning, causing relapse and emergence of drug-resistant bacteria. Therefore, it is necessary to shorten the treatment, and one possibility is the combined treatment antibiotics plus an immune-regulatory agent, such as in this case, CVP, blocking V1a and V2R activity. Mice on the 60th day of infection were treated daily with first-line antibiotics (AB) or AB plus CVP for 2 months. In comparison with animals treated only with antibiotics, mice that received the combined treatment showed a significant decrease in bacillary load at the start of treatment (2 weeks) (**Figure 3B**). Furthermore, reduced pneumonic areas were noted when animals were synergistically treated with AB plus CVP (**Figures 3C–G**), suggesting that this treatment may shorten the time of antibiotic therapy and improve clinical manifestations.

VP Inhibits Mycobacterial Clearance by Alveolar Macrophages

The highest VP immunostaining was exhibited by macrophages; hence, the cell line MH-S of murine alveolar macrophages was the most convenient for the *in vitro* experiments, infecting adherent

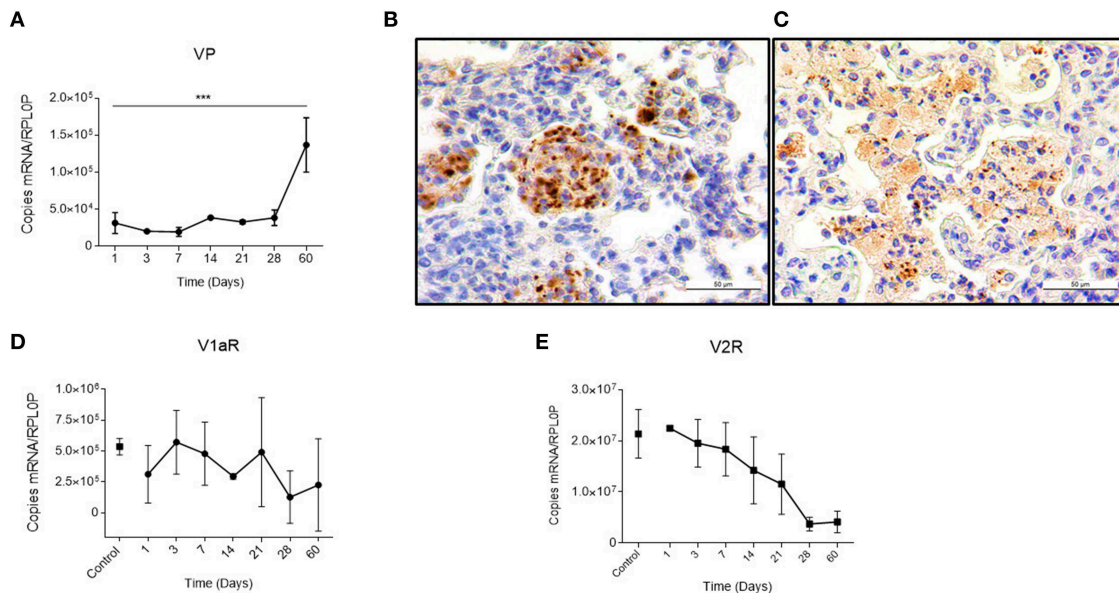


FIGURE 1 | Local kinetics of VP expression and VPR during pulmonary tuberculosis **(A)** Absolute expression of VP mRNA in lung homogenates during the course of infection. **(B)** Representative micrographs of immunohistochemistry with anti-VP antibody of the infected lung on day 14 showing immunopositive macrophages forming a granuloma (400×). As well as in foamy macrophages of pneumonic areas on day 60 post-infection **(C)**. **(D,E)** Absolute quantification of V1a and V2 mRNA, respectively, in lungs of healthy (control) and infected mice. Data are expressed as means ± SD of three different animals at each point. Asterisks represent statistical significance (*** $P < 0.0001$, one-tailed ANOVA).

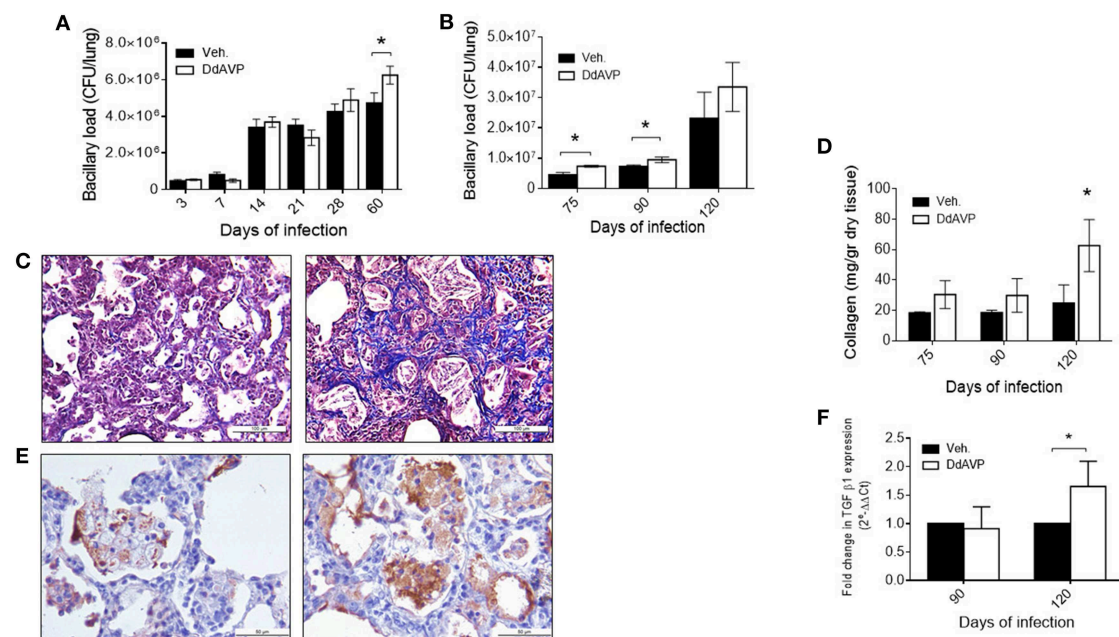


FIGURE 2 | Effect of vasopressin agonism during early and late infection in bacilli loads and histopathology **(A)** Bacillary loads of lung homogenates of mice infected with *M. tuberculosis* strain H37Rv and treated with DdAVP twice a day during early infection. **(B)** Bacillary loads at lungs of mice treated during late infection, starting from day 60 onwards. **(C)** Representative Masson's trichrome stain micrographs of lung of control-infected (left) and DdAVP-treated infected mice (right) on day 120 post-infection. **(D)** Collagen amount in lungs of infected mice treated during the late infection quantified by hydroxyproline assay. **(E)** Representative micrographs of lung immunohistochemistry anti-TGF-β1 of control-infected (left) and DdAVP-infected (right) mice after 60 days of treatment. **(F)** Relative expression of TGF-β mRNA in lungs of infected mice treated with DdAVP during the late infection. Days 75, 90, and 120 of infection correspond to 15, 30, and 60 days of treatment, respectively. Data are expressed as means ± SD of three different animals at each point. Asterisk represent statistical significance (* $P < 0.05$, two-way ANOVA).

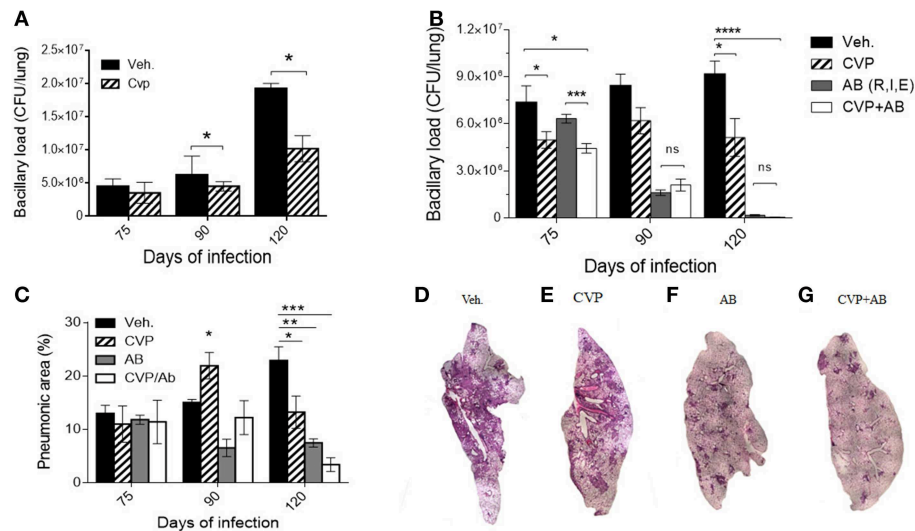


FIGURE 3 | Blockade of VP receptors decreased bacillary loads at lung. **(A)** Comparison of bacillary loads at lung homogenates of control mice treated with vehicle (black-filled bars) and treated with CVP (lined bars) from day 60. **(B)** Effect on bacillary loads of vehicle treated (black-filled bars), CVP (lined bars), the three antibiotics (AB, Rifampicin, Isoniazide, and Ethambutol, gray filled bars) and antibiotics plus CVP (AB + CVP, white bars), during late infection, from day 60. **(C)** Pneumonic areas of the infected lungs of mice treated with the different experimental conditions. **(D–G)** Representative micrographs of automatized reconstruction of infected lungs from vehicle, CVP, AB, and CVP plus AB, respectively. Days 75, 90, and 120 of infection correspond to 15, 30, and 60 days of treatment, respectively. Data are expressed as means \pm SD of three different animals at each point. Asterisk represent statistical significance (* P < 0.05, two-way ANOVA).

cells with Mtb and then three different doses of the synthetic agonist DdAVP or the antagonist CVP were added to RPMI medium. After 24 h of infection, repeated administration (at 0, 12, and 24 h) of the highest concentration of DdAVP produced an increase in the number of intracellular bacilli (**Figure 4A**) in a dose- and time-dependent manner, while CVP produced a significant decrease of bacillary loads when compared with the highest dose of DdAVP, suggesting that a *vasopressinergic tone* modifies the macrophage ability to kill mycobacteria. Moreover, infected macrophages supplemented with AVP (1×10^{-6} M) each for 24 h showed higher intracellular bacilli at days 1 and 3 post-infection (**Figure 4B**), in co-existence with decreased IL-6 in supernatants, which was totally reversed with CVP treatment (**Figure 4C**). TNF α , a protective cytokine during early mycobacterial infection, was found reduced with AVP treatment; nevertheless, CVP did not reverse the TNF inhibition mediated by VP completely (**Figure 4D**), suggesting a different mechanism regarding vasopressinergic modulation over macrophage cytokine production. It is important to mention that VP was not synthesized by cultured alveolar macrophages, as they do not express VP mRNA (**Supplementary Figure 2**).

Effect of Vasopressin on *M. tuberculosis*

Another aspect of interest was the possibility that VP could be exerting a direct effect on Mtb. To study this, bacteria were seeded in liquid medium in 96-well plates and incubated with lyophilized VP (Sigma-Aldrich) or DdAVP at different concentrations. As mentioned above, DdAVP is an isomer of VP that has an arginine in position D (unlike the position L in VP), which confers, in addition to a prolonged half-life, a greater affinity for the

V2 receptor; on the other hand, VP has a similar affinity for its three receptors. After 7 days of incubation, the bacteria that were incubated with VP transformed a greater amount of MTT-tetrazolium into formazan, which did not occur when the bacteria were incubated with DdAVP (**Figure 5A**) or the medium alone. This bacterial reaction is carried out by a reduction reaction of the compound NADH and is non-reversible, so that the intensity of the positivity indirectly indicates higher metabolic activity (or an increased number of bacteria) in Mtb incubated with VP. Unexpectedly, neither AVP nor DdAVP caused a change in the number of cultivable bacilli in the medium (**Figure 5B**).

DISCUSSION

The results shown here are a new example of the constant communication and superposition of neuroendocrine and immune functions during chronic infectious diseases. During ontogeny, the lung epithelium derives from neuroendocrine cells, and during the adult life for its adequate function, airway epithelium requires the influence of hormones and neuropeptides (44, 45). This also contributes to the distinctive characteristics that confirm the lung as an immune-privileged organ, since tolerance to environmental immunogens of the most diverse nature and origin is necessary; however, the lung is also an organ of entry and lodging of many highly evolved microorganisms, such as Mtb. Thus, the lungs need the contribution of well-balanced immune-neuroendocrine response to eliminate diverse infecting agents and efficient cellular mechanisms that repair and reconstitute the pulmonary tissue

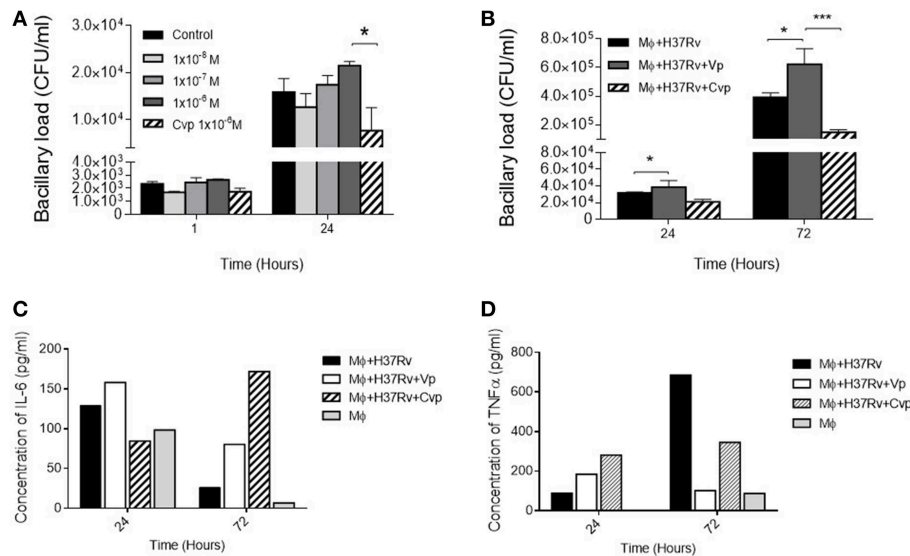


FIGURE 4 | Effects of VP and antagonist CVP on infected alveolar macrophages. **(A)** Number of cultivable intracellular bacilli expressed as CFU per milliliter at 1 and 24 h post-infection in RPMI controls (black bars), incubated with three different doses of DdAVP (1×10^{-8} M, white bars; 1×10^{-7} M gray bars, and 1×10^{-6} M dark gray bars) or CVP (1×10^{-6} M, lined bars). **(B)** Effect of VP or CVP on mycobacterial killing by MHS cells at 24 and 72 h post-infection. **(C)** Quantification of IL-6 and TNF α **(D)** in pools of supernatants of infected MHS cells detected by ELISA. Data are expressed as means \pm SEM of three different wells at each point. Asterisk represent statistical significance (* $P < 0.05$, two-way ANOVA).

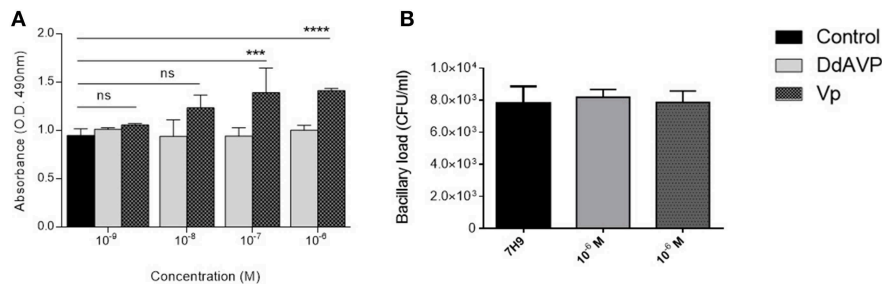


FIGURE 5 | Effects of VP on mycobacterial metabolism. **(A)** Reduction of MTS tetrazolium salts into colored compound formazan by Mtb H37Rv incubated in liquid 7H10 (black bars), medium plus DdAVP (clear gray bars), or medium plus VP (dark gray bars) for 7 days. **(B)** Number of cultivable bacilli in wells of the three experimental conditions. Data are expressed as means \pm SD of three wells in two independent experiments. Asterisk represent statistical significance (*** $P < 0.001$, **** $P < 0.0001$ two-way ANOVA).

after bacterial aggression. In this regard, VP could be a participating factor in the immunopathogenesis of pulmonary TB, considering that it is a pleiotropic hormone that exerts different effects on epithelial, immune, and fibroblast cells, and contributes to the regulation of different phenomena of resistance to inflammatory stress (31, 37, 46). On the other hand, its effects on phagocytosis, cytokine production, and apoptosis also suggest that vasopressinergic dysfunction could contribute to the pathogenesis of several infectious diseases, including TB. No less important is the association that exists between stress-mediated immunosuppression by VP and its relationship with infectious/inflammatory diseases (47–49), as VP is one of the main mediators of the hypothalamic–pituitary–adrenal axis, especially in periods of chronic stress resulting

in dysregulated cortisol production (25, 50). In fact, various inflammatory diseases exhibit an increased “vasopressinergic tone”; in particular, lung inflammation of different etiologies is accompanied by this hormonal characteristic (51–55).

In the present work, the existence of the so-called antidiuretic principle in pulmonary TB (13) is confirmed and corresponds to VP, as demonstrated by our immunohistochemical results; the intensity and the number of cells positive for VP in lung increased as the disease progressed, correlating with the extension of pneumonia, and interestingly, foamy macrophages that are the prevalent cell type in the pneumonic areas were those that showed the strongest VP immunostaining, which well-correlated with what was reported, that is, that these types of cells are distinctive in the advanced stage of the

disease and are characterized by having a large number of bacteria in their cytoplasm (56). The detection and progressive increase of VP transcripts in infected lungs during infection was seen, suggesting that VP has a significant activity in the infected organ, as there was no VP mRNA expression in the healthy lung.

The effects of VP are highly dependent on its concentration, time of action, type of organ, and target cell. Previously, it has been reported that VP disturbances occur in the pathophysiology of inflammatory diseases (24, 39); nevertheless, the anti-inflammatory effect of this hormone in the lungs has also been described, through the inhibition in the production of IL-6 (37). In addition, in heart, liver, and in fibroblasts, VP is an inducer of fibrosis, a mechanism partially dependent on TGF- β (42, 43, 57). To study the possible pathogenic effect in TB, experiments were carried out using vasopressinergic manipulation, with the synthetic agonist DdAVP, because its half-life is longer than VP, and CVP was used as a non-selective antagonist for the V1a and V2 receptors. The obtained results suggest that VP has anti-inflammatory/profibrotic effects, which should be important to reduce excessive inflammation and to promote the healing of irreversible damaged lung tissue in advanced active TB, which could be modulated by the expression of VP receptors that were lower expressed during progressive late disease, a phenomenon that has been reported previously in response to acute inflammation (58). However, it seems that sustained vasopressinergic activity, such as produced by the administration of DdAVP during late disease, has deleterious effects, as suggested by the higher number of live bacteria and the extensive fibrosis in the lungs of mice treated with this agonist compound. This effect can be mediated through the induction of TGF- β production since immunohistochemistry showed a higher number of strong TGF- β positive foamy macrophages surrounded by areas with extensive fibrosis, and higher gene expression of this cytokine was seen in the animals treated with the VP agonist. TGF- β is an important anti-inflammatory and immunosuppressive cytokine that is produced during active TB and has a significant effect in preventing excessive inflammation, but this activity is produced by inhibiting the TB protective Th1 pro-inflammatory response; hence, TGF- β has a deleterious effect in this disease (59). This cytokine also induces fibroblast activation and collagen secretion, being a key factor in the development of fibrosis. Thus, it seems that Mtb “takes advantage” of the physiological response of VP, which promotes anti-inflammation and tissue healing, leading to a non-protective immunity consequently. These functions can also be important to decrease the pulmonary functional capacity because of fibrosis.

The lower bacillary loads produced by the inhibition of VPR activity in advanced TB mice treated with CVP confirm the possible deleterious effect caused by the continuous and local production of VP on advanced infection and open the possibility of using these observations for therapeutic purposes, specifically the use of VP-blocking agents as adjuvants of antibiotic therapy. In that sense, it is interesting that animals with advanced progressive TB treated with first-line antibiotics and the VP receptor antagonist reduced significantly and more rapidly the bacillary loads in lungs than animals treated only

with antibiotics. However, it is important to mention that changes in diuresis and water intake in animals treated with CVP (**Supplementary Figure 1**) could be interfering with the antibiotic activity; thus, future investigations using selective blockers with no aquaretic activity could be useful. Although TB can be cured by chemotherapy, the treatment usually requires four specific drugs and 6 months of therapy in humans; this long treatment frequently produces significant compliance problems with the consequence of disease recrudescence and the arising of multi-drug resistant (MDR) strains. Thus, the possibility of shortening the conventional treatment is a basic strategy for the control of this disease. Indeed, the frequency of cases of MDR-TB is increasing, and its treatment is even more expensive and demanding, because it requires eight antibiotics administered during a year and a half. We are currently conducting experiments with mice infected with MDR bacteria and treated with second-line antibiotics and CVP, in order to determine if there is synergy and therefore possible shortening in the time of treatment of MDR-TB.

The results in the present study show for the first time the pathogenic importance of VS in experimental pulmonary TB, as far as we know. However, more experiments are needed to define in more detail the contribution of this hormone in the pathogenesis of TB, such as studying whether Mtb produces a VP-like molecule that causes aberrant biological effects that deregulate the mechanisms of the immune system, resulting in favor of the infection as well as the possibility that Mtb could be driving host VP system. Experimental procedures of this work used only male mice, which can be a limiting factor. It will be interesting to know whether female mice develop this vasopressinergic response in lungs, as differences between gender occur in the pathophysiology of TB (60) and also because of the known VP system differences between male and females. Also, it is necessary to study in detail the mechanisms underlying the decrease in bacillary load by blocking its activity *in vivo* or *in vitro*, since they could be caused by a lower rate of phagocytosis, antigen processing, or the inhibition of immunosuppressive effects of VP (mediated by TGF- β). It is also of interest to study if VP, in conjunction with other peptides and neurotransmitters, could be inducing effects directly on Mtb, influencing its virulence, as VP belongs to a huge group of regulatory peptides that have remained in evolution for more than 500 million years, and due to its pleiotropic effects, it is intuitive to think that a complex and well-adapted bacterium could be taking advantage of these host trophic factors. The results shown here with respect to the greater transformation of formazan by mycobacteria when treated with VP suggest this possibility and open discussion about some type of ancestral interaction between VS and Mtb, as this hormone can increase bacterial metabolism. This series of hypothetical possibilities are part of the perspectives of this work.

DATA AVAILABILITY

The datasets generated for this study are available on request to the corresponding author.

ETHICS STATEMENT

All the animal work was done according to the guidelines of the Mexican law NOM 061-Z00-1999, and approval of the Internal Committee for the Care and Use of Laboratory Animals (CICUAL) of the National Institute of Medical Sciences and Nutrition in México. Protocol number PAT-1861-16/20.

AUTHOR CONTRIBUTIONS

MZ, AQ-S, and RH-P contributed to the background work and conceived the experiments. MZ performed, organized, and analyzed the results. DM-E, BM-C, and JB-P contributed to the design and supervised experimental work. AQ-S provided DdAVP and CVP.

MZ and RH-P wrote the manuscript. RH-P provided the funds.

FUNDING

This study was supported by Consejo Nacional de Ciencia y Tecnología (CONACyT IFC 2015-1 Project number 115). MZ is a doctoral student from Programa de Doctorado en Ciencias Biomédicas, Universidad Nacional Autónoma de México (UNAM) and received fellowship 595244 from CONACyT.

SUPPLEMENTARY MATERIAL

The Supplementary Material for this article can be found online at: <https://www.frontiersin.org/articles/10.3389/fendo.2019.00351/full#supplementary-material>

REFERENCES

1. WHO. *Global Tuberculosis Report*. WHO (2018).
2. Hernandez-Pando R, Orozco H, Aguilar D. Factors that deregulate the protective immune response in tuberculosis. *Arch Immunol Ther Exp*. (2009) 57:355–67. doi: 10.1007/s00005-009-0042-9
3. Rajaram MVS, Ni B, Dodd CE, Schlesinger LS. Macrophage immunoregulatory pathways in tuberculosis. *Semin Immunol*. (2014) 26:471–85. doi: 10.1016/j.smim.2014.09.010
4. Malik BZA, Denning GM, Kusner DJ. Inhibition of Ca^{2+} signaling by *Mycobacterium tuberculosis* is associated with reduced phagosome-lysosome fusion and increased survival within human macrophages. *J Exp Med*. (2000) 191:287–302. doi: 10.1084/jem.191.2.287
5. Ehlers S, Schaible UE. The granuloma in tuberculosis: dynamics of a host-pathogen collusion. *Front Immunol*. (2012) 3:411. doi: 10.3389/fimmu.2012.00411
6. Hernández-Pando R, Orozco H, Sampieri A, Pavón L, Velasquillo C, Larriva-Sahd J, et al. Correlation between the kinetics of Th1, Th2 cells and pathology in a murine model of experimental pulmonary tuberculosis. *Immunology*. (1996) 89:26–33.
7. Bongiovanni B, Díaz A, D'Attilio L, Santucci N, Didoli G, Lioi S, et al. Changes in the immune and endocrine responses of patients with pulmonary tuberculosis undergoing specific treatment. *Ann N Y Acad Sci*. (2012) 1262:10–5. doi: 10.1111/j.1749-6632.2012.06643.x
8. Bottasso O, Bay ML, Besedovsky H, del Rey A. Adverse neuro-immune-endocrine interactions in patients with active tuberculosis. *Mol Cell Neurosci*. (2013) 53:77–85. doi: 10.1016/j.mcn.2012.11.002
9. Bottasso O, Bay ML, Besedovsky H, Del Rey A. Immunoendocrine alterations during human tuberculosis as an integrated view of disease pathology. *Neuroimmunomodulation*. (2009) 16:68–77. doi: 10.1159/000180261
10. Hernandez-Pando R, Orozco H, Honour J, Silva P, Leyva R, Rook GAW. Adrenal changes in murine pulmonary tuberculosis; a clue to pathogenesis? *FEMS Immunol Med Microbiol*. (1995) 12:63–72. doi: 10.1111/j.1574-695X.1995.tb00176.x
11. Weiss H, Katz S. Hyponatremia resulting from apparently inappropriate secretion of antidiuretic hormone in patients with pulmonary tuberculosis. *Am Rev Respir Dis*. (1965) 92:609–16.
12. Lee P, Ho KKY. Hyponatremia in pulmonary TB: evidence of ectopic antidiuretic hormone production. *Chest*. (2010) 137:207–8. doi: 10.1378/chest.09-0405
13. Vorherr H, Massry SG, Fallet R, Kaplan L, Kleeman CR. Antidiuretic principle in tuberculous lung tissue of a patient with pulmonary tuberculosis and hyponatremia. *Ann Intern Med*. (1970) 72:383–7. doi: 10.7326/0003-4819-72-3-383
14. Van Leeuwen FW, Caffé R, Van Der Sluis PJ, Sluiter AA, Van Der Woude TP, Seidah NG, et al. Propressophysin is present in neurones at multiple sites in Wistar and homozygous Brattleboro rat brain. *Brain Res*. (1986) 379:171–5. doi: 10.1016/0006-8993(86)90272-6
15. Keil LC, Severs WB. Reduction in plasma vasopressin levels of dehydrated rats following acute stress. *Endocrinology*. (2015) 100:30–8. doi: 10.1210/endo-100-1-30
16. Ma XM, Lightman SL. The arginine vasopressin and corticotrophin-releasing hormone gene transcription responses to varied frequencies of repeated stress in rats. *J Physiol*. (1998) 510:605–14. doi: 10.1111/j.1469-7793.1998.605bk.x
17. Morgenthaler NG, Müller B, Struck J, Bergmann A, Redl H, Christ-Crain M. Copeptin, a stable peptide of the arginine vasopressin precursor, is elevated in hemorrhagic and septic shock. *Shock*. (2007) 28:219–26. doi: 10.1097/SHK.0b013e318033e5da
18. Taveau C, Chollet C, Waeckel L, Desposito D, Bichet DG, Arthus MF, et al. Vasopressin and hydration play a major role in the development of glucose intolerance and hepatic steatosis in obese rats. *Diabetologia*. (2015) 58:1081–90. doi: 10.1007/s00125-015-3496-9
19. Palin K, Moreau ML, Sauviant J, Orcel H, Nadjar A, Duvoid-Guillou A, et al. Interleukin-6 activates arginine vasopressin neurons in the supraoptic nucleus during immune challenge in rats. *Am J Physiol Endocrinol Metab*. (2009) 296:E1289–99. doi: 10.1152/ajpendo.90489.2008
20. Raber J, Bloom FE. IL-2 induces vasopressin release from the hypothalamus and the amygdala: Role of nitric oxide-mediated signaling. *J Neurosci*. (1994) 14:6187–95. doi: 10.1523/JNEUROSCI.14-10-06187.1994
21. Maybauer MO, Maybauer DM, Enkhbaatar P, Traber DL. Physiology of the vasopressin receptors. *Best Pract Res Clin Anaesthesiol*. (2008) 22:253–63. doi: 10.1016/j.bpa.2008.03.003
22. Khagai II, Gulyaeva MA, Popova NA, Zakharova LA, Ivanova LN. Immune system in vasopressin-deficient rats during ontogeny. *Bull Exp Biol Med*. (2003) 136:448–50. doi: 10.1023/B:BEBM.0000017089.28428.1c
23. Zakharova LA, Karyagina AY, Popova NA, Khagai II, Ivanova ALN. Humoral immune response in ontogeny of the Brattleboro rats with a hereditary defect of vasopressin synthesis. *Doklady Biol Sci*. (2001) 376:70–1. doi: 10.1023/A:1018846514511
24. Chowdrey HS, Larsen PJ, Harbuz MS, Jessop DS, Aguilera G, Eckland DJ, et al. Evidence for arginine vasopressin as the primary activator of the HPA axis during adjuvant-induced arthritis. *Br J Pharmacol*. (1995) 116:2417–24. doi: 10.1111/j.1476-5381.1995.tb15089.x
25. de Goeij DCE, Jezova D, Tilders FJH. Repeated stress enhances vasopressin synthesis in corticotropin releasing factor neurons in the paraventricular nucleus. *Brain Res*. (1992) 577:165–8. doi: 10.1016/0006-8993(92)90552-K
26. Fodor A, Pinter O, Domokos A, Langnaese K, Barna I, Engelmann M, et al. Blunted HPA axis response in lactating, vasopressin-deficient Brattleboro rats. *J Endocrinol*. (2013) 219:89–100. doi: 10.1530/JOE-13-0224

27. Herman JP, Tasker JG. Paraventricular hypothalamic mechanisms of chronic stress adaptation. *Front Endocrinol.* (2016) 7:1–10. doi: 10.3389/fendo.2016.00137
28. Chang YY, Yang CH, Wang SC, Kao MC, Tsai PS, Huang CJ. Vasopressin inhibits endotoxin binding in activated macrophages. *J Surg Res.* (2015) 197:412–8. doi: 10.1016/j.jss.2015.04.042
29. Jan WC, Kao MC, Yang CH, Chang YY, Huang CJ. Phosphoinositide 3-kinase is involved in mediating the anti-inflammation effects of vasopressin. *Inflammation.* (2017) 40:435–41. doi: 10.1007/s10753-016-0489-x
30. Sigal F. Multiple effects of arginine vasopressin on prostaglandin E2 synthesis in fibroblasts. *Eur J Pharmacol.* (2004) 485:53–9. doi: 10.1016/j.ejphar.2003.11.049
31. Ekman R, Gobom J, Persson R, Mecocci P, Nilsson CL. Arginine vasopressin in the cytoplasm and nuclear fraction of lymphocytes from healthy donors and patients with depression or schizophrenia. *Peptides.* (2001) 22:67–72. doi: 10.1016/S0196-9781(00)00357-0
32. Johnson HM, Torres BA. A novel arginine vasopressin-binding peptide that blocks arginine vasopressin modulation of immune function. *J Immunol.* (1988) 141:2420–3.
33. Torres BA, Johnson HM. Arginine vasopressin (AVP) replacement of helper cell requirement in IFN-gamma production. Evidence for a novel AVP receptor on mouse lymphocytes. *J Immunol.* (1988) 140:2179–83.
34. Campos-Rodríguez R, Quintanar-Stephano A, Jarillo-Luna RA, Oliver-Aguillón G, Ventura-Juárez J, Rivera-Aguilar V, et al. Hypophysectomy and neurointermediate pituitary lobectomy reduce serum immunoglobulin M (IgM) and IgG and intestinal IgA responses to *Salmonella enterica* serovar typhimurium infection in rats. *Infect Immun.* (2006) 74:1883–9. doi: 10.1128/IAI.74.3.1883-1889.2006
35. Hu SB, Zhao ZS, Yhap C, Grinberg A, Huang SP, Westphal H, et al. Vasopressin receptor 1a-mediated negative regulation of B cell receptor signaling. *J Neuroimmunol.* (2003) 135:72–81. doi: 10.1016/S0165-5728(02)00442-3
36. Chassin C, Hornef MW, Bens M, Lotz M, Goujon J-M, Vimont S, et al. Hormonal control of the renal immune response and antibacterial host defense by arginine vasopressin. *J Exp Med.* (2007) 204:2837–52. doi: 10.1084/jem.20071032
37. Boyd JH, Holmes CL, Wang Y, Roberts H, Walley KR. Vasopressin decreases sepsis-induced pulmonary inflammation through the V2R. *Resuscitation.* (2008) 79:325–31. doi: 10.1016/j.resuscitation.2008.07.006
38. Schmittgen TD, Livak KJ. Analyzing real-time PCR data by the comparative C T method. *Nat Protoc.* (2008) 3:1101–8. doi: 10.1038/nprot.2008.73
39. Quintanar-Stephano A, Organista-Esparza A, Chavira-Ramírez R, Kovacs K, Berczi I. Effects of neurointermediate pituitary lobectomy and desmopressin on acute experimental autoimmune encephalomyelitis in Lewis rats. *Neuroimmunomodulation.* (2012) 19:148–57. doi: 10.1159/000330578
40. Bongiovanni B, Mata-espinosa D, Attilio LD, Leon-contreras JC, Marquez-velasco R, Bottasso O, et al. Effect of cortisol and/or DHEA on THP1-derived macrophages infected with *Mycobacterium tuberculosis*. *Tuberculosis.* (2015) 95:562–9. doi: 10.1016/j.tube.2015.05.011
41. Hundie GB, Woldemeskel D, Gessesse A. Evaluation of direct colorimetric MTT assay for rapid detection of rifampicin and isoniazid resistance in *Mycobacterium tuberculosis*. *PLoS ONE.* (2016) 11:1–14. doi: 10.1371/journal.pone.0169188
42. Quintanar-Stephano A, Ventura-Juárez J, Sánchez-Alemán E, Aldaba-Muruato LR, Cervantes-García D, Gonzalez-Blas D, et al. Liver cirrhosis reversion is improved in hamsters with a neurointermediate pituitary lobectomy. *Exp Toxicol Pathol.* (2016) 69:496–503. doi: 10.1016/j.etp.2017.04.006
43. Tahara A, Tsukada J, Tomura Y, Yatsu T, Shibasaki M. Vasopressin increases type IV collagen production through the induction of transforming growth factor-beta secretion in rat mesangial cells. *Pharmacol Res.* (2008) 57:142–50. doi: 10.1016/j.phrs.2008.01.003
44. Branchfield K, Nantie L, Verheyden JM, Sui P, Wienhold MD, Sun X. Pulmonary neuroendocrine cells function as airway sensors to control lung immune response. *Science.* (2015) 351:707–10. doi: 10.1126/science.aad7969
45. Van Lommel A. Pulmonary neuroendocrine cells (PNEC) and neuroepithelial bodies (NEB): Chemoreceptors and regulators of lung development. *Paediatr Respir Rev.* (2001) 2:171–6. doi: 10.1053/prrv.2000.0126
46. Brown L, Chen M. Vasopressin signal transduction in rat type II pneumocytes. *Am J Physiol.* (1990) 258:L301–7. doi: 10.1152/ajplung.1990.258.6.L301
47. Elenkov IJ, Chrousos GPG. Stress hormones, Th1/Th2 patterns, pro/anti-inflammatory cytokines and susceptibility to disease. *Trends Endocrinol Metab.* (1999) 10:359–68. doi: 10.1016/S1043-2760(99)00188-5
48. Marsland AL, Bachen EA, Cohen S, Rabin B, Manuck SB. Stress, immune reactivity and susceptibility to infectious disease. *Physiol Behav.* (2002) 77:711–6. doi: 10.1016/S0031-9384(02)00923-X
49. Martinez AN, Mehra S, Kaushal D. Role of interleukin 6 in innate immunity to *Mycobacterium tuberculosis* infection. *J Infect Dis.* (2013) 207:1253–61. doi: 10.1093/infdis/jit037
50. Engelmann M, Landgraf R, Wotjak CT. The hypothalamic–neurohypophysial system regulates the hypothalamic–pituitary–adrenal axis under stress: an old concept revisited. *Front Neuroendocrinol.* (2004) 25:132–49. doi: 10.1016/j.yfrne.2004.09.001
51. Bevilacqua M. Hyponatraemia in AIDS. *Baillieres Clin Endocrinol Metab.* (1994) 8:837–48. doi: 10.1016/S0950-351X(05)80304-0
52. Hoorn EJ, van Wolfswinkel ME, Hesselink DA, de Rijke YB, Koelewijn R, van Hellemond JJ, et al. Hyponatraemia in imported malaria: the pathophysiological role of vasopressin. *Malar J.* (2012) 11:26. doi: 10.1186/1475-2875-11-26
53. Hou L, Zhu L, Zhang M, Zhang X, Zhang G, Liu Z, et al. Participation of antidiuretic hormone (ADH) in asthma exacerbations induced by psychological stress via PKA/PKC signal pathway in airway-related vagal preganglionic neurons (AVPNs). *Cell Physiol Biochem.* (2017) 41:2230–41. doi: 10.1159/000475638
54. Park SJ, Shin J. I. Inflammation and hyponatremia: an underrecognized condition? *Korean J Pediatr.* (2013) 56:519–22. doi: 10.3345/kjp.2013.56.12.519
55. Rivers RPA, Forsling ML, Olver RP. Inappropriate secretion of antidiuretic hormone in infants with respiratory infections. *Arch Dis Child.* (1981) 56:358–63. doi: 10.1136/adc.56.5.358
56. Hernandez-Pando R, Orozco H, Arriaga K, Sampieri A, Larriva-Sahd J, Madrid-Marina V. Analysis of the local kinetics and localization of interleukin-1a, tumour necrosis factor- α and transforming growth factor- β , during the course of experimental pulmonary tuberculosis. *Immunology.* (1997) 90:607–17.
57. Yan-Ping H, Lian-You Z, Qiang-Sun Z, Shao-Wei L, Xiao-Yan Z, Xiao-Long L, et al. Mitogenic effect of arginine vasopressin on adult rat cardiac fibroblast: involvement of PKC-erk1/2 pathway. *J Cardiovasc Pharmacol.* (2008) 52:72–81. doi: 10.1097/FJC.0b013e31817f36b8
58. Grinevich V, Knepper MA, Verbalis J, Reyes I, Aguilera G. Acute endotoxemia in rats induces down-regulation of V2 vasopressin receptors and aquaporin-2 content in the kidney medulla. *Kidney Int.* (2004) 65:54–62. doi: 10.1111/j.1523-1755.2004.00378.x
59. Hernández-Pando R, Orozco-Esteves H, Maldonado HA, Aguilar-León D, Vilchis-Landeros MM, Mata-Espinosa DA, et al. A combination of a transforming growth factor- β antagonist and an inhibitor of cyclooxygenase is an effective treatment for murine pulmonary tuberculosis. *Clin Exp Immunol.* (2006) 144:264–72. doi: 10.1111/j.1365-2249.2006.03049.x
60. Bini EI, Mata Espinosa D, Marquina Castillo B, Barrios Payán J, Colucci D, Cruz AF, et al. The influence of sex steroid hormones in the immunopathology of experimental pulmonary tuberculosis. *PLoS ONE.* (2014) 9:e93831. doi: 10.1371/journal.pone.0093831

Conflict of Interest Statement: The authors declare that the research was conducted in the absence of any commercial or financial relationships that could be construed as a potential conflict of interest.

Copyright © 2019 Zetter, Barrios-Payán, Mata-Espinosa, Marquina-Castillo, Quintanar-Stephano and Hernández-Pando. This is an open-access article distributed under the terms of the Creative Commons Attribution License (CC BY). The use, distribution or reproduction in other forums is permitted, provided the original author(s) and the copyright owner(s) are credited and that the original publication in this journal is cited, in accordance with accepted academic practice. No use, distribution or reproduction is permitted which does not comply with these terms.



Pituitary Adenylate Cyclase-Activating Peptide (PACAP)-Glutamate Co-transmission Drives Circadian Phase-Advancing Responses to Intrinsically Photosensitive Retinal Ganglion Cell Projections by Suprachiasmatic Nucleus

OPEN ACCESS

Edited by:

Leo T. O. Lee,
University of Macau, China

Reviewed by:

Dora Reglodi,
University of Pécs, Hungary
Anderson O. L. Wong,
The University of Hong Kong,
Hong Kong

*Correspondence:

Martin K.-H. Schäfer
mkh.schafer@staff.uni-marburg.de
Lee E. Eiden
eidenl@mail.nih.gov
Martha U. Gillette
mgillett@illinois.edu

† Present address:

Peder T. Lindberg,
Department of Emergency Medicine,
Advocate Lutheran General Hospital,
Park Ridge, IL, United States
Penny W. Burgoon,
National Center for Advancing
Translational Sciences, National
Institutes of Health, Bethesda, MD,
United States
Christian Beaulé,
Strategic Project Management Group,
Office of the Vice-President of
Research, University of Ottawa,
Ottawa, ON, Canada

‡Work conducted in connection with
this report preceded this author's
federal employment

Specialty section:

This article was submitted to
Neuroendocrine Science,
a section of the journal
Frontiers in Neuroscience

Received: 13 July 2019

Accepted: 11 November 2019

Published: 06 December 2019

Peder T. Lindberg^{1†}, Jennifer W. Mitchell², Penny W. Burgoon^{2††}, Christian Beaulé^{2†},
Eberhard Weihe³, Martin K.-H. Schäfer^{3*}, Lee E. Eiden^{4*}, Sunny Z. Jiang⁴ and
Martha U. Gillette^{1,2*}

¹ Neuroscience Program, University of Illinois at Urbana-Champaign, Urbana, IL, United States, ² Department of Cell and Developmental Biology, University of Illinois at Urbana-Champaign, Urbana, IL, United States, ³ Institute of Anatomy and Cell Biology and Center of Mind, Brain and Behaviour, University of Marburg, Marburg, Germany, ⁴ Section on Molecular Neuroscience, Laboratory of Cellular and Molecular Regulation, National Institute of Mental Health, Bethesda, MD, United States

Results from a variety of sources indicate a role for pituitary adenylate cyclase-activating polypeptide (PACAP) in light/glutamate-induced phase resetting of the circadian clock mediated by the retinohypothalamic tract (RHT). Attempts to block or remove PACAP's contribution to clock-resetting have generated phenotypes that differ in their responses to light or glutamate. For example, previous studies of circadian behaviors found that period-maintenance and early-night phase delays are intact in PACAP-null mice, yet there is a consistent deficit in behavioral phase-resetting to light stimulation in the late night. Here we report rodent stimulus-response characteristics of PACAP release from the RHT, and map these to responses of the suprachiasmatic nucleus (SCN) in intact and PACAP-deficient mouse hypothalamus with regard to phase-resetting. SCN of PACAP-null mice exhibit normal circadian rhythms in neuronal activity, but are "blind" to glutamate stimulating phase-advance responses in late night, although not in early night, consistent with previously reported selective lack of late-night light behavioral responsiveness of these mice. Induction of CREB phosphorylation, a hallmark of the light/glutamate response of the SCN, also is absent in SCN-containing *ex vivo* slices from PACAP-deficient mouse hypothalamus. PACAP replacement to the SCN of PACAP-null mice restored wild-type phase-shifting of firing-rate patterns in response to glutamate applied to the SCN in late night. Likewise, *ex vivo* SCN of wild-type mice post-orbital enucleation are unresponsive to glutamate unless PACAP also is restored. Furthermore, we demonstrate that the period of efficacy of PACAP at SCN nerve terminals corresponds to waxing of PACAP mRNA expression in ipRGCs during the night, and waning during the day. These results validate the use of PACAP-deficient

mice in defining the role and specificity of PACAP as a co-transmitter with glutamate in ipRGC-RHT projections to SCN in phase advancing the SCN circadian rhythm in late night.

Keywords: PACAP, glutamate, suprachiasmatic nucleus, circadian rhythm, phase advance

INTRODUCTION

Internal circadian clocks must be both self-sustaining and flexible if they are to be useful in organizing behavior and physiology. Despite discoveries regarding peripheral oscillators, the circadian clock in the SCN is still considered one of the few sets of mammalian cells that maintains its own circadian rhythm relative to the external environment. It does this by responding to external time cues, the most important of which for mammals is light. This combination of internal rhythm generation and sensitivity to change makes the SCN an intriguing model of intrinsic mammalian brain function, and its adaptation to the environment.

In addition to the actions of glutamate (Ding et al., 1994) there is some evidence that PACAP plays a role in mammalian clock resetting. PACAP is a member of the secretin/glucagon/vasoactive intestinal peptide (VIP) family originally isolated from ovine hypothalamus (Miyata et al., 1989). Since its discovery only 18 years ago, several roles have been established for PACAP, including mediation of neurotransmitter release, vasodilation, bronchodilation, mediation of intestinal activity, increase of insulin and histamine secretion, and cell multiplication and differentiation (reviewed in Vaudry et al., 2000). PACAP has been co-localized with glutamate in the terminals of the RHT on the SCN (Hannibal et al., 1997, 2000, 2001b) and has been found to shift the clock under certain conditions (Hannibal et al., 1997). PACAP has also been shown to be associated with melanopsin, one of photopigments of the retina necessary for clock entrainment (Panda et al., 2002; Ruby et al., 2002).

Exogenous application of PACAP has been more controversial, alternately causing delays (Piggins et al., 2001), light-like shifts (Harrington et al., 1999), or no effect alone but modification of light or glutamate-induced shifts (Chen et al., 1999; Tischkau et al., 2000). In PACAP- and PACAP receptor-deficient mice, designed to test PACAP's circadian role, altered shifting that is not clearly consistent either with the previous pharmacological manipulations of PACAP in the SCN or with each other has been reported (Chen et al., 1999; Hannibal et al., 2001a; Kawaguchi et al., 2003; Colwell et al., 2004).

Another strain of mice was generated in 2002 that does not express detectable levels of PACAP (Hamelink et al., 2002). Like the Colwell model (Colwell et al., 2004), it was generated on the background of the C57BL6 mouse, but it eliminated only the PACAP-coding sequence, not the PRP sequence found in exon 4 (Okazaki et al., 1995). Thus, this

model may represent a more specific lesion of the PACAP peptide sequence and was generated on a background strain most easily comparable to other mice that have been described with respect to circadian phenotype (Buchanan, 2002; Abbott, 2005) including the PAC1-null mice (Hannibal et al., 2001a). Examination of this strain of mice was designed to complement previous experiments on PACAP transgenic mice and to extend findings into a new modality. By replicating some previous experiments we hope to shed light on an earlier controversy – the discrepancy of shifting in systems with a disruption of PACAP signaling. By introducing another level of examination – the brain-slice preparation – we sought to further test the reliability of behavioral results and to create another method to answer signaling questions at the level of the SCN.

Each examination of PACAP-deficient compared to wild-type mice tested the effect of light on a background of constant conditions. While each strain of mouse showed significant differences in light-induced phase resetting compared to wild-type mice, PACAP-receptor null mice differed in phenotype from PACAP null mice (Hannibal et al., 2001a; Kawaguchi et al., 2003; Colwell et al., 2004). The alternate lesions of a peptide and its receptor, with complementary results, are basic criteria that establish each animal as a preferred organism with which to study that peptide signaling system. This approach was championed by Harmar et al. (2002) for PACAP/VIP signaling in SCN (Shen et al., 2000; Cutler et al., 2003; Aton et al., 2005), and is extended here. We have previously reported that light exposure to mice specifically deficient in PACAP, but not lacking PACAP-related peptide (PrP) expression (Hamelink et al., 2002) results in shifts reminiscent of the original PACAP receptor null mice generated by Hannibal et al. (2001a), (Beaule et al., 2009).

We here examine SCN from PACAP-null, compared to wild-type mice, in a brain slice preparation, to extend our previous examination of the phase-shifting phenotype of PACAP-deficient mice *in vivo* to the mechanisms of PACAP action at the retinohypothalamic synapse in the SCN itself. In this slice preparation, the SCN expresses a peak in spontaneous firing rate during midday, between CT6 and 7. This peak recurs ~24 h later, at the same circadian time (Prosser and Gillette, 1989), and is shifted by a variety of stimuli in a manner consistent with the behavioral responses seen in the intact animal (Ding et al., 1994; Chen et al., 1999; Harrington et al., 1999; Tischkau et al., 2000; Buchanan and Gillette, 2005). Shifts represent a change in phase of the SCN, since peaks after a treatment recur ~24 h after the first (shifted) peak (Gillette and Prosser, 1988; Hannibal et al., 1997). This preparation applied to PACAP transgenic animals thus has the power to study altered

Abbreviations: PACAP, pituitary adenylate cyclase-activating polypeptide; SCN, suprachiasmatic nucleus; VGluT2, vesicular glutamate transporter isoform 2.

physiology in the same ways that it has previously been used to study relatively intact physiology and response to circadian signals of change. In the past, this preparation has been used to attempt to study a role of PACAP in circadian shifting (Chen et al., 1999). In PACAP-null mice, this preparation has the advantage of assured elimination of PACAP signaling. It is first important, however, to run appropriate controls for a system that has been otherwise lesioned over the course of the animals' development.

Since PACAP-null mice maintain an endogenous peak in spontaneous SCN firing-rate frequency that is similar to wild-type animals, it is possible to compare their response to glutamate applied directly to the SCN. Importantly, this preparation also allows the controlled replacement of PACAP into a system with otherwise undetectable levels of the peptide (Hamelink et al., 2002). This replacement makes possible an important control for transgenic animals that has not been performed in previous models, and suggests means of further characterizing the role of PACAP in the SCN.

MATERIALS AND METHODS

Materials

Peptides were purchased from AnaSpec (Fremont, CA, United States) unless otherwise noted. Antibodies were all obtained from commercial sources and these are indicated throughout the section "Results."

Animals

All manipulations were performed in accordance with the guidelines of the Institutional Animal Care and Use Committee and the Division of Animal Resources at the University of Illinois at Urbana-Champaign. Homozygote PACAP-null mice were derived as described previously (Hamelink et al., 2002) and bred onto a C57BL/6N background through 12 successive backcrossings (Hamelink et al., 2002). C57BL/6N mice were obtained from the same commercial source as the C57BL/6N mice used to establish the PACAP null backcross line (Charles River).

Hypothalamic tissue explants with optic nerves intact were obtained from rats (Long-Evans) and mice (C57BL/6) using previously described methods (Burgoon et al., 2004).

Enucleation Surgery and Circadian Timing

Mice 6–24 weeks old were housed under 12-h light:12-h dark (LD) cycles and provided food and water *ad libitum*. Zeitgeber time (ZT) is determined from the animal's LD cycle, with time of lights-on designated ZT 0. Because brain slices are maintained in constant conditions where the clock functions with a period of ~24-h without external time cues, the time of lights-on in the donor colony is designated as circadian time 0 (CT 0). Thus, subjective day (CT 0–12) corresponds to the light portion of the donor's former lighting schedule; subjective night (CT 12–24) corresponds to the dark portion of the donor's cycle. For animals in constant darkness (when

referred to in comparison to the studies performed here), onset of activity – designated by convention as CT12 – is used to determine period and indicate treatment times. Period is estimated by averaging the time between activity onsets for the 5 days prior to treatment. Treatment times are determined in circadian time to compensate for periods different than 24 h. For enucleated animals, onset of wheel-running activity – designated by convention as CT 12 – is used to determine period and treatment times (Beaule et al., 2009).

Bilateral orbital enucleation was performed on 8-week-old male C57BL/6J mice (Jackson Labs, Bar Harbor, ME, United States) under ketamine, medetomidine anesthesia, by severing the optic nerve, muscle and other connective tissues, and removing the eyes. The eye cavity was packed with sterile Gelfoam™ and the eyelid closed by suture. Mice recovered for an additional 8 weeks to ensure optic nerve degeneration.

Preparation, Chemical Treatment, and Single Unit Activity Recording of Brain Slices

Brain slices were prepared during the day, ≥ 2 h before the onset of the dark phase as preparation at night can alter clock phase (Gillette, 1986). The hypothalamus was blocked from the virgin brain and coronal slices were cut at 500 μm with a mechanical chopper. Slices containing the SCN were placed at the interface of a brain slice chamber (Prosser and Gillette, 1991) where they were perfused with glucose/bicarbonate/gentamicin-supplemented Earle's balanced salt solution (EBSS, Gibco BRL/Invitrogen, Carlsbad, CA, United States) while exposed to 95% O_2 :5% CO_2 at 35°C. This perfusion media was also used as the vehicle of chemical treatment of slices. Spontaneous single unit activity (SUA) was recorded extracellularly, under direct visual guidance of the recording electrode. SCN maintained in this way continue to generate a circadian rhythm of neuronal activity for up to 3 days in explant culture. The SCNs are clearly visible as translucent, ovoid structures at the base of the third ventricle, nestled in the optic chiasm.

Chemical treatment of a slice was applied via microdrop application under visual guidance. Before treatment, media flow was stopped and the media level in the slice chamber was lowered to expose the surface of the SCN. A 1 μl drop was applied to each SCN (two drops/slice) and the cover of the chamber was replaced to prevent evaporation. Glutamate was applied at 10 mM, a dose repeatedly shown to elicit consistent shifts in the mammalian SCN slice (Ding et al., 1994). PACAP was applied at varying concentrations, indicated in context. All treatments were dissolved in fresh, warm, oxygenated perfusion medium (supplemented EBSS) as a vehicle. Following 10 min after stimulus application, the slices were rinsed with fresh perfusion medium, and media flow was restored. At least 1 h was allowed to elapse following treatment before recording was resumed.

The spontaneous extracellular activity of neurons in the SCN was measured by means of a glass electrode filled with a 5-M NaCl solution. The electrode was positioned over the SCN

and is advanced slowly through the tissue. When a neuron was detected, its activity was recorded for 4 min. After each recording, the electrode was advanced until another neuron could be found or the slice had been fully penetrated. After a complete pass, the electrode was arbitrarily repositioned so as to sample the entire SCN area. Ensemble activity was determined by means of a 2-h running average grouped into 15-min bins. The peak of the running average was determined visually.

For electrical stimulation (rat), slices were stimulated using a suction electrode or a platinum bipolar electrode. To stimulate the RHT, optic nerves were pulled into the suction electrode or laid across the bipolar electrode. Nerves were stimulated for 5 min, and pulse frequency was set at 5, 10, and 20 Hz. Voltage strength was 2.5–10 V with a 0.05–1 ms pulse duration. SCN population spikes were observed during stimulation to confirm presence of P and N waves associated with post-synaptic responses and to detect possible current spread. If no P and N waves were detected, it was assumed that the nerves were damaged and that slice was not used for recording. Post-recording nerve crush followed by re-stimulation verified elimination of P and N waves. To verify the specificity of RHT activation on the circadian clock, a separate set of experiments stimulated the posterior hypothalamic areas instead of the optic nerves. A bipolar electrode was directed to the posterior hypothalamic area and the tissue was stimulated using the same stimulation parameters as those for the optic nerves.

Immunoreactivity of PACAP Releasate

Horizontal slices (400–450 μm) containing: (1) the ventral hypothalamus including the SCN, optic chiasm, and optic nerves or (2) a reduced slice (“nerve/chiasm” preparation) containing the SCN, optic chiasm, and optic nerves were prepared between CT 0–2 from Long-Evans rats using a vibrating slicer. Slices were incubated in EBSS supplemented with 24.6 mM glucose, 26.2 mM sodium bicarbonate plus 2.5 mg/l gentamicin, at pH 7.4. A protease inhibitor (CompleteTM, no EDTA, Roche Diagnostics) was added to the EBSS to prevent proteolysis. Slices stimulated in 0 Ca^{2+} were incubated in calcium-free EBSS, with CompleteTM containing EDTA, Roche Diagnostics).

Nitrocellulose filter paper was pre-wetted with 10–20 μl of EBSS to prevent slices adhering to the paper. Slices were placed SCN-side down on the paper and optic nerves were stimulated for 2 min with a bipolar electrode. Slices were gently removed, and the nitrocellulose was immediately fixed in paraformaldehyde vapor for 120–150 min and processed as previously published (Reimer et al., 1999). Briefly, the fixed paper was then incubated with the PACAP antibody (diluted 1:5) for 24 h at 4°C, and then washed in PBS + 0.1% Triton X-100 and incubated with a biotinylated rabbit anti-mouse antiserum (E464, Dako, Copenhagen, Denmark, diluted 1:800) for 1 h. After washing and incubating for 30 min at room temperature in ABC–streptavidin horseradish peroxidase complex diluted 1:125 (Dako, Denmark), the filter papers were washed, then incubated in biotinylated tyramide using a TSA-kit (Tyramide System Amplification; DuPont NEN., Boston, MA, United States) diluted 1:100. After another wash in PBS + 0.1% Triton X-100 and

a new incubation in ABC–streptavidin horseradish peroxidase complex as before, the papers were incubated in a solution of diaminobenzidine (DAB, Sigma, St. Louis, MO, United States) for 15 min. The reaction was terminated by washing the filter paper with tap water. Samples on each panel were processed for PACAP together. Images were cropped but not adjusted for brightness or contrast.

Relative staining intensity was quantified using NIH Image J software. Images of the nitrocellulose paper containing the “slice” and the PACAP “stain” were stacked together and an outline of the slice was traced. The stain image intensity was measured, using the slice image outline. Staining intensity was normalized against a 10- μM PACAP-38 microdrop control image. Values are reported as means \pm standard error.

Western Immunoblot

Suprachiasmatic nucleus slices were prepared as previously described, but were then reduced in size to an “SCN punch” by means of a 2-mm diameter sample corer. After treatment, punches were frozen on dry ice and subsequently homogenized by repeat pipetting in 50 μl ice-cold Tissue Protein Extraction Reagent (T-PER) with 1 \times Complete Protease Inhibitor Cocktail (PI, Roche) and 1 \times Phosphatase Inhibitor Cocktail (PhI, Cal Biochem, sets I and II). Samples were centrifuged at 10,000 rpm for 5 min at 4°C, and the protein supernatant transferred to a new chilled microfuge tube. Protein content of each sample was determined by the Micro BCA Protein Assay. Total protein (35 μg) was resolved by 4–15% SDS-PAGE and transferred to nitrocellulose. Each blot was probed with rabbit polyclonal antibodies to phosphorylated CREB and rabbit polyclonal anti-CREB (non-phospho-specific) from Upstate Biotechnology, Inc. (Lake Placid, NY, United States). HRP-linked antibodies against rabbit were used in conjunction with Supersignal chemiluminescent substrate (Pierce). Blots were digitally quantitated using the Biochemi Imaging system (UVP, Upland, CA, United States) and Labworks 4.0. pCREB-ir was compared to total CREB-ir to control for loading differences between wells, and this ratio was used to determine CREB phosphorylation. Average CREB phosphorylation in untreated slices of each blot was normalized to 1 to facilitate comparisons of induction.

Double Immunofluorescence

Immunofluorescence staining of coronal sections through the anterior diencephalon of FFPE brains of C57Bl/6 mice was carried out as previously described (Schafer et al., 2010), using the antibodies described and at the dilutions previously employed. Immunofluorescence signals were documented in a surface scan using a BX50WI confocal laser scanning microscope (Olympus Optical, Hamburg, Germany) and Olympus Fvoview 2.1 software, and stored as false color images (8-bit tiff format).

RNAScope Analysis of PACAP mRNA Expression in Retina

The eyeballs from three wild-type mice (C57BL/6N, $n = 3$) were freshly excised at each time point, frozen on Dry Ice, embedded

in freezing medium (TissueTec™) at -20°C and sectioned on a cryostat. Sagittal examine PACAP mRNA expression in retina by *in situ* histochemistry. The RNAscope 2.5 HD Reagent Kit-RED assay (Cat No. 322360, Advanced Cell Diagnostics, San Francisco, CA, United States) and mouse PACAP probe (Adcyap1, Cat No. 405911, Advanced Cell Diagnostics, San Francisco, CA, United States) were used for *in situ* hybridization of mouse retina sections following the user manual of the products. 50% hematoxylin staining solution was used for counterstaining. Slides with retina sections were image-captured with 20 \times objective with ZEISS Axio Scan (Carl Zeiss Microscopy, Thornwood, NY, United States) and images for sections from each animal were organized and converted to TIF files with BrainMaker (MBF Bioscience, Williston, VT, United States).

Data Quantitation and Statistical Analysis

Data for immunohistochemical investigations are presented as representative images to justify qualitative and comparative statements made in text about chemoanatomical features of PACAP circuitry. Single-plex images of RNAscope results were quantified with Fiji ImageJ. Briefly, color deconvolution was used to separate the single-plex images into different color channels: images for counter-stained nuclei were used to count cell number on retinal ganglion cell (RGC) layer and images for PACAP probe signals (RED) were used to quantify the integrated density (IntDen) of the signal within the RGC layer. Relative intensity of PACAP mRNA signal/cell at each time point was calculated as: IntDen of probe signal divided by cell number, then normalized by mean of the IntDen/cell at 11 AM (CT5). *Post hoc* Bonferroni analysis following one-way ANOVA using SigmaPlot 14.0 (Systat Software, Inc., San Jose, CA, United States) was conducted to compare PACAP mRNA expression between different time points.

For electrical recordings, the average time of peak activity of the neuronal ensemble was compared between each treatment and untreated animals to test the presence of a phase shift, and between experimental (PACAP-null, enucleated), and control (wild-type) animals for each condition using ANOVA. For western immunoblot, normalized densitometry was compared between control and each condition using ANOVA. Statistics are reported as the mean \pm SEM. Alpha was set at 0.05 for all statistical tests.

RESULTS

PACAP Release From the Retinohypothalamic Tract Onto the SCN and Phase Advance Elicited by Optic Nerve Stimulation Exhibit Identical Frequency-Dependence

A 20 Hz, 5 V, 2 min optic nerve stimulation invokes a phase advance in rodent horizontal brain slices (Atkins et al., 2018). Accordingly, to determine a correlation indicative of causality between PACAP release and phase advance elicited in the SCN

from the retinohypothalamic tract (RHT), we performed PACAP release experiments in rat SCN *ex vivo*, a preparation in which peptide secretion could technically be readily monitored. PACAP staining specific to the SCN was examined by using reduced horizontal slices containing the optic nerves, the optic chiasm, and its overlying hypothalamic tissue, including the SCN. PACAP release experiments revealed that 20 Hz stimulation to the optic nerves released PACAP (Figure 1). To determine if RHT-activated PACAP release was synaptic in nature, samples were also stimulated in the absence of external calcium, or after optic nerve crush. PACAP staining intensity was not different among sham-stimulated, 20 Hz in 0 Ca^{2+} , and nerve crush followed by 20 Hz stimulation samples. Only 20 Hz stimulated samples with normal extracellular calcium and intact optic nerve input exhibited significantly higher levels of PACAP staining compared to sham-stimulated controls (Figure 1).

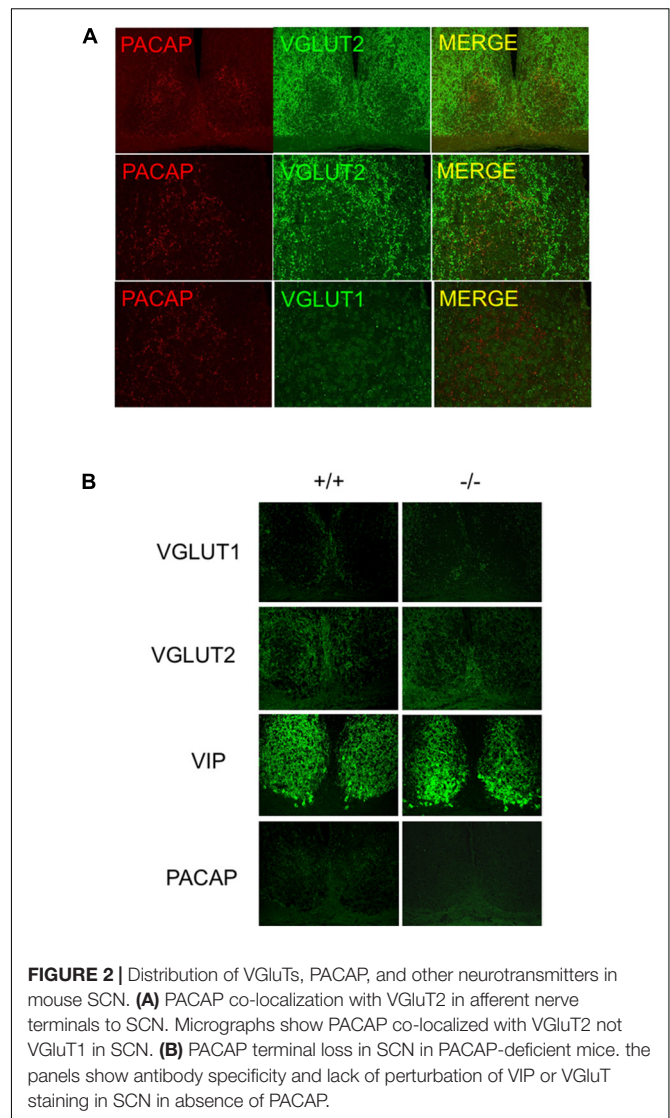
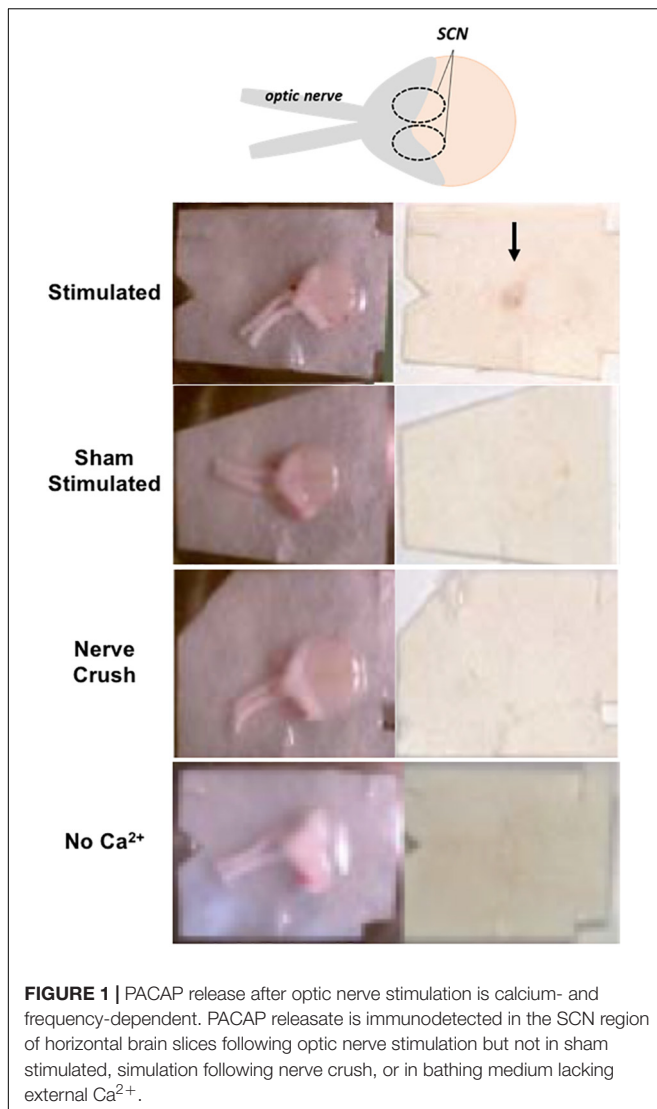
The results above establish a correlation between firing frequency of the retinohypothalamic inputs to the SCN, and PACAP release within the SCN itself. Thus, the circadian dependence of glutamate administration to trigger late-night phase shifting would be expected to show PACAP dependence in a system in which endogenous PACAP expression could be independently manipulated. We turned to the mouse *ex vivo* SCN slice preparation in order to answer this question.

Distribution and Glutamatergic Phenotype of PACAPergic Fibers to SCN in the Mouse

Pituitary adenylate cyclase-activating polypeptide innervation of the mouse SCN is coincident with the expression of VGLUT2 in SCN terminals (Figure 2A). Importantly, after removal of PACAP (i.e., in PACAP-deficient mice) the pattern of innervation by VGLUT2, and the pattern of expression of VIP in the cells of the SCN itself is unchanged (Figure 2B), demonstrating the SCN in PACAP-deficient mice remains essentially unchanged, save for the absence of PACAP itself. In addition, RHT innervation of the mouse SCN appears similar to that of other rodent species, and justifies at least limited generalization about the pattern and purpose of retinohypothalamic innervation of the SCN originating in intrinsically photosensitive retinal ganglion cells (ipRGCs) (Keenan et al., 2016).

Spontaneous Electrical Firing Rate Shifts Mirror Behavioral Rhythm Activity of SCN in the Mouse

Firing-rate patterns can be used to determine subjective time following chemical treatment of SCN that have been removed from mice and maintained in culture. This allows the examination of phase shifting following chemical application directly to SCN, despite the absence of wheel – running activity. As in behavioral experiments, untreated slices of wild-type, biorbitaly enucleated wild-type, and PACAP-deficient mice were recorded to determine whether and when each showed a spontaneous peak of firing-rate frequency. Each exhibited peaks between CT 6 and 7 [wild-type: CT 6.25 ± 0.12 h, PACAP-null: CT 6.54 ± 0.07 h (Figure 3); enucleated: CT 6.58 ± 0.17 ;

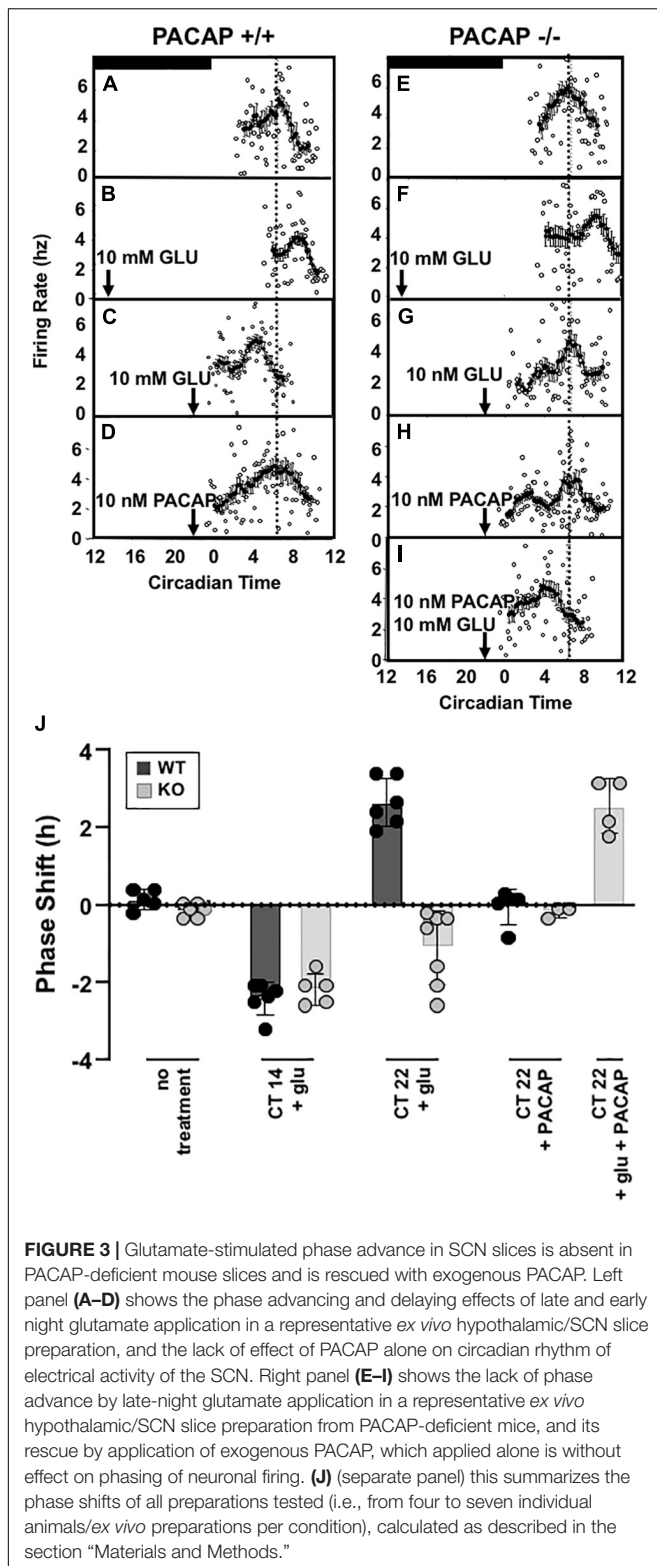


mean \pm SEM, $n = 5-6$]. These are consistent with previous electrical recordings in rat and mouse *ex vivo* hypothalamic slices (Green and Gillette, 1982; Shibata et al., 1982; Prosser et al., 1989; Burgoon et al., 2004). With these baseline characteristics established in the brain-slice preparation, we wished to determine whether exposure to glutamate would induce shifts in firing-rate patterns in slices, as exposure to light shifts wheel-running patterns in intact animals.

Applying glutamate to SCN of wild-type and PACAP-null mice is an approximation of natural phase shifting, but one step further “downstream” from simple light exposure. By isolating and exposing the SCN, neurotransmitters such as glutamate may be applied and SCN activity observed directly. To test whether or not PACAP-null mice would show intact shifts to direct glutamate application, we examined the glutamate responsiveness of wild-type and PACAP null mice at selected time-points of the early (CT 14) and late (CT 22) night, to determine if the PACAP dependence of light-induced phase

advance in circadian rhythm we reported in intact mice would persist in the *ex vivo* preparation. In that case, potential indirect effects of PACAP deficiency on SCN function, such as impaired sensory transduction from the retina secondary to pupillary reflex impairment, could be eliminated. SCN from wild-type mice respond to glutamate during the subjective night in a manner parallel to the response of intact animals to light in the mouse, as in the rat (Ding et al., 1994), with significant phase delays at CT 14 (Ding et al., 1994) and phase advances at CT 22 (2.81 ± 0.26 h, $n = 5$, **Figure 3**).

Consistent with results from wheel-running experiments, PACAP-deficient mice showed robust phase delays (131.5 ± 11.2 min, $n = 5$) in response to glutamate stimulation at CT 14. These delays were significantly different from untreated slices ($p < 0.001$ for each, *t*-test) but not significantly different from shifts seen in SCN, from wild-type mice, treated with glutamate at CT14 ($p > 0.2$, n.s., *t*-test). In contrast to the shifts seen in early night, and consistent with behavioral results, SCN



from PACAP-null mice failed to show the robust phase advance response to application of glutamate at CT22 seen in slices from wild-type mice. Thus, PACAP-deficient mouse slices showed

phase delays in response to glutamate at CT14 (75.5 ± 23.8 min, $p < 0.001$), but not phase advances in response to glutamate at CT22 (Figure 3). These shifts replicate alterations in light-responsiveness in intact, behaving mice, supporting the use of the brain-slice preparation to study further the mechanisms of PACAP-glutamate co-transmission in phase modulation of SCN rhythmicity.

Exogenous PACAP Rescues Late Night Phase Advancing Activity in PACAP-Null Mice

The results described above strongly suggest that PACAP plays an integral role in phase advances in response to light and glutamate during late night phase advance, but not early night phase delay. This is largely consistent with results seen in PAC1-R null mice (Hannibal et al., 2001a), but is not the same as results seen in other PACAP-null mouse models which demonstrate a diminished phase delay in early night (Kawaguchi et al., 2003; Colwell et al., 2004). One of the potential confounds of any genetically ablated animal model is the potential for wide-ranging, non-specific alterations as a result of a genetic lesion present during the entire course of development. An alternate explanation for altered shifting might suggest that such non-specific developmental disruptions result in altered shifting in the absence of a critical role for PACAP during the normal course of phase resetting. Fortunately, the PACAP-null mouse model holds the capacity to test such a hypothesis. Because exogenous PACAP may be replaced in the brain-slice preparation, the potential for PACAP to restore normal responses to glutamate may be directly tested.

A 1 μ l drop of 10 nM PACAP does not shift either wild-type or PACAP-null SCN slices when applied alone at CT 22. Peak times were not distinguishable from untreated slices ($p > 0.2$, not significant, Figure 3E). It has already been seen that 10 mM glutamate induces phase delays in PACAP-null mice. However, 10 nM PACAP, applied with 10 mM glutamate at CT 22, restored phase advances in PACAP-null mice that were significantly different than both untreated slices and slices treated only with PACAP, but not statistically different than those seen in wild-type mice (shift = 153.9 ± 21.1 min, $p > 0.2$, Figure 3).

Data accrued for individual experiments shown in Figure 3 are summarized in Figure 3J, where the overall early and late-night phase shifts induced by glutamate in wild-type and PACAP-null mice, and the effects of PACAP in rescuing defects in each case, are depicted graphically.

Dose-Response of PACAP Replacement on Glutamate-Induced Phase Shifting in PACAP-Null Mice

In order to examine glutamate signaling in the absence of confounding effects of PACAP, glutamate and PACAP were co-applied in PACAP-null mice using 1 pM and 10 nM PACAP concentrations, doses that had previously been shown to have no significant shifting effect on the clock. 10 nM PACAP, applied with 10 mM glutamate at CT 22, restored phase advances in

PACAP-null mice that were not statistically significantly different than those seen in wild-type mice (shift = 153.9 ± 21.1 min, $p > 0.2$). Co-application of glutamate and 1 pM PACAP also resulted in phase shifts, but these shifts were substantially larger than those induced by glutamate in wild-type mice (shift = 264.5 ± 34.6 min). These shifts were significantly larger than those seen either in glutamate-treated wild-type mice ($p \leq 0.014$) or PACAP-null mice exposed to glutamate and 10 nM PACAP ($p \leq 0.035$) (Figure 4).

Adult Lesion of PACAP via Biorbital Enucleation Demonstrates Similar Results to the PACAP-Null Mice

The importance of the retinal input of PACAP, rather than PACAP innervation from other sources, on the phase advance is demonstrated by the lack of a phase advance with glutamate application at CT 22 in SCN from biorbitally enucleated mice. These displayed no significant difference in their peak in firing rate between untreated (CT 6.58 ± 0.17) and those treated with a 10 mM glutamate application at CT 22 (CT 6.83 ± 0.20), unless PACAP was added to the preparation during glutamate administration (CT 3.83 ± 0.30) (Figure 5).

Glutamate-Induced pCREB Induction Is Attenuated in PACAP-Null Mice

As seen in other rodents (Ginty et al., 1993; Ding et al., 1997; McNulty et al., 1998; von Gall et al., 1998; Tischkau et al., 2003), glutamate treatment in wild-type mice elicited a significant two to threefold induction in phosphorylation of CREB (2.69 ± 0.51 -fold induction vs. untreated $p \leq 0.01$, $n = 5$). In PACAP-null mice, a slight induction was noted, although this induction was not significant. The lack of induction of pCREB in PACAP-null mice demonstrates a role for PACAP in the known internal signal transduction pathways stimulated by glutamate (Figure 6).

PACAP mRNA Expression in Retina Across the Circadian Period

The expression of endogenous PACAP in the retina has not previously been examined in C57Bl6 mice, although previous studies in PACAP-deficient and wild-type C57Bl6 mice have assumed that PACAP mRNA and peptide are expressed in ipRGCs of mice, and in this mouse strain, as previously reported in the rat, and as well, EGFP expression is found in ipRGCs of PACAP-EGFP transgenic mice (Condro et al., 2016). Surprisingly, we found a wide range in the intensity and number of PACAP mRNA-positive cells in the retina sampled at various times, and performed a systematic study across the circadian period to characterize this variation. The number of PACAP mRNA-positive ipRGCs increases dramatically during subjective night, compared to subjective day in the C57Bl/6N strain used in these studies (Figure 7). Changes in PACAP expression across the day have not previously been reported in any rodent species including mouse and rat, and further examination of this phenomenon in both rats and mice appears warranted.

DISCUSSION

The ability of the clock to entrain to external light and darkness is dependent upon photic transmission from eyes to the SCN via a subset of RGCs. Glutamate is accepted as a first message carrying light information from the RGCs to the SCN; however, the distribution of melanopsin in the RGCs reaching the SCN was also found to be identical to that for PACAP (Hannibal et al., 2002), implying a role for PACAP in light-entrainment of the clock. Investigations of PACAP and glutamate in circadian photic entrainment have revealed that these neuromodulators are co-stored in RGCs with innervation in the SCN (Hannibal et al., 2000).

Here, we have extended the detailed examination of the PACAP dependence of light-induced phase shifting *in vivo*, to the SCN slice preparation *ex vivo*. Firing-rate patterns are used to determine subjective time following chemical treatment of SCN that have been removed and maintained *ex vivo*, allowing examination of phase shifting following chemical application directly to SCN tissue. Applying glutamate to SCN slices, *ex vivo*, of wild-type and PACAP-null mice is an approximation of natural phase shifting one step removed from retinal light exposure. Overall, phase shifts in electrical activity replicate alterations in light-responsiveness in intact, behaving mice.

We show here that in the mouse SCN *ex vivo*, glutamate drives both late-night and early-night light exposure effects on circadian rhythm, and that the effect on late-night phase advance, as in the mouse *in vivo*, is PACAP-dependent, demonstrating that these phase-shifting modulatory effects of PACAP are dependent not on visual, but on non-visual photic sensory input to the SCN. The major expression of PACAP in the SCN is due to efferent connections from the retina via the RHT (Hannibal et al., 1998; Hannibal and Fahrenkrug, 2004). Severing the optic nerves and allowing degeneration of those nerves produces a PACAP “knockout” limited to the retinohypothalamic input to the SCN *in vivo*, and subsequently in the SCN-containing hypothalamic slice. We have recapitulated the effects of PACAP deficiency in hypothalamic slices from enucleated wild-type mice, in which retinohypothalamic inputs have degenerated, to demonstrate that it is specifically PACAP supplied from these inputs, rather than from other hypothalamic regions projecting to SCN, that is responsible for the modulation of glutamate-dependent non-visual photic regulation of circadian rhythmicity in SCN.

The results obtained here strongly suggest that PACAP plays an integral role in wild-type phase advances in response to light and glutamate during the late night. Our findings are inconsistent with a critical role of PACAP during the early night, as PACAP-null mice respond to light and glutamate with the same direction and magnitude of shift as wild-type mice despite the lack of PACAP expression. This is largely consistent with results seen in PAC1-R-deficient mice (Hannibal et al., 2001a), but is not the same as results seen in other PACAP-deficient mouse models (Kawaguchi et al., 2003; Colwell et al., 2004). One of the potential confounds of any genetically ablated animal model is the potential for wide-ranging, non-specific alterations as a result of a genetic lesion present during the entire course of development. An alternate explanation for altered shifting might

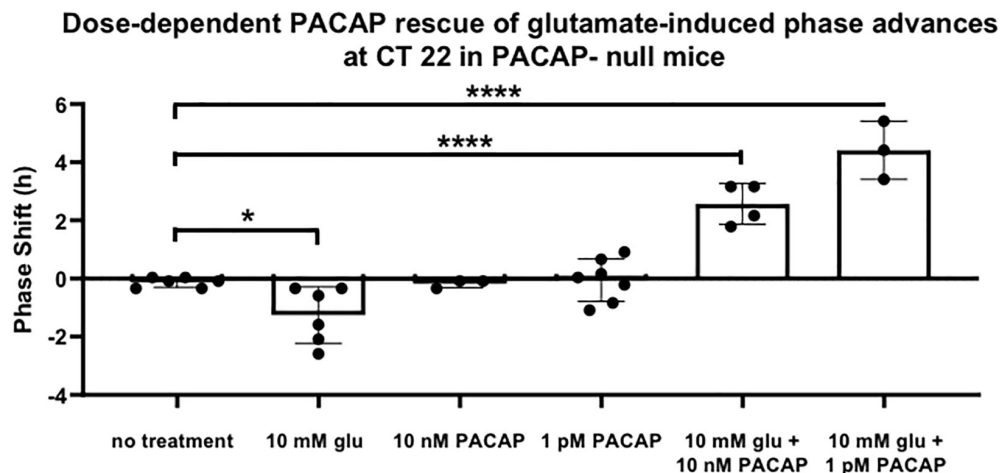


FIGURE 4 | PACAP rescues phase advances in PACAP-null mice with magnitudes that are dose-dependent. Neither glutamate nor PACAP induce phase advances when applied alone to PACAP-null SCN brain slices at CT 22. When they are applied together, they induce phase advances that are inversely related to PACAP dose. One-way ANOVA, Dunnett's *post hoc* test. * $p < 0.05$, **** $p < 0.0001$.

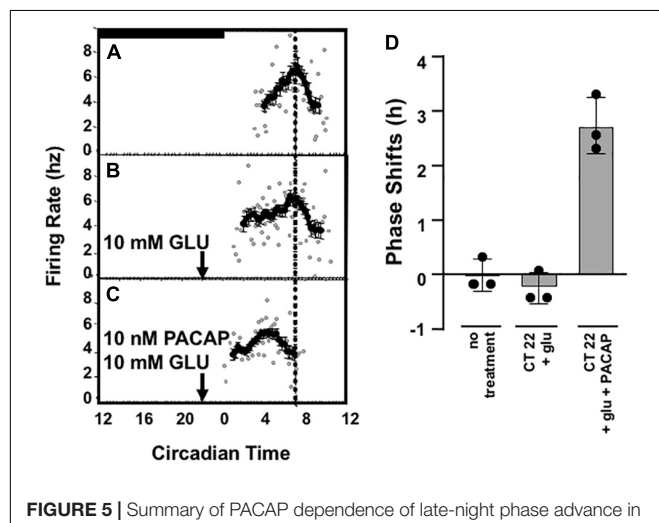


FIGURE 5 | Summary of PACAP dependence of late-night phase advance in slices from enucleated wild-type C57Bl/6 mice. Panels (A–C) depict PACAP dependence of glutamate-induced late-night phase advance using the doses of glutamate and PACAP shown to best mimic physiological phase-advance (i.e., phase advance observed *in vivo* in C57Bl/6 mice). Panel (D) summarizes the phase shift data obtained from preparations from three separate animals for each treatment condition. In enucleated mice, treatment with glutamate + PACAP is significantly induced as compared to no treatment or with glutamate alone. $p < 0.001$, One-way ANOVA, Tukey *post-hoc* test.

suggest that such non-specific developmental disruptions result in altered shifting in the absence of a critical role for PACAP during the normal course of phase resetting. Fortunately, the PACAP-deficient mouse model holds the capacity to test such a hypothesis. Because exogenous PACAP may be replaced in the brain-slice preparation, the potential for PACAP to restore normal responses to glutamate could be directly tested.

The data from these experiments are furthermore consistent with a surprisingly specific sensitivity of the SCN to PACAP.

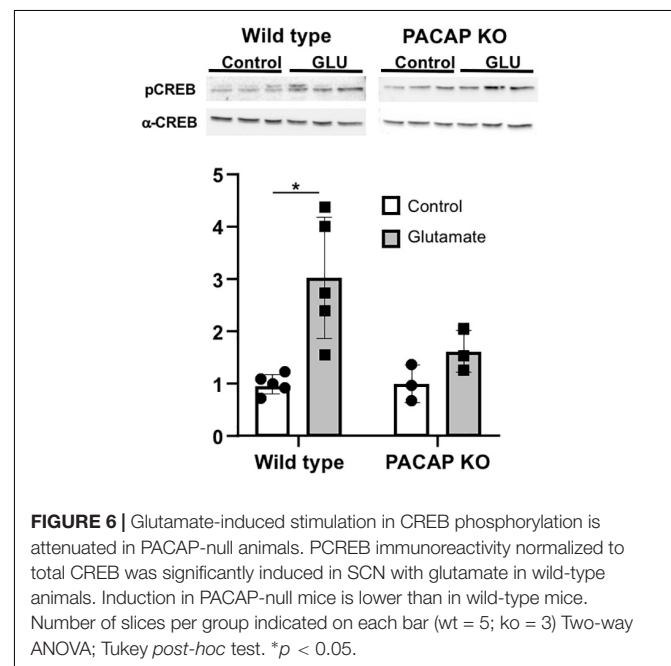
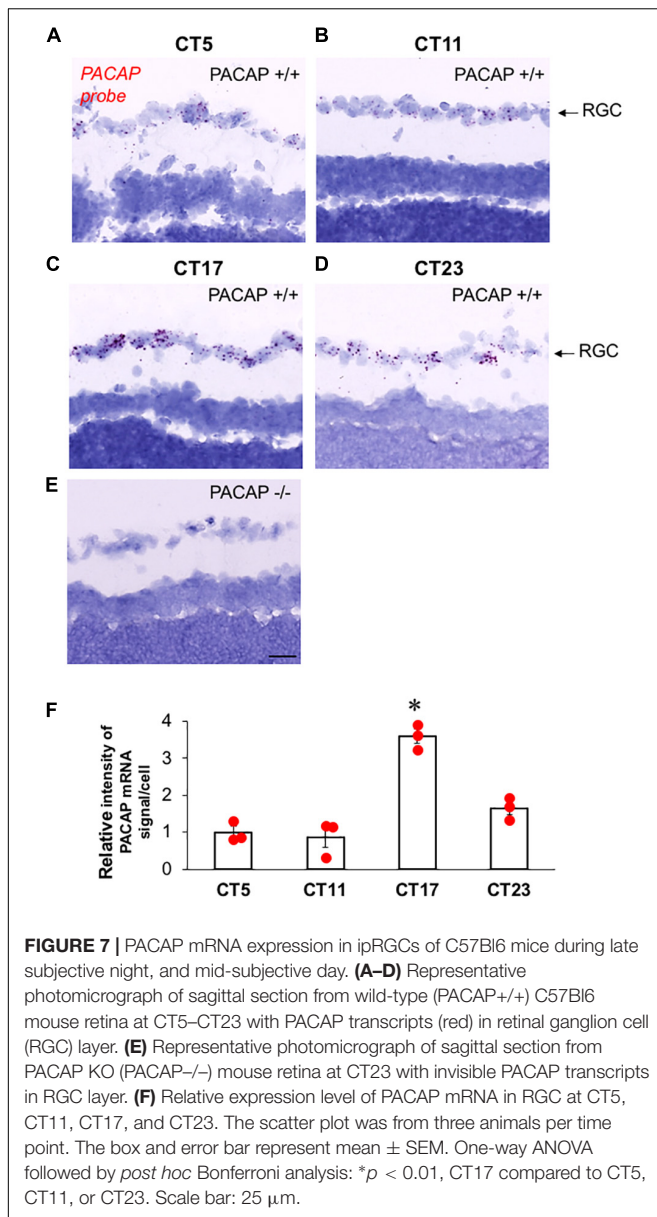


FIGURE 6 | Glutamate-induced stimulation in CREB phosphorylation is attenuated in PACAP-null animals. PCREB immunoreactivity normalized to total CREB was significantly induced in SCN with glutamate in wild-type animals. Induction in PACAP-null mice is lower than in wild-type mice. Number of slices per group indicated on each bar (wt = 5; ko = 3) Two-way ANOVA; Tukey *post-hoc* test. * $p < 0.05$.

The circadian clock, although able to maintain a near-24-h rhythm and appropriately delay during the early night, is nonetheless critically damaged during the late night in mice lacking PACAP. Replacing PACAP directly on the SCN brain slice, at only the time of glutamate application, and only in the area of the SCN, is sufficient to rescue wild-type shifting in the presence of glutamate. The most parsimonious conclusion supported by these data is that PACAP (or part of its signaling cascade) interacts with glutamate to shift the endogenous rhythm of the mammalian SCN during the late night. It will be of particular interest to examine in the *ex vivo* hypothalamic explant preparation the phenocopying of phase-shifting effects of



downstream components of glutamate signaling, such as cAMP and cGMP signaling (Tischkau et al., 2000, 2003), and their PACAP dependence, as this should provide valuable insights into how PACAP acts post-synaptically to allow glutamate phase-advance to occur in this preparation and, presumably, *in vivo*.

It will also be of critical interest to compare the effects of PACAP on pupillary constriction in the eye, apparently independently of glutamate transmission, and phase-shifting at the level of the SCN. Is PACAP released all night, or only when the SCN seems to require it? This question is of particular relevance in view of our novel observation of a circadian rhythm to the expression of PACAP itself (i.e., its mRNA) in the ipRGC, with significantly higher levels during subjective night than during subjective day. What is the intracellular response of PACAP as a function of time of day, as its receptor(s) appear to be

present throughout the day, and how does it interact with that of glutamate? Do all (or any) light pulses cause PACAP release, and when throughout the day is PACAP actually available for release in response to photic stimulation? The experimental system employed here affords the opportunity to study the nature of co-transmission in advances and delays more intimately, as well as to obtain greater insight into the mechanisms of species differences in phase shifting in response to light.

It is worthy of comment that the altered phase-shifting seen in these experiments reported here is similar to the results originally reported regarding mice with an altered PACAP receptor (PAC1-R). PAC1-R-null mice showed early-night responses that were similar to wild-type mice (although light-pulses at CT 20 induced longer delays in the PAC-1-R null mice). During the late night (CT23), however, PAC1-R-nulls showed phase delays opposite to the advances seen in wild-type mice (Hannibal et al., 2001a). These data are consistent with our previous results (Beaule et al., 2009).

How does PACAP modulation of glutamate signaling in SCN, and therefore potentially at other CNS synapses, compare to what is known about PACAP signaling from cell culture and other experiments? We have reported preliminarily (Zhang et al., 2018; Society for Neuroscience Annual Meeting, San Diego, CA, United States, November 2018) that PACAP seems to act downstream of glutamate signaling for late-night phase advance, in that the phase-shifting effects of cGMP, elevated by and mimicking the *ex vivo* effects of glutamate itself, are likewise blocked in PACAP-deficient slices, and this impairment is removed by direct application of PACAP together with glutamate at subjective late-night in the mouse SCN *ex vivo*. Other reports suggest that PACAP acts (Darvish and Russell, 1998; Chen et al., 1999; Michel et al., 2006) via non-specific calcium channel opening, downstream of elevation of cAMP, acknowledged to be the major intracellular effect of stimulation of the PAC1, VPAC1, and VPAC2 receptors through which PACAP acts. The fact that the modulatory effects of PACAP in “wild-type” SCN slices *ex vivo* can be restored, in PACAP-deficient mice, by addition of exogenous PACAP strongly suggests that, at least in the SCN, the effects of PACAP may be mediated either by glutamate-stimulated PACAP release at intact retinohypothalamic (psRGC) nerve terminals in the *ex vivo* preparation, or that a low level of spontaneous PACAP release is sufficient to “prime” late-night phase advancing effects within the SCN. In addition to concerted post-synaptic effects of glutamate and PACAP at this and other synapses, the possibility exists that PACAP modulates glutamate effects post-synaptically via PAC1-mediated activation of astroglial inputs at the post-synapse (Miyata Review, ANYAS, in press). PACAP also acts directly, in neurons and endocrine cells, to activate the mitogen-activated protein kinase ERK (Frödin et al., 1994; Barrie et al., 1997; Hashimoto et al., 2003; Butcher et al., 2005; Gerdin and Eiden, 2007; Ravi et al., 2008; Emery and Eiden, 2012; May et al., 2014), and this has recently been shown to occur via a novel cAMP effector, NCS-Rapgef2 (Emery et al., 2013; Missig et al., 2014, 2015). In any event, it seems that PACAP signaling may well shape glutamate responsivity, in addition to its own potential wholly independent effects at synapses at which there is no evidence

for glutamate co-transmission. It remains for future research to link glutamate/PACAP co-signaling to the effects of PACAP on metaplasticity in hippocampus (Macdonald et al., 2005; MacDonald et al., 2007; Costa et al., 2008), in fear processing in amygdala and hippocampus (Hammack and May, 2015; Schmidt et al., 2015), cocaine relapse in BNST (Miles et al., 2016, 2017), and multiple effects in projections from frontal cortex (Crestani et al., 2013).

As mentioned above, identifying the possible locus of PACAP action in modulation of glutamatergic signaling in the SCN by examining the PACAP dependence of late-night phase-shifting by downstream messengers activated by glutamate in SCN will be an important next step forward in full understanding of this glutamate-PACAP co-modulatory system (Gillette and Mitchell, 2002). At this time, we suggest that PACAP's physiological role, regardless of its mode of action, is to augment this signaling pathway during times when glutamate stimulation alone is insufficient. How and why PACAP expression waxes and wanes throughout the day in pigmented retina, and if this pattern is functionally related to PACAP circadian function, is a compelling question for future investigation, both for understanding of the full effects of retinal photosensitivity on sensory information processing and behavior in mammalian species, and for determining if the retinohypothalamic projection to the SCN is paradigmatic for PACAP neurotransmission in other brain regions.

DATA AVAILABILITY STATEMENT

All datasets generated for this study are included in the article/supplementary material.

REFERENCES

- Abbott, S. M. (2005). *Regulation of Circadian Rhythms by Sleep-Wake Centers in the Brainstem and Basal Forebrain*. Champaign, IL: University of Illinois.
- Atkins, N. Jr, Ren, S., Hatcher, N., Burgoon, P. W., Mitchell, J. W., Sweedler, J. V., et al. (2018). Functional peptidomics: stimulus- and time-of-day-specific peptide release in the mammalian circadian clock. *ACS Chem. Neurosci.* 9, 2001–2008. doi: 10.1021/acscchemneuro.8b00089
- Aton, S. J., Colwell, C. S., Harmar, A. J., Waschek, J., and Herzog, E. D. (2005). Vasoactive intestinal polypeptide mediates circadian rhythmicity and synchrony in mammalian clock neurons. *Nat. Neurosci.* 8, 476–483. doi: 10.1038/nn1419
- Barrie, A. P., Clohessy, A. M., Buensuceso, C. S., Rogers, M. V., and Allen, J. M. (1997). Pituitary adenylyl cyclase-activating peptide stimulates extracellular signal-regulated kinase 1 or 2 (ERK1/2) activity in a ras-independent, mitogen-activated protein kinase/ERK kinase 1 or 2-dependent manner in PC12 cells. *J. Biol. Chem.* 272, 19666–19671. doi: 10.1074/jbc.272.32.19666
- Beaulieu, C., Mitchell, J. W., Lindberg, P. T., Damadzic, R., Eiden, L. E., and Gillette, M. U. (2009). Temporally restricted role of retinal PACAP: integration of the phase-advancing light signal to the SCN. *J. Biol. Rhythms* 24, 126–134. doi: 10.1177/0748730409332037
- Buchanan, G. F. (2002). *Cholinergic Regulation of the Mammalian Circadian System: Analysis of Cholinergic-Induced Phase Shifting in vivo and in vitro in Wildtype and M1 Knockout Mice*. Champaign, IL: University of Illinois at Urbana-Champaign.

ETHICS STATEMENT

The animal study was reviewed and approved by the University of Illinois at Urbana-Champaign and the National Institutes of Health.

AUTHOR CONTRIBUTIONS

PL, JM, PB, CB, EW, MS, LE, and SJ contributed to the experimental data. LE, MG, JM, PL, and SJ wrote the manuscript.

FUNDING

This work was generously supported from the National Institutes of Health (United States): GM07143 (PL), NS11158 (JM), and HL08670, NS22155, and MH117377 (MG); from the Fonds de Recherche sur la Nature et les Technologies (Government of Québec) and Canadian Institutes of Health Research (CIHR) (CB); and from the NIMH-IRP: MH002386-21 (LE).

ACKNOWLEDGMENTS

We thank Jens Hannibal, Department of Clinical Biochemistry, Bispebjerg Hospital, Copenhagen, Denmark, for the kind gift of the PACAP antibody used for PACAP release experiments reported here. We also thank Dr. Limei Zhang, UNAM, for critical comments on the manuscript during preparation and Ms. Ann C. Benefiel, University of Illinois, for assistance with submission of the manuscript.

- Buchanan, G. F., and Gillette, M. U. (2005). New light on an old paradox: site-dependent effects of carbachol on circadian rhythms. *Exp. Neurol.* 193, 489–496. doi: 10.1016/j.expneurol.2005.01.008
- Burgoon, P. W., Lindberg, P. T., and Gillette, M. U. (2004). Different patterns of circadian oscillation in the suprachiasmatic nucleus of hamster, mouse, and rat. *J. Comp. Physiol. A Neuroethol. Sens. Neural. Behav. Physiol.* 190, 167–171. doi: 10.1007/s00359-003-0486-z
- Butcher, G. Q., Lee, B., Cheng, H.-Y. M., and Obrietan, K. (2005). Light stimulates MSK1 activation in the suprachiasmatic nucleus via a PACAP-ERK/MAP kinase-dependent mechanism. *J. Neurosci.* 25, 5305–5313. doi: 10.1523/jneurosci.4361-04.2005
- Chen, D., Buchanan, G. F., Ding, J. M., Hannibal, J., and Gillette, M. U. (1999). Pituitary adenylyl cyclase-activating peptide: a pivotal modulator of glutamatergic regulation of the suprachiasmatic circadian clock. *Proc. Natl. Acad. Sci. U.S.A.* 96, 13468–13473. doi: 10.1073/pnas.96.23.13468
- Colwell, C. S., Michel, S., Itri, J., Rodriguez, W., Tam, J., Lelievre, V., et al. (2004). Selective deficits in the circadian light response in mice lacking PACAP. *Am. J. Physiol. Regul. Integr. Comp. Physiol.* 287, R1194–R1201.
- Condro, M. C., Matynia, A., Foster, N. N., Ago, Y., Rajbhandari, A. K., Jayaram, B., et al. (2016). High-resolution characterization of a PACAP-EGFP transgenic mouse model for mapping PACAP-expressing neurons. *J. Comp. Neurol.* 524, 3827–3848. doi: 10.1002/cne.24035
- Costa, L., Santangelo, F., Li Volsi, G., and Ciranna, L. (2008). Modulation of AMPA receptor-mediated ion current by pituitary adenylyl cyclase-activating polypeptide (PACAP) in CA1 pyramidal neurons from rat hippocampus. *Hippocampus* 19, 99–109. doi: 10.1002/hipo.20488

- Crestani, C. C., Alves, F. H., Gomes, F. V., Resstel, L. B., Correa, F. M., and Herman, J. P. (2013). Mechanisms in the bed nucleus of the stria terminalis involved in control of autonomic and neuroendocrine functions: a review. *Curr. Neuropharmacol.* 11, 141–159. doi: 10.2174/1570159X11311020002
- Cutler, D. J., Haraura, M., Reed, H. E., Shen, S., Sheward, W. J., Morrison, C. F., et al. (2003). The mouse VPAC2 receptor confers suprachiasmatic nuclei cellular rhythmicity and responsiveness to vasoactive intestinal polypeptide in vitro. *Eur. J. Neurosci.* 17, 197–204. doi: 10.1046/j.1460-9568.2003.02425.x
- Darvish, N., and Russell, J. T. (1998). Neurotransmitter-induced novel modulation of a nonselective cation channel by a cAMP-dependent mechanisms in rat pineal cells. *J. Neurophysiol.* 79, 2546–2556. doi: 10.1152/jn.1998.79.5.2546
- Ding, J. M., Chen, D., Weber, E. T., Faiman, L. E., Rea, M. A., and Gillette, M. U. (1994). Resetting the biological clock: mediation of nocturnal circadian shifts by glutamate and NO. *Science* 266, 1713–1717. doi: 10.1126/science.7527589
- Ding, J. M., Faiman, L. E., Hurst, W. J., Kuriashkina, L. R., and Gillette, M. U. (1997). Resetting the biological clock: mediation of nocturnal CREB phosphorylation via light, glutamate, and nitric oxide. *J. Neurosci.* 17, 667–675. doi: 10.1523/jneurosci.17-02-00667.1997
- Emery, A., Eiden, M. V., Mustafa, T., and Eiden, L. E. (2013). GPCR-Gs signaling to ERK is controlled by the cAMP-sensing guanine nucleotide exchange factor NCS/Rapgef2 in neuronal and endocrine cells. *Sci. Signal.* 6:ra51. doi: 10.1126/scisignal.2003993
- Emery, A. C., and Eiden, L. E. (2012). Signaling through the neuropeptide GPCR PAC1 induces neuritogenesis via a single linear cAMP- and ERK-dependent pathway using a novel cAMP sensor. *FASEB J.* 26, 3199–3211. doi: 10.1096/fj.11-203042
- Frödin, M., Peraldi, P., and Van Obberghen, E. (1994). Cyclic AMP activates the mitogen-activated protein kinase cascade in PC12 cells. *J. Biol. Chem.* 269, 6207–6214.
- Gerdin, M. J., and Eiden, L. E. (2007). Regulation of PC12 cell differentiation by cAMP signaling to ERK independent of PKA: do all the connections add up? *Sci. STKE* 2007:15.
- Gillette, M. U. (1986). The suprachiasmatic nuclei: circadian phase-shifts induced at the time of hypothalamic slice preparation are preserved in vitro. *Brain Res.* 379, 176–181. doi: 10.1016/0006-8993(86)90273-8
- Gillette, M. U., and Mitchell, J. W. (2002). Signaling in the suprachiasmatic nucleus: selectively responsive and integrative. *Cell Tissue Res.* 309, 99–107. doi: 10.1007/s00441-002-0576-1
- Gillette, M. U., and Prosser, R. A. (1988). Circadian rhythm of the rat suprachiasmatic brain slice is rapidly reset by daytime application of cAMP analogs. *Brain Res.* 474, 348–352. doi: 10.1016/0006-8993(88)90449-0
- Ginty, D. D., Kornhauser, J. M., Thompson, M. A., Bading, H., Mayo, K. E., Takahashi, J. S., et al. (1993). Regulation of CREB phosphorylation in the suprachiasmatic nucleus by light and a circadian clock. *Science* 260, 238–241. doi: 10.1126/science.8097062
- Green, D. J., and Gillette, R. (1982). Circadian rhythm of firing rate recorded from single cells in the rat suprachiasmatic brain slice. *Brain Res.* 245, 198–200. doi: 10.1016/0006-8993(82)90361-4
- Hamelink, C., Tjurmina, O., Damadzic, R., Young, W. S., Weihe, E., Lee, H. W., et al. (2002). Pituitary adenylate cyclase-activating polypeptide is a sympathoadrenal neurotransmitter involved in catecholamine regulation and glucocorticosteroidogenesis. *Proc. Natl. Acad. Sci. U.S.A.* 99, 461–466. doi: 10.1073/pnas.012608999
- Hammack, S. E., and May, V. (2015). Pituitary adenylate cyclase activating polypeptide in stress-related disorders: data convergence from animal and human studies. *Biol. Psychiatry* 78, 167–177. doi: 10.1016/j.biopsych.2014.12.003
- Hannibal, J., Ding, J. M., Chen, D., Fahrenkrug, J., Larsen, P. J., Gillette, M. U., et al. (1997). Pituitary adenylate cyclase-activating peptide (PACAP) in the retinohypothalamic tract: a potential daytime regulator of the biological clock. *J. Neurosci.* 17, 2637–2644. doi: 10.1523/jneurosci.17-07-02637.1997
- Hannibal, J., Ding, J. M., Chen, D., Fahrenkrug, J., Larsen, P. J., Gillette, M. U., et al. (1998). Pituitary adenylate cyclase activating peptide (PACAP) in the retinohypothalamic tract: a daytime regulator of the biological clock. *Ann. N. Y. Acad. Sci.* 865, 197–206. doi: 10.1111/j.1749-6632.1998.tb11179.x
- Hannibal, J., and Fahrenkrug, J. (2004). Target areas innervated by PACAP-immunoreactive retinal ganglion cells. *Cell Tissue Res.* 316, 99–113. doi: 10.1007/s00441-004-0858-x
- Hannibal, J., Hindersson, P., Knudsen, S. M., Georg, B., and Fahrenkrug, J. (2002). The photopigment melanopsin is exclusively present in pituitary adenylate cyclase-activating polypeptide-containing retinal ganglion cells of the retinohypothalamic tract. *J. Neurosci.* 22:RC191.
- Hannibal, J., Jørgensen, F., Nielsen, H. S., Journot, L., Brabet, P., and Fahrenkrug, J. (2001a). Dissociation between light-induced phase shift of the circadian rhythm and clock gene expression in mice lacking the pituitary adenylate cyclase activating polypeptide type 1 receptor. *J. Neurosci.* 21, 4883–4890. doi: 10.1523/jneurosci.21-13-04883.2001
- Hannibal, J., Vrang, N., Card, J. P., and Fahrenkrug, J. (2001b). Light-dependent induction of cFos during subjective day and night in PACAP-containing ganglion cells of the retinohypothalamic tract. *J. Biol. Rhythms* 16, 457–470. doi: 10.1177/074873001129002132
- Hannibal, J., Møller, M., Ottersen, O. P., and Fahrenkrug, J. (2000). PACAP and glutamate are co-stored in the retinohypothalamic tract. *J. Comp. Neurol.* 418, 147–155. doi: 10.1002/(sici)1096-9861(20000306)418:2<147::aid-cne2>3.0.co;2-#
- Harmar, A. J., Marston, H. M., Shen, S., Spratt, C., West, K. M., Sheward, W. J., et al. (2002). The VPAC2 receptor is essential for circadian function in the mouse suprachiasmatic nuclei. *Cell* 109, 497–508. doi: 10.1016/s0092-8674(02)00736-5
- Harrington, M. E., Hoque, S., Hall, A., Golombek, D., and Biello, S. (1999). Pituitary adenylate cyclase activating peptide phase shifts circadian rhythms in a manner similar to light. *J. Neurosci.* 19, 6637–6642. doi: 10.1523/jneurosci.19-15-06637.1999
- Hashimoto, H., Kunugi, A., Arakawa, N., Shintani, N., Fujita, T., Kasai, A., et al. (2003). Possible involvement of a cyclic AMP-dependent mechanism in PACAP-induced proliferation and ERK activation in astrocytes. *Biochem. Biophys. Res. Commun.* 311, 337–343. doi: 10.1016/j.bbrc.2003.10.005
- Kawaguchi, C., Tanaka, K., Isojima, Y., Shintani, N., Hashimoto, H., Baba, A., et al. (2003). Changes in light-induced phase shift of circadian rhythm in mice lacking PACAP. *Biochem. Biophys. Res. Commun.* 310, 169–175. doi: 10.1016/j.bbrc.2003.09.004
- Keenan, W. T., Rupp, A. C., Ross, R. A., Somasundaram, P., Hiriyanna, S., Wu, Z., et al. (2016). A visual circuit uses complementary mechanisms to support transient and sustained pupil constriction. *eLife* 5:e15392. doi: 10.7554/eLife.15392
- Macdonald, D. S., Weerapura, M., Beazely, M. A., Martin, L., Czerwinski, W., Roder, J. C., et al. (2005). Modulation of NMDA receptors by pituitary adenylate cyclase activating peptide in CA1 neurons requires G α_q , protein kinase C, and activation of Src. *J. Neurosci.* 25, 11374–11384. doi: 10.1523/jneurosci.3871-05.2005
- MacDonald, J. F., Jackson, M. F., and Beazely, M. A. (2007). G protein-coupled receptors control NMDARs and metaplasticity in the hippocampus. *Biochim. Biophys. Acta* 1768, 941–951. doi: 10.1016/j.bbame.2006.12.006
- May, V., Buttolph, T. R., Girard, B. M., Clason, T. A., and Parsons, R. L. (2014). PACAP-induced ERK activation in HEK cells expressing PAC1 receptors involves both receptor internalization and PKC signaling. *Am. J. Physiol. Cell Physiol.* 306, C1068–C1079. doi: 10.1152/ajpcell.00001.2014
- McNulty, S., Schurov, I. L., Sloper, P. J., and Hastings, M. H. (1998). Stimuli which entrain the circadian clock of the neonatal Syrian hamster *in vivo* regulate the phosphorylation of the transcription factor CREB in the suprachiasmatic nucleus *in vitro*. *Eur. J. Neurosci.* 10, 1063–1072. doi: 10.1046/j.1460-9568.1998.00114.x
- Michel, S., Itri, J., Han, J. H., Gnietczynski, K., and Colwell, C. S. (2006). Regulation of glutamatergic signalling by PACAP in the mammalian suprachiasmatic nucleus. *BMC Neurosci.* 7:15. doi: 10.1186/1471-2202-7-15
- Miles, O., Thrallkill, E. A., Linden, A. K., May, V., Bouton, M. E., and Hammack, S. E. (2016). Cocaine self-Administration Alters Endogenous Pituitary Adenylate Cyclase Activating Peptide (PACAP) Levels in the Bed Nucleus of the Stria Terminalis (BNST). San Diego, CA: Society for Neuroscience.
- Miles, O. W., Thrallkill, E. A., Linden, A. K., May, V., Bouton, M. E., and Hammack, S. E. (2017). Pituitary adenylate cyclase-activating peptide in the bed nucleus of the stria terminalis mediates stress-induced reinstatement of cocaine seeking in rats. *Neuropsychopharmacology* 43, 978–986. doi: 10.1038/npp.2017.135

- Missig, G., Mei, L., Vizzard, M. A., Braas, K. M., Waschek, J. A., Ressler, K. J., et al. (2015). Parabrachial PACAP activation of amygdala endosomal ERK signaling regulates the emotional component of pain. *Biol. Psychiatr.* 81, 671–682. doi: 10.1016/j.biopsych.2016.08.025
- Missig, G., Roman, C. W., Vizzard, M. A., Braas, K. M., Hammack, S. E., and May, V. (2014). Parabrachial nucleus (PBN) pituitary adenylate cyclase activating polypeptide (PACAP) signaling in the amygdala: implication for the sensory and behavioral effects of pain. *Neuropharmacology* 86, 38–48. doi: 10.1016/j.neuropharm.2014.06.022
- Miyata, A., Arimura, A., Dahl, R. R., Minamino, N., Uehara, A., Jiang, L., et al. (1989). Isolation of a novel 38 residue-hypothalamic polypeptide which stimulates adenylate cyclase in pituitary cells. *Biochem. Biophys. Res. Commun.* 164, 567–574. doi: 10.1016/0006-291x(89)91757-9
- Okazaki, K., Itoh, Y., Ogi, K., Ohkubo, S., and Onda, H. (1995). Characterization of murine PACAP mRNA. *Peptides* 16, 1295–1299. doi: 10.1016/0196-9781(95)02018-r
- Panda, S., Sato, T. K., Castrucci, A. M., Rollag, M. D., DeGrip, W. J., Hogenesch, J. B., et al. (2002). Melanopsin (Opn4) requirement for normal light-induced circadian phase shifting. *Science* 298, 2213–2216. doi: 10.1126/science.1076848
- Piggins, H. D., Marchant, E. G., Goguen, D., and Rusak, B. (2001). Phase-shifting effects of pituitary adenylate cyclase activating polypeptide on hamster wheel-running rhythms. *Neurosci. Lett.* 305, 25–28. doi: 10.1016/s0304-3940(01)01796-7
- Prosser, R. A., and Gillette, M. U. (1989). The mammalian circadian clock in the suprachiasmatic nuclei is reset in vitro by cAMP. *J. Neurosci.* 9, 1073–1081. doi: 10.1523/jneurosci.09-03-01073.1989
- Prosser, R. A., and Gillette, M. U. (1991). Cyclic changes in cAMP concentration and phosphodiesterase activity in a mammalian circadian clock studied in vitro. *Brain Res.* 568, 185–192. doi: 10.1016/0006-8993(91)91396-i
- Prosser, R. A., McArthur, A. J., and Gillette, M. U. (1989). cGMP induces phase shifts of a mammalian circadian pacemaker at night, in antiphase to cAMP effects. *Proc. Natl. Acad. Sci. U.S.A.* 86, 6812–6815. doi: 10.1073/pnas.86.17.6812
- Ravni, A., Vaudry, D., Gerdin, M. J., Eiden, M. V., Falluel-Morel, A., Gonzalez, B., et al. (2008). A cAMP-dependent, PKA-independent signaling pathway mediating neuritogenesis through Egr1 in PC12 cells. *Mol. Pharmacol.* 73, 1688–1708. doi: 10.1124/mol.107.044792
- Reimer, M., Moller, K., Sundler, F., Hannibal, J., Fahrenkrug, J., and Kanje, M. (1999). Increased expression, axonal transport and release of pituitary adenylate cyclase-activating polypeptide in the cultured rat vagus nerve. *Neuroscience* 88, 213–222. doi: 10.1016/s0306-4522(98)00240-1
- Ruby, N. F., Brennan, T. J., Xie, X., Cao, V., Franken, P., Heller, H. C., et al. (2002). Role of melanopsin in circadian responses to light. *Science* 298, 2211–2213. doi: 10.1126/science.1076701
- Schafer, M. K., Mahata, S. K., Stroth, N., Eiden, L. E., and Weihe, E. (2010). Cellular distribution of chromogranin a in excitatory, inhibitory, aminergic and peptidergic neurons of the rodent central nervous system. *Regul. Pept.* 165, 36–44. doi: 10.1016/j.regpep.2009.11.021
- Schmidt, S. D., Myskiw, J. C., Furini, C. R., Schmidt, B. E., Cavalcante, L. E., and Izquierdo, I. (2015). PACAP modulates the consolidation and extinction of the contextual fear conditioning through NMDA receptors. *Neurobiol. Learn. Mem.* 118C, 120–124. doi: 10.1016/j.nlm.2014.11.014
- Shen, S., Spratt, C., Sheward, W. J., Kallo, I., West, K., Morrison, C. F., et al. (2000). Overexpression of the human VPAC2 receptor in the suprachiasmatic nucleus alters the circadian phenotype of mice. *Proc. Natl. Acad. Sci. U.S.A.* 97, 11575–11580. doi: 10.1073/pnas.97.21.11575
- Shibata, S., Oomura, Y., Kita, H., and Hattori, K. (1982). Circadian rhythmic changes of neuronal activity in the suprachiasmatic nucleus of the rat hypothalamic slice. *Brain Res.* 247, 154–158. doi: 10.1016/0006-8993(82)91041-1
- Tischkau, S. A., Gallman, E. A., Buchanan, G. F., and Gillette, M. U. (2000). Differential cAMP gating of glutamatergic signaling regulates long-term state changes in the suprachiasmatic circadian clock. *J. Neurosci.* 20, 7830–7837. doi: 10.1523/jneurosci.20-20-07830.2000
- Tischkau, S. A., Mitchell, J. W., Tyan, S. H., Buchanan, G. F., and Gillette, M. U. (2003). Ca2+/cAMP response element-binding protein (CREB)-dependent activation of Per1 is required for light-induced signaling in the suprachiasmatic nucleus circadian clock. *J. Biol. Chem.* 278, 718–723. doi: 10.1074/jbc.m209241200
- Vaudry, D., Gonzalez, B. J., Basille, M., Yon, L., Fournier, A., and Vaudry, H. (2000). Pituitary adenylate cyclase-activating polypeptide and its receptors: from structure to functions. *Pharmacol. Rev.* 52, 269–324.
- von Gall, C., Duffield, G. E., Hastings, M. H., Kopp, M. D., Dehghani, F., Korf, H. W., et al. (1998). “CREB in the mouse SCN: a molecular interface coding the phase-adjusting stimuli light, glutamate, PACAP, and melatonin for clockwork access. *J. Neurosci.* 18, 10389–10397. doi: 10.1523/jneurosci.18-24-10389.1998
- Zhang, L., Hernández, V. S., Weihe, E., Eiden, L. E., Jiang, S. Z., Lindberg, P. T., et al. (2018). *Conservation of Retinohypothalamic, Hippocampal, and Amygdalar PACAPergic Circuits in Mouse and Rat*. San Diego, CA: Society for Neuroscience Annual Meeting. Available at: <https://www.sfn.org/meetings/neuroscience-2018/abstracts/neuroscience-2018-abstracts>

Disclaimer: At least a portion of this work is authored by Lee E. Eiden on behalf of the U.S. Government and, as regards Dr. Eiden and the U.S. Government, is not subject to copyright protection in the United States. Foreign and other copyrights may apply.

Conflict of Interest: The authors declare that the research was conducted in the absence of any commercial or financial relationships that could be construed as a potential conflict of interest.

Citation: Lindberg PT, Mitchell JW, Burgoon PW, Beaulé C, Weihe E, Schäfer MK-H, Eiden LE, Jiang SZ and Gillette MU (2019) Pituitary Adenylate Cyclase-Activating Peptide (PACAP)-Glutamate Co-transmission Drives Circadian Phase-Advancing Responses to Intrinsically Photosensitive Retinal Ganglion Cell Projections by Suprachiasmatic Nucleus. *Front. Neurosci.* 13:1281. doi: 10.3389/fnins.2019.01281

Copyright © 2019 Lindberg, Mitchell, Burgoon, Beaulé, Weihe, Schäfer, Eiden, Jiang and Gillette. This is an open-access article distributed under the terms of the Creative Commons Attribution License (CC BY). The use, distribution or reproduction in other forums is permitted, provided the original author(s) and the copyright owner(s) are credited and that the original publication in this journal is cited, in accordance with accepted academic practice. No use, distribution or reproduction is permitted which does not comply with these terms.



The Roles of the Kisspeptin System in the Reproductive Physiology of the Lined Seahorse (*Hippocampus erectus*), an Ovoviviparous Fish With Male Pregnancy

Huixian Zhang¹, Bo Zhang^{1,2}, Geng Qin¹, Shuisheng Li³ and Qiang Lin^{1,2*}

¹ CAS Key Laboratory of Tropical Marine Bio-Resources and Ecology (LMB), Guangdong Provincial Key Laboratory of Applied Marine Biology (LAMB), South China Sea Institute of Oceanology, Institution of South China Sea Ecology and Environmental Engineering, Chinese Academy of Sciences, Guangzhou, China, ² University of Chinese Academy of Sciences, Beijing, China, ³ State Key Laboratory of Biocontrol, School of Life Sciences, Sun Yat-sen University, Guangzhou, China

OPEN ACCESS

Edited by:

Limei Zhang,
National Autonomous University
of Mexico, Mexico

Reviewed by:

Lee E. Eiden,
National Institutes of Health (NIH),
United States

Vito Salvador Hernandez,
National Autonomous University
of Mexico, Mexico

*Correspondence:

Qiang Lin
linqiang@scsio.ac.cn;
linqiangzsu@163.com

Specialty section:

This article was submitted to
Neuroendocrine Science,
a section of the journal
Frontiers in Neuroscience

Received: 11 September 2018

Accepted: 29 November 2018

Published: 11 December 2018

Citation:

Zhang H, Zhang B, Qin G, Li S
and Lin Q (2018) The Roles of the
Kisspeptin System
in the Reproductive Physiology of the
Lined Seahorse (*Hippocampus
erectus*), an Ovoviviparous Fish With
Male Pregnancy.
Front. Neurosci. 12:940.
doi: 10.3389/fnins.2018.00940

The kisspeptin/GPR54 system plays a crucial role in the regulation of the reproductive axis in vertebrates. Male pregnancy and ovoviviparity are special reproductive phenomena among vertebrates. To better understand the neuroendocrine mechanisms of male pregnancy, cDNAs encoding *kiss2* and GPR54 were cloned and functionally characterized from the lined seahorse, *Hippocampus erectus*, an ovoviviparous teleost with male pregnancy. The core mature peptide of seahorse Kiss2 is high conserved among seahorses, but unique among vertebrate Kiss orthologs. In the phylogenetic analysis, the seahorse Kiss clustered with the teleost Kiss2 clade. The *kiss2* transcripts were shown to be widely expressed in various tissues, notably in the brain and gonad of the seahorse, while GPR54-2 mRNA was expressed exclusively in the brain. In addition, *kiss2* mRNA found in male seahorse brain tissue increased significantly at the early pubertal stage, and decreased significantly during pregnancy. Intraperitoneal administration of seahorse Kiss2-10 to sexual mature male seahorses demonstrated to stimulate luteinizing hormone-releasing hormone (LHRH) and follicle-stimulating hormone (FSH) release and increased serum testosterone levels. In summary, we first identified the kisspeptin/GPR54 system in an ovoviviparous fish with male pregnancy, which might be involved in the regulation of the reproductive functions of pubertal onset, gonadal development, and male pregnancy via regulating the synthesis of both gonadotropin-releasing hormone (GHRH) and testosterone.

Keywords: kisspeptin, GPR54, seahorse, male pregnancy, ovoviviparity

INTRODUCTION

Kisspeptin is a novel neuropeptide product encoded by the *kiss* gene, which is now recognized as a key regulator of reproduction and involved in pubertal onset and neuroendocrine control of fertility in mammals (Tena-Sempere, 2010). Kisspeptin is a member of the hypothalamic RFamide family, as it possesses the Arg-Phe-amide motif at the C-terminal of the prepropeptide (Ukena and Tsutsui, 2005). Kisspeptin was first called metastin in consideration of

its suppressive effects on tumor growth and tumor metastasis (Lee et al., 1996). The receptor for kisspeptin was previously characterized as an orphan G protein-coupled receptor, GPR54 (Ohtaki et al., 2001). In late 2003, a mutation of GPR54 was found in an individual with hypogonadism, and caused the absence of puberty, indicating that the kisspeptin system plays a role in the regulation of reproductive function (Roux et al., 2003).

Many studies related to the kisspeptin system in vertebrates have been reported in the last decade. In most mammals, there is only one kisspeptin gene (*Kiss1*). However, the platypus, a mammalian monotreme, has two forms of kisspeptin genes (*Kiss1* and *Kiss2*) (Lee et al., 2009). In teleosts, multiple forms of kisspeptin genes have been identified. Most teleost fishes have two paralogous kisspeptin genes, named *kiss1* and *kiss2*. However, some fish species, including green puffer, tiger puffer, stickleback, and orange-spotted grouper, lack the *kiss1* gene and possess only *kiss2* (Tena-Sempere et al., 2012; Mechaly et al., 2013), whereas *Xenopus* carries three forms of kisspeptin gene, *kiss1a*, *kiss1b*, and *kiss2* (Moon et al., 2009).

The presence of two kisspeptin gene isoforms points to the concurrent existence of multiple forms of receptor. Multiple forms of GPR54 (GPR54-1 and GPR54-2) have been characterized in many vertebrate species, including zebrafish, medaka, goldfish, striped bass, sea bass, and chub mackerel. However, only GPR54-2 was identified in tiger puffer, green puffer, gray mullet, fatheted minnow, cobia, Nile tilapia, orange-spotted grouper, and half-smooth tongue sole (Tena-Sempere et al., 2012; Wang et al., 2017). In addition, *Xenopus* and European eel possess three receptor isoforms, GPR54-1a, GPR54-1b, and GPR54-2 (Moon et al., 2009; Pasquier et al., 2012a).

In mammals, many studies strongly suggest that the kisspeptin system regulates pubertal onset through the stimulation of gonadotropin-releasing hormone (GnRH) secretion. Mutations in the kiss receptor gene are related to an absence of pubertal onset and hypogonadism in human (Roux et al., 2003; Seminara et al., 2003). This abnormality was due to the disruption of the hypothalamic–pituitary–gonadal (HPG) axis, especially the kisspeptin–gonadotropin-releasing hormone (GnRH)–luteinizing hormone (LH) pathway. The GPR54 transcripts are colocalized with GnRH neurons, indicating that kisspeptin can directly stimulate gonadotropin-releasing hormone via GPR54 (Messenger et al., 2005).

In teleosts, there is debate on whether fish kisspeptin is an important regulator of the reproductive HPG axis or not. Many studies suggest that fish kisspeptin, similar to mammalian kisspeptin, is a key activator of the reproductive axis. In cichlid fish (e.g., *Oreochromis niloticus* and *Astatotilapia burtoni*), striped seabass, and chub mackerel, the kisspeptin receptor mRNA was expressed in GnRH1 neurons (Parhar et al., 2004; Ohga et al., 2017). Furthermore, the injection of Kiss2 peptide promotes the expression of gonadotropins (LH β and FSH β) both at the mRNA and plasma levels in several fish species (Li et al., 2009; Chang et al., 2012; Kim et al., 2014; Ohga et al., 2014). However, in zebrafish and medaka, kisspeptin and GPR54 knockout experiments showed that the kisspeptin system was dispensable

TABLE 1 | Information of primers used in this study.

Gene	Purpose	Primer	5'–3' sequence
Primer sequence			
kiss2	Partial cDNA	kiss2F1	CTCCCAAGATGAAGTT TGCAG
		kiss2R1	TCAGGTCAGCACCTC CAGTTG
	5'RACE	kiss2R2 (first)	AGATGGACGCATG ATTGTAG
		kiss2R3 (nest)	TTTGTTCCTGTGG TCGTTGC
	3'RACE	kiss2F2 (first)	CCTGAGCAGGAAT CACAGGG
		kiss2F3 (nest)	ACCTTTGTTTCTCC CTGATAG
	Real-time PCR	kiss2qF	ATCCCAACCTTTGT TTCTCC
		kiss2qR	AAATCTGCTTGTT CTGGCTCT
	GPR54-2	GPR54-2F1	GCAGCATCCCTTTCT TACCGA
		GPR54-2 R1	GACCTGGTAGTTGT TGCTCTC
GPR54-2	5'RACE	GPR54-2 R2 (first)	TGGTAGAGGATGAAG GCCCTC
		GPR54-2 R3 (nest)	CACCTGCTGCAAGAAG GCCAC
	3'RACE	GPR54-2 F2 (first)	AGGTCTCCAAGATG GTGGTCG
		GPR54-2 F3 (nest)	GATCAAGACGTGGGC AAACTG
	Real-time PCR	GPR54-2qF	AGCCAGGAGACAACA ACTACC
		GPR54-2qR	GAGGAGTTGGCATAA GACATG
sGnRH	Real-time PCR	sGnRHqF	CCTTGCGTAGCTGAGA TGGAG
		sGnRHqR	TACATTGTATGGTC GACGTCTC
LH β	Real-time PCR	LH β qF	CACAAGGAACCCAC TAAACC
		LH β qR	GAGGGTGCTTTCTT TATTCTG
FSH β	Real-time PCR	FSH β qF	GCAATGGGAACTGGA CCTAC
		FSH β qR	TGATTGATACGA GCAGCACA
β -actin	Real-time PCR	β -actin_qF	TTCACCACCACAG CCGAGA
		β -actin_qR	TGGTCTCGTGGA TTCCGCAG

for reproduction (Tang et al., 2015; Nakajo et al., 2018). In addition, GnRH neurons do not express kisspeptin receptor genes in medaka (Kanda et al., 2013) or European sea bass (Escobar et al., 2013). Taken together, the role of kisspeptin in fish reproduction remains controversial, and seems to differ depending on species.

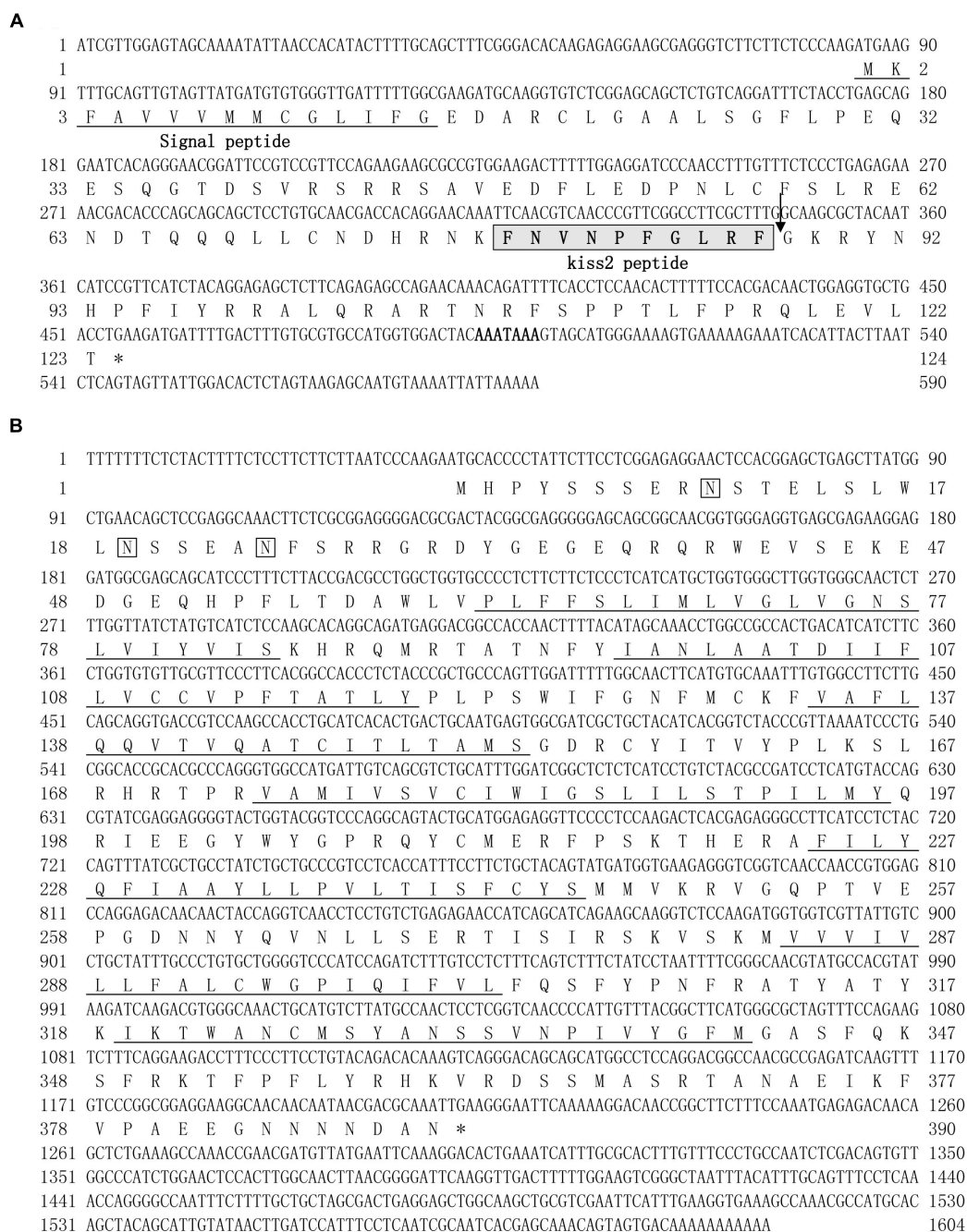


FIGURE 1 | cDNA and deduced amino acid sequence of lined seahorse *kiss2* and GPR54-2. **(A)** The nucleotide and deduced protein sequences of *kiss2* cDNA. The putative signal peptide is underlined. The mature peptide (kisspeptin-10) is boxed. **(B)** The nucleotide sequence and deduced protein sequence of GPR54-2 cDNA in lined seahorse. Seven putative hydrophobic transmembrane (TM) domains are underlined. Putative N-linked glycosylation sites are indicated by diamonds (CBS prediction server score > 0.50).

The lined seahorse (*Hippocampus erectus*) is a small marine fish with a special morphology, belonging to the order Syngnathiformes and the family Syngnathidae (fused jaws). The seahorse is an ovoviviparous fish and has a unique reproduction system with male pregnancy (Scobell and MacKenzie, 2011). The female seahorse deposits eggs into the male seahorse's special

organ called brood pouch, and the eggs get fertilized in the brood pouch. The male seahorse incubates developing embryos in the brood pouch, similar to the mammalian placenta, in which they are aerated, osmoregulated, protected, and provisioned before the hatching stage (Stolting and Wilson, 2007). The lumen of the brood pouch is rich in blood vessels and surrounded by

loose connective tissue, named pseudo-placenta. The embryos are embedded within individual compartments formed from the pseudo-placenta (Dzyuba et al., 2006). However, few studies have examined the underlying hormonal mechanisms that mediate the special reproductive behavior and male pregnancy in seahorses.

Our team has recently sequenced the whole genome of the lined seahorse (Lin et al., 2017). This helped in obtaining a series of genes involved in the endocrinology regulation of reproduction. To elucidate the roles of the kisspeptin system in reproduction and male pregnancy in seahorse, the kisspeptin gene was isolated from the lined seahorse, and the expression of the gene was analyzed in a variety of tissues in male and female seahorses, as well as in the brain and testis at different gonad developmental stages, or after treatment with Kiss2-10 injection.

MATERIALS AND METHODS

Animals and Tissue Sampling

The experimental lined seahorse individuals were collected from the Shenzhen Seahorse Center of the South China Sea Institute of Oceanology, Chinese Academy of Sciences (SCSIO-CAS), and animal ethics approval for experimentation was granted by the Chinese Academy of Sciences. The seahorses were maintained in recirculating holding tanks with seawater at room temperature under a cyclical light/dark photoperiod (16 h: 8 h). The seahorses were fed twice daily with frozen *Mysis* spp. The temperature, salinity, pH, light intensity, and dissolved oxygen (DO) were maintained at (mean \pm SD) $22 \pm 0.5^\circ\text{C}$, $25 \pm 1.0\text{‰}$, 7.9 ± 0.4 , 2000 lx, and $6.5 \pm 0.5 \text{ mg L}^{-1}$, respectively.

Cloning of the Seahorse Kisspeptin System

Adult seahorses were anesthetized with 0.05% MS222 (Sigma, Shanghai, China). Total RNA was extracted from the brain using TRIzol reagent (Invitrogen, CA, United States) according to the manufacturer's instructions. First-strand cDNA was synthesized using the PrimeScriptTM RT Reagent Kit with gDNA Eraser (Takara, Dalian, China). Partial cDNA fragments were obtained by PCR using primers (Table 1) designed based on the sequences of *kiss2* and GPR54-2 from the published genome data of lined seahorse (Lin et al., 2017). To obtain the full-length sequence of the cDNA of the kisspeptin gene in lined seahorse, 3' and 5' rapid amplification of cDNA ends (RACE) PCRs were conducted using the SMARTer RACE Kit (Clontech, CA, United States) according to the manufacturer's protocols. PCR amplification was performed using Taq DNA Polymerase Mix (TAKARA, Dalian, China), and PCR conditions were as follows: denaturation at 94°C for 5 min, followed by 35 cycles at 94°C for 30 s, 56°C for 30 s, 72°C for 2 min, and a final incubation at 72°C for 10 min. The PCR products were purified from an agarose gel and subcloned into a pGEM-T Easy Vector System (Promega, Fitchburg, WI, United States). The inserts were sequenced using an ABI 3700 sequencer (Applied Biosystems).

TABLE 2 | Amino acid sequence identities of the lined seahorse *kiss2* with *kiss* genes of various vertebrates.

Species	Accession no.	Amino acid sequence identities of Kiss (%)	
		Seahorse Kiss2	
Identity of vertebrate Kiss protein			
Human Kiss1	NP002247		10.6
Pig Kiss1	ACH68409.1		9.8
Bovine Kiss1	XM867473.1		13.2
Mouse Kiss1	AAI17047		13.8
Xenopus Kiss1	BX850386		13.7
Seabass Kiss1	FJ008914		8.2
Zebrafish Kiss1	ABV03802		12.8
Takifugu Kiss2	BAJ15497		47.1
Grouper Kiss2	ACT65993		58.2
Medaka Kiss2	AB439562		43.0
Seabass Kiss2	FJ008915		62.2
Zebrafish Kiss2	AB43956.1		26.9

Structural, Phylogenetic and Syntenic Analyses of Seahorse Kisspeptin System

The amino acid sequences of *kiss2* and GPR54-2 in lined seahorse were translated from the nucleotide sequence using DNASTAR software. The putative signal peptides were predicted by SignalP 4.1¹. The putative transmembrane domain of GPR54-2 was predicted using the TMHMM server V2.0². Multiple sequence alignments of amino acids were performed with ClustalX 2.0 (Larkin et al., 2007). Protein phylogeny analyses were conducted with MEGA6.0 (Tamura et al., 2013) using the neighbor-joining method with 1000 bootstrap replicates. TBLASTN searches against the genome assemblies of different vertebrate species, including human, zebrafish, medaka, and stickleback, and data retrieval for synteny analysis were performed using the Ensembl genome browser³.

Tissue Distribution of the Seahorse Kisspeptin System

To detect the tissue distribution of *kiss2* and GPR54-2 mRNA in lined seahorse, three adult female ($11.3 \pm 0.26 \text{ g}$, mean body weight) (8 months old) and male lined seahorses ($12.7 \pm 0.45 \text{ g}$) (8 months old) were anesthetized with 0.05% MS222, and decapitated. Tissue samples of the brain, gill, liver, intestine, kidney, muscle, brood pouch, skin, and gonads of male and female seahorses were quickly collected, snap frozen in liquid nitrogen, and stored at -80°C until RNA extraction. Different brain regions including telencephalon, cerebellum, optic tectum-thalamus, hypothalamus and pituitary were also detected. One micro gram of total RNA from each tissue was digested with a genome eraser and reverse-transcribed into cDNA using the PrimeScriptTM RT Reagent Kit with gDNA Eraser (Takara, Dalian, China).

¹www.cbs.dtu.dk/services/SignalP/

²www.cbs.dtu.dk/services/TMHMM/

³http://www.ensembl.org

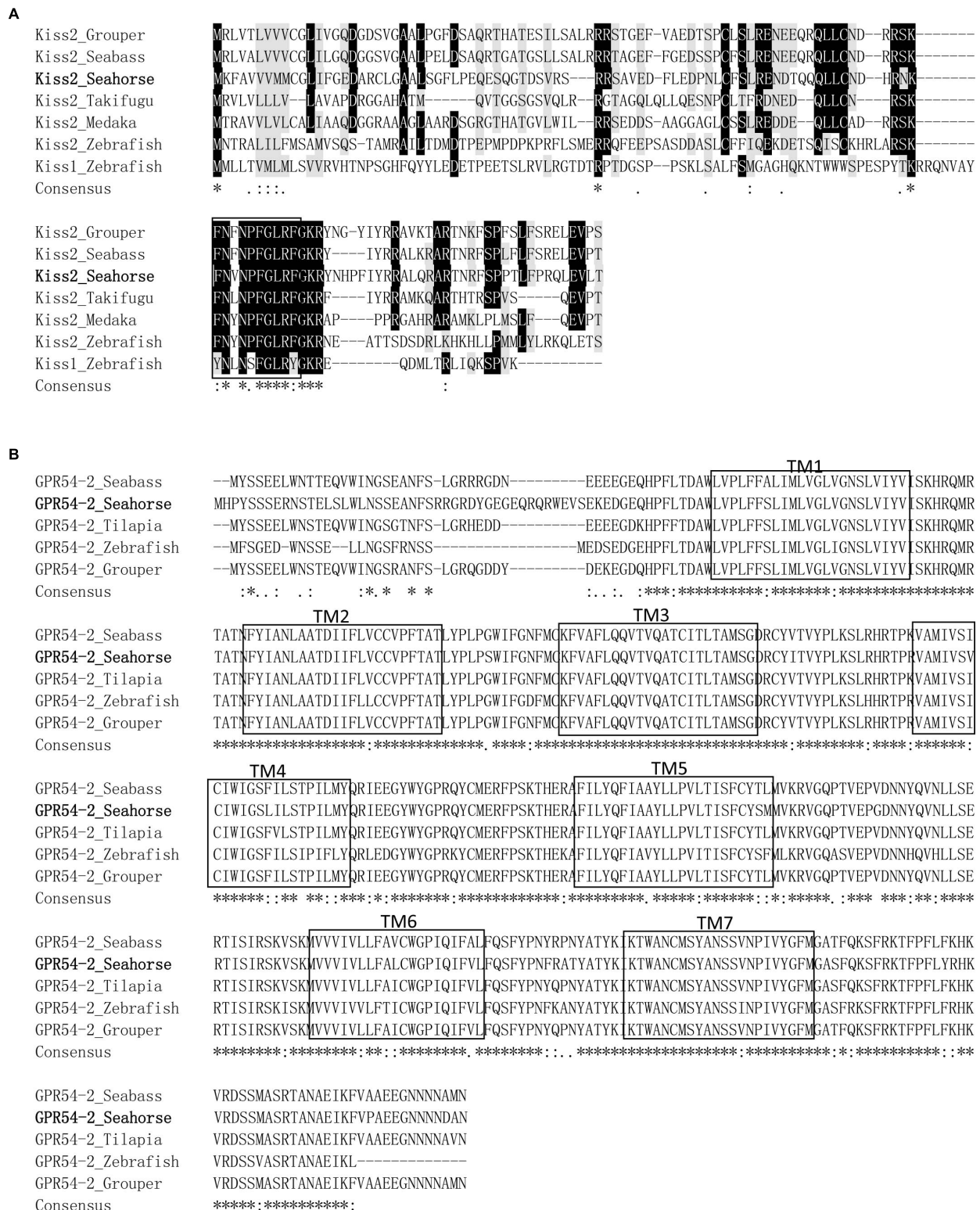
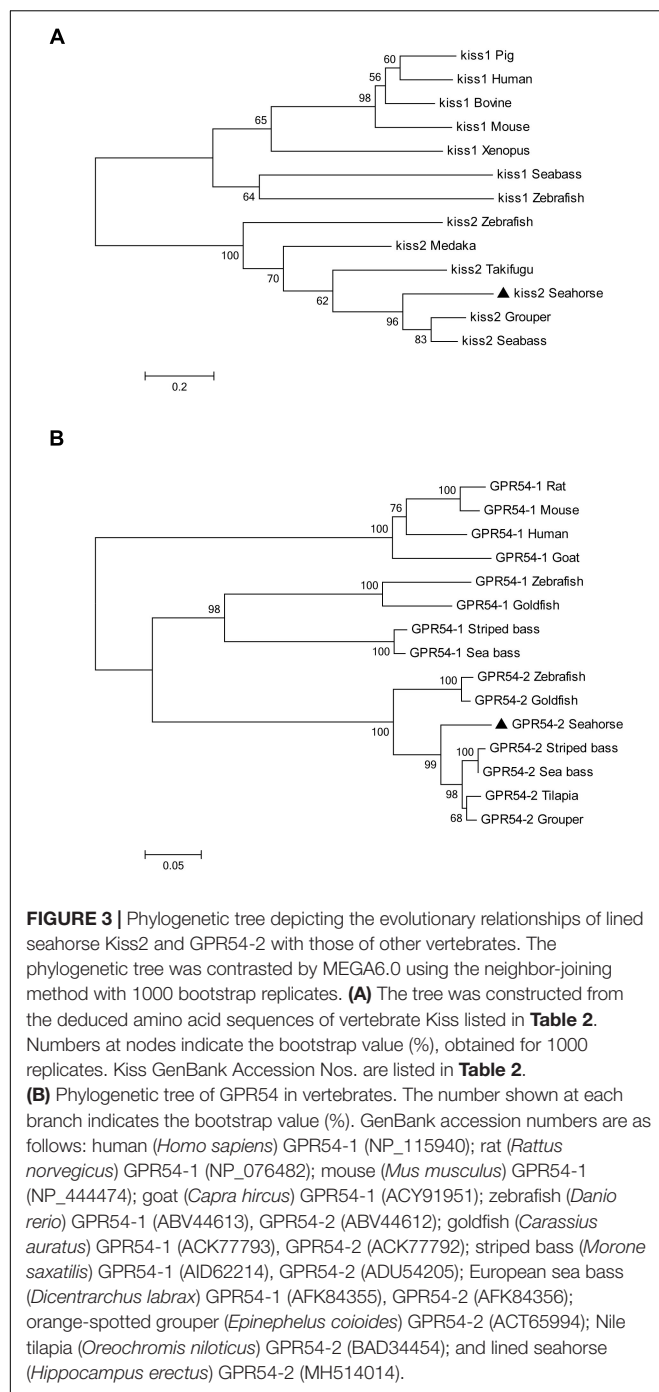


FIGURE 2 | Comparison of amino acid sequences of kisspeptin precursors and GPR54-2 from different species. **(A)** The mature peptides of Kiss2 are boxed. Multiple sequence alignment was performed by ClustalX 2.0. Identical sequences are indicated by asterisks. **(B)** Alignment of the amino acid sequences of GPR54-2 in different species. Gaps introduced in some sequences to maximize the alignment are indicated by hyphens. Identical sequences are indicated by asterisks. Putative TM domains are boxed. The GPR54-2 sequences of other teleosts were downloaded from GenBank (For detailed, see the legend for **Figure 3**).



Expression Profile of *kiss2* During Sexual Development Stages

The expression profile of seahorse *kiss2* was analyzed in the whole brain and testis of four different sexual development stages including immature (IMM), early puberty (EP), advanced puberty (AP), and mature (MAT) (3, 4, 5, and 6 months old) ($n = 8$) by real-time PCR. The gonad tissues of seahorses in different stages were fixed in Bouin's solution for 24 h. Then, the gonads were embedded in paraffin, cut into 10 μm sections,

and stained with hematoxylin and eosin. The classification of the gonad development stages was determined by light microscopy.

Expression Profile of *kiss2* During the Pregnancy Stages

Adult seahorses were allowed to mate freely before being subjected to a standardized assessment of pregnancy status on the basis of courtship behaviors. The pregnant seahorses (P stage) ($n = 8$) were maintained in the tank before euthanasia to sample the brain and testis tissues. Adult seahorses that were already mature were termed the pre-pregnancy group (PreP stage) ($n = 8$), and post-parturition (PostP stage) seahorses, in which the larval seahorses had hatched, were termed the post-pregnancy group (PostP stage) ($n = 8$).

Administration of Kisspeptin to Seahorse

Synthetic peptides corresponding to the lined seahorse Kiss2 decapeptide (Kiss2-10) (FNVNPFGLRF-NH₂) were provided by China Peptide Co., Ltd. (Shanghai, China) with a purity of 99.75%, as determined by HPLC. To evaluate the role of *kiss2* in the hypothalamus–pituitary axis, male lined seahorses were injected with Kiss2-10. The mRNA expression levels of GPR54 and sGnRH in the hypothalamus and FSH β and LH β in the pituitary were detected by real-time PCR. Sexually mature male seahorses, 12.5–14.0 g in body weight, were kept in indoor tanks supplied with recirculating sea water and feed with frozen *Mysis* spp. The test Kiss2-10 peptides were dissolved in a vehicle of 0.7% NaCl. Seahorses were anesthetized with 0.05% MS222 and intraperitoneally injected with Kiss2-10 (20 nmol/g body weight at a volume of 20 μL /g body weight) and saline (20 μL /g body weight) as a negative control. Eight seahorses from each group were collected randomly and killed by decapitation at 3 and 6 h post-injection. The hypothalamus and pituitaries were quickly dissected, frozen in liquid nitrogen, and stored at -80°C for subsequent RNA extraction. Blood samples were collected from tail vessels at 3 and 6 h post-injection. Serum samples were separated by centrifugation at $2,500 \times g$ for 30 min at 4°C , and stored at -20°C until the measurement of testosterone by ELISA as described in the manufacturer's protocol (Cayman Chemical Company, Ann Arbor, MI, United States).

RNA Extraction, Reverse-Transcription, and Real-Time Quantitative PCR

All experiments were performed according to the standard procedure in our lab (Zhang et al., 2016; Qin et al., 2018). In brief, total RNA was extracted using TRIzol reagent (Invitrogen, United States) according to the manufacturer's protocol. The purity and yield of RNA were detected by a NanoDrop 2000C spectrophotometer (Thermo Fisher Scientific, United States), and the integrity of RNA was determined by gel electrophoresis. One microgram of RNA was used as a template for the first strand cDNA synthesis using the reverse-transcription kit described above. Real-time quantitative PCR (qPCR) was performed on a Roche Light-Cycler 480 real time PCR system using SYBR Premix Ex TaqTM (TAKARA, Japan). qPCR conditions were as follows: denaturation at 94°C for 3 min, followed by 40 cycles at 94°C

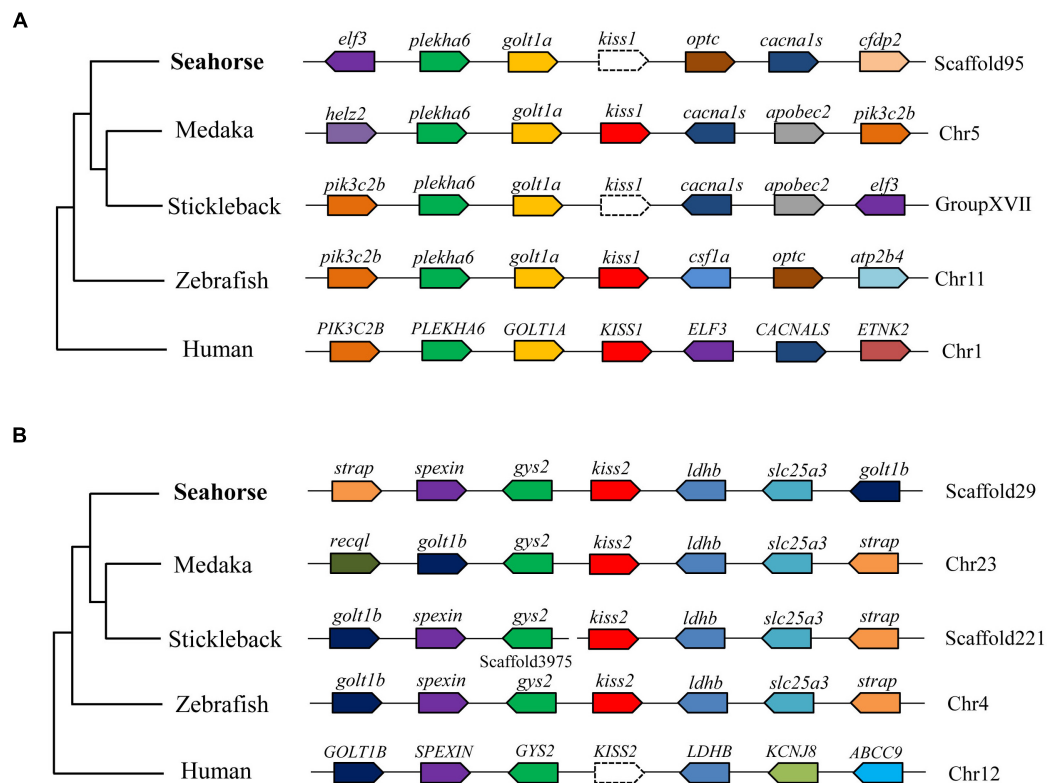


FIGURE 4 | Conserved synteny for the genomic region comprising *kiss1* (A) and *kiss2* (B) genes. Gene loci organizations in the genomic region containing the kisspeptin gene were obtained from the Ensembl genome browser (<http://www.ensembl.org>).

for 15 s, 55–58°C for 15 s, and 72°C for 20 s. At the end of the amplification, a melting curve analysis was generated to confirm the presence of a single PCR product. The housekeeping gene β -actin was used as an internal reference gene. The expression levels of each target gene analyzed via qPCR were determined using the comparative quantification method $2^{-\Delta\Delta CT}$ (Livak and Schmittgen, 2001).

Statistical Analyses

All the data were expressed as the means \pm standard error of mean (SEM) and evaluated by one way analysis of variance (ANOVA) followed by Duncan's multiple-range tests using Prism6.0 (GraphPad software, CA, United States) and SPSS 19.0 (IBM, United States). Differences between groups with $p < 0.05$ were considered statistically significant.

RESULTS

Cloning and Characterization of *kiss2* and GPR54-2 in Seahorse

A full-length cDNA encoding the *kiss2* precursor was isolated from the lined seahorse hypothalamus (GenBank Accession Number: MH514013). The open reading frame (ORF) encodes for the 124 amino acid (aa) precursor Kiss2 protein, with an N-terminal putative signal peptide sequence of 15 aa (Figure 1A).

Sequence alignment of deduced protein sequences shows that seahorse and other vertebrate Kiss precursors have relatively low identities with each other (Table 2). Homology analysis revealed that seahorse Kiss2 had the highest sequence identities with European seabass (62.2%) and orange-spotted grouper (58.2%) among Perciformes species. However, the mature decapeptide of Kiss (Kiss-10) and the C-terminal cleavage site (GKR) are conserved (Figure 2A). Interestingly, the decapeptide of seahorse Kiss2 (FNVNPFGLRF) is very unique. Phylogenetic analysis shows that Kiss cDNA sequences are clustered into two separate clades: *kiss1* and *kiss2*. The seahorse *kiss* is clustered with the *kiss2* clade and shares the highest similarity with seabass and grouper *kiss2* (Figure 3A). The synteny analysis of *kiss* shows that the *kiss2* gene is usually positioned in the genomic regions, including *golt1b*, *spexin*, *gys2*, and *ldhb*. The position of *kiss2* in seahorse and other teleost fishes is conserved (Figure 4B). The *kiss1* gene is usually positioned in the genomic regions containing common loci, including *plekha6*, *golt1a*, and *elf3*. While in this loci, the *kiss1* gene of seahorse is absent (Figure 4A).

The cloned full-length GPR54-2 cDNA sequence is 1604 bp (GenBank number: MH514014), including an ORF of 1173 bp, 39 bp of 5'UTR and 392 bp of 3'UTR. The deduced 390 amino acids contain an extracellular N-terminus, a seven transmembrane domain and a cytoplasmic C-terminus. Three potential N-linked glycosylation sites were predicted in the

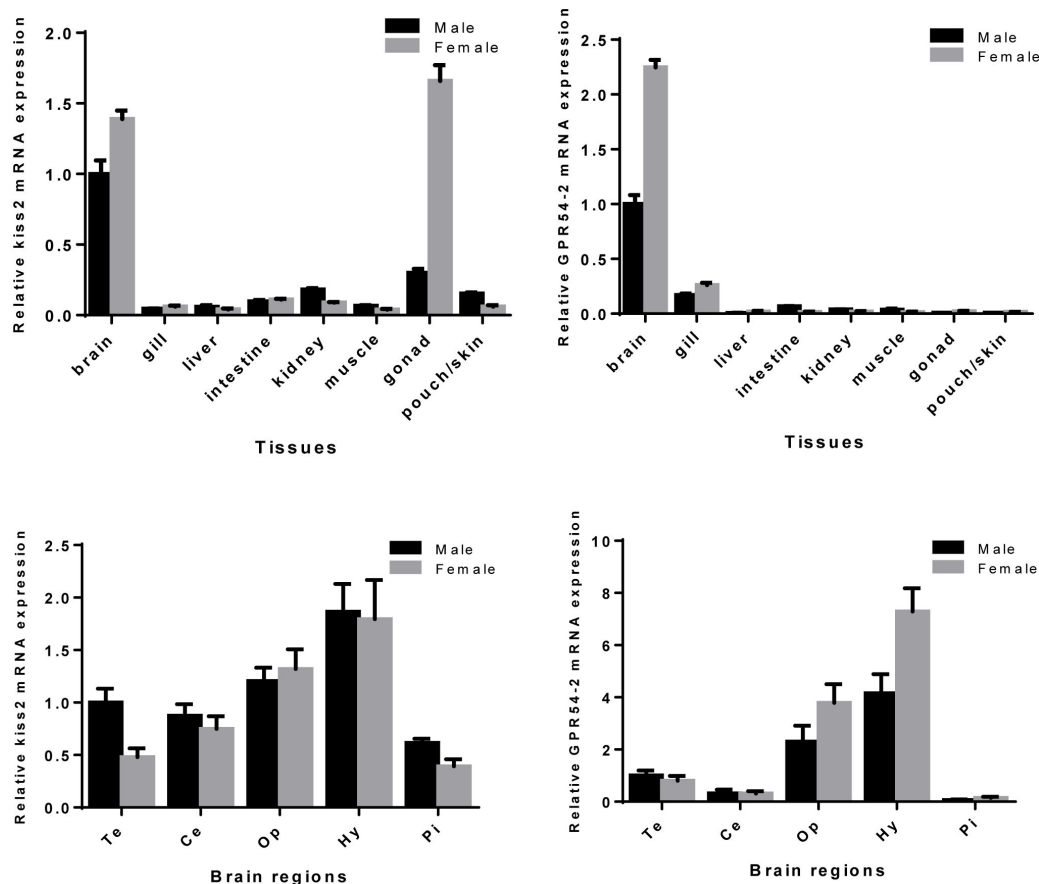


FIGURE 5 | Relative mRNA expression levels of *kiss2* and *GPR54-2* mRNA in various tissues and brain regions of male and female seahorses. The brain regions including: Te, telencephalon; Ce, cerebellum; Op, optic tectum-thalamus; Hy, hypothalamus; Pi, pituitary. The mRNA expression levels are identified by real-time PCR, normalized against the β -actin transcript, and presented as means \pm SEM.

extracellular N-terminus (Figure 1B). Multiple amino acid sequence alignments of *GPR54* showed that the identity of *GPR54* from different teleost species is very high except the extracellular N-terminus domain (Figure 2B). In the phylogenetic analysis, the seahorse *GPR54* clusters into *GPR54-2* clade (Figure 3B).

Tissue Distribution of *kiss2* and *GPR54-2* in Seahorse

Expression patterns of seahorse *kiss2* and *GPR54-2* in various tissues and brain regions were examined by real-time PCR. The *kiss2* mRNA was expressed in all detected tissues and was highly expressed in the brain and ovary (Figure 5 and Supplementary Figure S1). Interestingly, *kiss2* mRNA was expressed in the brood pouch of male seahorse. However, *GPR54-2* was expressed exclusively in the brain of seahorse, and the expression levels were close to the detection limits in the peripheral tissues. The *kiss2* and *GPR54-2* mRNA were highly expressed in the hypothalamus region of brain of both male and female seahorses, compared to other brain regions. In addition, *kiss2* and *GPR54-2* mRNA levels of expression in

the brain tissue were found to be higher in females than in males.

Expression Profile of *kiss2* During Sexual Development in Male Seahorse

Real-time quantitative PCR was used to quantify the expression of *kiss2* in the brain and testis of male seahorses during the gonadal developmental stages. The *kiss2* mRNA expression in the brain was significantly high in the early pubertal stage (4-month-old class) ($P = 0.0312$, $P < 0.05$), while there was no significant difference in the testis ($P = 0.764$) (Figure 6).

Expression Profile of *kiss2* During the Pregnancy Stages

The expression pattern of seahorse *kiss2* during the pregnancy stages was detected by real-time PCR. Both in the brain and testis, the expression level of *kiss2* mRNA was reduced significantly during pregnancy (P stage), and returned to the normal levels post-parturition (brain: $P = 0.0267$, $P < 0.05$; testis: $P = 0.0395$, $P < 0.05$). The *GPR54-2* mRNA was also downregulated during the pregnant stage ($P = 0.0452$, $P < 0.05$) (Figure 7).

Effects of Administration of Kiss2-10 on the Hypothalamus-Pituitary Axis in Seahorse

The intraperitoneal injection of Kiss2-10 significantly increased FSH β ($P = 0.00815$, $P < 0.01$) and LH β ($P = 0.0297$, $P < 0.05$) at 6 h post-injection. In addition, the mRNA expression of FSH β increased significantly at 3 h post-injection ($P = 0.0436$, $P < 0.05$). However, no significant difference was found in sGnRH ($P = 0.853$) and GPR54-2 ($P = 0.791$) mRNA levels (Figure 8). The serum testosterone concentration increased significantly at 6 h post-injection ($P = 0.0443$, $P < 0.05$) (Figure 9).

DISCUSSION

In the present study, one kisspeptin gene and its receptor were characterized and functionally evaluated in the lined seahorse. This is the first description of the kisspeptin system in an ovoviparous fish with male pregnancy. The deduced amino acid sequence of seahorse *kiss2* is poorly conserved compared to that of other vertebrate Kiss orthologs. However, the core putative mature peptide (decapeptide, Kiss2-10) and the GKR cleavage site were conserved. The Kiss2-10 is unique (FNVPFGLRF) among the vertebrate kisspeptins, while the sequence of Kiss2-10 in most vertebrates is FNFNPFGLRF (Pasquier et al., 2012b). The Kiss2-10 of the lined seahorse differed by only one amino acid to the Kiss2-10 of zebrafish (FNFNPFGLRF) and differed significantly by four aa to the Kiss1-10 of zebrafish (YNLNSFGLRY). The phylogeny tree showed that the *kiss2* of seahorse clustered with the teleost fish *kiss2* genes, and the synteny of *kiss2* in seahorse is conserved with other teleost fishes. These findings demonstrated that the cloned kisspeptin gene in seahorse is the orthologous gene of *kiss2* in the vertebrates.

Based on the genome and transcriptome databases of the lined seahorse, we searched for the *kiss1* gene in the lined seahorse genome and RNA-seq sequences by using tBLASTn search tool, and no *kiss1* gene was found. The synteny analysis of *kiss1* also showed that the *kiss1* gene was lost from the conserved locus of the lined seahorse. Similar results were found in several fish species with available genome databases, such as the stickleback (*Gasterosteus aculeatus*), tiger puffer (*Takifugu rubripes*), and green puffer (*Tetraodon nigroviridis*) (Felip et al., 2009). In addition, some fish species without sequenced genomes, such as orange-spotted grouper, grass puffer, Senegalese sole and Nile tilapia, also lacked the *kiss1* gene and possessed only the *kiss2* gene (Tena-Sempere et al., 2012). Moreover, in platy fish, another ovoviparous fish with an available genome database, we also found the *kiss2* gene on the scaffold JH556799.1, and the *kiss1* gene was absent. In addition, seahorse only possessed GPR54-2 and lacked GPR54-1, based on the genome data. Our study provides conclusive evidence for the loss of the *kiss1* system in the genome of several vertebrate species. Considering that the evolutionary rate of seahorse is very rapid (Lin et al., 2016), one of the duplicated copies (*kiss1* and GPR54-1) in seahorse appears to have been lost during evolution.

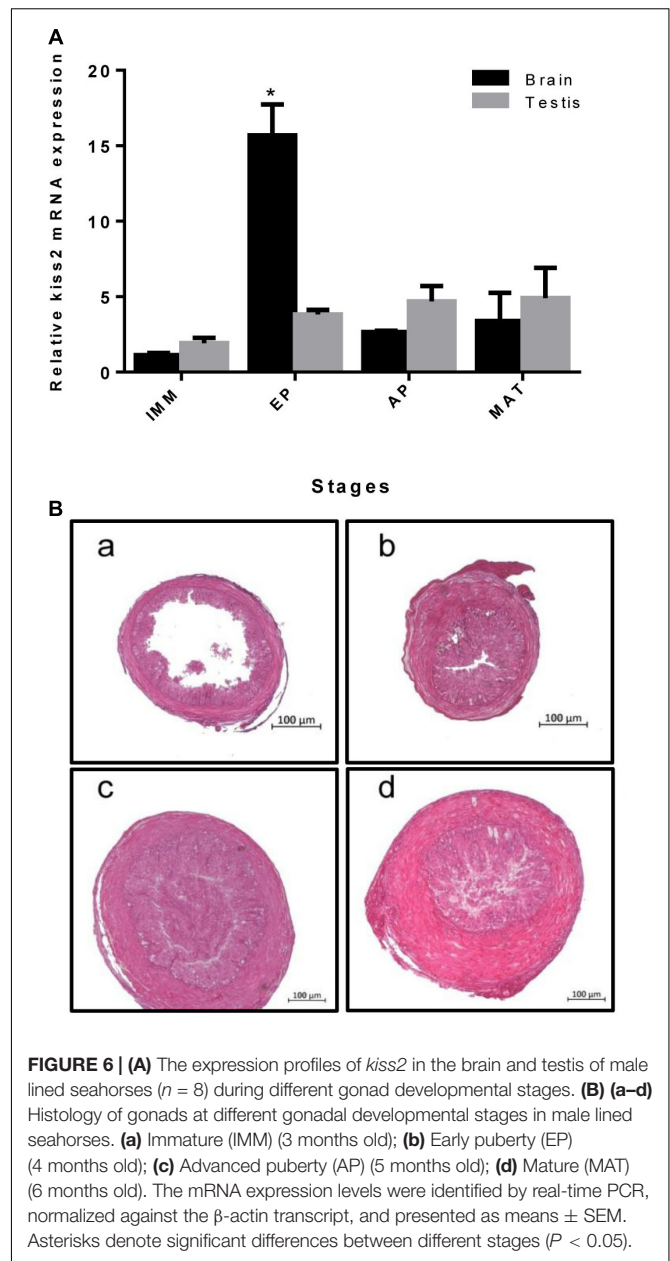


FIGURE 6 | (A) The expression profiles of *kiss2* in the brain and testis of male lined seahorses ($n = 8$) during different gonad developmental stages. **(B) (a–d)** Histology of gonads at different gonadal developmental stages in male lined seahorses. **(a)** Immature (IMM) (3 months old); **(b)** Early puberty (EP) (4 months old); **(c)** Advanced puberty (AP) (5 months old); **(d)** Mature (MAT) (6 months old). The mRNA expression levels were identified by real-time PCR, normalized against the β -actin transcript, and presented as means \pm SEM. Asterisks denote significant differences between different stages ($P < 0.05$).

It had been indicated that kisspeptin has been determined as an important regulator of the reproductive brain–pituitary–gonad (BPG) axis in mammals and teleosts (Ohga et al., 2018). Real-time PCR analysis supported this conclusion, showing that *kiss2* transcripts were highly expressed in the brain and gonad tissues in female and male seahorses. Interestingly, *kiss2* mRNA was expressed in the brood pouch of male seahorses. The brood pouch protected the embryos and provided them with oxygen and nutrients (Stolting and Wilson, 2007). This result suggested that kisspeptin may play a role in the regulation of male pregnancy in the lined seahorse. Moreover, GPR54-2 mRNA was mainly expressed in the brain while expressed much lower levels in the peripheral tissues of the lined seahorse. This expression pattern was consistent with previous studies.

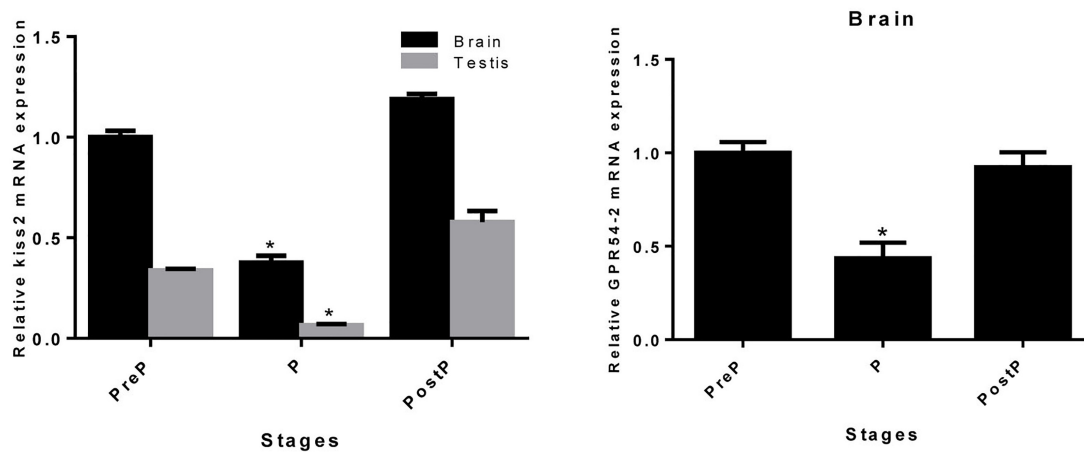


FIGURE 7 | The mRNA expressions of *kiss2* in the brain and testis ($n = 8$) and GPR54-2 in the brain of the male seahorses during different pregnant stages. PreP, pre-pregnant stage; P, pregnant stage; PostP, post parturition stage. The mRNA expression levels were identified by real-time PCR normalized against the β -actin transcript and presented as means \pm SEM. Asterisks denote significant differences between different stages ($P < 0.05$).

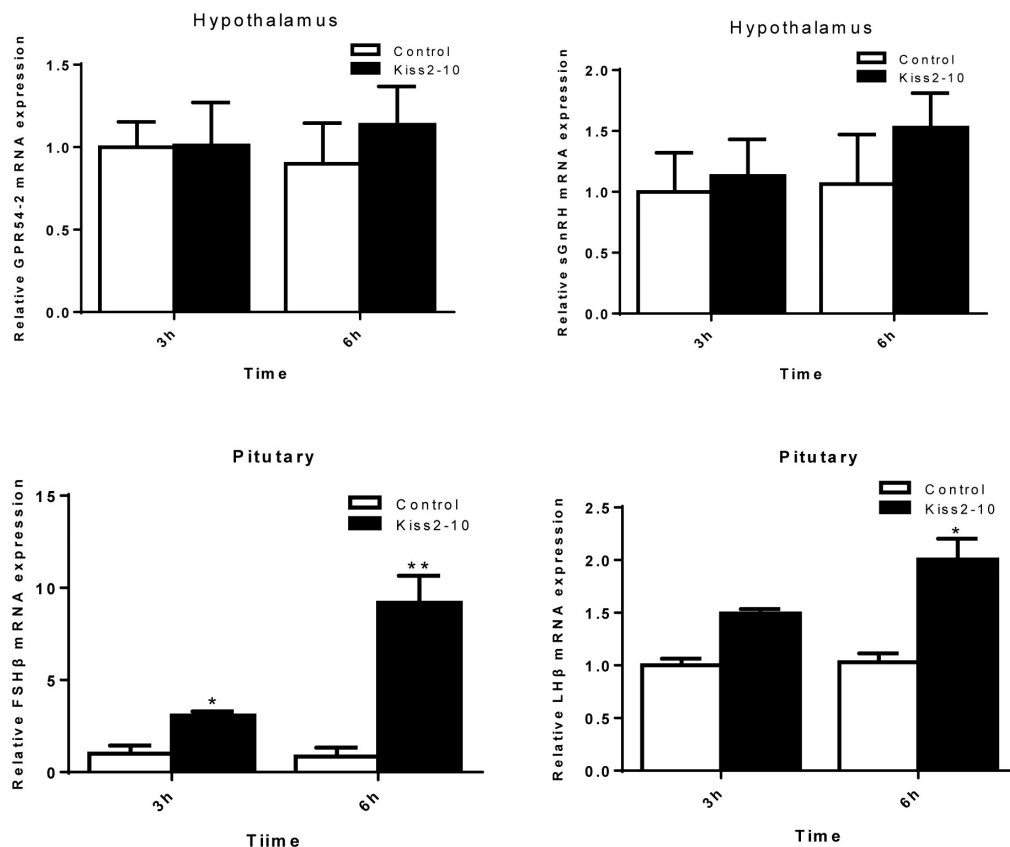
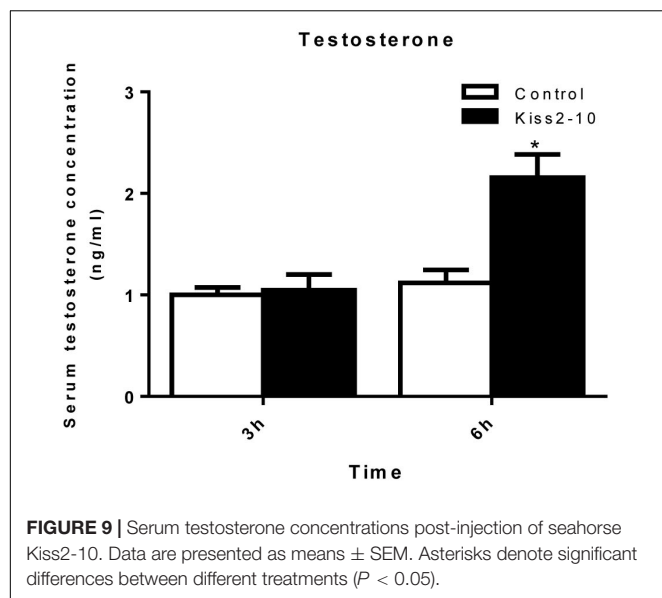


FIGURE 8 | Effects of administration of seahorse Kiss2-10 on the gene expressions for GPR54-2, sGnRH, FSH β , and LH β at 3 and 6 h post-injection in sexually mature male lined seahorses. The mRNA expression levels were identified by real-time PCR, normalized against the β -actin transcript, and presented as means \pm SEM. Asterisks denote significant differences between different treatments ($P < 0.05$).

The expression of GPR54 in the brain was much higher than the expression in the gonad and other peripheral tissues in most teleosts including zebrafish, fathead minnow, chub

mackerel and tongue sole (Wang et al., 2017; Ohga et al., 2018). The predominant expression of GPR54-2 mRNA in the brain indicated the potential involvement of seahorse kisspeptin



in neural functions of the HPG axis as a key regulator of reproduction.

Many studies have demonstrated that kisspeptin plays a critical role in pubertal onset in vertebrates (Seminara et al., 2003); (Cortes et al., 2015). However, the roles of kisspeptin in ovoviparous fishes are still widely underexplored. In the present study, we have detected the expression profile of *kiss2* during gonadal development in male lined seahorse. It is interesting to note that *kiss2* mRNA in the brain increased significantly at the early puberty stage in male seahorses, while there was no significant difference in the testis. This result indicated that seahorse *kiss2* was involved in the onset of puberty through the brain rather than the testis. In Atlantic halibut, kisspeptin was also involved in the onset of puberty (Mechaly et al., 2010). Moreover, in male chub mackerel, *kiss2* mRNA expression increased significantly just before the onset of meiosis in the testis (Ohga et al., 2018). These results suggest the positive involvement of the kisspeptin system in the pubertal process of teleosts, as is the case for mammals.

The mRNA expressions of *kiss2* in the brain and testis of seahorses were significantly reduced at the pregnancy stage. This result indicated that kisspeptin plays a role in the regulation of pregnancy in seahorses. In humans, the circulating kisspeptin levels are low in non-pregnant females, but dramatically increase during pregnancy (Horikoshi et al., 2003). However, kisspeptin does not appear to increase during pregnancy in many non-primate species, including rodents, sheep, and horses (Scott and Brown, 2013). It has been demonstrated that kisspeptin regulates the oxytocin system during pregnancy and lactation stages; however, the physiological role of circulating kisspeptin during pregnancy remains uncertain in mammals. To our knowledge, this is the first report that the expression of kisspeptin is reduced during pregnancy in an ovoviparous teleost (seahorse). This suggests that the physiological role of kisspeptin in pregnancy is different between ovoviparous teleosts and mammals.

In both mammals and teleosts, kisspeptin plays a crucial role in controlling reproductive activities by increasing gonadotropin release, which is mediated by stimulating GnRH release (Popa et al., 2008; Ohga et al., 2018). However, it is not known whether kisspeptin in ovoviparous teleosts serves the same role on the reproductive axis. In the present study, the *in vivo* administration of synthetic seahorse Kiss2-10 potentially stimulated the expression of FSH β and LH β in the pituitary of mature male seahorses, indicating that the stimulatory action of kisspeptin on GTH release is conserved among vertebrates. On the other hand, there is no stimulatory effect on the expression of GnRH in the hypothalamus, suggesting that Kiss2-10 does not act through GnRH releasing in seahorse, and can stimulate GTH expression directly. Moreover, seahorse Kiss2-10 injection can also stimulate the serum testosterone concentration at 6 h post-injection. In mammals, administration of kisspeptin potentially increased plasma LH and testosterone (Patterson et al., 2006). These observations indicated that kisspeptin may mediate its effects on the HPG axis by increasing the gonadotropin hormone and testosterone concentration in seahorses, serving the same role as that of its mammalian counterparts on the reproductive axis. In male fishes, FSH and LH can stimulate testicular Leydig cells to produce androgens including testosterone (T) and 11-ketotestosterone (11-KT). These androgens in turn promote spermatogenesis and development of secondary sexual characteristics in males (Knapp and Carlisle, 2011). In seahorses, the Leydig cells underwent a distant seasonal cycle of activation. A prolonged period of androgen synthesis that was maximal during proliferation of spermatocytes and development of the brood pouch, but suppressed during the pregnant stage (Scobell and MacKenzie, 2011). Our findings show that seahorse *kiss2* mRNA expression was upregulated during early puberty while it appeared to be downregulated during pregnancy. And the expression profiles of *kiss2* in early puberty and pregnant stages were constant with the androgen levels during these stages. This suggested that the seahorse kisspeptin levels are regulated to control the androgen level in the Leydig cells through stimulating FSH and LH.

In conclusion, we cloned *kiss2* and GPR54-2 cDNA sequences from the lined seahorse and investigated their expression profiles in various tissues and different reproductive stages. The putative mature peptide and protein cleavage sites of *kiss2* were well conserved among vertebrates. Tissue distribution showed that *kiss2* transcripts were highly expressed in the brain and gonad tissues in both female and male seahorses. However, GPR54-2 mRNA was exclusively expressed in the brain. In addition, the *kiss2* mRNA in the brain increased significantly at the early puberty stage of the male seahorse, and was reduced significantly at the pregnancy stage. We have demonstrated that seahorse Kiss2-10 stimulated LH and FSH release *in vivo*, and increased the serum testosterone concentration. Our results suggest that the kisspeptin/GPR54 system may be involved in the regulation of reproductive function of pubertal onset and gonadal development, as well as male pregnancy, by regulating both GTH and testosterone synthesis in the lined seahorse.

AUTHOR CONTRIBUTIONS

HZ and QL designed the research. HZ and BZ carried out the experiments. HZ, GQ, and SL analyzed the experiment data. QL provided lab space and equipment. All authors wrote the paper.

FUNDING

This work was supported by the National Natural Science Foundation of China (41825013, 41576145, and 41606170), the Pearl River S&T Nova Program of Guangzhou (201806010133), Guangdong Oceanic and Fisheries Science and Technology

Foundation (A201601D03), and the Science and Technology Planning Project of Guangdong Province (2017B030314052).

SUPPLEMENTARY MATERIAL

The Supplementary Material for this article can be found online at: <https://www.frontiersin.org/articles/10.3389/fnins.2018.00940/full#supplementary-material>

FIGURE S1 | RT-PCR analysis of tissue expression patterns of *kiss2* and GPR54-2 in male and female seahorses. Amplification of β -actin was used as house-keeping gene control. Br, brain; Li, liver; Gi, gill; In, intestine; Ki, kidney; Mu, muscle; Po, pouch; Sk, skin; Go, gonad; NC, negative control.

REFERENCES

- Chang, J. P., Mar, A., Wlasichuk, M., and Wong, A. O. L. (2012). Kisspeptin-1 directly stimulates LH and GH secretion from goldfish pituitary cells in a Ca²⁺-dependent manner. *Gen. Comp. Endocrinol.* 179, 38–46. doi: 10.1016/j.ygcen.2012.07.028
- Cortes, M. E., Carrera, B., Rioseco, H., Pablo del Rio, J., and Vigil, P. (2015). The role of kisspeptin in the onset of puberty and in the ovulatory mechanism: a mini-review. *J. Pediatr. Adolesc. Gynecol.* 28, 286–291. doi: 10.1016/j.jpaga.2014.09.017
- Dzyuba, B., Van Look, K. J. W., Cliffe, A., Koldewey, H. J., and Holt, W. V. (2006). Effect of parental age and associated size on fecundity, growth and survival in the yellow seahorse *Hippocampus kuda*. *J. Exp. Biol.* 209, 3055–3061. doi: 10.1242/jeb.02336
- Escobar, S., Servili, A., Espigares, F., Gueguen, M. M., Brocal, I., Felip, A., et al. (2013). Expression of kisspeptins and kiss receptors suggests a large range of functions for kisspeptin systems in the brain of the european sea bass. *PLoS One* 8:e70177. doi: 10.1371/journal.pone.0070177
- Felip, A., Zanuy, S., Pineda, R., Pinilla, L., Carrillo, M., Tena-Sempere, M., et al. (2009). Evidence for two distinct KiSS genes in non-placental vertebrates that encode kisspeptins with different gonadotropin-releasing activities in fish and mammals. *Mol. Cell. Endocrinol.* 312, 61–71. doi: 10.1016/j.mce.2008.11.017
- Horikoshi, Y., Matsumoto, H., Takatsu, Y., Ohtaki, T., Kitada, C., Usuki, S., et al. (2003). Dramatic elevation of plasma metastatin concentrations in human pregnancy: metastatin as a novel placenta-derived hormone in humans. *J. Clin. Endocrinol. Metab.* 88, 914–919. doi: 10.1210/jc.2002-021235
- Kanda, S., Akazome, Y., Mitani, Y., Okubo, K., and Oka, Y. (2013). Neuroanatomical evidence that kisspeptin directly regulates isotocin and vasotocin neurons. *PLoS One* 8:e62776. doi: 10.1371/journal.pone.0062776
- Kim, N. N., Shin, H. S., Choi, Y. J., and Choi, C. Y. (2014). Kisspeptin regulates the hypothalamus-pituitary-gonad axis gene expression during sexual maturation in the cinnamon clownfish, *Amphiprion melanopus*. *Comp. Biochem. Physiol. B Biochem. Mol. Biol.* 168, 19–32. doi: 10.1016/j.cbpb.2013.11.002
- Knapp, R., and Carlisle, S. L. (2011). "Chapter 3 – testicular function and hormonal regulation in fishes," in *Hormones and Reproduction of Vertebrates*, eds D. O. Norris and K. H. Lopez (London: Academic Press), 43–63.
- Larkin, M. A., Blackshields, G., Brown, N. P., Chenna, R., McGettigan, P. A., McWilliam, H., et al. (2007). Clustal W and Clustal X version 2.0. *Bioinformatics* 23, 2947–2948. doi: 10.1093/bioinformatics/btm404
- Lee, J. H., Miele, M. E., Hicks, D. J., Phillips, K. K., Trent, J. M., Weissman, B. E., et al. (1996). KiSS-1, a novel human malignant melanoma metastasis-suppressor gene. *J. Natl. Cancer Inst.* 88, 1731–1737. doi: 10.1093/jnci/88.23.1731
- Lee, Y. R., Tsunekawa, K., Moon, M. J., Um, H. N., Hwang, J. I., Osugi, T., et al. (2009). Molecular evolution of multiple forms of kisspeptins and gpr54 receptors in vertebrates. *Endocrinology* 150, 2837–2846. doi: 10.1210/en.2008-1679
- Li, S., Zhang, Y., Liu, Y., Huang, X., Huang, W., Lu, D., et al. (2009). Structural and functional multiplicity of the kisspeptin/GPR54 system in goldfish (*Carassius auratus*). *J. Endocrinol.* 201, 407–418. doi: 10.1677/JOE-09-0016
- Lin, Q., Fan, S., Zhang, Y., Xu, M., Zhang, H., Yang, Y., et al. (2016). The seahorse genome and the evolution of its specialized morphology. *Nature* 540, 395–399. doi: 10.1038/nature20595
- Lin, Q., Qiu, Y., Gu, R., Xu, M., Li, J., Bian, C., et al. (2017). Draft genome of the lined seahorse. *Hippocampus erectus*. *Gigascience* 6, 1–6. doi: 10.1093/gigascience/gix030
- Livak, K. J., and Schmittgen, T. D. (2001). Analysis of relative gene expression data using real-time quantitative PCR and the 2^{−ΔΔC_T} method. *Methods* 25, 402–408. doi: 10.1006/meth.2001.1262
- Mechaly, A. S., Vinas, J., Murphy, C., Reith, M., and Piferrer, F. (2010). Gene structure of the Kiss1 receptor-2 (Kiss1r-2) in the Atlantic halibut: insights into the evolution and regulation of Kiss1r genes. *Mol. Cell. Endocrinol.* 317, 78–89. doi: 10.1016/j.mce.2009.11.005
- Mechaly, A. S., Vinas, J., and Piferrer, F. (2013). The kisspeptin system genes in teleost fish, their structure and regulation, with particular attention to the situation in Pleuronectiformes. *Gen. Comp. Endocrinol.* 188, 258–268. doi: 10.1016/j.ygcen.2013.04.010
- Messenger, S., Chatzidakis, E. E., Ma, D., Hendrick, A. G., Zahn, D., Dixon, J., et al. (2005). Kisspeptin directly stimulates gonadotropin-releasing hormone release via G protein-coupled receptor 54. *Proc. Natl. Acad. Sci. U.S.A.* 102, 1761–1766. doi: 10.1073/pnas.0409330102
- Moon, J. S., Lee, Y. R., Oh, D. Y., Hwang, J. I., Lee, J. Y., Kim, J. I., et al. (2009). Molecular cloning of the bullfrog kisspeptin receptor GPR54 with high sensitivity to *Xenopus kisspeptin*. *Peptides* 30, 171–179. doi: 10.1016/j.peptides.2008.04.015
- Nakajo, M., Kanda, S., Karigo, T., Takahashi, A., Akazome, Y., Uenoyama, Y., et al. (2018). Evolutionally conserved function of kisspeptin neuronal system is nonreproductive regulation as revealed by nonmammalian study. *Endocrinology* 159, 163–183. doi: 10.1210/en.2017-00808
- Ohga, H., Adachi, H., Kitano, H., Yamaguchi, A., and Matsuyama, M. (2017). Kiss1 hexadecapeptide directly regulates gonadotropin-releasing hormone 1 in the scombroid fish, chub mackerel. *Biol. Reprod.* 96, 376–388. doi: 10.1095/biolreprod.116.142083
- Ohga, H., Selvaraj, S., Adachi, H., Imanaga, Y., Nyuji, M., Yamaguchi, A., et al. (2014). Functional analysis of kisspeptin peptides in adult immature chub mackerel (*Scomber japonicus*) using an intracerebroventricular administration method. *Neurosci. Lett.* 561, 203–207. doi: 10.1016/j.neulet.2013.12.072
- Ohga, H., Selvaraj, S., and Matsuyama, M. (2018). The roles of kisspeptin system in the reproductive physiology of fish with special reference to chub mackerel studies as main axis. *Front. Endocrinol.* 9:147. doi: 10.3389/fendo.2018.00147
- Ohtaki, T., Shintani, Y., Honda, S., Matsumoto, H., Hori, A., Kanehashi, K., et al. (2001). Metastasis suppressor gene KiSS-1 encodes peptide ligand of a G-protein-coupled receptor. *Nature* 411, 613–617. doi: 10.1038/35079135
- Parhar, I. S., Ogawa, S., and Sakuma, Y. (2004). Laser-captured single digoxigenin-labeled neurons of gonadotropin-releasing hormone types reveal a novel g protein-coupled receptor (Gpr54) during maturation in cichlid fish. *Endocrinology* 145, 3613–3618. doi: 10.1210/en.2004-0395
- Pasquier, J., Lafont, A. G., Jeng, S. R., Morini, M., Dirks, R., van den Thillart, G., et al. (2012a). Multiple kisspeptin receptors in early osteichthyans provide

- new insights into the evolution of this receptor family. *PLoS One* 7:e48931. doi: 10.1371/journal.pone.0048931
- Pasquier, J., Lafont, A. G., Tostivint, H., Vaudry, H., Rousseau, K., and Dufour, S. (2012b). Comparative evolutionary histories of kisspeptins and kisspeptin receptors in vertebrates reveal both parallel and divergent features. *Front. Endocrinol.* 3:173. doi: 10.3389/fendo.2012.00173
- Patterson, M., Murphy, K. G., Thompson, E. L., Patel, S., Ghatei, M. A., and Bloom, S. R. (2006). Administration of kisspeptin-54 into discrete regions of the hypothalamus potentially increases plasma luteinizing hormone and testosterone in male adult rats. *J. Neuroendocrinol.* 18, 349–354. doi: 10.1111/j.1365-2826.2006.01420.x
- Popa, S. M., Clifton, D. K., and Steiner, R. A. (2008). The role of kisspeptins and GPR54 in the neuroendocrine regulation of reproduction. *Annu. Rev. Physiol.* 70, 213–238. doi: 10.1146/annurev.physiol.70.113006.100540
- Qin, G., Johnson, C., Zhang, Y., Zhang, H., Yin, J., Miller, G., et al. (2018). Temperature-induced physiological stress and reproductive characteristics of the migratory seahorse *Hippocampus erectus* during a thermal stress simulation. *Biol. Open* 7:bio032888. doi: 10.1242/bio.032888
- Roux, N., Genin, E., Carel, J. C., Matsuda, F., Chaussain, J. L., and Milgrom, E. (2003). Hypogonadotropic hypogonadism due to loss of function of the KiSS1-derived peptide receptor GPR54. *Proc. Natl. Acad. Sci. U.S.A.* 100, 10972–10976. doi: 10.1073/pnas.1834399100
- Scobell, S. K., and MacKenzie, D. S. (2011). Reproductive endocrinology of Syngnathidae. *J. Fish Biol.* 78, 1662–1680. doi: 10.1111/j.1095-8649.2011.02994.x
- Scott, V., and Brown, C. H. (2013). “Beyond the GnRH Axis: kisspeptin regulation of the oxytocin system in pregnancy and lactation,” in *Kisspeptin Signaling in Reproductive Biology*, eds A. S. Kauffman and J. T. Smith (New York, NY: Springer), 201–218.
- Seminara, S. B., Messenger, S., Chatzidaki, E. E., Thresher, R. R., Acierno, J. S., Shagoury, J. K., et al. (2003). The GPR54 gene as a regulator of puberty. *New Engl. J. Med.* 349, 1614–U1618. doi: 10.1056/Nejmoa035322
- Stolting, K. N., and Wilson, A. B. (2007). Male pregnancy in seahorses and pipefish: beyond the mammalian model. *Bioessays* 29, 884–896. doi: 10.1002/bies.20626
- Tamura, K., Stecher, G., Peterson, D., Filipowski, A., and Kumar, S. (2013). MEGA6: Molecular Evolutionary Genetics Analysis version 6.0. *Mol. Biol. Evol.* 30, 2725–2729. doi: 10.1093/molbev/mst197
- Tang, H. P., Liu, Y., Luo, D. J., Ogawa, S., Yin, Y. K., Li, S. S., et al. (2015). The kiss/kissr systems are dispensable for zebrafish reproduction: evidence from gene knockout studies. *Endocrinology* 156, 589–599. doi: 10.1210/en.2014-1204
- Tena-Sempere, M. (2010). Roles of kisspeptins in the control of hypothalamic-gonadotropic function: focus on sexual differentiation and puberty onset. *Endocr. Dev.* 17, 52–62. doi: 10.1159/000262528
- Tena-Sempere, M., Felip, A., Gomez, A., Zanuy, S., and Carrillo, M. (2012). Comparative insights of the kisspeptin/kisspeptin receptor system: lessons from non-mammalian vertebrates. *Gen. Comp. Endocrinol.* 175, 234–243. doi: 10.1016/j.ygcen.2011.11.015
- Ukena, K., and Tsutsui, K. (2005). A new member of the hypothalamic RF-amide peptide family, LPXRF-amide peptides: structure, localization, and function. *Mass Spectrom. Rev.* 24, 469–486. doi: 10.1002/mas.20031
- Wang, B., Liu, Q., Liu, X., Xu, Y., and Shi, B. (2017). Molecular characterization of Kiss2 receptor and in vitro effects of Kiss2 on reproduction-related gene expression in the hypothalamus of half-smooth tongue sole (*Cynoglossus semilaevis*). *Gen. Comp. Endocrinol.* 249, 55–63. doi: 10.1016/j.ygcen.2017.04.006
- Zhang, H., Qin, G., Zhang, Y., Li, S., and Lin, Q. (2016). The leptin system and its expression at different nutritional and pregnant stages in lined seahorse (*Hippocampus erectus*). *Biol. Open* 5, 1508–1515. doi: 10.1242/bio.020750

Conflict of Interest Statement: The authors declare that the research was conducted in the absence of any commercial or financial relationships that could be construed as a potential conflict of interest.

The handling Editor and reviewer LE declared their involvement as co-editors in the Research Topic.

Copyright © 2018 Zhang, Zhang, Qin, Li and Lin. This is an open-access article distributed under the terms of the Creative Commons Attribution License (CC BY). The use, distribution or reproduction in other forums is permitted, provided the original author(s) and the copyright owner(s) are credited and that the original publication in this journal is cited, in accordance with accepted academic practice. No use, distribution or reproduction is permitted which does not comply with these terms.



Spexin-Based Galanin Receptor Type 2 Agonist for Comorbid Mood Disorders and Abnormal Body Weight

Seongsik Yun¹, Arfaxad Reyes-Alcaraz¹, Yoo-Na Lee¹, Hyo Jeong Yong¹, Jeewon Choi², Byung-Joo Ham³, Jong-Woo Sohn², Dong-Hoon Kim¹, Gi Hoon Son¹, Hyun Kim¹, Soon-Gu Kwon⁴, Dong Sik Kim⁴, Bong Chul Kim⁴, Jong-Ik Hwang¹ and Jae Young Seong^{1*}

¹ Graduate School of Medicine, Korea University, Seoul, South Korea, ² Graduate School of Medical Science and Engineering, Korea Advanced Institute of Science and Technology, Daejeon, South Korea, ³ Department of Psychiatry, College of Medicine, Korea University, Seoul, South Korea, ⁴ Neuracle Science Co., Ltd., Seoul, South Korea

OPEN ACCESS

Edited by:

David Vaudry,
Institut National de la Santé et de la
Recherche Médicale (INSERM),
France

Reviewed by:

Barbara Kofler,
University Hospital Salzburg, Austria
Zhaoxiang Bian,
Hong Kong Baptist University,
Hong Kong

*Correspondence:

Jae Young Seong
jyseong@korea.ac.kr

Specialty section:

This article was submitted to
Neuroendocrine Science,
a section of the journal
Frontiers in Neuroscience

Received: 19 February 2019

Accepted: 04 April 2019

Published: 18 April 2019

Citation:

Yun S, Reyes-Alcaraz A, Lee Y-N, Yong HJ, Choi J, Ham B-J, Sohn J-W, Kim D-H, Son GH, Kim H, Kwon S-G, Kim DS, Kim BC, Hwang J-I and Seong JY (2019) Spexin-Based Galanin Receptor Type 2 Agonist for Comorbid Mood Disorders and Abnormal Body Weight. *Front. Neurosci.* 13:391. doi: 10.3389/fnins.2019.00391

Despite the established comorbidity between mood disorders and abnormal eating behaviors, the underlying molecular mechanism and therapeutics remain to be resolved. Here, we show that a spexin-based galanin receptor type 2 agonist (SG2A) simultaneously normalized mood behaviors and body weight in corticosterone pellet-implanted (CORTI) mice, which are underweight and exhibit signs of anhedonia, increased anxiety, and depression. Administration of SG2A into the lateral ventricle produced antidepressive and anxiolytic effects in CORTI mice. Additionally, SG2A led to a recovery of body weight in CORTI mice while it induced significant weight loss in normal mice. In Pavlovian fear-conditioned mice, SG2A decreased contextual and auditory fear memory consolidation but accelerated the extinction of acquired fear memory without altering innate fear and recognition memory. The main action sites of SG2A in the brain may include serotonergic neurons in the dorsal raphe nucleus for mood control, and proopiomelanocortin/corticotropin-releasing hormone neurons in the hypothalamus for appetite and body weight control. Furthermore, intranasal administration of SG2A exerted the same anxiolytic and antidepressant-like effects and decreased food intake and body weight in a dose-dependent manner. Altogether, these results indicate that SG2A holds promise as a clinical treatment for patients with comorbid mood disorders and abnormal appetite/body weight.

Keywords: galanin receptor 2 agonist, depression, post-traumatic stress disorder, body weight, appetite, intranasal administration

INTRODUCTION

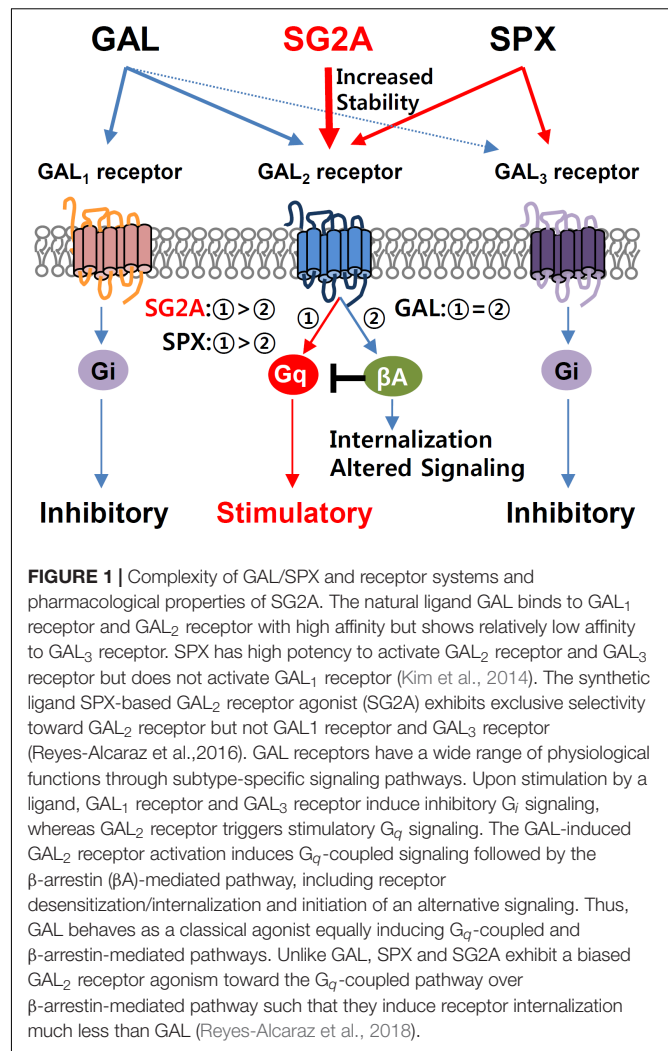
Mood disorders such as anxiety and depression are often associated with abnormal eating behaviors, leading to either obesity or a poor diet (Simon et al., 2006), and endocrine and metabolic conditions are both exacerbated in major depression (Simon et al., 2006; Marijnissen et al., 2011). Stress can promote either an increased consumption of palatable and rewarding foods leading to obesity or a diminished appetite causing weight loss (Adam and Epel, 2007), and individuals who

are underweight or obese are at a high risk for depression and anxiety (Carey et al., 2014). Therefore, mood disorders and abnormal appetite are reciprocally linked (Kloiber et al., 2007). This link has also been observed in animal models of mood disorders (Sharma et al., 2013), suggesting that a common signaling pathway underlies these phenotypes in humans and animals.

Recently, the novel neuropeptide spexin (SPX) and its receptors, galanin (GAL) receptor type 2 (GAL₂ receptor), and type 3 (GAL₃ receptor) (Kim et al., 2014; Yun et al., 2014), have gained attention for their possible involvement in the bidirectional regulation of mood and feeding behaviors. The function of SPX in feeding behavior is interesting, because it opposes the orexigenic function of GAL, a paralogous neuropeptide (Yun et al., 2015; Furlong and Seong, 2017). Whereas the SPX administration leads to weight loss in diet-induced obese rodents (Walewski et al., 2014) and decreased food intake in goldfish (Wong et al., 2013), GAL leads to an increase in food intake (Karatayev et al., 2009). SPX mRNA levels are markedly decreased in the fat tissues of obese humans (Walewski et al., 2014), whereas the circulating GAL levels, along with neuropeptide Y and leptin, are significantly higher in obese women (Baranowska et al., 1997). These differences likely reflect the activities of the targeted receptors: SPX binds with high affinity to GAL₂ receptor and GAL₃ receptor but not GAL₁ receptor, whereas GAL has high potencies for GAL₁ receptor and GAL₂ receptor but a low potency for GAL₃ receptor (Kim et al., 2014). In addition, the GAL₂ receptor-mediated downstream signaling induced by SPX and GAL differs. Whereas GAL exerts both G_q- and β -arrestin-mediated signaling of GAL₂ receptor, SPX shows a biased agonism favoring G-protein-mediated signaling (Reyes-Alcaraz et al., 2018).

When exogenously administered to rodents, GAL increases their immobility in the forced swim test (FST), suggesting an increase in depression-like behavior (Kuteeva et al., 2008). Studies using peptidergic or non-peptidergic compounds with selectivity for GAL receptor subtypes suggested that GAL₁/GAL₃ receptor-mediated signaling contributes to the prodepressive effect, whereas GAL₂ receptor-mediated signaling exerts antidepressive effects (Webling et al., 2012). For instance, M617, an agonist of GAL₁ receptor and GAL₂ receptor (GAL₁ receptor > GAL₂ receptor), induces depression-like behavior, but the non-peptidergic GAL₃ receptor antagonist SNAP37889 decreases anxiety- and depression-like behaviors (Swanson et al., 2005). AR-M1896 (Gal2-11), an agonist of GAL_{2/3} receptor (GAL₂ receptor > GAL₃ receptor), suppresses depression-like behaviors (Webling et al., 2012), but GAL₂ receptor knockout mice and GAL₂ receptor antagonist M871 injected mice exhibited anxiety- and depression-like behaviors (Bailey et al., 2007). Thus, steering SPX action through GAL₂ receptor is an optimal approach to simultaneously resolve both mood disorders and abnormal appetite/body weight.

We recently developed SPX-based GAL₂ receptor-selective agonists (SG2A) with a much longer half-life in serum than wild-type SPX (Figure 1; Reyes-Alcaraz et al., 2016, 2018). In addition, SG2A, like SPX but unlike GAL, preferentially induced G-protein-mediated signaling over β -arrestin-dependent



pathway (Reyes-Alcaraz et al., 2018), which avoids the drug tolerance or possible adverse side effects associated with classical agonists (Hausdorff et al., 1990; Yang and Tao, 2017). In the present study, we examined the beneficial effects of intracerebroventricularly (i.c.v.) administered SG2A on body weight and mood changes in mouse models of depression and anxiety disorder and investigated the putative neural networks activated by SG2A. We also examined whether intranasal (i.n.) administration of SG2A produces effects similar to those with i.c.v. administration, which would increase its potential clinical application for patients with comorbid mood disorders and abnormal body weight.

MATERIALS AND METHODS

Animals

Wild-type male C57BL/6J mice at 8-weeks old were obtained from Central Lab Animal (Seoul, South Korea) and proopiomelanocortin (POMC)-hrGFP mice were from Jackson Laboratory (#006421; Bar Harbor, ME, United States). All mice

were kept in temperature-controlled (22–23°C) rooms under a 12-h light-dark photoperiod. Standard mouse chow/water were available *ad libitum*. All animal procedures were approved by the Institutional Animal Care and Use Committee of Korea University (KOREA-2016-0050-C2) and Korea Advanced Institute of Science and Technology (KA2014-02).

Drug Application

For i.c.v. injections, the mice were anesthetized with a flow anesthesia system, mounted on a stereotaxic apparatus (Stoelting, Wood Dale, IL, United States), and unilaterally implanted with 26-gauge stainless steel guide cannulae (model C315G; Plastics One, Roanoke, VA, United States) in the lateral ventricles [(LV) AP, −0.55 mm; ML, 1.1 mm; and DV, −2.05 mm]. A 32-gauge dummy cannula was inserted into guide cannula to prevent clogging. Two jewelry screws were implanted into the skull as anchors, and the whole assembly was affixed to the skull with dental cement. Mice were allowed to recover for 2 weeks, singly housed. SG2A (PEG2-NWTdANAALYLFGPdQ-NH₂; AnyGen, Gwangju, South Korea) was dissolved in dimethyl sulfoxide (DMSO) to a concentration of 100 μM (170 ng/μl) and injected into the LV (0.5 μl/ventricle) 2–3 h before behavioral tests or 1–2 h before c-fos induction sampling with 33-gauge injector cannulae attached to 10-μl Hamilton syringes at a rate of 0.5 μl/min. For i.n. administration, a 10 mM stock solution of SG2A dissolved in DMSO was diluted with phosphate-buffered saline (PBS) to 1, 3, and 10 μg in 5 μl final volume, and 2.5 μl of this solution was delivered to each nostril with a pipette.

Behavioral Studies

Mice were handled for 5 min daily for 3 days before the behavioral tests. Recorded videos were analyzed with an ANY-maze video tracking program (Stoelting).

See **Supplementary Information** for body weight and food intake measurements, elevated plus maze test (EPMT), open field test (OFT), tail suspension test (TST), the FST, sucrose preference test (SPT), Pavlovian fear conditioning, unconditioned innate fear response, Y-maze test, and novel object recognition (NOR) test.

Corticosterone Pellet Implantation (CORTI) for the Depression Model

CORTI was performed as previously described (Demuyser et al., 2016). Mice were randomly assigned to two groups (Sham or CORTI). For the CORTI group, mice were anesthetized with a flow anesthesia system and two slow-release corticosterone pellets (21-day release, 5 mg/pellet; Innovative Research of America, Sarasota, FL, United States) were subcutaneously implanted in the neck to provide an equivalent total exposure of approximately 20 mg/kg/day corticosterone depending on the weight. Sham group, were treated equally but were not implanted. Cannulae for i.c.v. were then implanted into the LV of animals in both groups. Body weights were recorded every 3 days and every week.

Immunohistochemistry

Animals were perfused with 4% paraformaldehyde in PBS, and isolated brains were postfixed in the same fixative overnight. The brains were then cryoprotected in 30% sucrose, sectioned serially on a cryostat (40 μm), and stored in 50% glycerol/50% PBS at −20°C until use. Sections were blocked with 10% horse serum and 0.3% Triton X-100 for 30 min. Sections were incubated overnight at 4°C with primary antibodies against c-fos (Cell Signaling Technology, Danvers, MA, United States), CamKIIα (Millipore, Burlington, MA, United States), GAD67 (Millipore), tryptophan hydroxylase [(TPH) Sigma-Aldrich, St. Louis, MO, United States], tyrosine hydroxylase [(TH) Sigma-Aldrich], NeuN (Millipore), or corticotropin-releasing hormone [(CRH) Peninsula Laboratories, San Carlos, CA, United States]. After several washes with PBS, appropriate secondary antibodies, Alexa 488 and Cy3 with DAPI, were applied for 30 min. The sections were washed, mounted, and observed under a confocal microscope (Leica TCS SP8; Leica Microsystems, Buffalo Grove, IL, United States). For analysis of neurogenesis, mice were administered BrdU [100 mg/kg i.p.; 97% (+)-5'-bromo-2'-deoxyuridine; Sigma-Aldrich] twice per day (8-h interval) for 2 days prior to sacrifice. Before blocking, the brain sections were incubated with 1 N HCL for 30 min at 37°C and then incubated overnight with anti-BrdU (Abcam, Cambridge, United Kingdom) and anti-doublecortin [(DCX) Santa Cruz Biotechnology, Dallas, TX, United States] antibodies.

See **Supplementary Information** for Western blotting, electrophysiology and determination of α-MSH secretion in POMC neurons.

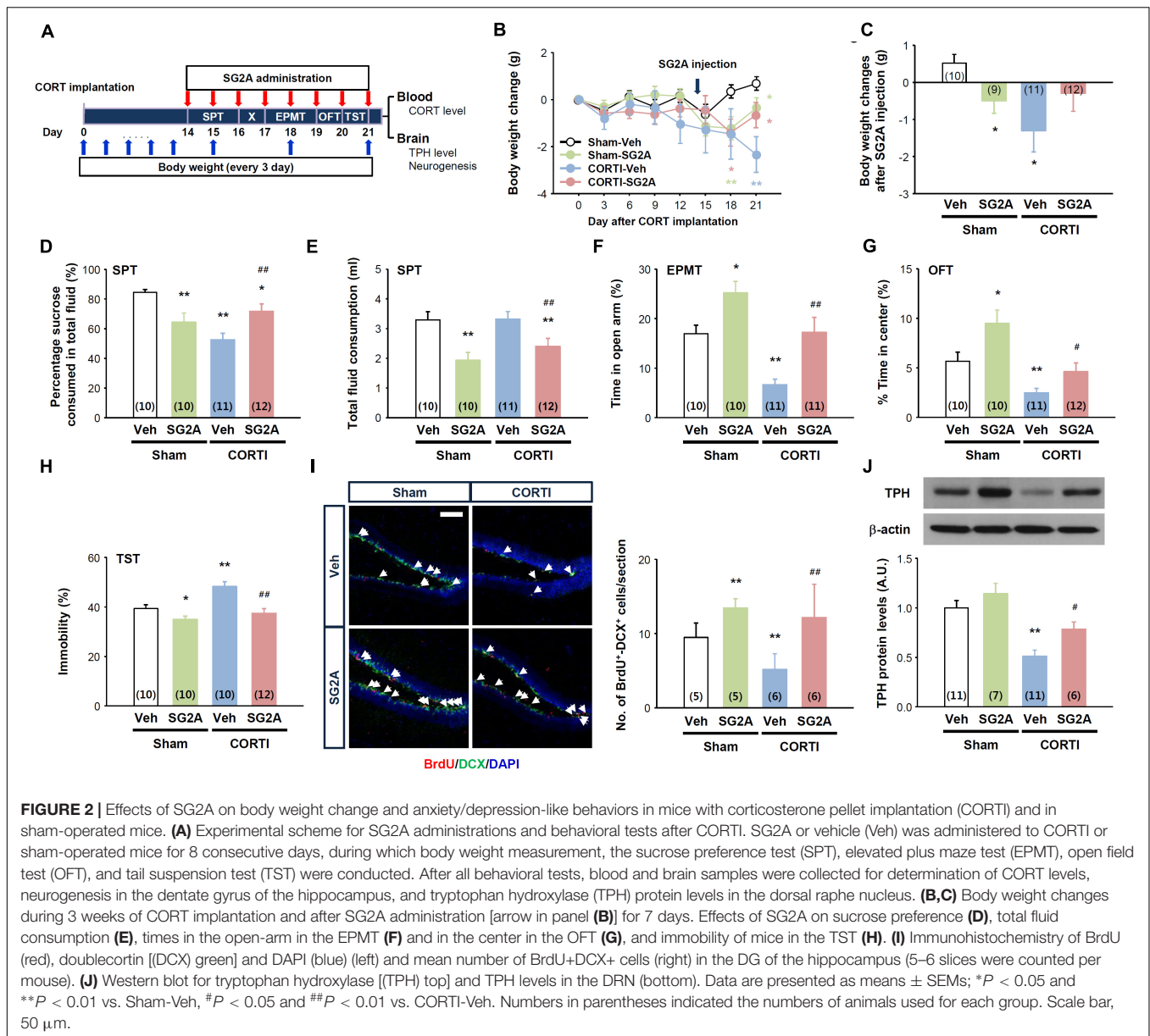
Statistical Analysis

The data are presented as means ± standard errors of the means (SEMs) from at least two independent experiments. Statistical differences between individual groups were evaluated using Student's *t*-tests and/or analyses of variance followed by Newman-Keuls tests as a *post hoc* comparison. Electrophysiology results were analyzed with Wilcoxon signed-rank tests. Fear memory extinction was evaluated by repeated-measures analyses of variance followed by Bonferroni tests. *P*-value of <0.05 was considered statistically significant.

RESULTS

Effects of SG2A in CORTI Mice

The effects of SG2A were first addressed in CORTI mice, which exhibit markedly lowered body weights and anhedonia-, anxiety-, and depression-like behaviors (**Figure 2**). The functional phenotype of these mice resembles the hypercortisolism, anhedonia, hypophagia, and weight loss in individuals with melancholic depression (Carroll et al., 2012), according to the Diagnostic and Statistical Manuals of Mental Disorders, 5th edition (American Psychiatric Association, 2013). 14 days after CORTI or sham operations, SG2A were administered i.c.v. for 8 consecutive days. During this time, the SPT was performed first for 2 days, followed by 1-day break, and then the EPMT was performed for 2 days, OFT for 1 day, and TST for 1 day. 3 to



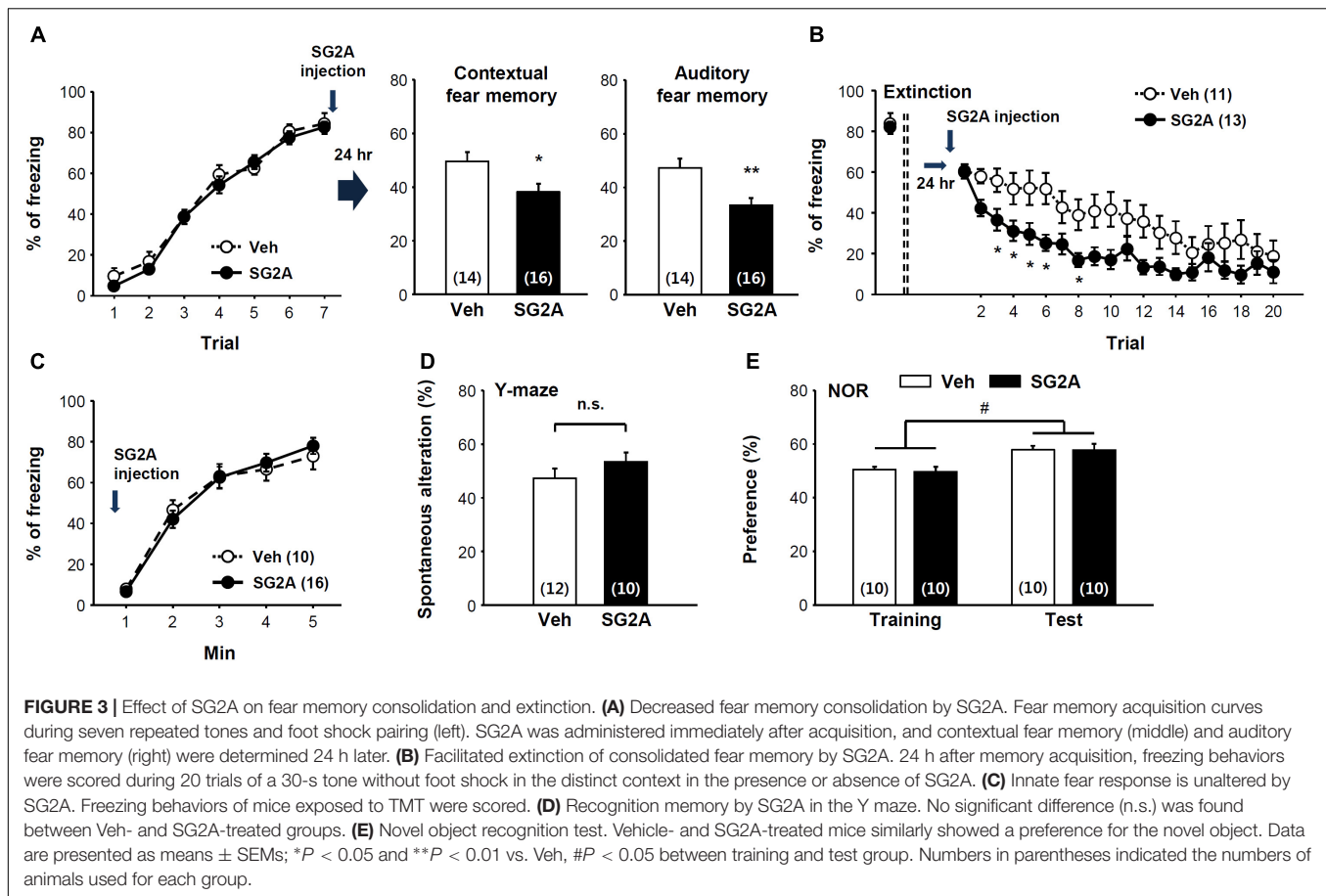
4 h after SG2A administration on the last day, blood and brain samples were collected (Figure 2A).

High levels of blood corticosterone were maintained for 21 days in CORTI mice, regardless of SG2A administration (Supplementary Figure 1A), and the body weights of CORTI mice were significantly lower than the sham-operated/vehicle-treated (Sham-Veh) mice (Figure 2B). Notably, the effect of SG2A on body weight differed between Sham and CORTI mice. The treatment of Sham mice with SG2A (Sham-SG2A) for 7 consecutive days led to a significant body weight loss, whereas the SG2A-treated CORTI mice partly recovered the body weights ($P = 0.08$, CORTI-SG2A vs. CORTI-Veh) and did not differ from those of Sham-Veh mice (Figure 2C).

The results of the SPT suggest that CORTI induces anhedonia, a major symptom of depression, as no sucrose preference was

observed in CORTI-Veh mice. SG2A administration significantly increased the sucrose preference rate in CORTI mice but induced a moderate but significant decrease in sucrose preference in Sham mice (Figure 2D). Notably, total fluid consumption did not differ between CORTI-Veh and Sham-Veh mice (Figure 2E), indicating that the decrease of sucrose preference in CORTI-Veh mice is likely due to anhedonia. By contrast, the decrease of sucrose preference in Sham-SG2A and CORTI-SG2A mice accompanied decreased total fluid (Figure 2E) and sucrose (Supplementary Figure 1B) consumption.

In the EPMT, CORT-Veh mice appeared to be very anxious, as their time in the open-arms was significantly less than that of Sham-Veh mice. SG2A administration increased the time in the open-arms for both groups (Figure 2F). In the OFT, CORTI-Veh mice spent less time in the center than Sham-Veh mice,



indicating increased anxiety. This anxiogenic effect of CORTI was rescued by SG2A administration (**Figure 2G**). Total activities were not significantly different among the experimental groups (**Supplementary Figure 1C**).

In the TST, the immobility of CORTI-Veh mice was significantly higher than that of Sham-Veh mice, indicating an increased depression-like behavior. SG2A reduced the immobility of both groups (**Figure 2H**).

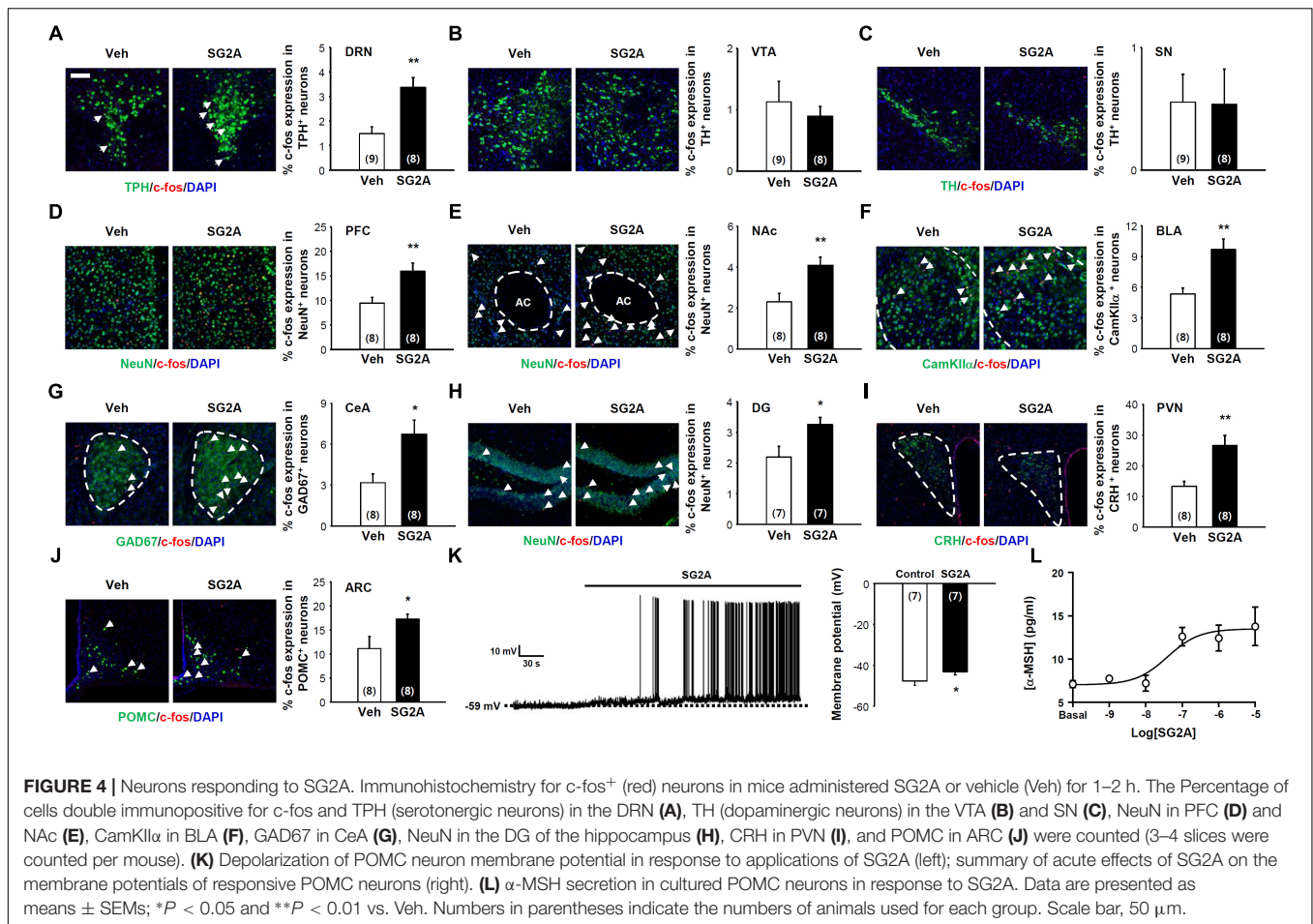
The DG of the hippocampus is particularly sensitive to highly sustained corticosterone, showing altered neural death and adult neurogenesis. Furthermore, neurogenesis in the DG is highly associated with depression, as antidepressant drugs increase neurogenesis (Schmidt and Duman, 2007). Thus, proliferating neural progenitors in the DG were examined by counting BrdU⁺DCX⁺ cells. The number of double-positive cells was significantly decreased in CORTI-Veh mice compared to that in Sham-Veh mice. SG2A treatment significantly augmented the number of BrdU⁺DCX⁺ cells in both groups (**Figure 2I**).

Depression-like behavior reflects an underactivity of monoaminergic transmission. We examined protein levels of TPH, the rate-limiting enzyme for serotonin (5-HT) synthesis, as our data, presented below, suggested that SG2A activates 5-HT neurons in the dorsal raphe nucleus (DRN) but not dopaminergic neurons in substantia nigra (SN) and the ventral tegmental area (VTA). CORTI markedly lowered TPH levels

compared to those of Sham-Veh mice. This decrease in TPH levels was rescued by SG2A (**Figure 2J**).

Effects of SG2A on Fear Memory Consolidation and Extinction

As SG2A exerted anxiolytic effects, we further determined the effects of SG2A on fear memory consolidation and extinction using the contextual and auditory-cued Pavlovian fear conditioning model. Seven trials of auditory cue with foot shock resulted in fear memory acquisition. Immediately after the last trial, SG2A or vehicle was administered into the LV of the mice (**Figure 3A**, left). The fear memory consolidation was determined 24 h later by placing the mice in the same chamber without auditory cues (context fear memory test) or in a different chamber with the auditory cues (auditory fear memory test). SG2A-administered mice spent significantly less time freezing than vehicle-treated mice in response to the context (**Figure 3A**, middle). Likewise, SG2A reduced the freezing rate responding to the auditory cue (**Figure 3A**, right). Thus, SG2A administration just after fear memory acquisition reduced both contextual and auditory fear memory consolidation after 24 h. Fear memory extinction was also examined at this time by determining the freezing rate in response to repeated auditory cues without foot-shock. SG2A or vehicle was administered 2–3 h

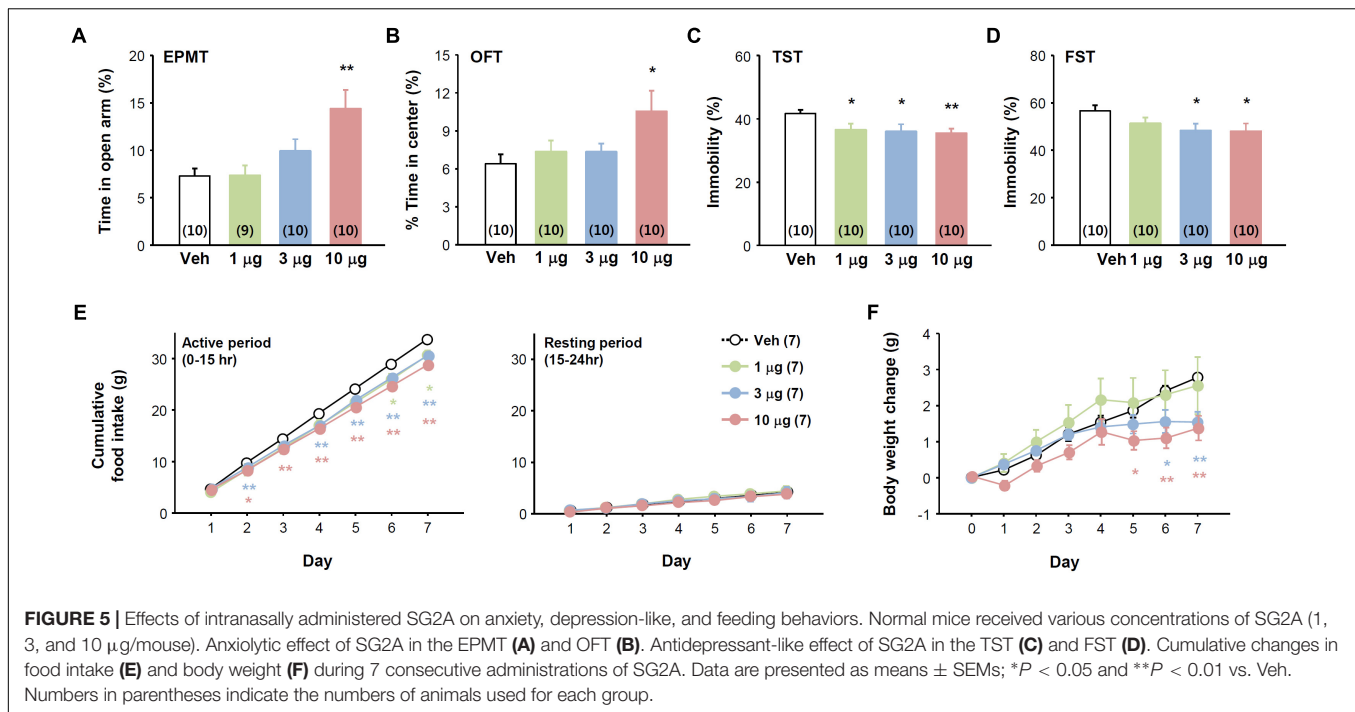


before the first auditory cue. Vehicle-treated mice showed a gradual decrease in freezing rate as the number of trials increased, and SG2A accelerated this decrease beginning at the second trial [treatment effect: $F(1,22) = 5.192$, $P < 0.05$; interaction: $F(1,22) = 1.773$, $P < 0.05$] (Figure 3B). These results suggest that SG2A facilitates the extinction of fear memories. Whether these effects were due to a decreased response to fear-causing environments (unconditioned fear response) or to impaired recognition memory was not clear. However, SG2A did not alter unconditioned fear responses, as freezing behaviors of mice exposed to TMT, a synthetic fox (predator) feces odor, did not differ (Figure 3C). The results from the Y-maze test suggest the SG2A does not alter spatial recognition memory, as there was no difference between vehicle- and SG2A-injected mice (Figure 3D). Furthermore, SG2A did not influence responding in the NOR test (Figure 3E). Thus the effects of SG2A on fear memory were not attributable to a decreased response to a fear environment or an impairment of recognition memory.

Neuronal Activation by SG2A

To determine the possible neural circuits for SG2A action, mRNA expression of SPX/GAL and GAL receptors were determined in the various brain regions using *in situ* hybridization assay and quantitative RT-PCR. SPX mRNA were strongly detected

in the medial habenula (mHb) and suprachiasmatic nucleus (SCN) of the hypothalamus. Interestingly, GAL₂ receptor mRNA levels were high in the hypothalamus, Hb, ventral midbrain (VMB), and DRN which are potential target regions of SPX action. In contrast, mRNA expressions of GAL, GAL₁ receptor, and GAL₃ receptor were mainly restricted in the hypothalamus (Supplementary Figure 2). To identify the neural circuits influenced by GAL₂ receptor activation, the numbers of c-fos⁺ neurons in various brain regions were determined at 1–2 h after a single i.c.v. administration of SG2A, which is sufficient to induce anxiolytic-, antidepressant-, and anorexic-like effects in normal and ob/ob mice (Supplementary Figure 3). We found that SG2A significantly increased the number of c-fos⁺TPH⁺ 5-HT neurons in the DRN (Figure 4A) but not the number of c-fos and TH double-positive dopaminergic neurons in the VTA (Figure 4B) and SN (Figure 4C). SG2A administration also induced c-fos in the prefrontal cortex (PFC) (Figure 4D) and the nucleus accumbens (NAc) (Figure 4E), regions implicated in the pathophysiology of depression and innervated by 5-HT neurons from the DRN (Challis and Berton, 2015). c-fos expression was also increased in the basolateral (BLA) and central amygdala (CeA). In particular, the number of neurons immunoreactive for both c-fos and CamKIIα (Figure 4F) or GAD67 (Figure 4G) was higher in SG2A-injected mice than in vehicle-treated mice. In the



hippocampus, SG2A increased the number of *c-fos*⁺ neurons in DG (Figure 4H) but not in CA1, CA2, or CA3 (Supplementary Figure 4). The activation of neurons in the amygdala and DG is implicated in regulating anxiety and fear memory (Sierra-Mercado et al., 2011). Increased *c-fos* immunoreactivity was also observed in CRH neurons in the paraventricular nucleus (PVN) (Figure 4I) and POMC neurons in the arcuate nucleus (ARC) (Figure 4J). However, other brain regions, such as Hb, lateral hypothalamus, and SCN, did not show *c-fos* induction after SG2A administration (Supplementary Figure 4).

As POMC neurons in the ARC are particularly important for regulating body weight via appetite and energy expenditure (Schwartz et al., 2000), we further examined whether SG2A can directly activate these neurons *ex vivo* and *in vitro*. POMC neurons in hypothalamic slices obtained from POMC-hrGFP transgenic mice can be identified by their green fluorescence (Sohn et al., 2011). As shown in Figure 4K, bath application of SG2A depolarized the membrane potentials of 7/18 (38.9%) POMC neurons by 4.6 ± 0.6 mV (from -47.7 ± 2.1 to -43.1 ± 1.5 mV, P < 0.05). The other 11 cells remained unresponsive to SG2A (from -46.8 ± 2.2 to -46.6 ± 2.2 mV, P > 0.05). These data demonstrate that GAL₂ receptor stimulation excites POMC neurons. *In vitro*, cultured POMC neurons exhibited dose-dependent SG2A-induced secretion of α -MSH, a major anorectic neuropeptide (Figure 4L; Yang and Tao, 2017).

Nasal Application of SG2A

The effects of SG2A in these animal models suggest it has therapeutic potential. Thus, we examined whether SG2A can be delivered to the CNS by i.n. administration, a

non-invasive route for enabling efficient crossing of the blood-brain barrier (Kageyama et al., 2016). Behavioral tests were performed 2–3 h after SG2A i.n. administration. Similar to that observed with i.c.v. administration, mice receiving i.n. SG2A spent more time in the open-arms in the EPMT (Figure 5A) and open field in OFT (Figure 5B) without significant changes in total movement (Supplementary Figure 5A) and significantly less immobility in the TST (Figure 5C) and FST (Figure 5D), suggesting that i.n. SG2A reduced anxiety- and depression-like behaviors. When administered for 7 days, i.n. SG2A significantly decreased cumulative food intake and body weight in a dose-dependent manner. SG2A decreased food intake during the active period when the mice mainly consume the chow, but not during the resting period (Figure 5E). These decreases corresponded to continual decreases in body weight, with a significant difference versus the vehicle-treated group observed beginning day 5 after SG2A administration for the 10 µg-treated group and day 6 for the 3 µg-treated group (Figure 5F).

Successful delivery of SG2A to the brain via the i.n. route was confirmed by *c-fos* induction in the brain regions that responded to i.c.v. administration. Specifically, i.n. administration of SG2A increased the numbers of *c-fos*⁺TPH⁺ 5-HT neurons in the DRN, *c-fos*⁺NeuN⁺ neurons in the PFC, NAC, and DG, *c-fos*⁺CamKII α ⁺ cells in the BLA, and *c-fos*⁺GAD67⁺ cells in the CeA (Supplementary Figure 5). Antidepressive and anxiolytic effects of SG2A i.n. administration were also examined in CORT1 mice. Nasal delivery of SG2A increased the time in the open-arm in the EPMT, increased time in the center in OFT, and decreased the time of immobility in the TST without any

differences in total activities (**Supplementary Figure 6**). Altogether, these results demonstrate that SG2A can be delivered to the CNS via an i.n. route to sufficiently evoke neurochemical and behavioral effects similar to those observed after i.c.v. administration.

DISCUSSION

Considering the cross-reactivity of SPX and GAL toward GAL receptors and the overall complexity of the GAL receptor subtype-specific signaling pathways (Kim et al., 2014; Yun et al., 2014), the development of subtype-selective GAL receptor agonists may help to elucidate GAL receptor subtype-specific physiological functions (Reyes-Alcaraz et al., 2016). Many different types of GAL receptor-targeting agonists/antagonists have been generated by using a variety of fragments from the GAL peptide. However, these agents maintained their substantial affinity toward other GAL receptor subtypes at high concentrations (Webling et al., 2012). Recently, we developed SG2A, an SPX-based GAL₂ receptor agonist that lacks activity toward GAL₁ receptor and GAL₃ receptor (Reyes-Alcaraz et al., 2016). The pharmacological relevance of SG2A is underscored by its biased agonism toward G-protein-dependent signaling over β -arrestin-mediated signaling, which is similar to SPX but different from GAL with unbiased activation (Reyes-Alcaraz et al., 2018). Probably due to β -arrestin-mediated signaling, classical agonists often result in contradictory results, such as with GAL for depression-like behaviors (Lu et al., 2005; Kuteeva et al., 2008) and the dichotomous action/dose-dependent inaction of galanin-like peptide in regulating food intake (Lawrence et al., 2002; Kageyama et al., 2016). By contrast, SG2A shows dose-dependent and consistent effects on mood and appetite behaviors during repetitive administrations. Thus, compared to the GAL-based agonist, the SPX-based agonist may have multiple pharmacological benefits, exerting its action on both mood and appetite/body weight.

SG2A administration (i.c.v./i.n.) produced rapid anxiolytic- and antidepressant-like behavioral effects. Thus, time required for onset of effects is different from selective serotonin reuptake inhibitors (SSRIs) that show a late onset of antidepressive effects. Nevertheless, the effect of SG2A is likely mediated by activation of 5-HT neurons in the DRN as shown in **Figure 4A**. It is of interesting to note that SPX mRNA is highly expressed in the mHb. Projection from mHb to interpeduncular nucleus (IPN) is connected to the serotonergic raphe nucleus which is implicated in the regulation of mood such as depression and anxiety (Yamaguchi et al., 2013). In addition, the DRN is known to express GAL₂ receptor which then promote TPH transcription (Xu et al., 1998; Lu et al., 2005; Mazarati et al., 2005). Indeed, our study showed that repetitive SG2A administration significantly increased TPH protein levels in the DRN of CORTI mice. Interestingly, chronic treatment of fluoxetine, an SSRI, increases GAL₂ receptor binding sites on the DRN (Lu et al., 2005). Thus, both SG2A and SSRI are involved in direct or indirect

activation of GAL₂ receptor for increased activities of 5-HT neurons in the DRN. In addition, SG2A, similar to SSRIs, increases neurogenesis in the DG of the hippocampus. The hippocampal neurogenesis is decreased by inescapable stress events resulting in a state of behavioral despair and this effect can be reversed by fluoxetine (Malberg and Duman, 2003). Disruption of fluoxetine-induced neurogenesis suppresses behavioral responses to antidepressants, therefore the increased neurogenesis is likely an essential process for antidepressive behavioral effects (Santarelli et al., 2003). Thus, increase in c-fos⁺TPH⁺ 5-HT neurons by SG2A and similarity of histochemical changes in the brain between SSRI and SG2A may suggest that antidepressive and anxiolytic effects of SG2A in CORTI mice are mainly mediated by activation of 5-HT neurons in the DRN.

One of the unexpected side effects of SSRIs is body weight changes (Levine et al., 1987; Uguz et al., 2015). A recent study showed that long-term treatment of escitalopram, an effective SSRI antidepressant that is associated with significant weight gain (Uguz et al., 2015), led to the downregulation of SPX expression in the rat hypothalamus. This suggests that the increased body mass by SSRI may be, at least in part, due to a decreased anorexic action of SPX in the hypothalamus (Palasz et al., 2016). Both POMC and CRH neurons in the hypothalamus are pivotal neuronal populations involved in appetite/body weight regulation (Schwartz et al., 2000). In goldfish, i.c.v. administration of SPX inhibited food intake accompanying increased mRNA levels of POMC and CRH (Wong et al., 2013). Our results also showed that SG2A reduced food consumption with induced c-fos expression in POMC- and CRH-positive neurons. As SG2A reduced body weight in normal and obese mice, SG2A treatment can circumvent SSRI-induced increase in body weight by direct activation of anorexic neuronal population in the hypothalamus. POMC and CRH neurons in the hypothalamus sense and integrate inputs not only from peripheral tissues (Schwartz et al., 2000) but also central inputs from brain areas involved in stress/mood/hedonic/reward control (Adam and Epel, 2007; Carroll et al., 2012). Moreover, hedonic or reward-based control can override homeostatic pathway for eating behaviors and body weight controls. In CORTI mice that already lost body weight, SG2A increased their body weight, likely via relieving anhedonia, anxiety, and depression. Thus, it seems likely that the antidepressive effects of SG2A overwhelms the anorexic effects of SG2A in CORTI mice. Together, SPX and GAL₂ receptor are likely connected to the key regulatory system controlling or linking appetite and mood behaviors, allowing optimal treatment for comorbid mood disorders and abnormal body weight.

Post-traumatic stress disorder (PTSD) is a severe anxiety disorder that involves an explicit conditioning episode (Dohrenwend et al., 2006; de Vries and Olff, 2009). Furthermore, PTSD and depression are commonly co-occurring mental disorders which reinforces each other. PTSD is frequently conceptualized as a memory disorder within a Pavlovian fear conditioning and extinction framework (Rubin et al., 2008;

Shin and Handwerker, 2009). This study also showed that SG2A contributes to fear memory consolidation and extinction in a PTSD animal model. Specifically, SG2A decreased both hippocampus-dependent contextual and amygdala-dependent auditory fear responses and facilitated fear extinction after fear memory acquisition. Accordingly, SG2A administration activated neurons in the amygdala, PFC, and DG which are major components of the neural circuits that regulate anxiety and fear memory (Sierra-Mercado et al., 2011). Although there are reports of impaired cognition induced by GAL (Rustay et al., 2005), SG2A did not induce memory deficits in the Y-maze and NOR tests in this study.

A major challenge for treatments involving peptide drugs is bypassing the blood-brain barrier. Over the last several decades, diverse formulations and devices have been developed to transport the drugs from the nose directly to the brain, showing promise for therapeutic efficacy based on animal models and clinical trials in humans (Craft et al., 2012; Striepen et al., 2013; Kageyama et al., 2016). Notably, i.n. administrations of GLP2, oxytocin, or other peptides produce antidepressive effects or improve social behavior, thereby attracting attention to the development of peptide drugs for the treatment of neuropsychiatric diseases (Sasaki-Hamada et al., 2017). The results of this study showed that SG2A can be successfully delivered to the CNS via the i.n. route, producing results comparable to those obtained with i.c.v. delivery.

CONCLUSION

In conclusion, SG2A exerts a rapid onset of effects toward relieving anxiety-, depression-like, and feeding behaviors and suppressing fear memory. These effects were maintained during repetitive SG2A administrations delivered either i.c.v./i.n. SG2A has potential for the clinical application to treat mood disorders and/or abnormal appetite/body weight.

REFERENCES

- Adam, T. C., and Epel, E. S. (2007). Stress, eating and the reward system. *Physiol. Behav.* 91, 449–458. doi: 10.1016/j.physbeh.2007.04.011
- American Psychiatric Association (2013). *Diagnostic and Statistical Manual of Mental Disorders*, 5th Edn. Arlington, VA: American Psychiatric Publishing.
- Bailey, K. R., Pavlova, M. N., Rohde, A. D., Hohmann, J. G., and Crawley, J. N. (2007). Galanin receptor subtype 2 (GalR2) null mutant mice display an anxiogenic-like phenotype specific to the elevated plus-maze. *Pharmacol. Biochem. Behav.* 86, 8–20. doi: 10.1016/j.pbb.2006.11.024
- Baranowska, B., Wasilewska-Dziubinska, E., Radzikowska, M., Plonowski, A., and Roguski, K. (1997). Neuropeptide Y, galanin, and leptin release in obese women and in women with anorexia nervosa. *Metabolism* 46, 1384–1389. doi: 10.1016/s0026-0495(97)90136-0
- Carey, M., Small, H., Yoong, S. L., Boyes, A., Bisquera, A., and Sanson-Fisher, R. (2014). Prevalence of comorbid depression and obesity in general practice: a cross-sectional survey. *Br. J. Gen. Pract.* 64, e122–e127. doi: 10.3399/bjgp14X677482
- Carroll, B. J., Iranmanesh, A., Keenan, D. M., Cassidy, F., Wilson, W. H., and Veldhuis, J. D. (2012). Pathophysiology of hypercortisolism in depression: pituitary and adrenal responses to low glucocorticoid feedback. *Acta. Psychiatr. Scand.* 125, 478–491. doi: 10.1111/j.1600-0447.2011.01821.x
- Challis, C., and Berton, O. (2015). Top-down control of serotonin systems by the prefrontal cortex: a path toward restored socioemotional function in depression. *ACS Chem. Neurosci.* 6, 1040–1054. doi: 10.1021/acschemneuro.5b00007
- Craft, S., Baker, L. D., Montine, T. J., Minoshima, S., Watson, G. S., Claxton, A., et al. (2012). Intranasal insulin therapy for Alzheimer disease and amnesic mild cognitive impairment: a pilot clinical trial. *Arch. Neurol.* 69, 29–38. doi: 10.1001/archneurol.2011.233
- de Vries, G. J., and Olff, M. (2009). The lifetime prevalence of traumatic events and posttraumatic stress disorder in the Netherlands. *J. Trauma Stress* 22, 259–267. doi: 10.1002/jts.20429
- Demuyser, T., Bentea, E., Deneyer, L., Albertini, G., Massie, A., and Smolders, I. (2016). Disruption of the HPA-axis through corticosterone-release pellets induces robust depressive-like behavior and reduced BDNF levels in mice. *Neurosci. Lett.* 626, 119–125. doi: 10.1016/j.neulet.2016.05.026
- Dohrenwend, B. P., Turner, J. B., Turse, N. A., Adams, B. G., Koenen, K. C., and Marshall, R. (2006). The psychological risks of Vietnam for U.S. veterans: a

DATA AVAILABILITY

All datasets generated for this study are included in the manuscript and/or the **Supplementary Files**.

ETHICS STATEMENT

All animal procedures were approved by the Institutional Animal Care and Use Committee of Korea University (KOREA-2016-0050-C2) and Korea Advanced Institute of Science and Technology (KA2014-02).

AUTHOR CONTRIBUTIONS

SY, AR-A, B-JH, J-WS, D-HK, GS, HK, S-GK, DK, and BK designed the research. SY, AR-A, Y-NL, HY, and JC performed the research. SY and AR-A analyzed the data. J-IH and JS wrote the manuscript. All authors read and approved the final manuscript.

FUNDING

This work was supported by grants from the Research Program of the National Research Foundation of Korea (NRF-2015M3A9E7029172) funded by the Ministry of Science, ICT, and Future Planning. Neuracle Science Co., Ltd., holds a Korean patent (10-1885238 and 10-1885241), United States (15/771,078), EPO (16871028.3), Australian (2016361783), Brazilian (11 2018 008315 1), Canada (3003262), China (201680062527.4), and Japan (2018-523789) patents.

SUPPLEMENTARY MATERIAL

The Supplementary Material for this article can be found online at: <https://www.frontiersin.org/articles/10.3389/fnins.2019.00391/full#supplementary-material>

- revisit with new data and methods. *Science* 313, 979–982. doi: 10.1126/science.1128944
- Furlong, M., and Seong, J. Y. (2017). Evolutionary and comparative genomics to drive rational drug design, with particular focus on neuropeptide seven-transmembrane receptors. *Biomol. Ther.* 25, 57–68. doi: 10.4062/biomolther.2016.199
- Hausdorff, W. P., Caron, M. G., and Lefkowitz, R. J. (1990). Turning off the signal: desensitization of beta-adrenergic receptor function. *FASEB J.* 4, 2881–2889. doi: 10.1096/fasebj.4.11.2165947
- Kageyama, H., Shiba, K., Hirako, S., Wada, N., Yamanaka, S., Nogi, Y., et al. (2016). Anti-obesity effect of intranasal administration of galanin-like peptide (GALP) in obese mice. *Sci. Rep.* 6:28200. doi: 10.1038/srep28200
- Karatayev, O., Baylan, J., and Leibowitz, S. F. (2009). Increased intake of ethanol and dietary fat in galanin overexpressing mice. *Alcohol* 43, 571–580. doi: 10.1016/j.alcohol.2009.09.025
- Kim, D. K., Yun, S., Son, G. H., Hwang, J. I., Park, C. R., Kim, J. I., et al. (2014). Coevolution of the spexin/galanin/kisspeptin family: spexin activates galanin receptor type II and III. *Endocrinology* 155, 1864–1873. doi: 10.1210/en.2013-2106
- Kloiber, S., Ising, M., Reppermund, S., Horstmann, S., Dose, T., Majer, M., et al. (2007). Overweight and obesity affect treatment response in major depression. *Biol. Psychiatry* 62, 321–326. doi: 10.1016/j.biopsych.2006.10.001
- Kuteeva, E., Hokfelt, T., Wardi, T., and Ogren, S. O. (2008). Galanin, galanin receptor subtypes and depression-like behaviour. *Cell. Mol. Life. Sci.* 65, 1854–1863. doi: 10.1007/s00018-008-8160-9
- Lawrence, C. B., Baudoin, F. M., and Luckman, S. M. (2002). Centrally administered galanin-like peptide modifies food intake in the rat: a comparison with galanin. *J. Neuroendocrinol.* 14, 853–860. doi: 10.1046/j.1365-2826.2002.00846.x
- Levine, L. R., Rosenblatt, S., and Bosomworth, J. (1987). Use of a serotonin re-uptake inhibitor, fluoxetine, in the treatment of obesity. *Int. J. Obes.* 11(Suppl. 3), 185–190.
- Lu, X., Barr, A. M., Kinney, J. W., Sanna, P., Conti, B., Behrens, M. M., et al. (2005). A role for galanin in antidepressant actions with a focus on the dorsal raphe nucleus. *Proc. Natl. Acad. Sci. U.S.A.* 102, 874–879. doi: 10.1073/pnas.0408891102
- Malberg, J. E., and Duman, R. S. (2003). Cell proliferation in adult hippocampus is decreased by inescapable stress: reversal by fluoxetine treatment. *Neuropsychopharmacology* 28, 1562–1571. doi: 10.1038/sj.npp.1300234
- Marijnissen, R. M., Bus, B. A., Holeywijn, S., Franke, B., Purandare, N., De Graaf, J., et al. (2011). Depressive symptom clusters are differentially associated with general and visceral obesity. *J. Am. Geriatr. Soc.* 59, 67–72. doi: 10.1111/j.1532-5415.2010.03228.x
- Mazarati, A. M., Baldwin, R. A., Shinmei, S., and Sankar, R. (2005). In vivo interaction between serotonin and galanin receptors types 1 and 2 in the dorsal raphe: implication for limbic seizures. *J. Neurochem.* 95, 1495–1503. doi: 10.1111/j.1471-4159.2005.03498.x
- Palasz, A., Suszka-Switek, A., Filipczyk, L., Bogus, K., Rojczyk, E., Worthington, J., et al. (2016). Escitalopram affects spexin expression in the rat hypothalamus, hippocampus and striatum. *Pharmacol. Rep.* 68, 1326–1331. doi: 10.1016/j.pharep.2016.09.002
- Reyes-Alcaraz, A., Lee, Y. N., Son, G. H., Kim, N. H., Kim, D. K., Yun, S., et al. (2016). Development of spexin-based human galanin receptor type II-specific agonists with increased stability in serum and anxiolytic effect in mice. *Sci. Rep.* 6:21453. doi: 10.1038/srep21453
- Reyes-Alcaraz, A., Lee, Y. N., Yun, S., Hwang, J. I., and Seong, J. Y. (2018). Conformational signatures in beta-arrestin2 reveal natural biased agonism at a G-protein-coupled receptor. *Commun. Biol.* 1:128. doi: 10.1038/s42003-018-0134-3
- Rubin, D. C., Berntsen, D., and Bohni, M. K. (2008). A memory-based model of posttraumatic stress disorder: evaluating basic assumptions underlying the PTSD diagnosis. *Psychol. Rev.* 115, 985–1011. doi: 10.1037/a0013397
- Rustay, N. R., Wrenn, C. C., Kinney, J. W., Holmes, A., Bailey, K. R., Sullivan, T. L., et al. (2005). Galanin impairs performance on learning and memory tasks: findings from galanin transgenic and GAL-R1 knockout mice. *Neuropeptides* 39, 239–243. doi: 10.1016/j.npep.2004.12.026
- Santarelli, L., Saxe, M., Gross, C., Surget, A., Battaglia, F., Dulawa, S., et al. (2003). Requirement of hippocampal neurogenesis for the behavioral effects of antidepressants. *Science* 301, 805–809. doi: 10.1126/science.1083328
- Sasaki-Hamada, S., Nakamura, R., Nakao, Y., Akimoto, T., Sanai, E., Nagai, M., et al. (2017). Antidepressant-like effects exerted by the intranasal administration of a glucagon-like peptide-2 derivative containing cell-penetrating peptides and a penetration-accelerating sequence in mice. *Peptides* 87, 64–70. doi: 10.1016/j.peptides.2016.11.013
- Schmidt, H. D., and Duman, R. S. (2007). The role of neurotrophic factors in adult hippocampal neurogenesis, antidepressant treatments and animal models of depressive-like behavior. *Behav. Pharmacol.* 18, 391–418. doi: 10.1097/FBP.0b013e3282ee2aa8
- Schwartz, M. W., Woods, S. C., Porte, D. Jr., Seeley, R. J., and Baskin, D. G. (2000). Central nervous system control of food intake. *Nature* 404, 661–671. doi: 10.1038/35007534
- Sharma, S., Fernandes, M. F., and Fulton, S. (2013). Adaptations in brain reward circuitry underlie palatable food cravings and anxiety induced by high-fat diet withdrawal. *Int. J. Obes.* 37, 1183–1191. doi: 10.1038/ijo.2012.197
- Shin, L. M., and Handwerker, K. (2009). Is posttraumatic stress disorder a stress-induced fear circuitry disorder? *J. Trauma Stress* 22, 409–415. doi: 10.1002/jts.20442
- Sierra-Mercado, D., Padilla-Coreano, N., and Quirk, G. J. (2011). Dissociable roles of prefrontal and infralimbic cortices, ventral hippocampus, and basolateral amygdala in the expression and extinction of conditioned fear. *Neuropsychopharmacology* 36, 529–538. doi: 10.1038/npp.2010.184
- Simon, G. E., Von Korff, M., Saunders, K., Miglioretti, D. L., Crane, P. K., Van Belle, G., et al. (2006). Association between obesity and psychiatric disorders in the US adult population. *Arch. Gen. Psychiatry* 63, 824–830. doi: 10.1001/archpsyc.63.7.824
- Sohn, J. W., Xu, Y., Jones, J. E., Wickman, K., Williams, K. W., and Elmquist, J. K. (2011). Serotonin 2C receptor activates a distinct population of arcuate pro-opiomelanocortin neurons via TRPC channels. *Neuron* 71, 488–497. doi: 10.1016/j.neuron.2011.06.012
- Striepen, N., Kendrick, K. M., Hanking, V., Landgraf, R., Wullner, U., Maier, W., et al. (2013). Elevated cerebrospinal fluid and blood concentrations of oxytocin following its intranasal administration in humans. *Sci. Rep.* 3:3440. doi: 10.1038/srep03440
- Swanson, C. J., Blackburn, T. P., Zhang, X., Zheng, K., Xu, Z. Q., Hokfelt, T., et al. (2005). Anxiolytic- and antidepressant-like profiles of the galanin-3 receptor (Gal3) antagonists SNAP 37889 and SNAP 398299. *Proc. Natl. Acad. Sci. U.S.A.* 102, 17489–17494. doi: 10.1073/pnas.0508970102
- Uguz, F., Sahingoz, M., Gungor, B., Aksoy, F., and Askin, R. (2015). Weight gain and associated factors in patients using newer antidepressant drugs. *Gen. Hosp. Psychiatry* 37, 46–48. doi: 10.1016/j.genhosppsych.2014.10.011
- Walewski, J. L., Ge, F., Lobdell, H. T., Levin, N., Schwartz, G. J., Vasselli, J. R., et al. (2014). Spexin is a novel human peptide that reduces adipocyte uptake of long chain fatty acids and causes weight loss in rodents with diet-induced obesity. *Obesity* 22, 1643–1652. doi: 10.1002/oby.20725
- Webbing, K. E., Runesson, J., Bartfai, T., and Langel, U. (2012). Galanin receptors and ligands. *Front. Endocrinol.* 3:146. doi: 10.3389/fendo.2012.00146
- Wong, M. K., Sze, K. H., Chen, T., Cho, C. K., Law, H. C., Chu, I. K., et al. (2013). Goldfish spexin: solution structure and novel function as a satiety factor in feeding control. *Am. J. Physiol. Endocrinol. Metab.* 305, E348–E366. doi: 10.1152/ajpendo.00141.2013
- Xu, Z. Q., Zhang, X., Pieribone, V. A., Grillner, S., and Hokfelt, T. (1998). Galanin-5-hydroxytryptamine interactions: electrophysiological, immunohistochemical and in situ hybridization studies on rat dorsal raphe neurons with a note on galanin R1 and R2 receptors. *Neuroscience* 87, 79–94. doi: 10.1016/s0306-4522(98)00151-1

- Yamaguchi, T., Danjo, T., Pastan, I., Hikida, T., and Nakanishi, S. (2013). Distinct roles of segregated transmission of the septo-habenular pathway in anxiety and fear. *Neuron* 78, 537–544. doi: 10.1016/j.neuron.2013.02.035
- Yang, L. K., and Tao, Y. X. (2017). Biased signaling at neural melanocortin receptors in regulation of energy homeostasis. *Biochim. Biophys. Acta* 1863, 2486–2495. doi: 10.1016/j.bbadis.2017.04.010
- Yun, S., Furlong, M., Sim, M., Cho, M., Park, S., Cho, E. B., et al. (2015). Prevertebrate local gene duplication facilitated expansion of the neuropeptide GPCR superfamily. *Mol. Biol. Evol.* 32, 2803–2817. doi: 10.1093/molbev/msv179
- Yun, S., Kim, D. K., Furlong, M., Hwang, J. I., Vaudry, H., and Seong, J. Y. (2014). Does kisspeptin belong to the proposed RF-amide peptide family? *Front. Endocrinol.* 5:134. doi: 10.3389/fendo.2014.00134

Conflict of Interest Statement: SY, AR-A, Y-NL, HY, GS, J-IH, and JS are shareholders. S-GK and DK are employees and shareholders. BK is a shareholder and the CEO of Neuracle Science Co., Ltd.

The remaining authors declare that the research was conducted in the absence of any commercial or financial relationships that could be construed as a potential conflict of interest.

Copyright © 2019 Yun, Reyes-Alcaraz, Lee, Yong, Choi, Ham, Sohn, Kim, Son, Kim, Kwon, Kim, Kim, Hwang and Seong. This is an open-access article distributed under the terms of the Creative Commons Attribution License (CC BY). The use, distribution or reproduction in other forums is permitted, provided the original author(s) and the copyright owner(s) are credited and that the original publication in this journal is cited, in accordance with accepted academic practice. No use, distribution or reproduction is permitted which does not comply with these terms.



Strategies for the Identification of Bioactive Neuropeptides in Vertebrates

Auriane Corbière¹, Hubert Vaudry^{1,2}, Philippe Chan³, Marie-Laure Walet-Balieu³, Thierry Lecroq⁴, Arnaud Lefebvre⁴, Charles Pineau⁵ and David Vaudry^{1,2,3*}

¹ Normandie Univ, UNIROUEN, Inserm, Laboratory of Neuronal and Neuroendocrine Communication and Differentiation, Neuropeptides, Neuronal Death and Cell Plasticity Team, Rouen, France, ² Normandie Univ, UNIROUEN, Regional Cell Imaging Platform of Normandy (PRIMACEN), Rouen, France, ³ Normandie Univ, UNIROUEN, Rouen Proteomic Platform (PISSARO), Institute for Research and Innovation in Biomedicine (IRIB), Rouen, France, ⁴ Normandie Univ, UNIROUEN, LITIS EA 4108, Information Processing in Biology & Health, Rouen, France, ⁵ Protim, Univ Rennes, Rennes Cedex, France

OPEN ACCESS

Edited by:

Dora Reglodi,
University of Pécs, Hungary

Reviewed by:

Liliane Schoofs,
KU Leuven, Belgium
Kazuhiro Takahashi,
Tohoku University, Japan
Andrea Tamas,
University of Pécs, Hungary

*Correspondence:

David Vaudry
david.vaudry@univ-rouen.fr

Specialty section:

This article was submitted to
Neuroendocrine Science,
a section of the journal
Frontiers in Neuroscience

Received: 26 June 2019

Accepted: 22 August 2019

Published: 18 September 2019

Citation:

Corbière A, Vaudry H, Chan P,
Walet-Balieu M-L, Lecroq T,
Lefebvre A, Pineau C and Vaudry D
(2019) Strategies for the Identification
of Bioactive Neuropeptides
in Vertebrates.
Front. Neurosci. 13:948.
doi: 10.3389/fnins.2019.00948

Neuropeptides exert essential functions in animal physiology by controlling e.g., reproduction, development, growth, energy homeostasis, cardiovascular activity and stress response. Thus, identification of neuropeptides has been a very active field of research over the last decades. This review article presents the various methods used to discover novel bioactive peptides in vertebrates. Initially identified on the basis of their biological activity, some neuropeptides have also been discovered for their ability to bind/activate a specific receptor or based on their biochemical characteristics such as C-terminal amidation which concerns half of the known neuropeptides. More recently, sequencing of the genome of many representative species has facilitated peptidomic approaches using mass spectrometry and *in silico* screening of genomic libraries. Through these different approaches, more than a hundred of bioactive neuropeptides have already been identified in vertebrates. Nevertheless, researchers continue to find new neuropeptides or to identify novel functions of neuropeptides that had not been detected previously, as it was recently the case for nociceptin.

Keywords: neuropeptide, identification, peptidomic approach, de novo, bioactivity, review

CHARACTERISTICS OF NEUROPEPTIDES

More than one hundred bioactive neuropeptides have been identified in vertebrates, varying in length from 3 amino acids, for thyrotropin-releasing hormone (TRH), up to several dozens of amino acids (82 for nesfatin-1). All neuropeptides are generated by cleavage of precursors of higher molecular weight that belong to three categories (**Figure 1**; Douglass et al., 1984). The first category includes mono-functional precursors that give rise to only one bioactive peptide flanked by one or two sequences called cryptic peptides, the function of which is generally unknown. Within these precursors, the bioactive peptide may be located at the N-terminal extremity upstream of the cryptic peptide as for neuropeptide Y (Cerdá-Reverter et al., 2000), in an intermediate position as for cholecystokinin (Beinfeld, 1997) or at the C-terminal extremity as for somatostatin and urotensin II (Vaudry et al., 2015; **Figure 1A**). The second category consists of mono-functional precursors with several copies of the bioactive peptide such as TRH, which exists in 5 copies within the same precursor in rat (Lee et al., 1988), resulting most likely from intragenic duplications during evolution (**Figure 1B**).

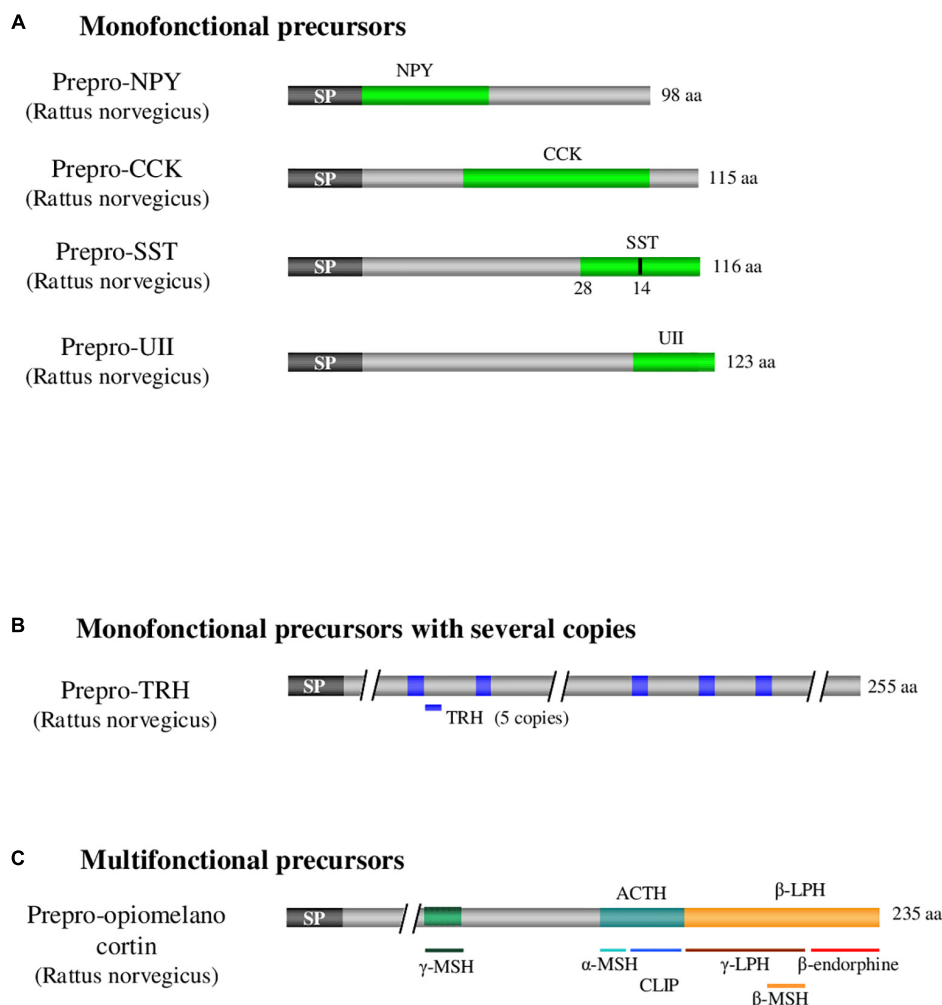


FIGURE 1 | Examples illustrating the 3 categories of neuropeptide precursors. **(A)** Illustration of monofunctional precursors with single copy of the peptide of interest as it is the case for CCK, UII, NPY, and SST. **(B)** Illustration of monofunctional precursors with several copies of the peptide of interest as it is the case for TRH. **(C)** Illustration of multifunctional precursors which express several different bioactive peptides as it is the case with POMC. ACTH: adrenocorticotrophic hormone. CCK: cholecystokinin. POMC: pro-opiomelanocortin. CLIP: corticotropin-like intermediate lobe peptide. LPH: lipotropic hormone. MSH: melanocyte-stimulating hormone. NPY: neuropeptide Y. SP: signal peptide. SST: somatostatin. TRH: thyrotropin-releasing hormone. UII: urotensin II. aa: aminoacid. Adapted from Neveu (2012).

The third category corresponds to multifunctional precursors giving rise to distinct bioactive peptides, the archetype being pro-opiomelanocortin (POMC), the precursor of adrenocorticotrophic hormone (ACTH), melanotropic hormones (α -, β - and γ -MSH) and β -endorphin (Figure 1C; Nakanishi et al., 1979). The precursors of the first category can eventually be reclassified in the third category if an activity for one of the cryptic peptides is discovered (Figures 1A,C). In fact, sequences initially considered cryptic may sometimes prove to have a biological effect, as it was the case for nocistatin, present in the same precursor as nociceptin and having an inverse effect on pain transmission (Okuda-Ashitaka and Ito, 2000).

The precursor polypeptide chains of neuropeptides exhibit several common structural features. First, a signal peptide consisting of a hydrophobic sequence of about twenty amino acids is located at the N-terminal extremity of the precursor.

This signal peptide allows the translocation of the polypeptide into the lumen of the endoplasmic reticulum (Coleman et al., 1985). Once the signal peptide is translated by the ribosome, the complex binds to a ribonucleoprotein associated with an RNA molecule, the signal recognition particle (Figure 2). This particle then binds to its receptor located on the reticulum membrane, allowing the elongation and translocation of the preprohormone polypeptide into the reticulum to continue (Walter et al., 1984). During translation, the signal peptide is cleaved off by an endopeptidase, the signal peptidase.

Precursors translocated in the lumen of the reticulum and subsequently transported in cell compartments of the secretory pathway, undergo various post-translational modifications, such as the formation of a disulfide bridge between two cysteines, phosphorylation of a serine or threonine residue, tyrosine sulfation, octanoylation, C-terminal amidation, and N-terminal

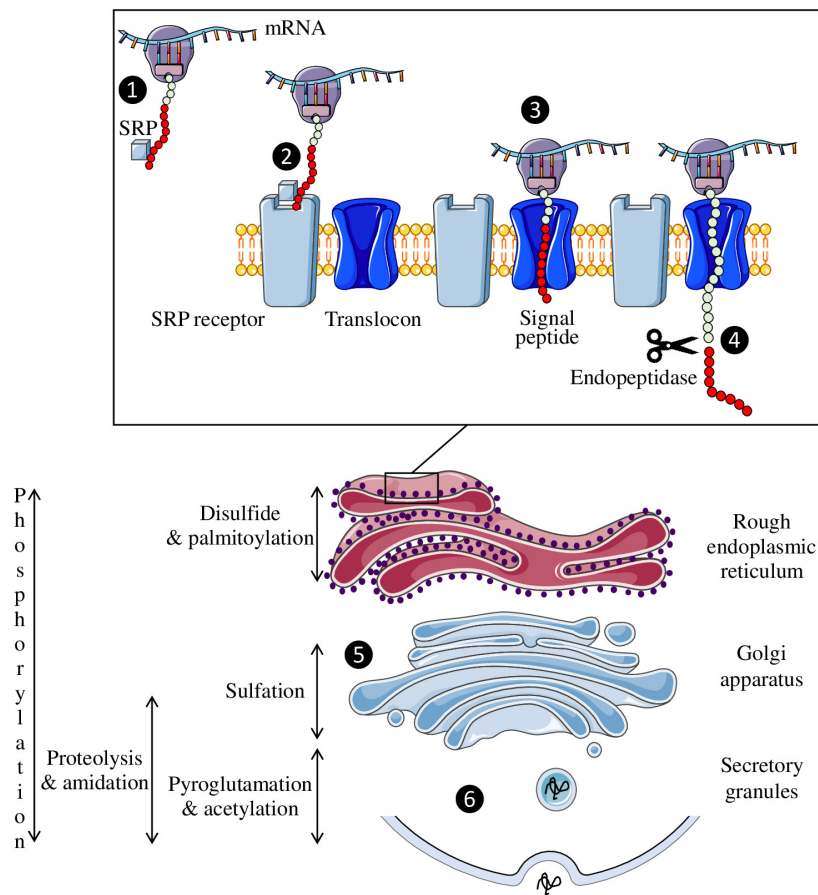


FIGURE 2 | Neuropeptide biosynthesis. The signal recognition particle (SRP) is fixed to the complex formed by the peptide, the ribosome and the mRNA (1) and then binds to its receptor on the endoplasmic reticulum membrane (2). This allows the peptide to enter the reticulum through the translocon so that peptide synthesis can continue (3). The signal peptide (red circles) is then cleaved off by an endopeptidase (4). Once synthesized, the neuropeptide will pass through the Golgi apparatus to undergo post-translational modifications (5) before being secreted in a regulated manner (6).

acetylation or pyroglutamylation. Each of these modifications can strongly affect the activity of the peptide and/or its resistance to enzymatic degradation. For example, sulfation of tyrosine in position 2 of cholecystokinin (Gigoux et al., 1998), N-octanoylation of the third serine residue of ghrelin (Kojima et al., 1999; Muccioli et al., 2001) or acetylation of the N-terminal serine of α -MSH (O'Donohue et al., 1981) significantly increases the affinity of these peptides for their receptors. Similarly, the presence of a disulfide bridge contributes to the spatial conformation of peptides, and its reduction usually leads to their inactivation as for oxytocin and urotensin II (Meraldi et al., 1977; Labarrère et al., 2003). These chemical modifications take place either during the transit of the precursor from the reticulum to the Golgi apparatus, or in the secretory vesicles. For example, disulfide bonds are formed in the endoplasmic reticulum, sulfation occurs in the Golgi apparatus and amidation, which concerns more than half of the neuropeptides, takes place in the secretory granules (Figure 2).

Once the precursors reach the trans-Golgi or secretory granules, they undergo specific cleavage by endoproteases called

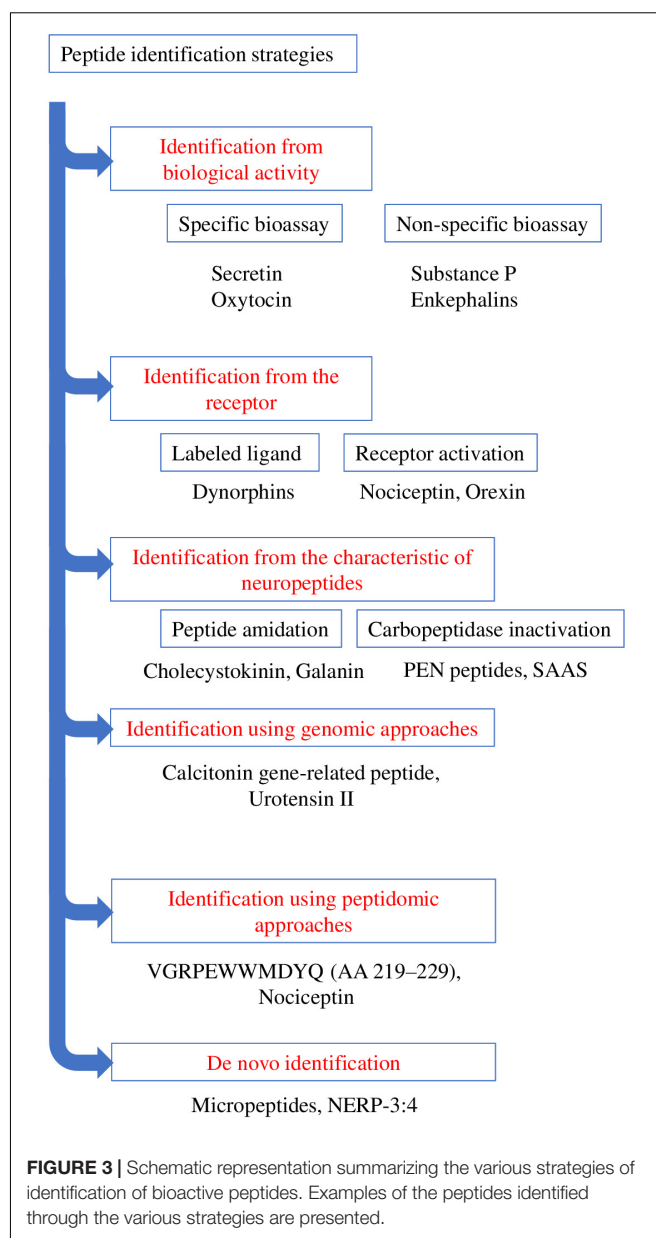
prohormone convertases (PCs) to give rise to biologically active peptides. There are 7 PCs in mammals: PC2 (Smeekens and Steiner, 1990), furin (van de Ven et al., 1990), PC1/3 (Seidah et al., 1991), PACE4 (Kiefer et al., 1991), PC4 (Nakayama et al., 1992), PC5/6 (Lusson et al., 1993) and PC7 (Tsuji et al., 1994). These 7 PCs share an affinity for substrates with basic amino acids (Fricker, 2012). The most common cleavage patterns consist of two basic amino acids such as a lysine-arginine and arginine-lysine doublets, two arginines or two lysines. PC1/3 and PC2, the most abundant enzymes, cleave the precursors downstream of these doublets and thus leave the two basic amino acids at the C-terminal extremity of the peptide. More rarely, the cleavage site may consist of a single basic amino acid as is the case for somatostatin-28 and the octadecaneuropeptide ODN (Barbaccia et al., 1990; Brakch et al., 1995). In the vast majority of cases, after cleavage, the basic residues are removed by carboxypeptidases (Fricker and Snyder, 1982; Song and Fricker, 1995), except for ODN and cortistatin (Ferrero et al., 1986; de Lecea et al., 1996). Two other PCs that do not cleave at basic sites have been

characterized: subtilisin-kexin-isozyme (Seidah et al., 1999) and proprotein convertase subtilisin-kexin isozyme (Seidah et al., 2003). Differential expression of PCs depending on the cell type leads to tissue-specific cleavages of the precursors. An illustrative example of differential maturation is given by POMC that generates distinct bioactive peptides according to the tissues. Thus, in corticotrope cells of the adenohypophysis, where just PC1/3 is present, only half of the 8 potential cleavage sites are processed, giving rise to ACTH and β -LPH, whereas in neurons of the arcuate nucleus and melanotrope cells of the intermediate lobe of the pituitary, which express both PC1/3 and PC2, the maturation is complete and leads to the formation of α -MSH and β -endorphin (Bicknell, 2008). After cleavage and post-translational modifications, the bioactive peptide(s) is (are) stored in secretory vesicles which, upon depolarization of the cell, merge with the plasma membrane to release their content in the extracellular space.

Neuropeptides, therefore, represent a particular type of intercellular signaling molecules. Indeed, they are produced by nerve cells (and often by other cell types including endocrine cells, skin cells...), they derive from the specific cleavage of a prehormone polypeptide harboring a signal peptide, and they are secreted in a controlled manner. Once released in the extracellular space, they act at low concentrations by binding to specific receptors before being degraded without reuptake, unlike neurotransmitters. These physical and biological characteristics can be exploited to identify novel neuropeptides. Since the first characterization of the neuropeptides oxytocin and vasopressin (Du Vigneaud, 1954), many research teams have set out strategies to discover novel neuropeptides. The techniques used for their identification are diverse and have evolved considerably over the last decades.

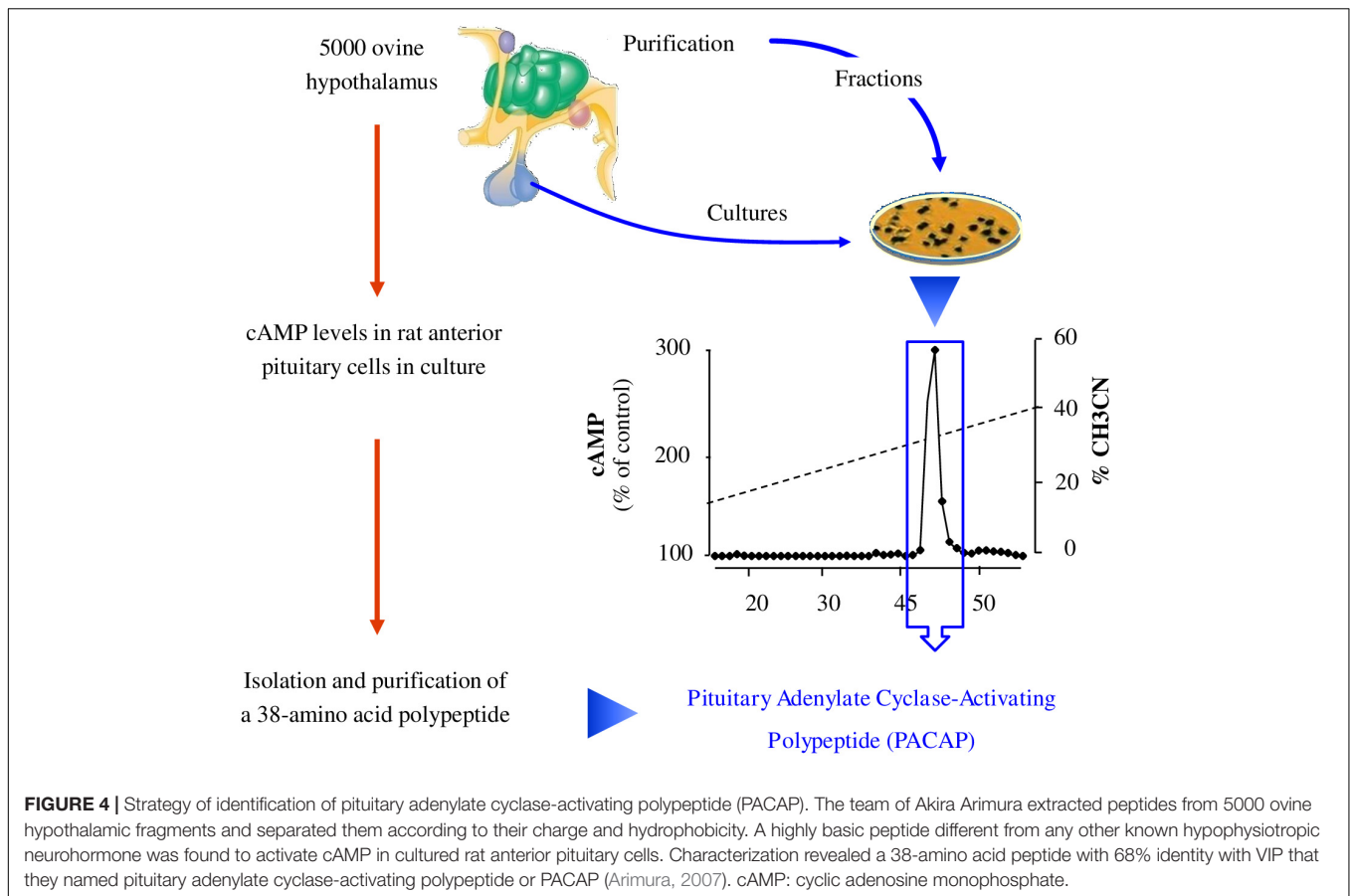
IDENTIFICATION FROM A BIOLOGICAL ACTIVITY

The initial method employed to discover bioactive peptides relies on a biological test, which consists of measuring the effect of tissue extracts, most often brain extracts for neuropeptides, on a physiological parameter. These extracts are then purified until a single compound is isolated. Two types of approaches can be distinguished for bioassays depending on whether the activity being tested corresponds to the “main function” of the peptide or to a mere pharmacological effect (Figure 3). Regarding the main function, it is through this approach that the first neuropeptide, oxytocin, was isolated by Du Vigneaud et al. (1953). Hypothalamic hypophysiotropic neuropeptides such as TRH, gonadotropin-releasing hormone and somatostatin have been discovered via the same approach by studying the ability of hypothalamic extracts to modulate the release of thyrotropin (Burgus et al., 1969), luteinizing hormone, follicle-stimulating hormone (Schally et al., 1971) and growth hormone (Brazeau et al., 1973). A similar strategy was also used to identify pituitary adenylate cyclase-activating polypeptide (PACAP) from a sheep hypothalamic extract by measuring the activation of adenylate



cyclase in pituitary cells, hence the name of this peptide (Miyata et al., 1989; Figure 4).

Besides, pharmacological (non-specific) activity tests were used to isolate other peptides such as substance P or enkephalins. For instance, the purification of substance P was carried out by measuring the effects of gut extracts, and later of brain extracts, on the contraction of intestine smooth muscles (Euler and Gaddum, 1931). However, it took four decades before the sequence of the peptide was determined (Chang et al., 1971). Regarding enkephalins, the test consisted in monitoring the effect of brain extracts on electrically evoked contractions of the mouse vas deferens and guinea pig ileum (Hughes et al., 1975). These inhibitory effects were completely antagonized by the opioid receptor antagonist naloxone.



Even though these approaches by biological tests have led to the identification of several neuropeptides, they are not devoid of drawbacks. In particular, the successive steps of purification and the activity tests until reaching a single bioactive compound can be very long. Furthermore, once a peptide such as PACAP has been characterized, decades of research are still necessary to identify its numerous functions (Vaudry et al., 2000, 2009) and decipher its mechanisms of action (Vaudry et al., 1998, 2002).

IDENTIFICATION FROM THE RECEPTOR

Large-scale cloning of G-protein coupled receptors (GPCRs), has led to the identification of numerous so-called orphan receptors, that is, receptors whose endogenous ligands have not yet been identified. The human genome encompasses ~800 genes encoding GPCRs of which 448 are sensory receptors (Mombaerts, 2004). Among the remaining ~350 GPCRs, ~140 still have no identified ligand (Stockert and Devi, 2015). Since about 50% of non-orphan GPCRs are activated by (neuro)peptides, a quick extrapolation indicates that approximately 70 orphan GPCRs should recognize one or several biologically active peptide(s) as natural ligand(s) (Alexander et al., 2011). These peptide-binding GPCRs thus represent very attractive targets for the identification of novel neuropeptides through a reversed pharmacology approach *via* the screening of tissue extracts or synthetic peptide

libraries. The search for the endogenous ligand(s) of an orphan GPCR necessitates the stable or transient expression of the receptor cDNA in a cell line in order to screen tissue extracts. The pairing of a potential neuropeptide to a receptor of interest can be carried out through two types of approaches (Figure 3). The first one uses a labeled ligand (most often radioactive) whose binding to the receptor is displaced by the endogenous ligand (Figure 3). In this case, an already known neuropeptide is used to identify novel related endogenous peptides that bind to the same receptor. This approach allowed the identification of several neuropeptides from prodynorphin, including different types of dynorphins (Pert et al., 1977; Goldstein et al., 1979). The main drawback of this technique is the requirement to label a peptidic ligand by adding a radioactive iodine atom to a tyrosine without dramatically altering its affinity. Alternatively, it is possible to label peptides with tritiated or deuterated atoms which do not impair the structure of the molecules (Allen et al., 1982). The second method focuses on the receptor activation, studied by measuring a physiological parameter such as cytosolic calcium level, second messenger formation, acidification, ... (Figure 3). It is through this approach that nociceptin and orexin were identified (Meunier et al., 1995; Reinscheid et al., 1995; Sakurai et al., 1998). Variants of this approach include imaging techniques that monitor *e.g.*, the internalization of the fluorochrome-labeled tagged receptor (De Mota et al., 2004) or microcalorimetry that reflect the interaction between the receptor and its ligand through

quantification of conformational change-induced temperature variations (Jerabek-Willemsen et al., 2014).

IDENTIFICATION FROM BIOCHEMICAL CHARACTERISTICS OF NEUROPEPTIDES

The methods presented above focus on the discovery of neuropeptides *via* their activity, either at the tissue or cell level. Besides this functional-based strategy, it is possible to identify novel neuropeptides according to their biochemical features. The main characteristic signature is peptide amidation, which can be studied by chemical precipitation steps of the amidated fragments prior to their purification. This approach has been used successfully by Viktor Mutt's team to isolate various neuropeptides, some of which had already been identified in other species, such as cholecystokinin (Tatemoto et al., 1984), while others were completely novel such as neuropeptide Y (Tatemoto et al., 1982) and galanin (Tatemoto et al., 1983). The main difficulty with this approach comes from the very large amount of material required: it took for example 400 kg of pig brain to purify and characterize neuropeptide Y. It should be noted that the continuous improvement of analytical instrument sensitivity can now greatly facilitate the identification steps. However, only about half of the known neuropeptides are amidated (Kim and Seong, 2001), implying that the other half cannot be identified by this technique. Other biochemical characteristics can be used to identify neuropeptides within precursors, such as the presence of cleavage sites for PCs, which has allowed to discover new peptides from precursors already known as it was the case for nocistatin (Okuda-Ashitaka et al., 1998). Finally, a method more rarely used is based on the activity of the enzymes involved in peptide biosynthesis, such as carboxypeptidase E (Hook and Loh, 1984). After cleavage of the precursor by PCs, carboxypeptidase E acts to remove the basic amino acids located at the C-terminal position. Inactivation of carboxypeptidase E results in the accumulation of an almost mature form of the putative neuropeptide that can then be more easily purified and sequenced. Such a strategy led to the identification of PEN peptides, derived from a precursor close to the granins, SAAS (Fricker et al., 2000), whose receptor has not yet been identified. This technique has the same limitations as the previous ones, namely not all neuropeptides are substrates of carboxypeptidase E. Moreover, it should be kept in mind that all these approaches to identify neuropeptides are only the first steps of a long research process since once the candidate has been purified and sequenced, it is necessary to identify its receptor(s) in order to investigate into details its functions.

IDENTIFICATION USING GENOMIC APPROACHES

Comparison of cDNA or genomic sequences between distant species has allowed the discovery, in mammals, of several

biologically active peptides previously identified in non-mammalian species. For instance, the cDNA of the calcium-regulating hormone stanniocalcin has been initially cloned in teleost fish (Butkus et al., 1987) and the human ortholog has been identified only a decade later (Olsen et al., 1996; Chang et al., 1998). Similarly, the cDNA of the hypertensive peptide urotensin II (UII) has been first characterized in frog, and has been subsequently used to identify the human UII cDNA sequence (Coulouarn et al., 1998). Theoretically, invertebrate genomic sequences could also be exploited for the identification of vertebrate neuropeptide cDNAs (Elphick et al., 2018). The comparative approach has also been used successfully at the peptidic level. Thus, melanin-concentrating hormone (MCH) which has been initially identified in fish as a pituitary hormone (Kawauchi et al., 1983) was subsequently sequenced in a rat hypothalamic extract (Vaughan et al., 1989) before its cDNA was finally cloned in rat (Nahon et al., 1989) and human (Presse et al., 1990).

The detection of possible alternative splicing events may also lead to the discovery of novel regulatory peptides. This was the case with the calcitonin primary transcript that, through tissue-specific processing, can give rise to two distinct mRNAs

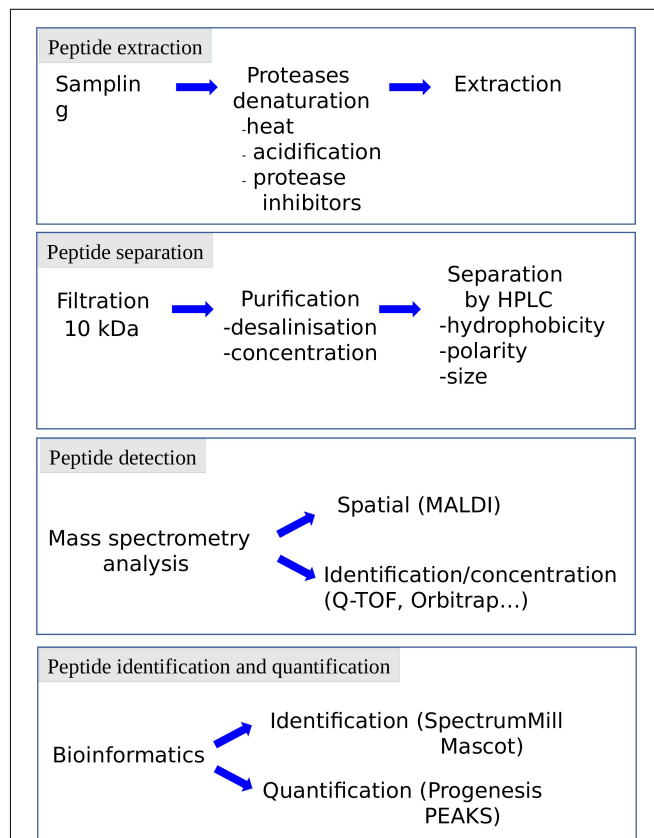


FIGURE 5 | Representation of the various steps of peptidomic studies. Each step can be adapted to the specificity of the peptide, the complexity of the matrix and the information needed (e.g., identification, quantification). HPLC: high pressure liquid chromatography.

i.e., calcitonin mRNA in thyroidal C cells and calcitonin gene-related peptide (CGRP) mRNA in neuronal cells (Amara et al., 1982; Rosenfeld et al., 1983). CGRP has thus been originally identified as an alternative splicing product of the calcitonin gene.

Genome sequencing of representative species of the different phyla has allowed the development of libraries containing almost all the genomic sequences of these species. However, the lack of gene annotations has made it necessary to create powerful computer tools to screen these libraries for the identification of novel neuropeptides. The developed softwares employ various strategies. First, sequence alignments can be used to compare non-annotated genes in one species with genes encoding neuropeptides in another species (Siepel et al., 2005). Thus, the genes that are conserved during evolution can be identified and are likely to exert an important function (Sonmez et al., 2009). Then, screening of cDNA libraries can identify sequences having common patterns with known neuropeptide families, such as the RFamide motif (Nathoo et al., 2001). Finally, it is possible to rely on the characteristics of neuropeptide precursors to screen genomic libraries for candidate sequences (Hewes and Taghert, 2001). These approaches use mathematical models like the Markov model, assigning a score to the sequences according to their correspondence with each of the criteria. It is then necessary to verify the expression of these sequences in neuronal cells and to look for an activity of the putative peptide. Nevertheless, *in silico* analysis can lead to a large number of predicted peptide candidates, which may require the synthesis of an important peptide library for subsequent biological screening (Liu et al., 2008; Shemesh et al., 2008; Kliger, 2010). But some

methods can help to reduce this number of candidates by using gene expression mapping to create peptide-receptor pairs (Williams et al., 2017).

It should be noted that these genomic techniques of identification of neuropeptides are progressively being supplanted by new and more efficient approaches. In particular, the evolution of mass spectrometry techniques has allowed the development of global peptidomic approaches for the discovery of novel biologically active peptides.

IDENTIFICATION USING PEPTIDOMIC APPROACHES

The term peptidomic appeared for the first time in 2001 in a study using mass spectrometry to develop a peptide profile in locusts (Clynen et al., 2001). Peptidomic methods (Figure 3) require a smaller amount of starting material and a shorter analysis time by reducing the successive purification steps. In addition, they make it possible to obtain more information on the candidate peptides, such as their sequence or the presence of post-translational modifications. Peptidomic studies are conventionally carried out in 4 steps, namely (i) peptides extraction, (ii) separation, (iii) detection and (iiii) identification and quantification (Figure 5).

The preservation of the peptides in their native state is crucial for peptidomic studies and must begin as soon as the sample is collected, to avoid the breakdown of proteins into peptides (false positives) or the degradation of the bioactive peptides (false negatives). Protection of the samples can be achieved

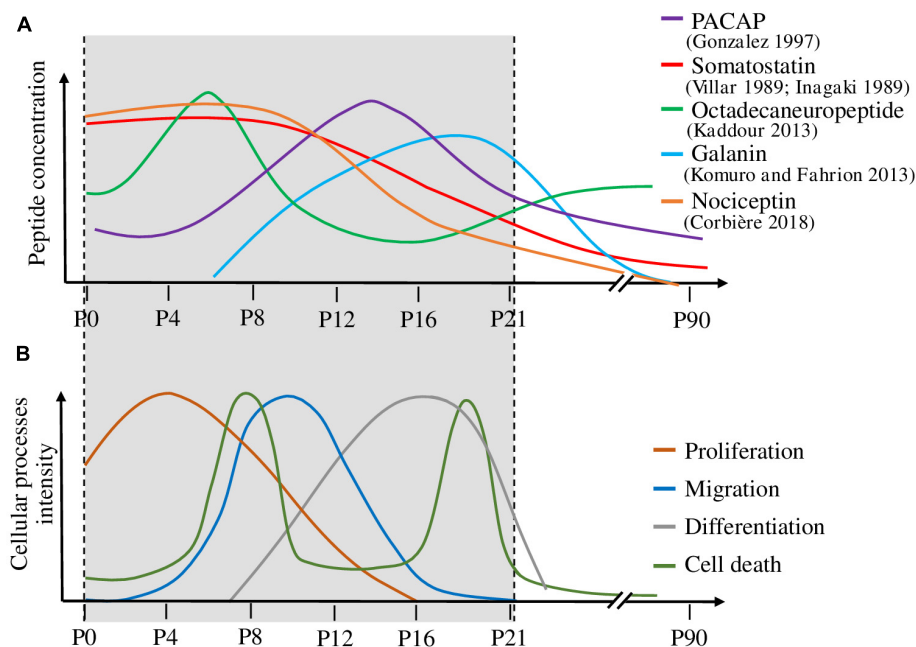


FIGURE 6 | Correlation between the expression level of various peptides and the mechanisms occurring during cerebellar cortex development. **(A)** Variation of five peptide concentrations during cerebellar development. **(B)** Temporal evolution of the cellular processes involved in cerebellar development, *i.e.*, proliferation, migration, differentiation and cell death. Peptide concentrations are high during the developmental processes on which they act. P: postnatal day. PACAP: pituitary adenylate cyclase-activating polypeptide.

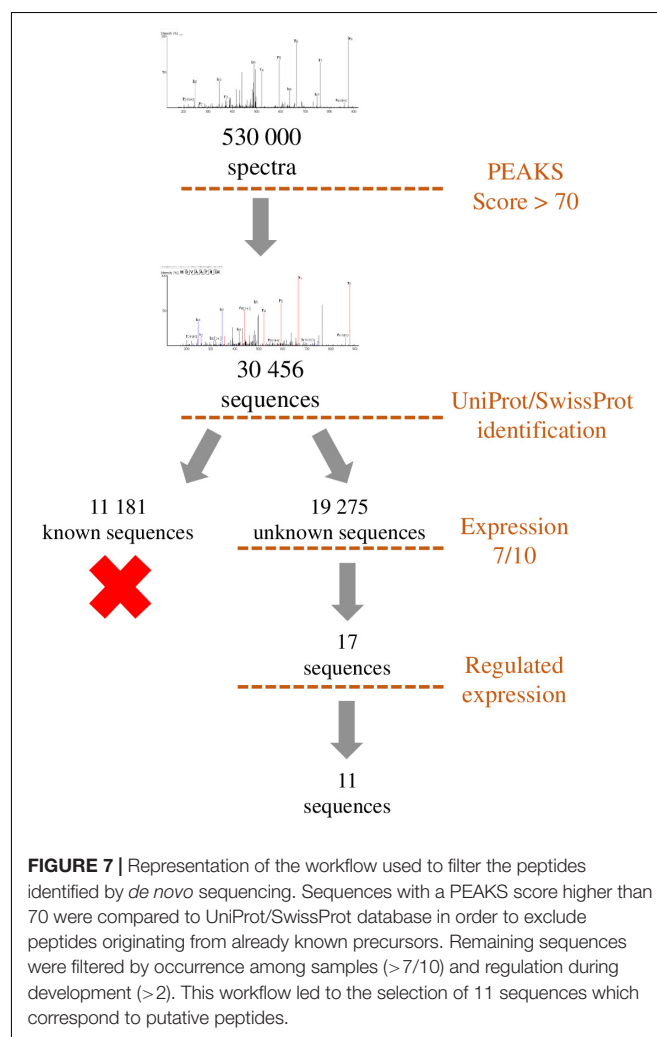
by heat denaturation of the proteolytic enzymes, acidification and/or addition of protease inhibitors. This can be done manually or using specific equipment such as the heat stabilization system Denator[®]. The extraction step has been refined and becomes more accessible and reproducible by the outbreak of commercial extraction tools. This step may include the use of centrifugal filters to remove larger proteins. The cut-off threshold conventionally used in peptidomics is 10 kDa, to get rid of proteins with a size greater than one hundred amino acids. The purification procedure is complemented using chromatography devices such as ZipTips[®] or Sep-Pak[®] to desalt, concentrate and purify samples.

The separation step, carried out upstream of the mass spectrometer, has been improved to allow the analysis of complex mixtures. Indeed, while it is possible to identify peptides via direct analysis of the sample by mass spectrometry, the presence of peptides and proteins of different molecular weight and variable concentrations in a complex matrix necessitates to include one or more separation steps upstream of the analyzer. This limitation can be circumvented by coupling the mass spectrometer to a separation method allowing the successive analysis of the various compounds of the sample by mass spectrometry. High performance liquid chromatography (HPLC) makes it possible to separate the peptides according to their hydrophobicity, polarity and/or size. The miniaturization of the columns (nanoHPLC) and the increase of the pressure (ultraHPLC), permit to increase the system sensitivity and resolution, and thus to improve the analyte separation. These ameliorations contribute to significantly reduce the amount of samples needed.

Peptide identification and quantification by mass spectrometry has also been considerably improved in recent years, particularly with the implementation in the proteomic platforms of devices such as high-resolution accurate-mass Orbitrap mass spectrometers which surpass the MALDI-TOF MS systems. The sensitivity level, acquisition rate, and range of analyzable masses have steadily increased through progress of ionization, ion trapping, and fragmentation (Eliuk and Makarov, 2015). In particular, the expansion of peptidomic techniques allowing the accumulation of information on peptide sequences and post-translational modifications has been facilitated by combination of fragmentation modes such as CID (Collision Induced Dissociation), HCD (Higher-Energy Collision Induced Dissociation) and ETD (Electron Transfer Dissociation) (Hayakawa et al., 2013). Peptide identification and quantification has also been made easier with advances in computer science. Indeed, the increase in the amount of data generated, that can reach for each experiment several tens of gigabytes, implies the development of bioinformatic databases and algorithms. In particular, data analysis is now facilitated by the development of powerful softwares to perform label-free quantitation (such as Progenesis), or database queries (such as Spectrum Mill or Mascot; Martens et al., 2005).

If peptidomic techniques were initially set up and still contribute to identify novel neuropeptides *de novo*, quantitative peptide profiling by mass spectrometry (also called differential peptidomics) is now used to screen and quantify already

characterized peptides in tissues where they were not known to be present and in different conditions. Such an approach was used to characterize peptides with daily regulation in the rat suprachiasmatic nucleus and led to the discovery that the peptide VGRPEWWMDYQ (AA 219–229), derived from proenkephalin A, is significantly increased at night-time (Lee et al., 2013). Still in the brain but during development, peptides acting on the ontogenesis of the cerebellar cortex (the external part of the cerebellum) often exhibit a specific pattern of expression with, in rodents, high expression over the first 2 postnatal weeks, and a decline at adulthood (Figure 6; Inagaki et al., 1989; Villar et al., 1989; Malagon et al., 1993; Tatsuno et al., 1994; Kaddour et al., 2013; Komuro and Fahrion, 2013). Based on this observation, it was possible to identify additional peptides exhibiting such a bell-shape expression profile (Corbière et al., 2018). Using a neuropeptide database, 33 peptides were identified in the cerebellum by mass spectrometry, among which 4 had a high expression level during development, which then decreased at adulthood. Further studies conducted on one of them, *i.e.*, nociceptin, confirmed that not only the peptide but also the expression



of its precursor gene and of its receptor are regulated during development. As the developing cerebellar cortex is composed of a dozen of cell types spread in 4 different well defined layers, an attempt was conducted to identify nociceptin by a MALDI-imaging approach. Although 8 compounds differentially expressed during cerebellar development could be detected through this approach, no peptide with an m/z corresponding to nociceptin could be unequivocally identified. Two peptides whose expression increased with cerebellar maturation may correspond to cerebellin-1 and [des-Ser1]-cerebellin but the measurement accuracy and the lack of fragmentation data show the limits of this approach (Belov et al., 2017). In fact, even if there are many developments around MALDI imaging, to date, only few bioactive peptides have been clearly identified through this approach (Ljungdahl et al., 2011; Hanrieder et al., 2012; Sui et al., 2017; Huber et al., 2018). To circumvent the problem, laser microdissection of the tissue coupled with real time PCR analysis was used to determine that both nociceptin and its receptor genes were mostly expressed in the internal granular layer of the cerebellar cortex, which mainly contains granule neurons. Subsequent functional studies showed that nociceptin exerts a neurotrophic effect on those granule neurons by increasing their survival and promoting their differentiation (Corbière et al., 2018; Figure 7). In an attempt to obtain information regarding cell specific peptide content, single cell neuropeptide profiling is a new challenge which has started to be developed (Jiménez et al., 2006; Neupert et al., 2012; Do et al., 2018).

DE NOVO IDENTIFICATION

To identify unknown peptides, *de novo* peptide sequencing of experimental data obtained by mass spectrometry can be carried out using softwares such as PEAKS. Nevertheless, some filters have to be applied to reduce the number of obtained sequences. A first step can be to eliminate all the sequences already present in SwissProt and/or UniProt databases coding for already known proteins and then to only retain sequences expressed recurrently and potentially regulated by a treatment, a disease or a developmental process. This allows the selection of several candidate peptides that are potentially bioactive in order to reverse-transcribe their sequence to identify the gene from which they are derived. Nevertheless, it remains to be determined whether some of these sequences can correspond to bioactive peptides. This can be achieved by looking at some selection criteria such as the presence of a sequence coding for a signal peptide upstream of the peptide of interest, the existence of basic doublets at the N- and C-terminal ends which may correspond to cleavage sites by PCs, and evolutionary conservation. If the peptide is under certain conditions regulated, it can be looked at the regulation of its gene expression and,

finally, possible functions should be investigated. This complex approach, which requires support from bioinformatics teams, has led to the identification of Neuroendocrine regulatory peptides (NERP-3; Sasaki et al., 2009) and other peptides derived from the VGF sequence (Sasaki et al., 2010). New methods of identification are also used to reduce the search space for spectral matching to improve the discrimination between correct peptide identification and false hit, and thus decrease the number of sequences (Hayakawa et al., 2013). Proteogenomics approaches are now also emerging to identify functional micropeptides produced from sORFs within cells of diverse species (Yeasmin et al., 2018). This approach often leads to a large number of peptide candidates that can nowadays be synthesized with dedicated robotic systems such as the Apex 396HT® Peptide Library Synthesizer.

The strategies developed in order to identify novel bioactive peptides have evolved considerably during the past decades. The successful but laborious pioneer tissue purifications combined to biological tests or immunoassays, that were rewarded by the attribution of several Nobel Prizes (Du Vigneaud, 1954; Guillemin, 1977; Schally, 1977; Yalow, 1977), are now supplanted by reverse pharmacology and peptidomic approaches which have already led to the discovery of several bioactive peptides. Owing to the raising interest of the pharmaceutical industry for peptide-based drugs (Fosgerau and Hoffmann, 2015; Henninot et al., 2018), the search of novel biologically active peptides is currently a very active domain. Rapid developments in bioinformatics, combined with powerful analytical methods and highly sophisticated mass spectrometers, should allow to de-orphanize the dozens of still orphan peptide-targeted GPCRs in vertebrates. These novel bioactive peptides will undoubtedly contribute to the rational design of innovative compounds either peptidergic analogs or small molecule-base drugs.

AUTHOR CONTRIBUTIONS

AC wrote the first draft of the manuscript. DV and HV corrected and completed the manuscript. PC, M-LW-B, TL, AL, and CP gave their technical knowledge to correct parts of the manuscript. All authors contributed to the manuscript revision, read and approved the submitted version.

FUNDING

AC was the recipient of a doctoral fellowship from Normandy Region. This work was supported by INSERM (U1239), Rouen University, Normandy Region and the European Union. Europe gets involved in Normandy with European Regional Development Fund (ERDF).

REFERENCES

- Alexander, S. P. H., Mathie, A., and Peters, J. A. (2011). Guide to receptors and channels (GRAC), 5th edition. *Br. J. Pharmacol.* 164(Suppl. 1), S1–S324. doi: 10.1111/j.1476-5381.2011.01649_1.x
- Allen, M. C., Brundish, D. E., Wade, R., Sandberg, B. E., Hanley, M. R., and Iversen, L. L. (1982). Tritiated peptides. 12. Synthesis and biological activity of [4-3H-Phe8]substance P. *J. Med. Chem.* 25, 1209–1213. doi: 10.1021/jm00352a022
- Amara, S. G., Jonas, V., Rosenfeld, M. G., Ong, E. S., and Evans, R. M. (1982). Alternative RNA processing in calcitonin gene expression generates mRNAs

- encoding different polypeptide products. *Nature* 298, 240–244. doi: 10.1038/298240a0
- Arimura, A. (2007). PACAP: the road to discovery. *Peptides* 28, 1617–1619. doi: 10.1016/j.peptides.2007.06.006
- Barbaccia, M. L., Berkovich, A., Guarneri, P., and Slobodyansky, E. (1990). DBI (diazepam binding inhibitor): the precursor of a family of endogenous modulators of GABAA receptor function. History, perspectives, and clinical implications. *Neurochem. Res.* 15, 161–168. doi: 10.1007/bf00972206
- Beinfeld, M. C. (1997). CCK biosynthesis and processing: recent progress and future challenges. *Life Sci.* 61, 2359–2366. doi: 10.1016/s0024-3205(97)00644-9
- Belov, M. E., Ellis, S. R., Dillillo, M., Paine, M. R. L., Danielson, W. F., Anderson, G. A., et al. (2017). Design and performance of a novel interface for combined matrix-assisted laser desorption/ionization at elevated pressure and electrospray ionization with orbitrap mass spectrometry. *Anal. Chem.* 89, 7493–7501. doi: 10.1021/acs.analchem.7b01168
- Bicknell, A. B. (2008). The tissue-specific processing of pro-opiomelanocortin. *J. Neuroendocrinol.* 20, 692–699. doi: 10.1111/j.1365-2826.2008.01709.x
- Brakch, N., Galanopoulou, A. S., Patel, Y. C., Boileau, G., and Seidah, N. G. (1995). Comparative proteolytic processing of rat prosomatostatin by the convertases PC1, PC2, furin, PACE4 and PC5 in constitutive and regulated secretory pathways. *FEBS Lett.* 362, 143–146. doi: 10.1016/0014-5793(95)00229-3
- Brazeau, P., Vale, W., Burgus, R., Ling, N., Butcher, M., Rivier, J., et al. (1973). Hypothalamic polypeptide that inhibits the secretion of immunoreactive pituitary growth hormone. *Science* 179, 77–79. doi: 10.1126/science.179.4068.77
- Burgus, R., Dunn, T. F., Desiderio, D., and Guillemin, R. (1969). Molecular structure of the hypothalamic hypophysiotropic TRF factor of ovine origin: mass spectrometry demonstration of the PCA-His-Pro-NH₂ sequence. *C. R. Acad. Sci. Hebd. Seances Acad. Sci. D.* 269, 1870–1873.
- Butkus, A., Roche, P. J., Fernley, R. T., Haralambidis, J., Penschow, J. D., Ryan, G. B., et al. (1987). Purification and cloning of a corpuscle of Stannius protein from *Anguilla australis*. *Mol. Cell. Endocrinol.* 54, 123–133. doi: 10.1016/0303-7207(87)90149-3
- Cerdá-Reverter, J. M., Martínez-Rodríguez, G., Zanuy, S., Carrillo, M., and Larhammar, D. (2000). Molecular evolution of the neuropeptide Y (NPY) family of peptides: cloning of three NPY-related peptides from the sea bass (*Dicentrarchus labrax*). *Regul. Pept.* 95, 25–34. doi: 10.1016/s0167-0115(00)00132-4
- Chang, A. C., Jeffrey, K. J., Tokutake, Y., Shimamoto, A., Neumann, A. A., Dunham, M. A., et al. (1998). Human stanniocalcin (STC): genomic structure, chromosomal localization, and the presence of CAG trinucleotide repeats. *Genomics* 47, 393–398. doi: 10.1006/geno.1997.5120
- Chang, M. M., Leeman, S. E., and Niall, H. D. (1971). Amino-acid sequence of substance P. *Nat. New Biol.* 232, 86–87. doi: 10.1038/newbio232086a0
- Clynen, E., Baggerman, G., Veelaert, D., Cersiaens, A., Van der Horst, D., Harthoorn, L., et al. (2001). Peptidomics of the pars intercerebralis-corpora cardiaca complex of the migratory locust, *Locusta migratoria*. *Eur. J. Biochem.* 268, 1929–1939. doi: 10.1046/j.1432-1327.2001.02067.x
- Coleman, J., Inukai, M., and Inouye, M. (1985). Dual functions of the signal peptide in protein transfer across the membrane. *Cell* 43, 351–360. doi: 10.1016/0092-8674(85)90040-6
- Corbière, A., Walet-Balieu, M.-L., Chan, P., Basille-Dugay, M., Hardouin, J., and Vaudry, D. (2018). A peptidomic approach to characterize peptides involved in cerebellar cortex development leads to the identification of the neurotrophic effects of nociceptin. *Mol. Cell. Proteomics* 17, 1737–1749. doi: 10.1074/mcp.RA117.000184
- Coulouarn, Y., Lihrmann, I., Jegou, S., Anouar, Y., Tostivint, H., Beauvillain, J. C., et al. (1998). Cloning of the cDNA encoding the urotensin II precursor in frog and human reveals intense expression of the urotensin II gene in motoneurons of the spinal cord. *Proc. Natl. Acad. Sci. U.S.A.* 95, 15803–15808. doi: 10.1073/pnas.95.26.15803
- de Lecea, L., Criado, J. R., Prospero-Garcia, O., Gautvik, K. M., Schweitzer, P., Danielson, P. E., et al. (1996). A cortical neuropeptide with neuronal depressant and sleep-modulating properties. *Nature* 381, 242–245. doi: 10.1038/381242a0
- De Mota, N., Reaux-Le Goazigo, A., El Messari, S., Chartrel, N., Roesch, D., Dujardin, C., et al. (2004). Apelin, a potent diuretic neuropeptide counteracting vasopressin actions through inhibition of vasopressin neuron activity and vasopressin release. *Proc. Natl. Acad. Sci. U.S.A.* 101, 10464–10469. doi: 10.1073/pnas.0403518101
- Do, T. D., Ellis, J. F., Neumann, E. K., Comi, T. J., Tillmaand, E. G., Lenhart, A. E., et al. (2018). Optically guided single cell mass spectrometry of rat dorsal root ganglia to profile lipids, peptides and proteins. *Chemphyschem. Eur. J. Chem. Phys. Phys. Chem.* 19, 1180–1191. doi: 10.1002/cphc.201701364
- Douglass, J., Civelli, O., and Herbert, E. (1984). Polyprotein gene expression: generation of diversity of neuroendocrine peptides. *Annu. Rev. Biochem.* 53, 665–715. doi: 10.1146/annurev.biochem.53.1.665
- Du Vigneaud, V. (1954). Hormones of the posterior pituitary gland: oxytocin and vasopressin. *Harvey Lect.* 50, 1–26.
- Du Vigneaud, V., Ressler, C., and Trippett, S. (1953). The sequence of amino acids in oxytocin, with a proposal for the structure of oxytocin. *J. Biol. Chem.* 205, 949–957.
- Eliuk, S., and Makarov, A. (2015). Evolution of orbitrap mass spectrometry instrumentation. *Annu. Rev. Anal. Chem.* 8, 61–80. doi: 10.1146/annurev-anchem-071114-040325
- Elphick, M. R., Mirabeau, O., and Larhammar, D. (2018). Evolution of neuropeptide signalling systems. *J. Exp. Biol.* 221:jeb151092. doi: 10.1242/jeb.151092
- Euler, U. S. V., and Gaddum, J. H. (1931). An unidentified depressor substance in certain tissue extracts. *J. Physiol.* 72, 74–87. doi: 10.1113/jphysiol.1931.sp002763
- Ferrero, P., Santi, M. R., Conti-Tronconi, B., Costa, E., and Guidotti, A. (1986). Study of an octadecaneuropeptide derived from diazepam binding inhibitor (DBI): biological activity and presence in rat brain. *Proc. Natl. Acad. Sci. U.S.A.* 83, 827–831. doi: 10.1073/pnas.83.3.827
- Fosgerau, K., and Hoffmann, T. (2015). Peptide therapeutics: current status and future directions. *Drug Discov. Today* 20, 122–128. doi: 10.1016/j.drudis.2014.10.003
- Fricker, L. D. (ed.). (2012). *Neuropeptides and Other Bioactive Peptides: From Discovery to Function*. San Rafael: Morgan & Claypool Publishers. doi: 10.4199/C00058ED1V01Y201205NPE003
- Fricker, L. D., McKinzie, A. A., Sun, J., Curran, E., Qian, Y., Yan, L., et al. (2000). Identification and characterization of proSAAS, a granin-like neuroendocrine peptide precursor that inhibits prohormone processing. *J. Neurosci. Off. J. Soc. Neurosci.* 20, 639–648. doi: 10.1523/jneurosci.20-02-00639.2000
- Fricker, L. D., and Snyder, S. H. (1982). Enkephalin convertase: purification and characterization of a specific enkephalin-synthesizing carboxypeptidase localized to adrenal chromaffin granules. *Proc. Natl. Acad. Sci. U.S.A.* 79, 3886–3890. doi: 10.1073/pnas.79.12.3886
- Gigoux, V., Escrieut, C., Silvente-Poirot, S., Maigret, B., Gouilleux, L., Fehrentz, J. A., et al. (1998). Met-195 of the cholecystokinin-A receptor interacts with the sulfated tyrosine of cholecystokinin and is crucial for receptor transition to high affinity state. *J. Biol. Chem.* 273, 14380–14386. doi: 10.1074/jbc.273.23.14380
- Goldstein, A., Tachibana, S., Lowney, L. I., Hunkapiller, M., and Hood, L. (1979). Dynorphin-(1-13), an extraordinarily potent opioid peptide. *Proc. Natl. Acad. Sci. U.S.A.* 76, 6666–6670. doi: 10.1073/pnas.76.12.6666
- Guillemin, R. (1977). Peptides in the brain: the new endocrinology of the neuron. *Science* 202, 390–402. doi: 10.1126/science.212832
- Hanrieder, R., Ljungdahl, A., and Andersson, M. (2012). MALDI imaging mass spectrometry of neuropeptides in Parkinson's disease. *J. Vis. Exp.* 60, 3445. doi: 10.3791/3445
- Hayakawa, E., Menschaert, G., De Bock, P.-J., Luyten, W., Gevaert, K., Baggerman, G., et al. (2013). Improving the identification rate of endogenous peptides using electron transfer dissociation and collision-induced dissociation. *J. Proteome Res.* 12, 5410–5421. doi: 10.1021/pr400446z
- Henninot, A., Collins, J. C., and Nuss, J. M. (2018). The current state of peptide drug discovery: back to the future? *J. Med. Chem.* 61, 1382–1414. doi: 10.1021/acs.jmedchem.7b00318
- Hewes, R. S., and Taghert, P. H. (2001). Neuropeptides and neuropeptide receptors in the *Drosophila melanogaster* genome. *Genome Res.* 11, 1126–1142. doi: 10.1101/gr.169901
- Hook, V. Y., and Loh, Y. P. (1984). Carboxypeptidase B-like converting enzyme activity in secretory granules of rat pituitary. *Proc. Natl. Acad. Sci. U.S.A.* 81, 2776–2780. doi: 10.1073/pnas.81.9.2776

- Huber, K., Khameghir-Silz, P., Schramm, T., Gorshkov, V., Spengler, B., and Römpf, A. (2018). Approaching cellular resolution and reliable identification in mass spectrometry imaging of tryptic peptides. *Anal. Bioanal. Chem.* 410, 5825–5837. doi: 10.1007/s00216-018-1199-z
- Hughes, J., Smith, T., Morgan, B., and Fothergill, L. (1975). Purification and properties of enkephalin - the possible endogenous ligand for the morphine receptor. *Life Sci.* 16, 1753–1758. doi: 10.1016/0024-3205(75)90268-4
- Inagaki, S., Shiosaka, S., Sekitani, M., Noguchi, K., Shimada, S., and Takagi, H. (1989). *In situ* hybridization analysis of the somatostatin-containing neuron system in developing cerebellum of rats. *Brain Res. Mol. Brain Res.* 6, 289–295. doi: 10.1016/0169-328x(89)90074-0
- Jerabek-Willemsen, M., André, T., Wanner, R., Roth, H. M., Dühr, S., Baaske, P., et al. (2014). MicroScale thermophoresis: interaction analysis and beyond. *J. Mol. Struct.* 1077, 101–113. doi: 10.1016/j.molstruc.2014.03.009
- Jiménez, C. R., Spijker, S., de Schipper, S., Lodder, J. C., Janse, C. K., Geraerts, W. P. M., et al. (2006). Peptidomics of a single identified neuron reveals diversity of multiple neuropeptides with convergent actions on cellular excitability. *J. Neurosci. Off. J. Soc. Neurosci.* 26, 518–529. doi: 10.1523/jneurosci.2566-05.2006
- Kaddour, H., Hamdi, Y., Vaudry, D., Basille, M., Desrues, L., Leprince, J., et al. (2013). The octadecanoneuropeptide ODN prevents 6-hydroxydopamine-induced apoptosis of cerebellar granule neurons through a PKC-MAPK-dependent pathway. *J. Neurochem.* 125, 620–633. doi: 10.1111/jnc.12140
- Kawauchi, H., Kawazoe, I., Tsubokawa, M., Kishida, M., and Baker, B. I. (1983). Characterization of melanin-concentrating hormone in chum salmon pituitaries. *Nature* 305, 321–323. doi: 10.1038/305321a0
- Kiefer, M. C., Tucker, J. E., Joh, R., Landsberg, K. E., Saltman, D., and Barr, P. J. (1991). Identification of a second human subtilisin-like protease gene in the fes/fps region of chromosome 15. *DNA Cell Biol.* 10, 757–769. doi: 10.1089/dna.1991.10.757
- Kim, K.-H., and Seong, B. L. (2001). Peptide amidation: production of peptide hormones *in vivo* and *in vitro*. *Biotechnol. Bioprocess. Eng.* 6, 244–251. doi: 10.1007/bf02931985
- Kliger, Y. (2010). Computational approaches to therapeutic peptide discovery. *Biopolymers* 94, 701–710. doi: 10.1002/bip.21458
- Kojima, M., Hosoda, H., Date, Y., Nakazato, M., Matsuo, H., and Kangawa, K. (1999). Ghrelin is a growth-hormone-releasing acylated peptide from stomach. *Nature* 402, 656–660. doi: 10.1038/45230
- Komuro, H., and Fahrion, J. (2013). *Role of Galanin in Neuronal Cell Migration After Brain Injury*. Cleveland, OH: Cleveland Clinic - Lerner Research Institute.
- Labarrère, P., Chatenet, D., Leprince, J., Marionneau, C., Loirand, G., Tonon, M.-C., et al. (2003). Structure-activity relationships of human urotensin II and related analogues on rat aortic ring contraction. *J. Enzyme. Inhib. Med. Chem.* 18, 77–88. doi: 10.1080/1475636031000093507
- Lee, J. E., Zamdborg, L., Southey, B. R., Atkins, N., Mitchell, J. W., Li, M., et al. (2013). Quantitative peptidomics for discovery of circadian-related peptides from the rat suprachiasmatic nucleus. *J. Proteome Res.* 12, 585–593. doi: 10.1021/pr300605p
- Lee, S. L., Stewart, K., and Goodman, R. H. (1988). Structure of the gene encoding rat thyrotropin releasing hormone. *J. Biol. Chem.* 263, 16604–16609.
- Liu, F., Baggerman, G., Schoofs, L., and Wets, G. (2008). The construction of a bioactive peptide database in Metazoa. *J. Proteome Res.* 7, 4119–4131. doi: 10.1021/pr800037n
- Ljungdahl, A., Hanrieder, J., Fälth, M., Bergquist, J., and Andersson, M. (2011). Imaging mass spectrometry reveals elevated nigral levels of dynorphin neuropeptides in L-DOPA-induced dyskinesia in rat model of Parkinson's disease. *PLoS One* 6:e25653. doi: 10.1371/journal.pone.0025653
- Lusson, J., Vieau, D., Hamelin, J., Day, R., Chrétien, M., and Seidah, N. G. (1993). cDNA structure of the mouse and rat subtilisin/kexin-like PC5: a candidate proprotein convertase expressed in endocrine and nonendocrine cells. *Proc. Natl. Acad. Sci. U.S.A.* 90, 6691–6695. doi: 10.1073/pnas.90.14.6691
- Malagon, M., Vaudry, H., Van Strien, F., Pelletier, G., Gracia-Navarro, F., and Tonon, M. C. (1993). Ontogeny of diazepam-binding inhibitor-related peptides (endozepines) in the rat brain. *Neuroscience* 57, 777–786. doi: 10.1016/0306-4522(93)90023-9
- Martens, L., Hermjakob, H., Jones, P., Adamski, M., Taylor, C., States, D., et al. (2005). PRIDE: the proteomics identifications database. *Proteomics* 5, 3537–3545. doi: 10.1002/pmic.200401303
- Meraldi, J. P., Hruby, V. J., and Brewster, A. I. (1977). Relative conformational rigidity in oxytocin and (1-penicillamine)-oxytocin: a proposal for the relationship of conformational flexibility to peptide hormone agonism and antagonism. *Proc. Natl. Acad. Sci. U.S.A.* 74, 1373–1377. doi: 10.1073/pnas.74.4.1373
- Meunier, J. C., Mollereau, C., Toll, L., Suaudeau, C., Moisand, C., Alvinerie, P., et al. (1995). Isolation and structure of the endogenous agonist of opioid receptor-like ORL1 receptor. *Nature* 377, 532–535. doi: 10.1038/377532a0
- Miyata, A., Arimura, A., Dahl, R. R., Minamino, N., Uehara, A., Jiang, L., et al. (1989). Isolation of a novel 38 residue-hypothalamic polypeptide which stimulates adenylate cyclase in pituitary cells. *Biochem. Biophys. Res. Commun.* 164, 567–574. doi: 10.1016/0006-291x(89)91757-9
- Mombaerts, P. (2004). Genes and ligands for odorant, vomeronasal and taste receptors. *Nat. Rev. Neurosci.* 5, 263–278. doi: 10.1038/nrn1365
- Muccioli, G., Papotti, M., Locatelli, V., Ghigo, E., and Deghenghi, R. (2001). Binding of 125I-labeled ghrelin to membranes from human hypothalamus and pituitary gland. *J. Endocrinol. Invest.* 24, RC7–RC9.
- Nahon, J. L., Schoepfer, R., and Vale, W. (1989). cDNA sequence of salmon melanin-concentrating hormone exhibits similarities with 7SL RNA. *Nucleic Acids Res.* 17:3598. doi: 10.1093/nar/17.9.3598
- Nakanishi, S., Inoue, A., Kita, T., Nakamura, M., Chang, A. C., Cohen, S. N., et al. (1979). Nucleotide sequence of cloned cDNA for bovine corticotropin-beta-lipotropin precursor. *Nature* 278, 423–427. doi: 10.1038/278423a0
- Nakayama, K., Kim, W. S., Torii, S., Hosaka, M., Nakagawa, T., Ikemizu, J., et al. (1992). Identification of the fourth member of the mammalian endoprotease family homologous to the yeast Kex2 protease. Its testis-specific expression. *J. Biol. Chem.* 267, 5897–5900.
- Nathoo, A. N., Moeller, R. A., Westlund, B. A., and Hart, A. C. (2001). Identification of neuropeptide-like protein gene families in *Caenorhabditis elegans* and other species. *Proc. Natl. Acad. Sci. U.S.A.* 98, 14000–14005. doi: 10.1073/pnas.241231298
- Neupert, S., Rubakhin, S. S., and Sweedler, J. V. (2012). Targeted single-cell microchemical analysis: MS-based peptidomics of individual paraformaldehyde-fixed and immunolabeled neurons. *Chem. Biol.* 19, 1010–1019. doi: 10.1016/j.chembiol.2012.05.023
- Neveu, C. (2012). *Contribution à l'étude des relations structure-activité du neuropeptide 26Rfa et des interactions avec son récepteur, le GPR103: approches in silico, in vitro et in vivo*. Ph.D. thesis, University of Rouen, Mont-Saint-Aignan.
- O'Donohue, T. L., Handelsmann, G. E., Chaconas, T., Miller, R. L., and Jacobowitz, D. M. (1981). Evidence that N-acetylation regulates the behavioral activity of alpha-MSH in the rat and human central nervous system. *Peptides* 2, 333–344. doi: 10.1016/s0196-9781(81)80126-x
- Okuda-Ashitaka, E., and Ito, S. (2000). Nocistatin: a novel neuropeptide encoded by the gene for the nociceptin/orphanin FQ precursor. *Peptides* 21, 1101–1109. doi: 10.1016/s0196-9781(00)00247-3
- Okuda-Ashitaka, E., Minami, T., Tachibana, S., Yoshihara, Y., Nishiuchi, Y., Kimura, T., et al. (1998). Nocistatin, a peptide that blocks nociceptin action in pain transmission. *Nature* 392, 286–289. doi: 10.1038/32660
- Olsen, H. S., Cepeda, M. A., Zhang, Q. Q., Rosen, C. A., and Vozzolo, B. L. (1996). Human stanniocalcin: a possible hormonal regulator of mineral metabolism. *Proc. Natl. Acad. Sci. U.S.A.* 93, 1792–1796. doi: 10.1073/pnas.93.5.1792
- Pert, A., Simantov, R., and Snyder, S. H. (1977). A morphine-like factor in mammalian brain: analgesic activity in rats. *Brain Res.* 136, 523–533. doi: 10.1016/0006-8993(77)90076-2
- Presse, F., Nahon, J. L., Fischer, W. H., and Vale, W. (1990). Structure of the human melanin concentrating hormone mRNA. *Mol. Endocrinol. Baltim. Md* 4, 632–637. doi: 10.1210/mend-4-4-632
- Reinscheid, R. K., Nothacker, H. P., Bourson, A., Ardati, A., Henningsen, R. A., Bunzow, J. R., et al. (1995). Orphanin FQ: a neuropeptide that activates an opioidlike G protein-coupled receptor. *Science* 270, 792–794. doi: 10.1126/science.270.5237.792
- Rosenfeld, M. G., Mermod, J.-J., Amara, S. G., Swanson, L. W., Sawchenko, P. E., Rivier, J., et al. (1983). Production of a novel neuropeptide encoded by the calcitonin gene via tissue-specific RNA processing. *Nature* 304, 129–135. doi: 10.1038/304129a0
- Sakurai, T., Amemiya, A., Ishii, M., Matsuzaki, I., Chemelli, R. M., Tanaka, H., et al. (1998). Orexins and orexin receptors: a family of hypothalamic neuropeptides

- and G protein-coupled receptors that regulate feeding behavior. *Cell* 92, 573–585. doi: 10.1016/s0092-8674(00)80949-6
- Sasaki, K., Satomi, Y., Takao, T., and Minamino, N. (2009). Snapshot peptidomics of the regulated secretory pathway. *Mol. Cell. Proteomics* 8, 1638–1647. doi: 10.1074/mcp.M900044-MCP200
- Sasaki, K., Takahashi, N., Satoh, M., Yamasaki, M., and Minamino, N. (2010). A peptidomics strategy for discovering endogenous bioactive peptides. *J. Proteome Res.* 9, 5047–5052. doi: 10.1021/pr1003455
- Schally, A. V. (1977). Aspects of hypothalamic regulation of the pituitary gland with major emphasis on its implications for the control of reproductive processes. *Lect. Nobel Prize Physiol. Med.* Available at: <https://www.nobelprize.org/prizes/medicine/1977/schally/lecture/>
- Schally, A. V., Arimura, A., Kastin, A. J., Matsuo, H., Baba, Y., Redding, T. W., et al. (1971). Gonadotropin-releasing hormone: one polypeptide regulates secretion of luteinizing and follicle-stimulating hormones. *Science* 173, 1036–1038. doi: 10.1126/science.173.4001.1036
- Seidah, N. G., Benjannet, S., Wickham, L., Marcinkiewicz, J., Jasmin, S. B., Stifani, S., et al. (2003). The secretory proprotein convertase neural apoptosis-regulated convertase 1 (NARC-1): liver regeneration and neuronal differentiation. *Proc. Natl. Acad. Sci. U.S.A.* 100, 928–933. doi: 10.1073/pnas.0335507100
- Seidah, N. G., Marcinkiewicz, M., Benjannet, S., Gaspar, L., Beaubien, G., Mattei, M. G., et al. (1991). Cloning and primary sequence of a mouse candidate prohormone convertase PC1 homologous to PC2, Furin, and Kex2: distinct chromosomal localization and messenger RNA distribution in brain and pituitary compared to PC2. *Mol. Endocrinol. Baltim. Md* 5, 111–122. doi: 10.1210/mend-5-1-111
- Seidah, N. G., Mowla, S. J., Hamelin, J., Mamarbachi, A. M., Benjannet, S., Touré, B. B., et al. (1999). Mammalian subtilisin/kexin isozyme SKI-1: a widely expressed proprotein convertase with a unique cleavage specificity and cellular localization. *Proc. Natl. Acad. Sci. U.S.A.* 96, 1321–1326. doi: 10.1073/pnas.96.4.1321
- Shemesh, R., Toporik, A., Levine, Z., Hecht, I., Rotman, G., Wool, A., et al. (2008). Discovery and validation of novel peptide agonists for G-protein-coupled receptors. *J. Biol. Chem.* 283, 34643–34649. doi: 10.1074/jbc.M805181200
- Siepel, A., Bejerano, G., Pedersen, J. S., Hinrichs, A. S., Hou, M., Rosenbloom, K., et al. (2005). Evolutionarily conserved elements in vertebrate, insect, worm, and yeast genomes. *Genome Res.* 15, 1034–1050. doi: 10.1101/gr.3715005
- Smekens, S. P., and Steiner, D. F. (1990). Identification of a human insulinoma cDNA encoding a novel mammalian protein structurally related to the yeast dibasic processing protease Kex2. *J. Biol. Chem.* 265, 2997–3000.
- Song, L., and Fricker, L. D. (1995). Purification and characterization of carboxypeptidase D, a novel carboxypeptidase E-like enzyme, from bovine pituitary. *J. Biol. Chem.* 270, 25007–25013. doi: 10.1074/jbc.270.42.25007
- Sonmez, K., Zaveri, N. T., Kerman, I. A., Burke, S., Neal, C. R., Xie, X., et al. (2009). Evolutionary sequence modeling for discovery of peptide hormones. *PLoS Comput. Biol.* 5:e1000258. doi: 10.1371/journal.pcbi.1000258
- Stockert, J. A., and Devi, L. A. (2015). Advancements in therapeutically targeting orphan GPCRs. *Front. Pharmacol.* 6:100. doi: 10.3389/fphar.2015.00100
- Sui, P., Watanabe, H., Artemenko, K., Sun, W., Bakalkin, G., Andersson, M., et al. (2017). Neuropeptide imaging in rat spinal cord with MALDI-TOF MS: method development for the application in pain-related disease studies. *Eur. J. Mass Spectrom. Chichester. Engl.* 23, 105–115. doi: 10.1177/1469066717703272
- Tatemoto, K., Carlquist, M., and Mutt, V. (1982). Neuropeptide Y—a novel brain peptide with structural similarities to peptide YY and pancreatic polypeptide. *Nature* 296, 659–660. doi: 10.1038/296659a0
- Tatemoto, K., Jörnvall, H., Siimesmaa, S., Halldén, G., and Mutt, V. (1984). Isolation and characterization of cholecystokinin-58 (CCK-58) from porcine brain. *FEBS Lett.* 174, 289–293. doi: 10.1016/0014-5793(84)81175-8
- Tatemoto, K., Rökæus, A., Jörnvall, H., McDonald, T. J., and Mutt, V. (1983). Galanin - a novel biologically active peptide from porcine intestine. *FEBS Lett.* 164, 124–128. doi: 10.1016/0014-5793(83)80033-7
- Tatsuno, I., Somogyvari-Vigh, A., and Arimura, A. (1994). Developmental changes of pituitary adenylate cyclase activating polypeptide (PACAP) and its receptor in the rat brain. *Peptides* 15, 55–60. doi: 10.1016/0196-9781(94)90170-8
- Tsuji, A., Hine, C., Mori, K., Tamai, Y., Higashine, K., Nagamune, H., et al. (1994). A novel member, PC7, of the mammalian kexin-like protease family: homology to PACE4A, its brain-specific expression and identification of isoforms. *Biochem. Biophys. Res. Commun.* 202, 1452–1459. doi: 10.1006/bbrc.1994.2094
- van de Ven, W. J., Voorberg, J., Fontijn, R., Pannekoek, H., van den Ouweland, A. M., van Duijnoven, H. L., et al. (1990). Furin is a subtilisin-like proprotein processing enzyme in higher eukaryotes. *Mol. Biol. Rep.* 14, 265–275. doi: 10.1007/bf00429896
- Vaudry, D., Basille, M., Anouar, Y., Fournier, A., Vaudry, H., and Gonzalez, B. J. (1998). The neurotrophic activity of PACAP on rat cerebellar granule cells is associated with activation of the protein kinase A pathway and c-fos gene expression. *Ann. N. Y. Acad. Sci.* 865, 92–99. doi: 10.1111/j.1749-6632.1998.tb11167.x
- Vaudry, D., Chen, Y., Hsu, C.-M., and Eiden, L. E. (2002). PC12 cells as a model to study the neurotrophic activities of PACAP. *Ann. N. Y. Acad. Sci.* 971, 491–496. doi: 10.1111/j.1749-6632.2002.tb04513.x
- Vaudry, D., Falluel-Morel, A., Bourgault, S., Basille, M., Burel, D., Wurtz, O., et al. (2009). Pituitary adenylate cyclase-activating polypeptide and its receptors: 20 years after the discovery. *Pharmacol. Rev.* 61, 283–357. doi: 10.1124/pr.109.001370
- Vaudry, D., Gonzalez, B. J., Basille, M., Pamantung, T. F., Fournier, A., and Vaudry, H. (2000). PACAP acts as a neurotrophic factor during histogenesis of the rat cerebellar cortex. *Ann. N. Y. Acad. Sci.* 921, 293–299. doi: 10.1111/j.1749-6632.2000.tb06980.x
- Vaudry, H., Leprince, J., Chatenet, D., Fournier, A., Lambert, D. G., Le Mével, J.-C., et al. (2015). International union of basic and clinical pharmacology. *XCII. Urotensin II, urotensin II-related peptide, and their receptor: from structure to function. Pharmacol. Rev.* 67, 214–258. doi: 10.1124/pr.114.009480
- Vaughan, J. M., Fischer, W. H., Hoeger, C., Rivier, J., and Vale, W. (1989). Characterization of melanin-concentrating hormone from rat hypothalamus. *Endocrinology* 125, 1660–1665. doi: 10.1210/endo-125-3-1660
- Villar, M. J., Hökfelt, T., and Brown, J. C. (1989). Somatostatin expression in the cerebellar cortex during postnatal development. An immunohistochemical study in the rat. *Anat. Embryol.* 179, 257–267. doi: 10.1007/bf00326591
- Walter, P., Gilmore, R., and Blobel, G. (1984). Protein translocation across the endoplasmic reticulum. *Cell* 38, 5–8. doi: 10.1016/0092-8674(84)90520-8
- Williams, E. A., Verasztó, C., Jasek, S., Conzelmann, M., Shahidi, R., Bauknecht, P., et al. (2017). Synaptic and peptidergic connectome of a neurosecretory center in the annelid brain. *eLife* 6:e26349. doi: 10.7554/eLife.26349
- Yalow, R. S. (1977). Radioimmunoassay: a probe for fine structure of biological systems. *Lect. Nobel Prize Physiol. Med.* Available at: <https://www.nobelprize.org/prizes/medicine/1977/yalow/lecture/>
- Yeasmin, F., Yada, T., and Akimitsu, N. (2018). Micropeptides encoded in transcripts previously identified as long noncoding RNAs: a new chapter in transcriptomics and proteomics. *Front. Genet.* 9:144. doi: 10.3389/fgene.2018.00144

Conflict of Interest Statement: The authors declare that the research was conducted in the absence of any commercial or financial relationships that could be construed as a potential conflict of interest.

Copyright © 2019 Corbière, Vaudry, Chan, Walet-Balieu, Lecroq, Lefebvre, Pineau and Vaudry. This is an open-access article distributed under the terms of the Creative Commons Attribution License (CC BY). The use, distribution or reproduction in other forums is permitted, provided the original author(s) and the copyright owner(s) are credited and that the original publication in this journal is cited, in accordance with accepted academic practice. No use, distribution or reproduction is permitted which does not comply with these terms.



Conceptualization of a Parasympathetic Endocrine System

Jonathan Gorky* and James Schwaber

Daniel Baugh Institute for Functional Genomics and Computational Biology, Thomas Jefferson University, Philadelphia, PA, United States

OPEN ACCESS

Edited by:

Lee E. Eiden,
National Institutes of Health (NIH),
United States

Reviewed by:

Limei Zhang,
National Autonomous University
of Mexico, Mexico
Sarah Haas Lockie,
Monash University, Australia
Vito Salvador Hernandez,
National Autonomous University
of Mexico, Mexico

*Correspondence:

Jonathan Gorky
jonathan.gorky@jefferson.edu

Specialty section:

This article was submitted to
Neuroendocrine Science,
a section of the journal
Frontiers in Neuroscience

Received: 09 March 2019

Accepted: 05 September 2019

Published: 23 September 2019

Citation:

Gorky J and Schwaber J (2019)
Conceptualization of a
Parasympathetic Endocrine System.
Front. Neurosci. 13:1008.
doi: 10.3389/fnins.2019.01008

We here propose a parasympathetic endocrine system (PES) comprised of circulating peptides released from secretory cells in the gut, significantly modulated by vagal projections from the dorsal motor nucleus of the vagus (DMV). While most of these gut peptides mediate well-described satiety and digestive effects that increase parasympathetic control of digestion (Lee et al., 1994; Gutzwiller et al., 1999; Klok et al., 2007), they also have actions that are far-reaching and increase parasympathetic signaling broadly throughout the body. The actions beyond satiety that peptides like somatostatin, cholecystokinin, glucagon-like peptide 1, and vasoactive intestinal peptide have been well-examined, but not in a systematic way. Consideration has been given to the idea that these and other gut-derived peptides are part of an endocrine system has been partially considered (Rehfeld, 2012; Drucker, 2016), but that it is coordinated through parasympathetic control and may act to increase the actions of parasympathetic projections has not been formalized before. Here only gut-derived hormones are included although there are potentially other parasympathetically mediated factors released from other sites like lung and liver (Drucker, 2016). The case for the existence of the PES with the DMV as its integrative controller will be made through examination of an anatomical substrate and evidence of physiological control mechanisms as well as direct examples of PES antagonism of sympathetic signaling in mammals, including humans. The implications for this conceptual understanding of a PES reframe diseases like metabolic syndrome and may help underscore the role of the autonomic nervous system in the associated symptoms.

Keywords: parasympathetic, autonomic, endocrine, gut, vagus

THE DMV AS THE PES CONTROLLER

Although there is evidence that more may participate, four effectors will be considered in this conceptualization: somatostatin (SST), cholecystokinin (CCK), glucagon-like peptide 1 (GLP-1), and vasoactive intestinal peptide (VIP). The system as hypothesized is shown in **Figure 1** with annotations as to each aspect of the connectivity. While all four are used as neurotransmitters and do not readily cross the blood brain barrier (Banks and Kastin, 1985), their presence in the circulatory system is able to mediate brain function through receptors in the hypothalamus and area postrema (van der Kooy, 1984; Shaffer and Moody, 1986; Breder et al., 1992; Yamamoto et al., 2003; Arora and Anubhuti, 2006), both of which prominently project to the dorsal motor nucleus

of the vagus (DMV) (Gray and Magnuson, 1987; Hyde et al., 1996; Zheng et al., 2005). This sets up a pathway by which DMV sensing for circulating peptide levels and their effects may be monitored and controlled. The DMV is capable of modulating secretion of each of these through direct and indirect means utilizing gut postganglionic and myenteric plexus neurons. The work on such vagal influence has not been fully investigated in any one species, so the literature cited here includes work done in rats, guinea pigs, dogs, and humans. VIP is secreted by a subset of secretomotor neurons under the influence of postganglionic parasympathetic neurons directly modulated by vagal efferents (Bitar et al., 1980; Kirchgeßner and Gershon, 1989; Yuan et al., 2005). SST is released from D-cells and is also under the influence of postganglionic parasympathetic neurons with vagal efferent projections having a demonstrable influence (Ahrén et al., 1986; Greenberg, 1993; Chisholm and Greenberg, 2002). CCK and GLP-1 secretion occurs under direct modulation by enteric neurons, which themselves have their influence from the postganglionic parasympathetic neurons. There is evidence that GLP-1 secretion can occur as a direct consequence of vagal efferent activity (Rocca and Brubaker, 1999). Although no such linear pathway has been described for CCK release as a result of vagal efferent activity, there is molecular and anatomical evidence that an indirect pathway exists. This pathway contains enteric secretomotor neurons that produce CCK and interactions with enteric neurons and possibly postganglionic neurons.

The DMV efferent projections are capable of modulating the release of several peptides in the gut, including the four enumerated above. Each of these four peptides are released through a complex network of local (gut sensing) and central (vagal) mechanisms. It is possible that the release of all gut peptides, including but not limited to the four discussed here, results from generic vagal efferent activity [release of acetylcholine (ACh)]. There is even evidence that changing the firing frequency can modulate peptide release of DMV efferents, which itself may be influenced by the transcriptional milieu of ion channels (Guzman et al., 1979; Nishi et al., 1985). DMV efferent neurons have the potential to express several other transmitters and peptides, the effects of which are still incompletely understood, especially with regard to local effects on signaling of gut projections.

ANTAGONISM OF THE SYMPATHETIC NERVOUS SYSTEM

The proposed parasympathetic endocrine system (PES) counterbalances the sympathetic nervous system broadly, not just with regard to digestion and orexigenic behavior. As the role of the four peptides examined here in digestion and satiety has been well-described (e.g., Arora and Anubhuti, 2006), we here focus on the other aspects of their control over visceral functions as they pertain to sympathetic antagonism. First, it is helpful to recall what the canonical effects of the sympathetic nervous system are. Sympathetic activation causes pupillary dilation, increased rate and contractility in the heart, bronchial dilation in the lungs, constriction of blood vessels generally,

fluid retention and Na⁺ reuptake in kidney, urinary bladder relaxation, and activation of sweat glands, and is generally proinflammatory (Grebe et al., 2010; Kreibitz, 2010). While not antagonistic to sympathetic activity, several PES peptides have the parasympathetic-like activity of enhancing erection induction, as will be discussed. What follows is evidence for sympathetic balancing in mammals from each of the PES effectors under consideration with these effects being summarized in **Figure 2**.

Somatostatin

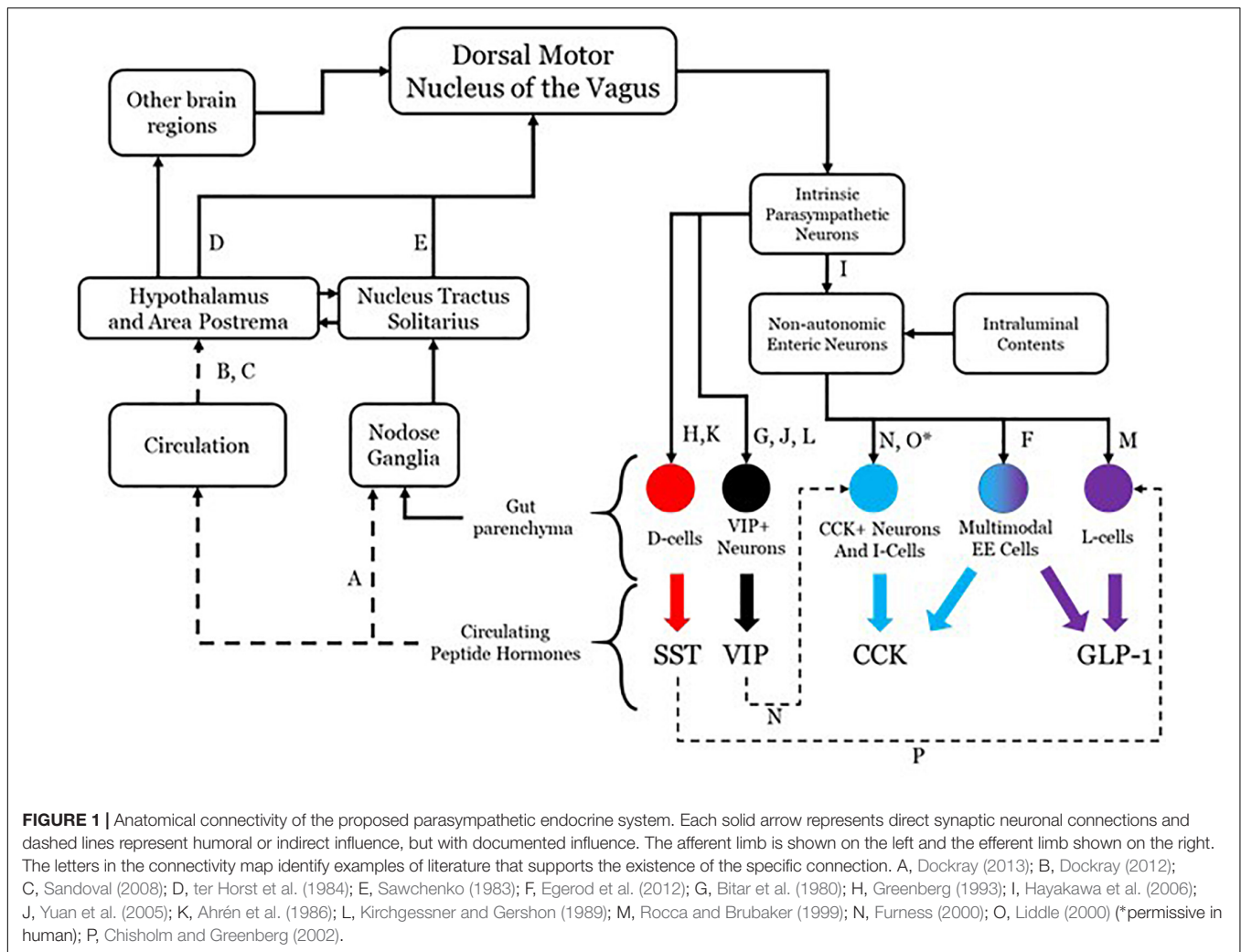
Somatostatin and neuronostatin, a closely related peptide derived from the same mRNA transcript, mediate broad sympathetic antagonism and parasympathetic potentiating effects. In the heart, SST reduces contractility in an ACh-dependent fashion (Franco-Cereceda et al., 1987; Yoshikawa et al., 1996) and directly antagonizes sympathetic adrenergic beta receptors (Murray et al., 2001). Neurostatin also diminishes contractility and has the net effect of reducing blood pressure when in circulation (Samson et al., 2008; Vainio et al., 2012). Central administration of SST causes apnea (Yamamoto et al., 1988) and local levels in the lungs result in bronchoconstriction (Barrios et al., 1987). SST also has broad anti-inflammatory effects (Hofland et al., 1999; Krantic, 2000; ten Bokum et al., 2000). In penile tissue, SST potentiates the effects of ACh induction of erection (Hedlund and Andersson, 1985). Even in the eye, SST alone causes minor pupillary constriction (Bito et al., 1982). Along with the effects mentioned above, SST is able to mimic the effects of parasympathetically mediated ischemic preconditioning in generating cardioprotection (Wang et al., 2005).

Cholecystokinin

The cardiovascular effects of CCK (Lovick, 2009) include reduction of heart rate (Kaczyńska and Szereda-Przestaszewska, 2015). CCK is also a vasodilator, acting locally (Sánchez-Fernández et al., 2004) or directly antagonizing neurons in rostral ventrolateral medulla (RVLM) and caudal ventrolateral medulla (CVLM) that selectively mediate vasoconstriction (Sartor and Verberne, 2002, 2006). Systemically administered CCK causes dyspnea with large enough doses in adults (Bradwejn et al., 1998) and can even induce panic attack like breathing patterns (Shlik et al., 1997). In the kidney, CCK decreases Na⁺ reuptake and reduces vascular resistance (von Schrenck et al., 2000) along with decreasing renal inflammation (Miyamoto et al., 2012). It has more broad anti-inflammatory effects via enhancement of vagal signaling (Luyer et al., 2005). CCK causes pupillary constriction, but only in primates and humans (Bill et al., 1990).

Glucagon-Like Peptide 1

In the lungs, GLP-1 stimulates macromolecule secretion, mimicking the effects of ACh, and increases pulmonary blood flow (Richter et al., 1993). In the kidney, GLP-1 inhibits Na⁺ reuptake, thus acting as a diuretic (Okerson and Chilton, 2012) and also induces diuresis in the bladder through contraction (Ahrén, 2004). Like SST, GLP-1 also enhances erectile function via direct binding of receptors in erectile tissue (Giagulli et al., 2015). GLP-1 has also been shown to mediate a robust cardioprotective response (Ban, 2010; Basalay et al., 2016).



Vasoactive Intestinal Peptide

Like the other peptides, VIP is a potent vasodilator capable of decreasing heart rate and conduction velocity (Henning and Sawmiller, 2001). Interestingly, there are more VIP receptors in the right ventricle compared with the left, although the functional implications of this is not well understood (Henning and Sawmiller, 2001). In the kidney, VIP increases Na⁺ excretion (Rosa et al., 1985) and can induce erection or vaginal lubrication (Sjöstrand et al., 1981; Ottesen et al., 1984, 1987; Hedlund and Andersson, 1985). There are several ways in which VIP mediates anti-inflammatory effects (Poza et al., 2000; Ganea and Delgado, 2002; Delgado et al., 2004): inhibits mast cell degranulation (Tunçel et al., 2000), decreases lymphocyte proliferation in Peyer's patches (Stanisz et al., 1986), induces Treg and regulatory dendritic cell expansion (Chorny et al., 2005), and is generally immunosuppressive in aqueous humor (Taylor et al., 1994). In contrast to the other peptides considered here, VIP is sympathomimetic in the lungs, antagonizing bronchoconstriction (Barnes and Dixon, 1984). On the balance, VIP has parasympathetic-like activity in spite of the respiratory function described here.

RECONSIDERING METABOLIC SYNDROME

There are likely more effectors of the PES than the four peptides explored above with partial or complete sympathetic antagonism. What makes this idea more than a collection of peptide functions is that it is coordinated by DMV projections. Reconsideration of disease processes in this context as a system may provide a foundation for new treatment approaches. Autonomic dysfunction accompanies many metabolic syndromes, including obesity and type II diabetes. There therefore may be some aspects of metabolic syndrome that are mediated, or at least modulated by autonomic functions via this parasympathetic endocrine system.

The diagnostic criteria for metabolic syndrome includes a combination of at least three of the following: abdominal obesity, hypertension, hyperglycemia, increased triglycerides, and decreased high-density lipoprotein (HDL) cholesterol (Alberti et al., 2005; Opie, 2007). The four peptides highlighted in this review each contribute to negating the effects of metabolic syndrome across these five criteria as shown in **Figure 3**, the

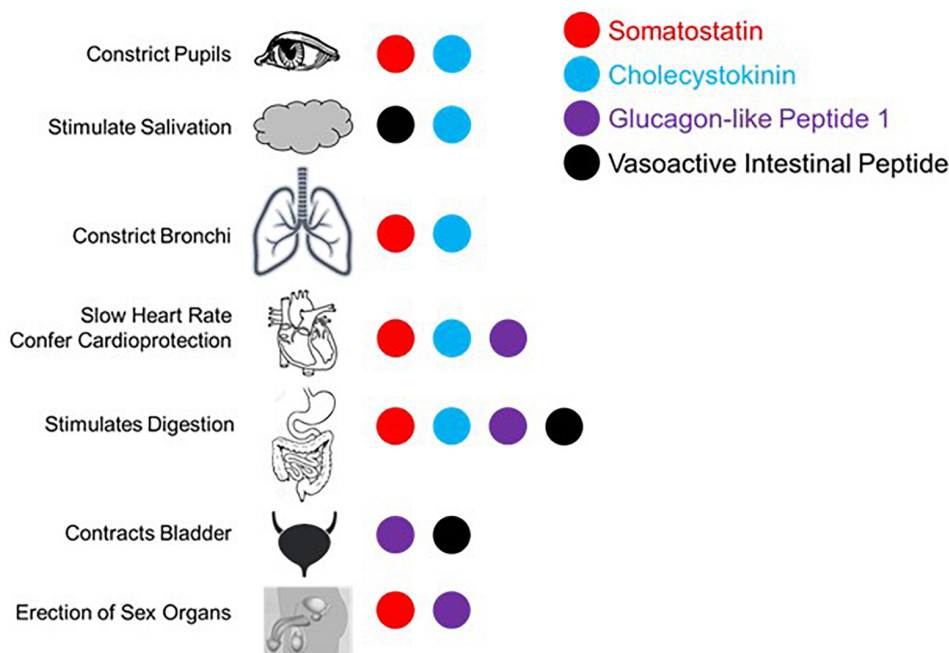


FIGURE 2 | Summary of published effects of four selected gut peptides and their effects in augmenting parasympathetic function canonically effected via the vagus nerve and/or sacral parasympathetic projections.

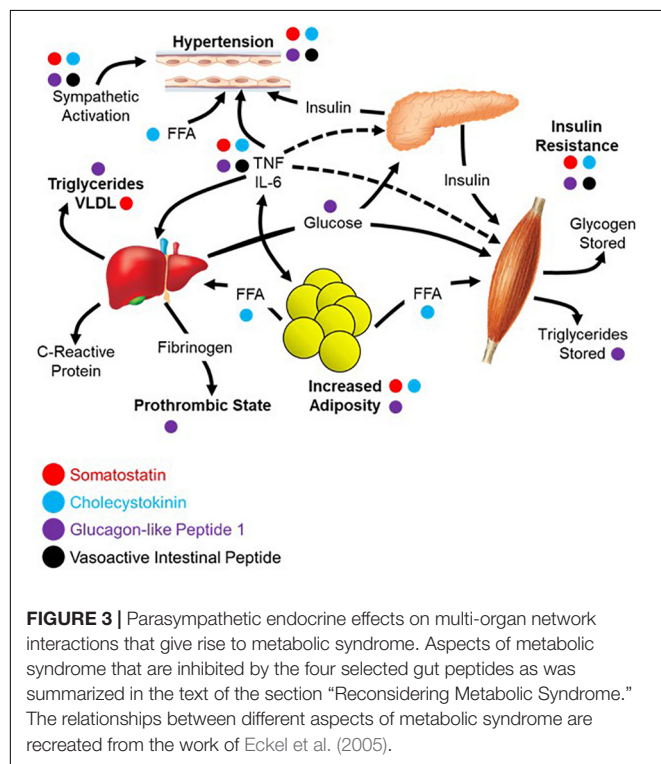


FIGURE 3 | Parasympathetic endocrine effects on multi-organ network interactions that give rise to metabolic syndrome. Aspects of metabolic syndrome that are inhibited by the four selected gut peptides as was summarized in the text of the section “Reconsidering Metabolic Syndrome.” The relationships between different aspects of metabolic syndrome are recreated from the work of Eckel et al. (2005).

underlying network being based largely on the work of Eckel et al. (2005). Abdominal obesity can be reduced/prevented through circulating SST (Lustig et al., 1999; Boehm and Lustig, 2002;

Boehm, 2003), CCK (Pi-Sunyer et al., 1982; Matson and Ritter, 1999; Neary and Batterham, 2009), or GLP-1 (Näslund et al., 1999; Day et al., 2009; Astrup et al., 2012). Hypertension can be ameliorated by all four peptides focused upon here; SST (Rosenthal et al., 1977; Carretta et al., 1989), CCK (Kagebayashi et al., 2012), GLP-1 (Wang et al., 2013; Katout et al., 2014), and VIP (Gao et al., 1994). All four peptides contribute to lowering fasting plasma glucose through a variety of mechanisms including stimulation of insulin secretion and inhibition of glucagon secretion; SST (Gerich et al., 1974, 1975; Wahren, 1976; Vergès, 2017), CCK (Cheung et al., 2009; Irwin et al., 2015), GLP-1 (Nauck et al., 1993; Toft-Nielsen et al., 1999; Irwin et al., 2015), and VIP (Kato et al., 1994). Effects on triglycerides and HDL cholesterol have less evidence to date, yet it has been demonstrated that GLP-1 can lower triglycerides (Qin et al., 2005; Meier et al., 2006) with CCK recently shown to have similar effects on absorption in a preclinical model (Plaza et al., 2018). Of the four, only GLP-1 can increase HDL cholesterol, although it appears to be mediated through a variety of other mechanisms as opposed to a direct effect on the production and processing of cholesterol (Ponzani et al., 2016).

Apart from the direct symptoms of metabolic syndrome, there is a broad sympathetic dominance across multiple organ systems (Tentolouris et al., 2006, 2008). This includes cardiovascular problems like resting tachycardia, reduced heart rate variability, and decreased baroreflex sensitivity (Garruti et al., 2012; Verrotti et al., 2014). Metabolic syndrome causes erectile dysfunction with a high incidence of comorbidity (Gündüz et al., 2004; Bal et al., 2007). Also in metabolic syndrome, there is a markedly decreased release of multiple gut peptides (Verrotti et al., 2014).

It is possible that the diminished gut peptide release contributes to the dysautonomia and sympathetic dominance through absence of antagonism. This may be due to physical changes in the gut or perturbations in the sensory mechanisms that otherwise mediate their release. If this is the case, it might be possible to replace these peptides and treat the autonomic symptoms. There is an example of this in a clinical trial showing that the use of SST analog treats diarrhea and orthostatic hypotension in patients with diabetes (Dudl et al., 1987). Moving forward, it may be helpful to assay for circulating peptide levels and use them either as biomarkers of disease or as indications to initiate peptide replacement therapy. It is likely that replacing the milieu of peptides rather than one or the other will be required for maximal clinical benefit.

CONCLUSION

The requirements of the PES laid out here were that it has a central controller, broadly counterbalances sympathetic effects, and can help explain disease pathology. The evidence provided suggests that there is a parasympathetic endocrine system that is coordinated by the DMV. The power lent by this concept derives from the network coordination of the four peptides discussed here and many additional circulating gut factors at the

level of the DMV where there can be integration of peripheral and central neuronal inputs and orchestration of multiple gut endocrine activities. This also enables identification via disease markers and interventions aimed at treating a network of factors at the central or peripheral level. The conceptualization of physiology laid out here goes beyond the boundaries of traditional medical specialties like gastroenterology, neurology, or cardiology and instead requires a systems approach to health and medicine. As the ability to deal with human health in a more comprehensive and complete way matures in the era of big data, clinicians must be ready to incorporate the growing complexity of the body as a system in the design and implementation of therapeutic intervention.

AUTHOR CONTRIBUTIONS

JG developed the main concepts and was the primary writer of the manuscript. JS provided the significant editorial contributions.

FUNDING

This work was made possible by grants from the National Institute of Health (5U01HL133360-02 and 3OT2OD023848).

REFERENCES

- Ahrén, B. (2004). GLP-1 and extra-islet effects. *Horm. Metab. Res.* 36, 842–845. doi: 10.1055/s-2004-826173
- Ahrén, B., Paquette, T. L., and Taborsky, G. J. (1986). Effect and mechanism of vagal nerve stimulation on somatostatin secretion in dogs. *Am. J. Physiol.* 250, E212–E217. doi: 10.1152/ajpendo.1986.250.2.E212
- Alberti, K. G., Zimmet, P., Shaw, J., and IDF Epidemiology Task Force Consensus Group. (2005). The metabolic syndrome—a new worldwide definition. *Lancet* 366, 1059–1062.
- Arora, S., and Anubhuti (2006). Role of neuropeptides in appetite regulation and obesity—a review. *Neuropeptides* 40, 375–401. doi: 10.1016/j.npep.2006.07.001
- Astrup, A., Carraro, R., Finer, N., Harper, A., Kunesova, M., Lean, M. E. J., et al. 1807 Investigators (2012). Safety, tolerability and sustained weight loss over 2 years with the once-daily human GLP-1 analog, liraglutide. *Int. J. Obes.* 36, 843–854. doi: 10.1038/ijo.2011.158
- Bal, K., Oder, M., Sahin, A. S., Karataş, C. T., Demir, O., Can, E., et al. (2007). Prevalence of metabolic syndrome and its association with erectile dysfunction among urologic patients: metabolic backgrounds of erectile dysfunction. *Urology* 69, 356–360. doi: 10.1016/j.urology.2006.09.057
- Ban, K. (2010). *Mechanisms Underlying Cardioprotective Effects of Glucagon like Peptide-1 in Ischemia-reperfusion Injury*. Ph. D Thesis, University of Toronto: Toronto, ON.
- Banks, W. A., and Kastin, A. J. (1985). Peptides and the blood-brain barrier: lipophilicity as a predictor of permeability. *Brain Res. Bull.* 15, 287–292. doi: 10.1016/0361-9230(85)90153-4
- Barnes, P. J., and Dixon, C. M. (1984). The effect of inhaled vasoactive intestinal peptide on bronchial reactivity to histamine in humans. *Am. Rev. Respir. Dis.* 130, 162–166. doi: 10.1164/arrd.1984.130.2.162
- Barrios, V., Fernandez Iriarte, M. C., Morcillo, E., Prieto, J. C., and Arilla, E. (1987). Effect of sensitization on somatostatin concentration and binding in cytosol from guinea pig airways. *Regul. Peptides* 19, 161–168. doi: 10.1016/0167-0115(87)90273-4
- Basalay, M. V., Mastitskaya, S., Mrochek, A., Ackland, G. L., Del Arroyo, A. G., Sanchez, J., et al. (2016). Glucagon-like peptide-1 (GLP-1) mediates cardioprotection by remote ischaemic conditioning. *Cardiovasc. Res.* 112, 669–676. doi: 10.1093/cvr/cvw216
- Bill, A., Andersson, S. E., and Almegård, B. (1990). Cholecystokinin causes contraction of the pupillary sphincter in monkeys but not in cats, rabbits, rats and guinea-pigs: antagonism by lorglumide. *Acta Physiol. Scand.* 138, 479–485. doi: 10.1111/j.1748-1716.1990.tb08875.x
- Bitar, K. N., Said, S. I., Weir, G. C., Saffouri, B., and Makhlof, G. M. (1980). Neural release of vasoactive intestinal peptide from the gut. *Gastroenterology* 79, 1288–1294. doi: 10.1016/0016-5085(80)90927-0
- Bito, L. Z., Nichols, R. R., and Baroody, R. A. (1982). A comparison of the mitotic and inflammatory effects of biologically active polypeptides and prostaglandin E2 on the rabbit eye. *Exp. Eye Res.* 34, 325–337. doi: 10.1016/0014-4835(82)90081-1
- Boehm, B. O. (2003). The therapeutic potential of somatostatin receptor ligands in the treatment of obesity and diabetes. *Expert Opin. Investig. Drugs* 12, 1501–1509. doi: 10.1517/eoid.12.9.1501.21813
- Boehm, B. O., and Lustig, R. H. (2002). Use of somatostatin receptor ligands in obesity and diabetic complications. *Best Pract. Res. Clin. Gastroenterol.* 16, 493–509. doi: 10.1053/bega.2002.0320
- Bradwejn, J., LeGrand, J. M., Koszycki, D., Bates, J. H., and Bourin, M. (1998). Effects of cholecystokinin tetrapeptide on respiratory function in healthy volunteers. *Am. J. Psychiatry* 155, 280–282.
- Breder, C. D., Yamada, Y., Yasuda, K., Seino, S., Saper, C. B., and Bell, G. I. (1992). Differential expression of somatostatin receptor subtypes in brain. *J. Neurosci.* 12, 3920–3934. doi: 10.1523/jneurosci.12-10-03920.1992
- Carretta, R., Fabris, B., Fischetti, F., Costantini, M., De Biasi, F., Muiesan, S., et al. (1989). Reduction of blood pressure in obese hyperinsulinaemic hypertensive patients during somatostatin infusion. *J. Hypertens. Suppl.* 7, S196–S197.
- Cheung, G. W. C., Kokorovic, A., Lam, C. K. L., Chari, M., and Lam, T. K. T. (2009). Intestinal cholecystokinin controls glucose production through a neuronal network. *Cell Metab.* 10, 99–109. doi: 10.1016/j.cmet.2009.07.005
- Chisholm, C., and Greenberg, G. R. (2002). Somatostatin-28 regulates GLP-1 secretion via somatostatin receptor subtype 5 in rat intestinal cultures. *Am. J. Physiol. Endocrinol. Metab.* 283, E311–E317. doi: 10.1152/ajpendo.00434.2001
- Chorny, A., Gonzalez-Rey, E., Fernandez-Martin, A., Pozo, D., Ganea, D., and Delgado, M. (2005). Vasoactive intestinal peptide induces regulatory dendritic

- cells with therapeutic effects on autoimmune disorders. *Proc. Natl. Acad. Sci. U.S.A.* 102, 13562–13567. doi: 10.1073/pnas.0504484102
- Day, J. W., Ottaway, N., Patterson, J. T., Gelfanov, V., Smiley, D., Gidda, J., et al. (2009). A new glucagon and GLP-1 co-agonist eliminates obesity in rodents. *Nat. Chem. Biol.* 5, 749–757. doi: 10.1038/nchembio.209
- Delgado, M., Pozo, D., and Ganea, D. (2004). The significance of vasoactive intestinal peptide in immunomodulation. *Pharmacol. Rev.* 56, 249–290. doi: 10.1124/pr.56.2.7
- Dockray, G. J. (2012). Cholecystokinin. *Curr. Opin. Endocrinol. Diabetes Obes.* 19, 8–12. doi: 10.1097/MED.0b013e32834eb77d
- Dockray, G. J. (2013). Enteroendocrine cell signalling via the vagus nerve. *Curr. Opin. Pharmacol.* 13, 954–958. doi: 10.1016/j.coph.2013.09.007
- Drucker, D. J. (2016). Evolving concepts and translational relevance of enteroendocrine cell biology. *J. Clin. Endocrinol. Metab.* 101, 778–786. doi: 10.1210/jc.2015-3449
- Dudl, R. J., Anderson, D. S., Forsythe, A. B., Ziegler, M. G., and O'Dorisio, T. M. (1987). Treatment of diabetic diarrhea and orthostatic hypotension with somatostatin analogue SMS 201-995. *Am. J. Med.* 83, 584–588. doi: 10.1016/0002-9343(87)90777-7
- Eckel, R. H., Grundy, S. M., and Zimmet, P. Z. (2005). The metabolic syndrome. *Lancet* 365, 1415–1428. doi: 10.1016/S0140-6736(05)66378-7
- Egerod, K. L., Engelstoft, M. S., Grunddal, K. V., Nøhr, M. K., Secher, A., Sakata, I., et al. (2012). A major lineage of enteroendocrine cells coexpress CCK, secretin, GIP, GLP-1, PYY, and neuropeptide but not somatostatin. *Endocrinology* 153, 5782–5795. doi: 10.1210/en.2012-1595
- Furness, J. B. (2000). Types of neurons in the enteric nervous system. *J. Auton. Nerv. Syst.* 81, 87–96. doi: 10.1016/S0165-1838(00)00127-2
- Franco-Cereceda, A., Bengtsson, L., and Lundberg, J. M. (1987). Inotropic effects of calcitonin gene-related peptide, vasoactive intestinal polypeptide and somatostatin on the human right atrium in vitro. *Eur. J. Pharmacol.* 134, 69–76. doi: 10.1016/0014-2999(87)90132-4
- Ganea, D., and Delgado, M. (2002). Vasoactive intestinal peptide (VIP) and pituitary adenylate cyclase-activating polypeptide (PACAP) as modulators of both innate and adaptive immunity. *Critic. Rev. Oral Biol. Med.* 13, 229–237.
- Gao, X., Noda, Y., Rubinstein, I., and Paul, S. (1994). Vasoactive intestinal peptide encapsulated in liposomes: effects on systemic arterial blood pressure. *Life Sci.* 54, L247–L252.
- Garruti, G., Giampetruzzi, F., Vita, M. G., Pellegrini, F., Lagioia, P., Stefanelli, G., et al. (2012). Links between metabolic syndrome and cardiovascular autonomic dysfunction. *Exp. Diabetes Res.* 2012:615835. doi: 10.1155/2012/615835
- Gerich, J. E., Lorenzi, M., Hane, S., Gustafson, G., Guillemin, R., and Forsham, P. H. (1975). Evidence for a physiologic role of pancreatic glucagon in human glucose homeostasis: studies with somatostatin. *Metab. Clin. Exp.* 24, 175–182. doi: 10.1016/0026-0495(75)90018-9
- Gerich, J. E., Lorenzi, M., Schneider, V., Karam, J. H., Rivier, J., Guillemin, R., et al. (1974). Effects of somatostatin on plasma glucose and glucagon levels in human diabetes mellitus. Pathophysiologic and therapeutic implications. *N. Engl. J. Med.* 291, 544–547. doi: 10.1056/nejm197409122911102
- Giagulli, V. A., Carbone, M. D., Ramunni, M. I., Licchelli, B., De Pergola, G., Sabbà, C., et al. (2015). Adding liraglutide to lifestyle changes, metformin and testosterone therapy boosts erectile function in diabetic obese men with overt hypogonadism. *Andrology* 3, 1094–1103. doi: 10.1111/andr.12099
- Gray, T. S., and Magnuson, D. J. (1987). Neuropeptide neuronal efferents from the bed nucleus of the stria terminalis and central amygdaloid nucleus to the dorsal vagal complex in the rat. *J. Comp. Neurol.* 262, 365–374. doi: 10.1002/cne.902620304
- Grebe, K. M., Takeda, K., Hickman, H. D., Bailey, A. L., Embry, A. C., Bennink, J. R., et al. (2010). Cutting edge: sympathetic nervous system increases proinflammatory cytokines and exacerbates influenza A virus pathogenesis. *J. Immunol.* 184, 540–544. doi: 10.4049/jimmunol.0903395
- Greenberg, G. R. (1993). Differential neural regulation of circulating somatostatin-14 and somatostatin-28 in conscious dogs. *Am. J. Physiol.* 264, G902–G909. doi: 10.1152/ajpgi.1993.264.5.G902
- Gündüz, M. I., Gümus, B. H., and Sekuri, C. (2004). Relationship between metabolic syndrome and erectile dysfunction. *Asian J. Androl.* 6, 355–358.
- Gutzwiller, J.-P., Drewe, J., Göke, B., Schmidt, H., Rohrer, B., Lareida, J., et al. (1999). Glucagon-like peptide-1 promotes satiety and reduces food intake in patients with diabetes mellitus type 2. *Am. J. Physiol. Regul. Integr. Comp. Physiol.* 276, R1541–R1544. doi: 10.1152/ajpregu.1999.276.5.R1541
- Guzman, S., Chayvialle, J. A., Banks, W. A., Rayford, P. L., and Thompson, J. C. (1979). Effect of vagal stimulation on pancreatic secretion and on blood levels of gastrin, cholecystokinin, secretin, vasoactive intestinal peptide, and somatostatin. *Surgery* 86, 329–336.
- Hayakawa, T., Kuwahara, S., Maeda, S., Tanaka, K., and Seki, M. (2006). Direct synaptic contacts on the myenteric ganglia of the rat stomach from the dorsal motor nucleus of the vagus. *J. Comp. Neurol.* 498, 352–362. doi: 10.1002/cne.21069
- Hedlund, H., and Andersson, K. E. (1985). Effects of some peptides on isolated human penile erectile tissue and cavernous artery. *Acta Physiol. Scand.* 124, 413–419. doi: 10.1111/j.1748-1716.1985.tb07677.x
- Henning, R. J., and Sawmiller, D. R. (2001). Vasoactive intestinal peptide: cardiovascular effects. *Cardiovasc. Res.* 49, 27–37. doi: 10.1016/s0008-6363(00)00229-7
- Holland, L. J., van Hagen, P. M., and Lamberts, S. W. (1999). Functional role of somatostatin receptors in neuroendocrine and immune cells. *Ann. Med.* 31(Suppl. 2), 23–27.
- Hyde, T. M., Knable, M. B., and Murray, A. M. (1996). Distribution of dopamine D1-D4 receptor subtypes in human dorsal vagal complex. *Synapse* 24, 224–232. doi: 10.1002/(sici)1098-2396(199611)24:3<224::aid-syn4>3.0.co;2-g
- Irwin, N., Pathak, V., and Flatt, P. R. (2015). A Novel CCK-8/GLP-1 hybrid peptide exhibiting prominent insulinotropic, glucose-lowering, and satiety actions with significant therapeutic potential in high-fat-fed Mice. *Diabetes Metab. Res. Rev.* 64, 2996–3009. doi: 10.2337/db15-0220
- Kaczynska, K., and Szereda-Przestaszewska, M. (2015). Contribution of CCK1 receptors to cardiovascular and respiratory effects of cholecystokinin in anesthetized rats. *Neuropeptides* 54, 29–34. doi: 10.1016/j.npep.2015.08.006
- Kagebayashi, T., Kontani, N., Yamada, Y., Mizushige, T., Arai, T., Kino, K., et al. (2012). Novel CCK-dependent vasorelaxing dipeptide, Arg-Phe, decreases blood pressure and food intake in rodents. *Mol. Nutr. Food Res.* 56, 1456–1463. doi: 10.1002/mnfr.201200168
- Kato, I., Suzuki, Y., Akabane, A., Yonekura, H., Tanaka, O., Kondo, H., et al. (1994). Transgenic mice overexpressing human vasoactive intestinal peptide (VIP) gene in pancreatic beta cells. Evidence for improved glucose tolerance and enhanced insulin secretion by VIP and PHM-27 in vivo. *J. Biol. Chem.* 269, 21223–21228.
- Katout, M., Zhu, H., Rutsky, J., Shah, P., Brook, R. D., Zhong, J., et al. (2014). Effect of GLP-1 mimetics on blood pressure and relationship to weight loss and glycemia lowering: results of a systematic meta-analysis and meta-regression. *Am. J. Hypertens.* 27, 130–139. doi: 10.1093/ajh/hpt196
- Kirchgessner, A. L., and Gershon, M. D. (1989). Identification of vagal efferent fibers and putative target neurons in the enteric nervous system of the rat. *J. Comp. Neurol.* 285, 38–53. doi: 10.1002/cne.902850105
- Klok, M. D., Jakobsdottir, S., and Drent, M. L. (2007). The role of leptin and ghrelin in the regulation of food intake and body weight in humans: a review. *Obes. Rev.* 8, 21–34. doi: 10.1111/j.1467-789x.2006.00270.x
- Krantic, S. (2000). Peptides as regulators of the immune system: emphasis on somatostatin. *Peptides* 21, 1941–1964. doi: 10.1016/s0196-9781(00)00347-8
- Kreibig, S. D. (2010). Autonomic nervous system activity in emotion: a review. *Biol. Psychol.* 84, 394–421. doi: 10.1016/j.biopsycho.2010.03.010
- Lee, M. C., Schiffman, S. S., and Pappas, T. N. (1994). Role of neuropeptides in the regulation of feeding behavior: a review of cholecystokinin, bombesin, neuropeptide Y, and galanin. *Neurosci. Biobehav. Rev.* 18, 313–323. doi: 10.1016/0149-7634(94)90045-0
- Liddle, R. A. (2000). Regulation of cholecystokinin secretion in humans. *J. Gastroenterol.* 35, 181–187. doi: 10.1007/s005350050328
- Lovick, T. A. (2009). CCK as a modulator of cardiovascular function. *J. Chem. Neuroanat.* 38, 176–184. doi: 10.1016/j.jchemneu.2009.06.007
- Lustig, R. H., Rose, S. R., Burghen, G. A., Velasquez-Miery, P., Broome, D. C., Smith, K., et al. (1999). Hypothalamic obesity caused by cranial insult in children: altered glucose and insulin dynamics and reversal by a somatostatin agonist. *J. Pediatr.* 135(2 Pt 1), 162–168. doi: 10.1016/s0022-3476(99)70017-x
- Luyer, M. D., Greve, J. W. M., Hadfoune, M., Jacobs, J. A., Dejong, C. H., and Buurman, W. A. (2005). Nutritional stimulation of cholecystokinin receptors inhibits inflammation via the vagus nerve. *J. Exp. Med.* 202, 1023–1029. doi: 10.1084/jem.20042397

- Matson, C. A., and Ritter, R. C. (1999). Long-term CCK-leptin synergy suggests a role for CCK in the regulation of body weight. *Am. J. Physiol. Regul. Integr. Comp. Physiol.* 276, R1038–R1045. doi: 10.1152/ajpregu.1999.276.4.R1038
- Meier, J. J., Gethmann, A., Götz, O., Gallwitz, B., Holst, J. J., Schmidt, W. E., et al. (2006). Glucagon-like peptide 1 abolishes the postprandial rise in triglyceride concentrations and lowers levels of non-esterified fatty acids in humans. *Diabetologia* 49, 452–458. doi: 10.1007/s00125-005-0126-y
- Miyamoto, S., Shikata, K., Miyasaka, K., Okada, S., Sasaki, M., Kodera, R., et al. (2012). Cholecystokinin plays a novel protective role in diabetic kidney through anti-inflammatory actions on macrophage: anti-inflammatory effect of cholecystokinin. *Diabetes Metab. Res. Rev.* 61, 897–907. doi: 10.2337/db11-0402
- Murray, F., Bell, D., Kelso, E. J., Millar, B. C., and McDermott, B. J. (2001). Positive and negative contractile effects of somatostatin-14 on rat ventricular cardiomyocytes. *J. Cardiovasc. Pharmacol.* 37, 324–332. doi: 10.1097/00005344-200103000-00011
- Näslund, E., Barkeling, B., King, N., Gutniak, M., Blundell, J. E., Holst, J. J., et al. (1999). Energy intake and appetite are suppressed by glucagon-like peptide-1 (GLP-1) in obese men. *Int. J. Obes. Relat. Metab. Disord.* 23, 304–311. doi: 10.1038/sj.ijo.0800818
- Nauck, M. A., Kleine, N., Orskov, C., Holst, J. J., Willms, B., and Creutzfeldt, W. (1993). Normalization of fasting hyperglycaemia by exogenous glucagon-like peptide 1 (7-36 amide) in type 2 (non-insulin-dependent) diabetic patients. *Diabetologia* 36, 741–744. doi: 10.1007/bf00401145
- Neary, M. T., and Batterham, R. L. (2009). Gut hormones: implications for the treatment of obesity. *Pharmacol. Ther.* 124, 44–56. doi: 10.1016/j.pharmthera.2009.06.005
- Nishi, S., Seino, Y., Takemura, J., Ishida, H., Seno, M., Chiba, T., et al. (1985). Vagal regulation of GRP, gastric somatostatin, and gastrin secretion in vitro. *Am. J. Physiol.* 248(4 Pt 1), E425–E431.
- Okerson, T., and Chilton, R. J. (2012). The cardiovascular effects of GLP-1 receptor agonists. *Cardiovasc. Ther.* 30, e146–e155. doi: 10.1111/j.1755-5922.2010.00256.x
- Opie, L. H. (2007). Metabolic syndrome. *Circulation* 115, e32–e35.
- Ottesen, B., Pedersen, B., Nielsen, J., Dalgaard, D., Wagner, G., and Fahrenkrug, J. (1987). Vasoactive intestinal polypeptide (VIP) provokes vaginal lubrication in normal women. *Peptides* 8, 797–800. doi: 10.1016/0196-9781(87)90061-1
- Ottesen, B., Wagner, G., Virag, R., and Fahrenkrug, J. (1984). Penile erection: possible role for vasoactive intestinal polypeptide as a neurotransmitter. *Br. Med. J.* 288, 9–11. doi: 10.1136/bmj.288.6410.9
- Pi-Sunyer, X., Kissileff, H. R., Thornton, J., and Smith, G. P. (1982). C-terminal octapeptide of cholecystokinin decreases food intake in obese men. *Physiol. Behav.* 29, 627–630. doi: 10.1016/0031-9384(82)90230-x
- Plaza, A., Merino, B., Cano, V., Domínguez, G., Pérez-Castells, J., Fernández-Alfonso, M. S., et al. (2018). Cholecystokinin is involved in triglyceride fatty acid uptake by rat adipose tissue. *J. Endocrinol.* 236, 137–150. doi: 10.1530/JOE-17-0580
- Ponzani, P., Scardapane, M., Nicolucci, A., and Rossi, M. C. (2016). Effectiveness and safety of liraglutide after three years of treatment. *Minerva Endocrinol.* 41, 35–42.
- Pozo, D., Delgado, M., Martínez, C., Guerrero, J. M., Leceta, J., Gomariz, R. P., et al. (2000). Immunobiology of vasoactive intestinal peptide (VIP). *Immunol. Today* 21, 7–11. doi: 10.1016/S0167-5699(99)01525-x
- Qin, X., Shen, H., Liu, M., Yang, Q., Zheng, S., Sabo, M., et al. (2005). GLP-1 reduces intestinal lymph flow, triglyceride absorption, and apolipoprotein production in rats. *Am. J. Physiol. Gastrointest. Liver Physiol.* 288, G943–G949.
- Rehfeld, J. F. (2012). Beginnings: a reflection on the history of gastrointestinal endocrinology. *Regul. Peptides* 177(Suppl.), S1–S5. doi: 10.1016/j.regpep.2012.05.087
- Richter, G., Feddersen, O., Wagner, U., Barth, P., Göke, R., and Göke, B. (1993). GLP-1 stimulates secretion of macromolecules from airways and relaxes pulmonary artery. *Am. J. Physiol.* 265(4 Pt 1), L374–L381.
- Rocca, A. S., and Brubaker, P. L. (1999). Role of the vagus nerve in mediating proximal nutrient-induced glucagon-like peptide-1 secretion. *Endocrinology* 140, 1687–1694. doi: 10.1210/endo.140.4.6643
- Rosa, R. M., Silva, P., Stoff, J. S., and Epstein, F. H. (1985). Effect of vasoactive intestinal peptide on isolated perfused rat kidney. *Am. J. Physiol.* 249(5 Pt 1), E494–E497.
- Rosenthal, J., Escobar-Jimenez, F., and Raptis, S. (1977). Prevention by somatostatin of rise in blood pressure and plasma renin mediated by beta-receptor stimulation. *Clin. Endocrinol.* 6, 455–462. doi: 10.1111/j.1365-2265.1977.tb03329.x
- Samson, W. K., Zhang, J. V., Avsian-Kretschmer, O., Cui, K., Yosten, G. L. C., Klein, C., et al. (2008). Neuronostatin encoded by the somatostatin gene regulates neuronal, cardiovascular, and metabolic functions. *J. Biol. Chem.* 283, 31949–31959. doi: 10.1074/jbc.M804784200
- Sánchez-Fernández, C., González, M. C., Beart, P. M., Mercer, L. D., Ruiz-Gayo, M., and Fernández-Alfonso, M. S. (2004). A novel role for cholecystokinin: regulation of mesenteric vascular resistance. *Regul. Peptides* 121, 145–153. doi: 10.1016/j.regpep.2004.04.018
- Sandoval, D. (2008). CNS GLP-1 regulation of peripheral glucose homeostasis. *Physiol. Behav.* 94, 670–674. doi: 10.1016/j.physbeh.2008.04.018
- Sartor, D. M., and Verberne, A. J. M. (2002). Cholecystokinin selectively affects presympathetic vasomotor neurons and sympathetic vasomotor outflow. *Am. J. Physiol. Regul. Integr. Comp. Physiol.* 282, R1174–R1184.
- Sartor, D. M., and Verberne, A. J. M. (2006). The sympathoinhibitory effects of systemic cholecystokinin are dependent on neurons in the caudal ventrolateral medulla in the rat. *Am. J. Physiol. Regul. Integr. Comp. Physiol.* 291, R1390–R1398.
- Sawchenko, P. E. (1983). Central connections of the sensory and motor nuclei of the vagus nerve. *J. Auton. Nerv. Syst.* 9, 13–26. doi: 10.1016/0165-1838(83)90129-7
- Shaffer, M. M., and Moody, T. W. (1986). Autoradiographic visualization of CNS receptors for vasoactive intestinal peptide. *Peptides* 7, 283–288. doi: 10.1016/0196-9781(86)90226-3
- Shlik, J., Vasar, V., Aluoja, A., Kingisepp, P. H., Jagomägi, K., Vasar, E., et al. (1997). The effect of cholecystokinin tetrapeptide on respiratory resistance in healthy volunteers. *Biol. Psychiatry* 42, 206–212. doi: 10.1016/S0006-3223(96)00334-4
- Sjöstrand, N. O., Klinge, E., and Himberg, J. J. (1981). Effects of VIP and other putative neurotransmitters on smooth muscle effectors of penile erection. *Acta Physiol. Scand.* 113, 403–405. doi: 10.1111/j.1748-1716.1981.tb06914.x
- Stanisz, A. M., Befus, D., and Bienenstock, J. (1986). Differential effects of vasoactive intestinal peptide, substance P, and somatostatin on immunoglobulin synthesis and proliferations by lymphocytes from Peyer's patches, mesenteric lymph nodes, and spleen. *J. Immunol.* 136, 152–156.
- Taylor, A. W., Streilein, J. W., and Cousins, S. W. (1994). Immunoreactive vasoactive intestinal peptide contributes to the immunosuppressive activity of normal aqueous humor. *J. Immunol.* 153, 1080–1086.
- ten Bokum, A. M., Hofland, L. J., and van Hagen, P. M. (2000). Somatostatin and somatostatin receptors in the immune system: a review. *Eur. Cytokine Netw.* 11, 161–176.
- ter Horst, G. J., Luiten, P. G. M., and Kuipers, F. (1984). Descending pathways from hypothalamus to dorsal motor vagus and ambiguous nuclei in the rat. *J. Auton. Nerv. Syst.* 11, 59–75. doi: 10.1016/0165-1838(84)90008-0
- Tentolouris, N., Argyrakopoulou, G., and Katsilambros, N. (2008). Perturbed autonomic nervous system function in metabolic syndrome. *Neuromol. Med.* 10, 169–178. doi: 10.1007/s12017-008-8022-5
- Tentolouris, N., Liatis, S., and Katsilambros, N. (2006). Sympathetic system activity in obesity and metabolic syndrome. *Ann. N. Y. Acad. Sci.* 1083, 129–152. doi: 10.1196/annals.1367.010
- Toft-Nielsen, M. B., Madsbad, S., and Holst, J. J. (1999). Continuous subcutaneous infusion of glucagon-like peptide 1 lowers plasma glucose and reduces appetite in type 2 diabetic patients. *Diabetes Care* 22, 1137–1143. doi: 10.2337/diacare.22.7.1137
- Tunçel, N., Töre, F., Şahintürk, V., Ak, D., and Tunçel, M. (2000). Vasoactive intestinal peptide inhibits degranulation and changes granular content of mast cells: a potential therapeutic strategy in controlling septic shock. *Peptides* 21, 81–89. doi: 10.1016/S0196-9781(99)00177-1
- Vainio, L., Perjes, A., Rytty, N., Magga, J., Alakoski, T., Serpi, R., et al. (2012). Neuronostatin, a novel peptide encoded by somatostatin gene, regulates cardiac contractile function and cardiomyocyte survival. *J. Biol. Chem.* 287, 4572–4580. doi: 10.1074/jbc.M111.289215

- van der Kooy, D. (1984). Area postrema: site where cholecystokinin acts to decrease food intake. *Brain Res.* 295, 345–347. doi: 10.1016/0006-8993(84)90982-x
- Vergès, B. (2017). Effects of anti-somatostatin agents on glucose metabolism. *Diabetes Metab.* 43, 411–415. doi: 10.1016/j.diabet.2017.05.003
- Verrotti, A., Prezioso, G., Scattoni, R., and Chiarelli, F. (2014). Autonomic neuropathy in diabetes mellitus. *Front. Endocrinol.* 5:205. doi: 10.3389/fendo.2014.00205
- von Schrenck, T., Ahrens, M., de Weerth, A., Bobrowski, C., Wolf, G., Jonas, L., et al. (2000). CCKB/gastrin receptors mediate changes in sodium and potassium absorption in the isolated perfused rat kidney. *Kidney Int.* 58, 995–1003. doi: 10.1046/j.1523-1755.2000.00257.x
- Wahren, J. (1976). Influence of somatostatin on carbohydrate disposal and absorption in diabetes mellitus. *Lancet* 2, 1213–1216. doi: 10.1016/s0140-6736(76)91142-9
- Wang, B., Zhong, J., Lin, H., Zhao, Z., Yan, Z., He, H., et al. (2013). Blood pressure-lowering effects of GLP-1 receptor agonists exenatide and liraglutide: a meta-analysis of clinical trials. *Diabetes Obes. Metab.* 15, 737–749. doi: 10.1111/dom.12085
- Wang, T.-L., Huang, Y.-H., and Chang, H. (2005). Somatostatin analogue mimics acute ischemic preconditioning in a rat model of myocardial infarction. *J. Cardiovasc. Pharmacol.* 45, 327–332. doi: 10.1097/01.fjc.0000156823.35210.21
- Yamamoto, H., Kishi, T., Lee, C. E., Choi, B. J., Fang, H., Hollenberg, A. N., et al. (2003). Glucagon-like peptide-1-responsive catecholamine neurons in the area postrema link peripheral glucagon-like peptide-1 with central autonomic control sites. *J. Neurosci.* 23, 2939–2946. doi: 10.1523/jneurosci.23-07-02939.2003
- Yamamoto, Y., Runold, M., Prabhakar, N., Pantaleo, T., and Lagercrantz, H. (1988). Somatostatin in the control of respiration. *Acta Physiol. Scand.* 134, 529–533. doi: 10.1111/j.1365-201x.1988.tb10631.x
- Yoshikawa, T., Port, J. D., Asano, K., Chidiak, P., Bouvier, M., Dutcher, D., et al. (1996). Cardiac adrenergic receptor effects of carvedilol. *Eur. Heart J.* 17(Suppl. B), 8–16. doi: 10.1093/eurheartj/17.suppl_b.8
- Yuan, P.-Q., Kimura, H., Million, M., Bellier, J.-P., Wang, L., Ohning, G. V., et al. (2005). Central vagal stimulation activates enteric cholinergic neurons in the stomach and VIP neurons in the duodenum in conscious rats. *Peptides* 26, 653–664. doi: 10.1016/j.peptides.2004.11.015
- Zheng, H., Patterson, L. M., and Berthoud, H.-R. (2005). Orexin-A projections to the caudal medulla and orexin-induced c-Fos expression, food intake, and autonomic function. *J. Comp. Neurol.* 485, 127–142. doi: 10.1002/cne.20515

Conflict of Interest Statement: The authors declare that the research was conducted in the absence of any commercial or financial relationships that could be construed as a potential conflict of interest.

Copyright © 2019 Gorky and Schwaber. This is an open-access article distributed under the terms of the Creative Commons Attribution License (CC BY). The use, distribution or reproduction in other forums is permitted, provided the original author(s) and the copyright owner(s) are credited and that the original publication in this journal is cited, in accordance with accepted academic practice. No use, distribution or reproduction is permitted which does not comply with these terms.



Neurotrophic, Gene Regulation, and Cognitive Functions of Carboxypeptidase E-Neurotrophic Factor- α 1 and Its Variants

Lan Xiao, Xuyu Yang and Y. Peng Loh*

Section on Cellular Neurobiology, Eunice Kennedy Shriver National Institute of Child Health and Human Development, National Institutes of Health, Bethesda, MD, United States

OPEN ACCESS

Edited by:

Limei Zhang,
National Autonomous University
of Mexico, Mexico

Reviewed by:

Illana Gozes,
Tel Aviv University, Israel
Maite Montero-Hadjadje,
Université de Rouen, France

*Correspondence:

Y. Peng Loh
lohpm@mail.nih.gov

Specialty section:

This article was submitted to
Neuroendocrine Science,
a section of the journal
Frontiers in Neuroscience

Received: 25 January 2019

Accepted: 01 March 2019

Published: 19 March 2019

Citation:

Xiao L, Yang X and Loh YP (2019)
Neurotrophic, Gene Regulation,
and Cognitive Functions
of Carboxypeptidase E-Neurotrophic
Factor- α 1 and Its Variants.
Front. Neurosci. 13:243.
doi: 10.3389/fnins.2019.00243

Carboxypeptidase E, also known as neurotrophic factor- α 1 (CPE-NF α 1), was first discovered as an exopeptidase and is known to work by cleaving C-terminal basic amino acids from prohormone intermediates to produce mature peptide hormones and neuropeptides in the endocrine and central nervous systems, respectively. CPE-NF α 1 also plays a critical role in prohormone sorting and secretory vesicle transportation. Recently, emerging studies have indicated that CPE-NF α 1 exerts multiple non-enzymatic physiological roles in maintaining normal central nervous system function and in neurodevelopment. This includes potent neuroprotective and anti-depressant activities, as well as stem cell differentiation functions. In addition, N-terminal truncated variants of CPE-NF α 1 have been identified to regulate expression of important neurodevelopmental genes. This mini-review summarizes recent advances in understanding the mechanisms underlying CPE-NF α 1's function in neuroprotection during stress and aspects of neurodevelopment.

Keywords: neuroprotection, neurotrophic factor, hippocampus, neurodevelopment, FGF2, BCL2, WNT/beta-catenin, stress

INTRODUCTION

CPE-NF α 1, a member of the M14 metallocarboxypeptidase family was discovered in 1982 in bovine adrenal medulla and named as enkephalin convertase due to its enzymatic activity in processing enkephalin precursor into its mature form (Fricker and Snyder, 1983). Since then, CPE-NF α 1 has been shown to cleave C-terminal basic amino acids from the intermediates generated by proprotein convertases' action on prohormones, thereby producing bioactive hormones and neuropeptides (Hook et al., 1982; Fricker and Snyder, 1983; Fricker, 1988). In the central nervous system, CPE-NF α 1 also functions as a regulated secretory pathway sorting receptor, secretory vesicle transport regulator and mediates synaptic vesicle localization to the active zone for release (Cawley et al., 2012; Ji et al., 2017). Recent studies have indicated that CPE-NF α 1 is a new neurotrophic factor functioning extracellularly, independent of its enzymatic activity, in the adult and embryonic central nervous system (Ji et al., 2017). Human mutations of CPE-NF α 1 have been associated with obesity, diabetes, infertility, learning disabilities, and Alzheimer's disease (AD) (Alsters et al., 2015; Cheng et al., 2016a). This review presents recent advances concerning the molecular structure,

distribution, and multifunctional roles of CPE-NF α 1 and its variants in the central nervous system in health and disease.

MOLECULAR STRUCTURE AND BIOSYNTHESIS OF CPE-NF α 1 AND ITS VARIANTS

In mammals, WT-CPE-NF α 1 gene consists of nine exons and encodes a 476 amino acid polypeptide (Jung et al., 1991; Cawley et al., 2012). Two CPE-NF α 1 mRNA transcripts, 2.4 and 1.7 kb in size, respectively, have been identified by Northern Blot analysis and DNA sequencing from human cancer cells. The 2.4 kb CPE-NF α 1 transcript encodes a 53 kD WT-CPE/NF α 1 and the 1.7 kb transcript encodes an N-terminal truncated 40 kD CPE-NF α 1 due to the intra-exonic splicing in exon1 (Yang et al., 2017). Both transcripts have also been detected in Northern blot of human hippocampal mRNA extract (Yang, our unpublished data). Three CPE-NF α 1 transcripts, a 2.3 kb WT transcript and two CPE-NF α 1 mRNA variants, 1.9 and 1.73 kb in size (**Figure 1**) have been identified in mouse embryonic brain. Unlike in human cancer cells, the two mouse CPE-NF α 1 mRNA variants are generated by using alternative transcription start sites, each of them encodes an N-terminal truncated CPE-NF α 1 with a molecular weight of 47 and 40 kD, respectively (Yang et al., 2017; Xiao et al., 2018).

The CPE-NF α 1 protein consists of a signal peptide, a catalytic domain, and a C-terminal domain. A 3-D structure model of CPE-NF α 1 shows a zinc binding site in the enzymatic domain, a prohormone sorting signal binding site, an amphipathic α -helical transmembrane domain, and a cytoplasmic tail that interacts with microtubule proteins for vesicle transport (Cawley et al., 2012). Mature CPE-NF α 1 has 476-amino acids. It is synthesized as preproCPE-NF α 1 that has a 25-amino acid signal peptide located at the N-terminal that directs proCPE-NF α 1 to the cisternae of the rough endoplasmic reticulum (ER) where it is removed (**Figure 2**). The proCPE-NF α 1 is then transported to the granules of the regulated secretory pathway through the Golgi complex where 17-amino acids comprising the pro-region are removed (Song and Fricker, 1995). Further processing at Arg455-Lysine 456 (Fricker and Devi, 1993) in the secretory granules yields a soluble form of CPE-NF α 1 (50 kDa), while the 53 kD unprocessed form is associated with the granule membrane, with some molecules assuming a transmembrane orientation (Cawley et al., 2012).

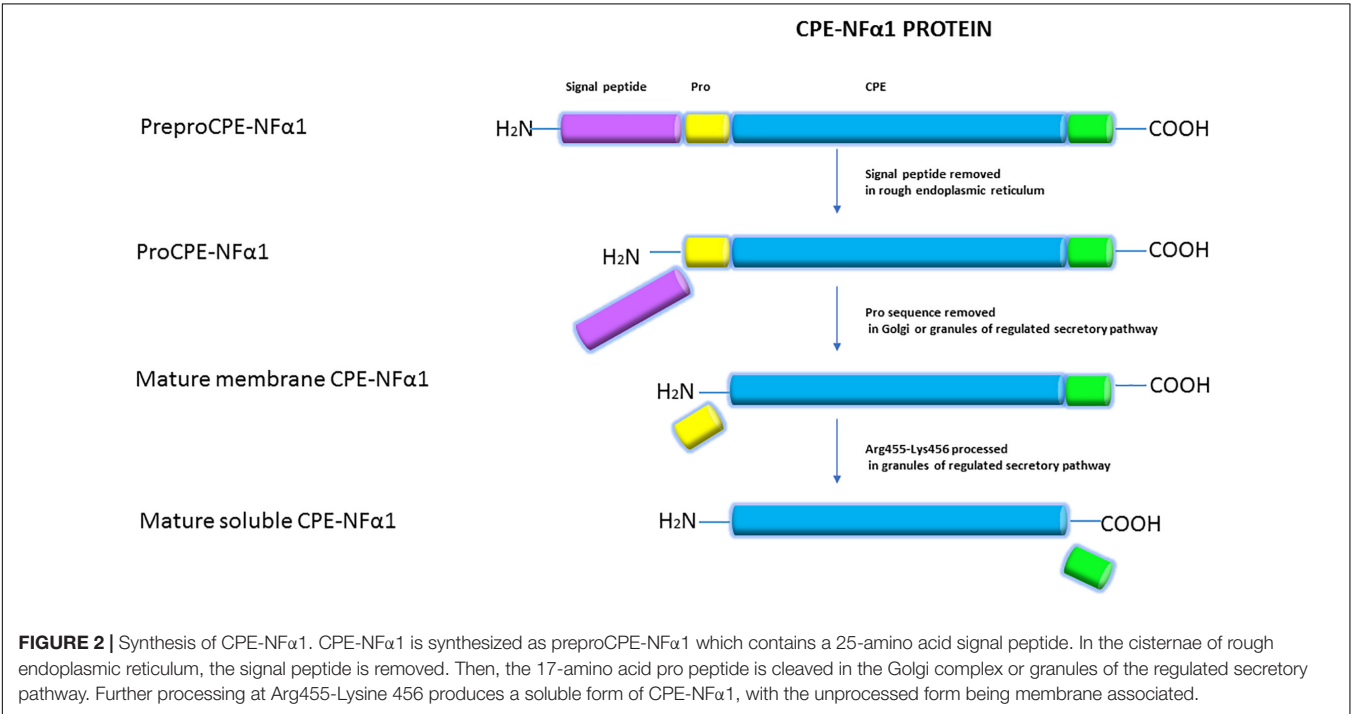
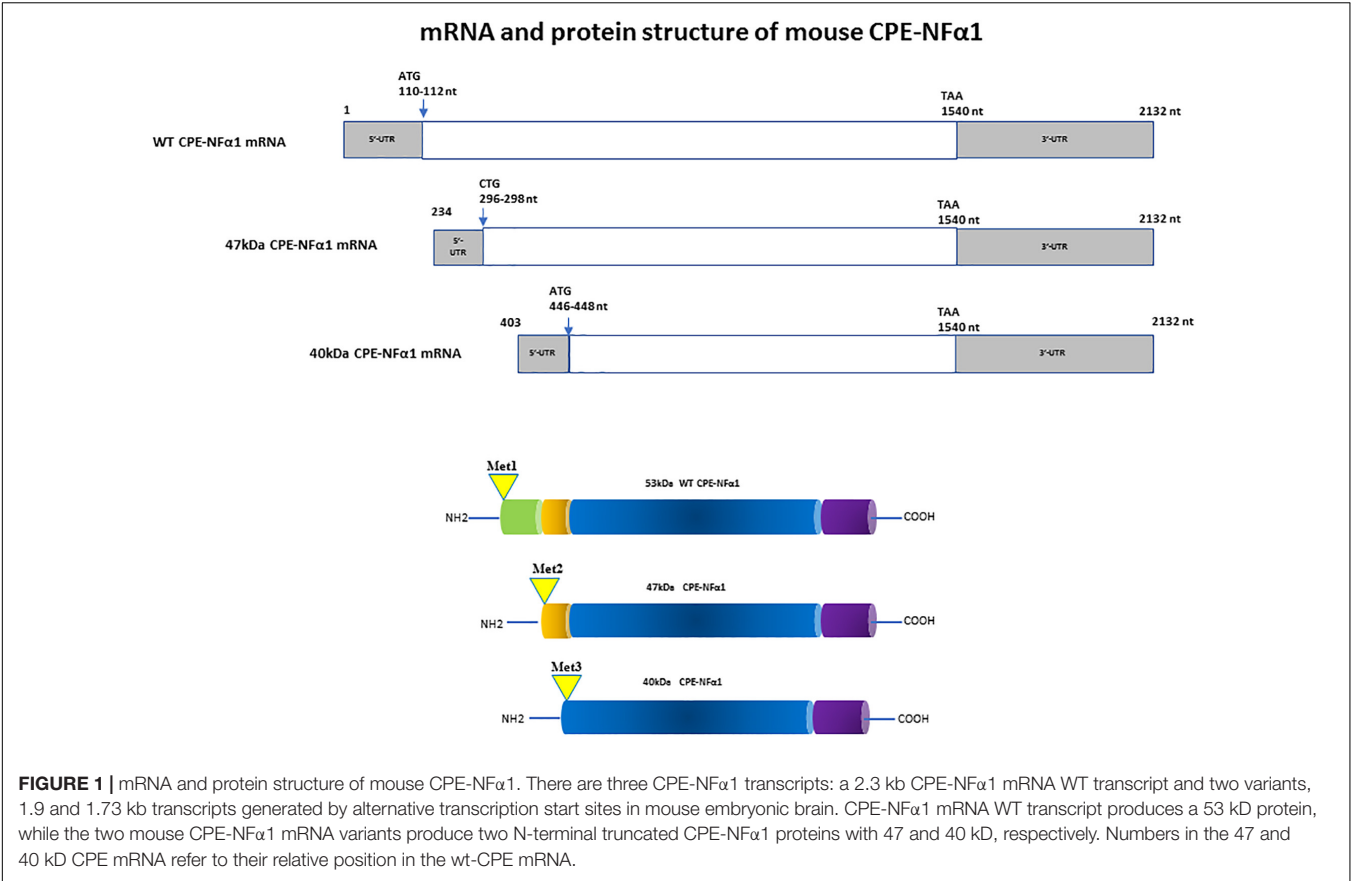
DISTRIBUTION OF CPE-NF α 1 AND CPE-NF α 1- Δ N

In mammals, CPE-NF α 1 is generally distributed in the endocrine and nervous system, with the highest concentration in the brain (Strittmatter et al., 1984). Immunohistochemical studies showed CPE-NF α 1 is located in neuropeptide-rich regions of the brain and endocrine system, for example, in the hypothalamus, pituitary, adrenal medulla, paraventricular nucleus, hippocampus, and amygdala (Hook et al., 1985; Lynch et al., 1990). Consistently, CPE-NF α 1 mRNA is also found

to be highly expressed in these brain regions (Birch et al., 1990; MacCumber et al., 1990; Zheng et al., 1994). The retina and olfactory bulb are also highly enriched in CPE-NF α 1 (Zhu et al., 2005). In the retina, CPE-NF α 1 is localized to the photoreceptors and is involved in synaptic transmission to the inner retina (Zhu et al., 2005). At the cellular level, CPE-NF α 1 is mainly distributed in the trans-Golgi network and dense core secretory granules of endocrine cells and peptidergic neurons (Cawley et al., 2012). CPE-NF α 1 exists as two active forms, the soluble and membrane form (**Figure 2**). The soluble form of CPE-NF α 1 functions as an enzyme that cleaves C-terminal basic residues such as arginine and lysine from intermediates derived from neuropeptide precursors or prohormones to produce biologically active peptides or hormones. The membrane form of CPE-NF α 1 acts as a sorting receptor at the trans-Golgi network to direct prohormones to the regulated secretory pathway granules, and mediates secretory granule movement (Cawley et al., 2012). In contrast, the N-terminal truncated (CPE-NF α 1- Δ N) forms which lack a signal peptide do not enter the secretory pathway. The 40 kD form of CPE-NF α 1- Δ N has been shown to be localized in the cytoplasm and to be able to translocate into the nucleus where it exerts its effects on gene regulation (Qin et al., 2014) (see summary in **Table 1**).

MICE AND HUMANS WITH CPE-NF α 1 MUTATION EXHIBIT NEUROLOGICAL DEFICITS

CPE-NF α 1 knockout (KO) mice, in addition to exhibiting endocrinological deficits such as obesity, diabetes, and infertility due to lack of enzyme activity, display a variety of behavioral abnormalities as evidenced by deficits in learning and memory in Morris water maze, object preference, and social transmission of food preference tests (Woronowicz et al., 2008). They also display depressive-like behavior (Cheng et al., 2015, 2016a). CPE^{fat/fat} mice which have a Ser202Pro mutation and lack CPE-NF α 1 have a similar phenotype to the knockout mouse and exhibit anxiety-like and depression-like behaviors (Rodríguez et al., 2013). Interestingly, a human with a null mutation also demonstrated similar symptoms, such as obesity, diabetes, hypogonadotropic hypogonadism, and impaired intellectual ability (Alsters et al., 2015). In another study, a human mutation of CPE-NF α 1 with three adenosines insertions was identified, this mutation was named QQ-CPE-NF α 1. Mice bearing this mutation showed neurodegeneration in the hippocampus and prefrontal cortex, deficits in neurogenesis at the dentate gyrus and hyperphosphorylation of tau (Cheng et al., 2016a). Another human CPE-NF α 1 mutation, T980C, which introduces a W235R change in the catalytic domain of CPE-NF α 1 caused a loss of enzyme activity, neurotoxic accumulation in the ER, resulting in ER stress and cell death when overexpressed in Neuro 2A cells. This novel single nucleotide polymorphism in the CPE-NF α 1 gene found in 12.5% of the AGI ASP population may confer neurological disorders in humans (Cong et al., 2017). These observations suggest that CPE-NF α 1 plays an important



role in neurological function, and mutation of this gene can lead to cognitive and neurodegenerative disorders.

CPE-NFα1 IN NEURODEGENERATIVE DISORDERS AND STRESS

In the cerebral cortex of AD patients, an abnormal accumulation of CPE-NF α1 was detected in dystrophic neurites surrounding amyloid plaques (Pla et al., 2013). In an AD animal model of APPswe/PS1dE9 mice, similar pattern of changes were also found. Amyloid plaques were surrounded by aberrant accumulation of CPE-NFα1 and Secretogranin III (SgIII) (Pla et al., 2013). Peptidase activity analysis of the postmortem brain from AD patients showed that soluble enzymatic activity of CPE-NFα1 was significantly increased in the Brodmann Area 21 compared with control (Weber et al., 1992). In a Cathepsins B and L double knockout mouse model that demonstrated early-onset neurodegeneration and reduction in brain size, the expression of CPE-NFα1 was upregulated by 10-fold (Stahl et al., 2007). In experimental autoimmune encephalomyelitis (EAE) animal model, CPE-NFα1 has been mapped as a EAE-linked trait loci which is associated to the severity of the disease and shown to be downregulated (Ibrahim et al., 2001; Mazon Pelaez et al., 2005). These observations suggest that CPE-NFα1 is associated to the pathophysiology of neurodegenerative diseases.

Studies have shown that CPE-NFα1 expression is up-regulated after different types of stress. CPE-NFα1 mRNA and protein were both increased in the rat hippocampal CA1, CA3, and cortex regions 15 min after transient global ischemia followed by 8 h reperfusion (Jin et al., 2001). An accumulation of CPE-NFα1 precursor was found in mouse cortex after focal cerebral ischemia *in vivo* and in ischemic cortical neurons *in vitro*.

Vice versa, mice lacking CPE-NFα1 were more vulnerable to focal cerebral ischemia (Zhou et al., 2004). Stress such as cat odor upregulated CPE-NFα1 gene expression in rat amygdala (Koks et al., 2004). Mild chronic restraint stress for 7 days up-regulated CPE-NF α1 expression in mouse hippocampal CA3 region (Murthy et al., 2013). Reduced levels of CPE-NFα1 were found in the offspring of pregnant ewes that experienced aversive interaction with human handling, along with abnormal corticolimbic dendritic spine morphology (Coulon et al., 2013). Primary cultured hippocampal neurons derived from CPE-NFα1-KO mice tend to die more rapidly than that from wild type (WT) mice (Cheng et al., 2013). Low-potassium-induced apoptosis in cultured primary cerebellar granule neurons from CPE-NFα1^{+/-} mice are much higher than that from CPE-NFα1^{+/+} mice (Koshimizu et al., 2009). Overexpression of CPE-NFα1 in rat primary hippocampal neurons prevented hydrogen peroxide-induced neurotoxicity (Woronowicz et al., 2008). All these studies indicate that stress modulates CPE-NFα1 expression in the central nervous system (CNS).

CPE-NFα1 AS A NEUROTROPHIC FACTOR IN NEUROPROTECTION AND ANTI-DEPRESSION

CPE-NFα1 plays multiple intracellular roles in the CNS independent of its enzymatic activity. It functions as a regulated secretory pathway sorting receptor for proneuropeptides (Cool et al., 1997) and proBDNF (Lou et al., 2005), mediates anterograde transport of neuropeptide and BDNF vesicles to the plasma membrane via cytoplasmic tail interaction with dynactin/dynein (Park et al., 2008), and localizes synaptic vesicles to the actin-rich pre-active zone in hypothalamic neurons through actin binding protein γ-adducin (Lou et al., 2010). While the mechanisms underlying these cell biological actions of CPE-NFα1 are well understood, those governing the neuroprotective effects of CPE-NFα1 during stress are just emerging. In 2013, a study showed that CPE-NFα1 secreted from hippocampal neurons, acts as a neuroprotective factor extracellularly, independent of its enzymatic activity (Cheng et al., 2013). Secreted rat WT CPE-NFα1 and CPE-NFα1-E300Q (mutant form with no enzymatic activity) (Qian et al., 1999) in medium from transduced cultured primary rat hippocampal neurons protected them from cell death induced by H₂O₂-mediated oxidative stress and glutamate excitotoxicity. Results from experiments with recombinant WT CPE-NFα1 or CPE-NFα1-E342Q (mouse homolog of E300Q) demonstrated similar effects. In addition, hippocampal neurons from CPE-NFα1-KO mice at embryonic day 17 (E17) in culture exhibited higher death rate than WT E17 neurons, and this was reversed by treatment with recombinant WT CPE-NFα1 (Cheng et al., 2013). Studies on the mechanism underlying the neuroprotective action of CPE-NFα1 using rat primary hippocampal neurons in culture revealed that when these cells were stressed with H₂O₂, it activated the ERK and AKT signaling pathways, presumably by binding to a cognate receptor, which then up-regulated expression of Bcl2, a pro-survival mitochondrial protein, and down-regulated

TABLE 1 | Comparison of CPE-NFα1 WT and CPE-NFα1-ΔN.

	CPE-NFα1 WT	CPE-NFα1-ΔN
Biosynthesis	First transcription start site	Alternative transcription start sites
Intracellular location	Regulated secretory vesicles	Cytoplasm and nucleus
Distribution	Endocrine and CNS. Embryonic and adult brain	Embryonic, not adult brain in mouse
Soluble and membrane forms	Soluble and membrane associated	Soluble
Extracellular secretion	Secreted from vesicles to extracellular space	Not secreted
Signal peptide	Yes	No
Structure	–	Lacking N-terminal
Enzymatic activity	Yes	Weak enzymatic activity
Intracellular sorting receptor to regulatory secreted pathway	Yes	No
Facilitates vesicle trafficking via cytoplasmic tail	Yes	No

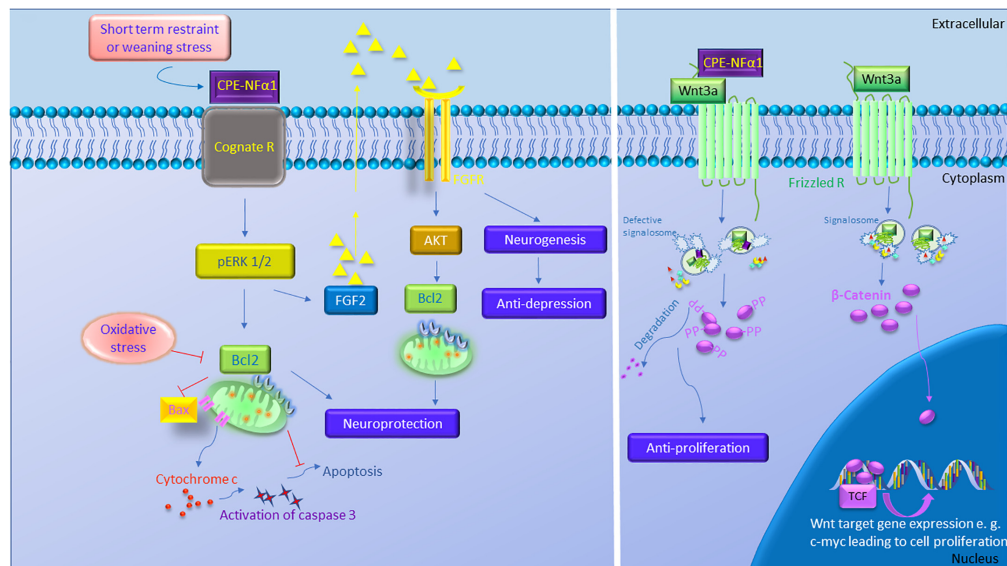


FIGURE 3 | The multiple functions of CPE-NF α 1 in the central nervous system (CNS). CPE-NF α 1 plays multiple functions in the CNS independent of its enzymatic activity. Short term restraint or weaning stress increases CPE-NF α 1 which binds to a cognate receptor and upregulates ERK1/2 and Bcl2, and decreases Bax and cytochrome c-induced activation of caspase 3 and apoptosis. CPE-NF α 1 also increases FGF2 that activates AKT and Bcl2 signaling and increases hippocampal neurogenesis and produces antidepressant-like effect. CPE-NF α 1 can also bind to Frizzled receptor – Wnt3a complex, enters the endosome that contains Wnt signaling factors and subsequently impairs the formation of signalosome. This results in β -catenin being degraded, rather than translocation into the nucleus and binds to T-cell factor transcription factor (TCF) to activate expression of Wnt target genes. Signalosome, Wnt, Fz, APC, GSK-3 β , Axin.

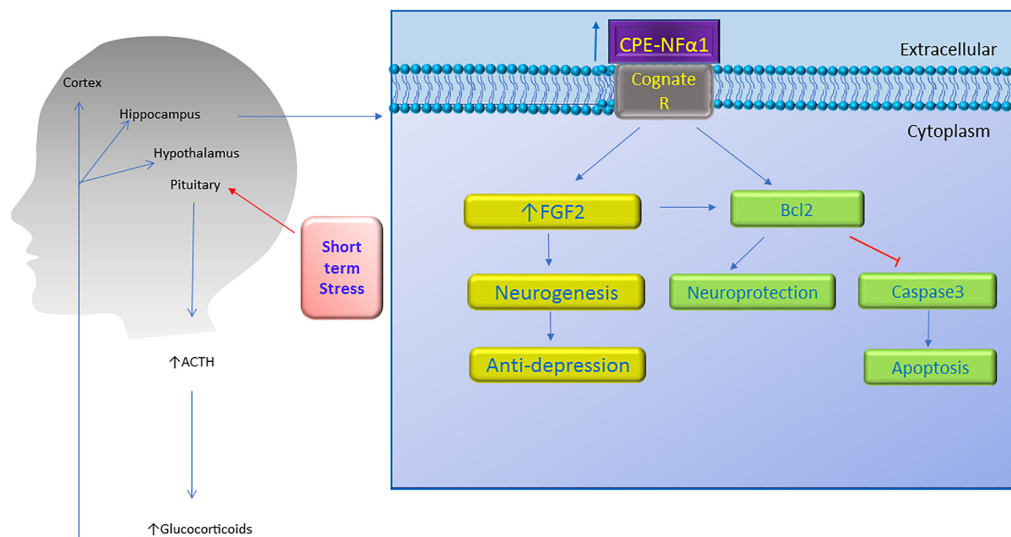


FIGURE 4 | Neuroprotective effect of CPE-NF α 1. Short term stress activates the hypothalamic-pituitary-adrenal axis which then increases ACTH and glucocorticoid secretion. The glucocorticoids upregulate CPE-NF α 1 expression via glucocorticoid regulatory elements (GRE) on the promoter. CPE-NF α 1 is secreted and possibly activates its cognate receptor which then produces antidepressant-like effects via increasing FGF2 expression and neurogenesis in the hippocampus. Additionally, CPE-NF α 1 protects against neurodegeneration through upregulating Bcl2, a mitochondrial pro-survival protein, by inhibiting caspase 3-mediated apoptosis.

expression of Caspase 3 to mediate neuroprotection (Cheng et al., 2013) (see Figure 3).

In an *in vivo* mouse model, complete degeneration of hippocampal CA3 region was observed in CPE-NF α 1-KO mice at 4-weeks of age after weaning stress which included maternal separation, ear tagging, and tail snipping at 3 weeks

of age (Woronowicz et al., 2008). CPE-NF α 1-KO mice that were not subjected to the weaning process at 3 weeks of age showed no degeneration of the CA3 region examined at week 4, indicating that this neurodegeneration was not due to a neurodevelopmental defect. Treatment with oral carbamazepine at 50 mg/kg daily for 2 weeks beginning at 2 weeks of age

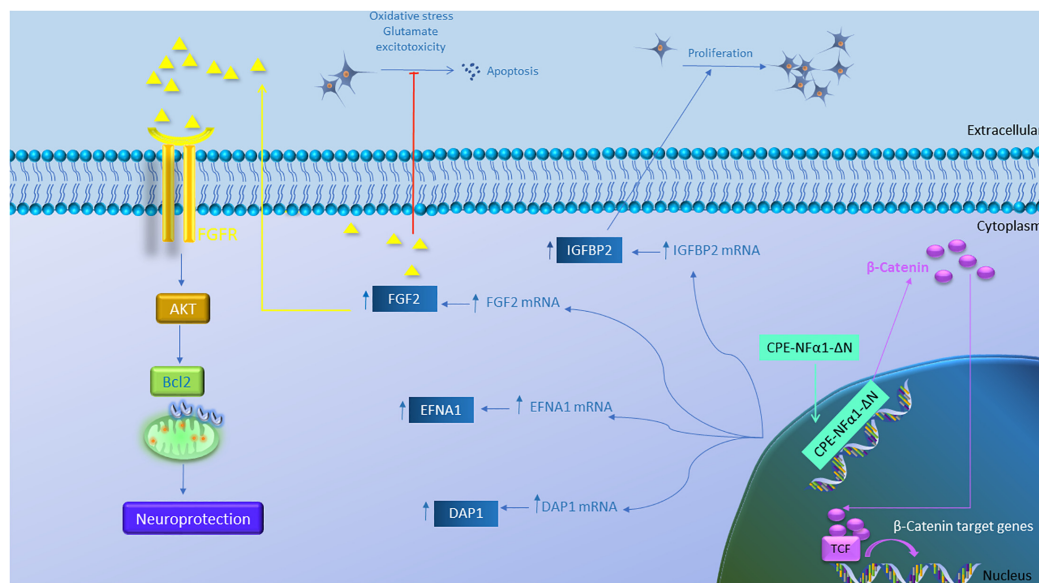


FIGURE 5 | Gene regulation function of CPE-NF α 1- Δ N in mouse embryonic neurons. CPE-NF α 1- Δ N increases expression of FGF2, IGFBP2, EFNA1, and DAP1 in mouse embryonic cortical and hippocampal neurons. IGFBP2 promotes neuronal proliferation while FGF2 inhibits oxidative stress or glutamate-induced excitotoxicity. FGF2 binds its receptor and induces neuroprotective effects via activating the AKT and Bcl2 signaling cascade. CPE-NF α 1- Δ N expressed in hippocampal neurons translocates into the nucleus and upregulates β -catenin expression. β -catenin then enters the nucleus and binds to T-cell factor (TCF) transcription factor to promote expression of Wnt target genes.

with the weaning process at 3 weeks of age, revealed no degeneration of the CA3 region when examined at 4 weeks of age (Woronowicz et al., 2012). These observations suggested that the CA3 pyramidal neurons underwent apoptosis due to glutamate excitotoxicity during the social and physical stress following the weaning protocol. In contrast, WT-mice, did not show any degeneration of the CA3 region after weaning stress. In another mouse model, adult CPE^{fat/fat} mice lacking CPE-NF α 1, also showed degeneration of the CA3 region (Zhou, personal communication). These findings together with the *in vitro* studies (Cheng et al., 2013) support the hypothesis that CPE-NF α 1 acts as a neurotrophic factor to protect the pyramidal neurons in the CA3 region in the hippocampus from stress-induced degeneration. Since BDNF is expressed in CPE-NF α 1-KO mice (Xiao et al., 2017), yet they showed neurodegeneration after weaning, indicates that BDNF could not protect the CA3 neurons in lieu of CPE-NF α 1. Further demonstration that CPE-NF α 1 is a neuroprotective factor *in vivo* during stress came from studies showing that chronic restraint stress of mice for 1 h/day for 7 days resulted in an increase in CPE-NF α 1 mRNA and protein expression in the hippocampus, with no evidence of neurodegeneration despite increased circulating corticosterone levels under this stress paradigm (Murthy et al., 2013). This up-regulation in expression of CPE-NF α 1 concurs with *in vitro* evidence showing that the CPE-NF α 1 promoter has a glucocorticoid binding domain and that dexamethasone up-regulated the expression of CPE-NF α 1 (Murthy et al., 2013). These mice also showed an increase in phosphorylation of Akt and Bcl2 expression; however, Bax, a pro-apoptotic mitochondria protein was decreased in the hippocampus (Murthy et al., 2013).

In contrast, CPE-NF α 1-KO mice subjected to the same stress paradigm showed no change in Akt phosphorylation, a decrease in expression of Bcl2 protein and an increase in Bax protein in the hippocampus compared to WT mice (Murthy et al., 2013). *In vitro* and *in vivo* evidence taken together indicate that during emotional and physical stress, secretion of glucocorticoid increases CPE-NF α 1 expression at the transcriptional and translational level in the hippocampus which in turn leads to neuroprotection of the CA1-3 neurons by acting extracellularly as a trophic factor to activate Erk or Akt signaling and increase Bcl2 pro-survival protein expression (see Figures 3, 4). CPE-NF α 1 also up-regulates the expression of FGF2 (Cheng et al., 2015), which has been shown to mediate protection against amyloid beta- or glutamate-induced neurotoxicity in hippocampal or cortical neurons via the Akt-Bcl2 signaling pathway (Qin et al., 2014; Cheng et al., 2016b; Figures 3, 5).

Behavioral analysis revealed that the CPE-NF α 1-KO and the Cpe^{fat/fat} mice exhibited depressive-like behavior as evidenced by increased immobility time in the forced-swimming test (Rodriguez et al., 2013; Cheng et al., 2015). CPE-NF α 1-KO mice showed decreased levels of FGF2 (Cheng et al., 2015), a protein demonstrated to be decreased in post mortem brains of patients with major depressive disorder (Evans et al., 2004). In addition, after long-term chronic restraint stress, mice showed depressive-like behavior, and reduced CPE-NF α 1, FGF2 and doublecortin, a marker for neuroblasts in their hippocampus. Interestingly, injection of 5 ng/g recombinant FGF2 into CPE-NF α 1-KO mouse for 30 consecutive days completely reversed the decreased number of doublecortin positive neurons in the subgranular zone of hippocampus and depressive-like behaviors as evidenced by

decreased immobility time in the forced-swim test (Cheng et al., 2015). *In vitro* studies showed that incubation of rat cultured hippocampal neurons with CPE-NF α 1 enhanced FGF2 mRNA and protein expression which was inhibited by the Sp1 inhibitor mithramycin A, a transcription inhibitor actinomycin, and ERK inhibitor U0126, suggesting that CPE-NF α 1 can upregulate FGF2 via ERK-Sp1 signaling cascade (Cheng et al., 2015). Thus, CPE-NF α 1 may act as an anti-depressant through up-regulating FGF2 expression in the hippocampus.

ROLE OF CPE-NF α 1 AND CPE-NF α 1- Δ N VARIANTS IN NEURODEVELOPMENT

In mice and rats, CPE-NF α 1 mRNA is expressed during embryogenesis as early as E5.5 mainly in the developing nervous system (Zheng et al., 1994; Selvaraj et al., 2017). In mice, the expression of CPE-NF α 1-WT and the two CPE-NF α 1- Δ N transcripts were detected in E8.5 embryonic brain and their expression peaked at embryonic day (E)10.5, then decreased from E12.5 to E16.5, and increased again at postnatal day 1 (P1). Interestingly, none of the CPE-NF α 1- Δ N mRNAs were found in adult mouse hippocampus or other organs such as liver, heart or lung, suggesting their critical role during embryonic neurodevelopment (Xiao et al., 2018). Studies of dendritic arborization in pyramidal layer V of cerebral cortex and hippocampal CA1 region in 14-week-old CPE-NF α 1-KO mice revealed abnormal dendritic pruning and increased number of non-functional D-type spines (Woronowicz et al., 2010), suggesting a role of CPE-NF α 1 in modeling the cytoarchitecture of the brain during development. Indeed, CPE-NF α 1 has been shown to regulate NGF-induced neurite outgrowth via interacting with Wnt-3a and Wnt-5a in PC12 cells and mouse primary cortical neurons (Selvaraj et al., 2015). CPE-NF α 1 is highly expressed in neural stem cells (Lee et al., 2012) and has been shown to inhibit embryonic neural stem cell proliferation by downregulating Wnt signaling pathway and β -catenin (Selvaraj et al., 2017). Studies have revealed that CPE-NF α 1 forms a complex with Wnt3a ligand and Frizzled receptor to inhibit the Wnt3a signaling cascade (Figure 3; Skalka et al., 2013). Moreover, exogenous application of CPE-NF α 1 and a non-enzymatic form of CPE-NF α 1(E300Q) induced differentiation of E14.5 cortical neural stem cells into astrocytes via activating the ERK1/2-Sox9 signaling pathway to enhance glial fibrillary acidic protein (GFAP) expression (Selvaraj et al., 2017). This corroborates the 49% decrease in astrocyte numbers observed in the neocortex of mouse neonates *in vivo* at postnatal day 1 (P1). In another study, electroporation of CPE-NF α 1 shRNA into E14.5 mouse embryos significantly decreased migration of neurons to cortex plate at E17.5, possibly due to the failure of transition from multipolar neurons into a bipolar morphology in the intermediate zone (Liang et al., 2018). Neuronal migration seems to depend on the function of the CPE-NF α 1 cytoplasmic tail which can interact with dynactin, an adaptor protein that interacts with microtubules. Furthermore, this study also showed that CPE-NF α 1 regulates dendrite morphology *in vivo* and in rat primary cultured hippocampal neurons (Liang et al., 2018).

While CPE-NF α 1 acts extracellularly as an embryonic stem cell differentiation and anti-proliferation factor, studies have indicated that CPE-NF α 1- Δ N could serve as a master regulator of genes involved in neurodevelopment (Figure 5 and Table 2). CPE-NF α 1- Δ N (40 kD variant), but not CPE-NF α 1 (Xiao, our unpublished data) was found to significantly up-regulate expression of four genes, fibroblast growth factor 2 (FGF2) (Qin et al., 2014), insulin-like growth factor binding protein2 (IGFBP2), death associated protein (DAP1), and EphrinA1 in HT22, a hippocampal cell line and in primary mouse cortical neurons (Xiao et al., 2018). These three genes are known to mediate neuronal proliferation, cell death and neuronal migration, respectively (Murphy et al., 1990; Deiss et al., 1995; Feinstein et al., 1995; Levy-Strumpf and Kimchi, 1998; Martinez et al., 2004; Martinez and Soriano, 2005; Russo et al., 2005; Zechel et al., 2010). Overexpressing of CPE-NF α 1- Δ N in HT22 cells promoted proliferation, but was inhibited by IGFBP2 siRNA, suggesting CPE-NF α 1- Δ N regulates embryonic neuronal proliferation through increasing IGFBP2. In addition, CPE-NF α 1- Δ N-induced FGF2 expression has a neuroprotective role against glutamate and H₂O₂ neurotoxicity in rat embryonic cortical neurons (Qin et al., 2014). Since FGF2 is also known to play a role in neuronal proliferation and neurogenesis in the developing mouse cortex, CPE-NF α 1- Δ N may also regulate these events in the embryonic brain (Raballo et al., 2000). Moreover, CPE-NF α 1- Δ N has been shown to up-regulate the expression of β -catenin in the Wnt pathway in HEK-293 cells (Skalka et al., 2013) and osteosarcoma cell lines, which promoted migration of these cells (Fan et al., 2018). We have shown that neuroprotection by CPE-NF α 1- Δ N against glutamate excitotoxicity may also involve β -catenin and Wnt pathway. Glutamate treatment resulted in a decrease in β -catenin

TABLE 2 | Neuroprotective and neurodevelopmental functions of CPE-NF α 1 WT and CPE-NF α 1- Δ N.

	Function	Reference
CPE-NF α 1 WT	Regulates NGF-induced neurite outgrowth	Selvaraj et al., 2015
	Inhibits neuronal stem cell proliferation	Selvaraj et al., 2017
	Induces differentiation of neural stem cells into astrocytes	Selvaraj et al., 2017
	Regulates cortical neuron migration and dendrite arborization	Liang et al., 2018
	Protects primary cultured rat hippocampal neurons from H ₂ O ₂ -induced oxidative stress	Cheng et al., 2013
	CA3 completely degenerated after weaning, ear tag and tail clipping at 3-week of age and prevented by carbamazepine	Woronowicz et al., 2008, 2012
	Upregulates FGF2 and produces antidepressant-like effects	Cheng et al., 2015
CPE-NF α 1- Δ N (40 kD)	Protects primary rat embryonic cortical neurons from glutamate and H ₂ O ₂ -induced apoptosis via FGF2	Qin et al., 2014
	Increases proliferation via upregulating IGFBP2	Xiao et al., 2018

level and poor cell viability compared to untreated control embryonic rat cortical neurons. However, in CPE-NF α 1- Δ N-transduced neurons treated with glutamate, this decrease in β -catenin did not occur and the cell viability was similar to control. Treatment of cortical neurons with XAV939 which stimulates degradation of β -catenin (Huang et al., 2009) showed that in the presence of XAV939, the neuroprotective effect of CPE-NF α 1- Δ N against glutamate neurotoxicity was abolished. This suggests that the activation of the Wnt/ β -catenin pathway may also contribute to the neuroprotective mechanism of CPE-NF α 1- Δ N in embryonic neurons (Qin et al., our unpublished data). Additionally, β -catenin has been reported to mediate neuronal proliferation and differentiation of stem cells (Israsena et al., 2004). Thus, CPE-NF α 1- Δ N may also regulate these processes during development via the Wnt signaling pathway.

CONCLUSION

CPE-NF α 1 is a multifunction protein (Table 2). In addition to being a prohormone and proneuropeptide processing enzyme, it is a sorting receptor and vesicle transport mediator. Recent studies have shown that it also plays a fundamental role in neurodevelopment, neurodegeneration, and cognitive functions. Null mutation of CPE-NF α 1 in animal models and a human both produced similar deficits, including obesity, diabetes, and compromised cognitive function and memory. In addition, abnormal accumulation in the ER of a human mutant of CPE-NF α 1 from an AD patient was found which caused neurotoxicity, neurodegeneration, and cognitive impairment in an animal model. *In vitro* studies using primary neurons in culture indicate that CPE-NF α 1 acts extracellularly as a trophic factor, independent of enzymatic activity to mediate neuroprotection via activating several pro-survival signaling cascades such as upregulating Bcl2 and FGF2 signaling. Studies to demonstrate the neurotrophic effect *in vivo* will be necessary using transgenic

mouse models to further support this hypothesis. Additionally, identifying a membrane receptor for CPE-NF α 1 will be required to substantiate a receptor-mediated mechanism for activating signaling pathways for neuroprotection and stem cell differentiation. Furthermore, CPE-NF α 1 and its derived peptides can be developed as potential therapeutic agents to treat neurodegenerative diseases. The 40 kD CPE-NF α 1- Δ N variant has been shown to activate genes involved in neurodevelopment (Table 2). Further studies will be required to determine the precise molecular mechanism underlying CPE-NF α 1- Δ N's role in activating such genes during embryonic development.

DATA AVAILABILITY

The datasets generated for this study are available on request to the corresponding author.

AUTHOR CONTRIBUTIONS

All authors listed have made a substantial, direct and intellectual contribution to the work, and approved it for publication.

FUNDING

This research was supported by the Intramural Research Program of the Eunice Kennedy Shriver National Institute of Child Health and Human Development (NICHD), National Institutes of Health, United States.

ACKNOWLEDGMENTS

We thank Drs. Hong Lou, Vinay Sharma, and Sangeetha Hareendran, (NICHD) for helpful discussions of the manuscript.

REFERENCES

- Alsters, S. I., Goldstone, A. P., Buxton, J. L., Zekavati, A., Sosinsky, A., Yiorakas, A. M., et al. (2015). Truncating Homozygous Mutation of Carboxypeptidase E (CPE) in a morbidly obese female with type 2 diabetes mellitus, intellectual disability and hypogonadotrophic hypogonadism. *PLoS One* 10:e0131417. doi: 10.1371/journal.pone.0131417
- Birch, N. P., Rodriguez, C., Dixon, J. E., and Mezey, E. (1990). Distribution of carboxypeptidase H messenger RNA in rat brain using in situ hybridization histochemistry: implications for neuropeptide biosynthesis. *Brain Res. Mol. Brain Res.* 7, 53–59. doi: 10.1016/0169-328X(90)90073-M
- Cawley, N. X., Wetsel, W. C., Murthy, S. R., Park, J. J., Pacak, K., and Loh, Y. P. (2012). New roles of carboxypeptidase E in endocrine and neural function and cancer. *Endocr. Rev.* 33, 216–253. doi: 10.1210/er.2011-1039
- Cheng, Y., Cawley, N. X., and Loh, Y. P. (2013). Carboxypeptidase E/NF α 1: a new neurotrophic factor against oxidative stress-induced apoptotic cell death mediated by ERK and PI3-K/AKT pathways. *PLoS One* 8:e71578. doi: 10.1371/journal.pone.0071578
- Cheng, Y., Cawley, N. X., Yanik, T., Murthy, S. R., Liu, C., Kasicki, F., et al. (2016a). A human carboxypeptidase E/NF- α 1 gene mutation in an Alzheimer's disease patient leads to dementia and depression in mice. *Transl. Psychiatry* 6:e973. doi: 10.1038/tp.2016.237
- Cheng, Y., Li, Z., Kardami, E., and Loh, Y. P. (2016b). Neuroprotective effects of LMW and HMW FGF2 against amyloid beta toxicity in primary cultured hippocampal neurons. *Neurosci. Lett.* 632, 109–113. doi: 10.1016/j.neulet.2016.08.031
- Cheng, Y., Rodriguez, R. M., Murthy, S. R., Senatorov, V., Thouennon, E., Cawley, N. X., et al. (2015). Neurotrophic factor- α 1 prevents stress-induced depression through enhancement of neurogenesis and is activated by rosiglitazone. *Mol. Psychiatry* 20, 744–754. doi: 10.1038/mp.2014.136
- Cong, L., Cheng, Y., Cawley, N. X., Murthy, S. R., and Loh, Y. P. (2017). A novel single nucleotide T980C polymorphism in the human carboxypeptidase E gene results in loss of neuroprotective function. *PLoS One* 12:e0170169. doi: 10.1371/journal.pone.0170169
- Cool, D. R., Normant, E., Shen, F., Chen, H. C., Pannell, L., Zhang, Y., et al. (1997). Carboxypeptidase E is a regulated secretory pathway sorting receptor: genetic obliteration leads to endocrine disorders in Cpe(fat) mice. *Cell* 88, 73–83. doi: 10.1016/S0092-8674(00)81860-7
- Coulon, M., Wellman, C. L., Marjara, I. S., Janczak, A. M., and Zanella, A. J. (2013). Early adverse experience alters dendritic spine density and gene expression in prefrontal cortex and hippocampus in lambs. *Psychoneuroendocrinology* 38, 1112–1121. doi: 10.1016/j.psyneuen.2012.10.018
- Deiss, L. P., Feinstein, E., Berissi, H., Cohen, O., and Kimchi, A. (1995). Identification of a novel serine/threonine kinase and a novel 15-kD protein as

- potential mediators of the gamma interferon-induced cell death. *Genes Dev.* 9, 15–30. doi: 10.1101/gad.9.1.15
- Evans, S. J., Choudary, P. V., Neal, C. R., Li, J. Z., Vawter, M. P., Tomita, H., et al. (2004). Dysregulation of the fibroblast growth factor system in major depression. *Proc. Natl. Acad. Sci. U.S.A.* 101, 15506–15511. doi: 10.1073/pnas.0406788101
- Fan, S., Gao, X., Chen, P., and Li, X. (2018). Carboxypeptidase E-DeltaN promotes migration, invasion and epithelial-mesenchymal transition of human osteosarcoma cell lines through the Wnt/beta-catenin pathway. *Biochem. Cell Biol.* doi: 10.1139/bcb-2018-0236 [Epub ahead of print].
- Feinstein, E., Druck, T., Kastury, K., Berissi, H., Goodart, S. A., Overhauser, J., et al. (1995). Assignment of DAPI and DAPK—genes that positively mediate programmed cell death triggered by IFN-gamma—to chromosome regions 5p12.2 and 9q34.1, respectively. *Genomics* 29, 305–307. doi: 10.1006/geno.1995.1255
- Fricker, L. D. (1988). Carboxypeptidase E. *Annu. Rev. Physiol.* 50, 309–321. doi: 10.1146/annurev.ph.50.030188.001521
- Fricker, L. D., and Devi, L. (1993). Posttranslational processing of carboxypeptidase E, a neuropeptide-processing enzyme, in AtT-20 cells and bovine pituitary secretory granules. *J. Neurochem.* 61, 1404–1415. doi: 10.1111/j.1471-4159.1993.tb13634.x
- Fricker, L. D., and Snyder, S. H. (1983). Purification and characterization of enkephalin convertase, an enkephalin-synthesizing carboxypeptidase. *J. Biol. Chem.* 258, 10950–10955.
- Hook, V. Y., Eiden, L. E., and Brownstein, M. J. (1982). A carboxypeptidase processing enzyme for enkephalin precursors. *Nature* 295, 341–342. doi: 10.1038/295341a0
- Hook, V. Y., Mezey, E., Fricker, L. D., Pruss, R. M., Siegel, R. E., and Brownstein, M. J. (1985). Immunochemical characterization of carboxypeptidase B-like peptide-hormone-processing enzyme. *Proc. Natl. Acad. Sci. U.S.A.* 82, 4745–4749. doi: 10.1073/pnas.82.14.4745
- Huang, S. M., Mishina, Y. M., Liu, S., Cheung, A., Stegmeier, F., Michaud, G. A., et al. (2009). Tankyrase inhibition stabilizes axin and antagonizes Wnt signalling. *Nature* 461, 614–620. doi: 10.1038/nature08356
- Ibrahim, S. M., Mix, E., Bottcher, T., Koczan, D., Gold, R., Rolfs, A., et al. (2001). Gene expression profiling of the nervous system in murine experimental autoimmune encephalomyelitis. *Brain* 124, 1927–1938. doi: 10.1093/brain/124.10.1927
- Israsena, N., Hu, M., Fu, W., Kan, L., and Kessler, J. A. (2004). The presence of FGF2 signaling determines whether beta-catenin exerts effects on proliferation or neuronal differentiation of neural stem cells. *Dev. Biol.* 268, 220–231. doi: 10.1016/j.ydbio.2003.12.024
- Ji, L., Wu, H. T., Qin, X. Y., and Lan, R. (2017). Dissecting carboxypeptidase E: properties, functions and pathophysiological roles in disease. *Endocr. Connect.* 6, R18–R38. doi: 10.1530/EC-17-0020
- Jin, K., Graham, S. H., Nagayama, T., Goldsmith, P. C., Greenberg, D. A., Zhou, A., et al. (2001). Altered expression of the neuropeptide-processing enzyme carboxypeptidase E in the rat brain after global ischemia. *J. Cereb. Blood Flow Metab.* 21, 1422–1429. doi: 10.1097/00004647-200112000-00006
- Jung, Y. K., Kunczt, C. J., Pearson, R. K., Dixon, J. E., and Fricker, L. D. (1991). Structural characterization of the rat carboxypeptidase-E gene. *Mol. Endocrinol.* 5, 1257–1268. doi: 10.1210/mend-5-9-1257
- Koks, S., Luuk, H., Nelovkov, A., Areda, T., and Vasar, E. (2004). A screen for genes induced in the amygdaloid area during cat odor exposure. *Genes Brain Behav.* 3, 80–89. doi: 10.1046/j.1601-183x.2003.00047.x
- Koshimizu, H., Senatorov, V., Loh, Y. P., and Gozes, I. (2009). Neuroprotective protein and carboxypeptidase E. *J. Mol. Neurosci.* 39, 1–8. doi: 10.1007/s12031-008-9164-5
- Lee, C., Hu, J., Ralls, S., Kitamura, T., Loh, Y. P., Yang, Y., et al. (2012). The molecular profiles of neural stem cell niche in the adult subventricular zone. *PLoS One* 7:e50501. doi: 10.1371/journal.pone.0050501
- Levy-Strumpf, N., and Kimchi, A. (1998). Death associated proteins (DAPs): from gene identification to the analysis of their apoptotic and tumor suppressive functions. *Oncogene* 17, 3331–3340. doi: 10.1038/sj.onc.1202588
- Liang, C., Carrel, D., Omelchenko, A., Kim, H., Patel, A., Fanget, I., et al. (2018). Cortical neuron migration and dendrite morphology are regulated by carboxypeptidase E. *Cereb. Cortex* doi: 10.1093/cercor/bhy155 [Epub ahead of print].
- Lou, H., Kim, S. K., Zaitsev, E., Snell, C. R., Lu, B., and Loh, Y. P. (2005). Sorting and activity-dependent secretion of BDNF require interaction of a specific motif with the sorting receptor Carboxypeptidase E. *Neuron* 45, 245–255. doi: 10.1016/j.neuron.2004.12.037
- Lou, H., Park, J. J., Cawley, N. X., Sarcon, A., Sun, L., Adams, T., et al. (2010). Carboxypeptidase E cytoplasmic tail mediates localization of synaptic vesicles to the pre-active zone in hypothalamic pre-synaptic terminals. *J. Neurochem.* 114, 886–896. doi: 10.1111/j.1471-4159.2010.06820.x
- Lynch, D. R., Braas, K. M., Hutton, J. C., and Snyder, S. H. (1990). Carboxypeptidase E (CPE): immunocytochemical localization in the rat central nervous system and pituitary gland. *J. Neurosci.* 10, 1592–1599. doi: 10.1523/JNEUROSCI.10-05-01592.1990
- MacCumber, M. W., Snyder, S. H., and Ross, C. A. (1990). Carboxypeptidase E (enkephalin convertase): mRNA distribution in rat brain by in situ hybridization. *J. Neurosci.* 10, 2850–2860. doi: 10.1523/JNEUROSCI.10-08-02850.1990
- Martinez, A., Otal, R., and Soriano Garcia, E. (2004). [Ephrins, neuronal development and plasticity]. *Rev. Neurol.* 38, 647–655. doi: 10.33588/rn.3807.2004068
- Martinez, A., and Soriano, E. (2005). Functions of ephrin/Eph interactions in the development of the nervous system: emphasis on the hippocampal system. *Brain Res. Brain Res. Rev.* 49, 211–226. doi: 10.1016/j.brainresrev.2005.02.001
- Mazon Pelaez, I., Vogler, S., Strauss, U., Wernhoff, P., Pahnke, J., Brockmann, G., et al. (2005). Identification of quantitative trait loci controlling cortical motor evoked potentials in experimental autoimmune encephalomyelitis: correlation with incidence, onset and severity of disease. *Hum. Mol. Genet.* 14, 1977–1989. doi: 10.1093/hmg/ddi203
- Murphy, M., Drago, J., and Bartlett, P. F. (1990). Fibroblast growth factor stimulates the proliferation and differentiation of neural precursor cells in vitro. *J. Neurosci. Res.* 25, 463–475. doi: 10.1002/jnr.490250404
- Murthy, S. R., Thouenon, E., Li, W. S., Cheng, Y., Bhupatkar, J., Cawley, N. X., et al. (2013). Carboxypeptidase E protects hippocampal neurons during stress in male mice by up-regulating prosurvival BCL2 protein expression. *Endocrinology* 154, 3284–3293. doi: 10.1210/en.2013-1118
- Park, J. J., Cawley, N. X., and Loh, Y. P. (2008). A bi-directional carboxypeptidase E-driven transport mechanism controls BDNF vesicle homeostasis in hippocampal neurons. *Mol. Cell. Neurosci.* 39, 63–73. doi: 10.1016/j.mcn.2008.05.016
- Pla, V., Paco, S., Ghezali, G., Ciria, V., Pozas, E., Ferrer, I., et al. (2013). Secretory sorting receptors carboxypeptidase E and secretogranin III in amyloid beta-associated neural degeneration in Alzheimer's disease. *Brain Pathol.* 23, 274–284. doi: 10.1111/j.1750-3639.2012.00644.x
- Qian, Y., Varlamov, O., and Fricker, L. D. (1999). Glu300 of rat carboxypeptidase E is essential for enzymatic activity but not substrate binding or routing to the regulated secretory pathway. *J. Biol. Chem.* 274, 11582–11586. doi: 10.1074/jbc.274.17.11582
- Qin, X. Y., Cheng, Y., Murthy, S. R., Selvaraj, P., and Loh, Y. P. (2014). carboxypeptidase E-DeltaN, a neuroprotein transiently expressed during development protects embryonic neurons against glutamate neurotoxicity. *PLoS One* 9:e112996. doi: 10.1371/journal.pone.0112996
- Raballo, R., Rhee, J., Lyn-Cook, R., Leckman, J. F., Schwartz, M. L., and Vaccarino, F. M. (2000). Basic fibroblast growth factor (Fgf2) is necessary for cell proliferation and neurogenesis in the developing cerebral cortex. *J. Neurosci.* 20, 5012–5023. doi: 10.1523/JNEUROSCI.20-13-05012.2000
- Rodriguez, R. M., Wilkins, J. J., Creson, T. K., Biswas, R., Berezniuk, I., Fricker, A. D., et al. (2013). Emergence of anxiety-like behaviours in depressive-like Cpe(fat/fat) mice. *Int. J. Neuropsychopharmacol.* 16, 1623–1634. doi: 10.1017/S1461145713000059
- Russo, V. C., Gluckman, P. D., Feldman, E. L., and Werther, G. A. (2005). The insulin-like growth factor system and its pleiotropic functions in brain. *Endocr. Rev.* 26, 916–943. doi: 10.1210/er.2004-0024
- Selvaraj, P., Huang, J. S., Chen, A., Skalka, N., Rosin-Arbesfeld, R., and Loh, Y. P. (2015). Neurotrophic factor-alpha1 modulates NGF-induced neurite outgrowth through interaction with Wnt-3a and Wnt-5a in PC12 cells and cortical neurons. *Mol. Cell. Neurosci.* 68, 222–233. doi: 10.1016/j.mcn.2015.08.005
- Selvaraj, P., Xiao, L., Lee, C., Murthy, S. R., Cawley, N. X., Lane, M., et al. (2017). Neurotrophic Factor-alpha1: a Key Wnt-beta-Catenin Dependent Anti-Proliferation Factor and ERK-Sox9 activated inducer of embryonic neural stem

- cell differentiation to astrocytes in neurodevelopment. *Stem Cells* 35, 557–571. doi: 10.1002/stem.2511
- Skalka, N., Caspi, M., Caspi, E., Loh, Y. P., and Rosin-Arbesfeld, R. (2013). Carboxypeptidase E: a negative regulator of the canonical Wnt signaling pathway. *Oncogene* 32, 2836–2847. doi: 10.1038/onc.2012.308
- Song, L., and Fricker, L. (1995). Processing of procarboxypeptidase E into carboxypeptidase E occurs in secretory vesicles. *J. Neurochem.* 65, 444–453. doi: 10.1046/j.1471-4159.1995.65010444.x
- Stahl, S., Reinders, Y., Asan, E., Mothes, W., Conzelmann, E., Sickmann, A., et al. (2007). Proteomic analysis of cathepsin B- and L-deficient mouse brain lysosomes. *Biochim. Biophys. Acta* 1774, 1237–1246. doi: 10.1016/j.bbapap.2007.07.004
- Strittmatter, S. M., Lynch, D. R., and Snyder, S. H. (1984). [3H]guanidinoethylmercaptosuccinic acid binding to tissue homogenates. Selective labeling of enkephalin convertase. *J. Biol. Chem.* 259, 11812–11817.
- Weber, S. J., Louis, R. B., Trombley, L., Bisette, G., Davies, P., and Davis, T. P. (1992). Metabolic half-life of somatostatin and peptidase activities are altered in Alzheimer's disease. *J. Gerontol.* 47, B18–B25.
- Woronowicz, A., Cawley, N. X., Chang, S. Y., Koshimizu, H., Phillips, A. W., Xiong, Z. G., et al. (2010). Carboxypeptidase E knockout mice exhibit abnormal dendritic arborization and spine morphology in central nervous system neurons. *J. Neurosci. Res.* 88, 64–72. doi: 10.1002/jnr.22174
- Woronowicz, A., Cawley, N. X., and Peng Loh, Y. (2012). Carbamazepine prevents hippocampal neurodegeneration in mice lacking the neuroprotective protein, Carboxypeptidase E. *Clin. Pharmacol. Biopharm. Suppl.* 1:2.
- Woronowicz, A., Koshimizu, H., Chang, S. Y., Cawley, N. X., Hill, J. M., Rodriguez, R. M., et al. (2008). Absence of carboxypeptidase E leads to adult hippocampal neuronal degeneration and memory deficits. *Hippocampus* 18, 1051–1063. doi: 10.1002/hipo.20462
- Xiao, L., Chang, S. Y., Xiong, Z. G., Selveraj, P., and Peng Loh, Y. (2017). Absence of Carboxypeptidase E/Neurotrophic Factor-Alpha1 in Knock-Out Mice Leads to Dysfunction of BDNF-TRKB Signaling in Hippocampus. *J. Mol. Neurosci.* 62, 79–87. doi: 10.1007/s12031-017-0914-0
- Xiao, L., Yang, X., Sharma, V. K., and Loh, Y. P. (2018). Cloning, gene regulation, and neuronal proliferation functions of novel N-terminal-truncated carboxypeptidase E/neurotrophic factor-alpha variants in embryonic mouse brain. *FASEB J.* 33, 808–820. doi: 10.1096/fj.201800359R
- Yang, X., Cong, L., Lou, H., and Loh, Y. P. (2017). A novel 40kDa CPE- Δ N isoform promotes proliferation and invasion in pancreatic cancer cells. *Cancer Res.* 77, 1967–1967. doi: 10.1158/1538-7445.AM2017-1967
- Zechel, S., Werner, S., Unsicker, K., and von Bohlen und Halbach, O. (2010). Expression and functions of fibroblast growth factor 2 (FGF-2) in hippocampal formation. *Neuroscientist* 16, 357–373. doi: 10.1177/1073858410371513
- Zheng, M., Streck, R. D., Scott, R. E., Seidah, N. G., and Pintar, J. E. (1994). The developmental expression in rat of proteases furin, PC1, PC2, and carboxypeptidase E: implications for early maturation of proteolytic processing capacity. *J. Neurosci.* 14, 4656–4673. doi: 10.1523/JNEUROSCI.14-08-04656.1994
- Zhou, A., Minami, M., Zhu, X., Bae, S., Minthorne, J., Lan, J., et al. (2004). Altered biosynthesis of neuropeptide processing enzyme carboxypeptidase E after brain ischemia: molecular mechanism and implication. *J. Cereb. Blood Flow Metab.* 24, 612–622. doi: 10.1097/01.WCB.0000118959.03453.17
- Zhu, X., Wu, K., Rife, L., Cawley, N. X., Brown, B., Adams, T., et al. (2005). Carboxypeptidase E is required for normal synaptic transmission from photoreceptors to the inner retina. *J. Neurochem.* 95, 1351–1362. doi: 10.1111/j.1471-4159.2005.03460.x

Conflict of Interest Statement: The authors declare that the research was conducted in the absence of any commercial or financial relationships that could be construed as a potential conflict of interest.

Copyright © 2019 Xiao, Yang and Loh. This is an open-access article distributed under the terms of the Creative Commons Attribution License (CC BY). The use, distribution or reproduction in other forums is permitted, provided the original author(s) and the copyright owner(s) are credited and that the original publication in this journal is cited, in accordance with accepted academic practice. No use, distribution or reproduction is permitted which does not comply with these terms.



Synthetic Peptides as Therapeutic Agents: Lessons Learned From Evolutionary Ancient Peptides and Their Transit Across Blood-Brain Barriers

David A. Lovejoy^{1,2*}, David W. Hogg¹, Thomas L. Dodsworth¹, Fernando R. Jurado¹, Casey C. Read¹, Andrea L. D'Aquila^{1,3} and Dalia Barsyte-Lovejoy⁴

¹ Department of Cell and Systems Biology, University of Toronto, Toronto, ON, Canada, ² Protagenic Therapeutics Inc., New York, NY, United States, ³ Department of Pediatrics, University of Alabama, Birmingham, AL, United States, ⁴ Structural Genomics Consortium, University of Toronto, Toronto, ON, Canada

OPEN ACCESS

Edited by:

David Vaudry,
Institut National de la Santé et de la
Recherche Médicale
(INSERM), France

Reviewed by:

Sergueï O. Fetissov,
Université de Rouen, France
Joao Carlos dos Reis Cardoso,
University of Algarve, Portugal
Yuri Ushkaryov,
University of Kent, United Kingdom

*Correspondence:

David A. Lovejoy
david.lovejoy@utoronto.ca

Specialty section:

This article was submitted to
Neuroendocrine Science,
a section of the journal
Frontiers in Endocrinology

Received: 17 April 2019

Accepted: 10 October 2019

Published: 12 November 2019

Citation:

Lovejoy DA, Hogg DW, Dodsworth TL,
Jurado FR, Read CC, D'Aquila AL and
Barsyte-Lovejoy D (2019) Synthetic
Peptides as Therapeutic Agents:
Lessons Learned From Evolutionary
Ancient Peptides and Their Transit
Across Blood-Brain Barriers.
Front. Endocrinol. 10:730.
doi: 10.3389/fendo.2019.00730

Peptides play a major role in the transmission of information to and from the central nervous system. However, because of their structural complexity, the development of pharmacological peptide-based therapeutics has been challenged by the lack of understanding of endogenous peptide evolution. The teneurin C-terminal associated peptides (TCAP) possess many of the required attributes of a practical peptide therapeutic. TCAPs, associated with the teneurin transmembrane proteins that bind to the latrophilins, members of the Adhesion family of G-protein-coupled receptors (GPCR). Together, this ligand-receptor unit plays an integral role in synaptogenesis, neurological development, and maintenance, and is present in most metazoans. TCAP has structural similarity to corticotropin-releasing factor (CRF), and related peptides, such as calcitonin and the secretin-based peptides and inhibits the (CRF)-associated stress response. Latrophilins are structurally related to the secretin family of GPCRs. TCAP is a soluble peptide that crosses the blood-brain barrier and regulates glucose transport into the brain. We posit that TCAP represents a phylogenetically older peptide system that evolved before the origin of the CRF-calcitonin-secretin clade of peptides and plays a fundamental role in the regulation of cell-to-cell energy homeostasis. Moreover, it may act as a phylogenetically older peptide system that evolved as a natural antagonist to the CRF-mediated stress response. Thus, TCAP's actions on the CNS may provide new insights into the development of peptide therapeutics for the treatment of CNS disorders.

Keywords: stress, latrophilin, receptor-ligand interaction, neuroplasticity, blood-brain barrier, G-protein coupled receptors, secretin, CRF

INTRODUCTION

The central nervous system (CNS) communicates information to the peripheral tissues primarily by neurotransmitter-mediated modulation of tonic and phasic ionic conductance among cells. Because of the large amount of information that can be encoded by this modulation, only a handful of small molecule neurotransmitters are required. However, secondarily, the CNS employs neurosecretory signals, mostly in the form of amphiphilic peptides that are

frequency- and amplitude-modulated to regulate the activity of proximal endocrine organs and tissues. Both transmission processes signal to the periphery and convey sensory information from the integration of in-coming external and internal organismal signals. As is the case with all transmission-reception systems, the CNS necessarily obtains feedback information regarding the physiological state of the peripheral tissues and organs. This receptive information occurs primarily via non-neural signals.

This CNS outflow of sensory information to the periphery combined with the counter-flow of information on the status of the peripheral tissues back to the CNS forms the basis of homeostatic regulation in all multicellular animals (metazoans). This system had to be functional in order for the first metazoans to evolve. Peripheral tissues, being non-neural in nature, can only provide feedback information to the brain by the release of secreted compounds that do not allow tonic or phasic information encoding. Moreover, given the number of specialized tissues that exist amongst the peripheral organs, their signal individuality can only be encoded by the suite of chemical compounds released into the interstitial space and vascular systems. Such signals provided coordination amongst peripheral tissues, and later became integrated into CNS communication. This integration occurred over much time that incorporated a number of evolutionary stages. The development of multicellular organisms led to a division of labor among cells. Further development led to the formation of functionally specific tissues and organs. Depending upon the available genome and associated gene expression in these tissues, the expressed secretory peptides had the potential to provide specific tissue and organ information back to the brain (**Figure 1**). However, because peripheral tissues evolved from shared common tissues and organs, and due to their associated genome, homeostatic information had to be encoded within the identity and structure of the secreted compounds. Peptides were particularly appropriate for this task as unique information could be encoded not only in frequency and amplitude modulation, but also within their primary amino acid sequences, and their subsequent secondary and tertiary structures [see (1) for discussion].

Reciprocal information exchange between the CNS and the periphery occurred before the evolution of CNS-vascular barriers. This was likely an evolutionary response to protect the integrity of intra-organismal information transmission from potential disruption of the homeostatic state by extra-organismal signals. As the blood brain barrier (BBB) evolved in the Metazoa, changes in its structure were evolutionarily selected to protect the organism from potentially noxious external signals while protecting incoming internal signals. For these reasons, the ability of synthetic therapeutic compounds, to transit across the BBB has been problematic, as these structures are unique to metazoan evolution over the last 600 million years, and therefore, frequently do not possess biological structures amenable to crossing the BBB. Natural peptides that evolved before the formation of the BBB co-evolved along with the development of the BBB, thus as a result, these peptides possessed the structural primary amino acid motifs and the subsequent secondary structures that were critical as essential recognizable regions by

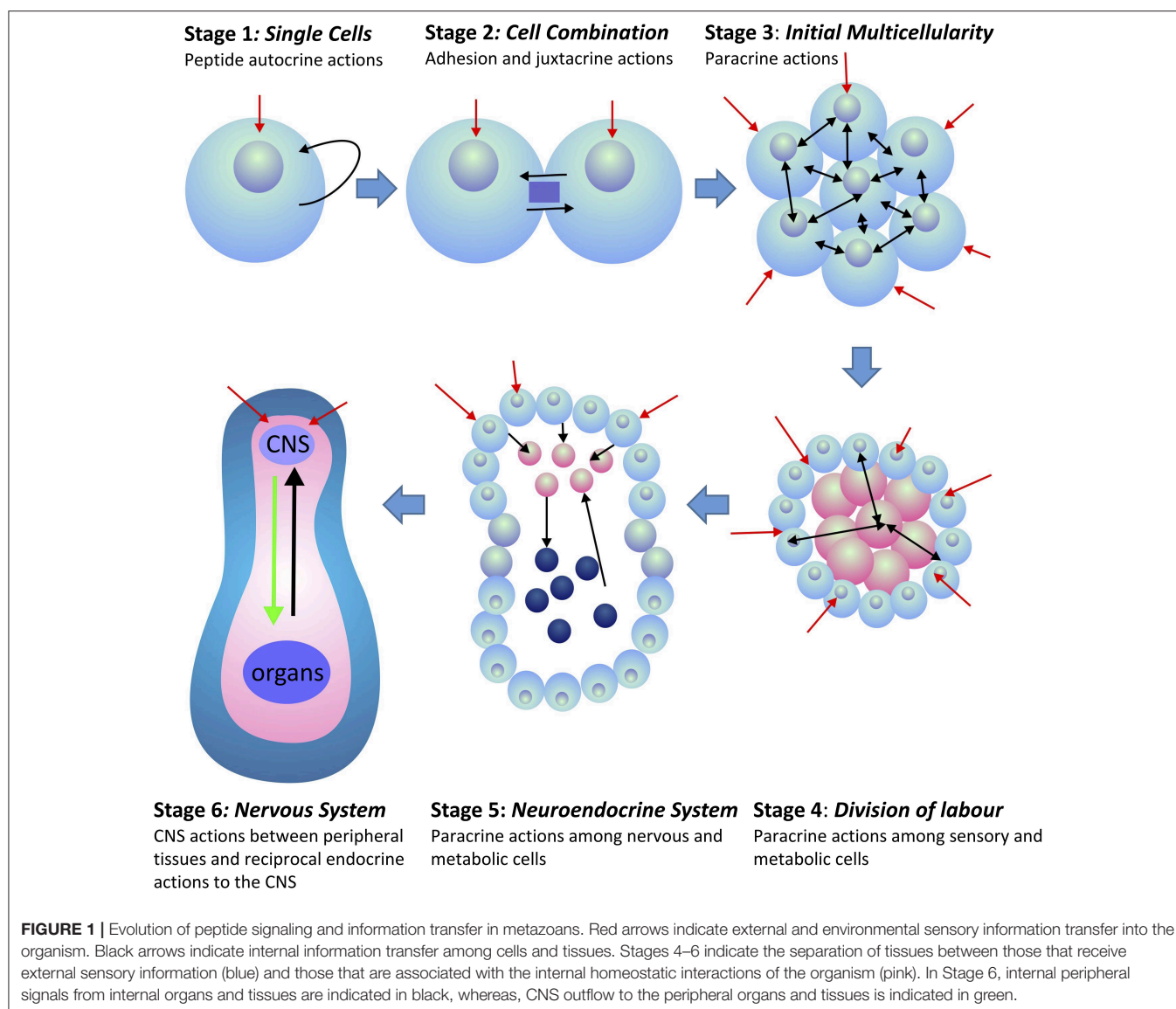
the early receptors and transporters that allowed transit across the BBB. Although numerous peptides do, in fact, cross the BBB, the lack of success of numerous synthetic pharmaceutical-based peptides is due, in part, to the focus on receptor-ligand binding *in vitro* as opposed to the requirements of a peptide to be soluble in different tissues, resistant to vascular-, and tissue-based peptidases, possess an extended resistency time in the target tissues, yet still be excreted by the organism.

However, recently, there has been more attention paid to the role of peptide-based therapeutics in the Pharma industry. Unfortunately, the inability of many of these synthetic peptides, novel to the biology of their target organisms (i.e., mammals, humans) to transit into the CNS has led to the misunderstanding that peptides, *per se*, do not enter CNS from the vasculature. Recent studies have identified numerous peptides that cross these vascular CNS barriers and have provided a rationale for this selective mechanism. The teneurin C-Terminal associated peptides (TCAP) evolved before the advent of various brain barriers, and is structurally related to many of the peptides that do cross the BBB. We posit that this is the reason for the success of TCAP-related peptides to transit among neural and peripheral tissues to achieve potent physiological and behavioral actions.

PEPTIDES AND THE BLOOD BRAIN BARRIERS

Historically, it was thought that peptides could not pass through the BBB. This early understanding was based on both the lack of understanding of the physiology of the BBB and the available technology to examine peptidergic transmission across the BBB (2, 3). However, by the last quarter of the twentieth century, Bloom (4) established that gastrointestinal peptides communicated with the brain, therefore, across the BBB, as part of a feedback mechanism to regulate organismal homeostasis. This was a major step forward in the understanding of inter-organ physiology and its relationship to the brain. The basic concept underlying this mechanism is that while the central nervous system (CNS) can communicate with non-neural tissues by nervous and neuroendocrine output, reciprocal efferent signals from these tissues must necessarily employ endocrine factors.

Since then, numerous peptides have been shown to cross the BBB by a combination of receptor and transporter mechanisms in specific vascular regions of the brain [see (2) for review]. However, despite the large number of studies confirming the transit of peptides across the BBB, numerous peptides do not cross. Because the BBB evolved to protect the brain from exogenous and potentially toxic compounds, yet needed to provide a portal to allow communication with endocrine signals from peripheral tissues, endogenous peptides that play a major role in homeostatic regulation are more likely to cross the BBB. A number of peptides such as insulin, leptin, ghrelin, and members of the secretin superfamily of peptides such as pituitary adenylate cyclase-activating polypeptide (PACAP), vasoactive intestinal peptide (VIP), and urocortin can cross the BBB (see below).



Vascular and Neural Access of Peptides to the CNS

Peptide action on the brain is regulated by a number of pharmacokinetic aspects that ultimately affect residency time in tissues. Residency time of a peripherally injected peptide in the brain is based on several factors. First, the clearance rate, including peptide degradation by plasma and endothelial associated peptidases, and elimination via the urinary system; second, transport into non-neural tissues; third, transport kinetics in the brain via the various neural blood barriers; and finally, efflux out of the brain.

Under natural conditions, most terrestrial vertebrates have three major routes that allow the intake of bioactive peptides from exogenous sources, including environmental (xenobiotics arising from natural products and anthropomorphic activities), nutrients (food) and pharmaceuticals (administered drugs). The

best studied of these routes is by ingestion. However, this method is not practical due to the high level of degradation that occurs in the gastrointestinal (GI) tract. Even those peptides that do survive and are taken up across the gut are further degraded by endothelial peptidases, and/or are eliminated by the kidney. Typically, most peptides have a half-life in the blood in the order of minutes and generally do not accumulate in the tissues (2). Thus, for the introduction of peptides into an organism that will ultimately enter the brain, an oral route is rarely practical. Although peptide ingestion by the gustatory route may provide limited access of some bioactive peptides that are relatively resistant to GI-associated degradation, this physiological system ultimately evolved to obtain nutrients that are safe to the organism. This complex transitory route is impractical for the learning of social interactive behaviors, as in many cases, the threat or invitation may be over by the time the low amounts of the remaining

intact bioactive compound has been perceived by the brain. Thus, for these reasons, other routes that provide a more direct route to the sensory integration regions of the CNS have evolved.

Over the last decade, peptide administration via nasal or oral mucosa administration has received greater attention. There are a number of reasons for this. Both the olfactory and vomeronasal (VNO) organs evolved specifically to take in chemical cues from the environment in an efficient manner and allow the organism to make rapid decisions that affect survival. The two sensory systems differ in that the olfactory organ is predisposed to sample volatile chemical signals, whereas the VNO is more sensitive to non-soluble and/or non-volatile compounds [see (1) for discussion]. Depending upon the species, these organ systems may be separate or integrated. Importantly, both organs are associated with a vascular network that is closely associated with the CNS, allowing for greater concentrations of the active compound to reach the CNS. The VNO is present in most vertebrates but possesses a number of specialized adaptations. Depending upon the species, access to the vasculature may occur via the dorsal oral mucosa or via the nasal epithelium. In those vertebrates that lack a VNO, evidence indicates that this a derived condition associated those lineages (5–7). Although this organ is well-developed in rodents, in humans, the VNO has been evolutionarily modified. The vomeronasal epithelium develops early in fetal life and is the embryonic tissue source of gonadotropin-releasing hormone (GnRH) neurons that migrate into the telecephalon to ultimately regulate the neuroendocrine aspects of the reproductive system (8). In the second half of pregnancy, the sensory aspects of the vomeronasal epithelium (VNE) degrades due, in part, to mutations of genes specific to VNO function (9). The adult human VNO possesses a number of features similar to that of the fetal VNE and that of non-human vertebrates, although it appears to have lost its sensory capacity (5–7, 10). However, in adult humans, there are a number of connections of VNO cells with the underlying capillaries, indicating that the VNO has evolved to take on a more endocrine function (11). Although the role of VNO with respect to peptide uptake in humans is equivocal, the actions of the main olfactory epithelium are less so. The sensory neurons of the olfactory epithelium extend their dendrites into the nasal cavity thus allowing these sensory neurons to come into direct contact with the external environment (12). As a result, olfactory signals can directly interact with the CNS.

Arguably, the least understood of these delivery methods are those that utilize the oral mucosa. In humans, these include the buccal mucosa (lining of the cheek), the sublingual mucosa (floor of mouth and underside of the tongue), and the gingival mucosa (associated with the teeth and aspects of the jaws). Transport of proteins and peptides across the oral mucosa occurs primarily by passive diffusion and avoids GI degradation via bypass of the initial hepatic metabolic processes (13). Transit of peptides through this route into the brain can be relatively efficient in comparison to other methods of administration, however, depending upon the peptide structure and solubility, can be limited by the comparatively small epithelial region and the difficulties in maintaining a constant delivery concentration (14).

CNS Blood Barriers

Although the vascular system of the olfactory, vomeronasal organs and oral mucosa indicates that peptides taken up via these routes gain a greater access to the CNS, they still need to navigate the various blood barriers of the CNS. There are three main barriers that control the molecular transport between the blood and the neural tissues: the blood brain barrier (BBB), which is formed by the cerebral vasculature epithelium between the blood and the brain's interstitial fluid; the choroid plexus epithelium between the blood and ventricular cerebrospinal fluid (CSF) barrier (2, 15, 16); and the arachnoid epithelium between the blood and the ventricular CSF. However, it is the BBB that has the greatest control of the proximal environment of brain cells (3).

There are two basic mechanisms by which a peripheral peptide can affect neuronal function. Peptides may be transported across the BBB via passive diffusion or saturable transport (2), resulting in activation of receptors at the cerebral vasculature level (17). Although it has been suggested that almost 100% of large molecules cannot cross the BBB (18), this number is misleading (3). Only about 0.05% of injected insulin reaches the brain (19). Previous studies lacked the technology and sensitivity to detect low amounts of the peptide in the brain. In the case of morphine, although it is not a peptide, about 0.02% of the injected dose can be detected in the brain (20). Thus, it is not appropriate to compare peptide transit across the BBB directly with other small bioactive molecules. It is likewise not reasonable to expect that peptide transit in the brain will occur via the circumventricular organs (CVOs). There is a 5,000–7,500-fold difference between the surface area of the CVOs as opposed to that of the BBB (21, 22). Moreover, the morphology of the capillaries associated with the CVOs do not allow significant penetration of peptides into the brain (16). As an example of this relationship, the transit of interleukin 1 alpha (IL-1 α) across the CVOs accounts for <5% of the peptide that enters the brain (2, 23).

Taken together, the previous studies of peptide transit across the various BBBs indicate several essential attributes of these barriers. Most importantly, this barrier evolved to ensure interactive transit between the peripheral tissues and the brain to ensure homeostatic communication among all tissues and organs of the organism. Secondly, the specificity of compounds that could transit the BBB was likely based on the suite of soluble proteinaceous and metabolic compounds as defined by the genomes of the species. Given this evolutionary scenario, it explains why the majority of natural xenobiotic compounds and novel artificially-derived compounds do not readily cross the BBB. In other words, after over 600 million years of selective evolution of the BBB, it is unlikely that a novel non-natural synthetic peptides that does not encompass the structural attributes for membrane transit, refractile to peptidases, yet still possesses a high affinity ($K_d < 1$ nM) for its target in the brain, will be successful. Peptide therapeutics based on the structure of natural peptides that possess a long evolutionary history are candidates for therapeutics that could be used for the treatment of mood disorders. The teneurin C-terminal associated peptide (TCAP) possesses the attributes that make it an excellent candidate for the treatment of mood disorders.

DISCOVERY OF THE TENEURINS AND THEIR RECEPTORS

The existence of the teneurins was reported independently in 1994 by two separate laboratories (24–26). Within a few years, the teneurin family was acknowledged as a type-II transmembrane protein that was highly expressed in the central nervous system (CNS) of almost all metazoans. The teneurins are complex multifunctional proteins consisting of numerous functional domains translated from a gene consisting of 20 to over 30 exons (27, 28) spanning over 600,000 bases in the genome. There are generally 4 teneurin paralogues found amongst chordates, thereby conforming to the 2R hypothesis that theorizes two major genome duplication events in the Chordata (29, 30). In contrast, there is typically only a single gene found in invertebrates with the exception of the Insecta, which possess two paralogues. Initial studies of the teneurins indicated a major role in neural development included cell adhesion, axonal pathfinding and cell proliferation (27, 28). The teneurins have now emerged as critical genes required for normal CNS function and maintenance.

For the first two decades following the discovery of the teneurins, the receptor mechanism was not clear. Initial studies indicated that the teneurins could homo- and hetero-dimerize to achieve activation (31–35). This teneurin activation stimulates the cleavage of its intracellular domain that leads to translocation and activation of the nuclear transcription factor zic-1 (31, 33). Although this may indeed be the case in some situations, new studies in the last decade have suggested an alternative hypothesis that the teneurins interact with a family of Adhesion family G-protein coupled receptor (GPCR) known as the latrophilins (LPHN). The LPHNs comprise a family of three paralogous receptors (36, 37). LPHN is also known as calcium-independent receptor for latrotoxin (CIRL), reflecting its binding capacity for α -latrotoxin (α -LTX) (38, 39). Their structure contains a long extracellular portion comprised of a lectin-like domain, an olfactomedin-like domain, a hormone-binding domain and a GPCR autoproteolysis inducing (GAIN) domain, which includes a GPCR proteolytic site [GPS; (39)]. This is followed by the seven-transmembrane domain that defines all GPCRs and, finally, a C-terminal intracellular tail. The LPHNs were first discovered in the search for the calcium-independent receptor of α -LTX, the principle vertebrate toxic component in the venom of the black widow spider (genus *Lactrodectus*) (38). Although α -LTX was initially shown to bind to the neurexins in an interaction that is calcium-dependent (40, 41); it also caused downstream effects in calcium-absent conditions, indicating another potential receptor mechanism at play (42). Davletov et al. (38) were the first to purify LPHN from detergent-solubilized bovine brain membranes and established that it bound α -LTX *in vitro* with high affinity in the absence of calcium, indicating a receptor-ligand interaction between the two molecules. This was further established via over-expression expression of LPHN in chromaffin cells, which resulted in increased cell sensitivity to α -LTX (39).

After their initial discovery, the three LPHN isoforms were classified as members of the Secretin GPCR family, as their hormone binding domains showed high sequence similarity to the signature hormone binding domains of the Secretin

GPCRs (43). These receptors have since been re-classified to the Adhesion GPCR family due to their long extracellular domains containing adhesion motifs and associated adhesion functions (44, 45). Recent phylogenetic analyses indicate that the Adhesion GPCR family is ancestral to the Secretin GPCR family, and that the Secretin GPCRs inherited their hormone binding domain from the Adhesion GPCRs (37, 46, 47). As this domain is critical to Secretin ligand binding, the ligands of the Adhesion GPCRs may have also been the progenitors to the Secretin GPCR ligands.

DISCOVERY AND CHARACTERIZATION OF THE TENEURIN C-TERMINAL ASSOCIATED PEPTIDES

Qian et al. (48) identified a clone from a rainbow trout hypothalamic cDNA library representing an ortholog of teneurin-3. This led to the discovery of a peptide-like sequence encoded at the carboxy-terminus in the last exon of the rainbow trout teneurin-3 gene. Because this sequence was annotated as part of the teneurin gene, this region was termed Teneurin C-terminal-associated peptide (TCAP)-3. TCAP-1, -2, and -4 were subsequently identified following *in silico* analyses of the available teneurin-1, -2, and -4 sequences, respectively (49). The TCAPs are approximately the same size as both CRF and its direct paralogues, urotensin-I (UI), and urocortin (Ucn), ranging from 40 to 41 residues in length. The TCAP and CRF families of peptides possess about 30% sequence similarity among homologous replacements (28, 50, 51). In addition, the TCAPs possess the cleavage motifs similar to CRF and related peptides (52). This primary structure similarity suggested that the TCAP family was distantly related to the CRF peptide families, and that they may share a common evolutionary origin (53, 54).

The CRF family of peptides belong to the Secretin family of peptides (28, 50, 54, 55). The CRF family consists of four to five paralogous peptides that mediate the stress response and regulate stress-associated energy metabolism. CRF is fundamentally responsible for regulating the hypothalamic-pituitary-adrenal (HPA) axis and coordinating the peripheral endocrine response to stress (56, 57). In vertebrates, the CRF family of ligands is highly conserved and integrated into a number of diverse physiological systems. This indicates significant selection pressures to maintain the CRF ligand-receptor signaling system due to the fundamental physiological roles it plays (58). The vertebrate CRF ligand family is comprised of two paralogous lineages: CRF and its direct paralogues as one lineage; and urocortin 2 and 3 that are included within a second paralogous lineage. The first paralogous lineage includes CRF and CRF2 [teleocortin; (55, 59–61)]; and a second lineage that includes mammalian urocortin (Ucn), amphibian sauvagine (Svga), and fish urotensin-I (UI) (62, 63). A second paralogous lineage to the CRF and UI family lineage includes urocortin 2 (Ucn2) and urocortin 3 (Ucn3) (64–66) (see **Figure 2**). Within invertebrates, the diuretic hormones (DHs) are orthologous to the CRF family of peptides, and are predominantly involved in osmoregulation and diuresis in insects (63, 67, 68). The secretin-related peptides are widely expressed in

deuterostomes and are also present to a limited degree in protostomes, however there are no clear data among lineages that evolved before the evolutionary divergence between these two lineages (55).

In contrast, evidence indicates that the teneurin-TCAP system predates the CRF-secretin peptide family by a few hundred million years. Comparative genomic and protein analyses support the theory that the teneurin/TCAP complex originated in metazoans through a horizontal gene transfer event from prokaryotes to a single-celled metazoan ancestor, likely a choanoflagellate (69–72). Prokaryotes contain unique proteinaceous polypeptide toxins (PPTs), which possess several characteristics similar to those of metazoan teneurins, including a type-II orientation and three main domains: an intracellular domain involved in secretion or cell signaling, a central domain involved in adhesion, and a C-terminal domain containing a toxin payload that could be released into neighboring cells (69, 72). The TCAP portion of teneurin, specifically, has high amino acid sequence similarity to the glycine-histidine-histidine (GHH) clade of the PPT C-terminal toxin domains (72). Additionally, the teneurins are the only metazoan genes to contain YD repeats, a motif common in certain aquatic bacteria and with similarity to bacterial RHS elements (70, 73). The recently resolved structures of chicken and human teneurin-2 and mouse teneurin-3 also show a striking similarity to that of bacterial Tc-toxins, with a cylindrical β -barrel domain encompassing a toxin-like C-terminal region corresponding to the TCAP region (74, 75). However, the teneurin extracellular domain itself also contains eight epidermal growth factor (EGF)-like repeats, which are a hallmark of the metazoan genes (71). Thus, the current theory regarding the evolution of the teneurins posits that a PPT was inherited by a choanoflagellate from a prokaryote via horizontal

gene transfer, and subsequently became associated with an EGF repeat domain, resulting in the formation and expression of a proto-teneurin gene containing an extended extracellular region and a bioactive C-terminal domain (69, 72). In bacterial PPT toxins, the encapsulated carboxy region containing the toxic payload (i.e., GHH and TCAP) is cleaved and released by proteases within the barrel domain (76). Although the function of the barrel domain in teneurins is yet to be determined, it may act on one of several known putative cleavage sites upstream to TCAP to allow for its release (75). Tucker (73) has postulated that the introduction of the teneurin protogenes into the choanoflagellates may have acted to increase the entrapment of their algae prey, thus linking the teneurins with nutrient acquisition and energy metabolism.

Although the dynamics of the interaction between Teneurin and TCAP as LPHN ligands was initially unclear, subsequent studies showed that Teneurin-2 bound with nanomolar affinity to the lectin-domain of LPHN1. Furthermore, a splice variant of C-terminal domain of Teneurin-2, termed LPHN1-associated synaptic surface organizer (Lasso), could also bind to LPHN1 at its C-terminal globular domain with high affinity, and with the implementation of antibodies against each of the ADGRL homologs, they demonstrated that LPHN1 is the primary ligand of Lasso (77). Furthermore, Teneurin-1 and Teneurin-4 also bind LPHN1 (78, 79). Because both the Teneurin paralogues and Lasso bind to LPHN1 with high affinity, it was presumed that TCAP could bind with the LPHN family. Transgenic over-expression of both TCAP-1 and the hormone-binding domain (HBD) of LPHN1 showed that both signals could be detected in immunoprecipitation studies. Moreover, the transfected cells experienced high levels of cytoskeletal rearrangement in the presence of TCAP-1 compared to wild-type cells (80). Together,

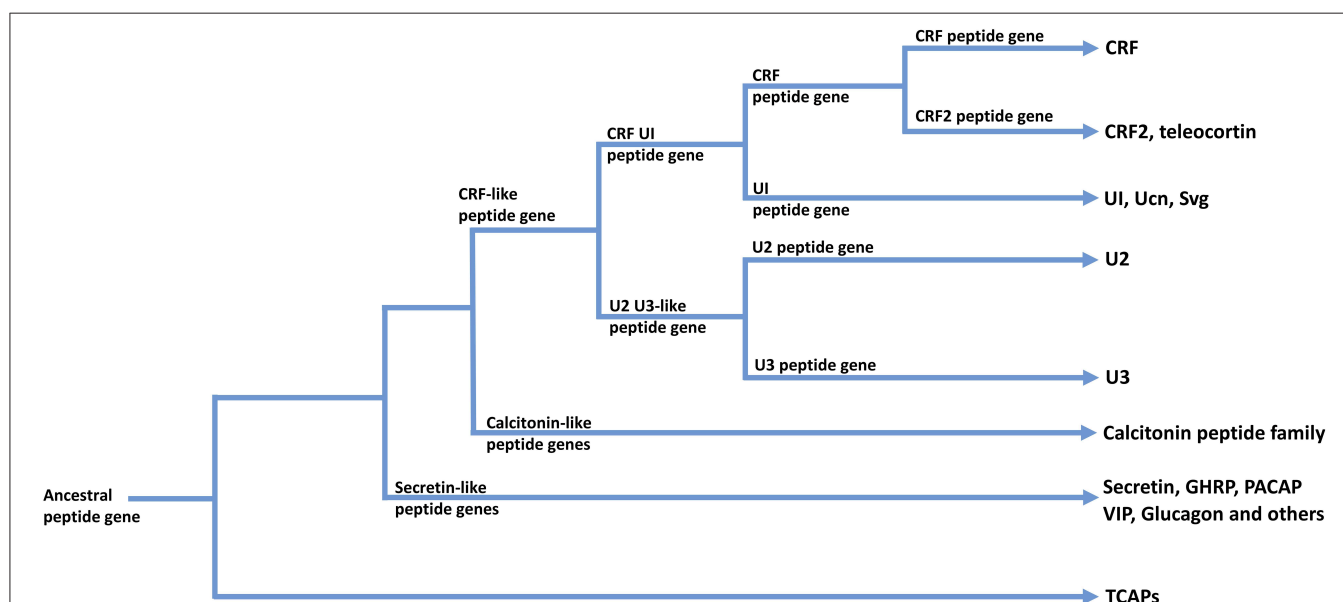


FIGURE 2 | A possible scheme for the phylogenetic relationships among TCAP-, CRF-, Calcitonin-, and Secretin-associated peptide families. Arrows indicate peptide families found in extant organisms.

these studies indicate that the extracellular region of teneurins, including TCAP-1, bind with LPHN1. Importantly however, these studies link TCAP-1 as a peptide to the Secretin family of peptides that bind to a receptor phylogenetically linked to the Secretin family of GPCRs. Given that both the teneurin/TCAP protein ligand and the LPHN receptor are the apparent result of lateral gene transfers from prokaryotes to a single celled metazoan ancestor (72), this suggests that this ligand-pair evolved well before the evolution of the Secretin-like ligands and associated receptor superfamilies.

TCAP, Secretin Peptides, and Relationship to Energy Metabolism

Further indication that TCAP is evolutionarily ancient and that it is a potential progenitor of secretin-like peptides along with the CRF and CRF-like peptides is supported by a number of physiological studies. Considerable evidence establishes a commonality among the secretin peptide and secretin receptor superfamilies (including CRF and calcitonin) in the regulation of energy metabolism for homeostasis (81–83). Much like the Secretin family of peptides, TCAP has been implicated in the regulation of both cellular and organismal energy metabolism (82, 84, 85). Recently, TCAP-1 has been demonstrated to induce glucose uptake in murine neuronal cells *in vitro* using ^3H -deoxyglucose (DG) (86). As glucose is the primary energy substrate in the brain, increased neural glucose uptake into rat brain using functional positron emission tomography with ^{18}F -DG indicates that TCAP-1 can regulate the supply component (i.e., glucose) of a cell's energy budget (86). Importantly, *in vitro* studies indicate that TCAP-1-mediated glucose uptake occurs through an insulin-independent pathway. Moreover, phylogenetic analyses suggest that TCAP evolution also predates insulin (86–88), this indicates that TCAP may be one of the first signaling peptides to regulate glucose uptake in metazoans.

If the fundamental role of TCAP was to regulate energy metabolism in the earliest metazoan ancestors, then it is possible that that TCAP's earliest functions were to stimulate aerobic metabolism, glucose, and other nutrient importation, and mitochondrial activity. This mechanism would necessarily be associated with cellular energy homeostasis given its evolutionary history before it was modified by the formation of novel functionally related paralogues arising from gene and genomic expansion by later multicellular organisms. Thus, we hypothesize that TCAPs original cellular role was to regulate cellular energy homeostasis, and that this mechanism has been conserved throughout the Metazoa. This supposition also suggests that the TCAPs should play a role in most metazoan tissues because the peptide evolved before the development of the multicellular animals and the subsequent differentiation of the various tissues and organs. It may also indicate that TCAP could play a greater role in the most highly energetic tissues.

TCAP and Transit Across Blood Brain Barriers

Assuming that TCAP evolved as a bioactive peptide in the earliest stages of metazoan evolution, then its presence in

metazoans predated the development of CNS-vascular barriers. Peptides structurally similar to TCAP [(54, 68); also see above] utilize a number of mechanisms that allows them to transit into neural tissues. CRF is relatively impermeable to the BBB although miniscule amounts do appear to cross (89). Unusually, CRF is transported out of the brain via a saturable transport system that allows peripheral actions (90). Urocortin-1, the direct paralogue of CRF in mammals, can cross the BBB in small amounts, but permeability is enhanced by co-administration of leptin. Urocortin-2, on the other hand, appears to cross by a passive diffusion mechanism (89). VIP, secretin and GLP-1 likely cross also by a non-saturable passive diffusion mechanism (91). In contrast, PACAP-38 enters the brain by a saturable transport system (3).

Likewise, evidence indicates that TCAP-1 also enters the brain, although the exact mechanism has not been determined. However, previous studies of an IV-administered fluorescein isothiocyanate (FITC)-TCAP1 variant were detected in capillaries and fiber tracts of the caudate putamen and alveolar hippocampus, as well as the anterior cingulate cortex, the cingulum and tracts leading to the choroid plexus (92). A number of the capillaries showed concentrations of fluorescence crossing the endothelial layer. Autoradiographic studies, utilizing IV-administered ^{125}I -labeled TCAP-1, similarly showed concentration in the caudate putamen, and cingulate cortex as well as regions of the nucleus accumbens, hippocampus and substantia nigra (86). Interestingly, neither study showed labeled TCAP-1 in any of the CVOs. Although these studies indicated that labeled TCAP-1 could be detected in the CNS after IV-administration, relative to the vehicle, FITC-only and ^{125}I -only controls, these studies do not confirm that the intact TCAP peptide was present in the labeled tissues as it is possible that peptide fragments bearing the label may be present.

However, the uptake of the intact TCAP into the brain is supported by a number of physiological studies. Peripheral administration of TCAP produces long-lasting actions that are not easily explained by its apparent short residency time in the CNS (49, 93–95). Several studies indicate that TCAP inhibits the long-term actions of CRF in the CNS. Peptides that do reach the CNS face particular challenges. Even among natural endogenous peptides, they are rapidly degraded by the peptidases of the vasculature and are eliminated via the urinary system. Of the small amount of the peptide that actually reaches its intended target in the CNS, it will be typically internalized and likely degraded. Therefore, this system has evolved to accept the smallest amount of the peptide to obtain a long-term action.

TCAP is an example of such a peptide. The biological half-life of IV-administered TCAP is similar to adrenocorticotrophic hormone (ACTH) and its plasma presence is typically removed via the kidneys and urinary tract. However, a single SC-administration of 10 nmol/kg can reduce plasma glucose by 40% for almost 1 week. A similar TCAP-1 administration significantly increases ^{18}F -deoxyglucose uptake into the brain after 3 days as assessed by functional positron emission

tomography (86). Moreover, *in vitro*, TCAP induces a significant uptake in ^3H -deoxyglucose in immortalized neurons due, in part, to a migration of glucose transporters to the plasma membrane. Long-term behavioral indications are similarly affected by TCAP. An ICV regimen of 30 pmols once per day over 5 days decreased the rat acoustic startle response (ASR) by 50% after 3 weeks (49). The ASR is typically used as a measure for anxiety. Using a similar dose/time regimen with either ICV or IV administration, TCAP-1 inhibited the CRF-induced reinstatement of cocaine seeking in rats (93–95).

Assuming the short residency time of TCAP on its CNS receptors, which occurs over a period of minutes, its mechanism may induce long-term synaptic plastic actions in order for these complex behaviors to endure. Evidence for neoplastic actions of TCAP in the brain has come from both *in vivo* and *in vitro* studies. *In vitro* studies utilizing primary and immortalized cell culture showed that TCAP was efficacious at regulating neurite and filopodia formation and axon fasciculation (92, 96). *In vivo*, IV-administration of TCAP-1 induced significant increases in dendritic spine density, and modulation of dendritic arborization (51, 97–99). These *in vivo* modifications of neuronal process development were corroborated *in vitro* by TCAP-mediated expression of a number of cytoskeletal protein mRNAs including β -tubulin α -actinin-4 and β -actin (92). Further studies indicate that the regulation of these mRNAs occurred via a TCAP-mediated phosphorylation of stathmin at serine-25 and filamin A at serine-2152 to stimulate actin and tubulin polymerization (96). Taken together, these studies indicate that TCAP-1 has efficacious neuroplastic actions that may provide an explanation for its long-term action on the CNS despite its expected low residency time on the CNS targets.

TCAP, CRF, AND MOOD DISORDERS

Teneurin C-terminal associated peptides evolved both before the formation of the CNS and the BBB and as a result of this, it could possess the necessary structural attributes to pass through a number of tissues and membranes. For this reason, the synthetic version of this peptide, when administered exogenously is efficacious at IV, ICV, and SC delivery. Moreover, this peptide possesses structural similarity to the CRF, calcitonin and secretin associated peptides and, likewise, can regulate glucose metabolism *in vivo*. CRF plays a fundamental role in the regulation of stress-associated energy metabolism and has been implicated in the etiology of mood disorders (100). Thus, taken together, these observations indicated that TCAP and related peptides could play a major role in the treatment of mood disorders including depression, anxiety, and post-traumatic-stress disorder, for example.

A number of TCAP-based studies support such a hypothesis. Initial studies using the acoustic startle reflex (ASR) model, a measure of anxiety, showed that animals with an initial strong response to the SRF showed an attenuation of the response when treated with TCAP. On the other hand animals with a

low initial ASR response showed an increased response in ASR (49). In a further study, when both high and low activity animals were combined, then TCAP pretreatment of the animals showed about a 50% decrease in the ASR after 3 weeks of treatment (49) indicating long lasting effects of TCAP. Further studies indicated that the attenuation of the anxiety response by TCAP was due, in part, to the inhibition of CRF actions. With respect to ASR, the expected increase in ASR by CRF could be entirely ablated by treatment with TCAP and could modulate elevated plus maze (EPM) and open field (OP) responses (101, 102). Particularly significant among these CRF-associated studies were the ablation studies of CRF-mediated cocaine seeking reinstatement by TCAP where TCAP inhibited cocaine seeking behavior in rats using both ICV and IV administration of TCAP (93–95). Furthermore, TCAP pretreatment *in vivo* in rats reduces CRF-mediated cfos expression in the limbic regions to basal levels (51, 99, 103).

Overall, TCAP is a natural peptide that possesses the key structural elements that can be used to develop new peptide analogs. The early evolution of TCAP could lead to the creation of a number of other related peptides that are essential for the internal regulation of metabolism and behavior. Although understanding the structural and physiological complexity of peptides will take some time to resolve, peptides in general, have the structural complexity and information transmission among tissues and organs that can act as the foundation for the next generation of drugs and may ultimately act to supplant the use of small molecule-based therapeutics which are typically used as front-line therapies.

The neuroanatomical substrates of mood and neuropsychiatric disorders do not corroborate well with the etiology of patients presenting with clinical symptoms of these conditions. The treatment of mood disorders using the current suite of frontline therapies rarely shows an improved prognosis in >50% of patients. Most of these pharmacological therapeutics incorporate small molecules to regulate monoamine and catecholamine neurotransmitters such as serotonin (5-HT), dopamine and norepinephrine. Despite their efficacy, these neurotransmitters only reach a subset of CNS regions. Because the range of neuroanatomical regions associated with each of these disorders is vast, rarely, if ever, can these therapeutics cover all affected regions of the CNS. Because of this, the medical community has resorted to electrical chemical therapies in the form of deep brain stimulation by transcranial electrode implantation (104), electroconvulsive therapy (ECT) (105), and transcranial magnetic stimulation (TMS) (106) to treat those patients whose conditions have been resistant to frontline pharmacologic therapies. Although the cellular and molecular mechanisms by which these therapies act is not understood, it does indicate that such approaches have a general effect beyond what is typically seen with any set of pharmacological therapeutics. Finding a commonality of the neuropathology amongst the range of mood disorders has been a particular challenge. One such commonality among all mood and psychiatric disorders is energy regulation. Recently, numerous studies have linked affective disorders such as major depression, anxiety, and post-traumatic stress disorders with CNS energy metabolism (107–110).

SUMMARY AND CONCLUSIONS

If we posit that homeostatic peptides regulate the synaptic plasticity of key regions of the CNS associated both with energy metabolism and reward- and fear-based learning behavior, then this indicates that bioactive peptides must, therefore, regulate the energy requirements of the associated neurons. TCAP-based peptides are phylogenetically ancient and are critical to the homeostasis of vertebrates. Because they and their receptor evolved in a single celled progenitor of multicellular organisms, they have become evolutionarily ensconced into numerous metabolic functions, notably within the CNS. In summary, the ancestral gene of TCAP evolved before the advent of the metazoans, and appears to have had a primary function in the regulation of energy metabolism. Its early appearance and maintenance in the genomes of extant metazoans indicates that was essential for the evolution of the Metazoa and may have acted as the ancestral gene that led to the evolution of CRF and the secretin family of peptides. Given this situation, the TCAPs may play a major role in energy metabolism of the brain and its associated pathology.

AUTHOR CONTRIBUTIONS

DL and DB-L: development and supervision of all research programs described in the paper. DH: senior PDF overseeing role of energy metabolism of TCAP and CRF. AD'A: developed methods for examining TCAPs role with respect to glycolysis and mitochondrial activity. CR: engaged in the direct role of TCAP on mitochondria. AD'A and CR: prepared the initial drafts of the role of TCAP, peptides, and pharmaceutical therapeutics with respect to the role of mitochondria. TD and FJ: prepared the initial drafts on the history of TCAP peptides.

FUNDING

This work was funded by grants from the Canadian Natural Sciences and Engineering Research Council (NSERC) and by Protogenic Therapeutics Inc. (PTI) to DL. DH was a recipient of Post-Doctoral Fellowship funding from PTI. In addition, TD was a recipient of an Ontario Graduate Scholarship (OGS) and AD'A was a former recipient of an NSERC doctoral scholarship.

REFERENCES

- Lovejoy DA. *Neuroendocrinology: An Integrated Approach*. Chichester: John Wiley & Sons Ltd. (2005).
- Kastin AJ, Pan W. Peptide transport across the blood-brain barrier. In: Prokai L, Prokai-Tatrai, editors. *Progress in Drug Research*. Vol 61. Basel: Birkhauser Verlag (2003). p. 81–100.
- Salameh TS, Banks WA. Delivery of therapeutic peptides and proteins to the CNS. *Adv Pharmacol*. (2014) 71:277–99. doi: 10.1016/bs.apha.2014.06.004
- Bloom SR. Hormonal peptides of the gastrointestinal tract. *Eur J Clin Invest*. (1979) 9:111–3. doi: 10.1111/j.1365-2362.1979.tb01676.x
- Witt M, Georgiewa B, Knecht M, Hummel T. On the chemosensory nature of the vomeronasal epithelium in adult humans. *Histochem Cell Biol*. (2002) 117:493–509. doi: 10.1007/s00418-002-0407-1
- Witt M, Hummel T. Vomeronasal versus olfactory epithelium: is there a cellular basis for human vomeronasal perception? *Int Rev Cytol*. (2006) 248: 209–59.
- D'Aniello B, Semin GR, Scandurra A, Pinelli C. The vomeronasal organ: a neglected organ. *Front Neuroanat*. (2017) 11:70. doi: 10.3389/fnana.2017.00070
- Wray S. From nose to brain: development of the gonadotropin-releasing neurones. *J Neuroendocrinol*. (2010) 22:743–53. doi: 10.1111/j.1365-2826.2010.02034.x
- Dulac C, Torello AT. Molecular detection of pheromone signals in mammals: from genes to behaviour. *Nat Rev Neurosci*. (2003) 4:551–62. doi: 10.1038/nrn1140
- Smith TD, Siegel MI, Burrows AM, Mooney MP, Burdi AR, Fabrizio PA, et al. Searching for the vomeronasal organ of adult humans: preliminary findings on location, structure and size. *Microsc Res Tech*. (1998) 41:483–91. doi: 10.1002/(SICI)1097-0029(19980615)41:6<483::AID-JEMT4>3.0.CO;2-O
- Wessels Q, Hoogland PV, Vorster W. Anatomical evidence for an endocrine activity of the vomeronasal organ in humans. *Clin Anat*. (2014) 27:856–60. doi: 10.1002/ca.22382
- Whelan JP, Wycocck CJ, Lampson LA. Distribution of beta 2-microglobulin in olfactory epithelium: a proliferating neuroepithelium not protected by a blood-tissue barrier. *J Immunol*. (1986) 137:2567–71.
- Senel S, Kremer M, Nagy K, Squier C. Delivery of bioactive peptides and proteins across oral (buccal) mucosa. *Curr Pharm Biotechnol*. (2001) 2:175–86. doi: 10.2174/1389201013378734
- Morales JO, Fathe KR, Brunaugh A, Ferati S, Li S, Montenegro-Nicolini M, et al. Challenges and future prospects for delivery of biologics: oral, mucosal, pulmonary and transdermal routes. *AAPS J*. (2017) 19:652–68. doi: 10.1208/s12248-017-0054-z
- Banks WA, Kastin AJ, Huang W, Jaspan JB, Maness LM. Leptin enters the brain by a saturable system independent of insulin. *Peptides*. (1996) 17:305–11. doi: 10.1016/0196-9781(96)00025-3
- Johansson CE, Stopa EG, McMillan PN. The blood-cerebrospinal fluid barrier: structure and functional significance. *Methods Mol Biol*. (2011) 686:101–31. doi: 10.1007/978-1-60761-938-3_4
- Kastin AJ, Fasold MB, Smith RR, Horner KA, Zadina JE. Saturable brain-to-blood transport of endomorphins. *Exp Brain Res*. (2001) 139:70–5. doi: 10.1007/s002210100736
- Jeffrey P, Summerfield SG. Challenges for the blood brain barrier screening. *Xenobiotica*. (2007) 37:1135–51. doi: 10.1080/00498250701570285
- Banks WA, Kastin AJ. Differential permeability of the blood-brain barrier to two pancreatic peptides: insulin and amylin. *Peptides*. (1998) 19:883–9. doi: 10.1016/S0196-9781(98)00018-7
- Advokat C, Gulati A. Spinal transections reduced both spinal antinociception and CNS concentration of systemically administered morphine in rats. *Brain Res*. (1991) 555:251–8. doi: 10.1016/0006-8993(91)90349-Z
- Strand F. *Neuropeptides: Regulators of Physiological Processes*. Cambridge: MIT Press (1999).
- Begley DJ. Peptides and the blood brain barrier: the status of our understanding. *Ann NY Acad Sci*. (1994) 739:89–100. doi: 10.1111/j.1749-6632.1994.tb19810.x
- Maness LM, Kastin AJ, Banks WA. Relative contributions of a CVO and the microvascular bed to delivery of blood-born IL-1 α to the brain. *Am J Physiol*. (1998) 275:E207–12. doi: 10.1152/ajpendo.1998.275.2.E207
- Baumgartner S, Chiquet-Ehrismann R. Ten-a, a drosophila gene related to tenascin, shows selective transcript localization. *Mech Dev*. (1993) 40:165–76. doi: 10.1016/0925-4773(93)90074-8
- Baumgartner S, Martin D, Hagios C, Chiquet-Ehrismann R. Ten-m, a Drosophila gene related to tenascin is a new pair-rule gene. *EMBO J*. (1994) 13:3728–40. doi: 10.1002/j.1460-2075.1994.tb06682.x
- Levine A, Bashan-Ahmed A, Budai-Hadrian O, Gartenberg D, Menasherow S, Wides R. Odd Oz: a novel Drosophila pair-rule gene. *Cell*. (1994) 77:587–98. doi: 10.1016/0092-8674(94)90220-8

27. Kenzelmann D, Chiquet-Ehrismann R, Tucker RP. Teneurins, a transmembrane protein family involved in cell communication during neuronal development. *Cell Mol Life Sci.* (2007) 64:1452–6. doi: 10.1007/s00018-007-7108-9
28. Lovejoy DA, Al Chawaf A, Cadinouche A. Teneurin C-terminal associated peptides: an enigmatic family of neuropeptides with structural similarity to the corticotrophin releasing factor and calcitonin family of peptides. *Gen Comp Endocrinol.* (2006) 148:299–305. doi: 10.1016/j.ygcen.2006.01.012
29. Holland PW, Garcia-Fernandez J. Hox genes and chordate evolution. *Dev Biol.* (1996) 173:282–395. doi: 10.1006/dbio.1996.0034
30. Lundin LG. Evolution of the vertebrate genome as reflected in paralogous chromosome regions in man and house mouse. *Genomics.* (1993) 16:1–19. doi: 10.1006/geno.1993.1133
31. Bagutti C, Forro G, Ferralli J, Rubin B, Chiquet-Ehrismann R. The intracellular domain of teneurin-2 has a nuclear function and represses zic-1-mediated transcription. *J Cell Sci.* (2003) 116:2957–66. doi: 10.1242/jcs.00603
32. Feng K, Zhou XH, Ohashi T, Morgelin M, Lustig A, Hirakawa S, et al. All four members of the ten-m/Odz family of transmembrane proteins form dimers. *J Biol Chem.* (2002) 277:26128–35. doi: 10.1074/jbc.M203722200
33. Nunes SM, Ferralli J, Choi K, Brown-Luedi M, Minet AD, Chiquet-Ehrismann R. The intracellular domain of teneurin-1 interacts with MBD1 and CAP/ponsin resulting in subcellular codistribution and translocation to the nuclear matrix. *Exp Cell Res.* (2005) 305:122–32. doi: 10.1016/j.yexcr.2004.12.020
34. Rubin BP, Tucker RP, Brown-Luedi M, Martin D, Chiquet-Ehrismann R. Teneurin 2 is expressed by the neurons of the thalamofugal visual system *in situ* and promotes homophilic cell-cell adhesion *in vitro*. *Development.* (2002) 129:4697–705.
35. Ohashi T, Zhou XH, Feng K, Richter B, Morgelin M, Perez MT, et al. Mouse ten-m/Odz is a new family of dimeric type II transmembrane proteins expressed in many tissues. *J Cell Biol.* (1999) 145:563–77. doi: 10.1083/jcb.145.3.563
36. Hamann J, Aust G, Arac D, Engel F, Formstone C, Fredriksson R, et al. International union of basic and clinical pharmacology. XCIV Adhesion G protein-coupled receptors. *Pharmacol Rev.* (2015) 67:338–67. doi: 10.1124/pr.114.009647
37. Nordstrom KVJ, Lagerstrom MC, Waller LM, Fredriksson R, Schiöth HB. The secretin GPCRs descended from the family of adhesion GPCRs. *Mol Biol Evol.* (2009) 26:71–84. doi: 10.1093/molbev/msn228
38. Davletov BA, Shamotienko OG, Lelianova VG, Grishin EG, Ushkaryov YA. Isolation and biochemical characterization of Ca²⁺-independent α -latrotoxin-binding protein. *J Biol Chem.* (1996) 271:23239–45. doi: 10.1074/jbc.271.38.23239
39. Krasnoperov VG, Bittner MA, Beavis R, Kuang T, Salinkow KV, Chepurny OG, et al. Alpha-latrotoxin stimulates exocytosis by the interaction with a neuronal G protein coupled receptor. *J Biol Chem.* (1997) 272:21504–8.
40. Petrenko AG, Kovalevko VA, Shamotienko OG, Surkova IN, Tarasyuk TA, Ushkaryov YA, et al. Isolation and properties of the alpha-latrotoxin receptor. *EMBO J.* (1990) 9:2023–7. doi: 10.1002/j.1460-2075.1990.tb08331.x
41. Ushkaryov YA, Petrenko AG, Geppert M, Südhof TC. Neurexins: synaptic cell surface proteins related to the alpha-latrotoxin receptor and laminin. *Science.* (1992) 257:50–6. doi: 10.1126/science.1621094
42. Rosenthal L, Zacchetti D, Madeddu L, Meldolesi J. Mode of action of alpha-latrotoxin: role of divalent cation in Ca²⁺-dependent and Ca²⁺-independent effects mediated by the toxin. *Mol Pharmacol.* (1990) 38:917–23.
43. Lelianova VG, Davletov BA, Sterling A, Rahman MA, Grishin EV, Totty NF, et al. α -Latrotoxin receptor, Latrophilin, is a novel member of the Secretin family of G protein-coupled receptors. *J Biol Chem.* (1997) 272:21504–8. doi: 10.1074/jbc.272.34.21504
44. Fredriksson R, Lagerström M, Lundin L, Schiöth H. The G-protein coupled receptors in the human genome form five main families. Phylogenetic analysis, paralogon groups and fingerprints. *Mol Pharmacol.* (2003) 63:1256–72. doi: 10.1124/mol.63.6.1256
45. Meza-Aguilar DG, Boucard AA. Latrophilins updated. *BioMol Concepts.* (2014) 5:457–78. doi: 10.1515/bmc-2014-0032
46. King N, Hittinger CT, Carroll SB. Evolution of key cell signaling and adhesion protein families predates animal origins. *Science.* (2003) 301:361–3. doi: 10.1126/science.1083853
47. Schiöth HB, Nordström KJ, Fredriksson R. The adhesion GPCRs: gene repertoire, phylogeny and evolution. *Adv Exp Med Biol.* (2010) 706:1–13. doi: 10.1007/978-1-4419-7913-1_1
48. Qian X, Barsyte-Lovejoy D, Wang L, Chewpoy B, Gautam N, Al Chawaf A, et al. Cloning and characterization of teneurin C-terminus associated peptide (TCAP)-3 from the hypothalamus of an adult rainbow trout (*Oncorhynchus mykiss*). *Gen Comp Endocrinol.* (2004) 137:205–16. doi: 10.1016/j.ygcen.2004.02.007
49. Wang L, Rotzinger S, Al Chawaf A, Elias C, Barsyte-Lovejoy D, Qian X, et al. Teneurin proteins possess a carboxy terminal sequence with neuromodulatory activity. *Mol Brain Res.* (2005) 133:253–65. doi: 10.1016/j.molbrainres.2004.10.019
50. Lovejoy DA. Structural evolution of urotensin-1: Reflections of life before corticotropin releasing factor. *Gen Comp Endocrinol.* (2009) 164:15–9. doi: 10.1016/j.ygcen.2009.04.014
51. Tan L, Chand D, De Almeida R, Xu M, De Lannoy L, Lovejoy D. Modulation of neuroplastic changes and corticotropin-releasing factor-associated behavior by a phylogenetically ancient and conserved peptide family. *Gen Comp Endocrinol.* (2012) 176:309–13. doi: 10.1016/j.ygcen.2011.11.011
52. Seidah NG, Chretien M. Proprotein and prohormone convertases: a family of subtilases generating diverse bioactive polypeptides. *Brain Res.* (1999) 848:45–62. doi: 10.1016/S0006-8993(99)01909-5
53. Chand D, Casatti CA, De Lannoy L, Song L, Kollara A, Barsyte-Lovejoy D, et al. C-terminal processing of the teneurin proteins: independent actions of a teneurin C-terminal associated peptide in hippocampal cells. *Mol Cell Neurosci.* (2013) 52:38–50. doi: 10.1016/j.mcn.2012.09.006
54. Lovejoy D, de Lannoy L. Evolution and phylogeny of the corticotropin-releasing factor (CRF) family of peptides: Expansion and specialization in the vertebrates. *J Chem Neuroanat.* (2013) 54:50–6. doi: 10.1016/j.jchemneu.2013.09.006
55. Cardoso JC, Bergqvist CA, Felix RC, Larhammar D. Corticotropin-releasing hormone family evolution: five ancestral genes remain in some lineages. *J Mol Endocrinol.* (2016) 57:73–86. doi: 10.1530/JME-16-0051
56. De Souza E. Corticotropin-releasing factor receptors: physiology, pharmacology, biochemistry and role in central nervous system and immune disorders. *Psychoneuroendocrinology.* (1995) 20:789–819. doi: 10.1016/0306-4530(95)00011-9
57. Owens M, Nemeroff C. Physiology and pharmacology of Corticotropin-releasing factor. *Pharmacol Rev.* (1991) 43:425–73.
58. Lovejoy DA. Chapter 101 - CRH family. In: Abba JK, editor. *Handbook of Biologically Active Peptides*. 2nd Edn. Boston, MA: Academic Press (2013). p. 752–9.
59. Grone BP, Marsuka KP. Divergent evolution of two corticotropin releasing hormone (CRH) genes in teleost fishes. *Front Neurosci.* (2015) 9:365. doi: 10.3389/fnins.2015.00365
60. Hosono K, Kikuchi Y, Miyaniishi H, Hiraki-Kajiyama T, Takeuchi A, Nakasone K, et al. Teleocortin: a novel member of the CRH family in teleost fish. *Endocrinology.* (2015) 156:2949–57. doi: 10.1210/en.2015-1042
61. Nock TG, Chand D, Lovejoy DA. Identification of members of the gonadotropin-releasing hormone (GnRH), corticotropin-releasing factor (CRF) families in the genome of the holocephalan, *Callorhynchus milii* (elephant shark). *Gen Comp Endocrinol.* (2011) 171:237–44. doi: 10.1016/j.ygcen.2011.02.001
62. Endsin MJ, Michalec O, Manzon LA, Lovejoy DA, Manzon RG. CRH peptide evolution occurred in three phases: evidence from characterizing sea lamprey CRH system members. *Gen Comp Endocrinol.* (2017) 240:162–73. doi: 10.1016/j.ygcen.2016.10.009
63. Hogg DW, Husic M, Lovejoy DA. Family of peptides: corticotropin-releasing hormone. In: Huhtaniemi IT, editor. *Encyclopedia of Endocrine Diseases, Vol. 3*. 2nd ed. San Diego, CA: Elsevier, Inc. (2018). p. 16–26.
64. Hsu SY, Hsueh AJ. Human stresscopin and stresscopin-related peptide are selective ligands for the type 2 corticotropin-releasing hormone. *Nat Med.* (2001) 7:605–11. doi: 10.1038/87936

65. Lewis K, Li C, Perrin MH, Blount A, Kunitake K, Donaldson C, et al. Identification of urocortin III, an additional member of the corticotropin-releasing factor (CRF) family with high affinity for the CRF2 receptor. *Proc Natl Acad Sci USA*. (2001) 98:7570–5. doi: 10.1073/pnas.121165198
66. Reyes TM, Lewis K, Perrin MH, Kunitake KS, Vaughan J, Arias CA, et al. Urocortin II: a member of the corticotropin-releasing factor (CRF) neuropeptide family that is selectively bound by type 2 CRF receptors. *Proc Natl Acad Sci USA*. (2001) 98:2843–8. doi: 10.1073/pnas.051626398
67. Coast G. Insect Diuretic peptides: structures, evolution and actions. *Am Zool*. (1998) 38:442–9. doi: 10.1093/icb/38.3.442
68. Lovejoy D, Jahan S. Phylogeny of the corticotropin-releasing factor family of peptides in the metazoa. *Gen Comp Endocrinol*. (2006) 146:1–8. doi: 10.1016/j.ygcen.2005.11.019
69. Chand D, De Lannoy L, Tucker R, Lovejoy D. Origin of chordate peptides by horizontal protozoan gene transfer on early metazoans and protists: evolution of the teneurin C-terminal associated peptides (TCAP). *Gen Comp Endocrinol*. (2013) 188:144–50. doi: 10.1016/j.ygcen.2013.02.006
70. Minet AD, Chiquet-Ehrismann R. Phylogenetic analysis of teneurin genes and comparison to the rearrangement hot spot elements of *E. coli*. *Gene*. (2000) 257:87–97. doi: 10.1016/S0378-1119(00)00388-7
71. Tucker RP, Beckmann J, Leachman NT, Schöler J, Chiquet-Ehrismann R. Phylogenetic analysis of the teneurins: conserved features and premetazoan ancestry. *Mol Biol Evol*. (2012) 29:1019–29. doi: 10.1093/molbev/msr271
72. Zhang D, de Souza RF, Anantharaman V, Iyer ALM. Polymorphic toxin systems: comprehensive characterization of trafficking modes, mechanism of action, immunity and ecology using comparative genomics. *Biol Direct*. (2012) 7:18. doi: 10.1186/1745-6150-7-18
73. Tucker RP. Horizontal gene transfer in choanoflagellates. *J Exp Zool B Mol Dev Evol*. (2013) 320:1–9. doi: 10.1002/jez.b.22480
74. Jackson VA, Meijer DH, Carrasquero M, van Bezouwen LS, Lowe ED, Kleanthous C, et al. Structures of Teneurin adhesion receptors reveal an ancient fold for cell-cell interaction. *Nat Commun*. (2018) 9:1079. doi: 10.1038/s41467-018-03460-0
75. Li J, Shalev-Benami M, Sando R, Jiang X, Kibrom A, Wang J, et al. Structural basis for teneurin function in circuit-wiring: a toxin motif at the synapse. *Cell*. (2018) 173:735–48. doi: 10.1016/j.cell.2018.03.036
76. Busby JN, Panjikar S, Landsberg MJ, Hurst MR, Lott JS. The BC component of ABC toxins is an RHS-repeat-containing protein encapsulation device. *Nature*. (2013) 501:547–50. doi: 10.1038/nature12465
77. Silva JP, Leilanova VG, Ermolyuk YS, Vysokov N, Hitchen PG, Berninghausen O, et al. Latrophilin 1 and its endogenous ligand Lasso/teneurin-2 form a high-affinity transsynaptic receptor pair with signaling capabilities. *Proc Natl Acad Sci USA*. (2011) 108:12113–8. doi: 10.1073/pnas.1019434108
78. Boucard AA, Maxeiner S, Sudhof TC. Latrophilins function as a heterophilic cell-adhesion molecules by binding to teneurins: regulation by alternative splicing. *J Biol Chem*. (2014) 289:387–402. doi: 10.1074/jbc.M113.504779
79. O'Sullivan ML, Martini F, von Daake S, Comoletti D, Ghosh A. LPHN3, a presynaptic adhesion-GPCR implicated in ADHD, regulates the strength of neocortical layer 2/3 synaptic input to layer 5. *Neural Dev*. (2014) 9:7. doi: 10.1186/1749-8104-9-7
80. Husic M, Baryte-Lovejoy D, Lovejoy DA. Teneurin C-terminal associated peptide (TCAP)-1 and latrophilin interaction in HEK293 cells: evidence for modulation for intercellular adhesion. *Front Endocrinol*. (2019) 10:22. doi: 10.3389/fendo.2019.00022
81. Lima WG, Marques-Oliveira GH, da Silva TM, Chaves VE. Role of calcitonin gene-related peptide in energy metabolism. *Endocrine*. (2017) 58:3–13. doi: 10.1007/s12020-017-1404-4
82. Lovejoy DA, Chang B, Lovejoy N, Del Castillo J. Molecular evolution and origin of the corticotropin-releasing hormone receptors. *J Mol Endocrinol*. (2014) 52:43–6079. doi: 10.1530/JME-13-0238
83. Sekar R, Chow BK. Role of secretin peptide family and their receptors in the hypothalamic control of energy homeostasis. *Horm Metab Res*. (2013) 45:945–54. doi: 10.1055/s-0033-1353155
84. Chen Y, Xu M, De Almeida R, Lovejoy DA. Teneurin C-terminal associated peptides (TCAP): modulators of corticotropin-releasing factor (CRF) physiology and behavior. *Front Neurosci*. (2013) 7:166. doi: 10.3389/fnins.2013.00166
85. D'Aquila AL, Hsieh A, Hsieh A, De Almeida R, Lovejoy SR, Lovejoy DA. Expression and actions of corticotropin-releasing factor/diuretic hormone-like peptide (CDLP) and teneurin C-terminal associated peptide (TCAP) in the vase tunicate, *Ciona intestinalis*: antagonism of the feeding response. *Gen Comp Endocrinol*. (2016) 246:105–15. doi: 10.1016/j.ygcen.2016.06.015
86. Hogg DW, Chen Y, D'Aquila AL, Xu M, Husic M, Tan LA, et al. A novel role of the corticotropin-releasing hormone (CRH) regulating peptide, teneurin C-terminal associated peptide (TCAP)-1 on glucose uptake into the brain. *J Neuroendocrinol*. (2018) 30:e12579. doi: 10.1111/jne.12579
87. Ebberink RH, Smit AB, Van Minnen J. The insulin family: evolution of structure and function in vertebrates and invertebrates. *Bio Bull*. (1989) 177:176–82. doi: 10.2307/1541928
88. Wimalawansa SJ. Amylin, calcitonin gene-related peptide, calcitonin, and adrenomedullin: a peptide superfamily. *Crit Rev Neurobiol*. (1997) 11:167–239. doi: 10.1615/CritRevNeurobiol.v11.i2.3.40
89. Kastin AJ, Akerstrom V. Differential interactions of the urocortin/corticotropin-releasing hormone peptides with the blood brain barrier. *Neuroendocrinology*. (2002) 75:367–74. doi: 10.1159/000059433
90. Martins JM, Banks WA, Kastin AJ. Transport of CRF from mouse brain directly affects peripheral production of β -endorphin by the spleen. *Am J Physiol*. (1997) 273:E1083–9. doi: 10.1152/ajpendo.1997.273.6.E1083
91. Dogrukul-Ak D, Tore F, Tuncel N. Passage of VIP/PACAP/secretin family across the blood-brain barrier: therapeutic effects. *Curr Pharm Des*. (2004) 10:1325–40. doi: 10.2174/1381612043384934
92. Al Chawaf A, St. Amant K, Belsham DD, Lovejoy DA. Regulation of neurite outgrowth in immortalized hypothalamic cells and hippocampal primary cultures by Teneurin C-terminal associated peptide-1 (TCAP-1). *Neuroscience*. (2007) 144:1241–54. doi: 10.1016/j.neuroscience.2006.09.062
93. Erb S, McPhee M, Brown ZJ, Kupferschmidt DA, Song L, Lovejoy DA. Repeated intravenous administrations of teneurin-C terminal associated peptide (TCAP)-1 attenuates reinstatement of cocaine seeking by corticotropin-releasing factor (CRF) in rats. *Beh Brain Res*. (2014) 269:1–5. doi: 10.1016/j.bbr.2014.04.013
94. Kupferschmidt DA, Lovejoy DA, Rotzinger S, Erb S. Teneurin C-terminal associated peptide (TCAP)-1 blocks the effects of corticotropin-releasing factor on reinstatement of cocaine seeking and on cocaine-induced behavioural sensitization. *Br J Pharmacol*. (2011) 162:574–83. doi: 10.1111/j.1476-5381.2010.01055.x
95. Kupferschmidt D, Lovejoy DA, Erb S. Teneurin C-terminal associated peptide (TCAP)-1 and corticotropin-releasing factor (CRF) interactions in the modulation of cocaine-related behaviour. In: Preedy V, editor. *The Neuroscience of Cocaine: Mechanisms and Treatment*. Cambridge, MA: Academic Press; Elsevier (2017). p. 195–203.
96. Chand D, Song L, De Lannoy L, Barsyte-Lovejoy D, Ackloo S, Boutros PC, et al. C-terminal region of Teneurin-1 co-localizes with dystroglycan and modulates cytoskeletal organization through an ERK-dependent stathmin- and filamin A-mediated mechanism in hippocampal cells. *Neuroscience*. (2012) 219:255–70. doi: 10.1016/j.neuroscience.2012.05.069
97. Rotzinger S, Lovejoy DA, Tan L. Behavioral effects of neuropeptide ligands in rodent models of depression and anxiety. *Peptides*. (2010) 31:736–56. doi: 10.1016/j.peptides.2009.12.015
98. Tan LA, Xu K, Vaccarino FJ, Lovejoy DA, Rotzinger S. Teneurin C-terminal associated peptide (TCAP)-1 attenuates corticotropin-releasing factor (CRF)-induced c-Fos expression in the limbic system and modulates anxiety behavior in male Wistar rats. *Behav Brain Res*. (2009) 201:198–206. doi: 10.1016/j.bbr.2009.02.013
99. Tan LA, Al Chawaf A, Vaccarino FJ, Boutros JC, Lovejoy DA. Teneurin C-terminal associated peptide (TCAP)-1 increases dendritic spine density in hippocampal neurons and decreases anxiety-like behaviors in rats. *Physiol Behav*. (2011). 104:199–204. doi: 10.1016/j.physbeh.2011.03.015
100. Deussing JM, Chen A. The corticotropin releasing factor family: Physiology of the stress response. *Physiol Rev*. (2018) 98:2225–86. doi: 10.1152/physrev.00042.2017
101. Rotzinger S, Tan L, Xu K, Lovejoy DA, Vaccarino FJ. TCAP-1 administration in rats modulates the anxiogenic effects of CRF in three tests of anxiety. *Neuropeptides*. (2006) 40:157–8. doi: 10.1016/j.npep.2006.09.042

102. Tan L, Xu K, Vaccarino F, Lovejoy DA, Rotzinger S. Repeated intracerebral Teneurin C-terminal associated peptide (TCAP)-1 injections produce enduring changes in behavioral responses to corticotropin-releasing factor (CRF) in rat models of anxiety. *Behav Brain Res.* (2008) 188:195–200. doi: 10.1016/j.bbr.2007.10.032
103. Tan L, Lovejoy DA. Neuroprotection, neuronal remodelling, and anxiety-like behaviour: The role of the teneurin and teneurin C-terminal associated peptide (TCAP) system in the hippocampus. *Am J Neuroprot Neuroregen.* (2009) 1:3–10. doi: 10.1166/ajnn.2009.1007
104. Staudt MD, Herring EZ, Gao K, Miller JP, Sweet JA. Evolution in the treatment of psychiatric disorders: from psychosurgery to psychopharmacology to neuromodulation. *Front Neurosci.* (2019) 13:108. doi: 10.3389/fnins.2019.00108
105. Baldinger-Melich P, Gryglewski G, Philippe C, James GM, Vranka C, Silberbauer L, et al. The effect of electroconvulsive therapy on cerebral monoamine oxidase A expression in treatment-resistant depression investigated using positron emission tomography. *Brain Stimul.* (2019) 12:714–23. doi: 10.1016/j.brs.2018.12.976
106. Škarabot J, Mesquita RNO, Brownstein CG, Ansdell P. Myths and methodologies: how loud is the story told by the transcranial magnetic stimulation-evoked silent period? *Exp Physiol.* (2019) 104:635–42. doi: 10.1113/EP087557
107. Allen J, Romay-Tallon R, Brymer KJ, Caruncho HK, Kalynchuk LE. Mitochondria and mood: Mitochondrial dysfunction as a key player in the manifestation of depression. *Front Neurosci.* (2018) 12:386. doi: 10.3389/fnins.2018.00386
108. Kim Y, Vadodaria KC, Lenkei Z, Kato T, Gage FH, Marchetto MC, et al. Mitochondria, metabolism, and redox mechanisms in psychiatric disorders. *Antioxid Redox Signal.* (2019) 31:275–317. doi: 10.1089/ars.2018.7606
109. Wallace DC. A mitochondrial etiology of neuropsychiatric disorders. *JAMA Psychiatry.* (2017) 74:863–4. doi: 10.1001/jamapsychiatry.2017.0397
110. Østergaard L, Jørgensen MB, Knudsen GM. Low on energy? An energy supply-demand perspective on stress and depression. *Neurosci Biobehav Rev.* (2018) 94:248–70. doi: 10.1016/j.neubiorev.2018.08.007

Conflict of Interest: DL is a co-founder of Protagenic Therapeutics, Inc., a biotechnology company that has a commercial interest in the therapeutic possibilities of the TCAPs.

The remaining authors declare that the research was conducted in the absence of any commercial or financial relationships that could be construed as a potential conflict of interest.

Copyright © 2019 Lovejoy, Hogg, Dodsworth, Jurado, Read, D'Aquila and Barsyte-Lovejoy. This is an open-access article distributed under the terms of the Creative Commons Attribution License (CC BY). The use, distribution or reproduction in other forums is permitted, provided the original author(s) and the copyright owner(s) are credited and that the original publication in this journal is cited, in accordance with accepted academic practice. No use, distribution or reproduction is permitted which does not comply with these terms.

Advantages of publishing in Frontiers



OPEN ACCESS

Articles are free to read
for greatest visibility
and readership



FAST PUBLICATION

Around 90 days
from submission
to decision



HIGH QUALITY PEER-REVIEW

Rigorous, collaborative,
and constructive
peer-review



TRANSPARENT PEER-REVIEW

Editors and reviewers
acknowledged by name
on published articles

Frontiers

Avenue du Tribunal-Fédéral 34
1005 Lausanne | Switzerland

Visit us: www.frontiersin.org

Contact us: info@frontiersin.org | +41 21 510 17 00



REPRODUCIBILITY OF RESEARCH

Support open data
and methods to enhance
research reproducibility



DIGITAL PUBLISHING

Articles designed
for optimal readership
across devices



FOLLOW US

@frontiersin



IMPACT METRICS

Advanced article metrics
track visibility across
digital media



EXTENSIVE PROMOTION

Marketing
and promotion
of impactful research



LOOP RESEARCH NETWORK

Our network
increases your
article's readership